CORA Cork Open Research Archive
Cartlann Taighde Oscailte Chorcaí

Title	Studies in derivatisation and direct arylation of heterocycles
Authors	Hickey, Aobha
Publication date	2022
Original Citation	Hickey, A. 2022. Studies in derivatisation and direct arylation of heterocycles. PhD Thesis, University College Cork.
Type of publication	Doctoral thesis
Rights	© 2022, Aobha Hickey. - https://creativecommons.org/licenses/by-nc-nd/4.0/
Download date	2026-11-06 23:03:42
Item downloaded from	https://hdl.handle.net/10468/13671



UCC
University College Cork, Ireland
Coláiste na hOllscoile Corcaigh

Studies in Derivatisation and Direct Arylation of Heterocycles



Aobha Hickey, B. Sc.

A thesis presented for the degree of

Doctor of Philosophy

to

NATIONAL UNIVERSITY OF IRELAND, CORK

School of Chemistry

University College Cork

Supervisor: Dr Gerard P. McGlacken

Head of School: Dr Humphrey Moynihan

2022

Table of Contents

Declaration v

Acknowledgements vi

Abstract ix

Preface x

Abbreviations and Acronyms xi

Chapter 1 Interspecies Activity of Alkyl-2-Pyrones 2

Introduction 2

1.1. 2-Pyrones 2

1.2. Quorum Sensing 3

1.3. Bacillus atropheaus 5

1.4. Pseudomonas aeruginosa 7

1.5. Interspecies and Interkingdom Activity of Autoinducers 7

Results and Discussion 9

1.6. Objectives 9

1.7. Chemistry 9

1.8. Biological Results 16

1.9. Further Developments 20

Conclusions and Future Work 22

Experimental 23

1.10. General Procedures 23

1.11. Synthesis of Alkyl-2-Pyrones 24

References 40

Chapter 2 Direct Arylation and Reversible Oxidative Addition of Bromophenoxyquinolines 43

Introduction 44
2.1. Quinolines 44
2.2. Aryl-Aryl Bond Formation 44
2.3. Direct Arylation of Nitrogen-Based Heterocycles 47
2.4. ^{1}H-^{15}N HMBC NMR Spectroscopy 48
2.5. One-Pot Reactions 49
2.6. Substrates with Multiple Halogens 50
2.7. Ultraviolet-Visible Absorption Spectroscopy 52
2.8. Fluorescence Spectroscopy 54
2.9. Fluorescent Quinolines 56
2.10. Potential for Reversible Oxidative Addition 57
2.11. Reversible Oxidative Addition in Synthesis 58
Results and Discussion 61
2.12. Objectives 61
2.13. Intramolecular Direct Arylation 62
2.14. One-Pot Tandem Cross-Coupling/Direct Arylation 64
2.15. Palladium-Quinoline Interaction 72
2.16. Photophysical Characterisation of One-Pot Products 88
2.17. Reversible Oxidative Addition 96
Conclusions 113
Experimental 114
2.18. General Procedures 114
2.19. Direct Arylation/One-Pot Substrates and Products 117
2.20. Reversible Oxidative Addition Substrates and Products 145
References 154
Chapter 3 Borylation of 6-Fluoroquinolines: Access to 6-Fluoroquinolones 157

Introduction 158

3.1. Fluoroquinolone Antibiotics 158

3.2. C-H Activation 161

3.3. Carbon-Boron Bond Formation 161

3.4. Iridium-Catalysed C-H Borylation 164

Results and Discussion 174

3.5. Objectives 174

3.6. Borylation of 2-Methylquinolones 175

3.7. Borylation of 6-Fluoroquinolones 178

3.8. Alternative Strategy for Borylation of 6-Fluoroquinolones 179

3.9. Purification of Borylated Products 183

3.10. Synthesis of Quinoline Starting Materials 188

3.11. Conversion of Substituted 4-Quinolines to 4-Quinolones 193

3.12. Borylation of 4-Substituted-Quinolines 197

3.13. Conversion of Functionalised 4-Substituted-Quinolines to 4-Quinolones 204

3.14. Functionalisation of 7-Borylated-4-Substituted-Quinolines 206

Conclusions and Future Work 215

Experimental 217

3.15. General Procedures 217

3.16. Compounds from Preliminary Studies 219

3.17. Substrates for Borylation 225

3.18. Borylation and Dervitisation of Quinoline Substrates 234

References 256

"Results! Why, man, I have gotten a lot of results. I know several thousand things that won't work!"

Thomas A. Edison

An té nach gcuireann san earrach ní bhaineann sé san fhómhar. (Whoever does not plant in the spring does not reap in the fall.)

Seanfhocal (Irish Proverb)

Declaration

This is to certify that the work I am submitting is my own and has not been submitted for another degree, either at University College Cork or elsewhere. All external references and sources are clearly acknowledged and identified within the contents. I have read and understood the regulations of University College Cork concerning plagiarism.

_____ 05May2022

Aobha Hickey

Acknowledgements

Firstly, I would like to express my gratitude to my supervisor, Dr Gerard McGlacken for giving me the opportunity to undertake these projects as part of his group, particularly for his continued support and guidance throughout my research. I greatly acknowledge The Irish Research Council for their generous funding, as well as the Higher Education Authority for granting a costed extension after on-site research was disrupted by the COVID-19 pandemic. I sincerely thank Dr Stuart Collins and Prof. Patrick Steel for examining this thesis.

Many thanks to all the technical officers that keep things running smoothly in the Kane – to Dr Lorraine Bateman, Dr Denis Lynch and Dr Dan McCarthy for NMR services, to Dr Florence McCarthy, Ryan Alam and Mick O'Shea for mass spectrometry analysis, to everyone who has worked in the Chemistry Office throughout my time here, to Noel Browne and all other staff in the School of Chemistry who make it possible for us researchers to get our work done. A special mention to Dr Tom O'Mahony for always being so willing to help and for the many hours of work that went into keeping all of our lab infrastructure afloat (no pun intended!). Sincerest thanks to Dr Trevor Carey and Dr Ian O'Connor for preventing my laptop from imploding and, most importantly, for keeping me up to date on the daily gossip! Big thank you to Dr Francis Harrington for your inventions and your advice in all things. Vielen Dank an Derry Kearney für seine kontroversen Meinungen und dafür, das er so viel von meinen Glaswaren gespart hat! Thank you also to Tina Kent and Denis Duggan for always putting a smile on my face and giving a helping hand wherever it was needed.

I also wish to acknowledge the many collaborations which evolved from the projects described herein. Thank you to Prof. John Sodeau for giving me a substantial crash course in photophysics, and to Prof. Fergal O'Gara and Dr F. Jerry Reen and their groups in the School of Microbiology here in UCC. A huge thank you to Prof Todd B. Marder and his research group in Universität Würzburg, and specifically to Dr Julia Merz, for taking such good care of me when I visited. It was a pleasure to work with you, danke schön für alles.

I have made many friends here over the course of this PhD programme, too many to list, but all of whom have contributed to the compilation of this thesis in some way; I am privileged to have worked alongside of you all. I thank you for helping me with queries, and for the chats, rants and cake in the write up area. A massive thank you to Dr Denis Lynch for everything that he does for all of the PhD students, without even a grumble of complaint, you have helped me in so many ways. Thanks to Amy L (the beesh) for many hugs, to Orla (hype girl, bestie) for all the organised fun and adventures, and to Edel for lots of laughs and several trips to the toilet! To my most unexpected friend, Aidan, I have thoroughly enjoyed getting to know you – just a shame you were so terrified of me at first! Also, I'm so glad I was able to help guide you on your chromatographic journey of discovery (lol).

A special thank you to my three 'lab moms' (it was a complicated but happy relationship) – Dr Leticia Pardo (original mom), Dr Rachel Shanahan (step-mom) and Dr Aisling Prendergast (other step-mom). Muchas gracias Leti para todo, you were my first lab mentor way back when I did my undergraduate summer placement. You have taught me so much and supported me in every way, with your sharp eyes, fresh perspective, café and pints of Beamish – even when you became an absent mother! Thanks to Rachel for sharing your wisdom, tips and tricks with me, listening to my endless raving and for teaching me how to cope when things aren't going so well. Thanks to Aisling for lending me your astuteness (wizardry) in all things IT and for being perfectly pedantic about corrections. A big thank you to Emma, Eimear and Mark for all of the laughs (with and at) and the pistachio bombolini-fuelled weight gain – Sicilian Delights will likely go into liquidation when we have all finished up! I honestly don't think I would have made it here without your advice and company (and voice notes) helping me on the worst of days. Eimear, you are one *feerse* girl — I have immensely enjoyed our many grub/coffee-related adventures and chats. A big thank you to Mark for always being so enthusiastic about chemistry, especially when the rest of us just simply couldn't be. Emma, we have been through the hoop together and have somehow managed to survive! You have been a very kind and generous friend and I am so grateful to you for that. To the rest of the GMG group past and present: Katrina, Pamela, Eoin, Robyn, David R, Marie Clara, Conor, Si-Lok,

Ella, Muireann and David J. Go raibh míle maith agaibh for putting up with my antics, including the persistent terrible singing, occasional cartwheeling and, of course, helping me with the many conundrums I have thrown at you all.

Finally, I express my utmost appreciation to my family and friends. To my siblings, Caoimhe, Kealan and Alannah – thank you for your encouragement and for never letting me forget my eternal student status! A particular mention to my mom and dad, Brid and Richard, who showed me the meaning of hard work and always prioritised our education. I am infinitely indebted to you both and dedicate this thesis to you. I also want to thank my Nanny Barbara (the Barb) to whom this thesis is also dedicated, for being so blindingly proud of everything we do; I hope this last day out in UCC will be the best of all (even if I am going to be the 'wrong' type of Dr!). I am massively grateful to my friends near and far who will probably never see this thesis: Róisín, Jen, Katie, Hazel, Úna, Maunsell, Eimear, Denise, Sophie and Kav – for being a constant reminder that there is a lot more to life than chemistry. Finally, Conor, I can't begin to thank you enough for keeping me sane (in ways). I would not have finished this without you.

There are some things you can't share without ending up liking each other, and knocking out a twelve-foot mountain troll is one of them.

J. K. Rowling
Harry Potter and the Philosophers Stone

For Brid, Richard and
the Barb

Abstract

Quorum sensing (QS) is a complex form of communication employed by bacterial species to coordinate group behaviours through the biosynthesis, secretion and detection of small molecules known as autoinducers (AIs). Understanding the mechanism *via* which these sophisticated networks operate could allow for the development of non-traditional therapies for the treatment of multi-drug resistant infections. Heerman and co-workers recently identified a group of 2-pyrones as AIs in the QS network of *Photorhabdus luminescens*. In Chapter 1, we synthesised 30 2-pyrone analogues, and explored whether these compounds could induce an interspecies response on a co-inhabiting microorganism, *Bacillus atropheaus*. One naturally occurring derivative dramatically enhanced the biofilm biomass of *B. atropheaus*. Contrastingly, all other natural and synthetic derivatives exhibited biofilm-inhibiting effects. Swarming motility was repressed by several analogues, with carbon chains between six and 10 units at the C-3 position proving optimal.

In Chapter 2 the palladium-catalysed, phosphine-free direct arylation of 4-phenoxyquinolines in air is described. Diverse benzofuroquinolines were synthesised with excellent yields. Further expansions of this reaction using multi-halogenated substrates allowed for two, mechanistically distinct reactions to occur in one-pot using the same pre-catalyst. Investigations employing ^{1}H-^{15}N HMBC spectroscopy led us to propose that the quinoline motif may be acting as an *N*-ligand to palladium in these transformations. The photophysical characteristics of the scaffolds constructed are reported. Attempts to build on recent breakthroughs in the area of reversible oxidative addition to preserve C-Br bonds are also described.

The quinoline nucleus is a versatile, nitrogen-based heterocycle which is found in numerous synthetic and naturally occurring pharmacologically active compounds. Structurally similar 6-fluoroquinolones account for a large portion of the antibiotic market. Chapter 3 involves the use of an iridium-catalysed C-H functionalisation/borylation strategy to selectively synthesise C-7 substituted 6-fluoroquinolines. The borylations proceed with very good yields and various important transformations utilising the installed boron group are demonstrated. Finally, the ubiquitous 6-fluoroquinolone moiety can be revealed through hydrolysis or hydrogenolysis of the 6-fluoro-4-substituted quinolines.

Preface

This thesis contains work which has been published after peer-review, or which is in the process of publication. Publications arising from this thesis are provided in Appendix II.

Abbreviations and Acronyms

A	absorbance
Å	ångström
Ac	acetyl
AcOH	acetic acid
Adm	1-adamantanecarboxylic acid
AHL	*N*-acyl homoserine lactone
anal.	analysis
approx.	approximately
aq.	aqueous
Ar	aryl
B_2pin_2	bis(pinacolato)diboron
Bcat	catechol boronic ester
BINAP	2,2'-bis(diphenylphosphino)-1,1'-binaphthalene
Bn	benzyl
Boc	*tert*-butyloxycarbonyl
Bpin	pinacol boronic ester
bpy	2,2'-bipyridine
bs	broad singlet
Bu	butyl
c	path length of a photon concentration
°C	Celsius degrees
^{13}C NMR	carbon nuclear magnetic resonance
ca.	*circa*, about
CA	citrate anion
CF	cystic fibrosis
COD	1,5-cyclooctadiene
COE	cyclooctene
conv.	conversion
COSY	correlation spectroscopy
Cp	cyclopentadienyl
Cp*	1,2,3,4,5-pentamethylcyclopentadienyl
CPME	cyclopentyl methyl ether
Cy	cyclohexyl
δ	NMR chemical shift
d	doublet
Da	dalton
DABCO	1,4-diazabicyclo[2.2.2]-octane
DavePhos	2-dicyclohexylphosphino-2'-(*N,N*-dimethylamino)biphenyl
dba	dibenzylideneacetone
DCE	1,2-dichloroethane
DCM	dichloromethane
dd	doublet of doublets
ddd	doublet of doublets of doublets
deg	degree
DEPT	distortionless enhancement by polarisation transfer

DG	directing group
dm	decimetre
DMA	*N,N*-dimethylacetamide
DMAP	*N,N*-dimethylaminopyridine
dmpe	1,2-bis(dimethylphosphino)ethane
DMF	*N,N*-dimethylformamide
DMSO	dimethylsulfoxide
DNA	deoxyribonucleic acid
dppe	1,2-bis(diphenylphosphino)ethane
dt	doublet of triplets
dtbpy	4,4'-di-*tert*-butyl-2,2'-bipyridine
EAS	electrophilic aromatic substitution
ee	enantiomeric excess
e.g.	for example
EDG	electron-donating group
equiv.	equivalent(s)
ESI	electrospray ionisation
Et	ethyl
et al.	and others
EWG	electron withdrawing group
FDA	Food and Drug Administration
FT-IR	Fourier-transform infrared spectroscopy
g	gram(s)
GC-MS	gas chromatography-mass spectrometry
gem	geminal
h	hour(s)
h	Planck's constant
^{1}H NMR	proton nuclear magnetic resonance
HBpin	pinacolborane
HBcat	catecholborane
(Het)Ar	heteroaryl
HFIP	1,1,1,3,3,3-hexafluoro-isopropanol
HHQ	2-heptyl-4-quinolone
HMBC	heteronuclear multiple-bond correlation spectroscopy
HMPA	hexamethyl-phosphoramide
HOMO	highest occupied molecular orbital
HPLC	high-performance liquid chromatography
HRMS	high-resolution mass spectrometry
HSQC	heteronuclear single-quantum correlation spectroscopy
Hz	Hertz
i	*iso*
i.e.	that is

ind	indenyl
IPr-HCl	1,3-bis(2,6-diisopropyl-phenyl)imidazolium chloride
IR	infrared
J	coupling constant
K	Kelvin
λ	wavelength
λ_{em}	wavelength of maximum emission
λ_{ex}	wavelength of excitation
λ_{max}	wavelength of maximum absorption
l	path length of a cell
L	litre ligand total orbital angular momentum
lit.	literature
LUMO	lowest unoccupied molecular orbital
LRMS	low resolution mass spectrometry
µ	micro (10^{-6})
m	milli (10^{-3}) multiplet
m	*meta*
M	molar
m/z	mass-to-charge ratio
max	maximum
mbar	millibar
m-CPBA	*meta*-chloroperoxy-benzoic acid
Me	methyl
mg	milligram
MH	Mizoroki-Heck
MHz	megahertz
min	minute
mL	millilitre
mmol	millimole
mol	mole
mol.	molecular
mol%	mole percent
m.p.	melting point
MS	mass spectrometry
MTBE	methyl *tert*-butyl ether
MW	microwave
n	non-bonding electrons
NEt_3	triethylamine
NMO	4-methylmorpholine *N*-oxide
ν	frequency
ν_{max}	frequency of maximum absorption
n-BuLi	*n*-butyllithium
nm	nanometres
NMP	*N*-methyl-2-pyrrolidone
NMR	nuclear magnetic resonance
o	*ortho*
OA	oxidative addition
OAc	acetate

o/n	overnight
OPiv	pivalate
p	*para*
PCC	pyridinium chlorochromate
Pd-Q	palladium-quinoline
π	pi
Ph	phenyl
phen	1,10-phenanthroline
piv	pivaloyl
PivOH	pivalic acid
PMP	pempidine
PPA	polyphosphoric acid
ppm	parts per million
PQS	*Pseudomonas* quinolone signal
Pr	propyl
p-TsOH	*p*-toluenesulfonic acid
q	quartet
QPhos	1,2,3,4,5-pentaphenyl-1'-(di-tert-butylphosphino)ferrocene
QPhos=O	1,2,3,4,5-pentaphenyl-1'-(di-tert-butylphosphine oxide)ferrocene
QS	quorum sensing
QSI	quorum sensing inhibition
rad	radian
RBF	round-bottomed flask
RDS	rate-determining step
RE	reductive elimination
ROA	reversible oxidative addition
(*R*,*S*)-Rev-Josiphos	(2*S*)-1-[(1*S*)-1-(Dicyclohexylphosphino)-ethyl]-2-(diphenylphosphino)-ferrocene
r.t.	room temperature
RuPhos	2-dicyclohexylphosphino-2',6'-diisopropoxybiphenyl
s	second singlet
σ	sigma
sat.	saturated
SMAP	silicon-constrained monodentate alkylphosphine
S	total spin quantum number
SM	Suzuki-Miyaura
SPhos	2-dicyclohexylphosphino-2',6'-dimethoxybiphenyl
t	triplet time
t, *tert*	tertiary
T	temperature Tesla
TBAB	Tetra-*n*-butylammonium bromide
TBS	*tert*-butyldimethylsilyl
Tf	trifluoromethanesulfonyl
TFA	trifluoroacetic acid trifluoroacetate

THF	tetrahydrofuran
TLC	thin-layer chromatography
TMB	1,3,5-trimethoxybenzene
TMEDA	*N,N,N*',*N*'-tetramethyl-ethylenediamine
TMS	tetramethylsilane, trimethylsilyl
TNT	trinitrotoluene
TOF LC-MS	time-of-flight liquid chromatography mass spectrometry
TPAP	tetrapropylammonium perruthenate
UTI	urinary tract infection
UV	ultraviolet
vis	visible
vs	versus
WHO	World Health Organisation
wt	weight
XANTphos	4,5-bis(diphenyl-phosphino)-9,9-dimethylxanthene
XPhos	2-dicyclohexylphosphino-2',4',6'-triisopropylbiphenyl

Chapter 1 Interspecies Activity of Alkyl-2-Pyrones

But man is a part of nature, and his war against nature is inevitably a war against himself.

Rachel L. Carson

Neantóg a dhóigh mé, copóg a leigheas mé.

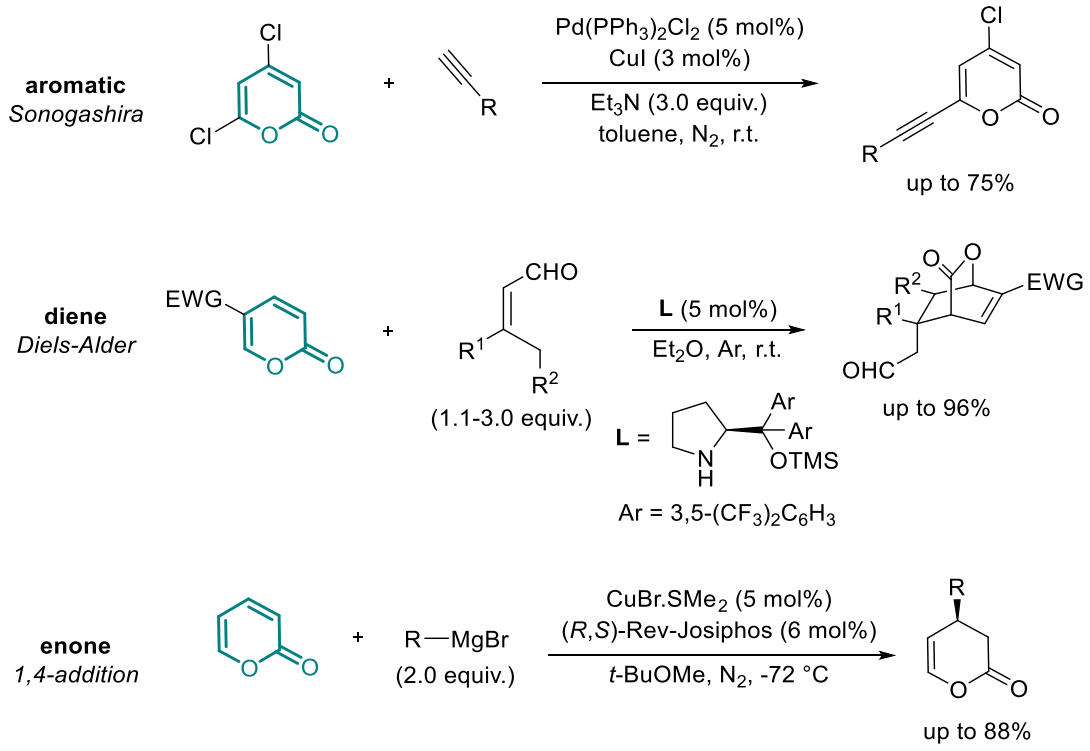
(*It's a nettle that stings me and a dock leaf that cures me.*)

Seanfhocal (Irish Proverb)

Introduction

1.1.2-Pyrones

Pyrones are a class of compounds which consist of six-membered, cyclic, unsaturated ester systems. There are two main structures in this class – the lactone-containing 2-pyrone (α-pyrone) and its vinylogous isomer, 4-pyrone (γ-pyrone).[1] Characteristically, these compounds possess an assortment of chemical and physical properties, with the 2-pyrone isomer exhibiting a mixture of aromatic,[2] diene[3] and enone[4] type reactivities (**Scheme 1.1**). This diversity allows the motif to undergo a multitude of transformations.[5-6]



Scheme 1.1 Various transformations of 2-pyrone compounds with the 2-pyrone nucleus highlighted in blue.

The 2-pyrone moiety is an important substructure found in numerous natural products and is a multifaceted building block used in the construction of synthetic molecules.[7-9] Pyrone-containing compounds are ubiquitous anti-proliferative agents with a diverse range of biological functions, including anti-fungal, anti-cancer, and anti-HIV activity, and are even being investigated for the treatment of Alzheimer's

disease.[6,10-12] Derivatives of the 2-pyrone motif have also exhibited cytotoxicity towards microbial pathogens including *Bacillus subtilis*, *Escherichia coli* and *Staphylococcus aureus*.[6,13-14]

A significant group of naturally occurring steroids called the bufadienolides encompass broad-scope biological properties dependent on the organism from which they are extracted.[15] These compounds include a 2-pyrone moiety bonded to the five-membered 'D' ring of the core steroidal structure. For example, bufalin (**Figure 1.1**) is isolated from a species of toad and possesses anaesthetic, blood pressure regulatory and anti-tumour effects.[13]

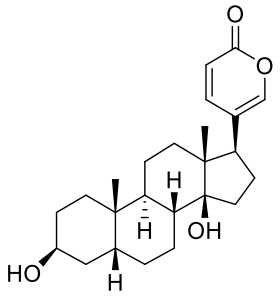


Figure 1.1 Bufalin.

1.2. Quorum Sensing

Several species of bacteria employ a method of communication known as quorum sensing (QS) to facilitate group behaviours.[16-18] This phenomenon was first discovered in the marine bacteria *Vibrio fischeri*, a bioluminescent species which exists symbiotically with the Hawaiian bobtail squid.[19] Bacteria within a colony synthesise, secrete and subsequently detect specific small molecules called autoinducers (AIs). Thus, the bacteria constantly monitor their extracellular environment, gauging population density through the number of AIs present. Once a threshold concentration/population is reached, the bacteria can vastly alter gene expression to generate a coordinated response. These interactions allow the colony to perform tasks as a single, multi-cellular unit which are essentially a waste of energy when carried out by an individual bacterium.[20] Such tasks typically include bioluminescence, secondary metabolite synthesis, biofilm formation and virulence factor production.[17,21-24] Biofilms are polymeric matrix structures that form through

attachment of microbial cells to biological or inert surfaces (**Figure 1.2**).[25] This community behaviour often allows the colony to circumvent the host immune system and also stimulates the development of resistance to antimicrobial treatments, giving rise to more potent pathogens.[26] The phenotype is adopted by up to 80% of infections in humans,[27] and can grow on anything from living tissue to medical devices.

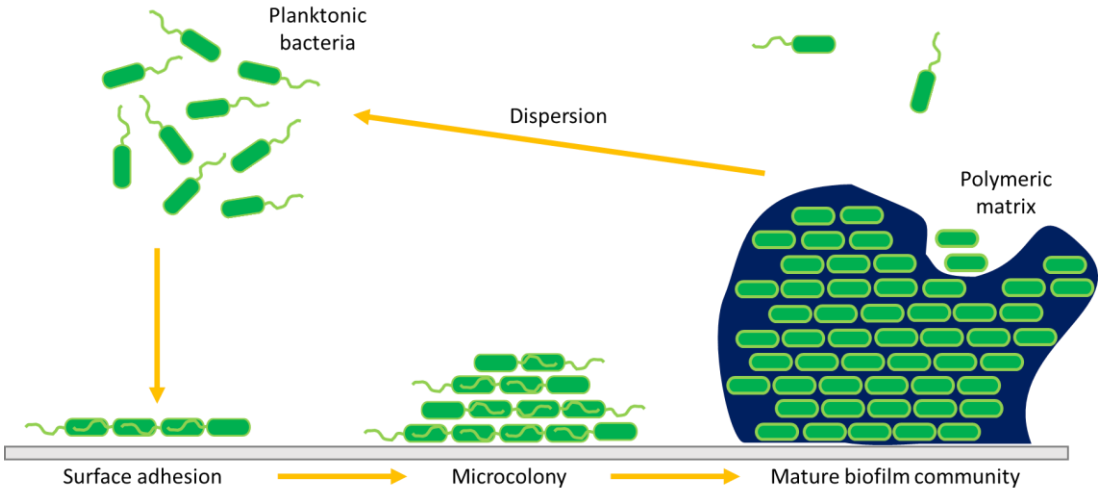


Figure 1.2 Formation of a biofilm through QS.

Bacterial swarming motility is also governed by a complex QS-based communication system, which directs multiple aspects of behaviour. Specifically, it encompasses the formation of head to tail connections between individual bacterial cells to allow for coordinated translocation of a bacterial colony across a surface.[28]

These multifaceted defence techniques make infection difficult to treat, highlighting the urgency for alternative medicines. Significant advances have been made in the area of antivirulence therapy, where interventions supress virulent bacterial phenotypes without inducing apoptosis.[29-31] This approach places far less selective pressure on the bacteria than other growth-limiting or biocidal methods and can therefore slow or completely preclude the evolution of resistance.[31-32] One such example is quorum sensing inhibition (QSI) which employs small molecules, structurally similar to native AIs, usually to 'confuse' and inhibit the bacterial QS pathways that control pathogenic behaviours. QSI is a rapidly growing area of research, although uses in a clinical setting remain a future-looking goal.[33-34]

The intricate process through which QS occurs has been thoroughly investigated and modelled. The typical network is comprised of a LuxI-type AI synthase and a LuxR-type receptor. The most predominant class of AIs synthesised and received by these proteins is the *N*-acyl homoserine lactones (AHLs) (**Figure 1.3**).[35]

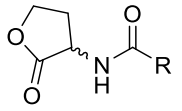
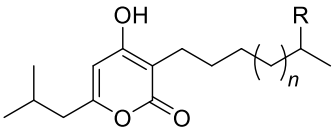


Figure 1.3 *N*-Acyl homoserine lactones.

It has been reported that systems lacking any LuxI-type AHL synthase can still bear proteins with properties analogous to LuxR-type receptors, called LuxR orphans or solos.[36-38] A report by Heerman and co-workers[39] demonstrated how the Gram-negative, insect pathogen *Photorhabdus luminescens* conducts its QS pathway. A number of 'photopyrones' (PPYs) are endogenously produced by a PPY synthase (PpyS) and operate as signalling molecules through LuxR orphan receptors (PluR). In response to threshold AI concentration, the quorum transcribes the operon responsible for cell clumping – a key pathogenic trait of this species. These findings comprise the first demonstration of 2-pyrones, specifically derivatives of 3-alkyl-4-hydroxy-6-isobutyl-2*H*-pyran-2-one (**Figure 1.4**), acting as potential signalling molecules in any bacterial strain.[39]



PPY	R	*n*
A	H	1
B	CH_3	1
C	H	3
D	CH_3	3
E	H	5
F	CH_3	5
G	H	7
H	CH_3	7

Figure 1.4 PPYs A–H isolated from *Photorhabdus luminescens*.

1.3. Bacillus atropheaus

Bacillus atropheaus is a Gram-positive, insecticidal, aerobic bacteria that is found in soil. As *B. atropheaus* is not considered pathogenic to humans, it is commonly used

as a surrogate to study the epidemiology and physiology of *B. anthracis* and other virulent species in the *B. cereus* family.[40] It is genetically similar to *B. subtilis* and is also known to utilise QS to coordinate gene expression to form biofilms and accommodate swarming, among other functions.[41] The main QS network in *B. atropheaus* is controlled by a much larger AI than those found in the majority of other QS circuits, namely the peptide ComX (~10,000 Da).[42] The specific amino acid residues are bonded and exported by a protein called ComQ and the resulting AIs are detected by the sensor protein kinase ComP. The kinase activates the response regulator ComA *via* phosphorylation and this in turn modulates group behaviours (**Figure 1.5**).[43] The pathway is consequently named ComQXPA and is shared by a multitude of other *Bacillus* species.[44]

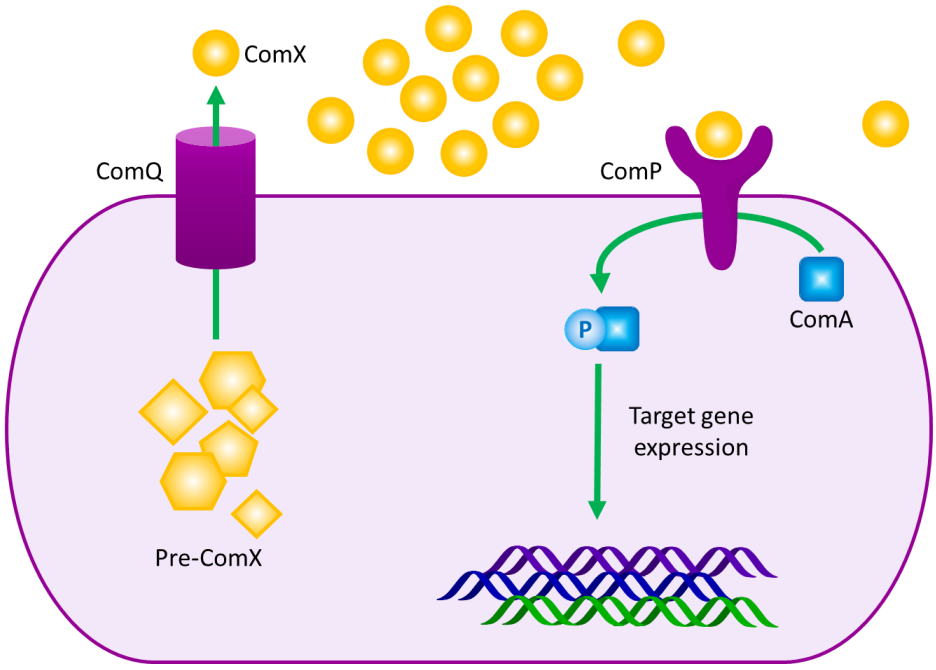


Figure 1.5 ComQXPA signalling pathway for the expression of group phenotypes at high population density.

Certain 2-pyrone derivatives have been shown to significantly impact the proliferation and pathogenic phenotypes of *Bacillus* species. The processes through which these inhibitions occur have are yet to be identified but could be related to the intricate QS networks operated by this genus of bacteria.[10,45-49]

1.4. Pseudomonas aeruginosa

Pseudomonas aeruginosa is a Gram-negative, nosocomial pathogen which primarily affects immunocompromised patients; for example it is the main source of mortality in people with cystic fibrosis (CF).[50] *P. aeruginosa* infections are notoriously difficult to treat as the bacterial colony rapidly forms a multi-drug resistant biofilm. Once a biofilm has been established on the surface of the lungs of CF patients, it becomes almost impossible to eradicate using antimicrobial therapy.[51] Thus, there is a critical need for the development of alternative strategies for the treatment of *P. aeruginosa* and other resistant bacterial strains.[52]

The McGlacken group, in collaboration with Dr F. Jerry Reen and Prof Fergal O'Gara from the School of Microbiology in UCC, has contributed several publications to the field of bacterial communication, with view to developing QSI strategies. The predominant focus of this research has been the QS networks employed by *P. aeruginosa*, specifically the *pqs* circuit, which is responsible for the expression of virulent phenotypes, *inter alia*, the release of virulence factors and biofilm formation.[34] This pathway is modulated by alkyl quinolone (AHQ) signalling molecules, 2-heptyl-4-quinolone (HHQ) and 2-heptyl-3-hydroxy-4-quinolone, or *Pseudomonas* quinolone signal (PQS) (**Figure 1.6**).[53] In depth structure-activity relationship studies have been carried out on derivatives of HHQ and PQS, and so the positional and electronic requirements for the operation and subsequent inhibition of the *pqs* pathway are well understood.[34,54-58]

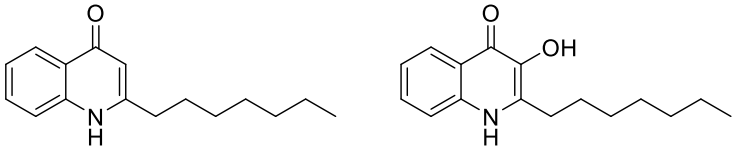


Figure 1.6 *P. aeruginosa* AHQ signalling molecules, HHQ and PQS.

1.5. Interspecies and Interkingdom Activity of Autoinducers

Bacteria often co-inhabit with other prokaryotic and eukaryotic organisms, forming diverse natural and infective ecosystems.[59] While the small, diffusible organic molecules used in QS are often species-specific, it is now known that communication

between species in a mixed microbial community is possible.[60-61] Consequently, interspecies and interkingdom interactions are mostly competitive and can greatly contribute to the pathogenicity of an infection.[62] The McGlacken group and its microbiology collaborators have again carried out multiple investigations on an assortment of pathogenic microbes and fungi that co-inhabit/co-infect with *P. aeruginosa*. Sophisticated interspecies and interkingdom influences were observed in response to analogues of HHQ and PQS in, for example, *V. vulnificus*, *B. subtilis*, *Aspergillus fumigatus* and *Candida albicans*.[62-65]

Results and Discussion

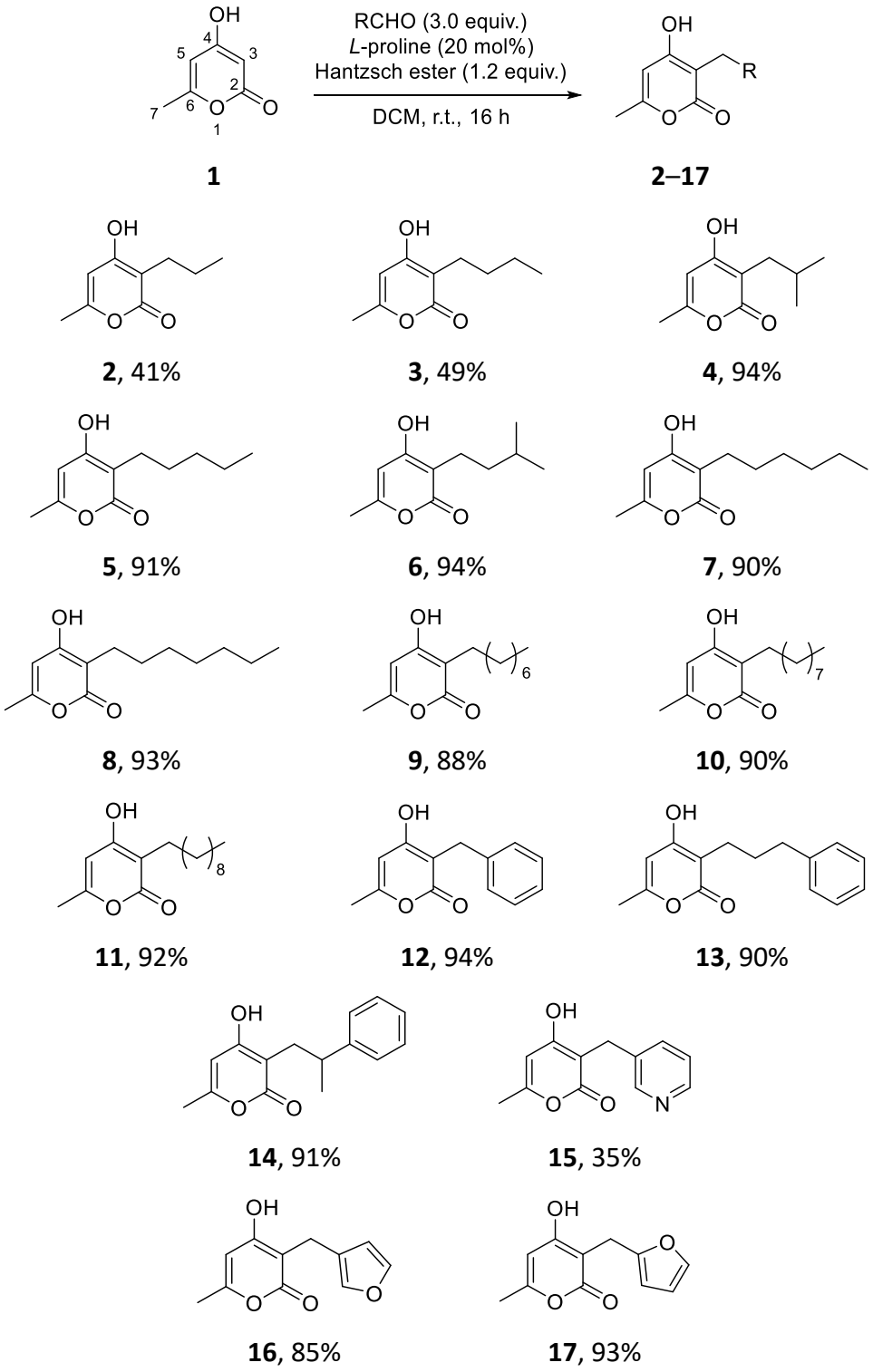
1.6. Objectives

Photorhabdus and *Bacillus* species co-inhabit soil environments and are known to exhibit a synergistic relationship in the infection of insects.[66-68] This interspecies co-operation led us to consider the possible signalling interactions that could be occurring between the two species. Thus, we wished to investigate if the 2-pyrone produced by *P. luminescens* (*vide supra*), or indeed synthetic derivatives of the native 2-pyrone would have any impact on the behaviour of a *B. atropheaus* colony.

1.7. Chemistry

1.7.1 Synthesis of 3-Alkyl-2-Pyrone Analogues

We wished to first investigate the effects of C-3 substitution alone, leaving the C-6-methyl group of the readily available 4-hydroxy-6-methyl-2*H*-pyran-2-one skeleton **1** untouched. Kraus *et al.*[69] described a method of selective pyrone functionalisation *via* reductive alkylation of **1** using various aldehydes to yield 3-alkyl-6-methyl-2-pyrones in excellent yields. We found this approach very appealing as it employs relatively inexpensive reagents and an assortment of aldehydes in a 'dump and stir' reaction at ambient temperature in air. Several analogues were accessed through this synthetic route in moderate to excellent yields (**Scheme 1.2**). Various straight chain and branched aliphatic aldehydes were tolerated (**2**–**11**), albeit with decreased yields for the shorter chained aldehydes (**2** and **3**). The reaction was also successful when aryl- (**12**–**14**) and heteroaryl-containing aldehydes were employed (**15**–**17**).

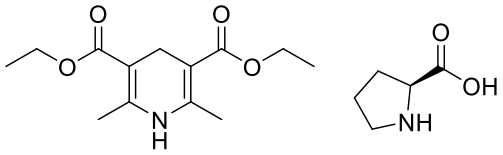


Scheme 1.2 Library of synthesised 3-alkyl-2-pyrones (2–17).

1.7.2 Mechanistic Considerations

This reaction proceeds *via* a reductive alkylation mechanism utilising 1,4-dihydropyridine **18** (Hantzsch ester) as the hydride source.[70] The role of *L*-proline **19** in the reaction is not definitive, though its rigid structural conformation lends itself

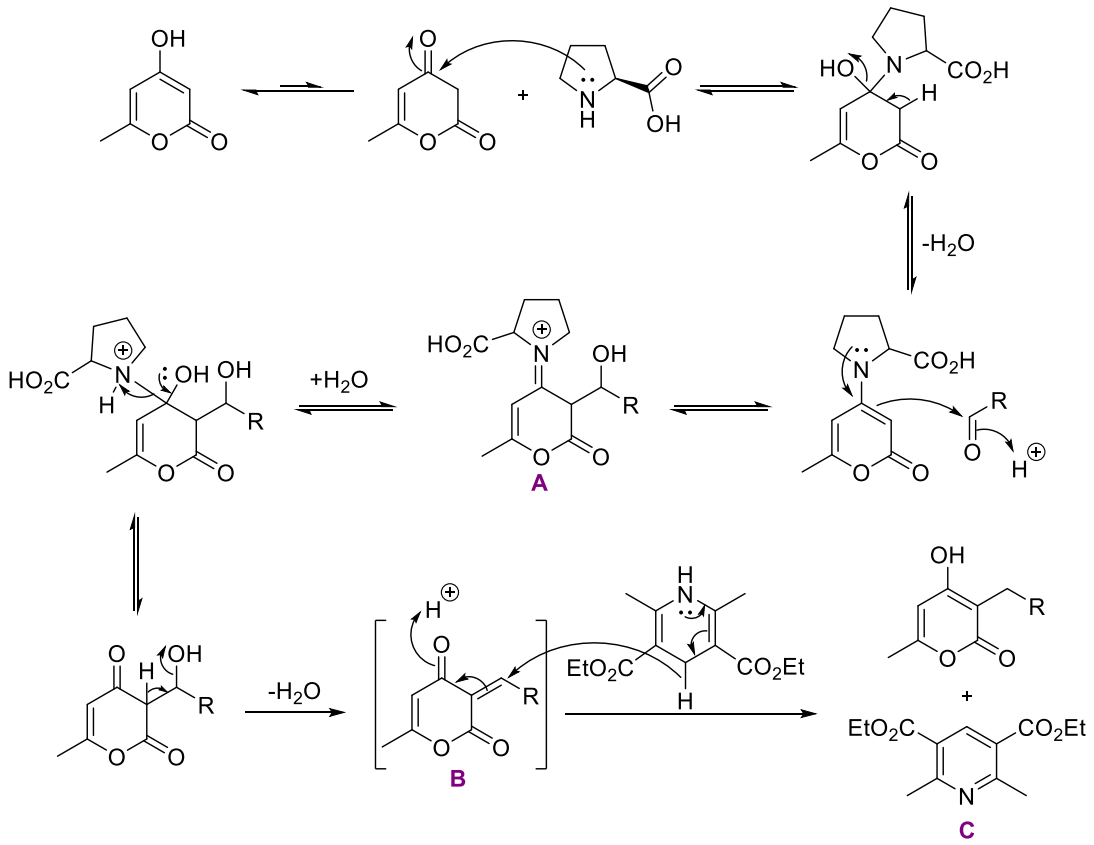
for use as an asymmetric organocatalyst in other systems (**Figure 1.7**).[71] It is also an autocatalytic proton source and has thus been used previously to catalyse aldol-type condensation reactions.[72] It is probable that it also works to promote regioselectivity through an enamine intermediate (*vide infra*).



18 **19**

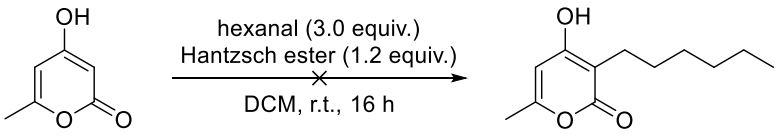
Figure 1.7 Hantzsch ester **18** and *L*-proline **19**.

The initial reaction observed here yields an aldol-type product **B** which could be formed when the enol moiety of **1** reacts with the polar carbonyl group of the aldehyde (**Scheme 1.3**). However, it is likely that this is not a simple enolate-carbonyl reaction, but rather that an enamine intermediate **A** forms *in situ* and reacts with the carbonyl moiety *via* a Mannich-type mechanism.[72]. Condensation product **B** is non-isolable,[69,73] and employing **18** as a hydride source allows for selective reduction of this double bond, yielding the desired 3-alkyl-6-methyl-2-pyrone and the corresponding Hantzsch pyridine **C** as a by-product.



Scheme 1.3 Proposed reductive alkylation mechanism.

Evidence pertaining to this mechanism was provided by a control experiment, which demonstrated no conversion by ^{1}H NMR analysis to alkylated product in the absence of **19** (**Scheme 1.4**). Under the standard conditions, once all reagents have been added, a cloudy suspension is initially observed. After ~15 min, an apparently homogenous, clear green solution forms. However, in the absence of *L*-proline, starting material **1** failed to dissolve and this ultimately contributed to the failure of the reaction.



1 **7**

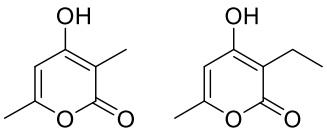
Scheme 1.4 Control experiment of **1** with hexanal in the absence of *L*-proline.

Considering *L*-proline has the propensity to react in any number of ways with the reagents involved, it is notable that no major yield-reducing side product was observed in the ^{1}H NMR analysis of the crude reaction mixture, nor isolated during

subsequent purifications. For example, self-condensation of the excess aldehyde or oxazolidinone formation are both possible.[74-76] Additionally, there appears to be no competitive reduction pathways which consume **18**.

1.7.3 Limitations of Methodology

Although the methodology proved robust for use with an array of substituted aldehydes, there were some from which the desired product could not be derived or isolated. Firstly, products with alkyl chains containing fewer than three carbons were difficult to purify, even when alternative methods were utilised. As the length of the chain at C-3 decreases, the target product becomes more similar to **1**, which is relatively insoluble in common organic solvents. The short chain products are significantly less soluble and are problematic to purify *via* either column chromatography or recrystallisation. Peaks consistent with **20** and **21** could be identified in the ^{1}H NMR spectra of the crude reaction mixtures, but neither were separated or characterised (**Figure 1.8**).



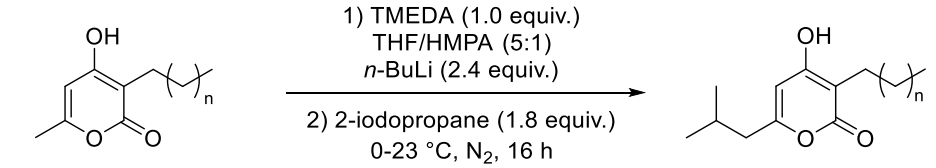
20 **21**

Figure 1.8. Short chain products which could not be purified.

Interestingly, when *p*-nitrobenzaldehyde was used, no alkylation occurred. This aldehyde is often used as a 'model substrate' in the optimisation of aldol-type reactions, and was expected to work well due to the electron-withdrawing nature of the nitro group.[77] However, solubility played an important role again here as even after several hours the reagents did not appear to have dissolved in DCM and only starting materials were present in the mixture, as observed by ^{1}H NMR analysis. Although generally requiring harsh reaction conditions, it is possible that the propensity for the nitro group to be reduced, consumes, or at least inhibits, the reductive action of **18** in the reaction. Further investigations would have to be carried out in order to identify and resolve this issue.

1.7.4 Synthesis of 6-Alkyl-2-Pyrone Analogues

In the report by Heerman and co-workers[39] all of the pyrones isolated include an isobutyl rather than a methyl group at the C-6 position, and we sought to investigate the biological impact of the addition of this group. PPYA, PPYB and PPYD represented the most active signalling molecules at nanomolar concentrations in *P. luminescens*[39] and so it was imperative to synthesise at least one of these as a positive standard for our biological evaluations. We also wanted to mimic the naturally occurring pyrones to examine compounds with varied chain length at the C-3 position in conjunction with the isobutyl group for biological activity. The synthesis of these molecules was achieved by using *n*-BuLi in TMEDA/THF/HMPA to deprotonate the appropriate starting material (**5**, **7**–**11**), which subsequently reacted with 2-iodopropane to give dialkylated products **22**–**27** in moderate isolated yields (**Scheme 1.5**).



5, 7–11 **22–27**

22, 45% **23**, 49% (PPYA) **24**, 45%

25, 45% (PPYC) **26**, 42% **27**, 37% (PPYE)

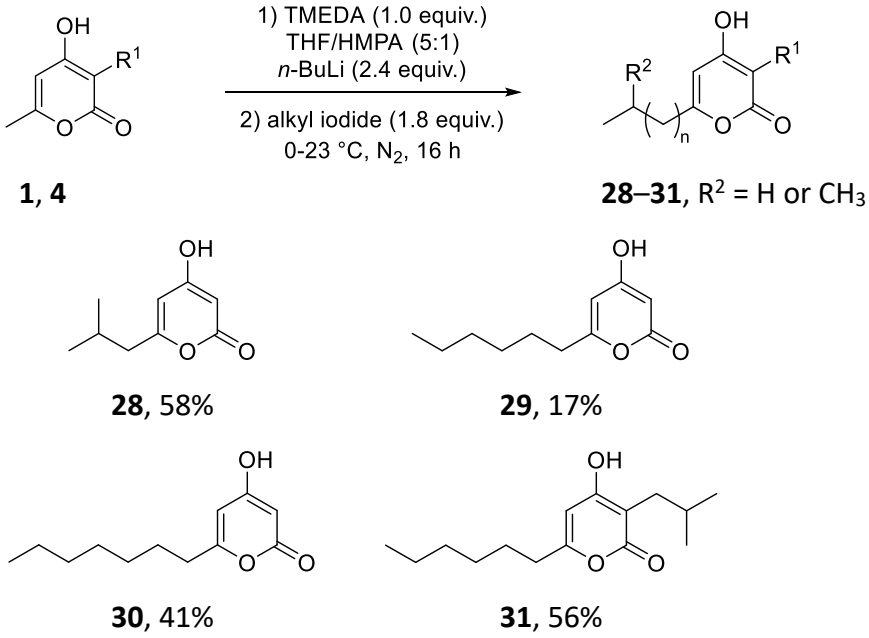
Scheme 1.5 Synthesis of the biological standards and other dialkylated 2-pyrones **22**–**27**.

As Heerman and co-workers[39] investigated the activity of 2-pyrones which were alkylated at both the C-3 and C-6 positions, we also wanted to examine the activity of derivatives substituted at C-6 only. Three 6-alkyl-2-pyrones, **28**–**30**, were constructed in yields of 58%, 17% and 41% respectively, using the methodology already described (**Scheme 1.6**). Attempts to lower the number of carbons in the

chain of the electrophilic partner failed to yield any viable product by both ^{1}H NMR and TLC analyses. Finally, dialkylated compound **31** was synthesised in moderate yield to investigate the positional significance of the alkyl chains relative to the oxygen moieties on the pyrone backbone.

Upon addition of *n*-BuLi to the mixture of the 2-pyrones in TMEDA/THF/HMPA, a deep red colour developed in solution. This colour change is indicative of dianion formation,[78] in this case at the 6-methyl group and at the 4-hydroxy position. TMEDA and HMPA normally act as donor ligands in these types of reactions to form active reaction aggregates with the alkyl lithium species.[78] Analysis of the side products revealed that *O*-alkylation, as well as a small fraction of di-alkylation of had taken place, accounting for some of the loss in yield.

Although it would seem intuitive to protect the 4-hydroxy position to promote anion formation at C-7 – preventing both competitive and di-alkylation, efforts made by a previous member of the group gave poorer yields than with the free OH group. For example, the parallel synthesis of **30** using a silyl-based protecting group strategy gave less than 5% isolated yield.[79]



Scheme 1.6 Alkylation at the C-6 position.

1.8. Biological Results

The analogues prepared above were tested for interspecies biological activity by Dr F. Jerry Reen at the School of Microbiology in UCC. The results of the studies are summarised below, although the experimental procedures and methods are outside the scope of this thesis. Full details of the biological experiments are published and included in **Appendix II** (*ACS Omega* **2021**, *6*, 33141-33148).

B. atropheaus is an insecticidal species of bacteria that co-inhabits with *P. luminescens* in soil-based environments. *Bacillus* species are known to operate QS networks to coordinate two main phenotypes critical to pathogenicity; biofilm formation and swarming motility.[80-82] Interference with these highly complex behaviours could result in a less competitive organism at the community level.[16,83-84]

Both phenotypes were investigated using *B. atropheaus.* Addition of the standard, PPYA, **23** (50 µM), to media prior to inoculation with *B. atropheaus* cultures led to a dramatic increase in attached biofilm biomass when compared with DMSO and untreated controls (**Figure 1.9 (a)**). In contrast, swarming motility was significantly repressed in the presence of **23** (**Figure 1.9 (b)**), with both results independent of any growth-related effects. The influence of **23** on biofilm formation and swarming motility suggests that it has the propensity to induce interspecies activity beyond that of its inherent role in the signal producing *Photorhabdus* species.[85]

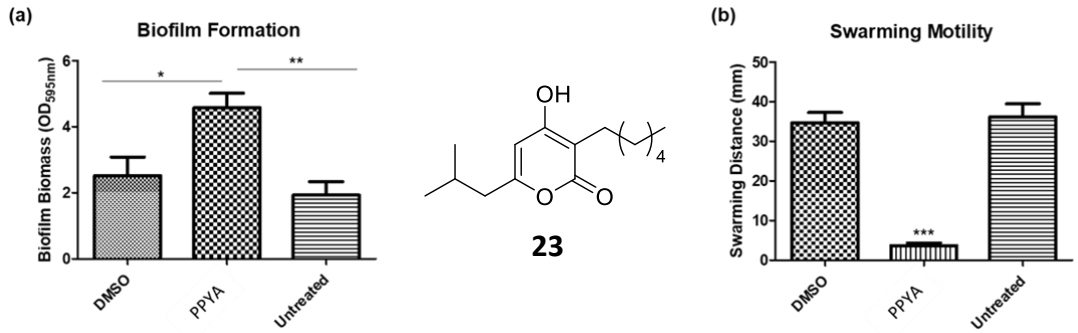


Figure 1.9 (a) Biofilm formation **(b)** Swarming motility of *B. atropheaus* in the presence of **23** at 50 µM in DMSO. Data presented is the average (+/- SEM) of three independent biological replicates. Statistical analysis was performed by One Way ANOVA with Bonferroni post-hoc corrective testing (* p≤0.05; ** p≤0.005; *** p≤0.001).[85]

Next, the impact of our synthetic mono-substituted 2-pyrone derivatives (**2**–**17**, **29**, **30**) on *B. atropheaus* was examined. Compounds **8**, **9**, **10** and **11** exhibited statistically significant anti-biofilm activity at 50 μM, in direct contrast to the biofilm enhancing properties exhibited by **23** (**Figure 1.10 (a)**). Pyrones **10** and **11** abolished, and pyrone **9** strongly suppressed swarming activity on semi-solid agar; the analogues in this case trending with the anti-swarming activity of **23** (**Figure 1.10 (b)**). To determine whether the influence on gene expression was simply a reflection of growth inhibition, *B. atropheaus* was grown in the presence of each compound. Growth was not comparably affected in the presence of pyrones **8** and **9** (**Figure 1.10 (c)**), delineating biofilm formation and growth for these derivatives. Growth inhibitory effects were observed with respect to compounds **10** and **11**. Interestingly, compound **7**, which possesses the same six-carbon chain at the C-3 position as carrier control compound **23**, induced little to no effect on either biofilm formation or swarming motility. This result indicates the apparent importance of the C6 isobutyl group for the biological activity of **23**.

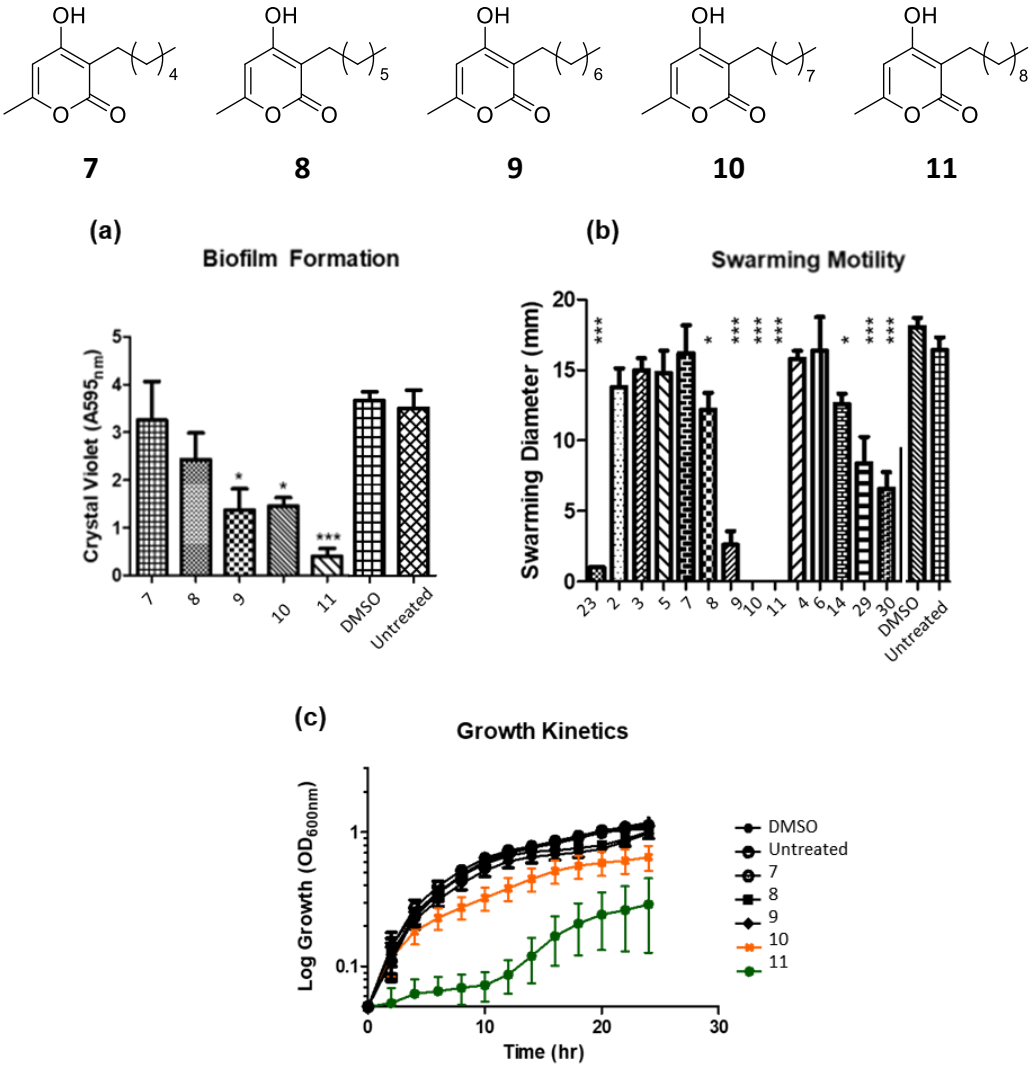


Figure 1.10 Relevant structures for biological data. **(a)** Anti-biofilm activity **(b)** Swarming motility of *B. atropheaus* with 50 µM compound or **23 (c)** Growth curve analysis of *B. atropheaus* in the presence of pyrone derivatives at 50 µM in DMSO. All data presented is the average (+/- SEM) of at least three independent biological replicates. Statistical analysis was performed by One way ANOVA with Bonferroni Multiple Comparison post-hoc corrective testing (* $p \leq 0.05$; ** $p \leq 0.005$; *** $p \leq 0.001$).[85]

We then considered the significance of the isobutyl group at C6 in the biological control **23**. We included this group alone on the core structure in compound **28**, and in conjunction with the 'best-performing' C3-alkyl chain lengths (**8**–**11**) to form compounds **22**, **24**–**27** and **31**. While these compounds did display anti-biofilm and anti-swarming properties, it is noted that growth kinetics of *B. atropheaus* was

affected in the presence of **22**, **24**–**28** and **31**, with the organism failing to reach final biomass achieved in the presence of the DMSO control (**Figure 1.11**).

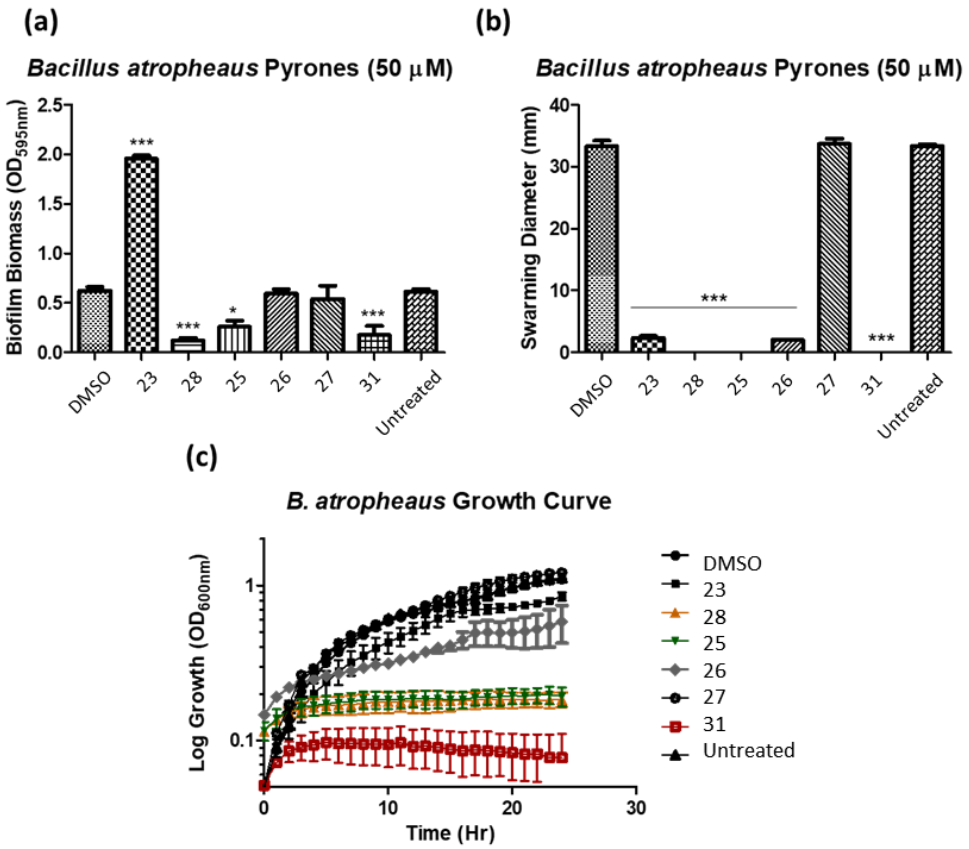


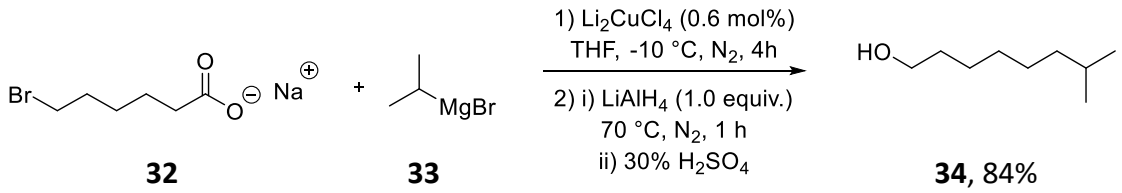
Figure 1.11 (a) Anti-biofilm activity **(b)** Swarming motility of *B. atropheaus* with 50 μM compound or **23 (c)** Growth curve analysis of *B. atropheaus* in the presence of pyrone derivatives at 50 μM in DMSO. All data presented is the average (+/- SEM) of at least three independent biological replicates. Statistical analysis was performed by One way ANOVA with Bonferroni post-hoc corrective testing (* $p \leq 0.05$, *** $p \leq 0.001$*** $p \leq 0.001$).[85]

Pyrones **8**, **9** are thus proposed as lead compounds for anti-biofilm/swarming activity, potentially working through interference with signalling mechanisms. None of the other compounds, with shorter or longer (linear, branched alkyl chains, aryl, heteroaryl) groups showed considerable anti-biofilm activity. Remarkably, the bioactivity of **23** towards *B. atropheaus* appears to be entirely specific to that exact structural arrangement.

1.9. Further Developments

Having discerned the unique interspecies role of PPYA, we considered it important to synthesise the other signalling molecules, PPYB and PPYD for any further biological studies. Although the majority of aldehydes employed were easily sourced, those required to construct PPYB and PPYD were not commercially available and needed to be freshly prepared from the corresponding alcohols.

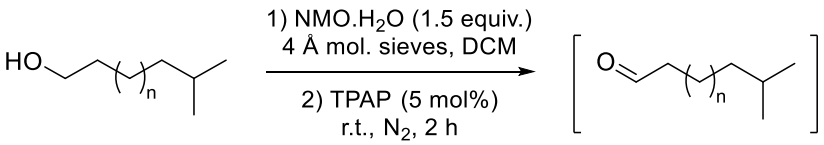
Firstly, 7-methyloctanol **34** was synthesised *via* the Grignard reaction of the sodium salt of 6-bromo-1-hexanoic acid **32** with freshly prepared isopropylmagnesium bromide **33** (**Scheme 1.7**). Subsequent *in situ* reduction of the branched chain intermediate using lithium aluminium hydride furnished alcohol **34** in good yield.[86-87]



32 **33** **34**, 84%

Scheme 1.7 Synthesis of 7-methyloctanol **34**.

Although there are a number of known methods for the oxidation of aliphatic alcohols to aldehydes (e.g. Swern oxidation, PCC), many of them utilise toxic and environmentally harmful reagents or proceed *via* radical-based mechanisms.[88] The Ley-Griffith reaction was chosen as the favoured protocol for this transformation – it is a ruthenium-catalysed oxidation which avoids radical formation and uses relatively mild conditions (**Scheme 1.8**).[89-91] The branched aldehydes **36** and **37** were observed by ^{1}H NMR analysis of the crude reaction mixtures and were found to be quite unstable, even when stored under a blanket of nitrogen in the freezer.

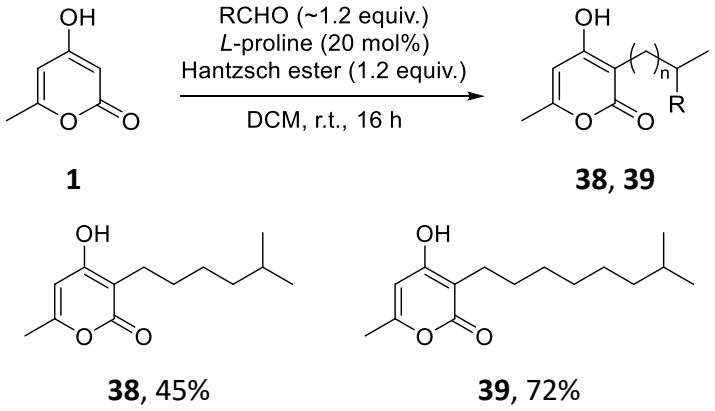


34, n = 3
35, n = 1

36, n = 3
37, n = 1

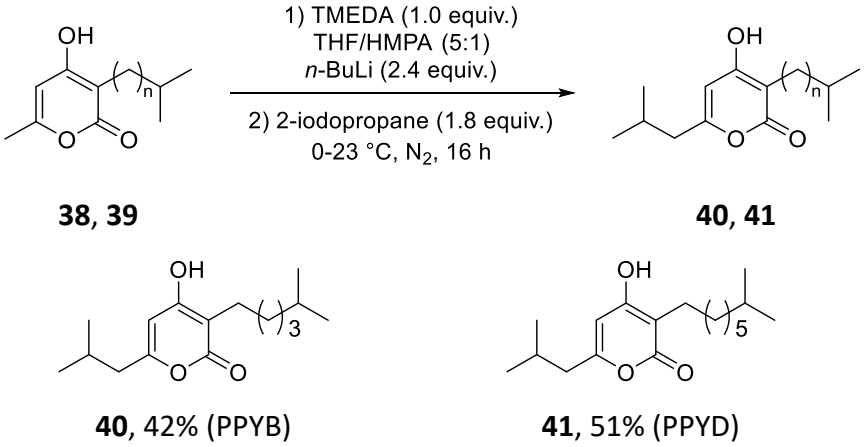
Scheme 1.8 Ley-Griffith oxidation of branched chain alcohols **34** and **35**.

Due to their instability, it was decided that the aldehydes would be immediately carried forward for reductive alkylation. Indeed, reaction of **36** and **37** with **1** provided the C-3-alkylated products **38** and **39** in moderate to good yields (**Scheme 1.9**).



Scheme 1.9 Synthesis of branched chain intermediates **38** and **39**.

With the C-3-alkylated products in hand, PPYB **40** and PPYD **41** were synthesised *via* the reaction of 2-iodopropane with **38** and **39** respectively, using the alkylation method previously described (**Scheme 1.10**). These compounds, along with PPYA, will act as important controls for all further biological studies on the entire library of pyrone compounds synthesised herein.



Scheme 1.10 Synthesis of PPYB **40** and PPYD **41**.

Conclusions and Future Work

A set of 30 mono- and di-substituted 2-pyrone compounds were synthesised through a series of alkylation procedures, including several novel, and known derivatives, as well as five naturally occurring analogues (PPYA **23**, PPYC **25**, PPYE **27**, PPYB **40**, PPYD **41**). Biological testing of these compounds was then carried out by our microbiology collaborators here in UCC on *B. atropheaus*. The activity of the naturally occurring analogue, PPYA **23**, used as a carrier control, appeared to have a novel influence on biofilm activity when compared to all other natural and non-natural compounds tested. Compounds with similar conformations and substitutions exhibited anti-biofilm activity, even those with just one CH_2 unit in the difference (compounds **22** and **24**). The isobutyl group at C-6 is also significant on compound **23** as compound **7**, which possesses the same six-carbon chain at the C-3 position displayed virtually no impact on either of the variables tested in *B. atropheaus*. Further potential analogues for this study may include the use of bioisosteric fluorine atoms at various positions, and the investigation of C-5 alkylation. These derivatives however will not be synthesised until a more in-depth structure-activity relationship is developed and the potential LuxR solo present in the *Bacillus* species can be identified. These studies are currently underway.

The influence the pyrone analogues had on the phenotypic behaviour of *Bacillus*, led our microbiology collaborators to investigate the possible impact of these signalling compounds on another very prevalent, co-inhabiting species, *Pseudomonas aeruginosa*.[92] This work is ongoing and will also be published in due course.

Experimental

1.10. General Procedures

Solvents and reagents were used as obtained from commercial sources and without purification, with the exception of THF, which was freshly distilled from sodium/benzophenone under nitrogen.

Melting points were measured in a Thomas Hoover Capillary Melting Point apparatus.

Infrared spectra were measured on a PerkinElmer FT-IR spectrometer as thin films in DCM.

Column chromatography was carried out using 60 Å (35-70 µm) silica. TLC was carried out on pre-coated silica gel plates (Merck 60 PF254) and the developed plates were visualised under UV light.

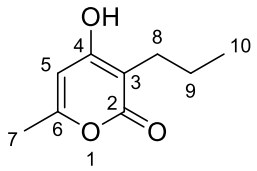
High resolution precise mass spectra (HRMS) were recorded on a Waters LCT Premier Tof LC-MS instrument in University College Cork. Samples were run in electrospray ionisation (ESI) mode using 50% acetonitrile-water containing 0.1% formic acid as eluent; samples were made up at a concentration of *ca*. 1 mg mL^{-1}. The Microanalysis Laboratory, National University of Ireland, Cork, performed elemental analysis using a PerkinElmer 240 and Exeter Analytical CE440 elemental analysers.

Nuclear Magnetic Resonance (NMR) samples were run in deuterated chloroform ($CDCl_3$), deuterated dimethyl sulfoxide ($(CD_3)_2SO$) or deuterated methanol (CD_3OD), as specified. ^1H NMR (300 MHz) spectra were recorded on a Bruker Avance III 300 NMR spectrometer in proton coupled mode. ^{13}C NMR (75 MHz) spectra were recorded on a Bruker Avance III 300 NMR spectrometer in proton decoupled mode at 300 K. Chemical shifts (δ) are expressed as parts per million (ppm), positive shift being downfield from TMS; coupling constants (*J*) are expressed in Hertz (Hz), are reported as observed and their values are uncorrected. Splitting patterns in ^1H NMR spectra are designated as: s (singlet), bs (broad singlet), d (doublet), dd (doublet of doublets), dt (doublet of triplets), t (triplet) and m (multiplet). Compounds were

numbered for ease of assignment and do not necessarily represent IUPAC nomenclature.

1.11. Synthesis of Alkyl-2-Pyrones

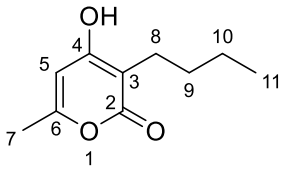
4-Hydroxy-6-methyl-3-propyl-2*H*-pyran-2-one (2)[69]



To a round bottom flask in open air was added 4-hydroxy-6-methyl-2*H*-pyran-2-one **1** (0.063 g, 0.5 mmol, 1.0 equiv.), propanal (0.11 mL, 1.5 mmol, 3.0 equiv.), diethyl 1,4-dihydro-2,6-dimethyl-3,5-pyridinedicarboxylate **18** (0.152 g, 0.6 mmol 1.2 equiv.) and DCM (7.5 mL). L-proline (0.012 g, 0.1 mmol, 20 mol%) was then added and the sides of the flask were rinsed again with DCM. The resulting reaction mixture was allowed to stir vigorously for 16 h at r.t. (~20 °C). The reaction mixture was then concentrated under reduced pressure.[69] Purification *via* column chromatography (hexanes:EtOAc 70:30 to 50:50) to yield **2** as a white crystalline solid (0.035 g, 41%); m.p. 148–151 °C (lit.[69] 148–151 °C); ^{1}H NMR (300 MHz, $CDCl_3$) δ: 6.20 (s, 1H, C(5)**H**), 2.50–2.35 (m, 2H, C(8)$\mathbf{H}_2$), 2.22 (s, 3H, C(7)$\mathbf{H}_3$), 1.63–1.43 (m, 2H, C(9)$\mathbf{H}_2$), 0.94 (t, *J* = 7.4 Hz, 3H, C(10)$\mathbf{H}_3$) ppm; ^{13}C NMR (75 MHz, $CDCl_3$) δ: 168.1, 166.9 (q**C**-2, q**C**-4), 159.9 (q**C**-6), 103.1 (q**C**-3), 101.5 (**C**(5)H), 24.9 (**C**(8)H_2), 21.3 (**C**(9)H_2), 19.7 (**C**(7)H_3), 13.9 (**C**(10)H_3) ppm; *m/z* (ES+): 169 ($(M+H)^+$ 100%).

Spectral characteristics were consistent with previously reported data.[69]

3-Butyl-4-hydroxy-6-methyl-2*H*-pyran-2-one (3)[93]

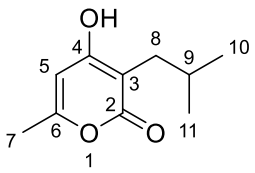


Compound **3** was prepared *via* the procedure described for **2** using butanal (0.14 mL, 1.5 mmol, 3.0 equiv.) to yield **3** as a white crystalline solid (0.045 g, 49%); m.p. 130–133 °C (lit.[93] 130–132 °C); IR (film) ν_{max} 3583 (broad OH stretch), 1650 (ester C=O stretch), 1575 (alkene C=C stretch), 1447 (aromatic C-C stretch), 1292 (ester C-O stretch), 1127 (alcohol C-O stretch) cm^{-1}; ^{1}H NMR (300 MHz, $CDCl_3$) δ: 9.73 (bs, 1H, O**H**), 6.18 (s, 1H, C(5)**H**), 2.56–2.35 (m, 2H, C(8)$\mathbf{H}_2$), 2.22 (s, 3H, C(7)$\mathbf{H}_3$), 1.61–1.20 (m, 4H, C(9)$\mathbf{H}_2$, C(10)$\mathbf{H}_2$), 0.91 (t, *J* = 7.2 Hz, 3H, C(11)$\mathbf{H}_3$) ppm; ^{13}C NMR (75 MHz, $CDCl_3$) δ: 168.5, 167.5 (q**C**-2, q**C**-4), 159.8 (q**C**-6), 103.4 (q**C**-3), 101.8 (**C**(5)H),

30.2 (**C**(9)H_2), 22.74 (**C**(8)H_2), 22.66 (**C**(10)H_2), 19.6 (**C**(7)H_3), 14.0 (**C**(11)H_3) ppm; *m/z* (ES+): 183 $(M+H)^+$ 86%).

Spectral characteristics were consistent with previously reported data.[93]

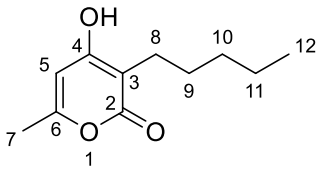
4-Hydroxy-3-isobutyl-6-methyl-2*H*-pyran-2-one (4)[69]



Compound **4** was prepared *via* the procedure described for **2** using *i*-butanal (0.27 mL, 3.0 mmol, 3.0 equiv.) to yield **4** as a white solid (0.171 g, 94%); m.p. 144–148 °C (lit.[69] 143–148 °C); ^{1}H NMR (300 MHz, $CDCl_3$) δ: 10.34 (s, 1H, O**H**), 6.18 (s, 1H, C(5)**H**), 2.28 (d, *J* = 7.3 Hz, 2H, C(8)**H**$_2$), 2.14 (s, 3H, C(7)**H**$_3$), 1.96–1.79 (m, 1H, C(9)**H**), 0.85 (d, *J* = 6.7 Hz, 6H, C(10)**H**$_3$, C(11)**H**$_3$) ppm; ^{13}C NMR (75 MHz, $CDCl_3$) δ: 168.8, 168.1 (q**C**-2, q**C**-4), 159.9 (q**C**-6), 102.4 (q**C**-3), 101.8 (**C**(5)H), 31.7 (**C**(8)H_2), 27.5 (**C**(9)H), 22.4 (2 × C, **C**(10)H_3, (**C**(11)H_3), 19.6 (**C**(7)H_3) ppm; *m/z* (ES+): 183 ($(M+H)^+$ 100%).

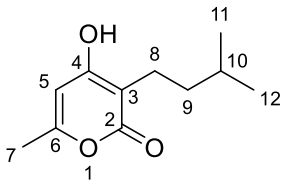
Spectral characteristics were consistent with previously reported data.[69]

4-Hydroxy-6-methyl-3-pentyl-2*H*-pyran-2-one (5)



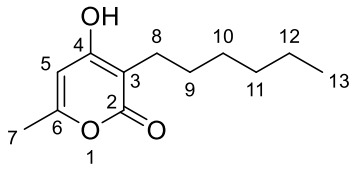
Compound **5** was prepared *via* the procedure described for **2** using pentanal (0.32 mL, 3.0 mmol, 3.0 equiv.) to yield **5** as an off-white solid (0.179 g, 91%); m.p. 132–136 °C; IR (film) ν_{max} 3208 (broad OH stretch), 1648 (ester C=O stretch), 1573, 1447 (alkene C=C stretch), 1274 (ester C-O stretch), 1128 (alcohol C-O stretch) cm^{-1}; ^{1}H NMR (300 MHz, $CDCl_3$) δ: 10.60 (bs, 1H, O**H**), 6.27 (s, 1H, C(5)**H**), 2.55–2.35 (m, 2H, C(8)**H**$_2$), 2.22 (s, 3H, C(7)**H**$_3$), 1.59–1.20 (m, 6H, C(9)**H**$_2$, C(10)**H**$_2$, C(11)**H**$_2$), 0.87 (t, *J* = 6.9 Hz, 3H, C(12)**H**$_3$) ppm; ^{13}C NMR (75 MHz, $CDCl_3$) δ: 168.6, 167.7 (q**C**-2, q**C**-4), 159.8 (q**C**-6), 103.4 (q**C**-3), 101.9 (**C**(5)H), 31.8 (**C**(10)H_2), 27.8 (**C**(9)H_2), 22.6 (**C**(8)H_2), 23.0 (**C**(11)H_2), 19.7 (**C**(7)H_3), 14.1 (**C**(12)H_3) ppm; HRMS (ESI-TOF) *m/z*: $[M+H]^+$ calcd for $C_{11}H_{17}O_3$: 197.1211; found: 197.1208.

4-Hydroxy-3-isopentyl-6-methyl-2*H*-pyran-2-one (6)



Compound **6** was prepared *via* the procedure described for **2** using *i*-pentanal (0.32 mL, 3.0 mmol, 3.0 equiv.) to yield **6** as a white crystalline solid (0.185 g, 94%); m.p. 149–155 °C; IR (film) ν_{max} 3429 (broad OH stretch), 1669 (ester C=O stretch), 1578, 1450 (alkene C=C stretch), 1249 (ester C-O stretch), 1131 (alcohol C-O stretch) cm^{-1}; ^{1}H NMR (300 MHz, $CDCl_3$) δ: 10.13 (bs, 1H, O**H**), 6.22 (s, 1H, C(5)**H**), 2.50–2.37 (m, 2H, C(8)$\mathbf{H}_2$), 2.22 (s, 3H, C(7)$\mathbf{H}_3$), 1.68–1.49 (m, 1H, C(10)**H**), 1.47–1.29 (m, 2H, C(9)$\mathbf{H}_2$), 0.92 (d, *J* = 6.6 Hz , 6H, C(12)$\mathbf{H}_3$, C(11)$\mathbf{H}_3$) ppm; ^{13}C NMR (75 MHz, $CDCl_3$) δ: 168.6, 167.6 (q**C**-2, q**C**-4), 159.7 (q**C**-6), 103.6 (q**C**-3), 101.9 (**C**(5)H), 37.0 (**C**(8)H_2), 22.5 (2 × C, **C**(11)H_3, **C**(12)H_3), 21.8 (**C**(10)H), 21.0 (**C**(9)H_2), 19.7 (**C**(7)H_3) ppm; HRMS (ESI-TOF) *m/z*: $[M+H]^+$ calcd for $C_{11}H_{17}O_3$: 197.1178; found: 197.1184.

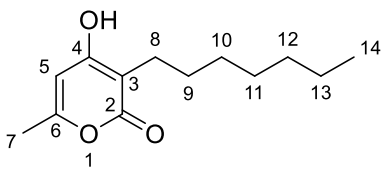
3-Hexyl-4-hydroxy-6-methyl-2*H*-pyran-2-one (7)[69]



Compound **7** was prepared *via* the procedure described for **2** using hexanal (0.74 mL, 6.0 mmol, 3.0 equiv.) to yield **7** as a white solid (0.376 g, 90%); m.p. 115-118 °C (lit.[69] 120–121 °C); ^{1}H NMR (300 MHz, $CDCl_3$) δ: 10.52 (bs, 1H, O**H**), 6.27 (s, 1H, C(5)**H**), 2.55–2.36 (m, 2H, C(8)$\mathbf{H}_2$), 2.22 (s, 3H, C(7)$\mathbf{H}_3$), 1.61–1.18 (m, 8H, C(9)$\mathbf{H}_2$, C(10)$\mathbf{H}_2$, C(11)$\mathbf{H}_2$, C(12)$\mathbf{H}_2$), 0.86 (t, *J* = 6.6 Hz, 3H, C(13)$\mathbf{H}_3$) ppm; ^{13}C NMR (75 MHz, $CDCl_3$) δ: 168.6, 167.6 (q**C**-2, q**C**-4), 159.8 (q**C**-6), 103.4 (q**C**-3), 101.9 (**C**(5)H), 31.8 (**C**(11)H_2, 29.3 (**C**(10)H_2), 28.0 (**C**(9)H_2), 23.0 (**C**(8)H_2), 22.7 (**C**(12)H_2), 19.6 (**C**(7)H_3), 14.1 (**C**(13)H_3) ppm; *m/z* (ES-): 209 ($(M-H)^-$ 100%).

Spectral characteristics were consistent with previously reported data.[69]

3-Heptyl-4-hydroxy-6-methyl-2*H*-pyran-2-one (8)[69]

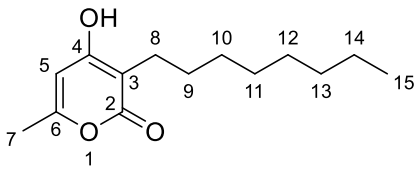


Compound **8** was prepared *via* the procedure described for **2** using heptanal (0.42 mL, 3.0 mmol, 3.0 equiv.) to yield **8** as an off-white solid (0.210 g, 93%); m.p. 119–124 °C; ^{1}H NMR (300 MHz, $CDCl_3$) δ:

10.38 (bs, 1H, O**H**), 6.24 (s, 1H, C(5)**H**), 2.50–2.41 (m, 2H, C(8)$\mathbf{H}_2$), 2.22 (s, 3H, C(7)$\mathbf{H}_3$), 1.64–1.40 (m, 2H, C(9)$\mathbf{H}_2$), 1.39–1.16 (m , 8H, C(10)$\mathbf{H}_2$, C(11)$\mathbf{H}_2$, C(12)$\mathbf{H}_2$, C(13)$\mathbf{H}_2$), 0.86 (t, *J* = 6.7 Hz, 3H, C(14)$\mathbf{H}_3$) ppm; ^{13}C NMR (75 MHz, $CDCl_3$) δ: 168.5, 167.6 (q**C**-2, q**C**-4), 159.7 (q**C**-6), 103.9 (q**C**-3), 101.8 (**C**(5)H), 31.9 (**C**(12)H_2), 29.6, 29.3 (**C**(10)H_2, **C**(11)H_2), 28.1 (**C**(9)H_2), 23.0 (**C**(8)H_2), 22.7 (**C**(13)H_2), 19.6 (**C**(7)H_3), 14.1 (**C**(14)H_3) ppm; *m/z* (ES+): 225 ($(M+H)^+$ 16%).

Spectral characteristics were consistent with previously reported data.[69]

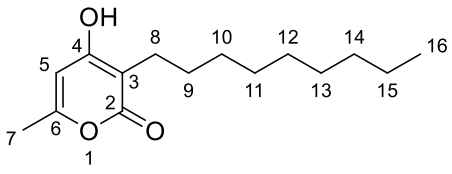
4-Hydroxy-6-methyl-3-octyl-2*H*-pyran-2-one (9)[94]



Compound **9** was prepared *via* the procedure described for **2** using octanal (0.47 mL, 3.0 mmol, 3.0 equiv.) to yield **9** as a white solid (0.211 g, 88%); m.p. 103–105 °C (lit.[94] 103–104.5 °C); ^{1}H NMR (300 MHz, $CDCl_3$) δ: 10.47 (bs, 1H, O**H**), 6.25 (s, 1H, C(5)**H**), 2.56–2.34 (m, 2H, C(8)$\mathbf{H}_2$), 2.22 (s, 3H, C(7)$\mathbf{H}_3$), 1.61–1.15 (m, 12H, C(9)$\mathbf{H}_2$, C(10)$\mathbf{H}_2$, C(11)$\mathbf{H}_2$, C(12)$\mathbf{H}_2$, C(13)$\mathbf{H}_2$, C(14)$\mathbf{H}_2$), 0.86 (t, *J* = 6.7 Hz, 3H, C(15)$\mathbf{H}_3$) ppm; ^{13}C NMR (75 MHz, $CDCl_3$) δ: 168.5, 167.5 (q**C**-2, q**C**-4), 159.7 (q**C**-6), 103.4 (q**C**-3), 101.8 (**C**(5)H), 31.9 (**C**(13)H_2), 29.7, 29.6, 29.3 (**C**(10)H_2, **C**(11)H_2, **C**(12)H_2), 28.1 (**C**(9)H_2), 23.0 (**C**(8)H_2), 22.7 (**C**(14)H_2), 19.6 (**C**(7)H_3), 14.1 (**C**(15)H_3) ppm; *m/z* (ES+): 239 ($(M+H)^+$ 98%).

Spectral characteristics were consistent with previously reported data.[94]

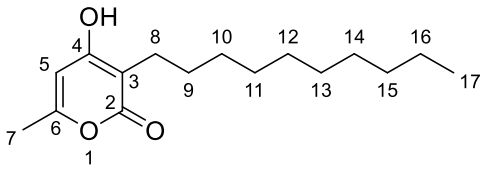
4-Hydroxy-6-methyl-3-nonyl-2*H*-pyran-2-one (10)



Compound **10** was prepared *via* the procedure described for **2** using nonanal (0.52 mL, 3.0 mmol, 3.0 equiv.) to yield **10** as a white solid (0.227 g, 90%); m.p. 93–96 °C; IR (film) ν_{max} 3410 (broad OH stretch), 1670 (ester C=O stretch), 1594, 1448 (alkene C=C stretch), 1249 (ester C-O stretch), 1129 (alcohol C-O stretch) cm^{-1}; ^{1}H NMR (300 MHz, $CDCl_3$) δ: 10.49 (bs, 1H, O**H**), 6.26 (s, 1H, C(5)**H**), 2.55–2.32 (m, 2H, C(8)$\mathbf{H}_2$), 2.22 (s, 3H, C(7)$\mathbf{H}_3$), 1.61–1.11 (m, 14H, C(9)$\mathbf{H}_2$, C(10)$\mathbf{H}_2$, C(11)$\mathbf{H}_2$, C(12)$\mathbf{H}_2$, C(13)$\mathbf{H}_2$, C(14)$\mathbf{H}_2$, C(15)$\mathbf{H}_2$), 0.86 (t, *J* = 6.7 Hz, 3H, C(16)$\mathbf{H}_3$) ppm; ^{13}C NMR (75 MHz, $CDCl_3$) δ: 168.5,

167.5 (q**C**-2, q**C**-4), 159.7 (q**C**-6), 103.4 (q**C**-3), 101.8 (**C**(5)H), 31.9 (**C**(14)H_2), 29.7 (2 × C), 29.6, 29.4 (**C**(10)H_2, **C**(11)H_2, **C**(12)H_2, **C**(13)H_2), 28.1 (**C**(9)H_2), 23.0 (**C**(8)H_2), 22.7 (**C**(15)H_2), 19.6 (**C**(7)H_3), 14.1 (**C**(16)H_3) ppm; HRMS (ESI-TOF) *m/z*: $[M+H]^+$ calcd for $C_{15}H_{25}O_3$: 253.1804; found: 253.1797; Anal. calcd for $C_{15}H_{24}O_3$: C, 71.39; H, 9.59; found C, 71.53; H, 9.55.

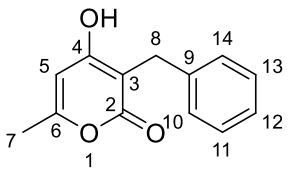
3-Decyl-4-hydroxy-6-methyl-2*H*-pyran-2-one (11)[94]



Compound **11** was prepared *via* the procedure described for **2** using decanal (0.57 mL, 3.0 mmol, 3.0 equiv.) to yield **11** as a white solid (0.246 g, 92%); m.p. 103–105 °C (lit.[94] 101.5–102.5 °C); ^{1}H NMR (300 MHz, $CDCl_3$) δ: 10.73 (bs, 1H, O**H**), 6.29 (s, 1H, C(5)**H**), 2.55–2.34 (m, 2H, C(8)**H**$_2$), 2.22 (s, 3H, C(7)**H**$_3$), 1.59–1.15 (m, 16H, C(9)**H**$_2$, C(10)**H**$_2$, C(11)**H**$_2$, C(12)**H**$_2$, C(13)**H**$_2$, C(14)**H**$_2$, C(15)**H**$_2$, C(16)**H**$_2$), 0.87 (t, *J* = 6.7 Hz, 3H, C(17)**H**$_3$) ppm; ^{13}C NMR (75 MHz, $CDCl_3$) δ: 168.6, 167.8 (q**C**-2, q**C**-4), 159.7 (q**C**-6), 103.4 (q**C**-3), 101.9 (**C**(5)H), 31.9 (**C**(15)H_2), 29.71, 29.67 (2 × C), 29.64, 29.4, (**C**(10)H_2, **C**(11)H_2, **C**(12)H_2, **C**(13)H_2, **C**(14)H_2), 28.1 (**C**(9)H_2), 23.0 (**C**(8)H_2), 22.7 (**C**(16)H_2), 19.6 (**C**(7)H_3), 14.1 (**C**(17)H_3) ppm; *m/z* (ES+): 267 ($(M+H)^+$ 100%).

Spectral characteristics were consistent with previously reported data.[94]

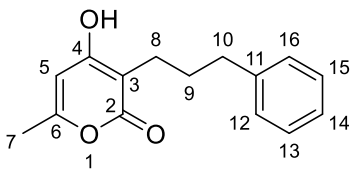
3-Benzyl-4-hydroxy-6-methyl-2H-pyran-2-one (12)[69]



Compound **12** was prepared *via* the procedure described for **2** using benzaldehyde (0.31 mL, 3.0 mmol, 3.0 equiv.) to yield **12** as a white solid (0.204 g, 94%); m.p. 167–170 °C (lit.[69] 156–158 °C); ^{1}H NMR (300 MHz, CD_3OD) δ: 7.29–7.01 (m, 5H, C(10)**H**, C(11)**H**, C(12)**H**, C(13)**H**, C(14)**H**), 6.02 (s, 1H, C(5)**H**), 3.69 (s, 2H, C(8)**H**$_2$), 2.19 (s, 3H, C(7)**H**$_3$) ppm; ^{13}C NMR (75 MHz, CD_3OD) δ: 168.5, 168.0 (q**C**-2, q**C**-4), 162.3 (q**C**-6), 141.7 (q**C**-9), 129.4 (2 × C, **C**(10)H, **C**(14)H), 129.0 (2 × C, **C**(11)H, **C**(13)H), 126.8 (**C**(12)H), 103.0 (q**C**-3), 101.4 (**C**(5)H), 29.5 (**C**(8)H_2), 19.5 (**C**(7)H_3) ppm; *m/z* (ES+): 217 ($(M+H)^+$ 54%).

Spectral characteristics were consistent with previously reported data.[69]

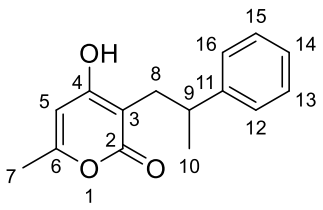
4-Hydroxy-6-methyl-3-(3-phenylpropyl)-2*H*-pyran-2-one (13)[93]



Compound **13** was prepared *via* the procedure described for **2** using hydrocinnamaldehyde (0.40 mL, 3.0 mmol, 3.0 equiv.) to yield **13** as an off-white solid (0.220 g, 90%); m.p. 129–130 °C (lit.[93] 129–131 °C); ^{1}H NMR (300 MHz, $CDCl_3$) δ: 10.70 (bs, 1H, O**H**), 7.36–6.98 (m, 5H, C(12)**H**, C(13)**H**, C(14)**H**, C(15)**H**, C(16)**H**), 6.25 (s, 1H, C(5)**H**), 2.84–2.37 (m, 4H, C(8)$\mathbf{H}_2$, C(10)$\mathbf{H}_2$), 2.16 (s, 3H, C(7)$\mathbf{H}_3$), 1.98–1.69 (m, 2H, C(9)$\mathbf{H}_2$) ppm; ^{13}C NMR (75 MHz, $CDCl_3$) δ: 168.6, 167.8 (q**C**-2, q**C**-4), 160.1 (q**C**-6), 142.5 (q**C**-11), 128.3 (2 × C), 128.2 (2 × C) (**C**(12)H, **C**(13)H, **C**(15)H, **C**(16)H), 125.6 (**C**(14)H), 102.9 (q**C**-3), 101.9 (**C**(5)H), 35.9 (**C**(10)H_2), 29.7 (**C**(9)H_2), 23.1 (**C**(8)H_2), 19.7 (**C**(7)H_3) ppm; *m/z* (ES+): 245 ($(M+H)^+$ 100%).

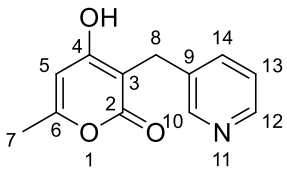
Spectral characteristics were consistent with previously reported data.[93]

4-Hydroxy-6-methyl-3-(2-phenylpropyl)-2*H*-pyran-2-one (14)



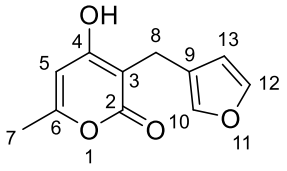
Compound **14** was prepared *via* the procedure described for **2** using 2-phenylpropanal (0.40 mL, 3.0 mmol, 3.0 equiv.) to yield **14** as a white solid (0.223 g, 91%); m.p. 184–186 °C; IR (film) ν_{max} 3389 (broad OH stretch), 1641 (ester C=O stretch), 1575 (alkene C=C stretch), 1445 (aromatic C-C stretch), 1257 (ester C-O stretch), 1122 (alcohol C-O stretch) cm^{-1}; ^{1}H NMR (300 MHz, $CD_3OD/CDCl_3$) δ: 7.34–7.05 (m, 5H, C(12)**H**, C(13)**H**, C(14)**H**, C(15)**H**, C(16)**H**), 5.90 (d, *J* = 0.8 Hz, 1H, C(5)**H**), 3.22–3.04 (m, 1H, C(9)**H**), 2.73–2.55 (m, 2H, C(8)$\mathbf{H}_2$), 2.18 (d, *J* = 0.8 Hz, 3H, C(7)$\mathbf{H}_3$), 1.23 (d, *J* = 7.0 Hz, 3H, C(10)$\mathbf{H}_3$) ppm; ^{13}C NMR (75 MHz, $CD_3OD/CDCl_3$) δ: 168.4, 167.7 (q**C**-2, q**C**-4), 161.0 (q**C**-6), 148.0 (q**C**-11), 128.6 (2 × C), 127.6 (2 × C) (**C**(12)H, **C**(13)H, **C**(15)H, **C**(16)H_2), 126.4 (**C**(14)H), 102.0 (q**C**-3), 101.2 (**C**(5)H), 38.8 (**C**(9)H), 32.3 (**C**(8)H_2), 21.3 (**C**(10)H_3), 19.7 (**C**(7)H_3) ppm; HRMS (ESI-TOF) *m/z*: $[M+H]^+$ calcd for $C_{15}H_{17}O_3$: 245.1178; found: 245.1170.

4-Hydroxy-6-methyl-3-(pyridin-3-ylmethyl)-*2H*-pyran-2-one (15)



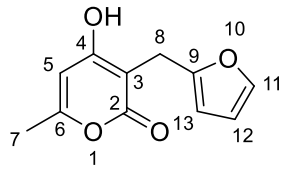
Compound **15** was prepared *via* the procedure described for **2** using nonanal (0.52 mL, 3.0 mmol, 3.0 equiv.) except that compound **15** precipitated out of the reaction mixture, was collected *via* suction filtration and was recrystallised from hot DCM/MeOH to yield **15** as a white crystalline solid (0.076 g, 35%); m.p. 202–205 °C; IR (film) ν_{max} 3382 (broad OH stretch), 1683 (ester C=O stretch), 1661 (C=N stretch), 1587 (alkene C=C stretch), 1448 (aromatic C-C stretch), 1270 (ester C-O stretch), 1120 (alcohol C-O stretch) cm^{-1}; ^{1}H NMR (300 MHz, $(CD_3)_2SO$) δ: 8.54–8.24 (m, 2H, C(10)**H**, C(12)**H**), 7.57 (dt, *J* = 7.8, 1.9 Hz, 1H, C(14)**H**), 7.26 (dd, *J* = 7.8, 4.8 Hz, 1H, C(13)**H**), 6.04 (s, 1H, C(5)**H**), 3.59 (s, 2H, C(8)$\mathbf{H}_2$), 2.16 (s, 3H, C(7)$\mathbf{H}_3$) ppm; ^{13}C NMR (75 MHz, $(CD_3)_2SO$) δ: 166.4, 165.2 (q**C**-2, q**C**-4), 161.2 (q**C**-6), 149.9 (**C**(10)H), 147.5 (**C**(12)H), 136.6 (q**C**-9), 136.0 (**C**(14)H), 123.8 (**C**(13)H), 100.3 (**C**(5)H), 100.1 (q**C**-3), 26.2 (**C**(8)H_2), 19.8 (**C**(7)H_3) ppm; HRMS (ESI-TOF) *m/z*: $[M+H]^+$ calcd for $C_{12}H_{12}NO_3$: 218.0817; found: 218.0810; Anal. calcd for $C_{12}H_{11}NO_3$: C, 66.35; H, 5.10; N, 6.45; found C, 65.06; H, 5.18; N, 6.73.

3-(Furan-3-ylmethyl)-4-hydroxy-6-methyl-2*H*-pyran-2-one (16)



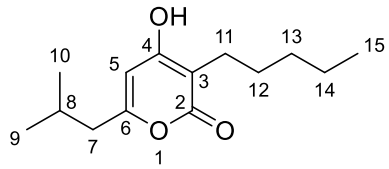
Compound **16** was prepared *via* the procedure described for **2** using 3-furaldehyde (0.26 mL, 3.0 mmol, 3.0 equiv.) to yield **16** as a beige crystalline solid (0.175 g, 85%); m.p. 187–189 °C; IR (film) ν_{max} 3401 (broad OH stretch), 1663 (ester C=O stretch), 1619 (furanyl C=C stretch), 1572, 1448 (alkene C=C stretch), 1262 (ester C-O stretch), 1124 (alcohol C-O stretch), 1018 (furanyl C-O stretch) cm^{-1}; ^{1}H NMR (300 MHz, $(CD_3)_2SO$) δ: 11.29 (bs, 1H, O**H**), 7.48 (t, *J* = 1.6 Hz, 1H, C(12)**H**), 7.34 (d, *J* = 0.5 Hz, 1H, C(10)**H**), 6.31 (d, *J* = 0.9 Hz, 1H, C(13)**H**), 6.02 (d, *J* = 0.7 Hz, 1H, C(5)**H**), 3.37 (s, 2H, C(8)$\mathbf{H}_2$), 2.15 (s, 3H, C(7)$\mathbf{H}_3$) ppm; ^{13}C NMR (75 MHz, $(CD_3)_2SO$) δ: 165.3, 164.6 (q**C**-2, q**C**-4), 160.3 (q**C**-6), 142.7 (**C**(12)H), 139.1 (**C**(10)H), 123.1 (q**C**-9), 111.4 (**C**(13)H), 100.0 (q**C**-3), 99.8 (**C**(5)H), 19.3 (**C**(7)H_3), 18.1 (**C**(8)H_2) ppm; HRMS (ESI-TOF) *m/z*: $[M+H]^+$ calcd for $C_{11}H_{11}O_4$: 207.0657; found: 207.0653.

3-(Furan-2-ylmethyl)-4-hydroxy-6-methyl-2*H*-pyran-2-one (17)



Compound **17** was prepared *via* the procedure described for **2** using 2-furaldehyde (0.25 mL, 3.0 mmol, 3.0 equiv.) to yield **17** as a yellow solid (0.194 g, 93%); m.p. 172–174 °C (lit.[73] 177–178 °C); IR (film) ν_{max} 3380 (broad OH stretch), 1664 (ester C=O stretch), 1621 (furanyl C=C stretch), 1573, 1449 (alkene C=C stretch), 1263 (ester C-O stretch), 1125 (alcohol C-O stretch), 1020 (furanyl C-O stretch) cm^{-1}; ^1H NMR (300 MHz, $(CD_3)_2SO$) δ: 7.43 (dd, *J* = 1.8, 0.8 Hz, 1H, C(11)**H**), 6.29 (dd, *J* = 3.1, 1.9 Hz, 1H, C(12)**H**), 6.03 (d, *J* = 0.9 Hz, 1H, C(5)**H**), 5.92 (dd, *J* = 3.1, 0.9 Hz, 1H, C(13)**H**), 3.58 (s, 2H, C(8)$\mathbf{H}_2$), 2.16 (d, *J* = 0.7 Hz, 3H, C(7)$\mathbf{H}_3$) ppm; ^{13}C NMR (75 MHz, $(CD_3)_2SO$) δ: 166.0, 164.4 (q**C**-2, q**C**-4), 160.7 (q**C**-6), 153.3 (q**C**-9), 140.9 (**C**(11)H), 110.3 (**C**(12)H), 105.0 (**C**(13)H), 99.8 (**C**(5)H), 97.3 (q**C**-3), 21.7 (**C**(8)H_2), 19.3 (**C**(7)H_3) ppm; HRMS (ESI-TOF) *m/z*: $[M+H]^+$ calcd for $C_{11}H_{11}O_4$: 207.0657; found: 207.0656.

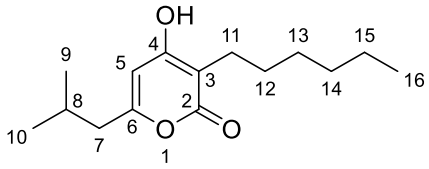
4-Hydroxy-6-isobutyl-3-pentyl-2*H*-pyran-2-one (22)



A Schlenk tube was heated under vacuum, cooled to r.t. and refilled with nitrogen three times. **5** (0.098 g, 0.5 mmol, 1.0 equiv.) was added, followed by dried and degassed THF (1.39 mL), the resulting white suspension was stirred at r.t. for 5 min. TMEDA (0.08 mL, 0.5 mmol, 1.0 equiv.) and HMPA (0.28 mL) were added and the resulting pale-yellow reaction mixture was cooled to 0 °C for 30 min. *n*-BuLi (0.95 mL, 1.265 M in hexanes) was added dropwise over 10 min giving a deep red reaction mixture that was stirred for a further 1 h at 0 °C, followed by the dropwise addition of 2-iodopropane (0.09 mL, 0.9 mmol, 1.8 equiv.). The orange reaction mixture was warmed to r.t. and stirred under nitrogen for 16 h. The reaction was acidified with 4 M HCl until the pH reached 2–3 and was then extracted with Et_2O (3 × 10 mL). The combined organic layers were washed with H_2O (3 × 10 mL) and brine (1 × 10 mL), dried over $MgSO_4$, filtered and concentrated under reduced pressure.[69] Purification *via* column chromatography (hexanes:EtOAc 70:30) to yield **22** as a white solid (0.054 g, 45%); m.p. 114–117 °C; IR (film) ν_{max} 3045 (broad OH stretch), 1663 (ester C=O stretch), 1569, 1433 (alkene C=C stretch), 1275 (ester C-O stretch), 1129 (alcohol C-O stretch) cm^{-1}; ^1H NMR (300

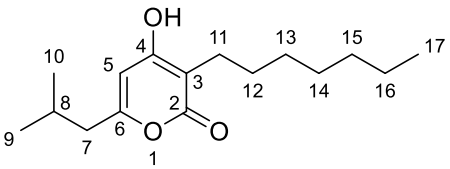
MHz, $CDCl_3$) δ: 10.12 (bs, 1H, O**H**), 6.17 (s, 1H, C(5)**H**), 2.55–2.37 (m, 2H, C(11)$\mathbf{H}_2$), 2.30 (d, *J* = 7.2 Hz, 2H, C(7)$\mathbf{H}_2$), 2.15–1.95 (m, 1H, C(8)**H**), 1.58–1.43 (m, 2H, C(12)$\mathbf{H}_2$), 1.41–1.16 (m, 4H, C(13)$\mathbf{H}_2$, C(14)$\mathbf{H}_2$), 1.02–0.80 (m, 9H, C(9)$\mathbf{H}_3$, C(10)$\mathbf{H}_3$, C(15)$\mathbf{H}_3$) ppm; ^{13}C NMR (75 MHz, $CDCl_3$) δ: 168.4, 167.0 (q**C**-2, q**C**-4), 162.7 (q**C**-6), 103.5 (q**C**-3), 101.9 (**C**(5)H), 42.6 (**C**(7)H_2), 31.8 (**C**(13)H_2), 27.7 (**C**(12)H_2), 26.8 (**C**(8)H), 23.0 (**C**(11)H_2), 22.6 (**C**(14)H_2), 22.2 (2 × C, **C**(9)H_3, **C**(10)H_3), 14.0 (**C**(15)H_3) ppm; HRMS (ESI-TOF) *m/z*: $[M+H]^+$ calcd for $C_{14}H_{23}O_3$: 239.1642; found: 239.1636.

3-Hexyl-4-hydroxy-6-isobutyl-2*H*-pyran-2-one (23, PPYA**)**[69]



Compound **23** was prepared *via* the procedure described for 22 using **7** (0.105 g, 0.5 mmol, 1.0 equiv.) to yield 23 as a pale yellow solid (0.060 g, 24%); m.p. 109–112 °C; ^{1}H NMR (300 MHz, $CDCl_3$) δ: 10.49 (bs, 1H, O**H**), 6.21 (s, 1H, C(5)**H**), 2.57–2.38 (m, 2H, C(11)$\mathbf{H}_2$), 2.30 (d, *J* = 7.2 Hz, 2H, C(7)$\mathbf{H}_2$), 2.15–1.94 (m, 1H, C(8)**H**), 1.55–1.22 (m, 8H, C(12)$\mathbf{H}_2$, C(13)$\mathbf{H}_2$, C(14)$\mathbf{H}_2$, C(15)$\mathbf{H}_2$), 1.01–0.75 (m, 9H, C(9)$\mathbf{H}_3$, C(10)$\mathbf{H}_3$, C(16)$\mathbf{H}_3$) ppm; ^{13}C NMR (75 MHz, $CDCl_3$) δ: 168.4, 167.4 (q**C**-2, q**C**-4), 162.6 (q**C**-6), 103.5 (q**C**-3), 102.0 (**C**(5)H), 42.6 (**C**(7)H_2), 31.8 (**C**(14)H_2), 29.1 (**C**(13)H_2), 28.0 (**C**(12)H_2), 26.2 (**C**(8)H), 23.1 (**C**(11)H_2), 22.7 (**C**(15)H_3), 22.2 (2 × C) (**C**(9)H_3, **C**(10)H_3), 14.1 (**C**(16)H_3) ppm; *m/z* (ES+): 253 ($(M+H)^+$ 100%); Anal. calcd for $C_{15}H_{24}O_3$: C, 71.39; H, 9.59; found C, 71.32; H, 9.39.

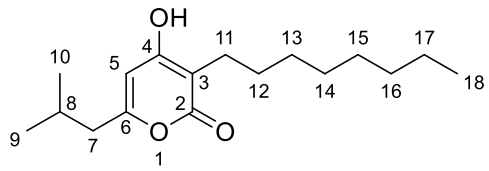
3-heptyl-4-hydroxy-6-isobutyl-*2H*-pyran-2-one (24)



Compound **24** was prepared *via* the procedure described for **22** using **8** (0.112 g, 0.5 mmol, 1.0 equiv.) to yield **24** as a yellow solid (0.060 g, 45%); m.p. 105–107 °C; IR (film) ν_{max} 3067 (broad OH stretch), 1663 (ester C=O stretch), 1569, 1433 (alkene C=C stretch), 1256 (ester C-O stretch), 1130 (alcohol C-O stretch) cm^{-1}; ^{1}H NMR (300 MHz, $CDCl_3$) δ: 9.88 (bs, 1H, O**H**), 6.15 (s, 1H, C(5)**H**), 2.54–2.37 (m, 2H, C(11)$\mathbf{H}_2$), 2.30 (d, *J* = 7.2 Hz, 2H, C(7)$\mathbf{H}_2$), 2.15–1.93 (m, 1H, C(8)**H**), 1.57–1.41 (m, 2H, C(12)$\mathbf{H}_2$), 1.40–1.16 (m, 8H, C(13)$\mathbf{H}_2$, C(14)$\mathbf{H}_2$, C(15)$\mathbf{H}_2$, C(16)$\mathbf{H}_2$), 1.02–0.78 (m, 9H, C(9)$\mathbf{H}_3$, C(10)$\mathbf{H}_3$, C(17)$\mathbf{H}_3$) ppm;

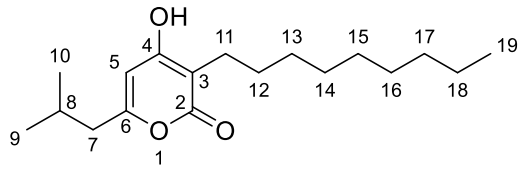
^{13}C NMR (75 MHz, $CDCl_3$) δ: 168.2, 166.8 (q**C**-2, q**C**-4), 162.7 (q**C**-6), 103.5 (q**C**-3), 101.8 (**C**(5)H), 42.6 (**C**(7)H_2), 31.9 (**C**(15)H_2), 29.7 (**C**(13)H_2), 29.3 (**C**(14)H_2), 28.1 (**C**(12)H_2), 26.8 (**C**(8)H), 23.1 (**C**(11)H_2), 22.7 (**C**(16)H_2), 22.2 (2 × C, **C**(9)H_3, **C**(10)H_3), 14.1 (**C**(17)H_3) ppm; HRMS (ESI-TOF) *m/z*: $[M+H]^+$ calcd for $C_{16}H_{27}O_3$: 267.1955; found: 267.1953.

4-Hydroxy-6-isobutyl-3-octyl-2*H*-pyran-2-one (25, PPYC**)**



Compound **25** was prepared *via* the procedure described for 22 using **9** (0.119 g, 0.5 mmol, 1.0 equiv.) to yield **25** as a white solid (0.063 g, 45%); m.p. 105–107 °C; IR (film) ν_{max} 3089 (broad OH stretch), 1663 (ester C=O stretch), 1569, 1433 (alkene C=C stretch), 1273 (ester C-O stretch), 1130 (alcohol C-O stretch) cm^{-1}; ^{1}H NMR (300 MHz, $CDCl_3$) δ: 9.58 (bs, 1H, O**H**), 6.13 (s, 1H, C(5)**H**), 2.57–2.37 (m, 2H, C(11)$\mathbf{H}_2$), 2.30 (d, *J* = 7.2 Hz, 2H, C(7)$\mathbf{H}_2$), 2.16–1.92 (m, 1H, C(8)**H**), 1.59–1.15 (m, 12H, C(12)$\mathbf{H}_2$, C(13)$\mathbf{H}_2$, C(14)$\mathbf{H}_2$, C(15)$\mathbf{H}_2$, C(16)$\mathbf{H}_2$, C(17)$\mathbf{H}_2$), 1.01–0.75 (m, 9H, C(9)$\mathbf{H}_3$, C(10)$\mathbf{H}_3$, C(18)$\mathbf{H}_3$) ppm; ^{13}C NMR (75 MHz, $CDCl_3$) δ: 168.4, 167.1 (q**C**-2, q**C**-4), 162.6 (q**C**-6), 103.5 (q**C**-3), 101.5 (**C**(5)H), 42.6 (**C**(7)H_2), 31.9 (**C**(16)H_2), 29.7, 29.6, 29.4 (**C**(13)H_2, **C**(14)H_2, **C**(15)H_2), 28.1 (**C**(12)H_2), 26.9 (**C**(8)H), 23.1 (**C**(11)H_2), 22.7 (**C**(17)H_2), 22.2 (2 × C, **C**(9)H_3, **C**(10)H_3), 14.1 (**C**(18)H_3) ppm; HRMS (ESI-TOF) *m/z*: $[M+H]^+$ calcd. for $C_{17}H_{29}O_3$: 281.2111; found: 281.2113.

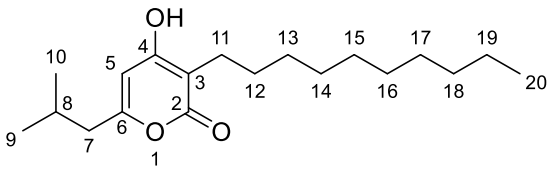
4-Hydroxy-6-isobutyl-3-nonyl-2*H*-pyran-2-one (26)



Compound **26** was prepared *via* the procedure described for **22** using **10** (0.126 g, 0.5 mmol, 1.0 equiv.) to yield **26** as a white solid (0.062 g, 42%); m.p. 98–100 °C; IR (film) ν_{max} 3044 (broad OH stretch), 1663 (ester C=O stretch), 1569, 1433 (alkene C=C stretch), 1265 (ester C-O stretch), 1130 (alcohol C-O stretch) cm^{-1}; ^{1}H NMR (300 MHz, $CDCl_3$) δ: 9.51 (bs, 1H, O**H**), 6.12 (s, 1H, C(5)**H**), 2.57–2.37 (m, 2H, C(11)$\mathbf{H}_2$), 2.30 (d, *J* = 7.2 Hz, 2H, C(7)$\mathbf{H}_2$), 2.17–1.92 (m, 1H, C(8)**H**), 1.64–1.15 (m, 14H, C(12)$\mathbf{H}_2$, C(13)$\mathbf{H}_2$, C(14)$\mathbf{H}_2$, C(15)$\mathbf{H}_2$, C(16)$\mathbf{H}_2$, C(17)$\mathbf{H}_2$, C(18)$\mathbf{H}_2$), 1.04–0.66 (m, 9H,

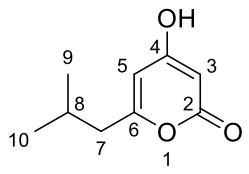
C(9)**H**$_3$, C(10)**H**$_3$, C(19)**H**$_3$) ppm; ^{13}C NMR (75 MHz, $CDCl_3$) δ: 168.5, 167.3 (q**C**-2, q**C**-4), 162.6 (q**C**-6), 103.5 (q**C**-3), 102.0 (**C**(5)H), 42.6 (**C**(7)H$_2$), 31.9 (**C**(17)H$_2$), 29.74, 29.66 (2 × C), 29.4 (**C**(13)H$_2$, **C**(14)H$_2$, **C**(15)H$_2$, **C**(16)H$_2$), 28.1 (**C**(12)H$_2$), 26.9 (**C**(8)H), 23.1 (**C**(11)H$_2$), 22.7 (**C**(18)H$_2$), 22.2 (2 × C, **C**(9)H$_3$, **C**(10)H$_3$), 14.1 (**C**(19)H$_3$) ppm; HRMS (ESI-TOF) *m/z*: $[M+H]^+$ calcd. for $C_{18}H_{31}O_3$: 295.2268; found: 295.2268.

3-Decyl-4-hydroxy-6-isobutyl-2*H*-pyran-2-one (27, PPYE**)**



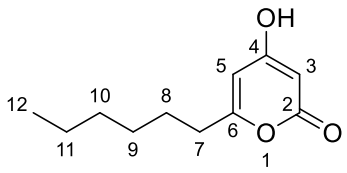
Compound **27** was prepared *via* the procedure described for **22** using **11** (0.133 g, 0.5 mmol, 1.0 equiv.) to yield **27** as a pale yellow solid (0.057 g, 37%); m.p. 95–96 °C; IR (film) ν_{max} 3090 (broad OH stretch), 1663 (ester C=O stretch), 1567, 1432 (alkene C=C stretch), 1258 (ester C-O stretch), 1130 (alcohol C-O stretch) cm^{-1}; ^{1}H NMR (300 MHz, $CDCl_3$) δ: 9.08 (bs, 1H, O**H**), 6.08 (s, 1H, C(5)**H**), 2.53–2.37 (m, 2H, C(11)**H**$_2$), 2.30 (d, *J* = 7.2 Hz, 2H, C(7)**H**$_2$), 2.16–1.96 (m, 1H, C(8)**H**), 1.60–1.12 (m, 16H, C(12)**H**$_2$, C(13)**H**$_2$, C(14)**H**$_2$, C(15)**H**$_2$, C(16)**H**$_2$, C(17)**H**$_2$, C(18)**H**$_2$, C(19)**H**$_2$), 0.99–0.79 (m, 9H, C(9)**H**$_3$, C(10)**H**$_3$, C(20)**H**$_3$) ppm; ^{13}C NMR (75 MHz, $CDCl_3$) δ: 168.4, 167.1 (q**C**-2, q**C**-4), 162.6 (q**C**-6), 103.5 (q**C**-3), 101.9 (**C**(5)H), 42.6 (**C**(7)H$_2$), 31.9 (**C**(18)H$_2$), 29.73, 29.71, 29.67, 29.66, 29.4 (**C**(13)H$_2$, **C**(14)H$_2$, **C**(15)H$_2$, **C**(16)H$_2$, **C**(17)H$_2$), 28.1 (**C**(12)H$_2$), 26.9 (**C**(8)H), 23.1 (**C**(11)H$_2$), 22.7 (**C**(19)H$_2$), 22.2 (2 × C, **C**(9)H$_3$, **C**(10)H$_3$), 14.1 (**C**(20)H$_3$) ppm; HRMS (ESI-TOF) *m/z*: $[M+H]^+$ calcd. for $C_{19}H_{33}O_3$: 309.2424; found: 309.2425.

4-Hydroxy-6-isobutyl-2*H*-pyran-2-one (28)[69]



Compound **28** was prepared *via* the procedure described for **22** using **1** (0.214 g, 1.7 mmol, 1.0 equiv.) to yield **28** as a white solid (0.165 g, 58%); m.p. 103–106 °C (lit.[95] 106–108 °C); ^{1}H NMR (300 MHz, $CDCl_3$) δ: 11.13 (bs, 1H, O**H**), 6.00 (d, *J* = 1.8 Hz, 1H, C(5)**H**), 5.60 (d, *J* = 1.8 Hz, 1H, C(3)**H**), 2.35 (d, *J* = 7.2 Hz, 2H, C(7)**H**$_2$), 2.15–1.94 (m, 1H, C(8)**H**), 0.95 (d, *J* = 6.6 Hz, 6H, C(9)**H**$_3$, C(10)**H**$_3$) ppm; ^{13}C NMR (75 MHz, $CDCl_3$) δ: 172.6, 168.5 (q**C**-2, q**C**-4), 166.4 (q**C**-6), 102.4 (**C**(5)H), 89.9 (**C**(3)H), 42.8 (**C**(7)H$_2$), 26.9 (**C**(8)H), 22.2 (2 × C, **C**(9)H$_3$, **C**(10)H$_3$) ppm; *m/z* (ES-): 167 ((M-H)$^-$ 100%).

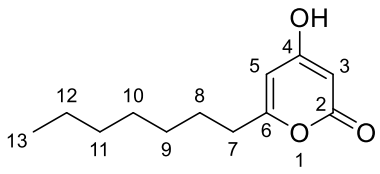
6-Hexyl-4-hydroxy-2*H*-pyran-2-one (29)[96]



Compound **29** was prepared *via* the procedure described for **22** using **1** (0.126 g, 1.0 mmol, 1.0 equiv.) and 1-iodopentane (0.23 mL, 1.8 mmol, 1.8 equiv.) to yield **29** as a yellow-orange solid (0.034 g, 17%); m.p. 44–46 °C (lit. 56–57 °C); ^{1}H NMR (300 MHz, $CDCl_3$) δ: 6.00 (s, 1H, C(5)**H**), 5.58 (bs, 1H, C(3)**H**), 2.47 (t, *J* = 7.6 Hz, 2H, C(7)**H**$_2$), 1.76–1.53 (m, 2H, C(8)**H**$_2$), 1.40–1.19 (m, 6H, C(9)**H**$_2$, C(10)**H**$_2$, C(11)**H**$_2$), 0.88 (t, *J* = 6.7 Hz, 3H, C(12)**H**$_3$) ppm; ^{13}C NMR (75 MHz, $CDCl_3$) δ: 172.7, 168.4 (q**C**-2, q**C**-4), 167.3 (q**C**-6), 101.3 (**C**(5)H), 89.8 (**C**(3)H), 33.6 (**C**(7)H_2), 31.4 (**C**(10)H_2), 28.6 (**C**(9)H_2), 26.6 (**C**(8)H_2), 22.4 (**C**(11)H_2), 14.0 (**C**(12)H_3) ppm; *m/z* (ES+): 197 ((M+H)$^+$ 70%).

Spectral characteristics were consistent with previously reported data.[96]

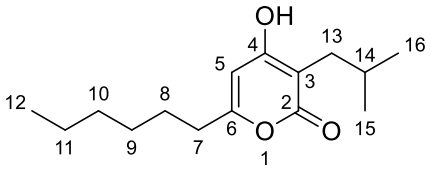
6-Heptyl-4-hydroxy-2*H*-pyran-2-one (30)[97]



Compound **30** was prepared *via* the procedure described for **22** using **1** (0.126 g, 1.0 mmol, 1.0 equiv.) and 1-iodohexane (0.27 mL, 1.8 mmol, 1.8 equiv.) to yield **30** as a yellow-orange solid (0.087 g, 41%); 68–70 °C (lit. 71–71.5 °C); ^{1}H NMR (300 MHz, $CDCl_3$) δ: 10.63 (bs, 1H, O**H**), 6.01 (s, 1H, C(5)**H**), 5.60 (bs, 1H, C(3)**H**), 2.48 (t, *J* = 7.3 Hz, 2H, C(7)**H**$_2$), 1.80–1.50 (m, 2H, C(8)**H**$_2$), 1.43–1.15 (m, 8H, C(9)**H**$_2$, C(10)**H**$_2$, C(11)**H**$_2$, C(12)**H**$_2$), 0.87 (t, *J* = 6.4 Hz, 3H, C(13)**H**$_3$) ppm; ^{13}C NMR (75 MHz, $CDCl_3$) δ: 172.8 (q**C**-2 or q**C**-4), 167.3 (q**C**-6), 166.9 (q**C**-2 or q**C**-4), 101.4 (**C**(5)H), 89.8 (**C**(3)H), 33.6 (**C**(7)H_2), 31.6 (**C**(11)H_2), 28.9 (2 × C, **C**(9)H_2, **C**(10)H_2), 26.7 (**C**(8)H_2), 22.6 **C**(12)H_2), 14.0 (**C**(13)H_3) ppm; m/z (ES+): 211 ((M+H)$^+$ 100%).

Spectral characteristics were consistent with previously reported data.[97]

6-Hexyl-4-hydroxy-3-isobutyl-2*H*-pyran-2-one (31)

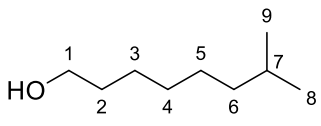


Compound **31** was prepared *via* the procedure described for **22** using **4** (0.091 g, 1.0 mmol, 1.0 equiv.) and 1-iodoheptane (0.12 mL,

0.9 mmol, 1.8 equiv.) to yield **31** as a pale yellow solid (0.071 g, 56%); m.p. 105–108 °C; IR (film) ν_{max} 3078 (broad OH stretch), 1664 (ester C=O stretch), 1573, 1435 (alkene C=C stretch), 1265 (ester C-O stretch), 1124 (alcohol C-O stretch) cm^{-1}; ^{1}H NMR (300 MHz, $CDCl_3$) δ: 10.01 (bs, 1H, O**H**), 6.18 (s, 1H, C(5)**H**), 2.55–2.26 (m, 4H, C(7)$\mathbf{H}_2$, C(13)$\mathbf{H}_2$), 2.10–1.86 (m, 1H, C(14)**H**), 1.73–1.53 (m, 2H, C(8)$\mathbf{H}_2$), 1.44–1.16 (m, 6H, C(9)$\mathbf{H}_2$, C(10)$\mathbf{H}_2$, C(11)$\mathbf{H}_2$), 1.03–0.79 (m, 9H, C(12)$\mathbf{H}_3$, C(15)$\mathbf{H}_3$, C(16)$\mathbf{H}_3$) ppm; ^{13}C NMR (75 MHz, $CDCl_3$) δ: 168.4, 167.5 (q**C**-2, q**C**-4), 163.7 (q**C**-6), 102.4 (q**C**-3), 100.7 (**C**(5)H), 33.5 (**C**(7)H_2), 31.9 (**C**(13)H_2), 31.4 (**C**(10)H_2), 28.7 (**C**(9)H_2), 27.5 (**C**(14)H), 26.7 (**C**(8)H_2), 22.45 (**C**(11)H_2), 22.44 (2 × C, **C**(15)H_3, **C**(16)H_3), 14.0 (**C**(12)H_3) ppm; HRMS (ESI-TOF) *m/z*: $[M+H]^+$ calcd. for $C_{15}H_{25}O_3$: 253.1798; found: 253.1800.

7-Methyloctan-1-ol (34)[86]

Stepwise procedure:[86]



1. Preparation of isopropylmagnesium bromide **33**

A solution of 2-bromopropane (0.73 mL, 7.81 mmol, 1.0 equiv.) in dry THF (1.6 mL) was added dropwise to a solution of magnesium turnings (0.191 g, 7.87 mmol, 1.01 equiv.) under nitrogen. The reaction was initiated by adding a crystal of iodine. The mixture was heated to reflux for 45 min to give a colourless solution of isopropylmagnesium bromide which was used immediately upon cooling.

2. Preparation of the catalyst Li_2CuCl_4

To a flame-dried 15 mL Schlenk flask, were added anhydrous LiCl (2.6 mg, 0.06 mmol, 1.2 mol%) and anhydrous $CuCl_2$ (4.2 mg, 0.03 mmol, 0.6 mol%). Dry THF (0.3 mL) was added to give an orange solution of Li_2CuCl_4 which was immediately consumed.

3. Preparation of 7-methyloctan-1-ol

Sodium 6-bromo-1-hexanoate **32** (1.09 g, 5 mmol, 1.0 equiv.) was suspended in dry THF (7.8 mL) in a flame-dried, 3-neck 100 mL RBF under a flow of nitrogen, and cooled to -10 °C. The Li_2CuCl_4 solution was added to the acid at -10 °C to give a blue-green mixture. The freshly prepared solution of isopropylmagnesium bromide **33** was then added with vigorous stirring, keeping the bath temperature below -5 °C. The resulting white solution was stirred at -10 °C for a further 4 h. The mixture was allowed to

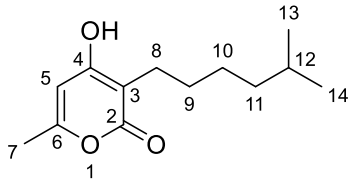
warm to r.t., $LiAlH_4$ (5 mL, 1 M in THF) was added dropwise and the solution was then heated to reflux for 1 h under nitrogen. The hot mixture was poured onto ice and the resulting white precipitate was dissolved by the addition of 30% H_2SO_4. The organic layer was separated, and the aqueous layer was extracted with Et_2O (3 × 10 mL). The combined organic layers were dried over $MgSO_4$, filtered and concentrated under reduced pressure to give compound **34** as a yellow liquid (0.605 g, 84%); ^{1}H NMR (300 MHz, $CDCl_3$) δ: 3.64 (t, *J* = 6.6 Hz, 2H, C(1)**H₂**), 1.92 (bs, 1H, O**H**), 1.63–1.05 (m, 11H, C(2)**H**$_2$, C(3)**H**$_2$, C(4)**H**$_2$, C(5)**H**$_2$, C(6)**H**$_2$, C(7)**H**), 0.86 (d, *J* = 6.6 Hz, 6H, C(8)**H**$_3$, C(9)**H**$_3$) ppm; ^{13}C NMR (75 MHz, $CDCl_3$) δ: 63.1, 38.9, 32.8, 29.7, 27.9, 27.3, 25.8, 22.6 (2 × C) ppm.

Spectral characteristics were consistent with previously reported data.[86]

5-Methylhexanal (37) and 7-methyloctanal (36)

A Schlenk tube was heated under vacuum, cooled to r.t. and refilled with nitrogen three times and NMO.H_2O (1.5 equiv.) was added. Dry DCM (2 mL/mmol), the alcohol (**34** or **35**, 1.0 equiv.) and powdered 4 Å mol. sieves (200 mg/mmol) were added and the suspension stirred at r.t. for 1 h under nitrogen. TPAP (5 mol%) was then added and the resulting mixture stirred for 30 min before being filtered through a short plug of silica and being concentrated under reduced pressure[90] to give crude reaction mixtures of 5-methylhexanal (**37**) and 7-methyloctanal (**36**) which were used directly for the next reaction without further purification.

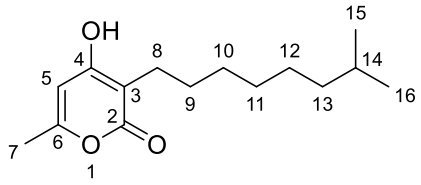
4-Hydroxy-6-methyl-3-(5-methylhexyl)-2*H*-pyran-2-one (38)



Compound **38** was prepared *via* the procedure described for **2** using 5-methylhexanal **37** (0.069 g, 0.6 mmol, 1.2 equiv.) to yield **38** as a white solid (0.050 g, 45%); m.p. 75–77 °C; IR (film) ν_{max} 3086 (broad OH stretch), 1669 (ester C=O stretch), 1574, 1448 (alkene C=C stretch), 1265 (ester C-O stretch), 1129 (alcohol C-O stretch) cm^{-1}; ^{1}H NMR (300 MHz, $CDCl_3$) δ: 10.27 (bs, 1H, O**H**), 6.23 (s, 1H, C(5)**H**), 2.59–2.34 (m, 2H, C(8)**H**$_2$), 2.23 (s, 3H, C(7)**H**$_3$), 1.64–1.05 (m, 7H, C(9)**H**$_2$, C(10)**H**$_2$, C(11)**H**$_2$, C(12)**H**), 0.85 (d, *J* = 6.6 Hz, 6H, C(13)**H**$_3$, C(14)**H**$_3$) ppm; ^{13}C NMR (75 MHz, $CDCl_3$) δ: 168.4, 167.3 (q**C**-2, q**C**-4), 159.8 (q**C**-6), 103.4 (q**C**-3), 101.7 (**C**(5)H), 38.9

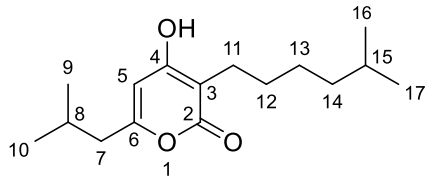
(**C**(11)H_2), 28.3 (**C**(9)H_2), 28.0 (**C**(12)H), 27.4 (**C**(10)H_2), 23.1 (**C**(8)H_2), 22.6 (2 × C, **C**(13)H_3, **C**(14)H_3), 19.6 (**C**(7)H_3) ppm; HRMS (ESI-TOF) *m/z*: $[M+H]^+$ calcd for $C_{13}H_{21}O_3$: 225.1485; found: 225.1483.

4-Hydroxy-6-methyl-3-(7-methyloctyl)-2*H*-pyran-2-one (39)



Compound **39** was prepared *via* the procedure described for **2** using 7-methyloctanal **36** (0.175 g, 1.2 mmol, 1.2 equiv.) to yield **39** as a white solid (0.182 g, 72%); m.p. 93–95 °C; IR (film) ν_{max} 3055 (broad OH stretch), 1669 (ester C=O stretch), 1574, 1448 (alkene C=C stretch), 1247 (ester C-O stretch), 1129 (alcohol C-O stretch) cm^{-1}; ^{1}H NMR (300 MHz, $CDCl_3$) δ: 10.00 (bs, 1H, O**H**), 6.21 (d, *J* = 0.6 Hz, 1H, C(5)**H**), 2.54–2.36 (m, 2H, C(8)**H**$_2$), 2.13 (s, 3H, C(7)**H**$_3$), 1.64–1.04 (m, 11H, C(9)**H**$_2$, C(10)**H**$_2$, C(11)**H**$_2$, C(12)**H**$_2$, C(13)**H**$_2$, C(14)**H**), 0.84 (d, *J* = 6.6 Hz, 6H, C(15)**H**$_3$, C(16)**H**$_3$) ppm; ^{13}C NMR (75 MHz, $CDCl_3$) δ: 168.2, 167.0 (q**C**-2, q**C**-4), 159.8 (q**C**-6), 103.4 (q**C**-3), 101.6 (**C**(5)H), 39.1 (**C**(13)H_2), 29.9 (**C**(11)H_2), 29.7 (**C**(10)H_2), 28.1 (**C**(9)H_2), 27.9 (**C**(14)H), 27.4 (**C**(12)H_2), 23.1 (**C**(8)H_2), 22.6 (2 × C, **C**(15)H_3, **C**(16)H_3), 19.6 (**C**(7)H_3) ppm; HRMS (ESI-TOF) *m/z*: $[M+H]^+$ calcd for $C_{15}H_{25}O_3$: 253.1798; found: 253.1799.

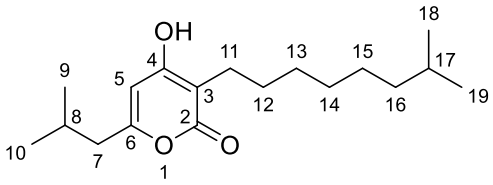
4-Hydroxy-6-isobutyl-3-(5-methylhexyl)-2*H*-pyran-2-one (40, PPYB**)**



Compound **40** was prepared *via* the procedure described for **22** using **38** (0.030 g, 0.134 mmol, 1.0 equiv.) to yield **40** as a white solid (0.015 g, 42%); m.p. 117–120 °C; IR (film) ν_{max} 3051 (broad OH stretch), 1663 (ester C=O stretch), 1570, 1433 (alkene C=C stretch), 1267 (ester C-O stretch), 1130 (alcohol C-O stretch) cm^{-1}; ^{1}H NMR (300 MHz, $CDCl_3$) δ: 9.72 (bs, 1H, O**H**), 6.13 (s, 1H, C(5)**H**), 2.57–2.38 (m, 2H, C(11)**H**$_2$), 2.29 (d, *J* = 7.2 Hz, 2H, C(7)**H**$_2$), 2.15–1.93 (m, 1H, C(8)**H**), 1.61–1.11 (m, 7H, C(12)**H**$_2$, C(13)**H**$_2$, C(14)**H**$_2$, C(15)**H**), 0.98–0.79 (m, 12H, C(9)**H**$_3$, C(10)**H**$_3$, C(16)**H**$_3$, C(17)**H**$_3$) ppm; ^{13}C NMR (75 MHz, $CDCl_3$) δ: 168.1, 166.7 (q**C**-2, q**C**-4), 162.7 (q**C**-6), 103.5 (q**C**-3), 101.7 (**C**(5)H), 42.6 (**C**(7)H_2), 38.9 (**C**(14)H_2), 28.3 (**C**(12)H_2), 28.0 (**C**(15)H), 27.5 (**C**(13)H_2), 26.8 (**C**(8)H), 23.2 (**C**(11)H_2), 22.6 (2 × C,

C(16)H_3, **C**(17)H_3), 22.2 (2 × C, **C**(9)H_3, **C**(10)H_3) ppm; HRMS (ESI-TOF) *m/z*: $[M+H]^+$ calcd for $C_{16}H_{27}O_3$: 267.1955; found: 267.1955.

4-Hydroxy-6-isobutyl-3-(7-methyloctyl)-2*H*-pyran-2-one (41, PPYD**)**



Compound **41** was prepared *via* the procedure described for **22** using **39** (0.101 g, 0.4 mmol, 1.0 equiv.) to yield **41** as a white solid (0.060 g, 51%); m.p. 97–98 °C; IR (film) ν_{max} 3059 (broad OH stretch), 1663 (ester C=O stretch), 1568, 1433 (alkene C=C stretch), 1253 (ester C-O stretch), 1129 (alcohol C-O stretch) cm^{-1}; ^{1}H NMR (300 MHz, $CDCl_3$) δ: 9.72 (bs, 1H, O**H**), 6.13 (s, 1H, C(5)**H**), 2.56–2.37 (m, 2H, C(11)**H**$_2$), 2.30 (d, *J* = 7.2 Hz, 2H, C(7)**H**$_2$), 2.17–1.93 (m, 1H, C(8)**H**), 1.61–1.06 (m, 11H, C(12)**H**$_2$, C(13)**H**$_2$, C(14)**H**$_2$, C(15)**H**$_2$, C(16)**H**$_2$, C(17)**H**), 0.93 (d, *J* = 6.6 Hz, 6H, C(9)**H**$_3$, C(10)**H**$_3$), 0.84 (d, *J* = 6.6 Hz, 6H, C(18)**H**$_3$, C(19)**H**$_3$) ppm; ^{13}C NMR (75 MHz, $CDCl_3$) δ: 168.1, 166.6 (q**C**-2, q**C**-4), 162.7 (q**C**-6), 103.5 (q**C**-3), 101.7 (**C**(5)H), 42.7 (**C**(7)H_2), 39.7 (**C**(16)H_2), 29.9 (**C**(14)H_2), 29.7 (**C**(13)H_2), 28.1 (**C**(12)H_2), 27.9 (**C**(17)H), 27.4 (**C**(15)H_2), 26.8 (**C**(8)H), 23.1 (**C**(11)H_2), 22.6 (2 × C, **C**(18)H_3, **C**(19)H_3), 22.2 (2 × C, **C**(9)H_3, **C**(10)H_3) ppm; HRMS (ESI-TOF) *m/z*: $[M+H]^+$ calcd for $C_{18}H_{31}O_3$: 295.2268; found: 295.2274.

References

1. Cavalieri, L. F. *Chem. Rev.* **1947**, *41*, 525-584.
2. Fairlamb, I. J. S., O'Brien, C. T., Lin, Z., Lam, K. C. *Org. Biomol. Chem.* **2006**, *4*, 1213-1216.
3. Cole, C. J. F., Fuentes, L., Snyder, S. A. *Chem. Sci.* **2020**, *11*, 2175-2180.
4. Mao, B., Fañanás-Mastral, M., Feringa, B. L. *Org. Lett.* **2013**, *15*, 286-289.
5. Lee, J. S. *Mar. Drugs* **2015**, *13*, 1581-1620.
6. McGlacken, G. P., Fairlamb, I. J. S. *Nat. Prod. Rep.* **2005**, *22*, 369-385.
7. Goel, A., Taneja, G., Raghuvanshi, A., Kant, R., Maulik, P. R. *Org. Biomol. Chem.* **2013**, *11*, 5239-5253.
8. Dickinson, J. M. *Nat. Prod. Rep.* **1993**, *10*, 71-98.
9. Pratap, R., Ram, V. J. *Tetrahedron* **2017**, *73*, 2529-2590.
10. Fairlamb, I. J. S., Marrison, L. R., Dickinson, J. M., Lu, F.-J., Schmidt, J. P. *Bioorg. Med. Chem.* **2004**, *12*, 4285-4299.
11. Clercq, E. D. *Med. Res. Rev.* **2002**, *22*, 531-565.
12. Bhat, Z. S., Rather, M. A., Maqbool, M., Lah, H. U. L., Yousuf, S. K., Ahmad, Z. *Biomed. Pharmacother.* **2017**, *91*, 265-277.
13. Takai, N., Kira, N., Ishii, T., Yoshida, T., Nishida, M., Nishida, Y., Nasu, K., Narahara, H. *Asian Pac. J. Cancer Prev.* **2012**, *13*, 399-402.
14. Storck, P., Aubertin, A.-M., Grierson, D. S. *Tetrahedron Lett.* **2005**, *46*, 2919-2922.
15. S. Steyn, P., R. van Heerden, F. *Nat. Prod. Rep.* **1998**, *15*, 397-413.
16. Rutherford, S. T., Bassler, B. L. *Cold Spring Harb. Perspect. Med.* **2012**, *2*, a012427.
17. Bassler, B. L. *Cell* **2002**, *109*, 421-424.
18. Bassler, B. L., Losick, R. *Cell* **2006**, *125*, 237-246.
19. Nealson, K. H., Platt, T., Hastings, J. W. *J. Bacteriol.* **1970**, *104*, 313-322.
20. Papenfort, K., Bassler, B. L. *Nat. Rev. Microbiol.* **2016**, *14*, 576-588.
21. Engebrecht, J., Nealson, K., Silverman, M. *Cell* **1983**, *32*, 773-781.

22. Barnard, A. M. L., Bowden, S. D., Burr, T., Coulthurst, S. J., Monson, R. E., Salmond, G. P. C. *Philos. Trans. R. Soc. Lond., B, Biol. Sci.* **2007**, *362*, 1165-1183.
23. Miller, M. B., Bassler, B. L. *Annu. Rev. Microbiol.* **2001**, *55*, 165-199.
24. de Kievit, T. R., Iglewski, B. H. *Infect. Immun.* **2000**, *68*, 4839-4849.
25. Hall-Stoodley, L., Costerton, J. W., Stoodley, P. *Nat. Rev. Microbiol.* **2004**, *2*, 95-108.
26. Davies, D. *Nat. Rev. Drug Discov.* **2003**, *2*, 114-122.
27. CDC. *Issues in Healthcare Settings: CDC's Seven Healthcare Safety Challenges*, United States Department of Health and Human Services, Atlanta, GA, **2001**.
28. Kearns, D. B. *Nat. Rev. Microbiol.* **2010**, *8*, 634-644.
29. Clatworthy, A. E., Pierson, E., Hung, D. T. *Nat. Chem. Bio.* **2007**, *3*, 541-548.
30. Fleitas Martínez, O., Cardoso, M. H., Ribeiro, S. M., Franco, O. L. *Front. Cell. Infect. Microbiol.* **2019**, *9*, 74.
31. Rasko, D. A., Sperandio, V. *Nat. Rev. Drug Discov.* **2010**, *9*, 117-128.
32. Dickey, S. W., Cheung, G. Y. C., Otto, M. *Nat. Rev. Drug Discov.* **2017**, *16*, 457-471.
33. Tang, K., Zhang, X.-H. *Mar. Drugs* **2014**, *12*, 3245-3282.
34. Ó Muimhneacháin, E., Reen, F. J., O'Gara, F., McGlacken, G. P. *Org. Biomol. Chem.* **2018**, *16*, 169-179.
35. Case, R. J., Labbate, M., Kjelleberg, S. *ISME J.* **2008**, *2*, 345-349.
36. Patankar, A. V., González, J. E. *FEMS Microbiol. Rev.* **2009**, *33*, 739-756.
37. Subramoni, S., Venturi, V. *Microbiology* **2009**, *155*, 1377-1385.
38. Brameyer, S., Heermann, R. *PLoS One* **2015**, *10*, e0124093.
39. Brachmann, A. O., Brameyer, S., Kresovic, D., Hitkova, I., Kopp, Y., Manske, C., Schubert, K., Bode, H. B., Heermann, R. *Nat. Chem. Bio.* **2013**, *9*, 573-578.
40. Greenberg, D. L., Busch, J. D., Keim, P., Wagner, D. M. *Investig. Genet.* **2010**, *1*, 4.
41. Burke, S. A., Wright, J. D., Robinson, M. K., Bronk, B. V., Warren, R. L. *Appl. Environ. Microbiol.* **2004**, *70*, 2786-2790.
42. Magnuson, R., Solomon, J., Grossman, A. D. *Cell* **1994**, *77*, 207-216.

43. Kalamara, M., Spacapan, M., Mandic-Mulec, I., Stanley-Wall, N. R. *Mol. Microbiol.* **2018**, *110*, 863-878.

44. Dogsa, I., Choudhary, K. S., Marsetic, Z., Hudaiberdiev, S., Vera, R., Pongor, S., Mandic-Mulec, I. *PLoS One* **2014**, *9*, e96122.

45. Cai, R., Chen, S., Liu, Z., Tan, C., Huang, X., She, Z. *Nat. Prod. Res.* **2017**, *31*, 124-130.

46. Helaly, S., Schneider, K., Nachtigall, J., Vikineswary, S., Tan, G. Y. A., Zinecker, H., Imhoff, J. F., Süssmuth, R. D., Fiedler, H.-P. *J. Antibiot.* **2009**, *62*, 445-452.

47. Ding, L., Ren, L., Li, S., Song, J., Han, Z., He, S., Xu, S. *Mar. Drugs* **2019**, *17*, 344.

48. El Awady, M., Boulis, A., Attia, A., Shaaban, M. *Egypt. Pharmaceut. J.* **2019**, *18*, 245-253.

49. Lai, D., Wang, A., Cao, Y., Zhou, K., Mao, Z., Dong, X., Tian, J., Xu, D., Dai, J., Peng, Y.*, et al. J. Nat. Prod.* **2016**, *79*, 2022-2031.

50. Govan, J. R., Deretic, V. *Microbiol. Rev.* **1996**, *60*, 539-574.

51. Høiby, N., Ciofu, O., Bjarnsholt, T. *Future Microbiol.* **2010**, *5*, 1663-1674.

52. Tacconelli, E., Carrara, E., Savoldi, A., Harbarth, S., Mendelson, M., Monnet, D. L., Pulcini, C., Kahlmeter, G., Kluytmans, J., Carmeli, Y.*, et al. Lancet Infect. Dis.* **2018**, *18*, 318-327.

53. Lee, J., Zhang, L. *Protein Cell* **2015**, *6*, 26-41.

54. Shanahan, R., Reen, F. J., Cano, R., O'Gara, F., McGlacken, G. P. *Org. Biomol. Chem.* **2017**, *15*, 306-310.

55. Hodgkinson, J., Bowden, S. D., Galloway, W. R. J. D., Spring, D. R., Welch, M. *J. Bacteriol.* **2010**, *192*, 3833-3837.

56. Hodgkinson, J. T., Galloway, W. R. J. D., Saraf, S., Baxendale, I. R., Ley, S. V., Ladlow, M., Welch, M., Spring, D. R. *Org. Biomol. Chem.* **2011**, *9*, 57-61.

57. McGlacken, G. P., McSweeney, C. M., O'Brien, T., Lawrence, S. E., Elcoate, C. J., Reen, F. J., O'Gara, F. *Tetrahedron Lett.* **2010**, *51*, 5919-5921.

58. Lu, C., Maurer, C. K., Kirsch, B., Steinbach, A., Hartmann, R. W. *Angew. Chem. Int. Ed.* **2014**, *53*, 1109-1112.

59. Clinton, A., Rumbaugh, K. P. *Isr. J. Chem.* **2016**, *56*, 265-272.

60. Ng, W.-L., Bassler, B. L. *Annu. Rev. Genet.* **2009**, *43*, 197-222.

61. Shiner, E. K., Rumbaugh, K. P., Williams, S. C. *FEMS Microbiol. Rev.* **2005**, *29*, 935-947.

62. Reen, F. J., Mooij, M. J., Holcombe, L. J., McSweeney, C. M., McGlacken, G. P., Morrissey, J. P., O'Gara, F. *FEMS Microbiol. Ecol.* **2011**, *77*, 413-428.

63. Reen, F. J., Clarke, S. L., Legendre, C., McSweeney, C. M., Eccles, K. S., Lawrence, S. E., O'Gara, F., McGlacken, G. P. *Org. Biomol. Chem.* **2012**, *10*, 8903-8910.

64. Reen, F. J., Phelan, J. P., Woods, D. F., Shanahan, R., Cano, R., Clarke, S., McGlacken, G. P., O'Gara, F. *Front. Microbiol.* **2016**, *7*, 2074.

65. Reen, F. J., Phelan, J. P., Gallagher, L., Woods, D. F., Shanahan, R. M., Cano, R., Ó Muimhneacháin, E., McGlacken, G. P., O'Gara, F. *Antimicrob. Agents Chemother.* **2016**, *60*, 5894-5905.

66. Jung, S., Kim, Y. *Environ. Entomol.* **2006**, *35*, 1584-1589.

67. Benfarhat-Touzri, D., Amira, A. B., Khedher, S. B., Givaudan, A., Jaoua, S., Tounsi, S. *J. Basic Microbiol.* **2014**, *54*, 1160-1165.

68. Blackburn, M. B., Martin, P. A. W., Kuhar, D., Farrar, R. R., Jr., Gundersen-Rindal, D. E. *PLoS One* **2011**, *6*, e18122.

69. Kraus, G. A., Basemann, K., Guney, T. *Tetrahedron Lett.* **2015**, *56*, 3494-3496.

70. Zheng, C., You, S.-L. *Chem. Soc. Rev.* **2012**, *41*, 2498-2518.

71. Mandalapu, D. *Synlett* **2015**, *26*, 707-708.

72. List, B., Lerner, R. A., Barbas, C. F. *J. Am. Chem. Soc.* **2000**, *122*, 2395-2396.

73. Moreno-Mañas, M., Pleixats, R. *Synthesis* **1984**, 430-431.

74. Orsini, F., Pelizzoni, F., Forte, M., Sisti, M., Bombieri, G., Benetollo, F. *J. Heterocycl. Chem.* **1989**, *26*, 837-841.

75. Seebach, D., Boes, M., Naef, R., Schweizer, W. B. *J. Am. Chem. Soc.* **1983**, *105*, 5390-5398.

76. Sharma, S. K., Parikh, P. A., Jasra, R. V. *J. Mol. Catal. A Chem.* **2007**, *278*, 135-144.

77. Gruttadauria, M., Giacalone, F., Marculescu, A. M., Salvo, A. M. P., Noto, R. *Arkivoc* **2009**, 5-15.

78. Reich, H. J. *J. Org. Chem.* **2012**, *77*, 5471-5491.

79. Zhang, X., McLaughlin, M., Muñoz, R. L. P., Hsung, R. P., Wang, J., Swidorski, J. *Synthesis* **2007**, 749-753.

80. Kearns, D. B., Losick, R. *Mol. Microbiol.* **2003**, *49*, 581-590.

81. Arnaouteli, S., Bamford, N. C., Stanley-Wall, N. R., Kovács, Á. T. *Nat. Rev. Microbiol.* **2021**, *19*, 600-614.

82. Bindel Connelly, M., Young, G. M., Sloma, A. *J. Bacteriol.* **2004**, *186*, 4159-4167.

83. Hibbing, M. E., Fuqua, C., Parsek, M. R., Peterson, S. B. *Nat. Rev. Microbiol.* **2010**, *8*, 15-25.

84. Reen, F. J., Shanahan, R., Cano, R., O'Gara, F., McGlacken, G. P. *Org. Biomol. Chem.* **2015**, *13*, 5537-5541.

85. Hickey, A., Pardo, L. M., Reen, F. J., McGlacken, G. P. *ACS Omega* **2021**, *6*, 33141-33148.

86. Klimentová, J., Kosák, P., Vávrová, K., Holas, T., Hrabálek, A. *Bioorg. Med. Chem.* **2006**, *14*, 7681-7687.

87. Yuasa, Y., Tsuruta, H. *Flavour Fragr. J.* **2004**, *19*, 199-204.

88. Tojo, G., Fernández, M. in *Oxidation of Alcohols to Aldehydes and Ketones: A Guide to Current Common Practice*, Springer US, Boston, MA, **2006**, pp. 1-179.

89. Griffith, W. P., Ley, S. V., Whitcombe, G. P., White, A. D. *J. Chem. Soc., Chem. Comm.* **1987**, 1625-1627.

90. Moore, P. W., Read, C. D. G., Bernhardt, P. V., Williams, C. M. *Chem. Eur. J.* **2018**, *24*, 4556-4561.

91. Zerk, T. J., Moore, P. W., Harbort, J. S., Chow, S., Byrne, L., Koutsantonis, G. A., Harmer, J. R., Martínez, M., Williams, C. M., Bernhardt, P. V. *Chem. Sci.* **2017**, *8*, 8435-8442.

92. Tashiro, Y., Ichikawa, S., Nakajima-Kambe, T., Uchiyama, H., Nomura, N. *Microbes Environ.* **2010**, *25*, 120-125.

93. Moreno-Manas, M., Ribas, J., Virgili, A. *J. Org. Chem.* **1988**, *53*, 5328-5335.

94. Tempone, A. G., Ferreira, D. D., Lima, M. L., Costa Silva, T. A., Borborema, S. E. T., Reimão, J. Q., Galuppo, M. K., Guerra, J. M., Russell, A. J., Wynne, G. M., *et al. Eur. J. Med. Chem.* **2017**, *139*, 947-960.

95. Pardo, L. M., Prendergast, A. M., Nolan, M.-T., Ó Muimhneacháin, E., McGlacken, G. P. *Eur. J. Org. Chem.* **2015**, 3540-3550.

96. Katritzky, A. R., Wang, Z., Wang, M., Hall, C. D., Suzuki, K. *J. Org. Chem.* **2005**, *70*, 4854-4856.

97. Giddens, A. C., Nielsen, L., Boshoff, H. I., Tasdemir, D., Perozzo, R., Kaiser, M., Wang, F., Sacchettini, J. C., Copp, B. R. *Tetrahedron* **2008**, *64*, 1242-1249.

Chapter 2 Direct Arylation and Reversible Oxidative Addition of Bromophenoxyquinolines

There's no limit to how complicated things can get, on account of one thing always leading to another.

E.B White

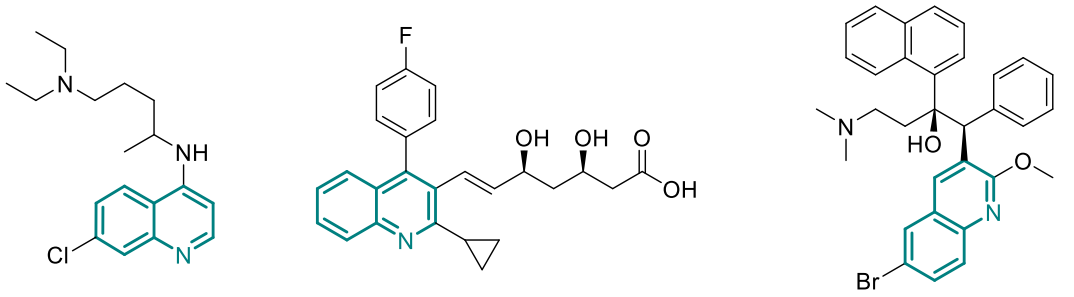
Tarraingíonn scéal scéal eile.
(*One story leads to another.*)

Seanfhocal (Irish Proverb)

Introduction

2.1. Quinolines

The quinoline nucleus is a versatile, nitrogen-based heterocycle which is found in numerous synthetic and naturally occurring pharmacologically active compounds (**Figure 2.1**).[1] It is ranked 22nd in the top 100 most frequently used ring systems in FDA approved drugs,[2] incorporating an assortment of biological activities, *inter alia*, anti-bacterial, anti-malarial and anti-fungal effects.[3-5] Most recently, several quinoline-based drugs were reported to have *in vitro* activity against SARS-CoV-2 (COVID-19).[6] These promising results however, were more likely related to the species' general anti-viral attributes, rather than specifically targeting the virus.[7-8] The quinoline backbone has been extensively derivatised through various methodologies, and displays reactivity similar to that of pyridine analogues.[9]



Chloroquine
anti-malarial

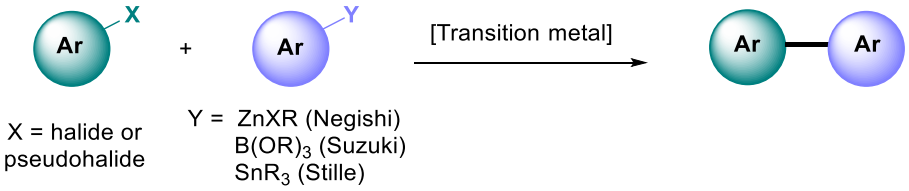
Pitavastatin
cholesterol-lowering

Bedaquiline
treatment of terberculosis

Figure 2.1 Quinoline-containing drugs – Chloroquine, Pitavastatin and Bedaquiline, with the quinoline nucleus highlighted in blue.

2.2. Aryl-Aryl Bond Formation

The biaryl motif is a pivotal substructure of many medicinally important compounds, thus making it a critical synthetic target.[10] There are a multitude of synthetic routes through which this coveted carbon-carbon bond can be formed,[11] e.g. the Negishi,[12] Mizoroki-Heck,[13-14] Suzuki-Miyaura[15] and Stille[16] coupling reactions. These transformations require the coupling of two 'pre-activated' aryl partners, typically an aryl halide with an organometallic reagent (**Scheme 2.1**).

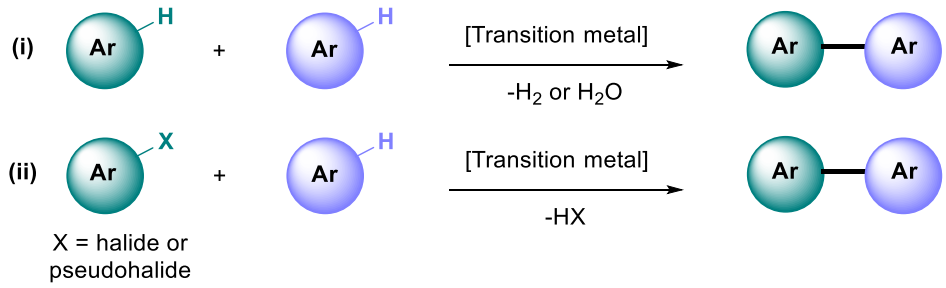


Scheme 2.1 Traditional cross-coupling reactions for the formation of aryl-aryl bonds.

Although practicable and effective, these reactions also come with some pervasive drawbacks. The necessity to pre-functionalise both coupling partners results in stoichiometric waste output of organometallic reagents (e.g. Sn for the Stille reaction), poor atom economy and an increase in general cost. In recent years, there have been significant advances toward more cost-effective and environmentally friendly methods of forming this moiety; through protocols that involve at least one C-H activation event, known as direct arylation. The main idea is to eliminate recourse to pre-activation of one or both coupling partners, thus increasing reaction efficacy and reducing waste output.[17-18] The ability to generate carbon-carbon bonds in this manner is an important synthetic tool, making it a key research area in 'green chemistry' for pharmaceutical manufacturers.[19]

The ideal scenario is where neither partner is pre-activated (**Scheme 2.2 (i)**), known as double C-H activation or dehydrogenative coupling, where the only by-products are hydrogen gas or water. However, this too comes with a set of obstacles; the most problematic being the large number of C-H sites available for activation on any given organic molecule, and the necessity for the systems to include a stoichiometric oxidant. Additionally, the reaction is thermodynamically disfavoured due to the strength of C-H bonds.[20-21] A common strategy used to influence this type of reaction is through the installation of a directing group or by exploitation of an intramolecular directing effect to maximise regioselectivity, although intermolecular dehydrogenative coupling has also been reported.[22-24] A 'chemical compromise' is often reached whereby one of the coupling partners is pre-activated, known as single C-H activation/functionalisation (**Scheme 2.2 (ii)**) – these terms are interchanged throughout the literature.[17] Single C-H activation transformations typically employ a transition metal catalyst to couple an activated species with a specific site on another aryl ring. Regioselectivity can be controlled by use of specific ligand/catalyst systems,

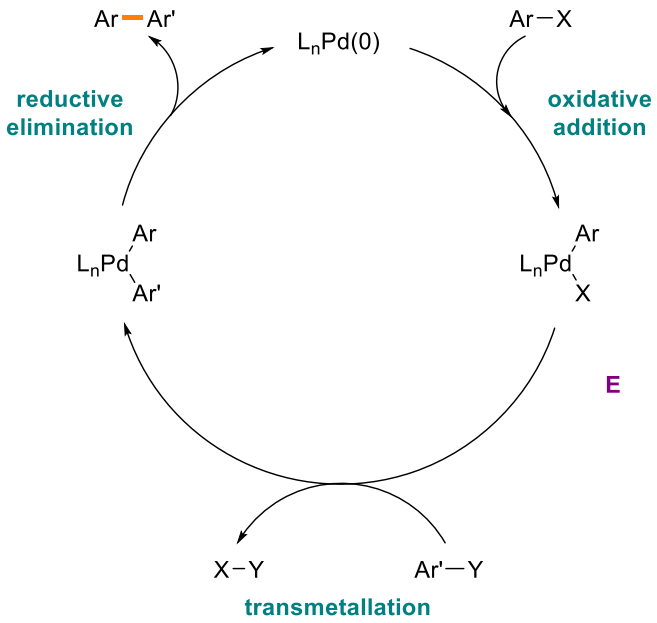
or the manipulation of steric effects and latent electronics inherent to the particular (hetero)aryl species.[25]



Scheme 2.2 Carbon-carbon bond formation *via* C-H activation.

Albeit an improvement in terms of cost, number of steps and atom economy, direct arylation methodologies are not widely used in late-stage functionalisation for a number of reasons. The conditions required are often harsh; employing strong oxidants, reductants, various additives and ligands, elevated temperatures and high loadings of transition metal catalysts.[18,21] This typically leads to low functional group tolerance and the specificity of the systems means they lack applicability to a broader scope of substrates. Efforts are being made to use 'milder' reaction conditions and make direct arylation a truly powerful synthetic tool,[18] with mildness being defined by Glorious and co-workers as a reaction that proceeds 'at or below ambient temperature, under neutral conditions and in the absence of strong oxidants and reductants'.[26]

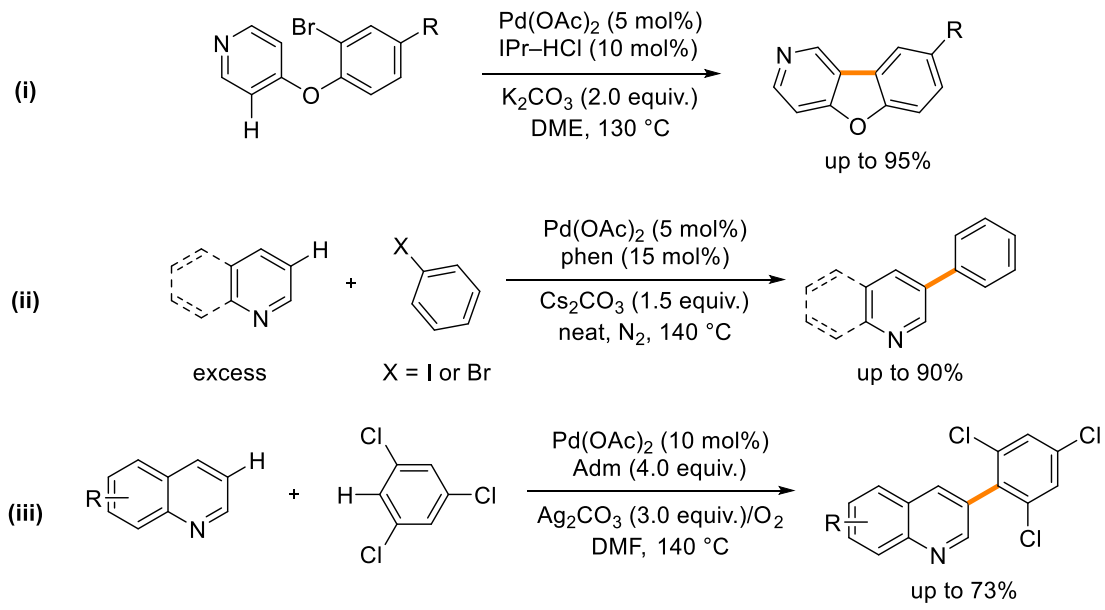
The mechanisms *via* which carbon-carbon bonds are formed follow the same general steps, whether considering the traditional cross-coupling or more modern direct arylation procedures (**Scheme 2.3**). The initial step involves the oxidative addition (OA) of a Pd(0) species to the C-X bond (X = halogen or H) of one coupling partner, giving a Pd(II) intermediate. The next step, transmetallation, installs the second aryl group on the metal centre. This species then undergoes reductive elimination (RE) to liberate the newly formed biaryl and regenerate the active Pd(0) catalyst.



Scheme 2.3 Generic catalytic cycle for palladium-catalysed cross-coupling reactions. L = ligand and X/Y = halogen, organometallic group or H.

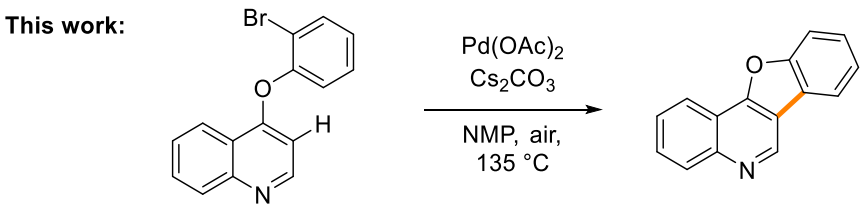
2.3. Direct Arylation of Nitrogen-Based Heterocycles

Within the field of direct arylation several methodologies have been developed and optimised for C-H activation reactions involving heteroaryls.[27-29] This thesis will focus on those which are palladium-catalysed and encompass nitrogen-based heterocycles, selective examples of which are described below.[30-33] Ha and co-workers[30] described the facile synthesis of benzofuro[3,2-*c*]pyridines through an intramolecular, palladium-catalysed direct arylation reaction in moderate to excellent yields (**Scheme 2.4 (i)**). An interesting report by Yu and co-workers[33] detailed the palladium-catalysed, intermolecular, C-3 selective arylation of pyridines and quinolines (**Scheme 2.4 (ii)**). This was the first report wherein access to the C-3 position was not promoted by a directing group or aided by the protection of the pyridine/quinoline substrates.[34-35] Following on from this, He *et al.*[31] developed conditions for the intermolecular dehydrogenative coupling of quinolines at C-3 with electron deficient arenes (**Scheme 2.4 (iii)**).



Scheme 2.4 Palladium catalysed C-H activation of pyridines and quinolines.

Although these examples represent significant breakthroughs in the direct arylation of nitrogen heterocycles, the methods are not directly transferable to other systems and the reaction conditions are considerably harsh. Each of the above protocols employs additional ligands, high temperatures and reaction times of up to 48 hours – strategies which permeate the literature for heteroaryl cross-couplings.[22] The work in Chapter 2 describes a palladium-catalysed, intramolecular direct arylation of 4-(2-bromophenoxy)quinolines (**Scheme 2.5**).[36] Arylation occurs at the C-3 position of the quinoline ring, is carried out in air and requires no added ligand.



Scheme 2.5 Intramolecular direct arylation of 4-(2-bromophenoxy)quinolines to construct benzofuro[3,2-*c*]quinolines.

2.4. ^{1}H-^{15}N HMBC NMR Spectroscopy

Considering that nitrogen heterocycles possess the propensity to act as ligands for palladium,[31,37-40] we suspected that our methodology was underpinned by palladium-quinoline (Pd-Q) coordination. This theory was investigated using ^{1}H-^{15}N

heteronuclear multiple bond correlation (HMBC) NMR spectroscopy. This technique was first developed and implemented in 1993[41] and has since been used to elucidate the coordinative structures of nitrogen-containing compounds with various metals.[42-44]

Despite the difficulties in observing the ^{15}N nucleus due to low natural abundance and gyromagnetic ratio, it is still preferred to the more abundant, quadrupolar ^{14}N nucleus, as it can produce more well-defined signals (**Table 2.1**). Indeed, enrichment of a sample with the ^{15}N-labelled substrate would expedite direct detection, but such compounds are very expensive to buy.[45] ^{1}H-^{15}N HMBC is a powerful technique which exploits the favourable properties of ^{1}H nuclei (**Table 2.1**) to indirectly detect the resonance of the ^{15}N nucleus.[46] Specific gradient-enhanced pulse sequences allow for suppression of t_1 noise from ^{1}H-^{14}N correlations as well as residual solvent signals. This acutely increases sensitivity and facilitates indirect detection *via* relatively weak long-range ^{1}H-^{15}N correlations.[47]

Table 2.1 Properties of ^{1}H, ^{14}N and ^{15}N which are relevant for NMR spectroscopy.[46]

nucleus	natural abundance (%)	spin number (I)	gyromagnetic ratio ($\gamma/10^7$, rad T^{-1} s^{-1})
^{1}H	99.99	½	26.75
^{14}N	99.64	1	1.93
^{15}N	0.37	½	-2.71

2.5. One-Pot Reactions

Protocols which integrate multiple chemical transformations in a single reaction vessel without isolation of intermediate species are considered 'the ultimate' in green catalytic methodologies.[48] These are often referred to as 'one-pot' processes, a term coined from the German word "Eintopf", which describes cooking an entire meal in a single pot.[49] Step-economic approaches can substantially reduce the number of reagents and amount of solvent required for the assembly of organic molecules, thus decreasing waste output, saving time and reducing costs. However, telescoping two or more processes in a single pot is by no means trivial, and

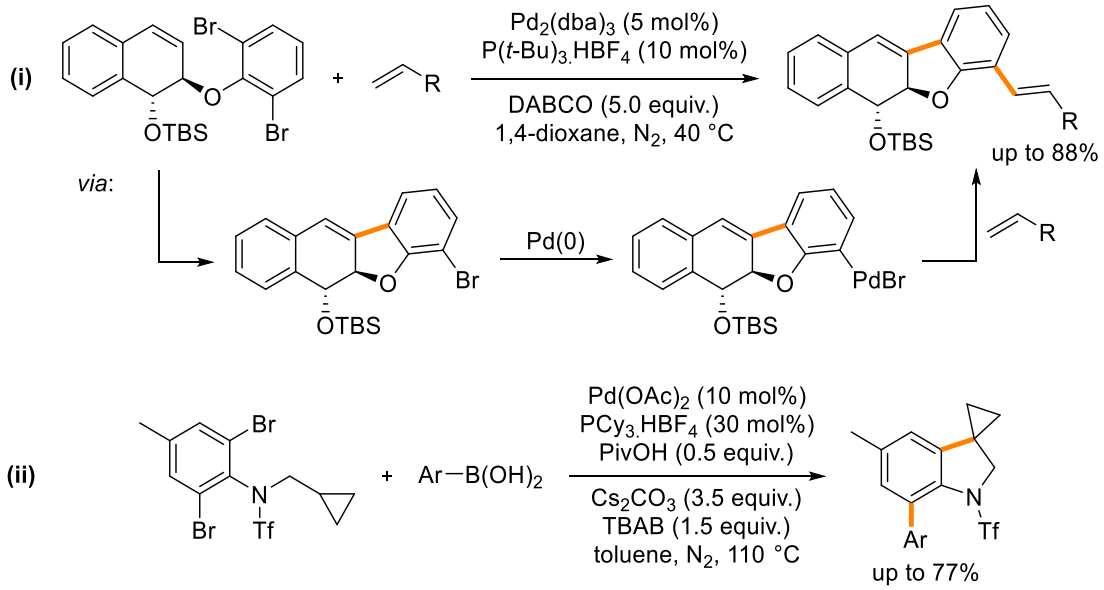
generates considerable challenges in terms of catalyst, reagent and solvent compatibilities.[50-51] One-pot systems are ubiquitous in the reported syntheses of natural products and pharmaceuticals and are often biomimetic in design.[52-53] While there is an extensive list of processes that have been telescoped to take place in the same vessel, this introduction will focus on the combination of a palladium-catalysed Suzuki-Miyaura or Mizoroki-Heck cross-coupling, with a direct arylation reaction, in one-pot. Given there are multiple terminologies applied to this type of transformation, the term 'tandem reaction' is most suitable for the protocols depicted here. It describes the sequential occurrence of one transformation directly after another.[51]

2.6. Substrates with Multiple Halogens

The reaction of the mono-brominated quinoline described above proceeded as anticipated, exclusively yielding one cyclised product (**Scheme 2.5**). Conversely, cross-coupling reactions involving substrates bearing more than one halogen are far less predictable in terms of chemo- and regioselectivity.[50,54-55] Selective C-H functionalisation in these cases is often promoted by utilising two different halogens.[56] The protocols exploit the attenuated reactivities of aromatic C-X bonds to control the initial OA step, given that the bond dissociation energies are consistent with the strength of the bonds, in the order of Ar-I < Ar-Br < Ar-Cl << Ar-F.[57]

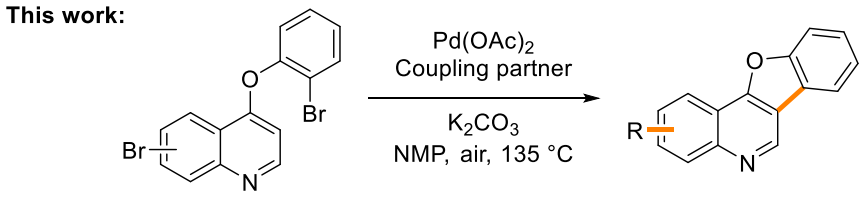
Using multiple halogens of the same type is significantly more challenging; differences in rate are considerably smaller and are not as easily harnessed. There are two main issues that can arise, depending on the electronic and steric properties of the substrate. If the reactivities of the C-X bonds are too similar, then both positions are equally likely to react and regioselectivity will not be achieved. On the other hand, if one site is considerably more labile, then the catalyst will primarily undergo OA into this position. However, if this site is not productive, it will inhibit the progression of any potential catalytic cycle at the other site. One way to overcome this issue is to introduce an intermolecular coupling partner and facilitate a one-pot, domino or tandem reaction. This strategy converts the non-productive OA species into a pivotal cross-coupling intermediate. The active catalyst is then regenerated and can facilitate a reaction at the second, inherently less reactive, C-X bond. Tandem

processes are often invoked after attempts to react di-halogenated compounds fail to go to completion. Selected examples from the Lautens and Cramer groups are shown below (**Scheme 2.6 (i)** and **(ii)** respectively).[58-59] Attempts to perform just the cyclisation reaction in both cases was hindered by the presence of a second halogen *via* product inhibition (**Scheme 2.6 (i)**). As outlined above, performing multiple reactions in a single pot is an appealing and efficient approach in the composition of complex molecular entities.



Scheme 2.6 One-pot reactions of di-halogenated compounds.

Similar to the above examples, attempts to cyclise di-brominated phenoxyquinoline substrates using the conditions described previously were unsuccessful. It was envisaged that OA into the C-Br bond on the quinoline ring was favoured over that on the phenoxy ring, constituting a catalytic dead-end. In an effort to liberate the palladium, phenylboronic acid was introduced into the reaction mixture, resulting (after optimisation) in a one-pot tandem Suzuki-Miyaura/direct arylation (SM/DA) reaction.[60] The work described herein focuses on the one-pot tandem Mizoroki-Heck/direct arylation (MH/DA) process for the same substrates.



Scheme 2.7 One-pot tandem SM/DA and MH/DA reactions.

There are several reported systems that combine a Suzuki-Miyaura or Mizoroki-Heck cross-coupling event with a direct arylation reaction.[61-65] However, we are aware of very few procedures where the one-pot process remains undisturbed i.e. by the subsequent addition of secondary reactants or catalysts.[66-70] Additionally, these protocols all employ phosphine ligands and an inert atmosphere, neither of which are required in our one-pot synthesis, making it a simple, attractive and cost-effective strategy. Novel, π-extended quinolines, with potentially useful photophysical features, were prepared through the one-pot MH/DA reaction.

2.7. Ultraviolet-Visible Absorption Spectroscopy

Radiation with a wavelength in the range of 100–800 nm falls in the category of ultraviolet-visible (UV-vis) spectroscopy, these transitions account for the existence of colours and our ability to see.[71] This range is a combination of three categories – the visible (400–800 nm), near UV (200–400 nm) and far or vacuum UV (<200 nm) regions.[72] Upon irradiation, the energy of a molecule will increase by an amount proportional to the energy of the absorbed photon. The energy of a photon is quantified using **Equation 2.1**, where *h* is Planck's constant, *c* is the pathlength travelled and λ is wavelength. Light absorption occurs at a rate of about 10^{-15} s, a time too short to allow comparable nuclear motion. It is therefore assumed that nuclei are in a fixed position before and after the transition, as outlined by the Franck-Condon principle.[73]

$$E = \frac{hc}{\lambda} \qquad \textbf{Equation 2.1}$$

Principles which dictate the probability of a transition occurring include the multiplicity of state (**Equation 2.2**) and orbital selection rules (**Equation 2.3**), where S is the total spin quantum number and L is the total orbital angular momentum.

These rules also predict the intensity of the 'allowed' transitions. Hence, promotions are allowed between orbitals of different symmetries when there is no change in electron spin, although weak spin- and orbit- 'forbidden' transitions can still occur.

$$\Delta \mathbf{S} = \mathbf{0} \qquad \textbf{Equation 2.2}$$

$$\Delta \mathbf{L} = \mathbf{0}, \pm \mathbf{1} \qquad \textbf{Equation 2.3}$$

According to the Beer-Lambert Law (**Equation 2.4**), the absorbance, *A*, of a solution is directly proportional to concentration, *c*, of the absorbing molecule, where ε is the molar extinction coefficient and l is the pathlength travelled by the light. Absorbance can be directly measured, based on the intensity of light that is transmitted through a sample compared to that transmitted through solvent alone. This allows for the calculation of ε, a measure of the efficacy of absorption.[74]

$$\boldsymbol{A = \varepsilon c l} \qquad \textbf{Equation 2.4}$$

For organic compounds, most observed absorptions are derived from π to π^*, n to σ^* and n to π^* transitions, where an electron is promoted from a (non-)bonding to an anti-bonding orbital. These transitions are all spin- and orbit-allowed and will therefore exhibit extinction coefficients in the range 10^3–10^6 ($dm^3\ mol^{-1}\ cm^{-1}$), with intensity for forbidden transitions displayed as low as 10^{-5}.

The electronically excitable part of the molecule is called the chromophore and it generally contains at least one degree of unsaturation i.e. a double bond. Longer chromophores yield higher intensity absorptions and greater ε values – increasing conjugation in a molecule decreases the gap between energy levels and lowers the energy required to promote an electron. There are two predominant strategies through which this extension can be achieved; the inclusion of further unsaturated bonds, and the addition of auxochromes. Auxochromes are groups which do not absorb UV-vis radiation themselves but can alter the intensity and/or position of absorption maxima when attached to a chromophore. Some examples include halogens, hydroxyl and amino groups, where conjugation is extended *via* resonance delocalisation of lone pairs.[74] Specific terminology is utilised for describing the changes generated by these substituents, as summarised below (**Figure 2.2**).

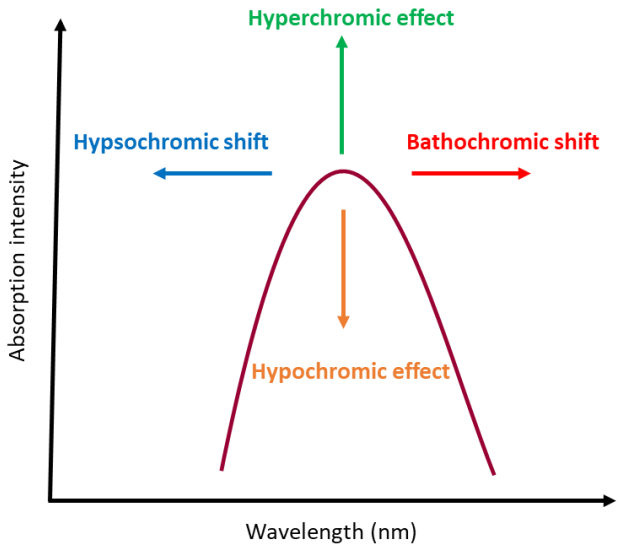


Figure 2.2 Substituent effects on position and intensity of absorption spectra.

2.8. Fluorescence Spectroscopy

Luminescence is the term used to describe all forms of light emission that are not exclusively conditioned by a rise in temperature (incandescence). It is divided into two categories based on the conformation of the excited state – fluorescence and phosphorescence. In excited singlet states, the electron in the higher energy orbital possesses a spin opposite to that of its paired electron in the ground state. The repopulation of the ground state is spin-allowed and so occurs rapidly (10^{-8} s) through the emission of a photon – this is known as fluorescence. The processes which occur between absorption and emission are summarised in a Jablonski diagram and are defined as either radiative or non-radiative (**Figure 2.3**).[73]

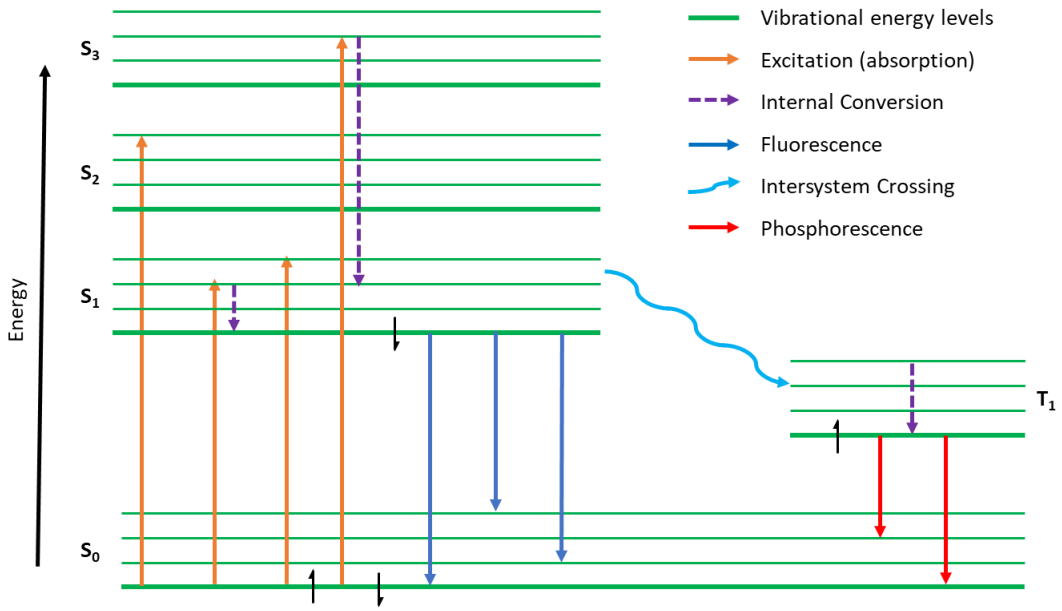


Figure 2.3 Jablonksi diagram with rotational levels omitted for clarity.

Small, conjugated organic molecules with the ability to emit fluorescent light can be exploited for a variety of applications. Natural or intrinsic fluorophores have been used for hundreds of years. Wood from a native Mexican tree, *Lignum nephriticum*, was an expensive medicinal commodity in 16th century Europe, used particularly for its diuretic properties. It was noted that infusions of the wood gave an unusual blue colour, a trait which was consequently utilised to determine the authenticity of samples.[75] This is the first known practical application of fluorescence and it wasn't until the 21st century that the structure of the fluorophore responsible was elucidated (**Figure 2.4**).[76]

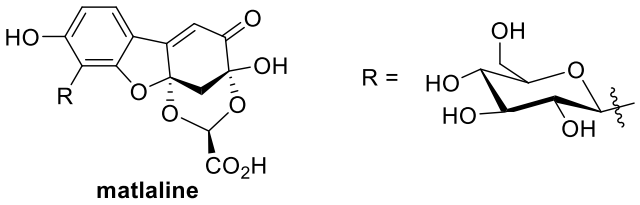


Figure 2.4 Active fluorophore, matlaline in *L. nephriticum.*

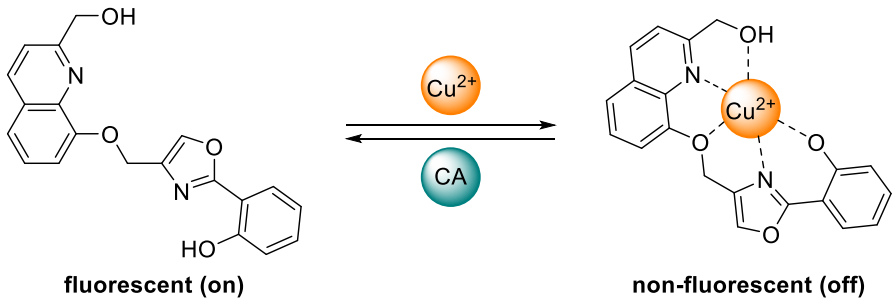
Over time, an intricate understanding of the complex structural requirements for fluorescence emission has been procured. Manipulation of this knowledge has resulted in a vast number of synthetic or extrinsic fluorophores being developed for myriad functions.[77] Some examples include their use in selective probes for ion

detection (chemosensors),[78] optoelectronic devices[79] and as dyes or tags in bioimaging.[80]

2.9. Fluorescent Quinolines

In recent years, the necessity for quantitative detection of various metal ions in environmental, medicinal and biological settings has been recognised. Fluorescence-based chemosensors are often developed for this purpose as they are typically highly sensitive, inexpensive to make/operate and provide real-time analysis.[81] Upon coordination of the analyte to the fluorescent probe, there are two different modes of detection that follow – either the frequency of emission is characteristically shifted, or the chelation acts as an 'on/off' switch for fluorescence.[82]

A number of quinoline-based ligands have been incorporated in fluorescent chemosensors.[83-84] For example, Pang and co-workers[85] developed a novel probe for the sequential detection of copper(II) and citrate ions in drinking water (**Scheme 2.8**). The molecules synthesised have multiple donor and acceptor sites which afford selective chelation sites. In the presence of excess Cu(II), emission intensity was comprehensively reduced and essentially turned off. Conversely, when excess citrate anion (CA) was added to a solution of the copper-ligand complex, emission was significantly enhanced or turned back on.

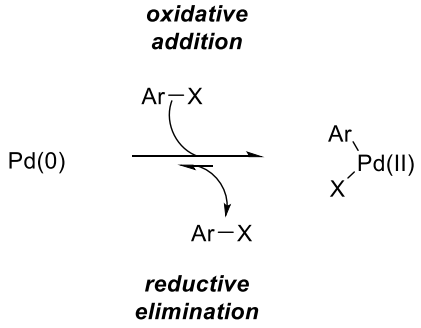


Scheme 2.8 Quinoline-based ligand as a selective fluorescent on/off switch for the detection of Cu(II) and citrate ions.

The photophysical characteristics of the π-extended quinolines constructed *via* the MH/DA pathway will be analysed herein.

2.10. Potential for Reversible Oxidative Addition

Palladium-catalysed cross-coupling reactions are ubiquitous transformations in the construction of novel entities. Although there are some variations, the systems are all considered to proceed *via* a generic Pd(0)/Pd(II) catalytic cycle (**Scheme 2.3**). The routes through which these systems progress have undergone extensive analyses and the intricate details for each elementary step have been accrued.[86-87] The oxidative addition (OA) step in many cases is postulated to be the rate-determining step (RDS) and was formerly treated as irreversible. OA spontaneously breaks the C-X bond and forms two new bonds to the metal centre (now oxidised to Pd(II)) and reformation of the C-X bond *via* reductive elimination (RE) is negligible. The reverse reaction is a highly endergonic process and is thus thermodynamically disfavoured (**Scheme 2.9**).



Scheme 2.9 Oxidative addition as an irreversible step. X = halogen, organometallic group or H.

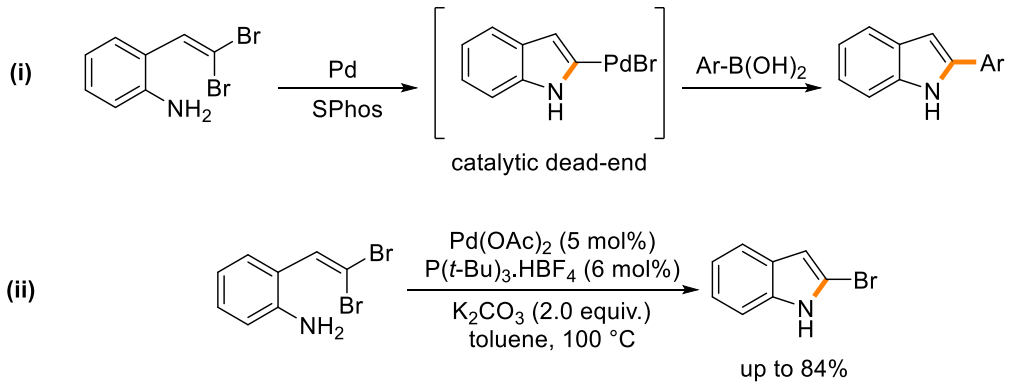
Seminal work by Hartwig and Roy demonstrated that large, bulky phosphine ligands could in fact promote RE and reform the aryl halide species. A series of mechanistic experiments were carried out on dimeric palladium-complexes, using an excess of sterically encumbered ligands to invoke a shift in equilibrium and form the free aryl halide species.[88-90] Two of the best-performing ligands were tri-*tert*-butylphosphine (P(*t*-Bu)$_3$) and 1,2,3,4,5-pentaphenyl-1'-(di-*tert*-butylphosphino)ferrocene (QPhos), both of which are electron-dense and possess considerable steric bulk. It is well documented that OA for electron-donating ligands is faster and more favourable than for those that are electron poor.[91] Therefore, it was concluded that the steric

congestion induced by these ligands was responsible for reversing the thermodynamics of the system, irrespective of their electronic capacities.[90]

2.11. Reversible Oxidative Addition in Synthesis

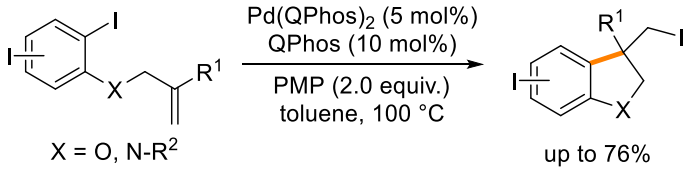
Using multi-halogenated substrates in cross-coupling reactions can cause chemo- and regioselectivity issues (*vide supra*), particularly if the palladium-catalyst is sequestered in a non-productive OA product. Turnover is often regenerated by the introduction of a suitable coupling partner, and although this is a practical strategy, it does not allow for the synthesis of halogenated species. However, a catalyst-ligand system capable of expediting both OA into and RE from a C-X bond, could accomplish site-selective cross-coupling reactions and in turn furnish halogen-containing molecules.

A salient extension of Hartwig's work was published by Lautens and Newman; detailing the palladium-catalysed cyclisation of *gem*-dibromoolefins using P(*t*-Bu)$_3$ as a key ligand, to furnish 2-bromoindoles in very good yields (**Scheme 2.10 (ii)**).[54] In their original report, a tandem synthesis had been employed to isolate highly functionalised indoles from what was a catalytic dead-end (**Scheme 2.10 (i)**).[92] By increasing the size of the ligand and enhancing steric crowding at the OA site, they were able to promote RE and thus isolate a halogen-containing scaffold. This site-selective cross-coupling was the first approach to harness reversible oxidative addition (ROA) for synthetic purposes.



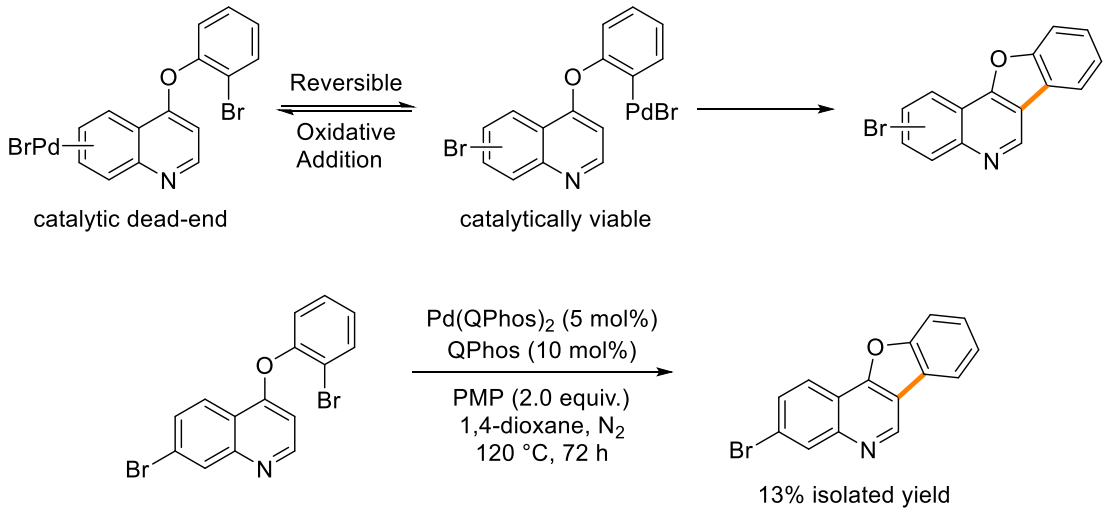
Scheme 2.10 Use of ROA in the production of halogenated indole products.

Several more examples followed on from this work, expanding the scope of bulky ligands which can facilitate ROA.[93-97] One such example extended the scope to include di-iodinated substrates, employing a combination of $Pd(QPhos)_2$ with added QPhos ligand. This strategy facilitates cyclisation, carboiodination and the isolation of a di-iodinated product. The iodide distal to the cyclisation site remains intact throughout the process (**Scheme 2.11**).[98]



Scheme 2.11 Example of sequential intramolecular carboiodination/MH reaction.

As we had encountered site-selectivity issues using multiple halogens in our direct arylation protocol, we envisaged the introduction of sterically encumbered ligands could induce ROA to give a cyclised, brominated benzofuroquinoline product.[60] Investigations carried out by another member of the group found the combination of QPhos and $Pd(QPhos)_2$ gave the desired brominated product, albeit with relatively low conversion by ^1H NMR analysis after 72 hours (**Scheme 2.12**).[60]



Scheme 2.12 Harnessing bulky ligands to isolate a brominated benzofuroquinoline product.

The aim of this chapter is to engender higher conversion to the cyclised benzofuroquinoline product, broaden the scope of the reaction and prove that ROA was actually responsible for the production of the brominated product in our case.

Results and Discussion

2.12. Objectives

Protocols that obviate the pre-functionalisation of one or both coupling partners in cross-coupling reactions are highly desirable. As described in the introduction, there are very few literature examples which directly target the C-3 position of quinoline or pyridine for arylation.[33] This section describes the palladium-catalysed direct arylation of 4-(2-bromophenoxy)quinolines at the C-3 position, and an extension of this methodology to a one-pot, tandem Mizoroki-Heck/direct arylation strategy. The reactions require no added ligand and are carried out in air, constructing diverse benzofuro[3,2-*c*]quinolines in excellent yields. Potential interaction between the substrate and catalyst are explored using ^{1}H-^{15}N HMBC NMR spectroscopy and the photophysical characteristics of the novel, π-extended entities are examined. The syntheses in this chapter were optimised by and carried out in conjunction with another member of the McGlacken group.[60]

Palladium-catalysed cross-coupling reactions have provided access to a vast assortment of products with exceptional functional group tolerance. Difficulties can however arise upon the addition of multiple halogens to the system. Palladium can add into a non-productive carbon-halogen bond and recent developments have induced reversibility of the oxidative addition step by the introduction of sterically encumbered phosphine ligands, allowing for the isolation of halogen-bearing products (*vide supra*). This section describes further investigation into the reversible oxidative addition reaction as well as optimisation towards the synthesis of brominated benzofuroquinoline products.

Note: Copies of the relevant ^{1}H, ^{13}C, and ^{1}H-^{15}N HMBC NMR spectra and HRMS data for metal-containing complexes, all details for X-ray crystallography studies, fluorescence emission and UV-Vis absorption data are included in **Appendix I**.

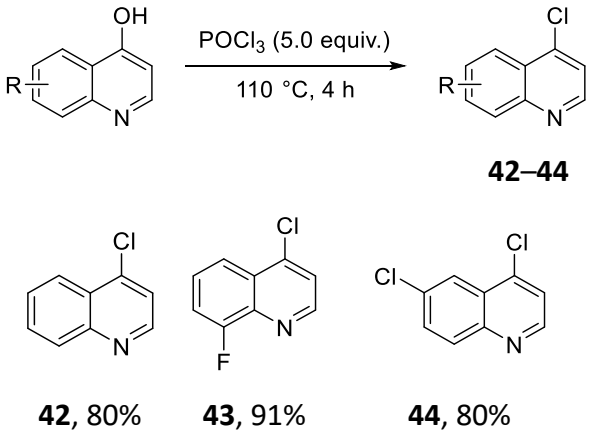
The term ‘yield by NMR’ is used throughout this section and is calculated from the ^{1}H NMR spectrum of a crude reaction mixture with 1,3,5-trimethoxybenzene as the internal standard for quantification.

2.13. Intramolecular Direct Arylation

To begin, a substrate scope for the palladium-catalysed, intramolecular direct arylation of 4-(2-bromophenoxy)quinolines was demonstrated.[36]

2.13.1 Preparation of Starting Materials

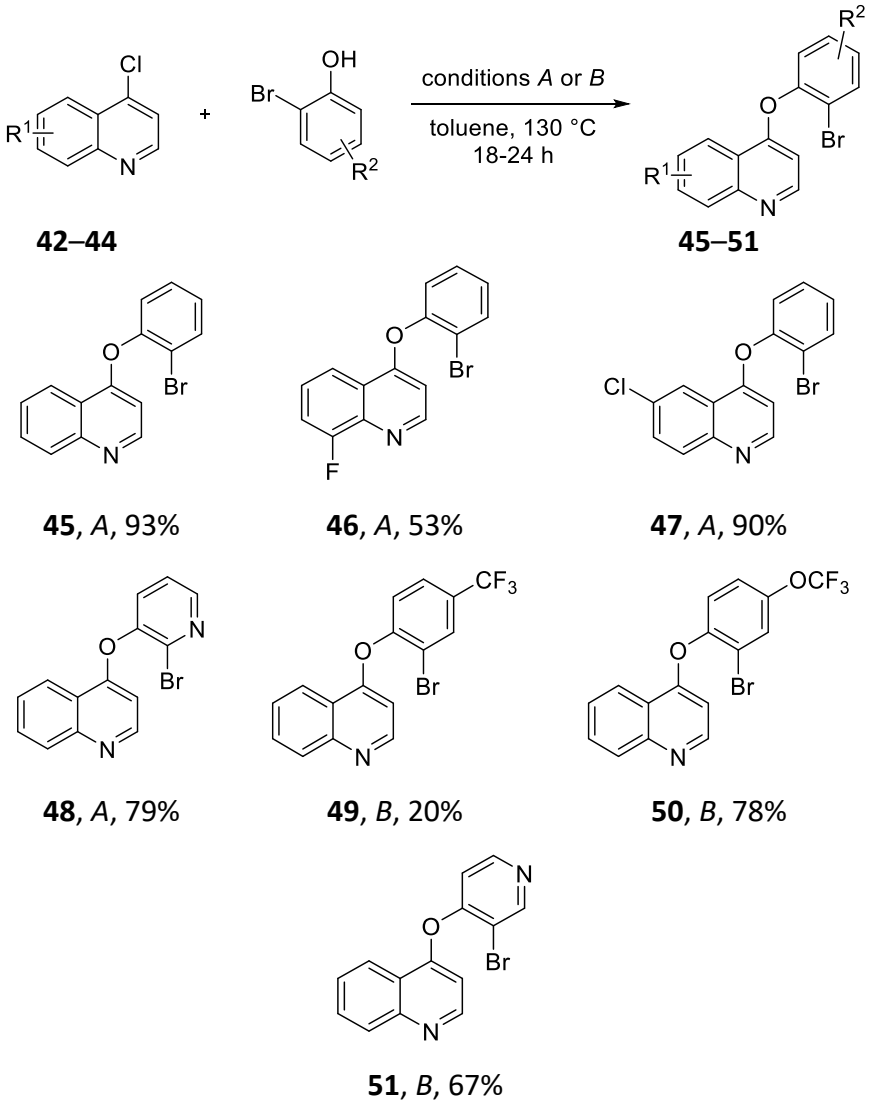
Substituted 4-chloroquinolines **42**–**44** were synthesised from the corresponding quinolin-4-ols using phosphorous oxychloride ($POCl_3$) in very good to excellent yields (**Scheme 2.13**).[99] $POCl_3$ is ubiquitously used to transform hydroxyl groups into the corresponding chlorides in nitrogen-based heterocycles.[100]



Scheme 2.13 Synthesis of 4-chloroquinolines.

4-Chloroquinolines **42**–**44** were subsequently reacted with various substituted phenols to give 4-(2-bromophenoxy)quinolines (**Scheme 2.14**). Compounds **45**–**48** were obtained using crushed NaOH pellets as base, with a large excess of 2-bromophenol/pyridinol and were isolated in moderate to excellent yields. Previous work by the group showed that upon substitution of the 2-bromophenol, it was necessary to employ *N,N*-dimethylaminopyridine (DMAP) as the base.[60] This method was used to form **49**, the isolated yield of which was relatively poor at 20%. Substrates **50** and **51** were also synthesised using this protocol with much higher yields of 78% and 67% respectively. These reactions are likely to proceed *via* nucleophilic aromatic substitution of the chloride with the phenoxide ion generated *in situ*. The poor yield of **49** is likely due to the electron-withdrawing effect of the trifluoromethyl group weakening the nucleophilicity of the phenoxide produced. It is possible that the DMAP acts as a nucleophilic catalyst in the reactions with

substituted 2-bromophenols i.e. it replaces the chloride and acts as a more labile leaving group.[101]

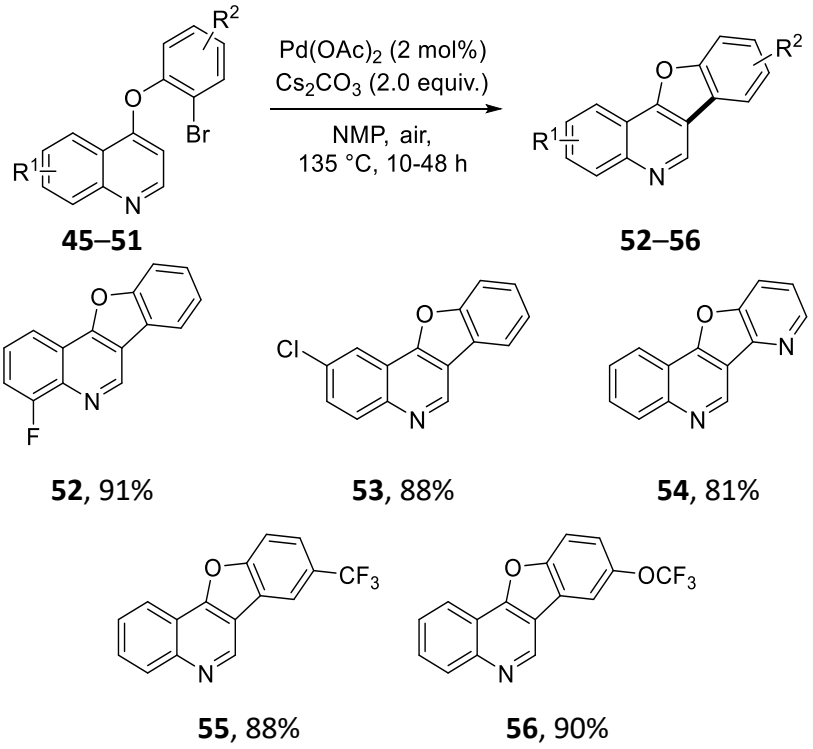


Scheme 2.14 Substituted 4-(2-bromophenoxy)quinoline substrates. *A*: NaOH (1.5 equiv.) and 2-bromophenol (5.0 equiv.). *B*: DMAP (3.0 equiv.) and substituted 2-bromophenol (1.5 equiv.).

2.13.2 Intramolecular Direct Arylation

Substrates **46**–**51** were all subjected to the optimised conditions to couple the C-3 position on the quinoline with the activated bromine site on the phenoxy ring (**Scheme 2.15**).[36] Under the standard conditions, **52**, **53**, **55** and **56** were furnished in excellent yields. Pleasingly, exchanging the simple aryl group for a *m*-pyridinyl group did not hinder the coupling reaction and **54** was obtained in 81% yield. Contrastingly,

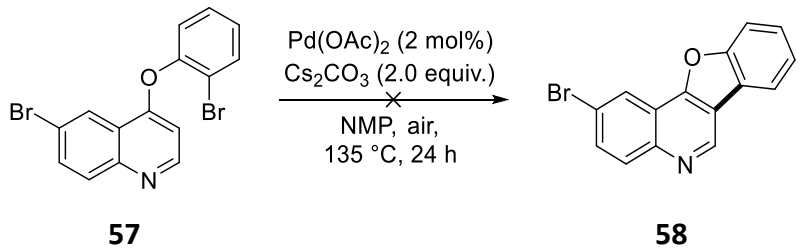
51 gave no conversion to cyclised product, with the *p*-pyridinyl moiety perhaps inhibiting the reaction pathway through interaction with the Pd-catalyst.



Scheme 2.15 Investigation of substrate scope. All yields are isolated.

2.14. One-Pot Tandem Cross-Coupling/Direct Arylation

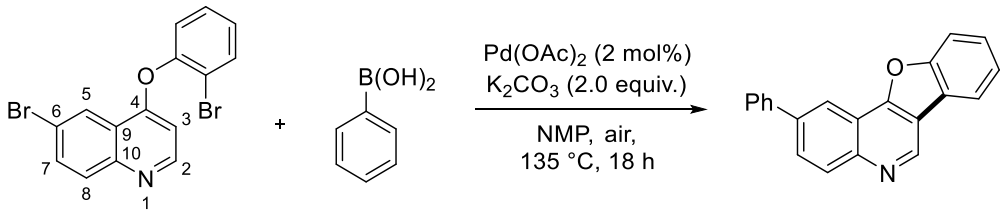
As is often the case, not all substrates in a scope form the desired product effectively. In this instance, the cyclisation of di-brominated quinoline **57** showed no conversion to **58** and only starting material was recovered after 24 hours (**Scheme 2.16**).[60]



Scheme 2.16 Failed cyclisation of di-brominated substrate.

It was unlikely that the bromine would affect the latent electronics of the C-3 position enough to completely prevent functionalisation, and it was therefore hypothesised that chemoselectivity issues were at play. We suspected that OA into the carbon-

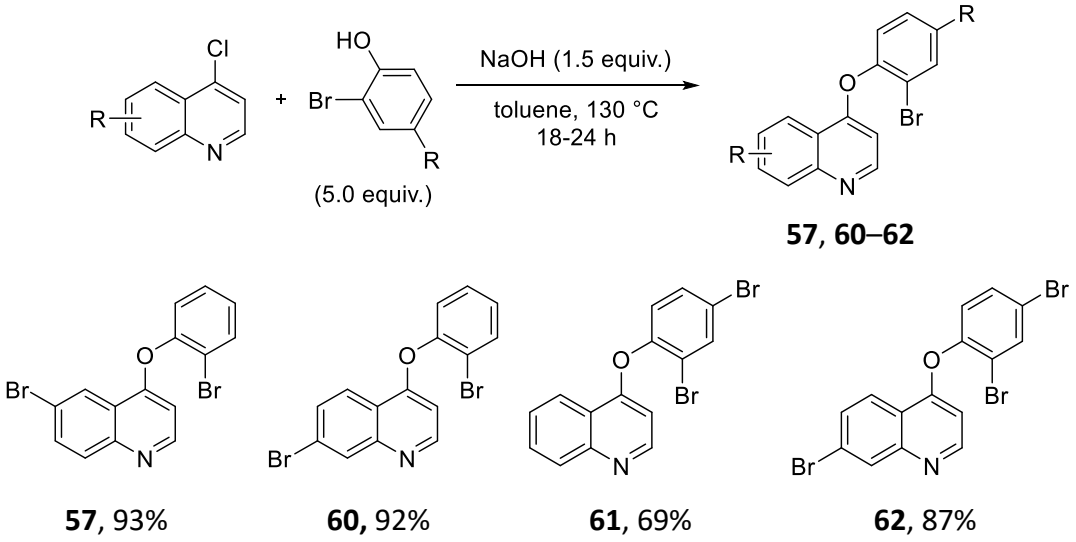
bromine bond on the quinoline ring was favoured over that on the phenoxy ring, sequestering the palladium in a catalytic dead-end.[102] It was envisaged, as inspired by Lautens[58] and Cramer,[59] that introduction of a suitable coupling partner could liberate the catalyst from the previously non-productive site and allow the cyclisation to take place. The addition of $PhB(OH)_2$, after a short optimisation, promoted the occurrence of a one-pot, tandem Suzuki-Miyaura/direct arylation reaction, with no added ligands, in air, to give **59** in 83% yield (**Scheme 2.17**).[102] Another member of the McGlacken group performed a substantial substrate scope on the SM/DA reaction to include a variety of electronically and sterically diverse phenyl boronic acids. The protocol was effective when the second bromine was positioned elsewhere on the structure (C-7, phenoxy) and also worked well on tri-brominated substrates with two equivalents of the coupling partner.[60,102]



57 **59**, 83%

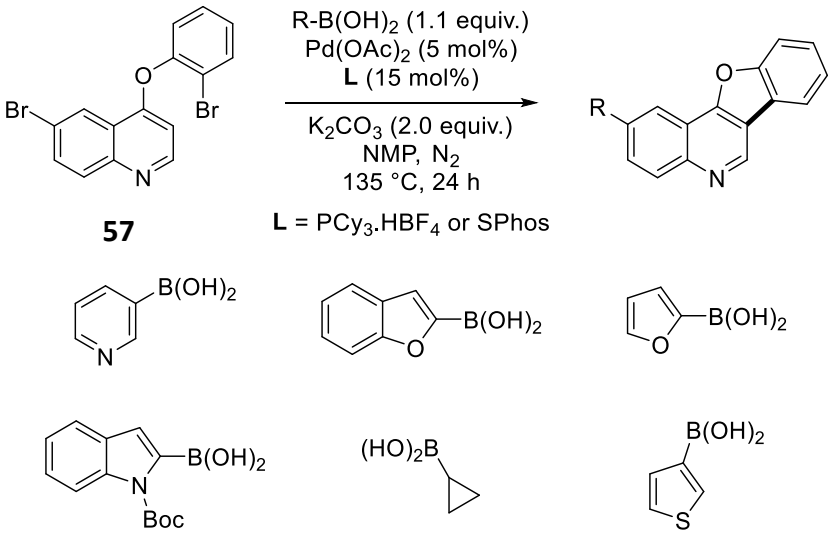
Scheme 2.17 One-pot, tandem SM/DA reaction.

We then looked at expanding the scope of the reaction to include other cross-coupling transformations. Firstly, a series of di- and tri-bromophenoxyquinolines were synthesised from commercially available 4-chloroquinolines and **42** (**Scheme 2.18**).



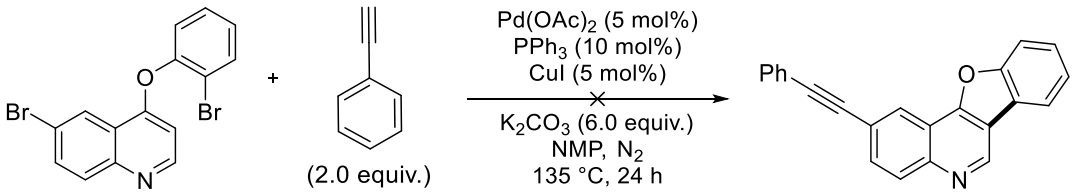
Scheme 2.18 Substituted di- and tri-bromophenoxyquinoline substrates.

Alkyl and heteroaromatic boronic acids were not tolerated by the one-pot system[60] and it was theorised that an additional ligand would aid the progression of such reactions. Based on previous work by the McGlacken group[103-104] and others[105-106] in the Suzuki-Miyaura cross-coupling of heteroaryl boronic acids, two ligands were chosen for the enhancement of these reactions: SPhos and tricyclohexylphosphine (PCy_3). Six boronic acids were selected for these small-scale test reactions, however little to no product was observed by ^1H NMR analysis in all cases (**Scheme 2.19**).



Scheme 2.19 Attempts to expand the SM/DA scope to include heteroaryl/alkyl boronic acids.

We also endeavoured to incorporate a Sonogashira-type coupling with our ring-closing reaction. Conditions published by Widchaya *et al.*[107] were integrated into our one-pot procedure but no conversion to cyclised product **63** was observed (**Scheme 2.20**).

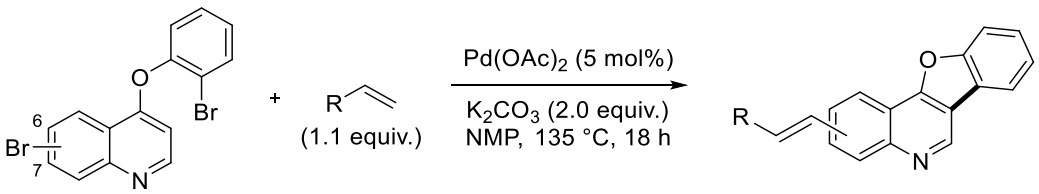


57 **63**

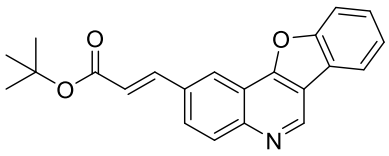
Scheme 2.20 Failed one-pot Sonogashira/direct arylation reaction.

2.14.1 One-Pot, Tandem Mizoroki-Heck/Direct Arylation

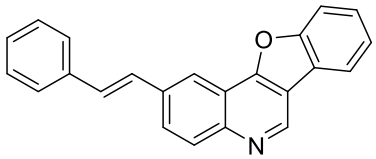
We were keen to elaborate upon the scope of cross-couplings compatible with the one-pot system and were finally able to combine the ring-closing reaction with a Mizoroki-Heck transformation. The MH/DA protocols were carried out using either *tert*-butyl acrylate or styrene derivatives in a single pot with no additional ligands or perturbation of the original reaction set-up required.[102] One-pot MH/DA reactions using styrene derivatives required increased catalytic loading (5 mol% $Pd(OAc)_2$) to ensure the complete consumption of starting material. The reactions performed well when the second bromine was positioned on the quinoline ring (C-6, C-7), constructing novel benzofuroquinolines **64**–**71** in good to excellent yields (**Scheme 2.21**).



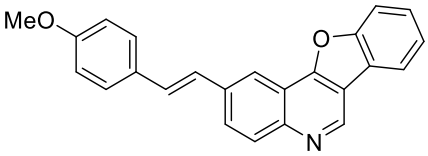
57, **60** **64–71**



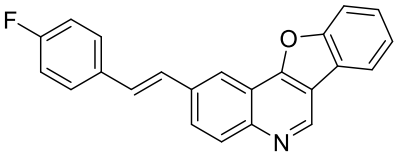
64, 78%[a]



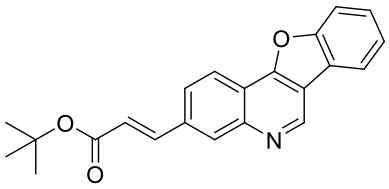
65, 73%



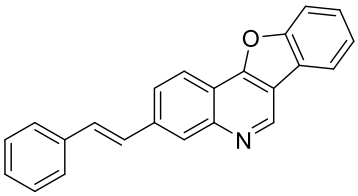
66, 82%



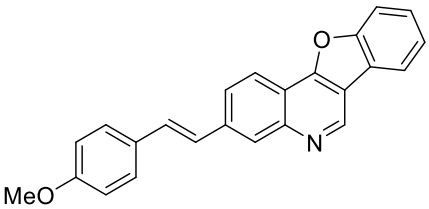
67, 80%



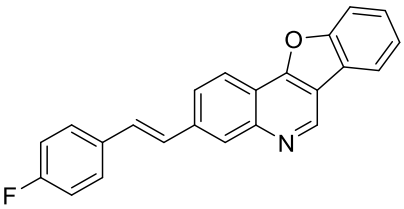
68, 79%[a]



69, 75%



70, 80%



71, 62%

Scheme 2.21 Substrate scope for tandem MH/DA reaction at the C-6 and C-7 positions on the quinoline ring. All yields are isolated. [a]Catalytic loading reduced to 2 mol%.

The structure of **68** was confirmed by X-ray diffraction analysis of single crystals which were obtained *via* vapour diffusion from a saturated solution of toluene in hexane (**Figure 2.5**).

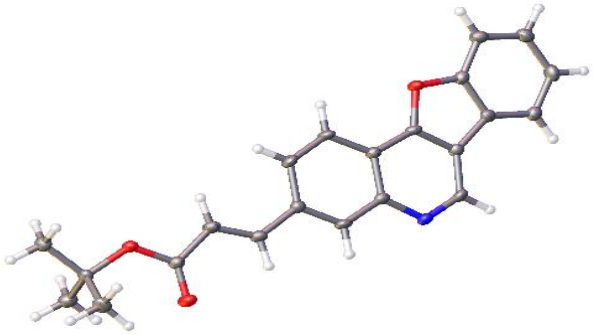
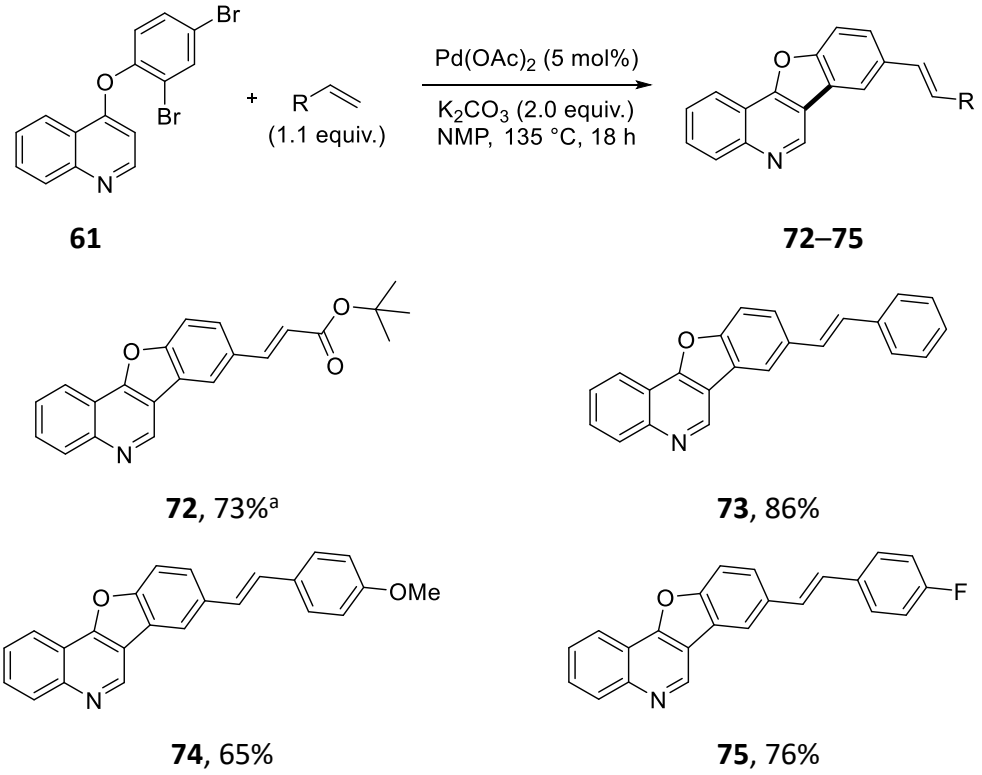


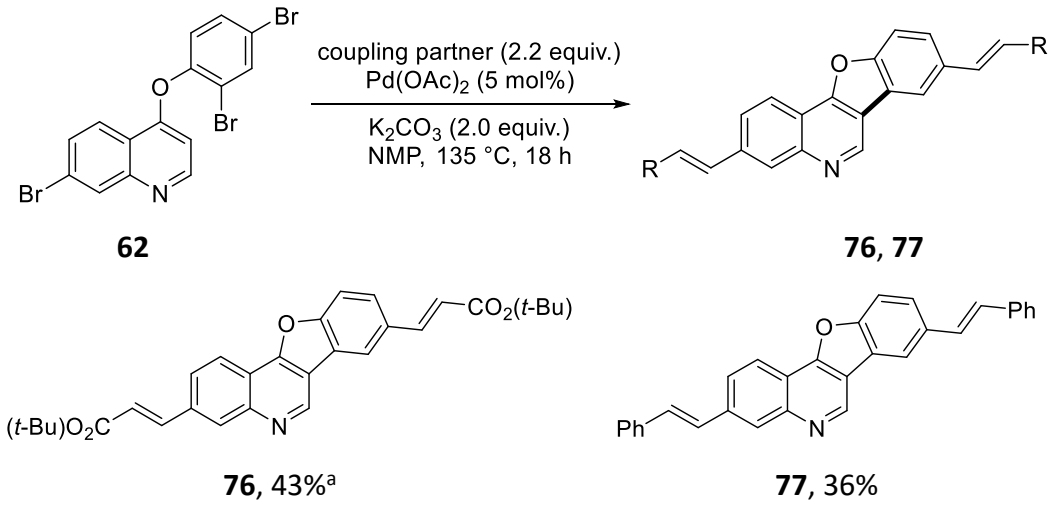
Figure 2.5 Crystal structure of **68**, thermal ellipsoids drawn at the 50% probability level.

The transformations were conducive to repositioning the second bromine onto the phenoxy ring, forming compounds **72**–**75** in excellent yields (**Scheme 2.22**).



Scheme 2.22 Substrate scope for tandem MH/DA reaction on the phenoxy ring. All yields are isolated. [a]Catalytic loading reduced to 2 mol%.

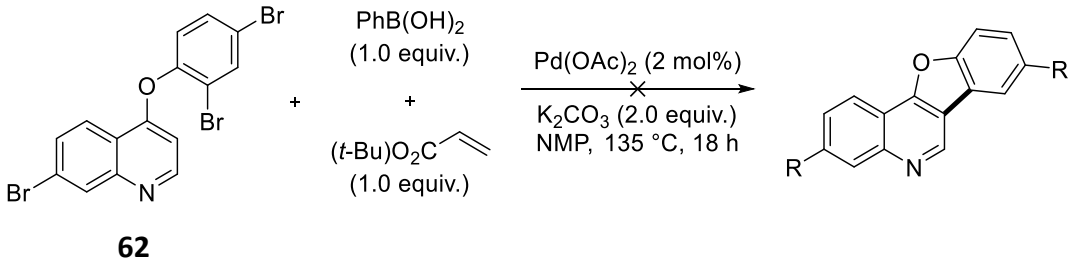
Finally, the protocol tolerated the inclusion of a third bromine for reaction with a second equivalent of coupling partner, albeit in lower yields than the reactions for di-brominated substrates (**Scheme 2.23**). Thus, this method allows for three transformations to be carried out in one-pot using a single pre-catalyst.



Scheme 2.23 Substrate scope for tandem MH/DA reaction on a tri-brominated quinoline substrate. All yields are isolated. [a]Catalytic loading reduced to 2 mol%.

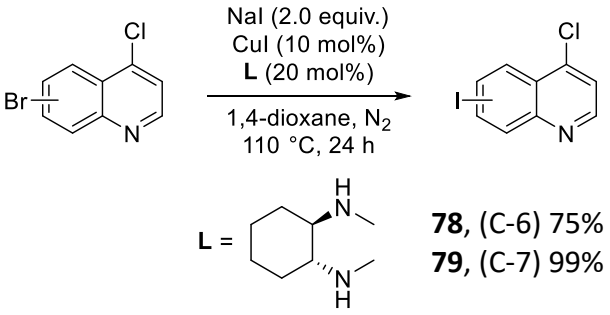
2.14.2 Potential for a One-Pot, Three-Component Strategy

Next, we wondered if the inherent electronics of the tri-brominated substrate could be manipulated to develop a one-pot process with three different systems i.e. tandem MH, SM and direct arylation reactions. Attempts to synthesise these more elaborate entities were unsuccessful and produced a complex mixture of cyclised products.



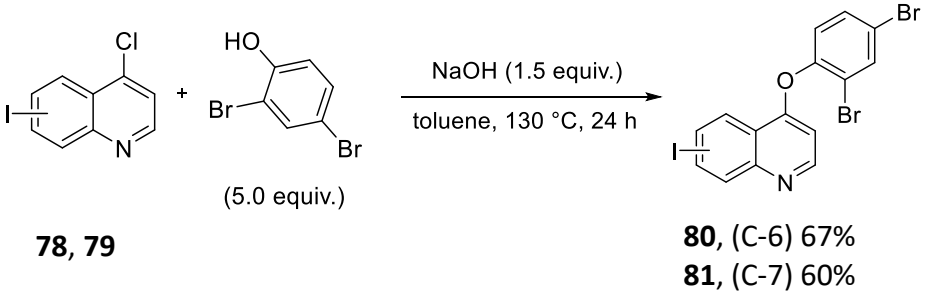
Scheme 2.24 Attempted three-component one-pot reaction.

It was then hypothesised that employing a more labile bond at one position could facilitate the three-component strategy. Iodinated 4-chloroquinolines **78** and **79** were thus furnished using a copper-catalysed aromatic Finkelstein reaction in excellent yields (**Scheme 2.25**).[108]



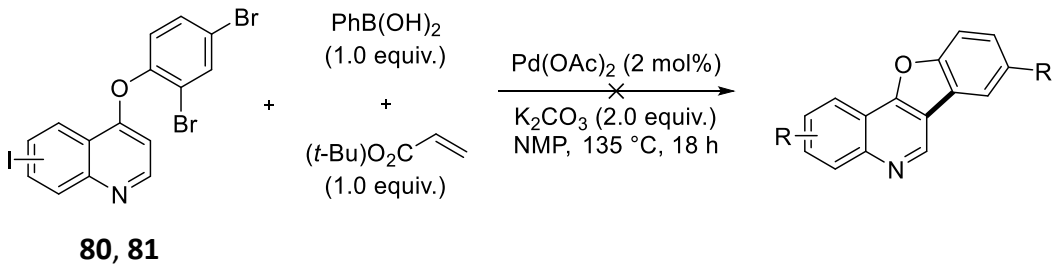
Scheme 2.25 Aromatic Finkelstein reaction of commercially available 6-bromo- and 7-bromo-4-chloroquinoline to form their respective iodinated equivalents.

These iodinated quinolines were then reacted with 2,4-dibromophenol to form the corresponding di-bromophenoxyquinolines **80** and **81** in moderate yields (**Scheme 2.26**).



Scheme 2.26 Synthesis of 6-iodo and 7-iodo 4-(2-bromophenoxy)quinolines.

These substrates were again subjected to our three-component, one-pot reaction. Although theoretically the C-I bond should be more labile, the reaction was again not selective, and a complex mixture of products was obtained (**Scheme 2.27**).



Scheme 2.27 Attempted three-component one-pot reaction using iodinated substrates.

2.15. Palladium-Quinoline Interaction

Considering that cross-coupling reactions which incorporate heteroaryl substrates usually require added ligand and inert atmosphere,[22] we wished to investigate why our direct arylation and one-pot protocols were without recourse to these additional parameters. There are several literature examples which utilise nitrogen-based ligands for the construction of carbon-carbon bonds,[31,37-40,109] and we suspected that the quinoline substrate was playing a similar role in our system.

2.15.1 ^{1}H-^{15}N NMR Spectroscopy

We wished to study the potential Pd-Q interaction using NMR spectroscopy, with the intention of measuring the resonance of the ^{15}N nucleus (at natural abundance) before and after the addition of the catalyst. Initially, the ^{1}H-^{15}N HMBC NMR spectra for substrates **45** and **60** were recorded in $CDCl_3$ (60 mg approx. of compound per sample). Pleasingly, only one ^{15}N NMR resonance was detected for each substrate, at 291.7 ppm and 290.5 ppm respectively. In both cases, the three ^{1}H-correlations to the nitrogen were identified as the protons at C-2, C-3 and C-8, as confirmed by two-dimensional NMR techniques which had been assigned previously (COSY, ^{1}H-^{13}C HSQC and ^{1}H-^{13}C HMBC) (**Figure 2.6**).

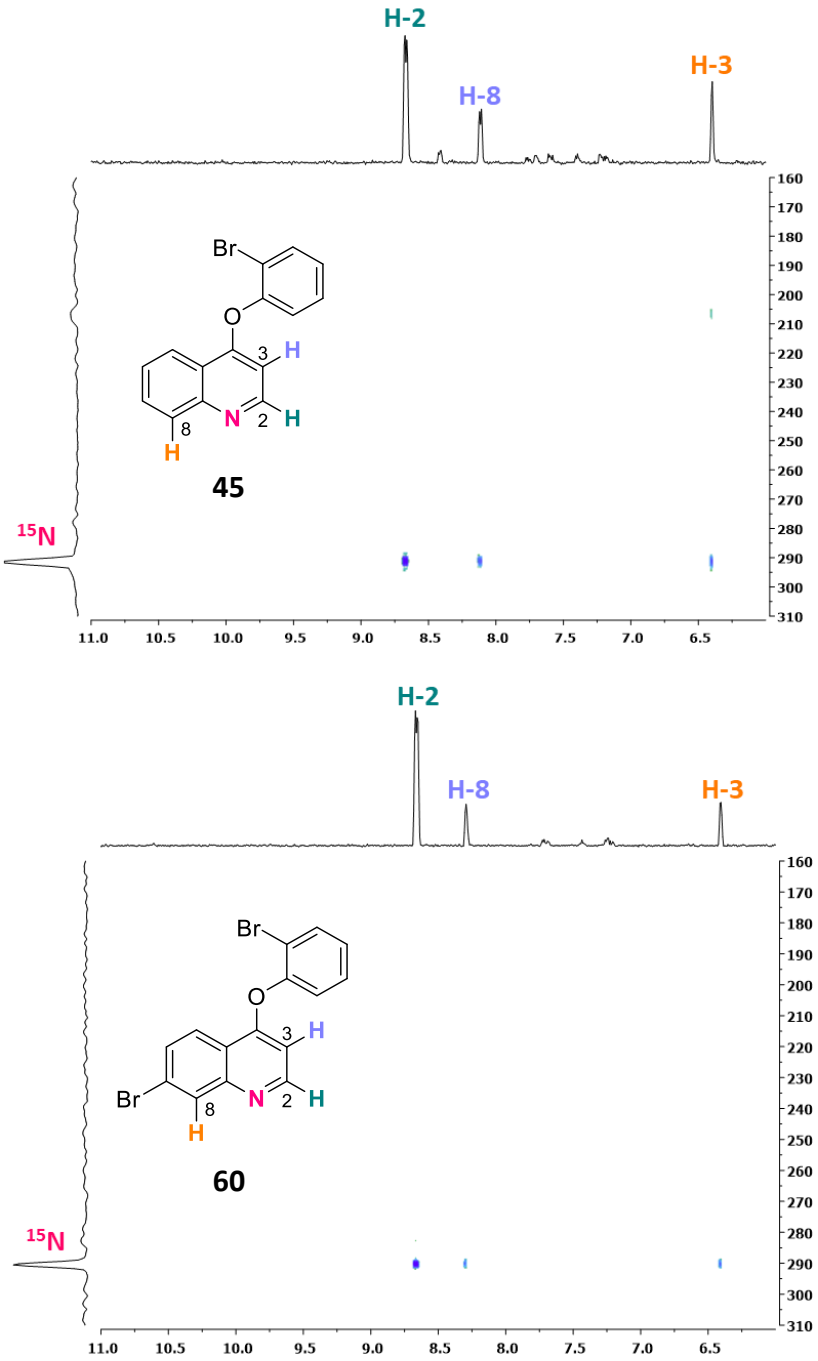


Figure 2.6 [Top] ^{1}H-^{15}N HMBC NMR spectrum for mono-bromo substrate **45**. [Bottom] ^{1}H-^{15}N NMR spectrum for di-bromo substrate **60**. Both spectra recorded at 600 MHz (^{1}H) and 60 MHz (^{15}N) in $CDCl_3$ at 300 K at a concentration of ~0.5 mol L^{-1}.

The high concentration of substrate already present in the NMR samples led us to contemplate the solubility issues that could arise upon the addition of the catalyst. Therefore, 0.5 equiv. of $Pd(OAc)_2$ was initially added to either sample and the ^{1}H, ^{13}C and ^{1}H-^{15}N HMBC NMR spectra were again recorded. To our surprise, complete

consumption of the starting materials was observed by ^{1}H NMR analysis. The formation of a new, single, quinoline-type entity was accompanied by downfield shifts in the protons at C-2, C-3 and C-8. The order of H-2 and H-8 was also reversed in both cases; this trend is indicative of direct Pd-N coordination in quinoline-based compounds (**Figure 2.7**).[43] It has also been shown previously that the largest variations in chemical shift are exhibited for the protons in the vicinity of the nitrogen atom when attached to a metal.[110-111] The reduction in electron density around the H-2 and H-8 nuclei is related to an inductive effect which is likely produced when the palladium moiety accepts the lone pair of electrons from the quinoline-nitrogen.[43] Larger coupling constants were also recorded for the vicinal ($^{3}J_{H,H}$) coupling between H-2 and H-3. This increase could also be attributed to a reduction in electron density at the nitrogen, along with a possible increase in angle strain caused by the new bond formed.[112] Similar shifts were discerned when the experiments were carried out in alternative solvents, namely 1,4-dioxane-d_8 and ACN-d_3 (see **Appendix I**).

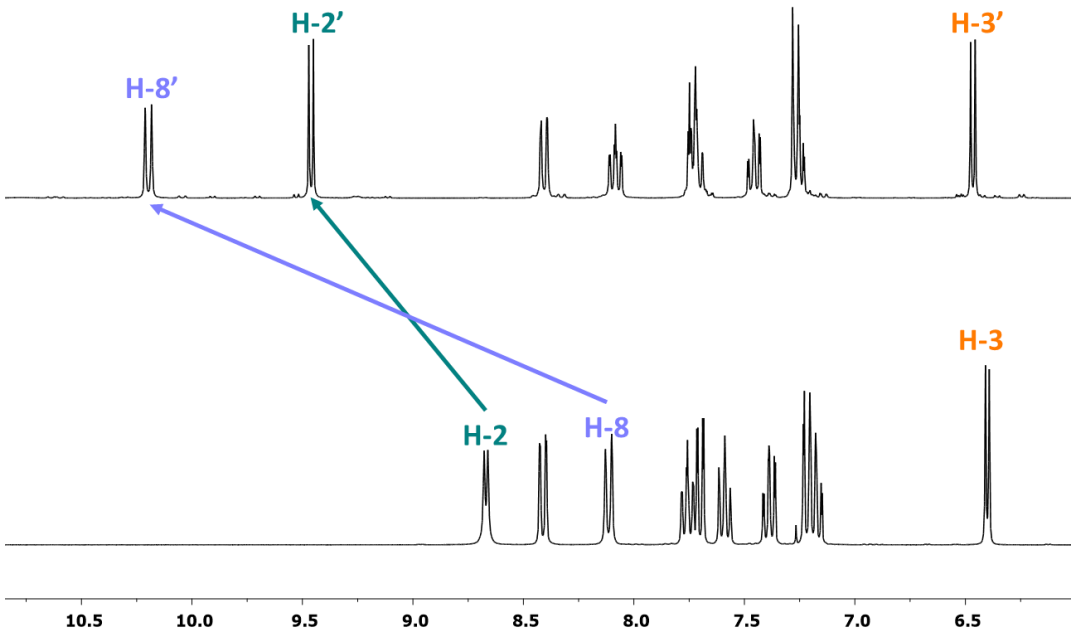


Figure 2.7 Excerpt from ^{1}H NMR spectra. [Bottom] Mono-bromo substrate **45**. [Top] Substrate **45** after addition of 0.5 equiv. $Pd(OAc)_2$. Both spectra were recorded at 600 MHz in $CDCl_3$ at 300 K.

Analysis of the ^{1}H-^{15}N HMBC NMR spectra revealed a dramatic upfield shift for the ^{15}N resonance of almost 100 ppm in both compounds. The significant shielding of the

^{15}N nucleus is also characteristic of complex formation between the quinoline-nitrogen and a heavy metal such as palladium.[42-44,113] The pertinent shifts in all recorded spectra are summarised below.(**Table 2.2**).

Table 2.2 Relevant chemical shifts for ^{1}H-^{15}N HMBC NMR spectra as recorded at 600 MHz (^{1}H) and 60 MHz (^{15}N) in $CDCl_3$ at 300 K. Concentration of ~0.5 mol L^{-1}. ^{15}N NMR shifts referenced externally to nitromethane at 380.2 ppm, the values of which are uncorrected. Chemical shifts δ reported in ppm and coupling constants (*J*) are reported in Hz.

compound	^{1}H-^{15}N HMBC[a]	relevant δ ^{1}H correlations	δ ^{15}N
45	3, 8, 2	6.40 (d, *J* = 5.1 Hz, 1H C(**3**)H) 8.12 (d, *J* = 8.5 Hz, 1H C(**8**)H) 8.67 (d, *J* = 5.1 Hz, 1H C(**2**)H)	291.7
45 + $Pd(OAc)_2$[b]	3', 2', 8'	6.47 (d, *J* = 6.2 Hz, 1H C(**3'**)H) 9.46 (d, *J* = 6.2 Hz, 1H C(**2'**)H) 10.20 (d, *J* = 8.6 Hz, 1H C(**8'**)H)	196.7
60	3, 8, 2	6.40 (d, *J* = 5.2 Hz, 1H C(**3**)H) 8.20–8.36 (m, 2H, C(**8**)H) 8.65 (d, *J* = 5.2 Hz, 1H C(**2**)H)	290.5
60 + $Pd(OAc)_2$[b]	3', 2', 8'	6.46 (d, *J* = 6.2 Hz, 1H C(**3'**)H) 9.43 (d, *J* = 6.2 Hz, 1H C(**2'**)H) 10.36 (d, *J* = 8.7 Hz, 1H C(**8'**)H)	194.2

[a]Protons correlated to the ^{15}N nucleus. [b]0.5 equiv. of $Pd(OAc)_2$ added.

The ^{13}C NMR spectra for these experiments are also noteworthy as the C-2 resonances are deshielded by ~5 ppm. Although C-8 does not experience a significant shift, the intensity of the signal is greatly reduced. This is probably as a result of an increase in relaxation time and the intensity of the signal could likely be enhanced by an increase in the relaxation delay in the ^{13}C NMR experiment. The appearance of two new carbons at ~178 ppm and ~22 ppm, were assumed to be from the incorporation of the acetate groups, representing the carbonyl and terminal methyl

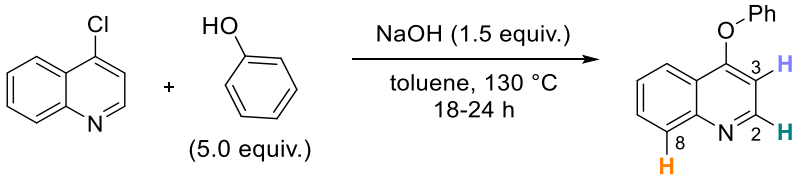
groups respectively (**Table 2.3**). The relative chemical shifts of these functionalities in the free $Pd(OAc)_2$ catalyst were measured to be 188.4 ppm and 22.8 ppm in $CDCl_3$.

Table 2.3 Relevant chemical shifts for ^{13}C NMR spectra as recorded at 150 MHz in $CDCl_3$ at 300 K. Chemical shifts δ reported in ppm.

compound	δ ^{13}C	compound	δ ^{13}C
45	151.1 (C(**2**)H)	**60**	152.2 (C(**2**)H)
	156.1 (C(**2'**)H)		157.4 (C(**2'**)H)
45 + $Pd(OAc)_2$[a]	178.3 (qC-**17'**)	**60** + $Pd(OAc)_2$[a]	178.4 (qC-**17'**)
	22.6 C(**18'**)H_3		22.7 C(**18'**)H_3

[a]0.5 equiv. of $Pd(OAc)_2$ added.

The non-halogenated 4-phenoxyquinoline motif **82** was also prepared, using the techniques previously described (**Scheme 2.28**).



42 **82**, 87%

Scheme 2.28 Synthesis of 4-phenxoyquinoline.

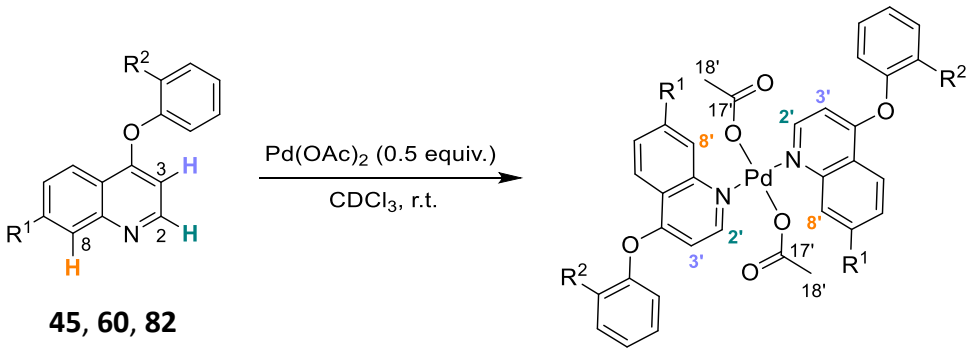
The NMR experiment was then repeated using **82** as the substrate. Shifts analogous to those observed in the reaction of **45** and **60** with 0.5 equiv. $Pd(OAc)_2$ were ascertained in the ^1H and ^{13}C NMR spectra (**Table 2.4**).

Table 2.4 Relevant chemical shifts for ^{1}H and ^{13}C NMR spectra as recorded at 300 MHz (^{1}H) and 75 MHz (^{13}C) in $CDCl_3$ at 300 K. Chemical shifts δ reported in ppm.

compound	relevant δ ^{1}H-NMR shifts	relevant δ ^{13}C NMR shifts
82	6.54 (d, *J* = 5.2 Hz, 1H C(**3**)H) 8.10 (d, *J* = 8.3 Hz, 1H C(**8**)H) 8.66 (d, *J* = 5.2 Hz, 1H C(**2**)H)	151.1 (C(**2**)H)
82 + $Pd(OAc)_2$[a]	6.58 (d, *J* = 6.2 Hz, 1H C(**3'**)H) 9.42 (d, *J* = 6.2 Hz, 1H C(**2'**)H) 10.16 (d, *J* = 8.6 Hz, 1H C(**8'**)H)	156.1 (C(**2'**)H) 178.3 (qC-**17'**) 22.7 C(**18'**)H_3

[a]0.5 equiv. of $Pd(OAc)_2$ added.

With all of this data in hand, we envisaged a dimeric complex forming in solution between two molecules of the phenoxyquinoline and one molecule of $Pd(OAc)_2$ (**Scheme 2.29**).



45, **60**, **82**

83 R^1 = H, R^2 = Br
84 R^1 = R^2 = Br
85 R^1 = R^2 = H

Scheme 2.29 Proposed formation and structure of the complex formed in solution, as elucidated by NMR spectroscopy.

As our suggested structure contained a 2:1 ratio of quinoline to $Pd(OAc)_2$, we repeated the experiment on substrate **45**, this time adding 0.25 equiv. of $Pd(OAc)_2$. Indeed, upon inspection of the ^{1}H NMR spectrum, an approximate 1:1 ratio of starting material:potential dimer was measured (**Figure 2.8**).

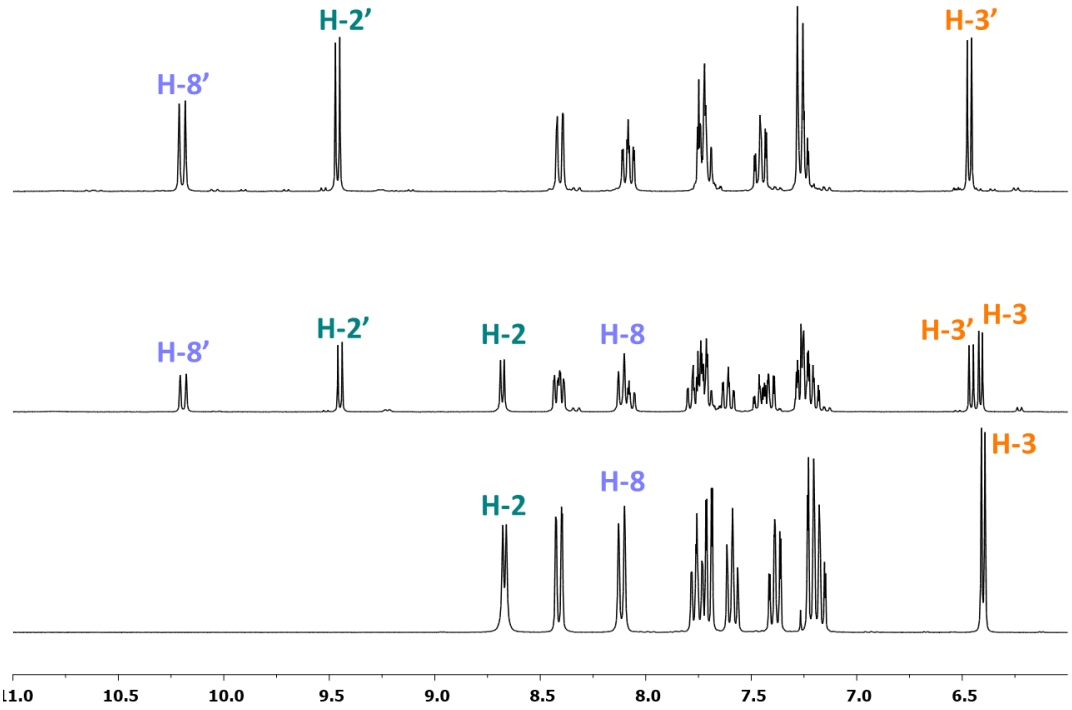
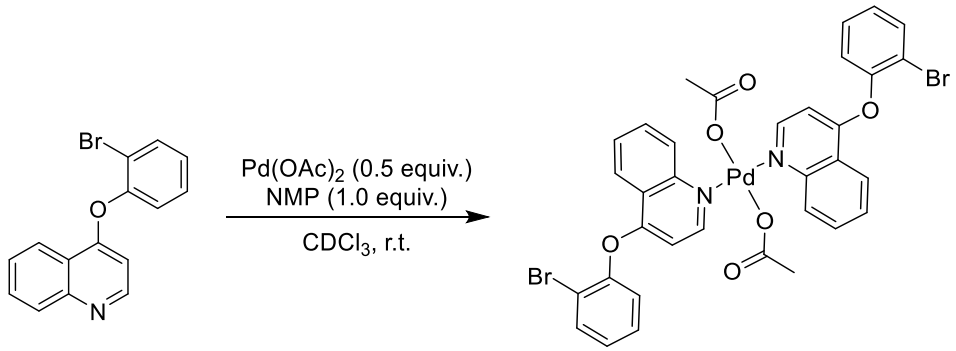


Figure 2.8 Excerpt from ^{1}H NMR spectra. [Bottom] Mono-bromo substrate **45**. [Middle] After addition of 0.25 equiv. $Pd(OAc)_2$ to **45**. [Top] Proposed complex, **83**. All spectra were recorded at 300 MHz in $CDCl_3$ at 300 K.

As it was not possible for the ^{1}H-^{15}N NMR experiments to be carried out in our reaction solvent, it is worth noting that the formation of mono-bromo Pd-Q complex **83** was not affected by the presence of NMP in solution (**Scheme 2.30**).



45 **83**

Scheme 2.30 Pd-Q coordination in the presence of NMP.

2.15.2 Further Analytical Data for Palladium Complexes

Further confirmation of these structures was achieved by HRMS analysis of the metal complexes in solution. ESI was employed as the mode of ionisation and the loss of a single acetate ion was apparent in all measured spectra; an attribute commonly observed in the literature for complexes of this type.[94,114-115] All complexes matched exactly the expected isotope pattern calculated for the $[M\text{-}OAc]^+$ ion, an example of which is shown below for complex **84** (**Figure 2.9**) (see **Appendix I** for other examples).

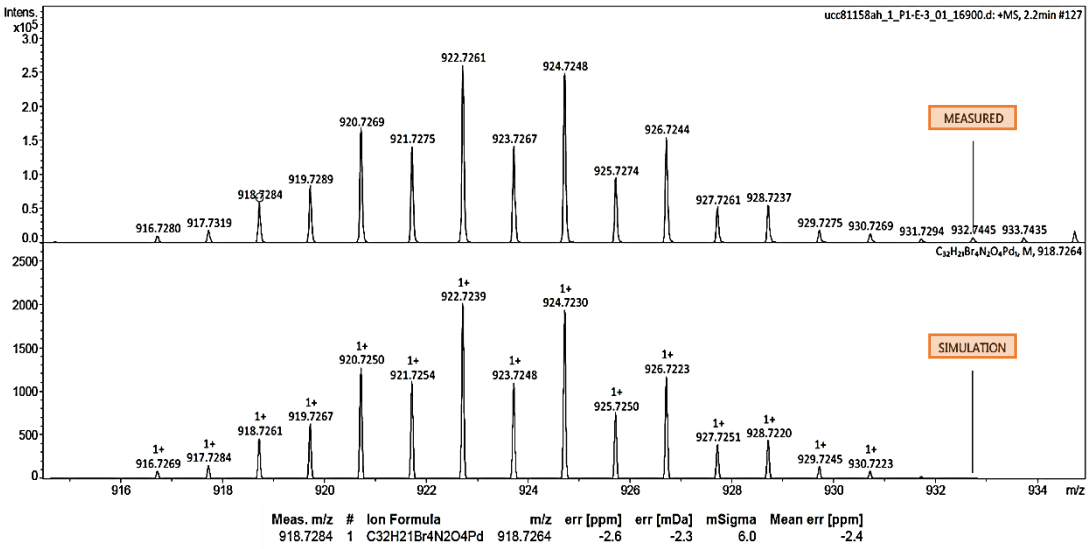


Figure 2.9 HRMS of di-bromo complex **84**. [Bottom] Predicted isotopic distribution. [Top] Actual isotopic distribution acquired. Spectrum measured on a Bruker compact TOF-MS at the University of York; samples were run in ESI mode using 50% $MeOH/H_2O$ as eluent.

Finally, X-ray quality crystals of complexes **83** and **85** were obtained *via* vapour diffusion from a saturated solution of toluene/methanol in hexane, unequivocally confirming the structures proposed (**Figure 2.10**).

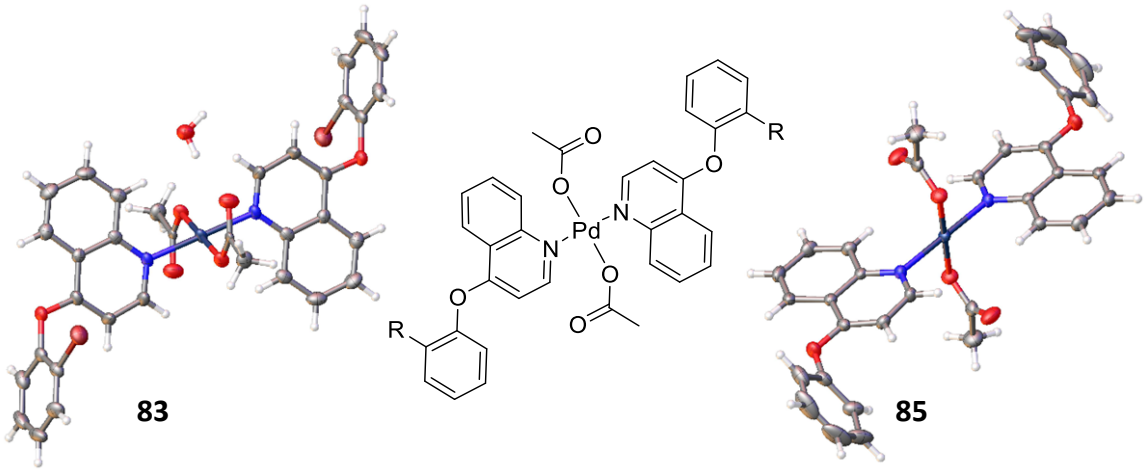
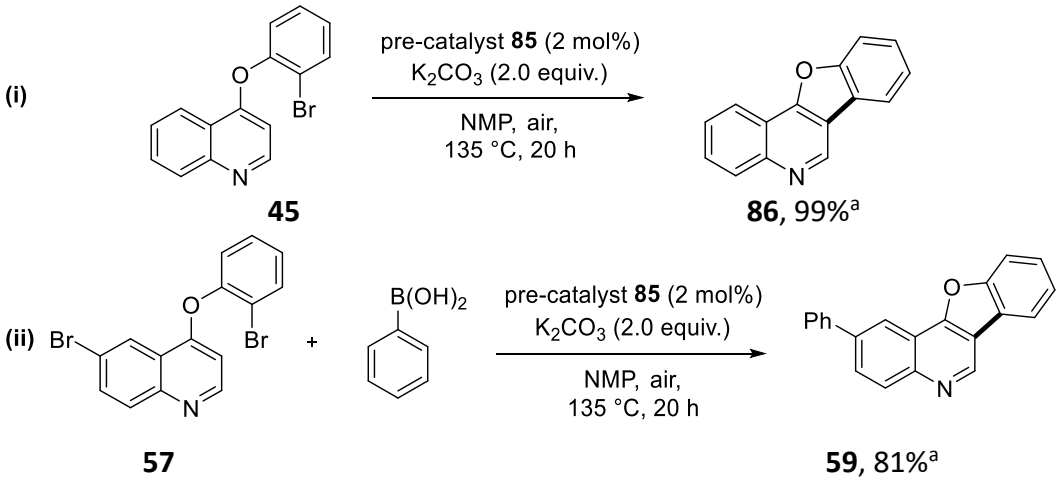


Figure 2.10 Crystal structures of **83** and **85**, thermal ellipsoids drawn at the 50% probability level. Disordered solvent (methanol) treated using solvent masking techniques for structure **85**.

2.15.3 Viability of Palladium-Quinoline Complexes

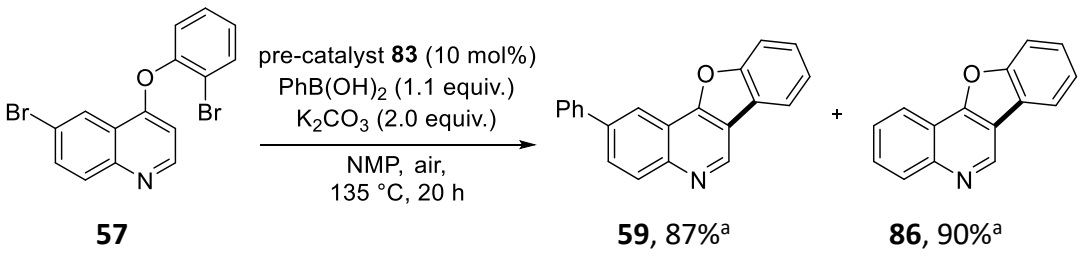
Although the role is undefined, the Pd-Q complexes formed are considered to play a critical role in the ring-closing system. In order to test their viability as pre-catalytic species, we undertook various experiments using the direct arylation and one-pot protocols, exploiting compounds **83–85** as the only palladium-source in the reactions.

Firstly, non-productive Pd-complex **85** was deemed a competent pre-catalyst for our cyclisation reaction, furnishing **86** in 99% yield by NMR (**Scheme 2.31 (i)**). The same complex also catalysed the SM/DA reaction of **57** with $PhB(OH)_2$, giving **59** in 81% yield by NMR (**Scheme 2.31 (ii)**).



Scheme 2.31 Pre-formed **85** as competent pre-catalyst for the direct arylation and SM/DA reactions. [a]Yields calculated from the ^{1}H NMR spectrum of the crude reaction mixture using 1,3,5-trimethoxybenzene as the internal standard.

Next, we wished to prove that the Pd-Q coordination was fluxional – in the case of added ligands, the ligating entities are not included in the final molecules, but rather facilitate the progression of the catalytic cycle to form the desired product(s). Productive, mono-bromo complex **83** was used as the only palladium-source for the SM/DA reaction (**Scheme 2.32**). An increased loading of 10 mol% was adopted to aid accuracy in the calculation of yields, and allow for clear diagnostic peaks to be identified by ^{1}H NMR analysis. Both the SM/DA and direct arylation products, **59** and **86**, were constructed in yields of 87% and 90% respectively by NMR. This experiment ruled out a spectator-only or sacrificial role for the quinoline ligands in the complexes formed, indicating the lability of the Pd-Q interaction.[43]

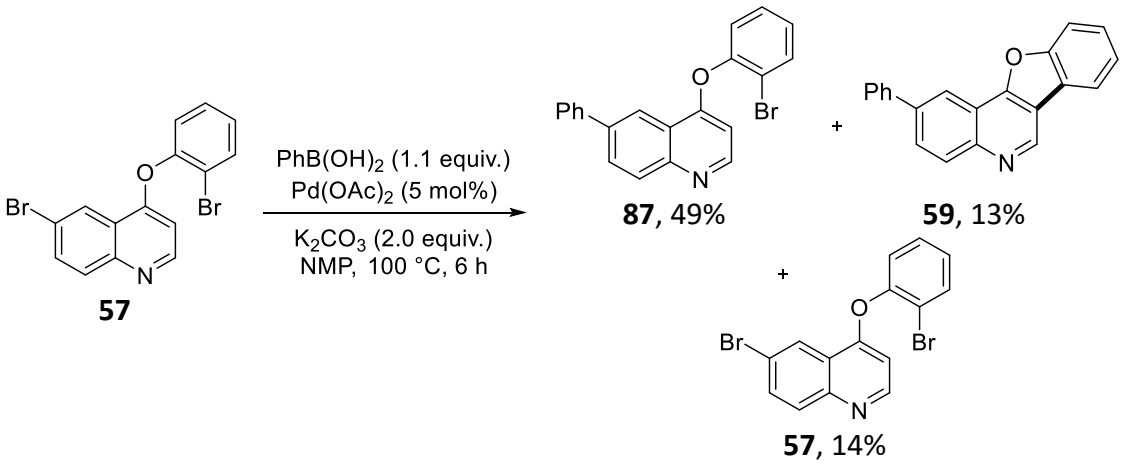


57 **59**, 87%[a] **86**, 90%[a]

Scheme 2.32 Pre-formed **83** as competent pre-catalyst for the SM/DA reaction. [a]Yields calculated from the ^{1}H NMR spectrum of the crude reaction mixture using 1,3,5-trimethoxybenzene as the internal standard.

2.15.1 Mechanistic Considerations

In terms of mechanism, we consider the SM and MH reactions to be the initial transformations in the one-pot system, progressing *via* the typical Pd(II)/Pd(0) mechanistic cycles.[116-117] Some evidence for this consideration was provided by an experiment carried out by another member of the group, from which SM-only product **87** was isolated (**Scheme 2.33**).[102]



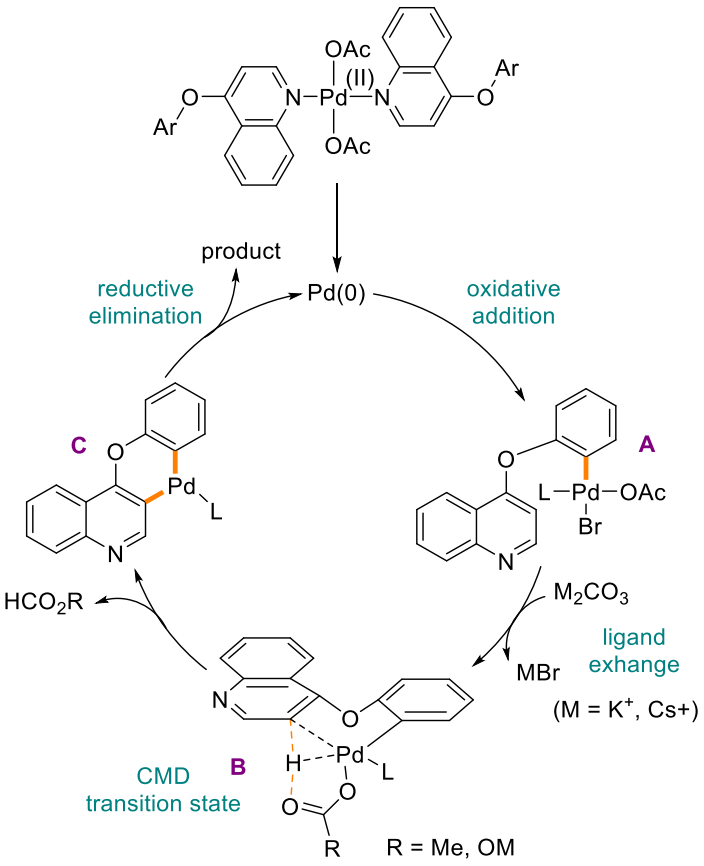
57 **87**, 49% **59**, 13% **57**, 14%

Scheme 2.33 Tandem reaction carried out at 100 °C.[102]

For the direct arylation step, three prospective scenarios are postulated.

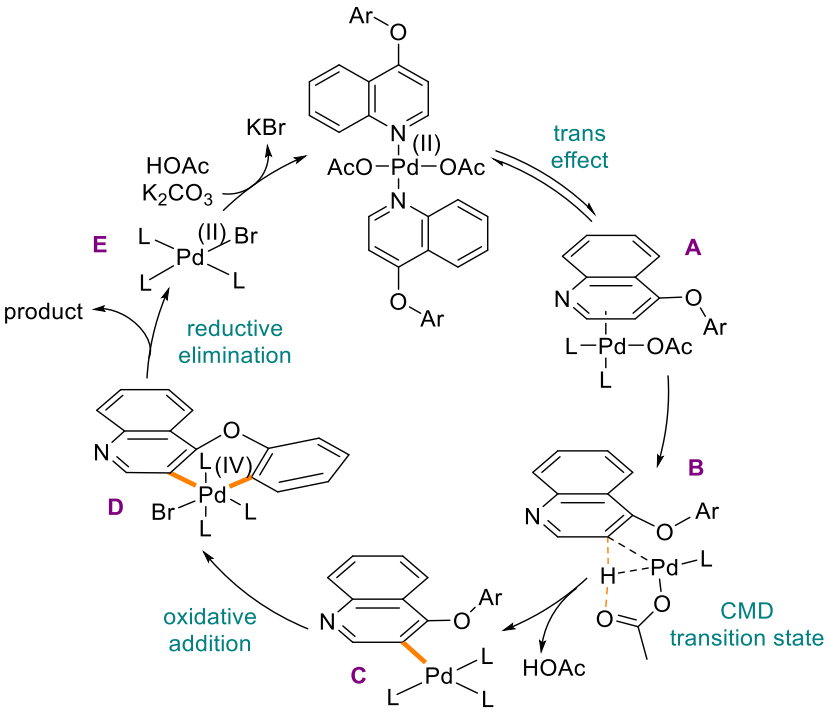
The first possibility is that the complexes are simply pre-catalysts and are subsequently transformed into an active Pd(0) species (**Scheme 2.34**). The first step would be OA into the aryl-bromine bond to give a 4-coordinate Pd(II) species (**A**). Next, C-H activation would arise *via*, for example, concerted metallation-deprotonation (CMD),[118-120] to give another palladacycle (**C**) (granting that other proton-abstraction mechanisms are also conceivable). As the name suggests, CMD is

a non-directed process in which metallation and proton-abstraction collectively occur, it is usually expedited by an intramolecular carboxylate base e.g. $^{-}$OAc.[121] This step is followed by RE to release the desired product and reform the active Pd(0) species.



Scheme 2.34 Plausible CMD-type catalytic cycle for the direct arylation reaction. Extra functional groups omitted for clarity. L = quinoline, OAc, NMP.

The second possibility involves the Pd-Q complexes as the active catalytic species, in a Pd(II)/Pd(IV) cycle (**Scheme 2.35**).[33,122] Under the steric influence of the two quinoline ligands, the complex reorients itself through a trans effect process, so that the palladium is bound through the π-system (**A**).[33] This invokes C-H activation at the C-3 position (**B**) again, *via*, for example, CMD, to give an aryl-Pd(II) species (**C**). This Pd(II) species undergoes OA into the aryl-bromine bond, thus furnishing a 6-cooridinate Pd(IV) species (**D**). Finally, RE liberates the cyclised product and a pre-catalytic intermediate (**E**) from which the active complex is regenerated.

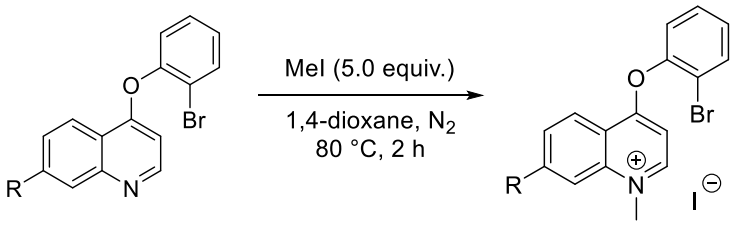


Scheme 2.35 Plausible Pd(II)/Pd(IV) catalytic cycle for the direct arylation reaction. Extra functional groups omitted for clarity. L = quinoline, $^{-}$OAc, NMP.

Another possibility is that the complexes play no direct role in the mechanism, but alternatively influence the consistent turnover of the catalytic cycle. The Pd-Q coordination could slow the decomposition of the active catalyst, retrieve off-cycle intermediates, stabilise reactive species or limit product inhibition.[40,123-127]

2.15.2 Importance and Role of Pd-Q Coordination

The role of the Pd-Q complexes in our ring-closing reaction was difficult to explicitly prove in our system, where it is not possible to omit or reintroduce the quinoline ligand. We did, however, create a situation whereby Pd-Q coordination was less available, through methylation of the nitrogen on the quinoline nucleus. This was achieved using methyl iodide as the electrophilic alkyl source to give **88** and **89** in excellent yields (**Scheme 2.38**).[128]

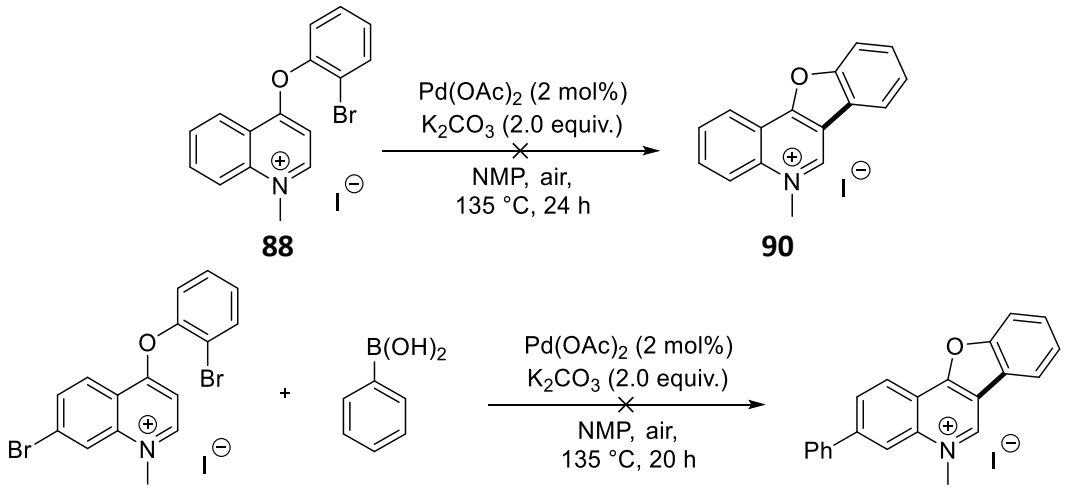


45, **60**

88, R = H 88%
89, R = Br 82%

Scheme 2.36 *N*-methylation of phenoxyquinoline substrates.

The methylated substrates were then subjected to the direct arylation and one-pot SM/DA reactions respectively, with neither showing any conversion to cyclised product by ^{1}H NMR analysis. Both compounds underwent degradation and gave a mixture of ring-open, quinoline-based products, none of which were specifically identified (**Scheme 2.37**). It is also crucial to recognise that the charged species formed upon methylation could dramatically alter the electronics of the system, and the iodide anion has the potential to coordinate to and poison the catalyst.[129] These reactions are not conclusive but do provide evidence pertaining to the pivotal role of the Pd-Q interaction.



88 **90**

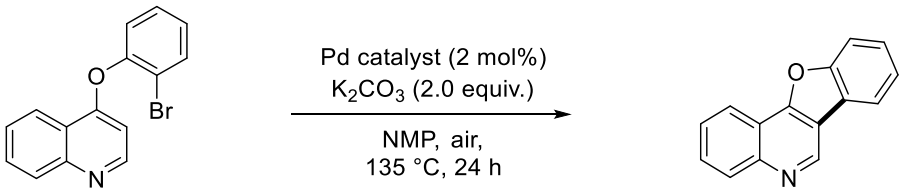
89 **91**

Scheme 2.37 Direct arylation and SM/DA reactions of *N*-methylated phenoxyquinoline compounds.

Interestingly, no Pd-Q complexation was observed when the NMR experiments were repeated using a number of Pd(0) compounds. These Pd(0) catalysts were

consequently utilised in the ring-closing reaction, with none proving as efficient as $Pd(OAc)_2$ (**Table 2.5**).[36] Other Pd(II) sources ($Pd(OPiv)_2$, $Pd(TFA)_2$, $PdCl_2$) all yielded >85% conversion to cyclised product under the same conditions. The lack of conversion to cyclised product using Pd(0) sources could elude to the necessity of Pd-Q coordination in this direct arylation system. While $Pd_2(dba)_3$ did give good conversion to cyclised product, this transformation is likely to proceed through an alternative mechanism to that proposed for our Pd(II) source.

Table 2.5 Use of Pd(0) catalysts for the direct arylation reaction.

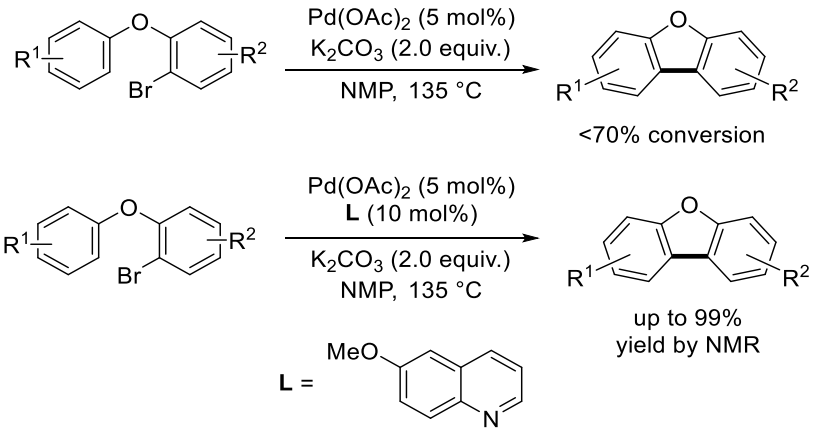


45 **86**

catalyst	complex formed?	yield **86**[a] (%)	% remaining **45**[a] (%)
$Pd(OAc)_2$	yes	95[b]	–
Pd/C	no	9	76
Pd/Al_2O_3	no	0	86
$Pd_2(dba)_3$	no	80	0
$Pd(dba)_2$	no	53	37

[a]Yields calculated from the ^{1}H NMR spectrum of the crude reaction mixture using 1,3,5-trimethoxybenzene as the internal standard. [b]Isolated yield.

At this stage, we were interested to determine if the Pd-Q complex could be employed as a pre-catalyst in other systems. Thus, studies were carried out by other members of the group on the intramolecular direct arylation of simple diaryl ether species.[130] Following on from the discovery of our Pd-Q complexes, it was established that addition of quinoline-type ligands, specifically 6-methoxyquinoline, lead to a significant increase in conversion to the cyclised, dibenzofuran products (**Scheme 2.38**). This was a critical development as the starting materials and products in these reactions are inseparable using traditional purification techniques.[130]



Scheme 2.38 Direct arylation reaction of diaryl ethers improved by the addition of a quinoline-based ligand.

2.16. Photophysical Characterisation of One-Pot Products

Polymeric and π-extended quinolines possess eminently useful optical and electronic properties. They are energetically stable and in steady oxidation states, making them very attractive candidates for inclusion in electronic and photonic materials for various applications.[131] Organic π-systems that are capped by an electron-donor and electron-acceptor at either end are known as push-pull systems. The new interaction between the two groups can bring about distinct photophysical properties compared to the mono- or un-functionalised system.[132]

During chromatographic purification of the one-pot MH/DA reaction mixtures, a particularly intense 'glow' was noted in the TLC of the product-containing fractions. Solutions of the purified products were also seen to emit light when irradiated with UV light (**Figure 2.11**), and so we decided to further investigate the electroluminescent properties of some one-pot MH/DA products.

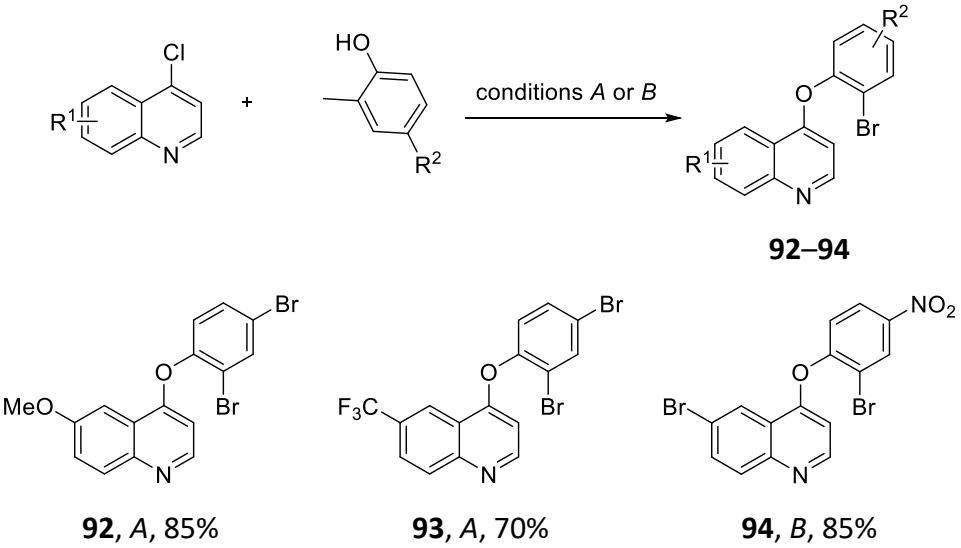
Note: For the purpose of this discussion litre (L) will be exchanged for cubic decimetres (dm^3), the more common unit used for the description of photophysical measurements.



Figure 2.11 Example of a one-pot MH/DA product in DCM under UV light.

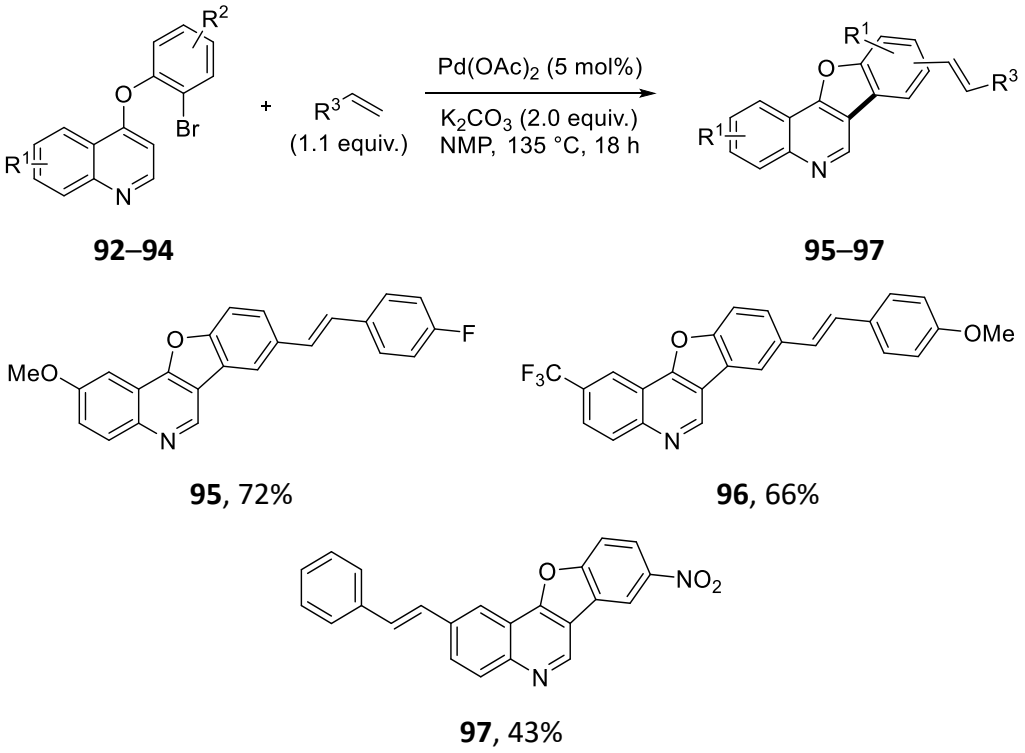
Upon discovery of the emissive capabilities of the π-extended compounds, we prepared three more di-bromophenoxyquinoline compounds **92**–**94**, with their potential photophysical characteristics in mind (**Scheme 2.39**). Compounds **92** and

93 were synthesised with the intention of creating a push-pull system i.e. cross-coupling of **92** with 4-fluorostyrene and **93** with 4-methoxystyrene. Nitro-groups have the propensity to weaken or fully quench fluorescent activity in organic molecules[133-134] and substrate **94** was constructed with the intention of demonstrating this phenomenon.



Scheme 2.39 Substituted di-bromophenoxyquinoline substrates. Conditions: *A* NaOH (1.5 equiv.) and 2,4-dibromophenol (5.0 equiv.) in toluene (0.5 mL $mmol^{-1}$) at 130 °C for 24 h. *B* NaOH (1.5 equiv.) and 2-bromo-4-nitrophenol (2.0 equiv.) in 1,2-dichlorobenzene (4.0 mL $mmol^{-1}$) at 150 °C for 24 h.

These substrates were subsequently reacted with styrene derivatives in one-pot MH/DA reactions to construct three new benzofuroquinoline scaffolds with potentially interesting photophysical capacities (**Scheme 2.40**).

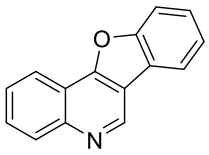


Scheme 2.40 Extended substrate scope for tandem MH/DA reaction. All yields are isolated.

The UV-vis absorption and fluorescence emission properties of each styrene-functionalised MH/DA product were investigated. The UV-vis data collected provided the maximum wavelength of absorption (λ_{max}) for each compound and the corresponding molar extinction coefficient (ε) was calculated (*vide supra*). The maximum wavelength of emission (λ_{em}) upon excitation is also quoted. UV-vis spectra of the substrates were measured on solutions of *ca*. 10^{-5} mol dm^{-3} in DCM and emission spectra were measured from the appropriate dilutions of the same samples (10^{-6}–10^{-8} mol dm^{-3}). Although other suitable solvents are available (ACN, cyclohexane, EtOH, etc.), DCM was chosen to maximise solubility.

First, benzofuro[3,2-*c*]quinoline **86** was characterised for comparative purposes (**Table 2.6**). This compound absorbed in the near UV region and emitted fluorescent light at concentrations of 10^{-6} mol dm^{-3} in the blue light part of the spectrum.

Table 2.6 UV−Vis data and calculated ε values for benzofuro[3,2-*c*]quinoline.



86

compound	λ_{max} (nm)	ε^a ($dm^3\ mol^{-1}\ cm^{-1}$)	λ_{em} (nm)
86	257	63300	353

[a]ε calculated at 8×10^{-6} mol dm^{-3}

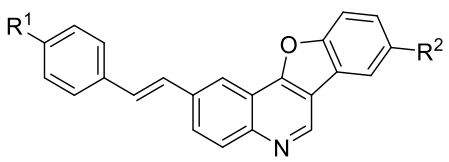
Ordinarily, when carrying out these photophysical measurements, the wavelength at which the sample is excited (λ_{ex}) is decided by the value of λ_{max} from the UV-vis spectrum of that sample. However, we irradiated all compounds at 257 nm, the λ_{max} value observed in the UV-vis spectrum of **86**. In the interest of clarity, the products will be grouped and compared with those that have the same substitution pattern.

Adding a styrene moiety to the C-6 position (**65**) induces a red shift (higher wavenumber, lower energy) with respect to the λ_{max} of **86**. Further functionalisation of the styrene group yielded competing effects on the absorption maxima. Introduction of an electron donating group (*p*-OMe, **66**) induced a hypsochromic shift relative to **65**, whereas the more electronically poor substrate (*p*-F, **67**) was blue shifted by a single nanometre. Substitution of the phenoxy ring with a nitro group (**97**) increased the concentration at which UV activity was observed (>10^{-5} mol dm^{-3}) and lowered λ_{max} with respect to **65**. The ε values calculated are all in the order of 10^4 $dm^3\ mol^{-1}\ cm^{-1}$, indicating that all electronic transitions are both spin- and orbit-allowed (**Table 2.7**).

Substitution of **86** with styrene at the C-6 position (**65**) generated a bathochromic shift in λ_{em} and decreased the concentration at which fluorescence could be measured by a factor of 10 (10^{-6} vs 10^{-7} mol dm^{-3}). The electron releasing derivative (*p*-OMe, **66**) emitted at an even higher wavelength and although the electron poor derivative (*p*-F, **67**) was not significantly shifted, an increase in emission intensity was observed. Fluorescence was completely eliminated upon the addition of a nitro

group (**97**); the electronic excitation energy is rapidly dissipated in the presence of this moiety (**Table 2.7**).[135]

Table 2.7 UV−Vis data, calculated ε values and fluorescence emission data for compounds functionalised at the C-6 position.



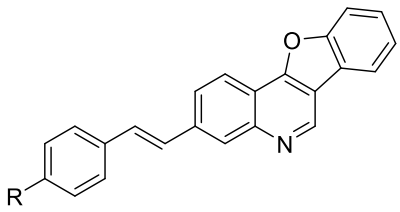
65, $R^1 = R^2 = H$
66, $R^1 = OMe$, $R^2 = H$
67, $R^1 = F$, $R^2 = H$
97, $R^1 = H$, $R^2 = NO_2$

compound	λ_{max} (nm)	ε^a ($dm^3\ mol^{-1}\ cm^{-1}$)	λ_{em} (nm)
86	257	63300	353
65	301	45188	389
66	259	38338	416
67	300	42000	388
97	285	18185	–

[a]ε calculated at 8×10^{-6} mol dm^{-3} with the exception of **97** which was calculated at 2×10^{-5} mol dm^{-3} due to a lack of UV activity below this concentration.

Virtually identical trends were observed for the substitution of the C-7 position with the same styrene derivatives in both absorption and emission spectra. Functionalisation at this position yielded a slightly larger red shift in λ_{max} and λ_{em} for the styrene (**69**) and fluorostyrene (**71**) derivatives. The electron poor substrate (*p*-F, **71**) also exhibited a notable hyperchromic effect with respect to **69** (**Table 2.8**).

Table 2.8 UV−Vis data, calculated ε values and fluorescence emission data for compounds functionalised at the C-7 position.



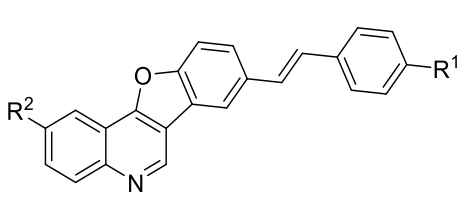
69, R = H
70, R = OMe
71, R = F

compound	λ_{max} (nm)	ε^a ($dm^3\ mol^{-1}\ cm^{-1}$)	λ_{em} (nm)
86	257	63300	353
69	337	38500	387
70	260	31700	421
71	336	43638	386

[a]ε calculated at 8×10^{-6} mol dm^{-3}.

Addition of styrene derivatives to the phenoxy ring produced complementary absorption spectra, with λ_{max} just a single nm longer than **86** in each case. Shifts analogous to those noted in the cases of C-6 and C-7 substitution were observed here, with the electron poor substrate (*p*-F, **75**) exhibiting fluorescence activity at concentrations as low as 6×10^{-8} mol dm^{-3}. Formation of a push-pull system with a methoxy group at C-6 and a fluorine on the styrene (**95**) induced a red shift in λ_{max} relative to the fluorostyrene derivative (**75**). This combination did not cause any considerable shift in λ_{em} but did increase the intensity at which emission occurred. The push-pull system formed in the opposite direction, with a trifluoromethyl group at C-6 and a methoxy group on the styrene (**96**) induced a very slight hypsochromic shift on λ_{max} compared to the absorption spectrum of the vinylanisole derivative (**74**). The λ_{em} for this compound was the lowest energy emission recorded throughout the series but was only fluorescent at concentrations higher than any of the other functionalised compounds (**Table 2.9**).

Table 2.9 UV−Vis data, calculated ε values and fluorescence emission data for compounds functionalised on the phenoxy ring.



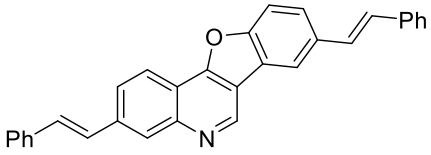
73, $R^1 = R^2 = H$
74, $R^1 = OMe$, $R^2 = H$
75, $R^1 = F$, $R^2 = H$
95, $R^1 = OMe$, $R^2 = F$
96, $R^1 = CF_3$, $R^2 = OMe$

compound	λ_{max} (nm)	ε^a ($dm^3\ mol^{-1}\ cm^{-1}$)	λ_{em} (nm)
86	257	63300	353
73	258	36538	382
74	258	42688	409
75	258	39788	381
95	268	13025	382
96	256	32238	463

[a]ε calculated at 8×10^{-6} mol dm^{-3}.

The disubstituted analogue (**77**) exhibited a bathochromic shift in λ_{max} compared to **86** and again gave a large value for ε. It is the only compound which demonstrates a hypsochromic shift in emission intensity, albeit by less than 10 nm compared to **86**.

Table 2.10 UV−Vis data and calculated ε values for the disubstituted structure.



77

compound	λ_{max} (nm)	ε^a ($dm^3\ mol^{-1}\ cm^{-1}$)	λ_{em} (nm)
86	257	63300	353
77	343	51075	346

[a]ε calculated at 8×10^{-6} mol dm^{-3}

All compounds exhibit their λ_{max} in the near UV region and are red-shifted (lower wavelength, higher energy) compared to **86**, with the exception of **96**. All calculated ε values are in the range of $10^4\ dm^3\ mol^{-1}\ cm^{-1}$, indicating that the electronic

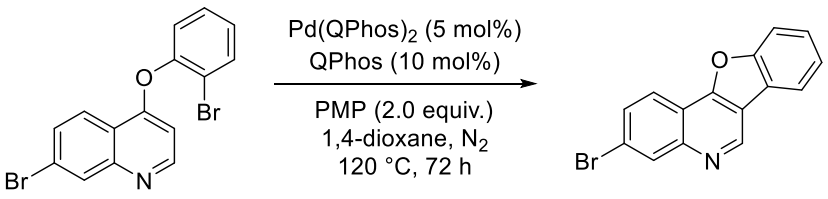
transitions are both spin- and orbit- allowed, albeit not as efficiently as those in **86**. The addition of further auxochromes to the substituted frameworks resulted in different shifts in absorption and emission maxima. Increases in emission intensity were ascertained for certain molecules as well as a decrease in the concentration at which fluorescence could occur.

2.17. Reversible Oxidative Addition

Palladium-catalysed cross-coupling reactions have provided access to an assortment of products with exceptional functional group tolerance. As remarked by Lautens however, polyhalogenated substrates are 'notably absent' from the scopes of these catalytic systems.[54] Regio- and chemo-selectivity issues are often encountered as the metal can undergo oxidative addition into a non-productive carbon-halogen bond. Formerly, this process resulted in a catalytic dead-end, as the OA step was considered irreversible. This limitation has been addressed in recent years through the development of catalyst/ligand systems that can promote both addition to and elimination from a single carbon-halogen bond. In particular, the use of sterically encumbered phosphine ligands has allowed for the isolation of halogen-bearing products in several cases (*vide supra*). This section describes how di-bromophenoxyquinolines can undergo direct arylation with retention of one of the carbon-bromine bonds – we suspect reversible oxidative addition (ROA) is at play in this system.

2.17.1 Previous Work

As described previously, di-bromophenoxyquinolines such as **57** and **60** failed to undergo the intramolecular C-H functionalisation/cyclisation reaction using $Pd(OAc)_2$. An irreversible OA of the metal into the C-Br bond on the quinoline backbone was suspected. We hoped that under certain conditions this OA step could be rendered reversible, facilitating the DA reaction while retaining the quinoline C-Br bond on the cyclised product. Another member of the McGlacken group carried out the initial studies on this work.[60] Various sterically bulky ligands were tried in conjunction with $Pd(OAc)_2$ on di-bromo substrates **57** and **60**, as well as the 6- and 7-iodo 4-(2-bromophenoxy)quinolines **80** and **81**. Finally, the combination of QPhos ligand with $Pd(QPhos)_2$ gave the cyclised, brominated product **98** in 13% isolated yield (**Scheme 2.41**). [60,98] The isolated yield does not represent the entire conversion of starting material to product (~20%) as the polarities of the substrate and cyclised quinoline are very similar, and separation was reported to be difficult.



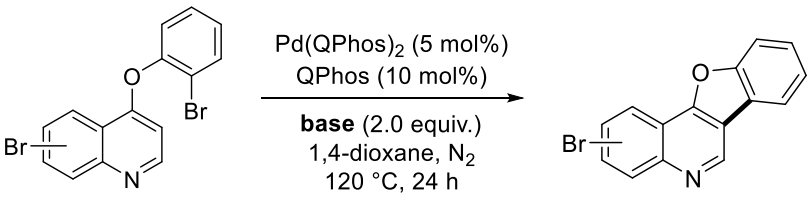
60 **98**, 13%

Scheme 2.41 Suspected reversible oxidative addition of **60**, as optimised by Dr Rachel Shanahan. Yield is isolated.[60]

2.17.2 Optimisation Attempts

To promote the cyclisation process, we sought to optimise the conditions used by Lautens and co-workers,[98] first turning to the reagents employed in our optimised DA and one-pot protocols. Initially, Cs_2CO_3 was trialled as an alternative base to PMP, with both **57** and **60**. The latter substrate proved slightly more promising by ^{1}H NMR analysis of the crude reaction mixtures (**Table 2.11**). Switching the base to K_2CO_3 increased the yield by NMR, and **98** was isolated in 22% yield.

Table 2.11 Attempted ring-closing reaction of **57** and **60** using a carbonate base.



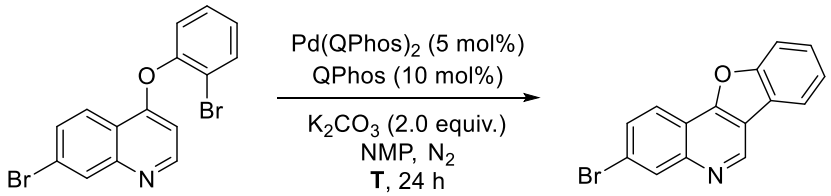
57, **60** **98**, **99**

substrate	base	yield (%)[a]
57 (C-6)	Cs_2CO_3	**99**, 31
60 (C-7)	Cs_2CO_3	**98**, 38
60 (C-7)	K_2CO_3	**98**, 55 (22)

[a]Yield calculated from the ^{1}H NMR spectrum of the crude reaction mixture using 1,3,5-trimethoxybenzene as the internal standard, isolated yield in parentheses.

Next, we turned to the solvent which gave the highest yield in our DA reactions, NMP at 135 °C.[60] Complete degradation of di-bromoquinoline starting material **60**, and no evidence of cyclised product was observed by ^{1}H NMR analysis after 24 hours. This reaction was repeated at 120 °C to give **98** in 15% yield by NMR (**Table 2.12**).

Table 2.12 Attempted ring-closing reaction of **60** in NMP.



60 **98**

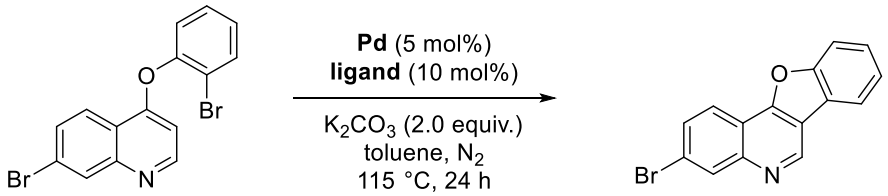
temperature (°C)	yield (%)[a]
135	0
120	15

[a]Yield calculated from the ^{1}H NMR spectrum of the crude reaction mixture using 1,3,5-trimethoxybenzene as the internal standard.

We then turned our attention to performing a further set of optimisation reactions with various catalyst and ligand combinations on substrate **60** (**Table 2.13**). A significant number of reported ROA protocols adopt toluene as solvent,[54,93,95-98] and so this was primarily used in the screen. Previously published work had also shown that a stoichiometric amount of iodide could stimulate ROA in aryl bromides, obviating the need to use expensive aryl iodides for this type of protocol.[96] The most effective source was found to be potassium iodide, which allowed for halogen exchange and promoted catalytic turnover through reductive elimination.[96] Another paper by Lautens and co-workers[97] outlined how using NEt_3 as an additive in toluene almost doubled the yield of their iodinated products, although the reason for this increase remains unclear.

Interestingly, ROA can be achieved using $Pd(QPhos)_2$ in the absence of extra QPhos ligand (**Table 2.13**, entry 2, 16). Also noteworthy is that increasing the reaction time from 24 to 72 hours enhanced conversion to cyclised product in toluene with NEt_3 (entry 3 and 4), but the same effect was not observed in 1,4-dioxane (entry 13). None of the conditions screened in toluene improved upon the previous result in 1,4-dioxane. The addition of NEt_3 (entry 15), an extra equivalent of base (entry 14) and the inclusion of KI in the system (entry 17) did not improve the yields observed by ^{1}H NMR analysis.

Table 2.13 Attempted optimisation of ring-closing conditions.



60 **98**

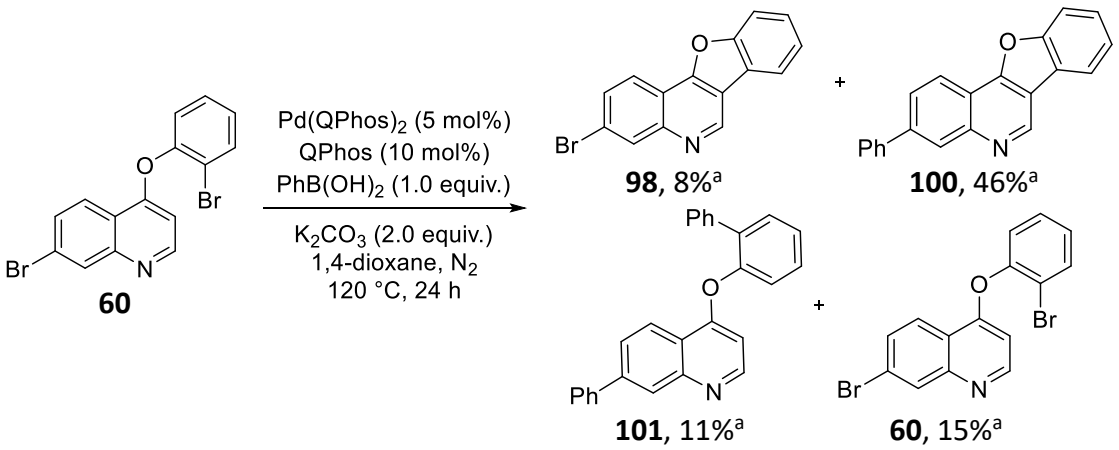
entry	catalyst	ligand	additive	yield (%)[a]
1	$Pd(QPhos)_2$	QPhos	–	32
2	$Pd(QPhos)_2$	–	–	24
3	$Pd(QPhos)_2$	QPhos	NEt_3 1.0 equiv.	17
4[b]	$Pd(QPhos)_2$	QPhos	NEt_3 1.0 equiv.	43
5	$Pd(dba)_2$	QPhos	–	8
6	$Pd(dba)_2$	QPhos	NEt_3 1.0 equiv.	5
7	$Pd(OAc)_2$	P(*t*-Bu)$_3$.HBF_4	–	1
8	$Pd(OAc)_2$	P(*t*-Bu)$_3$.HBF_4	NEt_3 1.0 equiv.	0
9	$Pd(OAc)_2$	QPhos	–	0
10	$Pd(OAc)_2$	QPhos	NEt_3 1.0 equiv.	0
11	$Pd(P(t\text{-}Bu)_3)_2$	P(*t*-Bu)$_3$.HBF_4	–	3
12	$Pd(P(t\text{-}Bu)_3)_2$	–	–	5
13[b,c]	$Pd(QPhos)_2$	QPhos	–	24
14[c,d]	$Pd(QPhos)_2$	QPhos	–	19
15[c]	$Pd(QPhos)_2$	QPhos	NEt_3 1.0 equiv.	21
16[c]	$Pd(QPhos)_2$	–	–	48
17[c]	$Pd(QPhos)_2$	QPhos	KI 2.0 equiv.	29
18[c]	$Pd(dba)_2$	QPhos	–	20
19[c]	$Pd_2(dba)_3$	QPhos	–	10
20[c]	$Pd_2(dba)_3$	P(*t*-Bu)$_3$.HBF_4	–	1
21[c]	$Pd(P(t\text{-}Bu)_3)_2$	P(*t*-Bu)$_3$.HBF_4	–	1

[a]Yields calculated from the ^{1}H NMR spectrum of the crude reaction mixture using 1,3,5-trimethoxybenzene as the internal standard. [b]Reaction time increased to 72 h. [c]Reaction carried out at 120 °C in 1,4-dioxane. [d]3.0 equiv. K_2CO_3 used.

2.17.3 Investigation of Carbon-Bromine Bond Reactivity

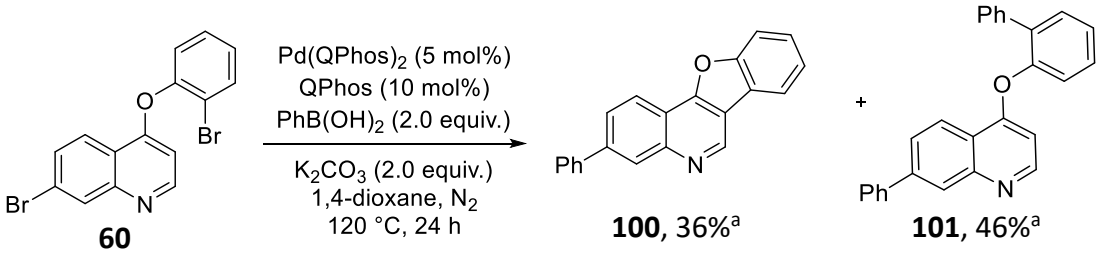
As no combination of ligand, catalyst and additive appeared to improve upon a 55% yield by NMR, we decided to examine the reactivity of the two C-Br bonds. We firstly wanted to confirm that ROA was occurring, as we were aware that the Pd(QPhos) system could simply favour OA at the phenoxy C-Br bond over that on the quinoline backbone. We also considered that ROA could ensue in the C-Br bond on the phenoxy ring, instead of, or as well as on the quinoline ring, possibly inhibiting the desired ring-closing pathway. To investigate these hypotheses, a number of experiments were undertaken employing the $Pd(QPhos)_2$/QPhos system.

Firstly, we looked at the addition of a single equivalent of phenyl boronic acid to our reaction (0.5 equiv. relative to the number of C-Br bonds). The minor product of this experiment was ring-closed compound **98**, with the reaction predominantly yielding SM/DA product **100** (**Scheme 2.42**). A small amount of another ring-open quinoline was produced, postulated to be di-arylated product **101**. As described previously when using $Pd(OAc)_2$ (albeit with C-Br at C-6, **Scheme 2.33**), the SM reaction takes place first, exclusively at the quinoline C-Br bond and no brominated cyclised product was observed. The below experiment verifies that OA at the quinoline bromide is also possible using $Pd(QPhos)_2$. SM/DA product **100** is observed in reasonable yield, although it is difficult to conclude which of the two steps comes first, particularly given the presence of **98** in the reaction mixture. It is possible that DA occurs first with the expelled palladium then adding to the C-Br bond on the quinoline, or that the SM reaction occurs on the quinoline first and the DA reaction follows to yield **100**. Also worth noting is that the yields calculated by NMR in this case give a total of 80%, suggesting that some of the reaction components undergo decomposition, or are not decipherable by ^{1}H NMR analysis.



Scheme 2.42 Use of 1.0 equiv. $PhB(OH)_2$ to probe the reactivity of C-Br bonds in the di-bromophenoxyquinoline system. [a]Yields calculated from the ^1H NMR spectrum of the crude reaction mixture using 1,3,5-trimethoxybenzene as the internal standard.

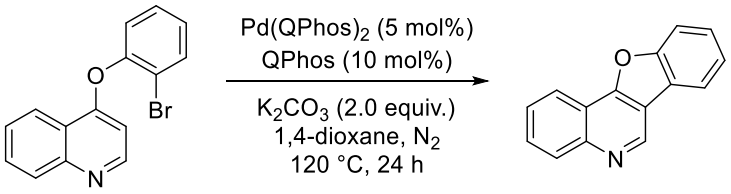
Given the limited amount of coupling partner in the reaction above, we wished to offer sufficient boronic acid to both C-Br sites and so we introduced a second equivalent of $PhB(OH)_2$ to the experiment. Only **100** and **101** were observed by ^1H NMR analysis of the crude reaction mixture (**Scheme 2.43**). From this experiment, a portion of **101** was successfully isolated and its structure confirmed by ^1H and ^{13}C NMR analysis. Di-arylated product **101** had never been identified as a side product in our one-pot SM/DA reactions using $Pd(OAc)_2$ and NMP. We therefore concluded that the addition of palladium to both C-Br bonds was possible and likely under these conditions.



Scheme 2.43 Use of 2.0 equiv. $PhB(OH)_2$ to probe the reactivity of C-Br bonds in the di-bromophenoxyquinoline system. [a]Yields calculated from the ^1H NMR spectrum of the crude reaction mixture using 1,3,5-trimethoxybenzene as the internal standard.

Next, we proceeded to investigate the success of the SM and DA reactions individually using the $Pd(QPhos)_2$ system. First, we applied the catalyst/ligand combination to mono-bromophenoxyquinoline **45** to gauge the success of the ring-

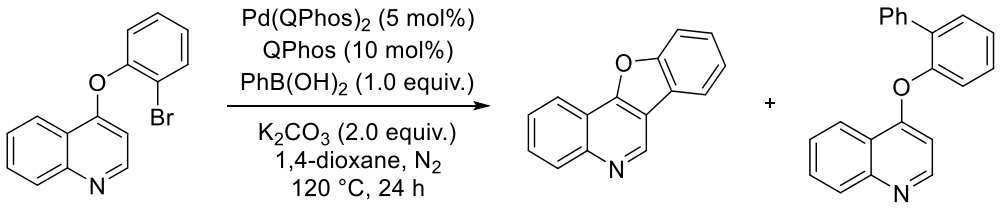
closing step under these conditions (**Scheme 2.44**). As already discussed, catalytic Pd(0) sources proved less productive than Pd(II) sources in the ring-closing reaction (**Table 2.5**). $Pd(QPhos)_2$ was no exception, furnishing the benzofuroquinoline **86** in 22% yield by NMR. Effectively, although OA is facile at this position, the actual ring-closing step is sluggish when using $Pd(QPhos)_2$. This may indicate why the SM reaction is made possible at the phenoxy C-Br of **60** in the presence of a $PhB(OH)_2$.



45 **86**, 22%[a]

Scheme 2.44 DA reaction using $Pd(QPhos)_2$ and QPhos in 1,4-dioxane. [a]Yield calculated from the ^1H NMR spectrum of the crude reaction mixture using 1,3,5-trimethoxybenzene as the internal standard.

More evidence pertaining to the theory that a SM reaction will outcompete cyclisation under the $Pd(QPhos)_2$/dioxane conditions was provided by a further reaction involving the addition of $PhB(OH)_2$. Similarly to the reaction of **60** described above, a small portion of cyclised product **86** and a ring-open quinoline were observed by ^1H NMR analysis (**Scheme 2.45**). Ring-open species **102** was isolated in 81% yield, affirming the occurrence of a SM reaction on the phenoxy ring. From this we confirmed that OA is facile at the phenoxy C-Br bond using $Pd(QPhos)_2$. The resulting carbopalladated species is either influenced by the QPhos ligand to induce a conformation more susceptible to SM coupling, or, the ring-closing reaction is slowed by the presence of the QPhos ligand.

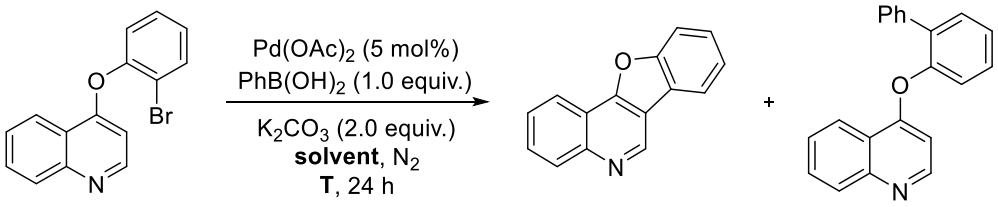


45 **86**, 20%[a] **102**, 81%

Scheme 2.45 Investigating the progression of the DA reaction in the presence of 1.0 equiv. $PhB(OH)_2$. [a]Yield calculated from the ^1H NMR spectrum of the crude reaction mixture using 1,3,5-trimethoxybenzene as the internal standard.

We next considered the difference in solvent and catalyst used between the above reactions and the optimised DA and one-pot protocols ($Pd(OAc)_2$/NMP). Three experiments were performed using $Pd(OAc)_2$ (**Table 2.14**). Firstly, one equivalent of $PhB(OH)_2$ was added to the standard ring-closing reaction at 135 °C. No conversion to **102** was observed. The same experiment was carried out in 1,4-dioxane at 120 °C and a complete reverse in reactivity was obtained, giving 73% yield by NMR of **102** and only 27% of the fused benzofuroquinoline **86**. Finally, the experiment was repeated using NMP at 120 °C to give **86** in 79% and **102** in 18% yield by NMR. Thus, the SM reaction is favoured in 1,4-dioxane and the cyclisation reaction is favoured at either temperature in NMP, suggesting that NMP is a non-innocent solvent in the DA reaction.

Table 2.14 Addition of $PhB(OH)_2$ to the DA reaction with $Pd(OAc)_2$.



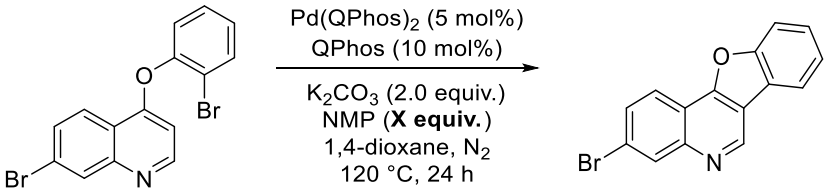
45 **86** **102**

solvent	temperature (°C)	yield **86** (%)[a]	yield **102** (%)[a]
NMP	135	86	–
1,4-dioxane	120	27	73
NMP	120	79	18

[a]Yields calculated from the ^{1}H NMR spectrum of the crude reaction mixture using 1,3,5-trimethoxybenzene as the internal standard.

From these experiments it was evident that NMP was an important component for the ring-closing reaction. Using NMP as the solvent had proved ineffective for this system (*vide supra*) and we therefore employed it as an additive in 1,4-dioxane for the ROA reaction (**Table 2.15**). Disappointingly, varying amounts of NMP did not aid the cyclisation reaction, but rather inhibited it.

Table 2.15 Use of NMP as an additive in the ROA reaction.



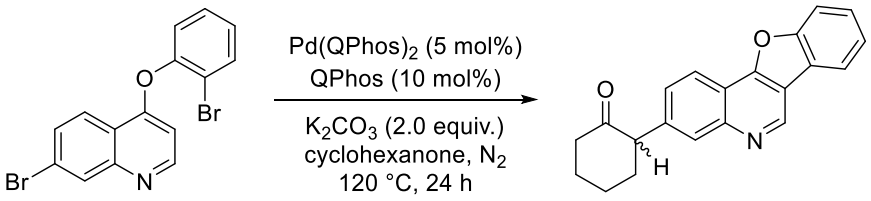
60 **98**

NMP	yield (%)[a]
2.0 equiv.	24
10.0 equiv.	~8[b]
20.0 equiv.	~6[b]

[a]Yields calculated from the ^{1}H NMR spectrum of the crude reaction mixture using 1,3,5-trimethoxybenzene as the internal standard. [b]More than one cyclised product and degradation of starting material detected.

Then, we sought to encourage the C-H cleavage step through utilisation of additives reported to promote such reactions.[18] The hydrogen bonding capacity of HFIP makes it an excellent candidate for use as a solvent/co-solvent in C-H functionalisation reactions,[136] PivOH and $ZnCl_2$ are commonly exploited as acidic co-catalysts,[137-139] and Ag_2CO_3 is used an external oxidant to mediate C-H cleavage, or to (re)generate an active catalytic species.[129,140] All of these additives were trialled in conjuction with our Pd(QPhos)/QPhos system; none seemed to enhance the cyclisation reaction however, mostly yielding starting material and degradation products as observed by ^{1}H NMR analysis of the crude reaction mixtures.

Other high boiling point solvents such as DMA and DMF were also applied to the system but neither gave any conversion to **98** at 120 °C, as evident by ^{1}H NMR analysis. Cyclohexanone was also adopted as a solvent for the ROA reaction. Although this system did not yield any of the desired product **98**, another cyclised product **103** was observed by ^{1}H NMR analysis. Isolation and characterisation of this species elucidated the occurrence of a one-pot α- arylation/DA reaction (**Scheme 2.46**). The palladium-catalysed α-arylation of ketones with quinolines and pyrdines has been reported previously in the literature,[141-146] but to the best of our knowledge there are no studies which detail the combination of α- arylation with a DA step.



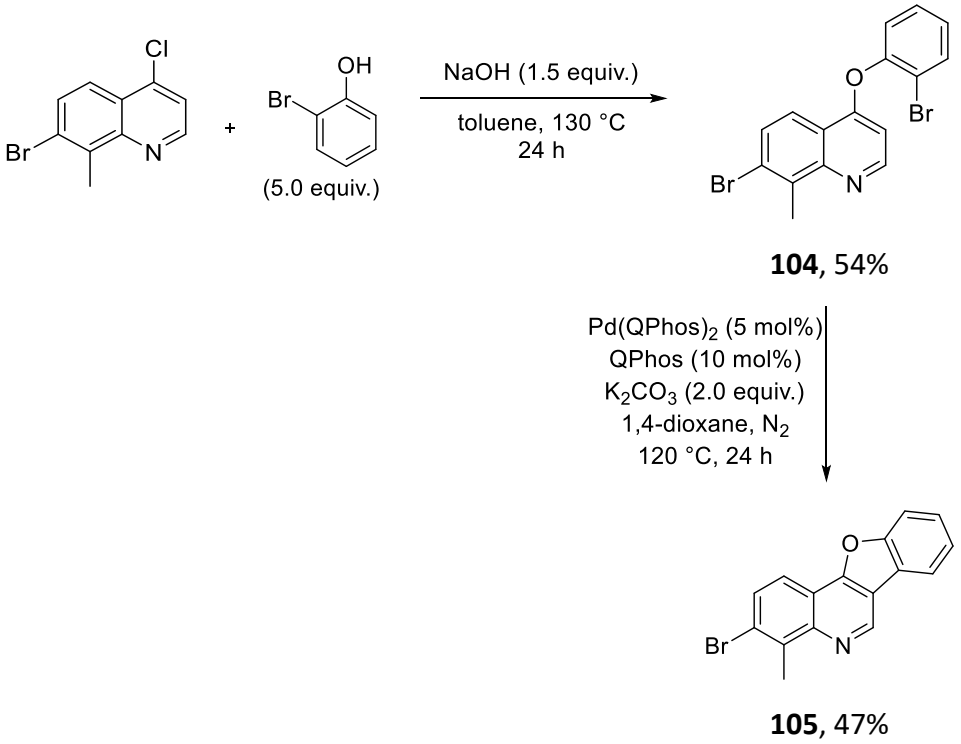
60 **103**, 73%

Scheme 2.46 One-pot α- arylation/DA reaction in cyclohexanone. Yield is isolated.

2.17.4 Substrate Modifications

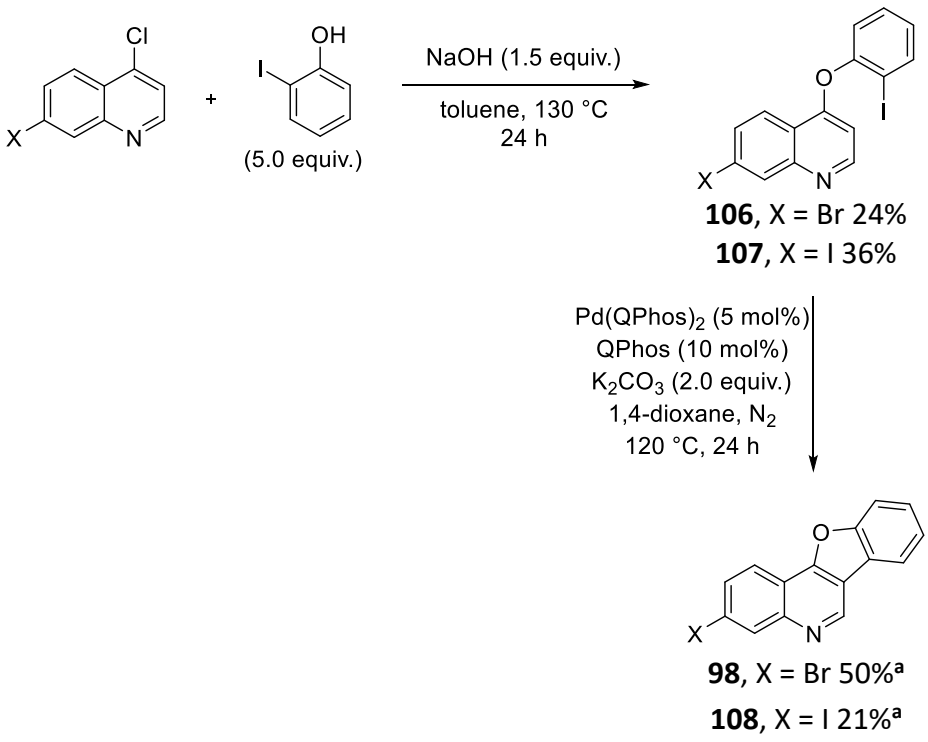
As none of the endeavours to promote the DA reaction were successful, we then moved to modify the substrate in order to improve the yield of a halogen-bearing, cyclised product. We envisaged that substitution of the quinoline ring proximal to the C-Br bond could promote the key RE step. Compound **104** was synthesised using the methods described previously from the commercially available 4-chloroquinoline

starting material. Substrate **104** was then subjected to the $Pd(QPhos)_2$ system and brominated product **105** was isolated in 47% yield (**Scheme 2.47**). It is worth noting that addition of phenyl boronic acid to the reaction mixture allowed for a SM reaction to take place at the quinoline C-Br site, verifying that OA is possible here.



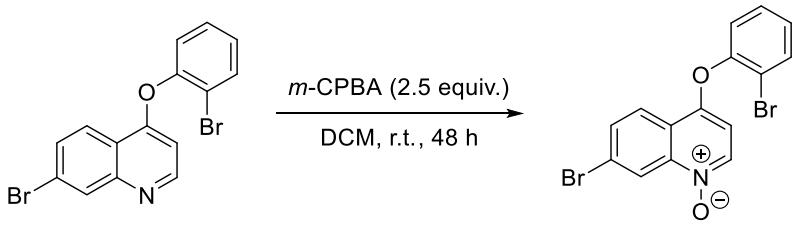
Scheme 2.47 Synthesis of a sterically hindered starting material and subsequent reaction of a substrate sterically encumbered proximal to the C-Br bond on the quinoline ring.

Next, we looked to promote the reaction through use of weaker carbon-iodine bonds on either ring.[147] Substrates **106** and **107** were synthesised using the methods described previously and subjected to the standard conditions. Again, the introduction of this labile bond did not induce an increase in conversion to cyclised product in either case, as observed by ^{1}H NMR analysis. In fact, in the case of **107**, the yield was reduced when compared to the reaction of dibromo substrate **60** (**Scheme 2.48**).



Scheme 2.48 Use of labile C-I bond on the phenoxy ring in an attempt to promote the ring-closing reaction. [a]Yield calculated from the ^{1}H NMR spectrum of the crude reaction mixture using 1,3,5-trimethoxybenzene as the internal standard.

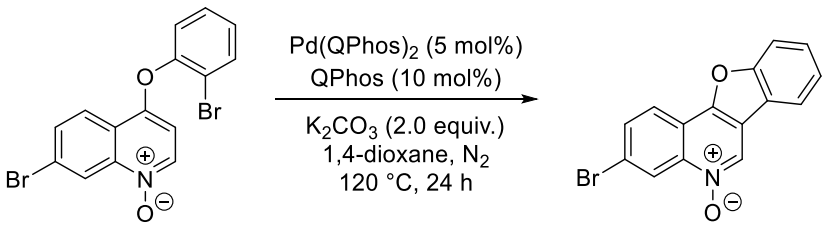
When this strategy did not improve conversion, we considered increasing the acidity, and perhaps weakening the strength of the C-H bond at the C-3 position by altering the electronics of the system. First di-bromophenoxyquinoline *N*-oxide **109** was synthesised using *m*-CPBA in excellent yield (**Scheme 2.49**).



60 **109**, 96%

Scheme 2.49 Synthesis of a di-bromophenoxyquinoline *N*-oxide.

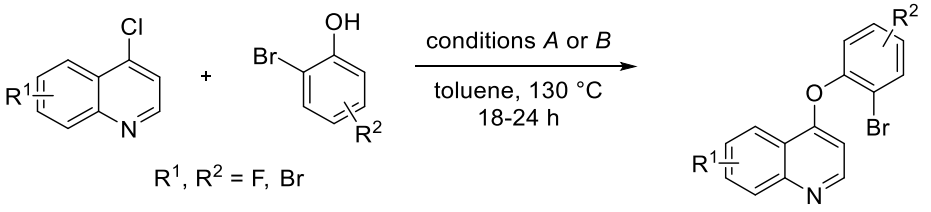
Disappointingly, the introduction of an oxide did not enhance the reversible oxidative addition reaction and the cyclised, brominated product **110** was detected in only 35% yield by NMR (**Scheme 2.50**).



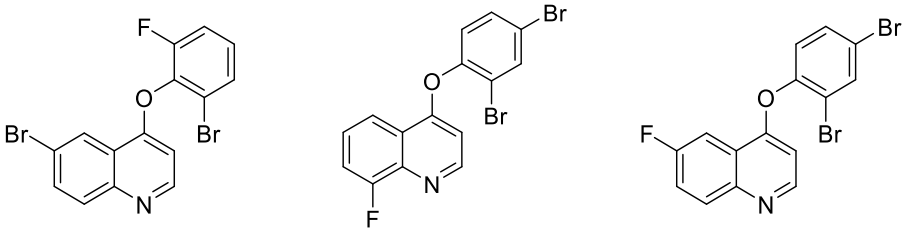
109 **110**, 35%

Scheme 2.50 Use of di-bromophenoxyquinoline *N*-oxide in an attempt to promote the ring-closing reaction. Yield calculated from the ^{1}H NMR spectrum of the crude reaction mixture using 1,3,5-trimethoxybenzene as the internal standard.

Next, we looked at placing various electron-withdrawing substituents on both the phenoxy and the quinoline rings to decrease the strength of the C-H bond at C-3, and thus encourage cyclisation (**Scheme 2.51**). This modification assumes a CMD-type mechanism is at play for the ring-closing step (**Scheme 2.34**).[118-120]



111–113

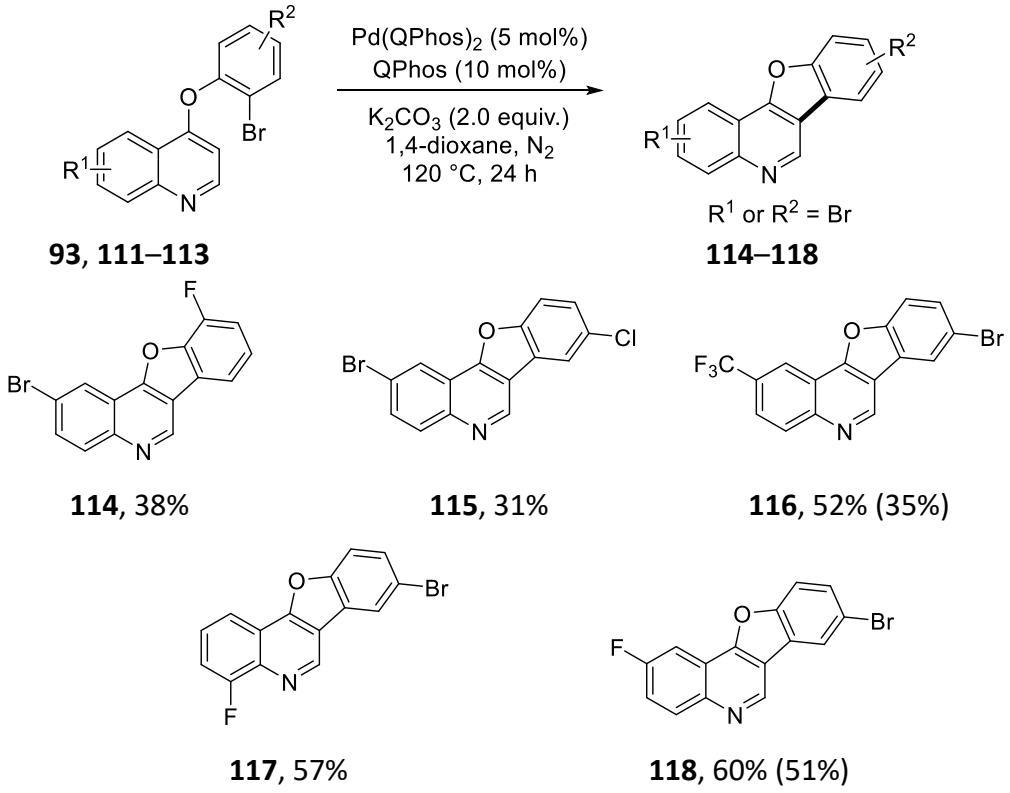


111, *A*, 91% **112**, *B*, 74% **113**, *B*, 54%

Scheme 2.51 Substituted 4-(2-bromophenoxy)quinoline substrates. *A*: DMAP (3.0 equiv.) and substituted 2-bromophenol (1.5 equiv.). *B*: NaOH (1.5 equiv.) and 2-bromophenol (5.0 equiv.).

These substrates were then subjected to the Pd(QPhos)$_2$ conditions (**Scheme 2.52**). Introduction of a fluorine onto the phenoxy ring did not increase conversion to brominated product **114**. The installation of a chlorine on this ring also did not encourage the cyclisation reaction to form **115** (starting material synthesised by

another member of the group[60]). Compound **93**, which had been synthesised previously, gave appreciable conversion to brominated product **116**, which was isolated in 35% yield. The addition of a fluorine to the quinoline ring appeared to have a positive impact on the conversion to brominated products **116**–**118**, and **118** was isolated in 51% yield.



93, **111**–**113**

114–**118**

114, 38%

115, 31%

116, 52% (35%)

117, 57%

118, 60% (51%)

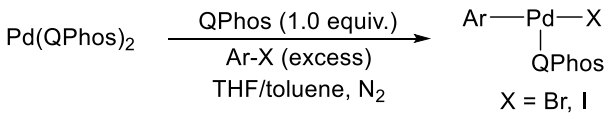
Scheme 2.52 ROA of substituted di-bromophenoxyquinoline substrates. Yields calculated from the ^{1}H NMR spectrum of the crude reaction mixture using 1,3,5-trimethoxybenzene as the internal standard. Isolated yields in parentheses.

2.17.5 Attempted Isolation of the Oxidative Addition Product

To prove that the halide on the quinoline ring was retained through a reversible OA pathway, we sought to prove the occurence of the transient, non-productive OA complex Ar-Pd-Br in our catalytic cycle. Efforts to identify and isolate this species proved unsuccessful, however, a summary of our attempts is given below.

Based on the literature, we envisaged the existence of a 3-coordinate palladium complex (**Scheme 2.53**). We hoped to isolate the species using careful manipulation techniques,[148-149] or identify it *in situ* using NMR spectroscopy (^{1}H, ^{31}P).[54,89,150] These

compounds require careful handling under an inert atmosphere and, in general, are synthesised by employing the palladium source as the limiting reagent, the phosphine ligand in slight excess and the aryl-halide in excess (sometimes as solvent) in either THF or toluene. Experiments that identify the species *in situ* usually involve benzene-d_6 or THF-d_8 as the solvents of choice.

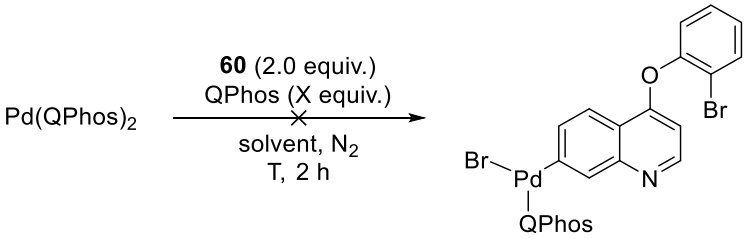


Scheme 2.53 General scheme for the isolation of a 3-coordinate palladium complex.

Once identified, we intended to use the palladium complex to prove that ROA was occuring in our system by subjecting the species to our optimised conditions to induce RE and observe reformation of the aryl halide Ar-X. This could also be achieved by using the isolated complex as the only Pd-source for the reaction, where progression to the cyclised product would only ensue if an active palladium species could be released *via* RE from the complex.

Our initial studies looked at isolating 3-coordinate species **119** that we suspected was formed in the reaction of **60** to give **98**, in either THF or toluene (**Table 2.16**). As the ^{1}H NMR spectra of the crude reaction mixtures were crowded by excess substrate **60** and ligand, the reaction was analysed using ^{31}P NMR. Much to our disappointment, the only peaks present in the ^{31}P spectra of the concentrated mixtures in $CDCl_3$ were those attributed to $Pd(QPhos)_2$ (62.4 ppm) and the free QPhos ligand (26.4 ppm).

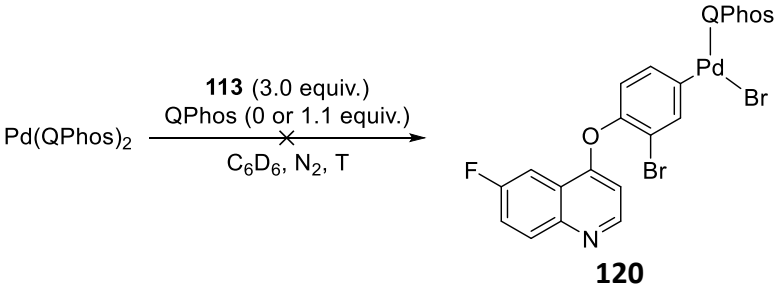
Table 2.16 Attempted isolation of 3-coordinate palladium complex **119**.



119

QPhos (equiv.)	solvent	temperature (°C)
1.1	THF	70
1.1	toluene	100
–	THF	70
–	toluene	100

Next, we looked at using our 'most active' substrate **113**, which had given a 60% yield by NMR of cyclised, brominated product **118**. This time we wished to observe the *in situ* generation of complex **120** by both ^{31}P and ^{19}F NMR analysis. The solutions in this case were prepared in a Schlenk tube in C_6D_6 and were then transferred into NMR tubes under an inert atmosphere (**Scheme 2.54**). The samples were analysed periodically over 48 hours by NMR and when no change was observed, were heated to 65 °C for 24 hours. The samples were then cooled to r.t. and analysed again over 48 hours but only peaks representative of $Pd(QPhos)_2$ (62.4 ppm), QPhos ligand (25.3 ppm) and QPhos=O (60.8 ppm) were observed. No new species was identified by ^{19}F NMR analysis.

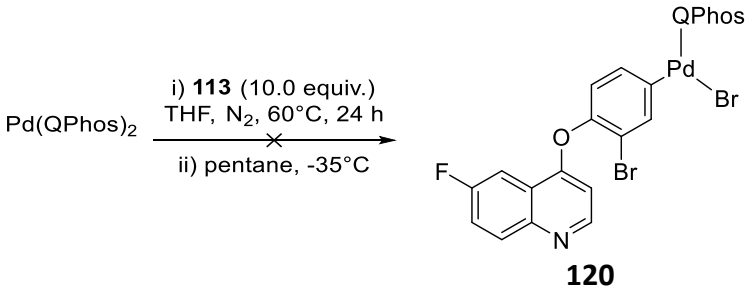


120

Scheme 2.54 NMR experiments to identify 3-coordinate palladium complex **120**.

The isolation of similar OA products often employ a large excess of the halogen-containing reagent. In an attempt to mimic these conditions, 10.0 equiv. of **113** was

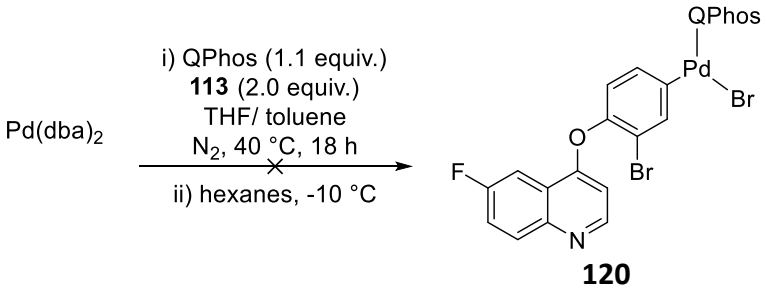
added to the reaction mixture.[149] Reported conditions involve cooling the mixture to cryogenic temperatures in pentane in order to precipitate out the desired complexes. In our hands however, no solid was observed and again, no new peaks were evident by NMR analysis.



120

Scheme 2.55 Attempted isolation of 3-coordinate palladium complex **120**.

Although $Pd(QPhos)_2$ is the catalyst of choice for these reactions, we considered the possibility of using an alternative Pd-source to isolate **120**, as demonstrated by Hartwig for a similar system.[148] This strategy was applied using $Pd(dba)_2$ in THF/toluene at 40 °C for 18 hours (**Scheme 2.56**). Upon addition of hexanes and cooling to -18 °C, a brown precipitate was observed, which was isolated by suction filtration. Analysis of both the solid and filtrate gave no indication of the presence of complex **120**, but rather showed peaks representative of $Pd(QPhos)_2$ and QPhos by ^{31}P NMR and only quinoline starting material **113** by ^{19}F NMR (-111 ppm).



120

Scheme 2.56 Attempted isolation of 3-coordinate palladium complex **120** using $Pd(dba)_2$ as the Pd source in THF and toluene.

Further investigations are necessary for the elucidation of the OA complexes present in these reactions and an internal referencing standard (e.g. triphenylphosphine oxide) should likely be added to future experiments/controls. This will help to avoid ambiguity and potential misinterpretation of results, considering that the difference

in resonance between ligated palladium species and complexed palladacycles is reported to be roughly 3 ppm by ^{31}P NMR.[54,89]

Conclusions and Future Work

The direct arylation of 4-(2-bromophenoxy)quinoline compounds to form fused benzofuroquinolines was demonstrated. From this methodology was developed a novel, one-pot, tandem Mizoroki-Heck/direct arylation strategy. Both procedures required no added ligand and the possible interaction between the palladium catalyst and quinoline substrate was examined using advanced NMR techniques. The structures of the palladium-quinoline complexes formed in solution were confirmed by HRMS and X-ray crystallography and this analysis elucidated the possible ligating role of the quinoline. The photophysical capacities of the functionalised benzofuroquinoline products were also investigated. Both the position and intensity of the absorption and emission maxima were tuneable, subject to the inclusion of various functional groups. Finally, a reversible oxidative addition protocol to allow for the isolation of cyclised, brominated quinoline products was explored.

Future work on this project will be mainly carried on from the ROA section of the Chapter. The potential for a one-pot arylation/DA reaction will be further explored and pursued. A major goal still lies in the identification and isolation of the suggested 3-cooridnate palladium complex. This complex will be utilised in a series of experiments to unequivocally prove the occurrence of reversible oxidative addition in the system.

Experimental

2.18. General Procedures

K_2CO_3 and Cs_2CO_3 were stored in an oven at 150 °C. 1,4-Dioxane was distilled over sodium/benzophenone under nitrogen and stored over flame-dried 4 Å molecular sieves. NaI was dried *via* Kugelrohr distillation before use. All other solvents and reagents were used as obtained from commercial sources and without purification.

Melting points were measured in a Thomas Hoover Capillary Melting Point apparatus.

Infrared spectra were measured on a Perkin-Elmer FT-IR spectrometer. Samples were dissolved in DCM and dispersed as thin films on NaCl plates, and the dichloromethane allowed to evaporate before measurement of sample.

Column chromatography was carried out using 60 Å (35-70 µm) silica. TLC was carried out on pre-coated silica gel plates (Merck 60 PF254). The developed plates were visualised under UV light.

High resolution precise mass spectra (HRMS) were recorded on a Waters LCT Premier Tof LC-MS instrument in University College Cork. Samples were run in electrospray ionisation (ESI) mode using 50% acetonitrile-water containing 0.1% formic acid as eluent; samples were made up at a concentration of *ca*. 1 mg mL^{-1}. HRMS of metal-containing complexes were recorded on a Bruker compact TOF-MS in the University of York. Samples were run in electrospray ionisation (ESI) mode using 50% MeOH-water as eluent; samples were made up at a concentration of *ca*. 1 mg mL^{-1}. Acquisitions were internally calibrated using sodium formate clusters.

Nuclear Magnetic Resonance (NMR) samples were run in deuterated chloroform ($CDCl_3$), deuterated dimethylsulfoxide ($(CD_3)_2SO$), deuterated dioxane ($C_4D_8O_2$), deuterated acetonitrile (C_2D_3N) or deuterated benzene (C_6D_6) as specified. ^1H NMR (600 MHz), ^1H NMR (400 MHz) ^1H NMR (300 MHz) spectra were recorded on Bruker Avance III 600, Bruker Avance 400 and Bruker Avance III 300 NMR spectrometers, respectively, in proton coupled mode using tetramethysilane (TMS) as the internal standard. ^{13}C NMR (150 MHz), ^{13}C NMR (100 MHz) and ^{13}C NMR (75 MHz) spectra

were recorded on Bruker Avance III 600, Bruker Avance 400 and Bruker Avance III 300 NMR spectrometers, respectively, in proton decoupled mode at 300 K using TMS as the internal standard. ^{19}F NMR (282 MHz) spectra were recorded on a Bruker Avance III 300 NMR spectrometer in proton decoupled mode at 300 K. ^{31}P NMR (121.5 MHz) spectra were recorded on a Bruker Avance III 300 NMR spectrometer in proton decoupled mode at 300 K. ^{1}H-^{15}N HMBC NMR spectra were recorded on a Bruker Avance III 600 NMR spectrometer [600 MHz (^{1}H), 60 MHz (^{15}N)], equipped with Bruker BBFO cryoprobe. All spectra recorded at 300 K and referenced externally to nitromethane at 380.2 ppm, the value of which was uncorrected. ^{1}H-^{15}N HMBC spectra were acquired using the Bruker HMBCqpndqf pulse program (2D H-1/X correlation *via* heteronuclear zero and double quantum coherence optimised on long range couplings), with 4 scans and spectral width of 600–650 ppm. All spectra were run at University College Cork. Chemical shifts (δ) are expressed as parts per million (ppm), positive shift being downfield from TMS; coupling constants (*J*) are expressed in Hertz (Hz), are reported as observed and their values are uncorrected. Splitting patterns in ^{1}H-NMR spectra are designated as: s (singlet), bs (broad singlet), d (doublet), dd (doublet of doublets), ddd (doublet of doublets of doublets), t (triplet), td (triplet of doublets), q (quartet), quin (quintet) and m (multiplet). Compounds were numbered for ease of assignment and do not necessarily represent IUPAC nomenclature.

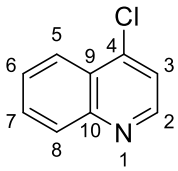
Single-crystal X-ray analysis was performed on a Rigaku AFC12 FRE-HF diffractometer equipped with an Oxford Cryosystems low-temperature device. The crystals were kept at a steady *T* = 100(2) K during data collection. The structures were solved with the **ShelXT**[151] structure solution program using the Intrinsic Phasing solution method and by using **Olex2**[152] as the graphical interface. The models were refined with version 2016/6 of **ShelXL**[151] using Least Squares minimisation. Cell parameters were retrieved and refined using the **CrysAlisPro** (Rigaku, V1.171.40.37a, 2019). All non-hydrogen atoms were refined anisotropically. Hydrogen atom positions were calculated geometrically and refined using the riding model.

UV-Visible absorption was measured on a Thermo Scientific Evolution 60S UV-Visible Spectrophotometer. All solutions were made up in DCM and measurements were

performed in high precision Quartz cells 10 mm in pathlength. A baseline in DCM was recorded by an internal reference detector. Molar absorption values were calculated using Beer's law at a concentration of 8×10^{-6} mol dm^{-3}. Fluorescence intensities were measured on PerkinElmer Fluorescence Spectrometer LS 55. All solutions were made up in DCM and measurements were performed in high precision Quartz cells 10 × 10 mm in pathlength. Spectra were recorded in the range 200–700 nm and compounds were excited at 257 nm.

2.19. Direct Arylation/One-Pot Substrates and Products

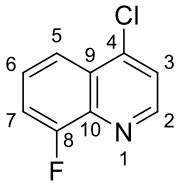
4-Chloroquinoline (42)[153]



Quinolin-4-ol (0.726 g, 5.0 mmol, 1.0 equiv.) was added to a Schlenk tube, dissolved in phosphoryl chloride (2.32 mL, 25.0 mmol, 5.0 equiv.) and the mixture was stirred at 110 °C, until all the starting material was consumed (4 h), as evident by TLC (DCM:MeOH 90:10). The cooled reaction mixture was slowly added to iced water (20 mL) with stirring. Solid $NaHCO_3$ was then added gradually until pH ~ 7 and the mixture was allowed to stir until effervescence ceased.[99] The mixture was transferred to a separating funnel and the organic layer was collected. The aq. layer was extracted with DCM (3 × 15 mL). The combined organic layers were washed with saturated $NaHCO_3$ solution (15 mL), H_2O (15 mL), and brine (20 mL), dried over $MgSO_4$, filtered and concentrated under reduced pressure to yield **42** as a pink solid (0.709 g, 87%); m.p. 31–32 °C (lit.[154] 28–31 °C); ^{1}H NMR (300 MHz, $CDCl_3$) δ: 8.79 (d, *J* = 4.6 Hz, 1H, C(2)**H**), 8.24 (dd, *J* = 8.4, 1.0 Hz, 1H, C(5)**H**), 8.13 (d, *J* = 8.4 Hz, 1H, C(8)**H**), 7.79 (ddd, *J* = 8.4, 6.9, 1.2 Hz, 1H, C(7)**H**), 7.66 (ddd, J = 8.2, 6.9, 1.2 Hz, 1H, C(6)**H**), 7.50 (d, *J* = 4.7 Hz, 1H, C(3)**H**) ppm; ^{13}C NMR (75 MHz, $CDCl_3$) δ: 149.9 (**C**(2)H), 149.1 (q**C**-4), 142.7 (q**C**-10), 130.4 (**C**(7)H), 129.9 (**C**(8)H), 127.6 (**C**(6)H), 126.5 (q**C**-9), 124.2 (**C**(5)H), 121.3 (**C**(3)H) ppm; *m/z* (ES+): 164 ($(M+H)^+$ 100%).

Spectral characteristics were consistent with previously reported data.[153]

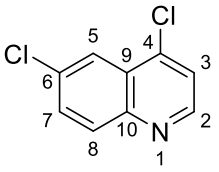
4-Chloro-8-fluoroquinoline (43)



Compound **43** was prepared *via* the procedure described for **42** using 8-fluoroquinolin-4-ol (0.571 g, 3.5 mmol, 1.0 equiv.) to yield **43** as a beige solid (0.623 g, 91%); m.p. 93–95 °C; IR (film) ν_{max} 1642 (C=N stretch), 1492 (aromatic C=C stretch), 1072, 666 cm^{-1}; ^{1}H NMR (300 MHz, $CDCl_3$) δ: 8.84 (d, *J* = 4.7 Hz, 1H, C(2)**H**), 8.03 (dt, *J* = 8.5, 1.1 Hz, 1H, C(5)**H**), 7.66–7.40 (m, 2H, C(3)**H**, C(6)**H**), 7.54–7.43 (m, 1H, C(7)**H**) ppm; ^{13}C NMR (75 MHz, $CDCl_3$) δ: 158.0 (d, $^1J_{(C,F)}$ = 258 Hz, q**C**(8)F), 149.9 (**C**(2)H), 142.6 (d, $^4J_{(C,F)}$ = 5 Hz, q**C**(4)Cl), 139.4 (d, $^2J_{(C,F)}$ = 12 Hz, q**C**-10), 128.0 (q**C**-9), 127.3 (d, $^3J_{(C,F)}$ = 8 Hz, **C**(6)H), 122.2 (**C**(3)H), 119.8 (d, $^4J_{(C,F)}$ = 5 Hz, **C**(5)H), 114.5 (d, $^2J_{(C,F)}$ = 19 Hz, **C**(7)H) ppm;

^{19}F NMR (282 MHz, $CDCl_3$) δ: -124 ppm; HRMS (ESI-TOF) *m/z*: $[M+H]^+$ calcd for C_9H_6ClFN: 182.0173; found: 182.0164.

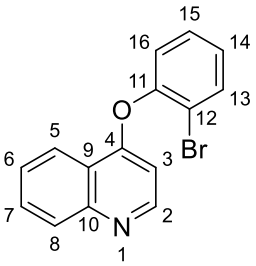
4,6-Dichloroquinoline (44)[155]



Compound **44** was prepared *via* the procedure described for **42** using 6-chloroquinolin-4-ol (0.629 g, 3.5 mmol. 1.0 equiv.) to yield **44** as a beige solid (0.552 g, 80%); m.p. 97–100 °C (lit.[155] 101–104 °C); IR (film) ν_{max} 1643 (C=N), 1487 (aromatic C=C), 646 (C-Cl) cm^{-1}; ^{1}H NMR (300 MHz, $CDCl_3$) δ: 8.77 (d, *J* = 4.7 Hz, 1H, C(2)**H**), 8.22 (d, *J* = 2.3 Hz, 1H, C(5)**H**), 8.07 (d, *J* = 9.0 Hz, 1H, C(8)**H**), 7.71 (dd, *J* = 9.0, 2.3 Hz, 1H, C(7)**H**), 7.52 (d, *J* = 4.7 Hz, 1H, C(3)**H**) ppm; ^{13}C NMR (75 MHz, $CDCl_3$) δ: 150.2 (**C**(2)H), 147.5 (q**C**-10), 141.6 (q**C**(4)Cl), 133.8 (q**C**(6)Cl), 131.5 (**C**(5)H), 131.4 (**C**(7)H), 127.3 (q**C**-9), 123.2 (**C**(8)H), 122.0 (**C**(3)H) ppm; *m/z* (ES+): 198 ($(M+H)^+$ 100%).

Spectral characteristics were consistent with previously reported data.[155]

4-(2-Bromophenoxy)quinoline (45)[36]

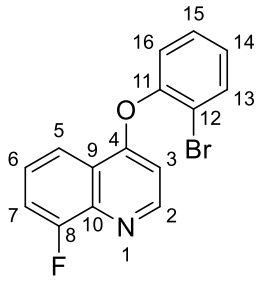


A mixture of **42** (0.164 g, 1.0 mmol, 1.0 equiv.), 2-bromophenol (0.58 mL, 5.0 mmol, 5.0 equiv.), crushed NaOH pellets (0.060 g, 1.5 mmol, 1.5 equiv.) and toluene (0.5 mL) was stirred in a sealed vial at 130 °C, until the reaction was complete (24 h), as evident by TLC (hexanes:EtOAc 90:10–80:20). The cooled reaction mixture was diluted with 10% aq. NaOH (5 mL) and stirred at r.t. for 1 h. The aq. layer was extracted with DCM (3 × 10 mL). The combined organic layers were washed with 6 M NaOH (2 × 10 mL), H_2O (10 mL), and brine (15 mL), dried over $MgSO_4$, filtered and concentrated under reduced pressure. Purification *via* column chromatography (hexanes:EtOAc 80:20) to yield **45** as a pale yellow solid (0.280 g, 93%); m.p. 61–63 °C (lit.[36] 62–64 °C); ^{1}H NMR (300 MHz, $CDCl_3$) δ: 8.67 (d, *J* = 5.1 Hz, 1H, C(2)**H**), 8.42 (dd, *J* = 8.4, 1.2 Hz, 1H, C(5)**H**), 8.11 (d, *J* = 8.5 Hz, 1H, C(8)**H**), 7.84–7.66 (m, 2H, C(7)**H**, C(13)**H**), 7.60 (ddd, *J* = 8.1, 7.0, 1.0 Hz, 1H, C(6)**H**), 7.41 (ddd, *J* = 8.1, 7.4, 1.6 Hz, 1H, C(15)**H**), 7.31–7.08 (m, 2H, C(14)**H**, C(16)**H**), 6.41 (d, *J* = 5.1 Hz, 1H, C(3)**H**) ppm; ^{13}C NMR (75 MHz, $CDCl_3$) δ: 160.7 (q**C**-4), 151.2 (q**C**-11), 151.0 (**C**(2)H), 149.8 (q**C**-10), 134.3 (**C**(13)H), 130.2 (**C**(7)H), 129.2 (**C**(15)H),

129.1 (**C**(8)H), 127.3 (**C**(14)H), 126.3 (**C**(6)H), 123.2 (**C**(16)H), 121.9 (**C**(5)H), 121.1 (q**C**-9), 116.4 (q**C**(12)Br), 103.7 (**C**(3)H) ppm; *m/z* (ES+): 301 ((M+H)+ 100%).

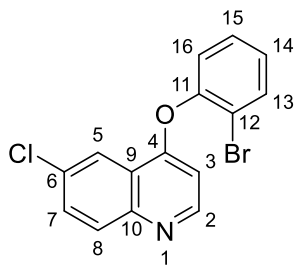
Spectral characteristics were consistent with previously reported data.

4-(2-Bromophenoxy)-8-fluoroquinoline (46)



Compound **46** was prepared *via* the procedure described for **45** using **43** (0.272 g, 1.5 mmol, 1.0 equiv.) to yield **46** as a pale yellow crystalline solid (0.252 g, 53%); m.p. 87–90 °C; IR (film) ν_{max} 1631 (C=N stretch), 1597 (aromatic C=C stretch), 1264, 1224, 949, 612 cm^{-1}; ^{1}H NMR (300 MHz, $CDCl_3$) δ: 8.71 (d, *J* = 5.1 Hz, 1H, C(2)**H**), 8.19 (d, *J* = 8.0 Hz, 1H, C(5)**H**), 7.70 (dd, *J* = 8.0, 1.4 Hz, 1H, C(13)**H**), 7.58–7.34 (m, 3H, C(6)**H**, C(7)**H**, C(15)**H**), 7.29–7.12 (m, 2H, C(14)**H**, C(16)**H**), 6.45 (d, *J* = 5.1 Hz, 1H, C(3)**H**) ppm; ^{13}C NMR (75 MHz, $CDCl_3$) δ: 160.6 (d, $^{4}J_{(C,F)}$ = 4 Hz, q**C**-4), 157.9 (d, $^{1}J_{(C,F)}$ = 256 Hz, q**C**(8)F), 151.2 (**C**(2)H), 150.7 (q**C**-11), 140.0 (d, $^{2}J_{(C,F)}$ = 13 Hz, q**C**-10), 134.3 (**C**(13)H), 129.3 (**C**(15)H), 127.6 (**C**(14)H), 126.0 (d, $^{3}J_{(C,F)}$ = 8 Hz, **C**(6)H), 123.2 (**C**(16)H), 122.7 (d, $^{3}J_{(C,F)}$ = 3 Hz, q**C**-9), 117.7 (d, $^{4}J_{(C,F)}$ = 5 Hz, **C**(5)H), 116.2 (q**C**(12)Br), 114.3 (d, $^{2}J_{(C,F)}$ = 19 Hz, **C**(7)H), 104.4 (**C**(3)H) ppm; ^{19}F NMR (282 MHz, $CDCl_3$) δ: -125 ppm; HRMS (ESI-TOF) *m/z*: $[M+H]^+$ calcd for $C_{15}H_{10}BrFNO$: 317.9930; found: 317.9918.

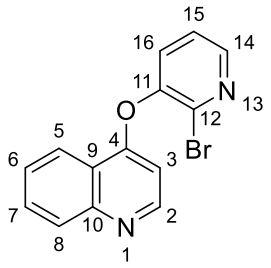
4-(2-Bromophenoxy)-6-chloroquinoline (47)



Compound **47** was prepared *via* the procedure described for **45** using **44** (0.297 g, 1.5 mmol, 1.0 equiv.) to yield **47** as an off-white solid (0.453 g, 90%); m.p. 89–90 °C; IR (film) ν_{max} 1642 (C=N stretch), 1563 (aromatic C=C stretch), 1262, 1222, 666, 643 cm^{-1}; ^{1}H NMR (300 MHz, $CDCl_3$) δ: 8.66 (d, *J* = 5.2 Hz, 1H, C(2)**H**), 8.40 (d, *J* = 2.3 Hz, 1H, C(5)**H**), 8.04 (d, *J* = 9.0 Hz, 1H, C(8)**H**), 7.79–7.65 (m, 2H, C(7)**H,** C(13)**H**), 7.44 (ddd, *J* = 8.2, 7.3, 1.6 Hz, 1H, C(15)**H**), 7.30–7.17 (m, 2H, C(14)**H**, C(16)**H**), 6.41 (d, *J* = 5.2 Hz, 1H, C(3)**H**) ppm; ^{13}C NMR (75 MHz, $CDCl_3$) δ: 159.9 (q**C**-4), 151.2 (**C**(2)H), 150.7 (q**C**-11), 148.1 (q**C**-10), 134.3 (**C**(13)H), 132.2 (q**C**(6)Cl), 131.1 (**C**(7)H), 130.8 (**C**(8)H), 129.3 (**C**(15)H), 127.5 (**C**(14)H), 123.2

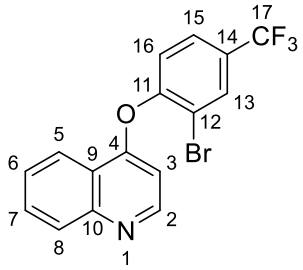
(**C**(16)H), 121.6 (q**C**-9), 121.0 (**C**(5)H), 116.3 (q**C**(12)Br), 104.2 (**C**(3)H) ppm; HRMS (ESI-TOF) *m/z*: $[M+H]^+$ calcd for $C_{15}H_{10}BrClNO$: 333.9634; found: 333.9628.

4-((2-Bromopyridin-3-yl)oxy)quinoline (48)



Compound **48** was prepared *via* the procedure described for **45** using 4-chloroquinoline (0.164 g, 1.0 mmol, 1.0 equiv.) and 2-bromo-3-hydroxypyridine (0.261 g, 1.5 mmol, 1.5 equiv.) to yield **48** as an off-white solid (0.238 g, 79%); m.p. 170–173 °C; IR (film) ν_{max} 1639, 1503 (C=N stretch), 1448 (aromatic C=C stretch), 1305, 1268, 666 cm^{-1}; ^1H NMR (300 MHz, $CDCl_3$) δ: 8.72 (d, *J* = 5.1 Hz, 1H, C(2)**H**), 8.47–8.28 (m, 2H, C(5)**H,** C(14)**H**), 8.13 (d, *J* = 8.5 Hz, 1H, C(8)**H**), 7.79 (ddd, *J* = 8.4, 7.0, 1.4 Hz, 1H, C(7)**H**), 7.70–7.47 (m, 2H, C(6)**H**, C(16)**H**), 7.38 (dd, *J* = 8.0, 4.6 Hz, 1H, C(15)**H**), 6.45 (d, *J* = 5.1 Hz, 1H, C(3)**H**) ppm; ^{13}C NMR (75 MHz, $CDCl_3$) δ: 159.9 (q**C**-4), 150.9 (**C**(2)H), 149.9 (q**C**-10), 148.7 (q**C**-11), 147.0 (**C**(14)H), 136.6 (q**C**(12)Br), 130.49 (**C**(7)H), 130.46 (**C**(16)H), 129.2 (**C**(8)H), 126.7 (**C**(6)H), 124.0 (**C**(15)H), 121.7 (**C**(5)H), 121.0 (q**C**-9), 104.1 (**C**(3)H) ppm; HRMS (ESI-TOF) *m/z*: $[M+H]^+$ calcd for $C_{14}H_{10}BrN_2O$: 300.9976; found: 300.9986.

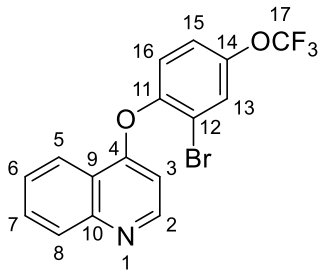
4-(2-Bromo-4-(trifluoromethyl)phenoxy)quinoline (49)



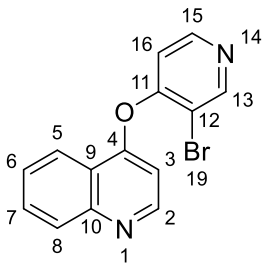
A mixture of **42** (0.164 g, 1.5 mmol, 1.0 equiv.), 2-bromo-4-(trifluoromethyl)phenol (0.362 g, 1.5 mmol, 1.5 equiv.), DMAP (0.367 g, 3.0 mmol, 3.0 equiv.) and toluene (0.5 mL) was stirred in a sealed vial at 120 °C, until the reaction was complete (24 h), as evident by TLC (hexanes:EtOAc 80:20).[60] The cooled reaction mixture was diluted with 10% aq. NaOH (5 mL) and stirred at r.t. for 1 h. The aq. layer was extracted with DCM (3 × 10 mL). The combined organic layers were washed with 6 M NaOH (2 × 10 mL), 1 M HCl (10 mL), H_2O (10 mL), and brine (15 mL), dried over $MgSO_4$, filtered and concentrated under reduced pressure. Purification *via* column chromatography (hexanes:EtOAc 80:20) to yield **49** as a sticky colourless oil (0.073 g, 20%); IR (film) ν_{max} 1623 (C=N stretch), 1492 (aromatic C=C stretch), 1320, 1263, 1231, 1130, 588 cm^{-1}; ^1H NMR (300 MHz, $CDCl_3$) δ: 8.73 (d, *J* = 4.9 Hz, 1H, C(2)**H**), 8.34 (dd, *J* = 8.4, 0.9

Hz, 1H, C(5)**H**), 8.14 (d, *J* = 8.5 Hz, 1H, C(8)**H**), 8.00 (d, *J* = 1.7 Hz, 1H, C(13)**H**), 7.79 (ddd, *J* = 8.4, 6.9, 1.4 Hz, 1H, C(7)**H**), 7.70–7.54 (m, 2H, C(6)**H,** C(15)**H**), 7.28 (d, *J* = 8.5 Hz, 1H, C(16)**H**), 6.50 (d, *J* = 5.1 Hz, 1H, C(3)**H**) ppm; ^{13}C NMR (75 MHz, $CDCl_3$) δ: 159.8 (q**C**-4), 154.4 (q**C**-11), 150.9 (**C**(2)H), 150.0 (q**C**-10), 131.7 (q, $^3J_{(C,F)}$ = 4 Hz, **C**(13)H), 130.5 (**C**(7)H), 129.3 (**C**(8)H), 129.2 (q, $^2J_{(C,F)}$ = 34 Hz, q**C**(14)CF_3), 126.7 (**C**(6)H), 126.4 (q, $^3J_{(C,F)}$ = 4 Hz, **C**(15)H), 122.9 (q, $^1J_{(C,F)}$ = 272 Hz, q**C**(17)F_3), 122.6 (**C**(16)H), 121.7 (**C**(5)H), 121.0 (q**C**-9), 116.5 (q**C**(12)Br), 104.7 (**C**(3)H) ppm; ^{19}F NMR (282 MHz, $CDCl_3$) δ: -62 ppm; HRMS (ESI-TOF) *m/z*: $[M+H]^+$ calcd for $C_{16}H_{10}BrF_3NO$: 367.9898; found: 367.9886.

4-(2-Bromo-4-(trifluoromethoxy)phenoxy)quinoline (50)



Compound **50** was prepared *via* the procedure described for **49** using 2-bromo-4-(trifluoromethoxy)phenol (0.386 g, 1.5 mmol, 1.5 equiv.) to yield **50** as a pale yellow solid (0.302 g, 78%); m.p. 50–52 °C; IR (film) ν_{max} 1640 (C=N stretch), 1481 (aromatic C=C stretch), 1306, 1253, 1218, 1187, 567 cm^{-1}; ^{1}H NMR (300 MHz, $CDCl_3$) δ: 8.71 (d, *J* = 5.1 Hz, 1H, C(2)**H**), 8.38 (dd, *J* = 8.4, 0.9 Hz, 1H, C(5)**H**), 8.13 (d, *J* = 8.4 Hz, 1H, C(8)**H**), 7.79 (ddd, *J* = 8.5, 6.9, 1.5 Hz, 1H, C(7)**H**), 7.69–7.55 (m, 2H, C(6)**H**, C(13)**H**), 7.39–7.25 (m, 2H, C(15)**H,** C(16)**H**), 6.44 (d, *J* = 5.1 Hz, 1H, C(3)**H**) ppm; ^{13}C NMR (75 MHz, $CDCl_3$) δ: 160.3 (q**C**-4), 151.0 (**C**(2)H), 150.0 (q**C**-14), 149.9 (q**C**-10), 146.6 (q**C**-11), 130.4 (**C**(7)H), 129.2 (**C**(8)H), 127.0 (**C**(13)H), 126.5 (**C**(6)H), 123.7 (**C**(16)H), 121.8 (**C**(15)H), 121.7 (**C**(5)H), 120.9 (q**C**-9), 120.4 (q, $^1J_{(C,F)}$ = 259 Hz, q**C**(17)F_3), 116.9 (q**C**(12)Br), 103.8 (**C**(3)H) ppm; ^{19}F NMR (282 MHz, $CDCl_3$) δ: -58 ppm; HRMS (ESI-TOF) *m/z*: $[M+H]^+$ calcd for $C_{16}H_{10}BrF_3NO_2$: 383.9847; found: 383.9843.

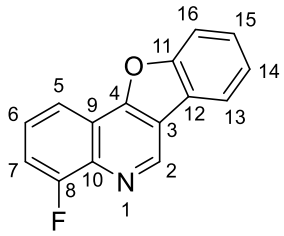


4-((3-Bromopyridin-4-yl)oxy)quinoline (51)

Compound **51** was prepared *via* the procedure described for **49** using 3-bromo-4-pyridinol (0.261 g, 1.5 mmol, 1.5 equiv.) to yield **50** as a yellow solid (0.203 g, 67%); m.p. 245–247 °C. IR (film) ν_{max} 1632, 1593 (C=N stretch), 1564 (aromatic C=C stretch), 1301, 1273, 667 cm^{-1}. ^{1}H NMR (600 MHz, $(CD_3)_2SO$) δ: 915 (d, *J* = 4.6 Hz, 1H,

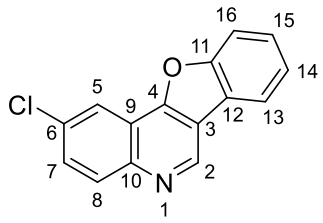
C(2)**H**), 8.70 (d, *J* = 2.2 Hz, 1H, C(13)**H**), 8.27 (d, *J* = 8.4 Hz, 1H, C(8)**H**), 8.13 (dd, *J* = 7.5, 2.2 Hz, 1H, C(15)**H**), 8.04-7.94 (m, 1H, C(7)**H**), 7.88 (d, *J* = 4.6 Hz, 1H, C(3)**H**), 7.86-7.76 (m, 2H, C(5)**H**, C(6)**H**), 6.52 (d, *J* = 7.5 Hz, 1H, C(16)**H**) ppm; ^{13}C NMR (150 MHz, $(CD_3)_2SO$) δ: 172.3 (q**C**-11), 151.6 (**C**(2)H), 149.4 (q**C**-10), 146.3 (q**C**-4), 142.0 (**C**(13)H), 141.6 (**C**(15)H), 131.2 (**C**(7)H), 130.1 (**C**(8)H), 129.1 (**C**(6)H), 123.5 (q**C**-9), 122.5 (**C**(5)H), 119.1 (**C**(3)H), 116.1 (**C**(16)H), 115.3 (q**C**(12)Br) ppm; HRMS (ESI-TOF) *m/z*: $[M+H]^+$ calcd. for $C_{14}H_{10}BrN_2O$: 300.9976; found 300.9971.

4-Fluorobenzofuro[3,2-*c*]quinoline (52)



A mixture of **46** (0.106 g, 0.33 mmol, 1.0 equiv.), $Pd(OAc)_2$ (1.5 mg, 0.0067 mmol, 2 mol%) and anhydrous Cs_2CO_3 (0.218 g, 0.67 mmol, 2.0 equiv.) in anhydrous NMP (0.5 mL) was stirred at 135 °C in a sealed reaction tube until the reaction was completed as evident by ^{1}H-NMR analysis (24 h). The cooled reaction mixture was diluted with DCM, filtered through a short plug of Celite, rinsed with DCM and the filtrate concentrated under reduced pressure. Purification *via* column chromatography (DCM 100 to DCM:EtOAc 95:5) to yield **52** as a white crystalline solid (0.072 g, 91%); m.p. 153–155 °C; IR (film) ν_{max} 1640 (C=N stretch), 1596 (aromatic C=C stretch), 1300, 1249, 949 cm^{-1}; ^{1}H NMR (300 MHz, $CDCl_3$) δ: 9.52 (s, 1H, C(2)**H**), 8.27–7.99 (m, 2H, C(5)**H**, C(13)**H**), 7.75 (d, *J* = 8.1 Hz, 1H, C(16)**H**), 7.68–7.40 (m, 4H, C(6)**H**, C(7)**H**, C(14)**H**, C(15)**H**) ppm; ^{13}C NMR (100 MHz, $CDCl_3$) δ: 158.6 (d, $^1J_{(C,F)}$ = 257 Hz, q**C**(8)F), 157.0 (d, $^4J_{(C,F)}$ = 5 Hz, q**C**-4), 156.0 (q**C**-11), 144.6 (**C**(2)H), 137.3 (d, $^2J_{(C,F)}$ = 12 Hz, q**C**-10), 127.7 (**C**(15)H), 127.1 (d, $^3J_{(C,F)}$ = 8 Hz, **C**(6)H), 124.3 (**C**(14)H), 122.4 (q**C**-12), 120.9 (**C**(13)H), 118.9 (d, $^3J_{(C,F)}$ = 3 Hz, q**C**-9), 117.3 (q**C**-3), 116.6 (d, $^4J_{(C,F)}$ = 5 Hz, **C**(5)H), 113.7 (d, $^2J_{(C,F)}$ = 19 Hz, **C**(7)H), 112.2 (**C**(16)H) ppm; ^{19}F NMR (282 MHz, $CDCl_3$) δ: -122 ppm; HRMS (ESI-TOF) *m/z*: $[M+H]^+$ calcd for $C_{15}H_9FNO$: 238.0668; found 238.0661.

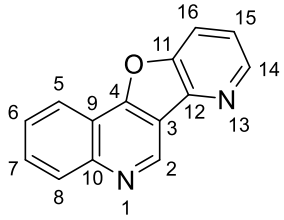
2-Chlorobenzofuro[3,2-*c*]quinoline (53)[156]



Compound **53** was prepared *via* the procedure described for **52** using **47** (0.084 g, 0.25 mmol, 1.0 equiv.) to yield **53** as a white crystalline solid (0.056 g, 88%); m.p. 141–142 °C (lit.[156] 139–141 °C); ^{1}H NMR (300 MHz, $CDCl_3$) δ: 9.38 (s, 1H, C(2)**H**), 8.27 (d, *J* = 2.3 Hz, 1H, C(5)**H**), 8.12 (d, *J* = 9.0 Hz, 1H, C(8)**H**), 8.02 (dd, *J* = 7.6, 0.6 Hz, 1H, C(13)**H**), 7.76–7.59 (m, 2H, C(7)**H**, C(16)**H**), 7.58–7.38 (m, 2H, C(14)**H**, C(15)**H**) ppm; ^{13}C NMR (75 MHz, $CDCl_3$) δ: 156.3 (q**C**-4), 156.0 (q**C**-11), 145.5 (q**C**-10), 144.4 (**C**(2)H), 132.9 (q**C**(6)Cl), 131.4 (**C**(8)H), 130.0 (**C**(7)H), 127.6 (**C**(15)H), 124.2 (**C**(14)H), 122.3 (q**C**-12), 120.7 (**C**(13)H), 119.8 (**C**(5)H), 117.7 (q**C**-9), 116.9 (q**C**-3), 112.2 (**C**(16)H) ppm; *m/z* (ES+): 254 ($(M+H)^+$ 100%).

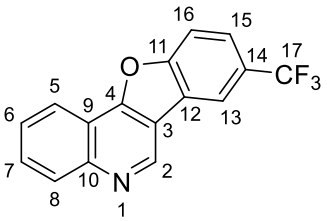
Spectral characteristics were consistent with previously reported data.[156]

Pyrido[2',3':4,5]furo[3,2-*c*]quinoline (54)



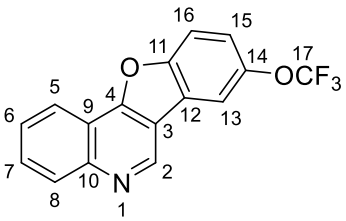
Compound **54** was prepared *via* the procedure described for **52** except that it was stirred for 10 h using **48** (0.151 g, 0.50 mmol, 1.0 equiv.) to yield **54** as a pale yellow solid (0.090 g, 81%); m.p. 174–175 °C; IR (film) ν_{max} 1637, 1570 (C=N stretch), 1437 (aromatic C=C stretch), 1306, 1264 cm^{-1}; ^{1}H NMR (300 MHz, $CDCl_3$) δ: 9.66 (s, 1H, C(2)**H**), 8.71 (dd, *J* = 4.8, 1.2 Hz, 1H, C(14)**H**), 8.43–8.17 (m, 2H, C(5)**H,** C(8)**H**), 7.96 (dd, *J* = 8.4, 1.3 Hz, 1H, C(16)**H**), 7.86–7.60 (m, 2H, C(6)**H,** C(7)**H**), 7.42 (dd, *J* = 8.4, 4.8 Hz, 1H, C(15)**H**) ppm; ^{13}C NMR (75 MHz, $CDCl_3$) δ: 159.1 (q**C**-4), 149.2 (q**C**-11), 148.2 (q**C**-10), 146.6 (**C**(14)H), 144.4 (**C**(2)H), 142.8 (q**C**-12), 130.2 (**C**(7)H), 130.0 (**C**(8)H), 127.3 (**C**(6)H), 121.3 (**C**(15)H), 120.6 (**C**(5)H), 119.0 (**C**(16)H), 116.9 (q**C**-9), 115.3 (q**C**-3) ppm; HRMS (ESI-TOF) *m/z*: $[M+H]^+$ calcd for $C_{14}H_9N_2O$: 221.0715; found: 221.0710.

8-(Trifluoromethyl)benzofuro[3,2-*c*]quinoline (55)



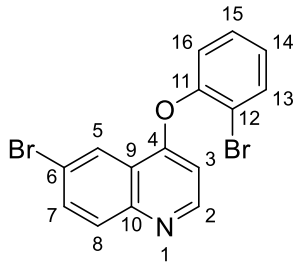
Compound **55** was prepared *via* the procedure described for **52** using **49** (0.073 g, 0.30 mmol, 1.0 equiv.), except that it was stirred for 18 h, to yield **55** as a white crystalline solid (0.053 g, 88%); m.p. 170–173 °C; IR (film) ν_{max} 1627 (C=N stretch), 1567 (aromatic C=C stretch), 1333, 1310, 1151, 1110 cm^{-1}; ^{1}H NMR (400 MHz, $CDCl_3$) δ: 9.52 (s, 1H, C(2)**H**), 8.48–8.35 (m, 2H, C(5)**H**, C(13)**H**), 8.29 (d, *J* = 8.5 Hz, 1H, C(8)**H**) 7.91–7.65 (m, 4H, C(6)**H**, C(7)**H**, C(15)**H**, C(16)**H**) ppm; ^{13}C NMR (75 MHz, $CDCl_3$) δ: 158.4 (q**C**-4), 157.2 (q**C**-11), 147.8 (q**C**-10), 144.1 (**C**(2)H), 130.0 (**C**(8)H), 129.9 (**C**(7)H), 127.4 (**C**(6)H), 126.8 (q, $^{2}J_{(C,F)}$ = 33 Hz, q**C**(14)CF_3), 124.29 (q, $^{3}J_{(C,F)}$ = 4 Hz, **C**(15)H), 124.28 (q, $^{1}J_{(C,F)}$ = 272 Hz, q**C**(17)F_3), 123.0 (q**C**-12), 120.7 (**C**(5)H), 118.3 (q, $^{3}J_{(C,F)}$ = 4 Hz, **C**(13)H), 116.8 (q**C**-9), 115.4 (q**C**-3), 112.5 (**C**(16)H) ppm; ^{19}F NMR (282 MHz, $CDCl_3$) δ: -61 ppm; HRMS (ESI-TOF) *m/z*: $[M+H]^+$ calcd for $C_{16}H_9F_3NO$: 254.0373; found: 254.0368.

8-(Trifluoromethoxy)benzofuro[3,2-*c*]quinoline (56)



Compound **56** was prepared *via* the procedure described for **52** using **50** (0.192 g, 0.50 mmol, 1.0 equiv.), except that it was stirred for 20 h, to yield **56** as a white crystalline solid (0.137 g, 90%); m.p. 124–126 °C; IR (film) ν_{max} 1641 (C=N stretch), 1512 (aromatic C=C stretch), 1280, 1247, 1206, 1141, 1156 cm^{-1}; ^{1}H NMR (300 MHz, $CDCl_3$) δ: 9.47 (s, 1H, C(2)**H**), 8.41 (dd, *J* = 8.1, 1.0 Hz, 1H, C(5)**H**), 8.28 (d, *J* = 8.4 Hz, 1H, C(8)**H**), 7.95 (d, *J* = 1.1 Hz, 1H, C(13)**H**), 7.88–7.64 (m, 3H, C(6)**H,** C(7)**H,** C(16)**H**), 7.41 (dd, *J* = 8.9, 0.9 Hz, 1H, C(15)**H**) ppm; ^{13}C NMR (75 MHz, $CDCl_3$) δ: 158.7 (q**C**-4), 153.9 (q**C**-14), 147.8 (q**C**-10), 145.8 (q**C**-11), 144.2 (**C**(2)H), 130.0 (**C**(8)H), 129.9 (**C**(7)H), 127.4 (**C**(6)H), 123.8 (q**C**-12), 120.8 (**C**(5)H), 120.7 (**C**(15)H), 120.6 (q, $^{1}J_{(C,F)}$ = 257 Hz, **C**(17)F_3), 117.0 (q**C**-9), 115.9 (q**C**-3), 113.6 (**C**(13)H), 113.0 (**C**(16)H) ppm; ^{19}F NMR (282 MHz, $CDCl_3$) δ: -58 ppm; HRMS (ESI-TOF) *m/z*: $[M+H]^+$ calcd for $C_{16}H_9F_3NO_2$: 304.0585; found: 304.0574.

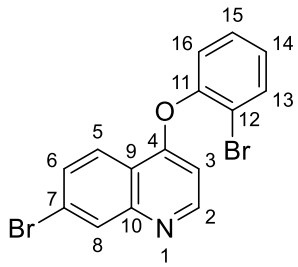
6-Bromo-4-(2-bromophenoxy)quinoline (57)[102]



Compound **57** was prepared *via* the procedure described for **45** using 6-bromo-4-chloroquinoline (0.970 g, 4.0 mmol, 1.0 equiv.) and 2-bromophenol (2.32 mL, 20.0 mmol, 5.0 equiv.) to yield **57** as a pale yellow solid (1.406 g, 93%); m.p. 95–97 °C (lit.[102] 97–98 °C); ^{1}H NMR (300 MHz, $CDCl_3$) δ: 8.67 (d, *J* = 5.2 Hz, 1H, C(2)**H**), 8.58 (d, *J* = 2.2 Hz, 1H, C(5)**H**), 7.97 (d, *J* = 9.0 Hz, 1H, C(8)**H**), 7.83 (dd, *J* = 9.0, 2.2 Hz, 1H, C(7)**H**), 7.78–7.67 (m, 1H, C(13)**H**), 7.44 (ddd, *J* = 8.2, 7.3, 1.6 Hz, 1H, C(15)**H**), 7.30–7.14 (m, 2H, C(14)**H**, C(16)**H**), 6.40 (d, *J* = 5.2 Hz, 1H, C(3)**H**) ppm; ^{13}C NMR (75 MHz, $CDCl_3$) δ: 159.8 (q**C**-4), 151.4 (**C**(2)H), 150.8 (q**C**-11), 148.4 (q**C**-10), 134.4 (**C**(13)H), 133.7 (**C**(7)H), 130.9 (**C**(8)H), 129.3 (**C**(15)H), 127.6 (**C**(14)H), 124.3 (**C**(5)H), 123.3 (**C**(16)H), 122.2 (q**C**-9), 120.3 (q**C**(6)Br), 116.4 (q**C**(12)Br), 104.2 (**C**(3)H) ppm; *m/z* (ES+): 380 ($(M+H)^+$ 100%).

Spectral characteristics were consistent with previously reported data.[102]

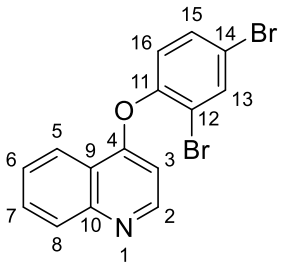
7-Bromo-4-(2-bromophenoxy)quinoline (60)[102]



Compound **60** was prepared *via* the procedure described for **45** using 7-bromo-4-chloroquinoline (0.970 g, 4.0 mmol, 1.0 equiv.) and 2-bromophenol (2.32 mL, 20.0 mmol, 5.0 equiv.) to yield **60** as a pale yellow solid (1.397 g, 92%); m.p. 72–74 °C (lit.[102] 73–74 °C); ^{1}H NMR (300 MHz, $CDCl_3$) δ: 8.66 (d, *J* = 5.2 Hz, 1H, C(2)**H**), 8.39–8.19 (m, 2H, C(5)**H**, C(8)**H**), 7.79–7.61 (m, 2H, C(6)**H**, C(13)**H**), 7.44 (ddd, *J* = 8.2, 7.3, 1.6 Hz, 1H, C(15)**H**), 7.33–7.16 (m, 2H, C(14)**H**, C(16)**H**), 6.40 (d, *J* = 5.2 Hz, 1H, C(3)**H**) ppm; ^{13}C NMR (75 MHz, $CDCl_3$) δ: 160.9 (q**C**-4), 152.1 (**C**(2)H), 150.8 (q**C**-11), 150.5 (q**C**-10), 134.4 (**C**(13)H), 131.4 (**C**(8)H), 129.8 (**C**(6)H), 129.3 (**C**(15)H), 127.6 (**C**(14)H), 124.6 (q**C**(7)Br), 123.5 (**C**(5)H), 123.3 (**C**(16)H), 119.7 (q**C**-9), 116.3 (q**C**(12)Br), 103.9 (**C**(3)H) ppm; *m/z* (ES+): 380 ($(M+H)^+$ 100%).

Spectral characteristics were consistent with previously reported data.[102]

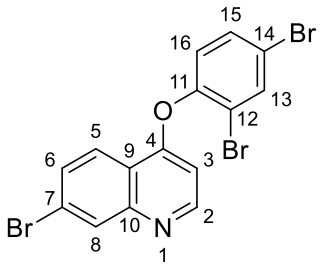
4-(2,4-Dibromophenoxy)quinoline (61)[102]



Compound **61** was prepared *via* the procedure described for **45** using **42** (0.164 g, 1.0 mmol, 1.0 equiv.) and 2,4-dibromophenol (1.26 g, 5.0 mmol, 5.0 equiv.) to yield **61** as a white solid (0.261 g, 69%); m.p. 124–125 °C (lit.[102] 125–126 °C); ^{1}H NMR (300 MHz, $CDCl_3$) δ: 8.69 (d, *J* = 5.1 Hz, 1H, C(2)**H**), 8.37 (dd, *J* = 8.3, 0.9 Hz, 1H, C(5)**H**), 8.12 (d, *J* = 8.5 Hz, 1H, C(8)**H**), 7.87 (d, *J* = 2.3 Hz, 1H, C(13)**H**), 7.78 (ddd, *J* = 8.5, 6.9, 1.5 Hz, 1H, C(7)**H**), 7.67–7.46 (m, 2H, C(6)**H**, C(15)**H**), 7.11 (d, *J* = 8.6 Hz, 1H, C(16)**H**), 6.43 (d, *J* = 5.1 Hz, 1H, C(3)**H**) ppm; ^{13}C NMR (75 MHz, $CDCl_3$) δ: 160.3 (q**C**-4), 151.0 (**C**(2)H), 150.6 (q**C**-11), 149.9 (q**C**-10), 136.6 (**C**(13)H), 132.3 (**C**(15)H), 130.3 (**C**(7)H), 129.2 (**C**(8)H), 126.5 (**C**(6)H), 124.2 (**C**(16)H), 121.7 (**C**(5)H), 120.9 (q**C**-9), 119.3 (q**C**(14)Br), 117.3 (q**C**(12)Br), 103.8 (**C**(3)H) ppm; *m/z* (ES+): 380 ($(M+H)^+$ 100%).

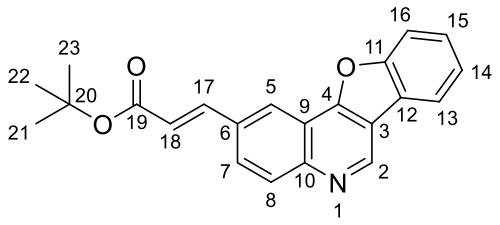
Spectral characteristics were consistent with previously reported data.[102]

7-Bromo-4-(2,4-dibromophenoxy)quinoline (62)



Compound **62** was prepared *via* the procedure described for **45** using 7-bromo-4-chloroquinoline (0.243 g, 1.0 mmol, 1.0 equiv.) and 2,4-dibromophenol (1.26 g, 5.0 mmol, 5.0 equiv.) to yield **62** as a white solid (0.398 g, 87%); m.p. 140–142 °C; IR (film) ν_{max} 1615 (C=N stretch), 1559 (aromatic C=C stretch), 1302, 1096 (ether C-O stretch), 716, 666 (C-Br stretch) cm^{-1}; ^{1}H NMR (300 MHz, $CDCl_3$) δ: 8.68 (d, *J* = 5.2 Hz, 1H, C(2)**H**), 8.36–8.18 (m, 2H, C(5)**H**, C(8)**H**), 7.88 (d, *J* = 2.3 Hz, 1H, C(13)**H**), 7.70 (dd, *J* = 8.9, 1.9 Hz, 1H, C(6)**H**), 7.56 (dd, *J* = 8.6, 2.3 Hz, 1H, C(15)**H**), 7.13 (d, *J* = 8.6 Hz, 1H, C(16)**H**), 6.42 (d, *J* = 5.2 Hz, 1H, C(3)**H**) ppm; ^{13}C NMR (75 MHz, $CDCl_3$) δ: 160.5 (q**C**-4), 152.1 (**C**(2)H), 150.5 (q**C**-10), 150.2 (q**C**-11), 136.7 (**C**(13)H), 132.4 (**C**(15)H), 131.5 (**C**(8)H), 130.0 (**C**(6)H), 124.7 (q**C**(7)Br), 124.4 (**C**(16)H), 123.3 (**C**(5)H), 119.7 (q**C**(14)Br), 119.6 (q**C**-9), 117.4 (q**C**(12)Br), 103.9 (**C**(3)H) ppm; HRMS (ESI-TOF) *m/z*: $[M+H]^+$ calcd for $C_{15}H_9Br_3NO$: 455.8229; found: 455.8233.

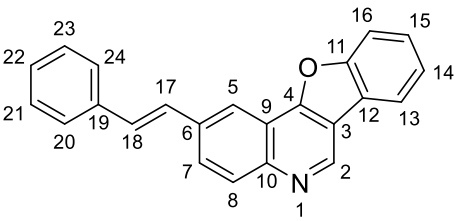
***tert*-Butyl (*E*)-3-(benzofuro[3,2-*c*]quinolin-2-yl)acrylate (64)**[102]



A mixture of **57** (0.190 g, 0.50 mmol, 1.0 equiv.), *tert*-butyl acrylate (0.08 mL, 0.55 mmol, 1.1 equiv.), $Pd(OAc)_2$ (2.2 mg, 0.01 mmol, 2 mol%) and anhydrous K_2CO_3 (0.138 g, 1.0 mmol, 2.0 equiv.) in anhydrous NMP (0.75 mL) was stirred at 135 °C in a sealed reaction tube until the reaction was completed as evident by ^{1}H-NMR analysis (18 h). The cooled reaction mixture was diluted with DCM, filtered through a short plug of Celite, rinsed with DCM and the filtrate concentrated under reduced pressure. Purification *via* column chromatography (DCM:EtOAc 99:1–95:5) to yield **64** as a white solid (0.134 g, 78%); m.p. 167–169 °C (lit.[102] 169–170 °C); ^{1}H NMR (300 MHz, $CDCl_3$) δ: 9.43 (s, 1H, C(2)**H**), 8.43 (d, *J* = 1.6 Hz, 1H, C(5)**H**), 8.20 (d, *J* = 8.8 Hz, 1H, C(8)**H**), 8.06 (dd, *J* = 7.6, 0.7 Hz, 1H, C(13)**H**), 7.96–7.65 (m, 3H, C(7)**H**, C(16)**H**, C(17)**H**), 7.63–7.36 (m, 2H, C(14)**H**, C(15)**H**), 6.57 (d, *J* = 16.0 Hz, 1H, C(18)**H**), 1.59 (s, 9H, C(21)$\mathbf{H}_3$, C(22)$\mathbf{H}_3$, C(23)$\mathbf{H}_3$) ppm; ^{13}C NMR (75 MHz, $CDCl_3$) δ: 166.0 (q**C**-19), 157.4 (q**C**-4), 156.0 (q**C**-11), 147.8 (q**C**-10), 145.0 (**C**(2)H), 142.4 (**C**(17)H), 133.3 (q**C**-6), 130.4 (**C**(8)H), 127.5 (**C**(15)H), 127.4 (**C**(7)H), 124.4 (**C**(14)H), 122.4 (q**C**-12), 122.0 (**C**(18)H), 121.5 (**C**(5)H), 120.7 (**C**(13)H), 117.2 (q**C**-9), 116.9 (q**C**-3), 112.2 (**C**(16)H), 80.8 (q**C**-20), 28.2 (3 × C, **C**(21)H_3, **C**(22)H_3, **C**(23)H_3) ppm; *m/z* (ES+): 346 ($(M+H)^+$ 100%).

Spectral characteristics were consistent with previously reported data.[102]

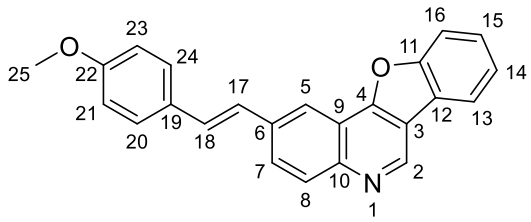
(*E*)-2-Styrylbenzofuro[3,2-*c*]quinoline (65)



A mixture of **57** (0.114 g, 0.30 mmol, 1.0 equiv.), styrene (0.04 mL, 0.33 mmol, 1.1 equiv.), $Pd(OAc)_2$ (3.4 mg, 0.015 mmol, 5 mol%) and anhydrous K_2CO_3 (0.083 g, 0.60 mmol, 2.0 equiv.) in anhydrous NMP (0.5 mL) was stirred at 135 °C in a sealed reaction tube until the reaction was completed as evident by ^{1}H-NMR analysis (18 h). The cooled reaction mixture was diluted with DCM, filtered through a short plug of Celite, rinsed with DCM and the filtrate concentrated under reduced pressure.

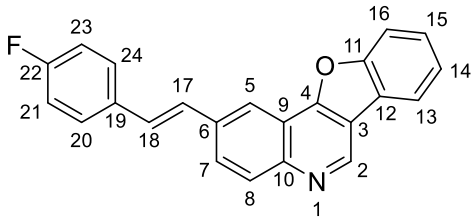
Purification *via* column chromatography (DCM:EtOAc 99:1–95:5) to yield **65** as a white solid (0.070 g, 73%); m.p. 201–202 °C; IR (film) ν_{max} 1662 (trans alkene C=C stretch), 1649 (C=N stretch), 1561 (aromatic C=C stretch), 1377, 1188 (ether C-O stretch) cm^{-1}; ^{1}H NMR (300 MHz, $CDCl_3$) δ: 9.41 (s, 1H, C(2)**H**), 8.39 (d, *J* = 1.8 Hz, 1H, C(5)**H**), 8.22 (d, *J* = 8.9 Hz, 1H, C(8)**H**), 8.07 (dd, *J* = 7.6, 0.8 Hz, 1H, C(13)**H**), 7.98 (dd, *J* = 8.9, 2.0 Hz, 1H, C(7)**H**), 7.76 (d, *J* = 8.1 Hz, 1H, C(16)**H**), 7.66–7.22 (m, 9H, C(14)**H**, C(15)**H**, C(17)**H**, C(18)**H**, C(20)**H**, C(21)**H**, C(22)**H**, C(23)**H**, C(24)**H**) ppm; ^{13}C NMR (75 MHz, $CDCl_3$) δ: 157.4 (q**C**-4), 156.0 (q**C**-11), 147.0 (q**C**-10), 143.9 (**C**(2)H), 137.0 (q**C**-19), 136.1 (q**C**-6), 130.6 (**C**(18)H), 130.1 (**C**(8)H), 128.8 (2 × C, **C**(21)H, **C**(23)H), 128.1 (**C**(22)H), 127.8 (**C**(17)H), 127.3 (**C**(15)H), 127.2 (**C**(7)H), 126.8 (2 × C, **C**(20)H, **C**(24)H), 124.1 (**C**(14)H), 122.7 (q**C**-12), 120.7 (**C**(13)H), 118.6 (**C**(5)H), 117.4 (q**C**-9), 116.7 (q**C**-3), 112.1 (**C**(16)H) ppm; HRMS (ESI-TOF) *m/z*: $[M+H]^+$ calcd for $C_{23}H_{16}NO$: 322.1226; found: 322.1223.

(*E*)-2-(4-Methoxystyryl)benzofuro[3,2-*c*]quinoline (66)



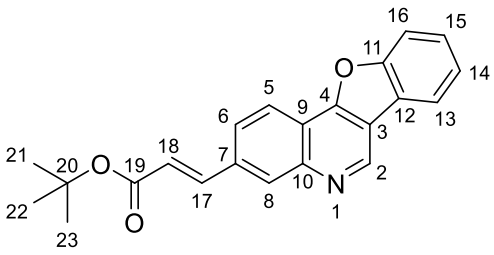
Compound **66** was prepared *via* the procedure described for **65** using 4-vinylanisole (0.04 mL, 0.33 mmol, 1.1 equiv.) to yield **66** as a white solid (0.086 g, 82%); m.p. 190–192 °C; IR (film) ν_{max} 1656 (trans alkene C=C stretch), 1602 (C=N stretch), 1562 (aromatic C=C stretch), 1346, 1250, 1110 (ether C-O stretch) cm^{-1}; ^{1}H NMR (300 MHz, $CDCl_3$) δ: 9.41 (s, 1H, C(2)**H**), 8.38 (d, *J* = 1.7 Hz, 1H, C(5)**H**), 8.21 (d, *J* = 8.9 Hz, 1H, C(8)**H**), 8.09 (d, *J* = 7.4 Hz, 1H, C(13)**H**), 7.97 (dd, *J* = 8.9, 1.8 Hz, 1H, C(7)**H**), 7.76 (d, *J* = 8.1 Hz, 1H, C(16)**H**), 7.65–7.40 (m, 4H, C(14)**H**, C(15)**H**, C(20)**H**, C(24)**H**), 7.38–7.12 (m, 2H, C(17)**H**, C(18)**H**), 7.04–6.84 (m, 2H, C(21)**H**, C(23)**H**), 3.86 (s, 3H, C(25)**H₃**) ppm; ^{13}C NMR (75 MHz, $CDCl_3$) δ: 159.7 (q**C**-22), 157.4 (q**C**-4), 156.0 (q**C**-11), 146.9 (q**C**-10), 143.7 (**C**(2)H), 136.5 (q**C**-6), 130.2 (**C**(18)H), 130.1 (**C**(8)H), 129.8 (q**C**-19), 128.0 (2 × C, **C**(20)H, **C**(24)H), 127.3 (**C**(15)H), 127.2 (**C**(7)H), 125.7 (**C**(17)H), 124.1 (**C**(14)H), 122.8 (q**C**-12), 120.7 (**C**(13)H), 118.1 (**C**(5)H), 117.5 (q**C**-9), 116.7 (q**C**-3), 114.3 (2 × C, **C**(21)H, **C**(23)H), 112.1 (**C**(16)H), 55.4 (**C**(25)H_3) ppm; HRMS (ESI-TOF) *m/z*: $[M+H]^+$ calcd for $C_{24}H_{18}NO_2$: 352.1332; found: 352.1328.

(*E*)-2-(4-Fluorostyryl)benzofuro[3,2-*c*]quinoline (67)



Compound **67** was prepared *via* the procedure described for **65** using 4-fluorostyrene (0.04 mL, 0.33 mmol, 1.1 equiv.) to yield **67** as a yellow solid (0.082 g, 80%); m.p. 189–191 °C; IR (film) ν_{max} 1676 (trans alkene C=C stretch), 1598 (C=N stretch), 1559 (aromatic C=C stretch), 1346, 1234, (ether C-O stretch), 1158 (C-F stretch), 1096 (ether C-O stretch) cm^{-1}; ^{1}H NMR (300 MHz, $CDCl_3$) δ: 9.41 (s, 1H, C(2)**H**), 8.37 (d, *J* = 1.8 Hz, 1H, C(5)**H**), 8.21 (d, *J* = 8.9 Hz, 1H, C(8)**H**), 8.07 (d, *J* = 7.5 Hz, 1H, C(13)**H**), 7.95 (dd, *J* = 8.9, 2.0 Hz, 1H, C(7)**H**), 7.75 (d, *J* = 8.1 Hz, 1H, C(16)**H**), 7.63–7.41 (m, 4H, C(14)**H**, C(15)**H**, C(20)**H**, C(24)**H**), 7.34–7.17 (m, 2H, C(17)**H**, C(18)**H**), 7.15–7.00 (m, 2H, C(21)**H**, C(23)**H**) ppm; ^{13}C NMR (75 MHz, $CDCl_3$) δ: 162.6 (d, $^{1}J_{(C,F)}$ = 248 Hz, q**C**(22)F), 157.4 (q**C**-4), 156.0 (q**C**-11), 147.0 (q**C**-10), 144.0 (**C**(2)H), 135.9 (q**C**-6), 133.2 (d, $^{4}J_{(C,F)}$ = 3 Hz, q**C**-19), 130.2 (**C**(8)H), 129.4 (**C**(18)H), 128.3 (d, $^{3}J_{(C,F)}$ = 8 Hz, 2 × C, **C**(20)H, **C**(24)H), 127.6 (d, $^{6}J_{(C,F)}$ = 2 Hz, **C**(17)H), 127.3 (**C**(15)H), 127.1 (**C**(7)H), 124.1 (**C**(14)H), 122.7 (q**C**-12), 120.7 (**C**(13)H), 118.6 (**C**(5)H), 117.4 (q**C**-9), 116.7 (q**C**-3), 115.8 (d, $^{2}J_{(C,F)}$ = 22 Hz, 2 × C, **C**(21)H, **C**(23)H), 112.1 (**C**(16)H) ppm; ^{19}F NMR (282 MHz, $CDCl_3$) δ: -113 ppm; HRMS (ESI-TOF) *m/z*: $[M+H]^+$ calcd for $C_{23}H_{15}FNO$: 340.1132; found: 340.1135.

***tert*-Butyl (*E*)-3-(benzofuro[3,2-*c*]quinolin-3-yl)acrylate (68)**[102]

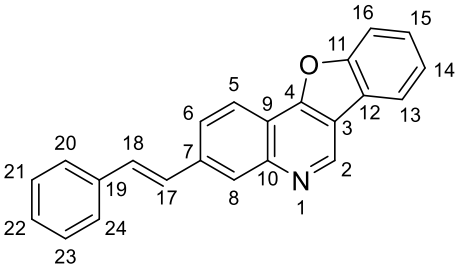


Compound **68** was prepared *via* the procedure described for **64** using **60** (0.190 g, 0.50 mmol, 1.0 equiv.) to yield **68** as a white solid (0.137 g, 79%); m.p. 164–165 °C (lit.[102] 160–162 °C); ^{1}H NMR (300 MHz, $CDCl_3$) δ: 9.49 (s, 1H, C(2)**H**), 8.55–8.24 (m, 2H, C(5)**H**, C(8)**H**), 8.09 (dd, *J* = 7.6, 0.8 Hz, 1H, C(13)**H**), 7.93–7.69 (m, 3H, C(6)**H**, C(16)**H**, C(17)**H**), 7.64–7.35 (m, 2H, C(14)**H**, C(15)**H**), 6.58 (d, *J* = 16.0 Hz, 1H, C(18)**H**), 1.58 (s, 9H, C(21)$\mathbf{H}_3$, C(22)$\mathbf{H}_3$, C(23)$\mathbf{H}_3$) ppm; ^{13}C NMR (75 MHz, $CDCl_3$) δ: 166.0 (q**C**-19), 157.1 (q**C**-4), 156.2 (q**C**-11), 147.4 (q**C**-10), 145.1 (**C**(2)H), 142.8 (**C**(17)H), 135.6 (q**C**-7), 130.7 (**C**(8)H), 127.6 (**C**(15)H), 125.1 (**C**(6)H), 124.3 (**C**(14)H), 122.5 (q**C**-12), 122.0 (**C**(18)H), 121.5 (**C**(5)H),

120.8 (**C**(13)H), 117.7 (q**C**-9), 117.1 (q**C**-3), 112.2 (**C**(16)H), 80.9 (q**C**-20), 28.2 (3 × C, **C**(21)H_3, **C**(22)H_3, **C**(23)H_3) ppm; *m/z* (ES+): 346 ($(M+H)^+$ 100%).

Spectral characteristics were consistent with previously reported data.[102]

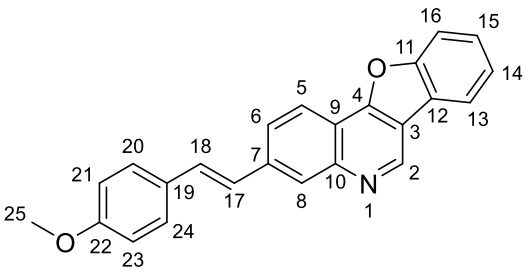
(*E*)-3-Styrylbenzofuro[3,2-*c*]quinoline (69)



Compound **69** was prepared *via* the procedure described for **65** using **60** (0.114 g, 0.30 mmol, 1.0 equiv.) to yield **69** as an off-white solid (0.072 g, 75%); m.p. 179–182 °C; IR (film) ν_{max} 1656 (trans alkene C=C stretch), 1632 (C=N stretch), 1561 (aromatic C=C stretch), 1348, 1190 (ether C-O stretch) cm^{-1}; ^{1}H NMR (300 MHz, $CDCl_3$) δ: 9.46 (s, 1H, C(2)**H**), 8.36 (d, *J* = 8.6 Hz, 1H, C(5)**H**), 8.27 (d, *J* = 1.3 Hz, 1H, C(8)**H**), 8.07 (dd, *J* = 7.5, 0.9 Hz, 1H, C(13)**H**), 7.91 (dd, *J* = 8.6, 1.5 Hz, 1H, C(6)**H**), 7.74 (d, *J* = 7.9 Hz, 1H, C(16)**H**), 7.65–7.20 (m, 9H, C(14)**H**, C(15)**H**, C(17)**H**, C(18)**H**, C(20)**H**, C(21)**H**, C(22)**H**, C(23)**H**, C(24)**H**) ppm; ^{13}C NMR (75 MHz, $CDCl_3$) δ: 157.4 (q**C**-4), 156.1 (q**C**-11), 147.9 (q**C**-10), 144.8 (**C**(2)H), 138.5 (q**C**-7), 137.0 (q**C**-19), 130.7 (**C**(18)H), 128.8 (2 × C, **C**(21)H, **C**(23)H), 128.1 (2 × C, **C**(17)H, (**C**(22)H), 128.0 (**C**(8)H), 127.2 (**C**(15)H), 126.8 (2 × C, **C**(20)H, **C**(24)H), 124.9 (**C**(6)H), 124.1 (**C**(14)H), 122.7 (q**C**-12), 121.1 (**C**(5)H), 120.6 (**C**(13)H), 116.3 (2 × C, q**C**-3, q**C**-9), 112.1 (**C**(16)H) ppm; HRMS (ESI-TOF) *m/z*: $[M+H]^+$ calcd for $C_{23}H_{16}NO$: 322.1226; found: 322.1227.

Note: ^{13}C-NMR shifts at 116.3 and 128.1 ppm represent two individual carbon signals each, as confirmed by 2D NMR experiments.

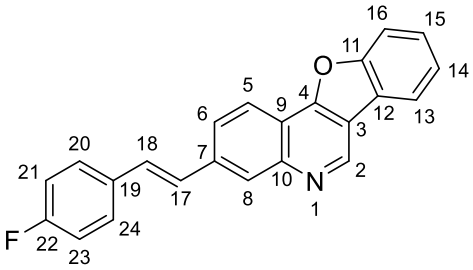
(*E*)-3-(4-Methoxystyryl)benzofuro[3,2-*c*]quinoline (70)



Compound **70** was prepared *via* the procedure described for **65** using **60** (0.114 g, 0.30 mmol, 1.0 equiv.) and 4-vinylanisole (0.04 mL, 0.33 mmol, 1.1 equiv.) to yield **70** as a yellow solid (0.084 g, 80%); m.p. 168–170 °C; IR (film) ν_{max} 1687 (trans alkene C=C stretch), 1603 (C=N stretch), 1560 (aromatic C=C stretch), 1347, 1176, 1033 (ether C-O stretch) cm^{-}

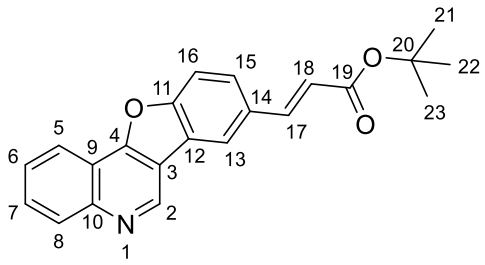
^{1}; ^{1}H NMR (300 MHz, $CDCl_3$) δ: 9.47 (s, 1H, C(2)**H**), 8.38 (d, *J* = 8.6 Hz, 1H, C(5)**H**), 8.27 (d, *J* = 1.2 Hz, 1H, C(8)**H**), 8.09 (dd, *J* = 7.2, 1.3 Hz, 1H, C(13)**H**), 7.92 (dd, *J* = 8.6, 1.5 Hz, 1H, C(6)**H**), 7.75 (d, *J* = 7.8 Hz, 1H, C(16)**H**), 7.65–7.42 (m, 4H, C(14)**H**, C(15)**H**, C(20)**H**, C(24)**H**), 7.39–7.13 (m, 2H, C(17)**H**, C(18)**H**), 7.00–6.89 (m, 2H, C(21)**H**, C(23)**H**), 3.86 (s, 3H, C(25)**H₃**) ppm; ^{13}C NMR (75 MHz, $CDCl_3$) δ: 159.7 (q**C**-22), 157.4 (q**C**-4), 156.0 (q**C**-11), 148.0 (q**C**-10), 144.7 (**C**(2)H), 138.9 (q**C**-7), 130.3 (**C**(18)H), 129.8 (q**C**-19), 128.1 (2 × C, **C**(20)H, **C**(24)H), 127.5 (**C**(8)H), 127.1 (**C**(15)H), 126.0 (**C**(17)H), 124.8 (**C**(6)H), 124.1 (**C**(14)H), 122.8 (q**C**-12), 121.0 (**C**(5)H), 120.5 (**C**(13)H), 116.2 (q**C**-3), 116.0 (q**C**-9), 114.3 (2 × C, **C**(21)H, **C**(23)H), 112.1 (**C**(16)H), 55.4 (**C**(25)H_3) ppm; HRMS (ESI-TOF) *m/z*: $[M+H]^+$ calcd for $C_{24}H_{18}NO_2$: 352.1332; found: 352.1333.

(*E*)-3-(4-Fluorostyryl)benzofuro[3,2-*c*]quinoline (71)



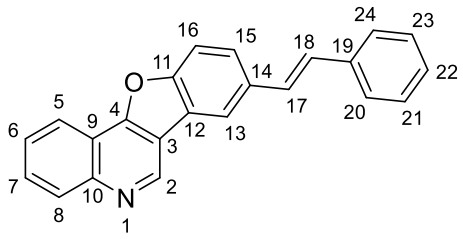
Compound **71** was prepared *via* the procedure described for **65** using **60** (0.114 g, 0.30 mmol, 1.0 equiv.) and 4-fluorostyrene (0.04 mL, 0.33 mmol, 1.1 equiv.) to yield **71** as a yellow solid (0.063 g, 62%); m.p. 209–211 °C; IR (film) ν_{max} 1682 (trans alkene C=C stretch), 1637 (C=N stretch), 1508 (aromatic C=C stretch), 1347, 1228 (ether C-O stretch), 1158 (C-F stretch), 1012 (ether C-O stretch) cm^{-1}; ^{1}H NMR (300 MHz, $CDCl_3$) δ: 9.48 (s, 1H, C(2)**H**), 8.39 (d, *J* = 8.6 Hz, 1H, C(5)**H**), 8.28 (d, *J* = 1.4 Hz, 1H, C(8)**H**), 8.15–8.04 (m, 1H, C(13)**H**), 7.91 (dd, *J* = 8.6, 1.6 Hz, 1H, C(6)**H**), 7.76 (dd, *J* = 7.6, 0.7 Hz, 1H, C(16)**H**), 7.64–7.42 (m, 4H, C(14)**H**, C(15)**H**, C(20)**H**, C(24)**H**), 7.38–7.20 (m, 2H, C(17)**H**, C(18)**H**), 7.16–7.02 (m, 2H, C(21)**H**, C(23)**H**) ppm; ^{13}C NMR (75 MHz, $CDCl_3$) δ: 162.6 (d, $^{1}J_{(C,F)}$ = 248 Hz, q**C**(22)F), 157.4 (q**C**-4), 156.0 (q**C**-11), 147.9 (q**C**-10), 144.8 (**C**(2)H), 138.3 (q**C**-7), 133.2 (d, $^{4}J_{(C,F)}$ = 3 Hz, q**C**-19), 129.4 (**C**(18)H), 128.3 (d, $^{3}J_{(C,F)}$ = 8 Hz, 2 × C, **C**(20)H, **C**(24)H), 127.89, 127.86 (**C**(8)H, **C**(17)H), 127.3 (**C**(15)H), 124.8 (**C**(6)H), 124.1 (**C**(14)H), 122.7 (q**C**-12), 121.1 (**C**(5)H), 120.6 (**C**(13)H), 116.34, 116.31 (q**C**-3, q**C**-9), 115.8 (d, $^{2}J_{(C,F)}$ = 22 Hz, 2 × C, **C**(21)H, **C**(23)H), 112.1 (**C**(16)H) ppm; ^{19}F NMR (282 MHz, $CDCl_3$) δ: -113 ppm; HRMS (ESI-TOF) *m/z*: $[M+H]^+$ calcd for $C_{23}H_{15}FNO$: 340.1132; found: 340.1134.

tert-Butyl (_E_)-3-(benzofuro[3,2-_c_]quinolin-8-yl)acrylate (72)



Compound **72** was prepared *via* the procedure described for **64** using **61** (0.076 g, 0.20 mmol, 1.0 equiv.) to yield **72** as a white solid (0.050 g, 73%); m.p. 157–158 °C; IR (film) ν_{max} 1703 (ester C=O stretch), 1638 (trans alkene C=C stretch), 1594 (C=N stretch), 1566 (aromatic C=C stretch), 1367, 1203 (ether C-O stretch), 1151 (ester C-O stretch) cm^{-1}; ^{1}H NMR (300 MHz, $CDCl_3$) δ: 9.45 (s, 1H, C(2)**H**), 8.36 (dd, *J* = 8.1, 1.1 Hz, 1H, C(5)**H**), 8.30–8.09 (m, 2H, C(8)**H**, C(13)**H**), 7.89–7.50 (m, 5H, C(6)**H**, C(7)**H**, C(15)**H**, C(16)**H**, C(17)**H**), 6.47 (d, *J* = 15.9 Hz, 1H, C(18)**H**), 1.58 (s, 9H, C(21)$\mathbf{H}_3$, C(22)$\mathbf{H}_3$, C(23)$\mathbf{H}_3$) ppm; ^{13}C NMR (75 MHz, $CDCl_3$) δ: 166.2 (q**C**-19), 158.2 (q**C**-4), 156.7 (q**C**-11), 147.7 (q**C**-10), 144.3 (**C**(2)H), 143.0 (**C**(17)H), 131.2 (q**C**-14), 130.0 (**C**(8)H), 129.6 (**C**(7)H), 127.24 (**C**(6)H), 127.22 (**C**(15)H), 123.5 (q**C**-12), 120.8 (**C**(5)H), 120.4 (**C**(18)H), 120.2 (**C**(13)H), 117.1 (q**C**-9), 115.9 (q**C**-3), 112.5 (**C**(16)H), 80.7 (q**C**-20), 28.3 (3 × C, **C**(21)H_3, **C**(22)H_3, **C**(23)H_3) ppm; HRMS (ESI-TOF) *m/z*: $[M+H]^+$ $C_{22}H_{20}NO_3$: 346.1438; found: 346.1430.

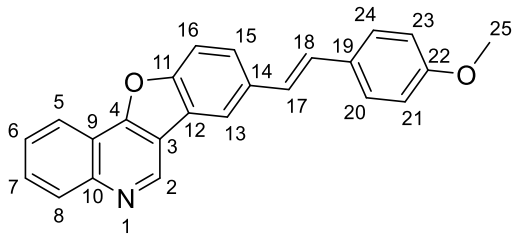
(_E_)-8-Styrylbenzofuro[3,2-_c_]quinoline (73)



Compound **73** was prepared *via* the procedure described for **65** using **61** (0.114 g, 0.30 mmol, 1.0 equiv.) to yield **73** as a yellow solid (0.083 g, 86%); m.p. 200–203 °C; IR (film) ν_{max} 1650 (trans alkene C=C stretch), 1598 (C=N stretch), 1567 (aromatic C=C stretch), 1324, 1195 (ether C-O stretch) cm^{-1}; ^{1}H NMR (300 MHz, $CDCl_3$) δ: 9.50 (s, 1H, C(2)**H**), 8.39 (dd, *J* = 8.1, 1.3 Hz, 1H, C(5)**H**), 8.32–8.11 (m, 2H, C(8)**H**), C(13)**H**), 7.87–7.63 (m, 4H, C(6)**H**, C(7)**H**, C(15)**H**, C(16)**H**), 7.61–7.55 (m, 2H, C(20)**H**, C(24)**H**), 7.47–7.11 (m, 5H, C(17)**H**, C(18)**H**, C(21)**H**, C(22)**H**, C(23)**H**) ppm; ^{13}C NMR (75 MHz, $CDCl_3$) δ: 158.0 (q**C**-4), 155.6 (q**C**-11), 147.5 (q**C**-10), 144.4 (**C**(2)H), 137.2 (q**C**-19), 133.9 (q**C**-14), 129.9 (**C**(8)H), 129.4 (**C**(7)H), 128.9 (**C**(18)H), 128.8 (2 × C, **C**(21)H, **C**(23)H), 128.1 (**C**(17)H), 127.8 (**C**(22)H) 127.1 (**C**(6)H), 126.5 (2 × C, **C**(20)H, **C**(24)H), 126.0 (**C**(15)H), 123.3 (q**C**-12), 120.8 (**C**(5)H), 118.2 (**C**(13)H),

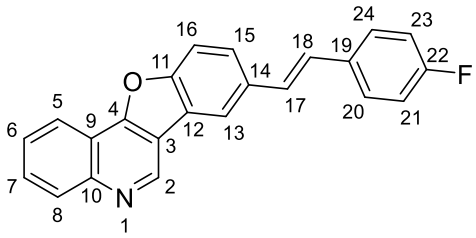
117.2 (q**C**-9), 116.2 (q**C**-3), 112.2 (**C**(16)H) ppm; HRMS (ESI-TOF) *m/z*: $[M+H]^+$ calcd for $C_{23}H_{16}NO$: 322.1226; found: 322.1223.

(*E*)-8-(4-Methoxystyryl)benzofuro[3,2-*c*]quinoline (74)



Compound **74** was prepared *via* the procedure described for **65** using **61** (0.114 g, 0.30 mmol, 1.0 equiv.) and 4-vinylanisole (0.04 mL, 0.33 mmol, 1.1 equiv.) to yield **74** as a white solid (0.068 g, 65%); m.p. 204–206 °C; IR (film) ν_{max} 1637 (trans alkene C=C stretch), 1605 (C=N stretch), 1567 (aromatic C=C stretch), 1323, 1253, 1046 (ether C-O stretch) cm^{-1}; ^1H NMR (300 MHz, $CDCl_3$) δ: 9.52 (s, 1H, C(2)**H**), 8.42 (d, *J* = 8.1 Hz, 1H, C(5)**H**), 8.29 (d, *J* = 8.5 Hz, 1H, C(8)**H**), 8.19 (d, *J* = 0.9 Hz, 1H, C(13)**H**), 7.88–7.61 (m, 4H, C(6)**H**, C(7)**H**, C(15)**H**, C(16)**H**), 7.58–7.43 (m, 2H, C(20)**H**, C(24)**H**), 7.16 (app. s, 2H, C(17)**H**, C(18)**H**), 7.02–6.86 (m, 2H, C(21)**H**, C(23)**H**), 3.86 (s, 3H, C(25)**H₃**) ppm; ^{13}C NMR (75 MHz, $CDCl_3$) δ: 159.4 (q**C**-22), 158.0 (q**C**-4), 155.4 (q**C**-11), 147.5 (q**C**-10), 144.4 (**C**(2)H), 134.3 (q**C**-14), 130.0 (q**C**-19), 129.9 (**C**(8)H), 129.4 (**C**(7)H), 128.5 (**C**(18)H), 127.7 (2 × C, **C**(20)H, **C**(24)H), 127.1 (**C**(6)H), 126.1 (**C**(17)H), 125.8 (**C**(15)H), 123.2 (q**C**-12), 120.8 (**C**(5)H), 117.9 (**C**(13)H), 117.2 (q**C**-9), 116.3 (q**C**-3), 112.2 (**C**(16)H), 114.2 (2 × C, **C**(21)H, **C**(23)H), 55.4 (**C**(25)H_3) ppm; HRMS (ESI-TOF) *m/z*: $[M+H]^+$ calcd for $C_{24}H_{18}NO_2$: 352.1332; found: 352.1337.

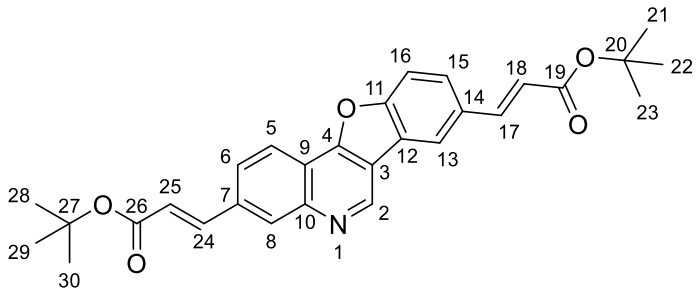
(*E*)-8-(4-Fluorostyryl)benzofuro[3,2-*c*]quinoline (75)



Compound **75** was prepared *via* the procedure described for **65** using **61** (0.114 g, 0.30 mmol, 1.0 equiv.) and 4-fluorostyrene (0.04 mL, 0.33 mmol, 1.1 equiv.) to yield **75** as a white solid (0.077 g, 76%); m.p. 202–205 °C; IR (film) ν_{max} 1640 (trans alkene C=C stretch), 1598 (C=N stretch), 1569 (aromatic C=C stretch), 1325, 1234 (ether C-O stretch), 1159 (C-F stretch), 1196 (ether C-O stretch) cm^{-1}; ^1H NMR (300 MHz, $CDCl_3$) δ: 9.51 (s, 1H, C(2)**H**), 8.40 (dd, *J* = 8.2, 0.9 Hz, 1H, C(5)**H**), 8.28 (d, *J* = 8.4 Hz, 1H, C(8)**H**), 8.18 (d, *J* = 1.1 Hz, 1H, C(13)**H**),

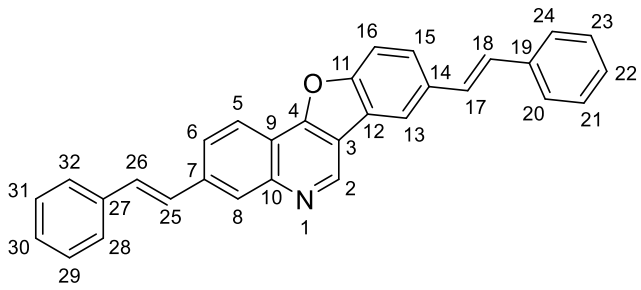
7.88–7.61 (m, 4H, C(6)**H**, C(7)**H**, C(15)**H**, C(16)**H**), 7.60–7.44 (m, 2H, C(20)**H**, C(24)**H**), 7.24–7.01 (m, 4H, C(17)**H**, C(18)**H**, C(21)**H**, C(23)**H**) ppm; ^{13}C NMR (75 MHz, $CDCl_3$) δ: 162.4 (d, $^1J_{(C,F)}$ = 248 Hz, q**C**(22)F), 157.9 (q**C**-4), 155.5 (q**C**-11), 147.5 (q**C**-10), 144.3 (**C**(2)H), 133.7 (q**C**-14), 133.4 (d, $^4J_{(C,F)}$ = 3 Hz, q**C**-19), 129.9 (**C**(8)H), 129.4 (**C**(7)H), 128.0 (d, $^3J_{(C,F)}$ = 8 Hz, 2 × C, **C**(20)H, **C**(24)H), 127.9 (d, $^6J_{(C,F)}$ = 2 Hz, **C**(17)H), 127.6 (**C**(18)H), 125.9 (**C**(15)H), 123.2 (q**C**-12), 120.8 (**C**(5)H), 118.0 (**C**(13)H), 117.1 (q**C**-9), 116.2 (q**C**-3), 115.7 (d, $^2J_{(C,F)}$ = 22 Hz, 2 × C, **C**(21)H, **C**(23)H), 112.2 (**C**(16)H) ppm; ^{19}F NMR (282 MHz, $CDCl_3$) δ: -114 ppm; HRMS (ESI-TOF) *m/z*: $[M+H]^+$ calcd for $C_{23}H_{15}FNO$: 340.1132; found: 340.1135.

Di-*tert*-butyl 3,3'-(benzofuro[3,2-*c*]quinoline-3,8-diyl)(2*E*,2'*E*)-diacrylate (76)



Compound **76** was prepared *via* the procedure described for **64** using **62** (0.050 g, 0.11 mmol, 1.0 equiv.) and *tert*-butyl acrylate (0.03 mL, 0.22 mmol, 2.2 equiv.) to yield **76** as a white solid (0.023 g, 43%); m.p. 217–219 °C; IR (film) ν_{max} 1703 (ester C=O stretch), 1638 (trans alkene C=C stretch), 1559 (C=N stretch), 1512 (aromatic C=C stretch), 1368, 1201 (ether C-O stretch), 1148 (ester C-O stretch) cm^{-1}; ^{1}H NMR (300 MHz, $CDCl_3$) δ: 9.49 (s, 1H, C(2)**H**), 8.44–8.29 (m, 2H, C(5)**H**, C(8)**H**), 8.23 (d, *J* = 0.8 Hz, 1H, C(13)**H**), 7.94–7.66 (m, 5H, C(6)**H**, C(15)**H**, C(16)**H**, C(17)**H**, C(24)**H**), 6.67–6.40 (m, 2H, C(18)**H**, C(25)**H**), 1.61–1.50 (m, 18H, C(21)**H**$_3$, C(22)**H**$_3$, C(23)**H**$_3$, C(28)**H**$_3$, C(29)**H**$_3$, C(30)**H**$_3$) ppm; ^{13}C NMR (75 MHz, $CDCl_3$) δ: 166.1 (q**C**-19), 166.0 (q**C**-26), 157.8 (q**C**-4), 156.9 (q**C**-11), 147.7 (q**C**-10), 145.0 (**C**(2)H), 142.8 (**C**(17)H), 142.7 (**C**(24)H), 136.0 (q**C**-7), 131.4 (q**C**-14), 130.7 (**C**(8)H), 127.5 (**C**(15)H), 125.3 (**C**(6)H), 123.3 (q**C**-12), 122.3 (**C**(25)H), 121.4 (**C**(5)H), 120.5 (**C**(18)H), 120.3 (**C**(13)H), 117.6 (q**C**-9), 116.6 (q**C**-3), 112.6 (**C**(16)H), 80.9, 80.7 (q**C**-20, q**C**-27), 28.24, 28.22 (6 × C, **C**(21)H$_3$, **C**(22)H$_3$, **C**(23)H$_3$, **C**(28)H$_3$, **C**(29)H$_3$, **C**(30)H$_3$) ppm; HRMS (ESI-TOF) *m/z*: $[M+H]^+$ calcd for $C_{29}H_{30}NO_5$: 472.2118; found: 472.2117.

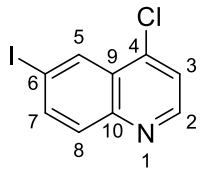
3,8-Di((*E*)-styryl)benzofuro[3,2-*c*]quinoline (77)



Compound **77** was prepared *via* the procedure described for **64** using **62** (0.115 g, 0.25 mmol, 1.0 equiv.) and styrene (0.06 mL, 0.55 mmol, 2.2 equiv.) to yield **77** as a white solid (0.076 g, 36%); m.p. >250 °C; IR (film) ν_{max} 1691 (trans alkene C=C stretch), 1594 (C=N stretch), 1560 (aromatic C=C stretch), 1326, 1044 (ether C-O stretch) cm^{-1}; ^{1}H NMR (600 MHz, $(CD_3)_2SO$) δ: 9.69 (s, 1H, C(2)**H**), 8.61 (d, *J* = 1.5 Hz, 1H, C(13)**H**), 8.41 (d, *J* = 8.5 Hz, 1H, C(5)**H**), 8.35 (d, *J* = 1.3 Hz, 1H, C(8)**H**), 8.17 (dd, *J* = 8.7, 1.4 Hz, 1H, C(6)**H**), 7.94 (d, *J* = 8.5 Hz, 1H, C(16)**H**), 7.87 (dd, *J* = 8.6, 1.6 Hz, 1H, C(13)**H**), 7.75–7.63 (m, 4H, 4 × Ar-C**H**), 7.59 (app. s, 2H, C(25)**H**, C(26)**H**), 7.54–7.20 (m, 8H, C(17)**H**, C(18)**H**, 6 × Ar-C**H**) ppm; ^{13}C NMR (150 MHz, $(CD_3)_2SO$) δ: 157.4 (q**C**-4), 155.5 (q**C**-11), 148.1 (q**C**-10), 146.0 (**C**(2)H), 139.0 (q**C**-7), 137.5, 137.3 (q**C**-19, q**C**-27), 134.3 (q**C**-14), 131.2 (**C**(26)H),129.3, 129.0, 128.6, 128.33, 128.29, 127.3, 127.2, 127.0 (**C**(17)H, **C**(18)H, **C**(25)H, 11 × Ar-**C**H), 125.6 (**C**(6)H), 123.2 (q**C**-12), 121.4 (**C**(5)H), 119.1 (**C**(13)H), 116.4 (q**C**-3), 115.9 (q**C**-9), 112.8 (**C**(16)H) ppm; HRMS (ESI-TOF) *m/z*: $[M+H]^+$ calcd for $C_{31}H_{22}NO$: 424.1696; found: 424.1690.

Note: This compound was highly insoluble, spectra were acquired on <2 mg after heating in $(CD_3)_2SO$ and it was difficult to directly assign. As with other compounds, some ^{13}C shifts from this spectrum represent more than one signal as confirmed by 2D NMR experiments.

4-Chloro-6-iodoquinoline (78)[157]

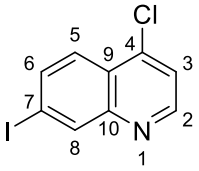


To a Schlenk tube under nitrogen atmosphere were added CuI (0.019 g, 0.10 mmol, 10 mol%), 6-bromo-4-chloroquinoline (0.243 g, 1.0 mmol, 1.0 equiv.), anhydrous NaI (0.300 g, 2.0 mmol, 2.0 equiv.) and *trans*-*N*,*N*'-dimethylcyclohexane-1,2-diamine (0.028 g, 0.20 mmol, 20 mol%). The Schlenk was placed under vacuum and then refilled once with nitrogen. Anhydrous 1,4-dioxane (1 mL) was added and the reaction mixture was degassed with a bubble of nitrogen for 10 min. The resulting

green/blue mixture was stirred at 110 °C for 24 h under a nitrogen atmosphere.[108] The cooled reaction mixture was slowly added to iced water (15 mL) and extracted with DCM (3 × 10 mL). The combined organic layers were washed with sat. $Na_2S_2O_3$ (10 mL), H_2O (10 mL), and brine (15 mL), dried over $MgSO_4$, filtered and concentrated under reduced pressure to give **78** as a white solid (0.216 g, 75%); 138–139 °C (lit.[158] 138–139.5 °C); ^{1}H NMR (300 MHz, $CDCl_3$) δ: 8.78 (d, *J* = 4.7 Hz, 1H, C(2)**H**), 8.62 (d, *J* = 1.9 Hz, 1H, C(5)**H**), 8.01 (dd, *J* = 8.9, 1.9 Hz, 1H, C(7)**H**), 7.83 (d, *J* = 8.9 Hz, 1H, C(8)**H**), 7.49 (d, *J* = 4.7 Hz, 1H, C(3)**H**) ppm; ^{13}C NMR (75 MHz, $CDCl_3$) δ: 150.4 (**C**(2)H), 148.1 (q**C**-10), 141.3 (q**C**(4)Cl), 139.3 (**C**(7)H), 133.1 (**C**(5)H), 131.4 (**C**(8)H), 128.0 (q**C**-9), 121.8 (**C**(3)H), 93.6 (q**C**(6)I) ppm; *m/z* (ES+): 290 ((M+H)$^+$ 100%).

Spectral characteristics were consistent with previously reported data.[157]

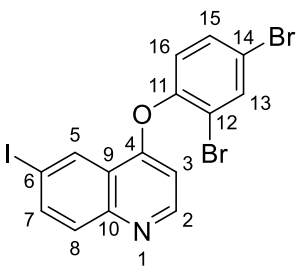
4-Chloro-7-iodoquinoline (79)[159]



Compound **79** was prepared *via* the procedure described for **78** using 7-bromo-4-chloroquinoline (0.243 g, 1.0 mmol, 1.0 equiv.), to yield **79** as a white solid (0.287 g, 99%); m.p. 98–100 °C (lit.[159] 102.3–102.7 °C); ^{1}H NMR (300 MHz, $CDCl_3$) δ: 8.76 (d, *J* = 4.7 Hz, 1H, C(2)**H**), 8.55 (dd, *J* = 1.5, 0.5 Hz, 1H, C(8)**H**), 7.97–7.83 (m, 2H, C(5)**H**, C(6)**H**), 7.50 (d, *J* = 4.7 Hz, 1H, C(3)**H**) ppm; ^{13}C NMR (75 MHz, $CDCl_3$) δ: 150.6 (**C**(2)H), 149.7 (q**C**-10), 142.8 (q**C**(4)Cl), 138.8 (**C**(8)H), 136.4 (**C**(6)H), 125.7 (q**C**-9), 125.4 (**C**(5)H), 121.7 (**C**(3)H), 96.8 (q**C**(7)I) ppm; *m/z* (ES+): 290 ((M+H)$^+$ 100%).

Spectral characteristics were consistent with previously reported data.[159]

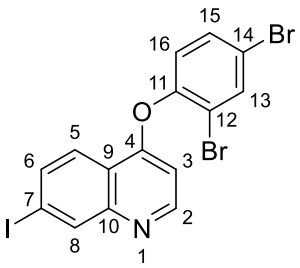
4-(2,4-Dibromophenoxy)-6-iodoquinoline (80)



Compound **80** was prepared *via* the procedure described for **45** using **78** (0.145 g, 0.50 mmol, 1.0 equiv.) and 2,4-dibromophenol (0.630 g, 2.5 mmol, 5.0 equiv.) to yield **80** as a brown solid (0.168 g, 67%); m.p. 175–177 °C; IR (film) 1658 (C=N stretch), 1558 (aromatic C=C stretch), 1348, 1048 (ether C-O stretch), 705, 665 (C-Br stretch), 630 (C-I stretch) cm^{-1}; ^{1}H NMR (300 MHz, $CDCl_3$) δ: 8.85–8.58 (m, 2H, C(2)**H**, C(5)**H**), 8.01 (dd, *J* = 8.9, 2.0 Hz, 1H,

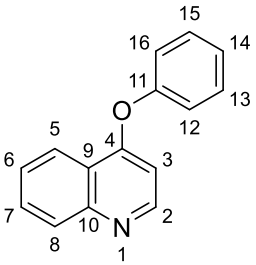
C(7)**H**), 7.95–7.75 (m, 2H, C(8)**H**, C(13)**H**), 7.56 (dd, *J* = 8.6, 2.3 Hz, 1H, C(15)**H**), 7.12 (d, *J* = 8.6 Hz, 1H, C(16)**H**), 6.40 (d, *J* = 5.1 Hz, 1H, C(3)**H**) ppm; ^{13}C NMR (75 MHz, $CDCl_3$) δ: 159.2 (q**C**-4), 151.5 (**C**(2)H), 150.1 (q**C**-11), 148.8 (q**C**-10), 139.1 (**C**(7)H), 136.7 (**C**(13)H), 132.4 (**C**(15)H), 130.9 (**C**(8)H), 130.8 (**C**(5)H), 124.4 (**C**(16)H), 122.5 (q**C**-9), 119.7 (q**C**(14)Br), 117.4 (q**C**(12)Br), 104.1 (**C**(3)H), 92.0 (q**C**(6)I) ppm; HRMS (ESI-TOF) *m/z*: $[M+H]^+$ calcd for $C_{15}H_9Br_2INO$: 503.8090; found: 503.8093.

4-(2,4-Dibromophenoxy)-7-iodoquinoline (81)



Compound **81** was prepared *via* the procedure described for **45** using **79** (0.145 g, 0.50 mmol, 1.0 equiv.) and 2,4-dibromophenol (0.630 g, 2.5 mmol, 5.0 equiv.) to yield **81** as a beige solid (0.220 g, 60%); m.p. 152–154 °C; IR (film) ν_{max} 1652 (C=N stretch), 1584 (aromatic C=C stretch), 1289, 1047 (ether C-O stretch), 750, 666 (C-Br stretch), 554 (C-I stretch) cm^{-1}; ^{1}H NMR (300 MHz, $CDCl_3$) δ: 8.66 (d, *J* = 5.1 Hz, 1H, C(2)**H**), 8.54 (d, *J* = 1.5 Hz, 1H, C(8)**H**), 8.09 (d, *J* = 8.8 Hz, 1H, C(5)**H**), 7.96–7.80 (m, 2H, C(6)**H**, C(13)**H**), 7.55 (dd, *J* = 8.6, 2.3 Hz, 1H, C(15)**H**), 7.12 (d, *J* = 8.6 Hz, 1H, C(16)**H**), 6.42 (d, *J* = 5.1 Hz, 1H, C(3)**H**) ppm; ^{13}C NMR (75 MHz, $CDCl_3$) δ: 160.5 (q**C**-4), 151.8 (**C**(2)H), 150.5 (q**C**-10), 150.2 (q**C**-11), 138.2 (**C**(8)H), 136.7 (**C**(13)H), 135.2 (**C**(6)H), 132.4 (**C**(15)H), 124.4 (**C**(16)H), 123.1 (**C**(5)H), 120.0 (q**C**-9), 119.7 (q**C**(14)Br), 117.3 (q**C**(12)Br), 104.1 (**C**(3)H), 96.8 (q**C**(7)I) ppm; HRMS (ESI-TOF) *m/z*: $[M+H]^+$ calcd for $C_{15}H_9Br_2INO$: 503.8090; found: 503.8094.

4-Phenoxyquinoline (82)[160]

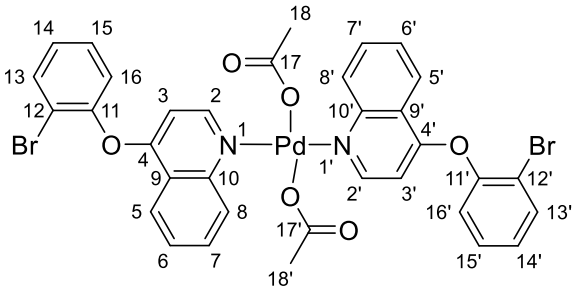


Compound **82** was prepared *via* the procedure described for **45** using **42** (0.164 g, 1.0 mmol, 1.0 equiv.) and phenol (0.471 g, 5.0 mmol, 5.0 equiv.) to yield **82** as a yellow oil (0.192 g, 87%); ^{1}H NMR (300 MHz, $CDCl_3$) δ: 8.66 (d, *J* = 5.1 Hz, 1H, C(2)**H**), 8.36 (dd, *J* = 8.4, 1.1 Hz, 1H, C(5)**H**), 8.10 (d, *J* = 8.3 Hz, 1H, C(8)**H**), 7.74 (ddd, *J* = 8.5, 6.9, 1.5 Hz, 1H, C(7)**H**), 7.56 (ddd, *J* = 8.2, 6.9, 1.1 Hz, 1H, C(6)**H**), 7.50–7.39 (m, 2H, C(13)**H**, C(15)**H**), 7.33–7.23 (m, 1H, C(14)**H**), 7.22-7.13 (m, 2H, C(12)**H**, C(16)**H**), 6.54 (d, *J* = 5.2 Hz, 1H, C(3)**H**) ppm; ^{13}C NMR (75 MHz, $CDCl_3$) δ: 161.9 (q**C**-4), 154.4 (q**C**-11), 151.1 (**C**(2)H), 149.8 (q**C**-10), 130.3 (2 × C,

C(13)H, **C**(15)H), 130.1 (**C**(7)H), 129.1 (**C**(8)H), 126.1 (**C**(6)H), 125.6 (**C**(14)H), 121.8 (**C**(5)H), 121.5 (q**C**-9), 121.1 (2 × C, **C**(12)H, **C**(16)H), 104.4 (**C**(3)H) ppm; *m/z* (ES+): 222 ($(M+H)^+$ 100%).

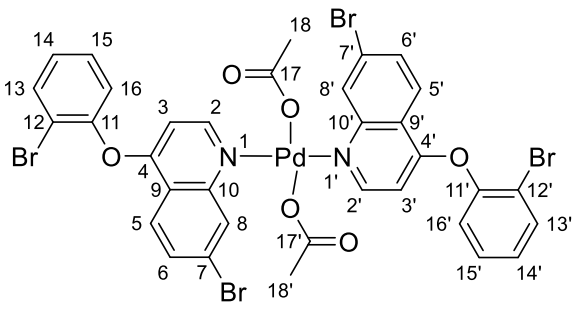
Spectral characteristics were consistent with previously reported data.[160]

4-(2-Bromophenoxy)quinoline Palladium Diacetate Dimer (83)



To an NMR tube at r.t. were added **45** (61.5 mg, 0.20 mmol, 1.0 equiv.), $Pd(OAc)_2$ (22.9 mg, 0.10 mmol, 0.50 equiv.) and $CDCl_3$ (0.6 mL) to give **83**; decomposition >150°C; IR (film) ν_{max} 1615 (ester C=O stretch), 1589 (C=N stretch), 1573 (aromatic C=C stretch), 1303 (ether C-O stretch), 1217 (ester C-O stretch), 1075 (ether C-O stretch), 695 (C-Br stretch) cm^{-1}; ^{1}H NMR (300 MHz, $CDCl_3$) δ: 10.20 (d, *J* = 8.6 Hz, 2H, C(8)**H**, C(8')**H**), 9.46 (d, *J* = 6.2 Hz, 2H, C(2)**H**, C(2')**H**), 8.41 (dd, *J* = 8.1, 0.9 Hz, 2H, C(5)**H**, C(5')**H**), 8.08 (ddd, *J* = 8.6, 7.0, 1.4 Hz, 2H, C(7)**H**, C(7')**H**), 7.84–7.59 (m, 4H, C(6)**H**, C(6')**H** C(13)**H**, C(13')**H**), 7.54–7.37 (m, 2H, C(15)**H**, C(15')**H**), 7.34–7.11 (m, 4H, C(14)**H**, C(14')**H** C(16)**H**, C(16')**H**), 6.47 (d, *J* = 6.2 Hz, 2H, C(3)**H**, C(3')**H**), 1.53 (s, 6H, C(18)$\mathbf{H_3}$, C(18')$\mathbf{H_3}$) ppm; ^{13}C NMR (150 MHz, $CDCl_3$) δ: 178.3 (q**C**-17, q**C**-17'), 162.6 (q**C**-4, q**C**-4'), 156.1 (**C**(2)H, **C**(2')H), 150.2 (q**C**-11, q**C**-11'), 147.9 (q**C**-10, q**C**-11'), 134.5 (**C**(13)H, **C**(13')H), 132.1 (**C**(7)H, **C**(7')H), 129.4 (**C**(15)H, **C**(15')H), 129.0 (**C**(8)H, **C**(8')H), 128.1 (**C**(14)H, **C**(14')H), 127.4 (**C**(6)H, **C**(6')H), 123.4 (**C**(16)H, **C**(16')H), 122.0 (**C**(5)H, **C**(5')H), 121.3 (q**C**-9, q**C**-9'), 116.2 (q**C**(12)Br, q**C**(12')Br), 103.9 (**C**(3)H, **C**(3')H), 22.6 (**C**(18)H_3, **C**(18')H_3) ppm; HRMS (ESI-TOF) *m/z*: $[M\text{-}OAc]^+$ calcd for for $C_{32}H_{23}Br_2N_2O_4Pd$ 762.9054; found: 762.9081.

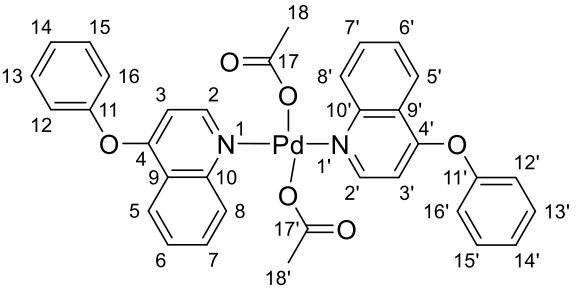
7-Bromo-4-(2-bromophenoxy)quinoline Palladium Diacetate Dimer (84)



To an NMR tube at r.t. were added **60** (60.8 mg, 0.16 mmol, 1.0 equiv.), $Pd(OAc)_2$ (18.0 mg, 0.08 mmol, 0.50 equiv.) and $CDCl_3$ (0.6 mL) to give **84**; decomposition >190°C; IR (film) ν_{max} 1623 (ester C=O stretch), 1590 (C=N stretch), 1511 (aromatic C=C stretch), 1306 (ether C-O stretch), 1219 (ester C-O stretch), 1063 (ether C-O stretch), 733, 693 (C-Br stretch) cm^{-1}; ^1H NMR (600 MHz, $CDCl_3$) δ: 10.36 (d, *J* = 1.7 Hz, 2H, C(8)**H**, C(8')**H**), 9.43 (d, *J* = 6.2 Hz, 2H, C(2)**H**, C(2')**H**), 8.29 (d, *J* = 8.8 Hz, 2H, C(5)**H**, C(5')**H**), 7.93–7.66 (m, 4H, C(6)**H**, C(6')**H**, C(13)**H**, C(13')**H**), 7.57–7.41 (m, 2H, C(15)**H**, C(15')**H**), 7.37–7.16 (m, 4H, C(14)**H**, C(14')**H**, C(16)**H**, C(16')**H**), 6.46 (d, *J* = 6.2 Hz, 2H, C(3)**H**, C(3)**H**), 1.59 (s, 6H, C(18)$\mathbf{H_3}$, C(18')$\mathbf{H_3}$) ppm; ^{13}C NMR (150 MHz, $CDCl_3$) δ: 178.4 (q**C**-17, q**C**-17'), 162.8 (q**C**-4, q**C**-4'), 157.4 (**C**(2)H, **C**(2')H), 149.9 (q**C**-11, q**C**-11'), 148.4 (q**C**-10, q**C**-10'), 134.6 (**C**(13)H, **C**(13')H), 131.2 (**C**(8)H, **C**(8')H), **C**(6)H, **C**(6')H), 129.6 (**C**(15)H, **C**(15')H), 128.4 (**C**(14)H, **C**(14')H), 127.0 (q**C**(7)Br, q**C**(7')Br), 123.5 (**C**(5)H, **C**(5')H), 123.3 (**C**(16)H, **C**(16')H), 120.1 (q**C**-9, q**C**-9'), 116.1 (q**C**(12)Br, q**C**(12')Br), 104.2 (**C**(3)H, **C**(3')H), 22.7 (**C**(18)H_3, **C**(18')H_3) ppm; HRMS (ESI-TOF) *m/z*: $[M\text{-}OAc]^+$ calcd for $C_{32}H_{21}Br_4N_2O_4Pd$ 918.7264; found: 918.7284.

Note: ^{13}C-NMR shift at 131.2 ppm represents two individual carbon signals as confirmed by 2D NMR experiments.

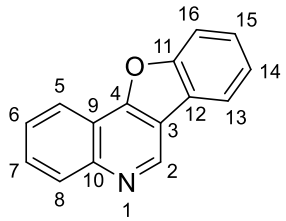
4-Phenoxyquinoline Palladium Diacetate Dimer (85)



To 25 mL RBF at r.t. were added **82** (55.0 mg, 0.25 mmol, 1.0 equiv.), $Pd(OAc)_2$ (27.9 mg, 0.12 mmol, 0.50 equiv.) and $CDCl_3$ (2.0 mL) to give **85**; decomposition >150°C; IR (film) ν_{max} 1621 (ester C=O stretch), 1595 (C=N stretch), 1512 (aromatic C=C stretch), 1305 (ether C-O stretch), 1203 (ester C-O

stretch), 1063 (ether C-O stretch) cm^{-1}; ^{1}H NMR (300 MHz, $CDCl_3$) δ: 10.08 (d, *J* = 8.6 Hz, 2H, C(8)**H**, C(8')**H**), 9.34 (d, *J* = 6.2 Hz, 2H, C(2)**H**, C(2')**H**), 8.28 (dd, *J* = 8.4, 1.0 Hz, 2H, C(5)**H**, C(5')**H**), 7.99 (ddd, *J* = 8.6, 7.0, 1.4 Hz, 2H, C(7)**H**, C(7')**H**), 7.61 (ddd, *J* = 8.2, 7.0, 1.0 Hz, 2H, C(6)**H**, C(6')**H**), 7.51–7.23 (m, 6H, C(13)**H**, C(13')**H**, C(14)**H**, C(14')**H**, C(15)**H**, C(15')**H**), 7.21–7.03 (m, 4H, C(12)**H**, C(12')**H** C(16)**H**, C(16')**H**), 6.50 (d, *J* = 6.2 Hz, 2H, C(3)**H**, C(3')**H**), 1.53 (s, 6H, C(18)**H₃**, C(18')**H₃**) ppm; ^{13}C NMR (75 MHz, $CDCl_3$) δ: 178.3 (q**C**-17, q**C**-17'), 163.9 (q**C**-4, q**C**-4'), 156.1 (**C**(2)H, **C**(2')H), 153.4 (q**C**-11, q**C**-11'), 148.0 (q**C**-10, q**C**-11'), 132.0 (**C**(7)H, **C**(7')H), 130.7 (**C**(13)H, **C**(13')H, **C**(15)H, **C**(15')H), 129.1 (**C**(8)H, **C**(8')H), 127.3 (**C**(6)H, **C**(6')H), 126.7 (**C**(14)H, **C**(14')H), 122.0 (**C**(5)H, **C**(5')H), 121.8 (q**C**-9, q**C**-9'), 121.4 (**C**(12)H, **C**(12')H, **C**(16)H, **C**(16')H), 104.3 (**C**(3)H, **C**(3')H), 22.7 (**C**(18)H_3, **C**(18')H_3) ppm; HRMS (ESI-TOF) *m/z*: $[M\text{-}OAc]^+$ calcd for $C_{32}H_{25}N_2O_4Pd$ 607.0844; found: 607.0849.

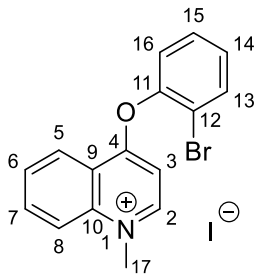
Benzofuro[3,2-*c*]quinoline (86)[156]



Compound **86** was prepared *via* the procedure described for **52** using **45** (0.270 g, 0.90 mmol, 1.0 equiv.), except that the $Pd(OAc)_2$ loading was reduced to 2 mol% (4.0 mg, 0.018 mmol) and it was stirred for 24 h, to yield **86** as a white solid (0.170 g, 87%); m.p. 124–127 °C (lit.[156] 124–126 °C); ^{1}H NMR (300 MHz, $CDCl_3$) δ: 9.43 (s, 1H, C(2)**H**), 8.35 (dd, *J* = 8.1, 1.1 Hz, 1H, C(5)**H**), 8.24 (d, *J* = 8.4 Hz, 1H, C(8)**H**), 8.03 (dd, *J* = 7.6, 0.8 Hz, 1H, C(13)**H**), 7.84–7.58 (m, 3H, C(6)**H**, C(7)**H**, C(16)**H**), 7.57–7.33 (m, 2H, C(14)**H**, C(15)**H**); ^{13}C NMR (75 MHz, $CDCl_3$) δ: 157.4 (q**C**-4), 155.9 (q**C**-11), 147.4 (q**C**-10), 144.3 (**C**(2)H), 129.8 (**C**(8)H), 129.3 (**C**(7)H), 127.2 (**C**(15)H), 127.0 (**C**(6)H), 124.0 (**C**(14)H), 122.7 (q**C**-12), 120.8 (**C**(5)H), 120.6 (**C**(13)H), 117.1 (q**C**-9), 116.3 (q**C**-3), 112.1 (**C**(16)H) ppm; *m/z* (ES+): 220 ($(M+H)^+$ 100%).

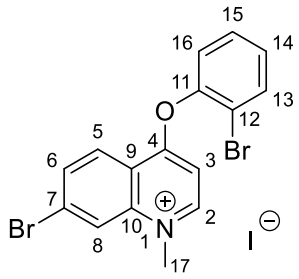
Spectral characteristics were consistent with previously reported data.[156]

4-(2-Bromophenoxy)-*N*-methylquinolin-1-ium iodide (88)



To a 15 mL Schlenk tube under nitrogen atmosphere was added **45** (0.080 g, 0.27 mmol, 1.0 equiv.), followed by methyl iodide (0.08 mL, 1.33 mmol, 5.0 equiv.) and anhydrous 1,4-dioxane (0.7 mL). The flask was sealed, and the reaction mixture was stirred at 80 °C for 2 h. The reaction mixture was cooled to r.t., filtered *via* suction filtration, washed with Et_2O (2× 5 mL) and dried under vacuum[128] to yield **88** as a yellow solid (0.105 g, 88%); m.p. 205–208 °C; IR (film) ν_{max} 1642 (C=N stretch), 1532 (aromatic C=C stretch), 1273, 1043 (ether C-O stretch), 782 (C-Br stretch) cm^{-1}; ^1H NMR (300 MHz, $CDCl_3$) δ: 10.28 (d, *J* = 7.0 Hz, 1H, C(2)**H**), 8.73 (dd, *J* = 8.4, 0.8 Hz, 1H, C(5)**H**), 8.40 (d, *J* = 8.8 Hz, 1H, C(8)**H**), 8.34–8.22 (m, 1H, C(7)**H**), 8.13–7.93 (m, 1H, C(6)**H**), 7.79 (dd, *J* = 8.4, 1.4, Hz, 1H, C(13)**H**), 7.63–7.49 (m, 1H, C(15)**H**), 7.46–7.32 (m, 2H, C(14)**H**, C(16)**H**), 6.88 (d, *J* = 7.0 Hz, 1H, C(3)**H**), 4.81 (s, 3H, C(17)$\mathbf{H_3}$) ppm; ^{13}C NMR (75 MHz, $CDCl_3$) δ: 167.0 (q**C**-4), 152.1 (**C**(2)H), 149.0 (q**C**-11), 140.2 (q**C**-10), 136.5 (**C**(7)H), 134.9 (**C**(13)H), 130.2 (**C**(15)H), 129.8 (**C**(6)H), 129.5 (**C**(14)H), 124.4 (**C**(5)H), 123.1 (**C**(16)H), 121.1 (q**C**-9), 118.9 (**C**(8)H), 115.4 (q**C**(12)Br), 104.2 (**C**(3)H), 45.3 (**C**(17)H_3) ppm; HRMS (ESI-TOF) *m/z*: $[M+H]^+$ calcd for $C_{16}H_{13}BrNO^+$: 314.0175; found: 314.0168.

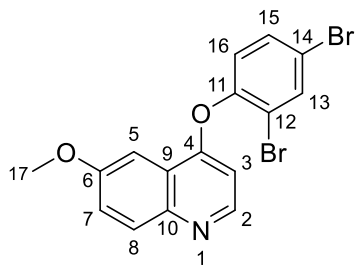
7-Bromo-4-(2-bromophenoxy)-*N*-methylquinolin-1-ium iodide (89)



Compound **89** was prepared *via* the procedure described for **88** using **60** (0.114 g, 0.30 mmol, 1.0 equiv.) to yield **89** as a yellow solid (0.128 g, 82%); m.p. 229–232 °C; IR (film) ν_{max} 1623 (C=N stretch), 1518 (aromatic C=C stretch), 1271, 1043 (ether C-O stretch), 789, 751 (C-Br stretch) cm^{-1}; ^1H NMR (300 MHz, $CDCl_3$) δ: 10.43 (d, *J* = 7.0 Hz, 1H, C(2)**H**), 8.59 (d, *J* = 8.9 Hz, 1H, C(5)**H**), 8.39 (d, *J* = 1.5 Hz, 1H, C(8)**H**), 8.09 (dd, *J* = 8.9, 1.6 Hz, 1H, C(6)**H**), 7.88–7.72 (m, 1H, C(13)**H**), 7.65–7.49 (m, 1H, C(15)**H**), 7.47–7.33 (m, 2H, C(14)**H**, C(16)**H**), 6.91 (d, *J* = 7.0 Hz, 1H, C(3)**H**), 4.74 (s, 3H, C(17)$\mathbf{H_3}$) ppm; ^{13}C NMR (75 MHz, $CDCl_3$) δ: 167.1 (q**C**-4), 153.5 (**C**(2)H), 148.8 (q**C**-11), 140.6 (q**C**-10), 134.9 (**C**(13)H), 133.6 (**C**(6)H), 132.1 (q**C**(7)Br), 130.3 (**C**(15)H), 129.7 (**C**(14)H), 125.9 (**C**(5)H), 123.0 (**C**(16)H), 121.0 (**C**(8)H), 119.9 (q**C**-9), 115.2 (q**C**(12)Br), 104.8 (**C**(3)H), 44.9

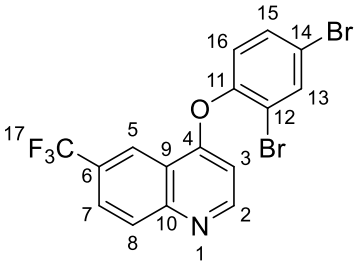
(**C**(17)H_3) ppm; HRMS (ESI-TOF) *m/z*: $[M+H]^+$ calcd for $C_{16}H_{12}Br_2NO^+$: 391.9280; found: 391.9281.

4-(2,4-Dibromophenoxy)-6-methoxyquinoline (92)



Compound **92** was prepared *via* the procedure described for **45** using 4-chloro-6-methoxyquinoline (0.194 g, 1.0 mmol, 1.0 equiv.) and 2,4-dibromophenol (1.26 g, 5.0 mmol, 5.0 equiv.) to yield **92** as a white solid (0.346 g, 85%); m.p. 112–113 °C; ν_{max} 1624 (C=N stretch), 1566 (aromatic C=C stretch), 1365, 1234, 1080 (ether C-O stretch), 726, 677 (C-Br stretch) cm^{-1}; ^{1}H NMR (300 MHz, $CDCl_3$) δ: 8.54 (d, *J* = 5.0 Hz, 1H, C(2)**H**), 8.01 (d, *J* = 9.2 Hz, 1H, C(8)**H**), 7.86 (d, *J* = 2.3 Hz, 1H, C(13)**H**), 7.63–7.47 (m, 2H, C(5)**H**, C(15)**H**), 7.41 (dd, *J* = 9.2, 2.8 Hz, 1H, C(7)**H**), 7.09 (d, *J* = 8.6 Hz, 1H, C(16)**H**), 6.40 (d, *J* = 5.1 Hz, 1H, C(3)**H**), 3.96 (s, 3H, C(17)**H$_3$**) ppm; ^{13}C NMR (75 MHz, $CDCl_3$) δ: 159.3 (q**C**-4), 157.9 (q**C**-14), 150.7 (q**C**-11), 148.3 (**C**(2)H), 146.0 (q**C**-10), 136.6 (**C**(13)H), 132.3 (**C**(15)H), 130.7 (**C**(8)H), 124.2 (**C**(16)H), 123.0 (**C**(13)H), 121.7 (q**C**-9), 119.1 (q**C**(14)Br), 117.3 (q**C**(12)Br), 104.3 (**C**(3)H), 99.3 (**C**(5)H), 55.7 (**C**(17)H_3) ppm; HRMS (ESI-TOF) *m/z*: $[M+H]^+$ calcd for $C_{16}H_{12}Br_2NO_2$: 407.9229; found: 407.9240.

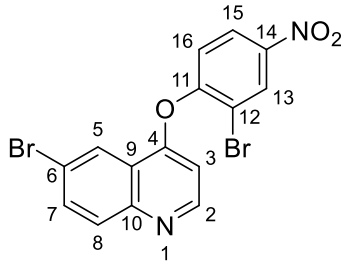
4-(2,4-Dibromophenoxy)-6-(trifluoromethyl)quinoline (93)



Compound **93** was prepared *via* the procedure described for **45** using 4-chloro-6-(trifluoromethyl)quinoline (0.232 g, 1.0 mmol, 1.0 equiv.) and 2,4-dibromophenol (1.26 g, 5.0 mmol, 5.0 equiv.) to yield **93** as a white solid (0.334 g, 70%); m.p. 116–119 °C; IR (film) ν_{max} 1637 (C=N stretch), 1568 (aromatic C=C stretch), 1366, 1225 (ether C-O stretch), 1165 (C-F stretch), 1096 (ether C-O stretch), 717, 620 (C-Br stretch) cm^{-1}; ^{1}H NMR (300 MHz, $CDCl_3$) δ: 8.89–8.64 (m, 2H, C(2)**H**, C(5)**H**), 8.24 (d, *J* = 8.9 Hz, 1H, C(8)**H**), 8.02–7.84 (m, 2H, C(7)**H**, C(13)**H**), 7.58 (dd, *J* = 8.6, 2.3 Hz, 1H, C(15)**H**), 7.16 (d, *J* = 8.6 Hz, 1H, C(16)**H**), 6.48 (d, *J* = 5.2 Hz, 1H, C(3)**H**) ppm; ^{13}C NMR (75 MHz, $CDCl_3$) δ: 160.9 (q**C**-4), 153.1 (**C**(2)H), 150.7 (q**C**-10), 149.9 (q**C**-11), 136.8 (**C**(13)H), 132.5 (**C**(15)H), 130.4 (**C**(8)H), 128.3 (q, $^2J_{(C,F)}$ = 33 Hz, q**C**-6),

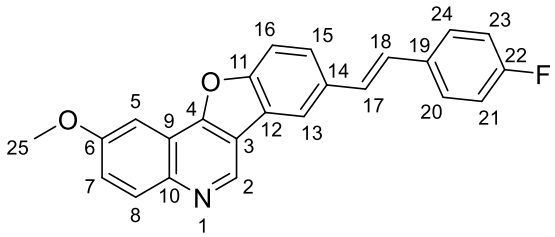
126.1 (q, $^{3}J_{(C,F)}$ = 3 Hz, **C**(7)H), 124.5 (**C**(16)H), 124.0 (q, $^{1}J_{(C,F)}$ = 272 Hz, q**C**(17)F_3), 120.1 (q, $^{3}J_{(C,F)}$ = 4 Hz, **C**(5)H), 120.0 (2 × C, q**C**-9, q**C**(14)Br), 117.5 (q**C**(12)Br), 104.3 (**C**(3)H) ppm; ^{19}F NMR (282 MHz, $CDCl_3$) δ: -62 ppm; HRMS (ESI-TOF) *m/z*: $[M+H]^+$ calcd for $C_{16}H_9Br_2F_3NO$: 445.8998; found: 445.8997.

6-Bromo-4-(2-bromo-4-nitrophenoxy)quinoline (94)



Compound **94** was prepared *via* the procedure described for **45** using 6-bromo-4-chloroquinoline (0.121 g, 0.5 mmol, 1.0 equiv.) and 2-bromo-4-nitrophenol (0.218 g, 1.0 mmol, 2.0 equiv.), except that it was stirred in 1,2-dichlorobenzene (2 mL) at 150 °C to yield **94** as a white solid (0.181 g, 85%); m.p. 209–211 °C; ν_{max} 1641 (C=N stretch), 1561 (aromatic C=C stretch), 1520, 1299 (N-O stretch), 1347, 1264, 1096 (ether C-O stretch), 739, 622 (C-Br stretch) cm^{-1}; ^{1}H NMR (300 MHz, $CDCl_3$) δ: 8.77 (d, *J* = 4.5 Hz, 1H, C(2)**H**), 8.65 (d, *J* = 2.7 Hz, 1H, C(13)**H**), 8.47 (d, *J* = 2.2 Hz, 1H, C(5)**H**), 8.29 (dd, *J* = 9.0, 2.2 Hz, 1H, C(7)**H**), 7.24 (d, *J* = 2.9 Hz, 1H, C(13)**H**), 7.16 (d, *J* = 8.9 Hz, 1H, C(16)**H**), 6.96 (dd, *J* = 8.9, 2.7 Hz, 1H, C(15)**H**), 8.03 (d, *J* = 9.0 Hz, 1H, C(8)**H**), 7.88 (dd, *J* = 9.0, 2.2 Hz, 1H, C(7)**H**), 7.38–7.21 (m, 1H, C(16)**H**), 6.57 (d, *J* = 5.0 Hz, 1H, C(8)**H**) ppm; ^{13}C NMR (75 MHz, $CDCl_3$) δ: 158.4 (q**C**-4), 156.5 (q**C**-11), 151.2 (**C**(2)H), 148.7 (q**C**-10), 145.4 (q**C**-14), 134.2 (**C**(7)H), 131.2 (**C**(8)H), 130.0 (**C**(13)H), 124.7 (**C**(15)H), 123.9 (**C**(5)H), 122.1 (q**C**-9), 121.9 (**C**(16)H), 121.1 (q**C**(6)Br), 116.4 (q**C**(12)Br), 105.8 (**C**(3)H) ppm; HRMS (ESI-TOF) *m/z*: $[M+H]^+$ calcd for $C_{15}H_9Br_2N_2O_3$: 422.8974; found: 422.8973.

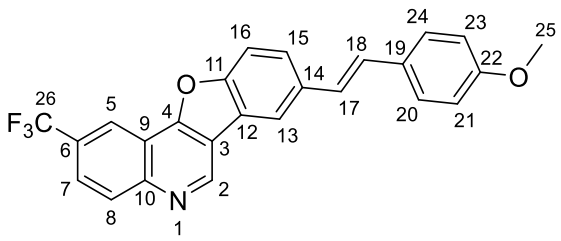
(*E*)-8-(4-Fluorostyryl)-2-methoxybenzofuro[3,2-*c*]quinoline (95)



Compound **95** was prepared *via* the procedure described for **65** using **92** (0.205 g, 0.50 mmol, 1.0 equiv.) and 4-fluorostyrene (0.07 mL, 0.55 mmol, 1.1 equiv.) to yield **95** as a pale yellow solid (0.133g, 72%); m.p. 183–186 °C; IR (film) ν_{max} 1638 (trans alkene C=C stretch), 1598 (C=N stretch), 1509 (aromatic C=C stretch), 1331, 1228 (ether C-O stretch), 1158

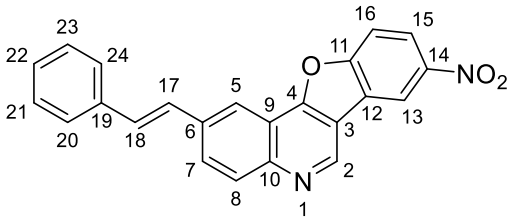
(C-F stretch), 1044 (ether C-O stretch) cm^{-1}; ^{1}H NMR (300 MHz, $CDCl_3$) δ: 9.24 (s, 1H, C(2)**H**), 8.10 (d, *J* = 9.2 Hz, 1H, C(5)**H**), 7.99 (d, *J* = 0.8 Hz, 1H, C(13)**H**), 7.64–7.41 (m, 5H, C(5)**H**, C(15)**H**, C(16)**H**, C(20)**H**, C(24)**H**), 7.35 (dd, *J* = 9.2, 2.8 Hz, 1H, C(7)**H**), 7.13–6.97 (m, 4H, C(17)**H**, C(18)**H**, C(21)**H**, C(23)**H**), 3.96 (s, 3H, C(17)$\mathbf{H_3}$) ppm; ^{13}C NMR (75 MHz, $CDCl_3$) δ: 162.4 (d, $^{1}J_{(C,F)}$ = 248 Hz, q**C**(22)F), 158.2 (q**C**-6), 157.2 (q**C**-4), 155.4 (q**C**-11), 143.4 (q**C**-10), 141.5 (**C**(2)H), 133.5 (q**C**-14), 133.4 (d, $^{4}J_{(C,F)}$ = 3 Hz, q**C**-19), 131.3 (**C**(8)H), 127.9 (d, $^{3}J_{(C,F)}$ = 8 Hz, 2 × C, **C**(20)H, **C**(24)H), 127.8 (d, $^{6}J_{(C,F)}$ = 2 Hz, **C**(17)H), 127.4 (**C**(18)H), 125.8 (**C**(15)H), 123.3 (q**C**-12), 121.8 (**C**(7)H), 118.1 (**C**(13)H), 117.8 (q**C**-9), 116.2 (q**C**-3), 115.7 (d, $^{2}J_{(C,F)}$ = 22 Hz, 2 × C, **C**(21)H, **C**(23)H), 112.0 (**C**(16)H), 98.6 (**C**(5)H), 55.7 (**C**(25)H_3) ppm; ^{19}F NMR (282 MHz, $CDCl_3$) δ: -114 ppm; HRMS (ESI-TOF) *m/z*: $[M+H]^+$ calcd for $C_{24}H_{17}Br_2NO_2$: 370.1238; found: 370.1235.

(*E*)-8-(4-methoxystyryl)-2-(trifluoromethyl)benzofuro[3,2-*c*]quinoline (96)



Compound **96** was prepared *via* the procedure described for **65** using **93** (0.99 g, 0.22 mmol, 1.0 equiv.) and 4-vinylanisole (0.03 mL, 0.24 mmol, 1.1 equiv.) to yield **96** as a white solid (0.066 g, 71%); m.p. 239–241 °C; IR (film) ν_{max} 1643 (trans alkene C=C stretch), 1567 (C=N stretch), 1512 (aromatic C=C stretch), 1335, 1253 (ether C-O stretch), 1166 (C-F stretch), 1046 (ether C-O stretch) cm^{-1}; ^{1}H NMR (300 MHz, $CDCl_3$) δ: 9.31 (s, 1H, C(2)**H**), 8.20–8.01 (m, 2H, C(5)**H**, C(13)**H**), 7.73–7.45 (m, 5H, C(5)**H**, C(15)**H**, C(16)**H**, C(20)**H**, C(24)**H**), 7.39 (dd, *J* = 9.2, 2.8 Hz, 1H, C(7)**H**), 7.19–6.99 (m, 4H, C(17)**H**, C(18)**H**, C(21)**H**, C(23)**H**), 4.01 (s, 3H, C(17)$\mathbf{H_3}$) ppm; ^{13}C NMR (150 MHz, $CDCl_3$) δ: 159.5 (q**C**-22), 158.0 (q**C**-4), 155.5 (q**C**-11), 148.1 (q**C**-10), 146.4 (**C**(2)H), 134.7 (q**C**-14), 131.0 (**C**(8)H), 129.8 (q**C**-19), 128.9 (q, $^{2}J_{(C,F)}$ = 33 Hz, q**C**-6), 128.8 (**C**(18)H), 127.8 (2 × C, **C**(20)H, **C**(24)H), 126.5 (**C**(15)H), 125.7 (**C**(17)H), 125.0 (app. d, $^{3}J_{(C,F)}$ = 2 Hz, **C**(7)H), 123.9 (q, $^{1}J_{(C,F)}$ = 273 Hz, q**C**(26)F_3), 122.7 (q**C**-12), 119.1 (q, $^{3}J_{(C,F)}$ = 4 Hz, **C**(5)H), 118.0 (**C**(13)H), 117.4 (q**C**-3), 116.4 (q**C**-9), 114.2 (2 × C, **C**(21)H, **C**(23)H), 112.4 (**C**(16)H) 55.4 (**C**(25)H_3) ppm; ^{19}F NMR (282 MHz, $CDCl_3$) δ: -62 ppm; HRMS (ESI-TOF) *m/z*: $[M+H]^+$ calcd for $C_{25}H_{17}F_3NO_2$: 407.9229; found: 407.9229.

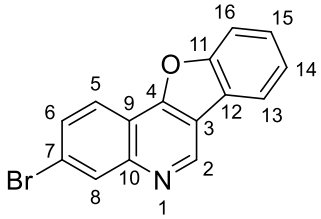
(*E*)-8-nitro-2-styrylbenzofuro[3,2-*c*]quinoline (97)



Compound **97** was prepared *via* the procedure described for **65** using **94** (0.041 g, 0.096 mmol, 1.0 equiv.) and styrene (0.01 mL, 0.11 mmol, 1.1 equiv.) to yield **97** as an off-white solid (0.015 g, 43%); m.p. >250°C; IR (film) ν_{max} 1642 (trans alkene C=C stretch), 1561 (C=N stretch), 1523 (nitro N-O stretch), 1461 (aromatic C=C stretch), 1343 (ether C-O stretch), 1254 (nitro N-O stretch), 1205, 1040 (ether C-O stretch) cm^{-1}; ^{1}H NMR (600 MHz, $CDCl_3$) δ: 9.78 (s, 1H, C(2)**H**), 9.36 (d, *J* = 2.4 Hz, 1H, C(13)**H**), 8.55–8.44 (m, 2H, C(5)**H**, C(15)**H**), 8.27–8.19 (m, 2H, C(7)**H**, C(8)**H**), 8.17 (d, *J* = 9.0 Hz, 1H, C(16)**H**), 7.78–7.66 (m, 2H, C(20)**H**, C(24)**H**), 7.63–7.52 (m, 2H, C(17)**H**, C(18)**H**), 7.48–7.40 (m, 2H, C(21)**H**, C(23)**H**), 7.37–7.30 (m, 1H, C(22)**H**) ppm; ^{13}C NMR (150 MHz, $CDCl_3$) δ: 158.71, 158.67 (q**C**-4, q**C**-11), 147.4 (q**C**-10), 145.6 (**C**(2)H), 145.0 (q**C**-14), 137.2 (q**C**-19), 137.0 (q**C**-6), 131.4 (**C**(18)H), 130.5 (**C**(8)H), 129.3 (2 × C, **C**(21)H, **C**(23)H), 128.7 (**C**(22)H), 128.6 (**C**(7)H), 127.8 (**C**(17)H), 127.3 (2 × C, **C**(20)H, **C**(24)H), 123.8 (**C**(15)H), 123.7 (q**C**-12), 118.8 (**C**(5)H), 118.6 (**C**(13)H), 116.8 (q**C**-9), 116.2 (q**C**-3), 113.6 (**C**(16)H) ppm; HRMS (ESI-TOF) *m/z*: $[M+H]^+$ calcd for $C_{23}H_{15}N_2O_3$: 367.1077; found: 367.1081.

2.20. Reversible Oxidative Addition Substrates and Products

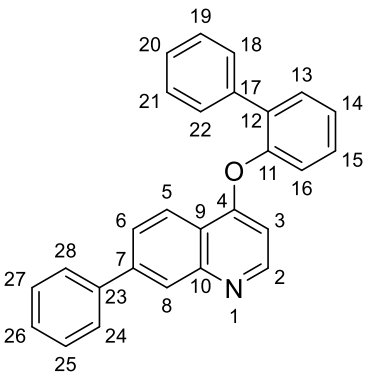
3-Bromo-4-methylbenzofuro[3,2-*c*]quinoline (98)[60]



A 15 mL Schlenk was flame-dried and cooled to r.t. under vacuum. The Schlenk was refilled with nitrogen and **60** (0.030 g, 0.08 mmol, 1.0 equiv.), QPhos (5.6 mg, 0.008 mmol, 10 mol%), QPhos (6.1 mg, 0.004 mmol, 5 mol%) and K_2CO_3 (0.022 g, 0.16 mmol, 2.0 equiv.) were added and the Schlenk placed under vacuum once more for ~10 min. The Schlenk was evacuated and refilled with nitrogen three times and distilled 1,4-dioxane (0.5 mL) was added *via* septum. The Schlenk was sealed, and the resulting mixture stirred at 125 °C for 24 h. The cooled reaction mixture was diluted with DCM, filtered through a short plug of Celite,

rinsed with DCM and the filtrate concentrated under reduced pressure. Purification *via* column chromatography (DCM 100 to DCM:EtOAc 99:1, unless otherwise stated) to yield **98** as a white solid (0.005 g, 22%); m.p. 165–167 °C; ν_{max} 1614 (C=N stretch), 1560 (aromatic C=C stretch), 1261, 1096 (ether C-O stretch), 739 (C-Br stretch) cm^{-1}; ^{1}H NMR (500 MHz, $CDCl_3$) δ: 9.49 (s, 1H, C(2)**H**), 8.49 (d, *J* = 1.3 Hz, 1H, C(8)**H**), 8.29 (d, *J* = 8.7 Hz, 1H, C(5)**H**), 8.10 (d, *J* = 7.3 Hz, 1H, C(13)**H**), 7.86–7.69 (m, 2H, C(6)**H**, C(16)**H**), 7.58 (app. t, *J* = 7.8 Hz, 1H, C(15)**H**), 7.50 (app. t, *J* = 7.2 Hz, 1H, C(14)**H**) ppm; ^{13}C NMR (125 MHz, $CDCl_3$) δ: 157.7 (q**C**-4), 156.3 (q**C**-11), 147.7 (q**C**-10), 145.4 (**C**(2)H), 132.2 (**C**(8)H), 130.8 (**C**(6)H), 127.9 (**C**(15)H), 124.6 (**C**(14)H), 123.8 (q**C**(7)Br), 122.5 (q**C**-12), 122.4 (**C**(5)H), 121.0 (**C**(13)H), 117.0 (q**C**-3), 116.0 (q**C**-9), 112.4 (**C**(16)H) ppm; HRMS (ESI-TOF) *m/z*: $[M+H]^+$ calcd for $C_{15}H_9BrNO$: 297.9862; found: 297.9859.

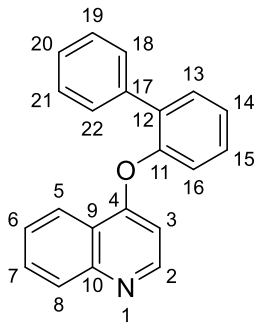
4-([1,1'-Biphenyl]-2-yloxy)-7-phenylquinoline (101)



Compound **101** was prepared *via* the procedure described for **98** using **60** (0.038 g, 0.1 mmol, 1.0 equiv.) except that phenyl boronic acid (0.024 g, 0.2 mmol, 2.0 equiv.), was also added to yield both **100** and **101**. ^{1}H NMR (300 MHz, $CDCl_3$) δ: 8.60 (d, *J* = 5.2 Hz, 1H, C(2)**H**), 8.36 (d, *J* = 8.7 Hz, 1H, C(5)**H**), 8.24 (d, *J* = 1.5 Hz, 1H, C(8)**H**), 7.87–7.67 (m, 3H, C(6)**H**, C(24)**H**, C(28)**H**), 7.62–7.36 (m, 8H, C(13)**H**, C(14)**H**, C(15)**H**, C(18)**H**, C(22)**H**, C(25)**H**, C(26)**H**, C(27)**H**), 7.33–7.15 (m, 4H, C(16)**H**, C(19)**H**, C(20)**H**, C(21)**H**), 6.44 (d, *J* = 5.2 Hz, 1H, C(3)**H**) ppm; ^{13}C NMR (75 MHz, $CDCl_3$) δ: 161.6 (q**C**-4), 151.5 (**C**(2)H), 150.9 (q**C**-11), 150.0 (q**C**-10), 142.7 (q**C**-7), 140.3 (q**C**-23), 136.8 (q**C**-17), 135.0 (q**C**-12), 131.7 (**C**(13)H), 129.2 (**C**(15)H), 129.0 (2 × C, **C**(25)H, **C**(27)H), 128.8 (2 × C, **C**(18)H, **C**(22)H), 128.3 (2 × C, **C**(19)H, **C**(21)H), 127.9 (**C**(26)H), 127.6 (**C**(20)H), 127.5 (2 × C, **C**(24)H, **C**(28)H), 126.6 (**C**(8)H), 126.4 (**C**(14)H), 125.6 (**C**(6)H), 122.36, 122.35 (**C**(5)H, **C**(16)H), 120.2 (q**C**-9), 103.9 (**C**(3)H) ppm; HRMS (ESI-TOF) *m/z*: $[M+H]^+$ calcd for $C_{27}H_{20}NO$: 374.1539; found: 374.1529.

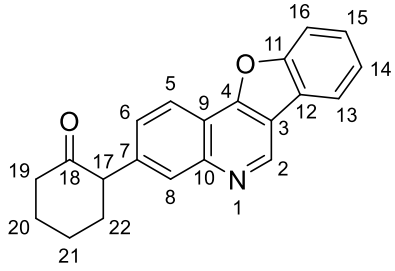
Note: Compound was not sufficiently pure for complete analysis or calculation of yield.

4-([1,1'-Biphenyl]-2-yloxy)quinoline (102)



Compound **102** was prepared *via* the procedure described for **98** using **45** (0.030 g, 0.1 mmol, 1.0 equiv.), except that phenyl boronic acid (0.012 g, 0.1 mmol, 1.0 equiv.) was also added to yield **102** as a beige solid (0.024 g, 81%); m.p. 69–71 °C; IR (film) ν_{max} 1591 (C=N stretch), 1501, 1478 (aromatic C=C stretch), 1254, 1113 (ether C-O stretch) cm^{-1}; ^{1}H NMR (300 MHz, $CDCl_3$) δ: 8.57 (d, *J* = 5.2 Hz, 1H, C(2)**H**), 8.29 (dd, *J* = 8.3, 1.1 Hz, 1H, C(5)**H**), 8.02 (d, *J* = 8.4 Hz, 1H, C(8)**H**), 7.70 (ddd, *J* = 8.4, 6.9, 1.5 Hz, 1H, C(7)**H**), 7.63–7.32 (m, 6H, C(6)**H**, C(13)**H**, C(14)**H**, C(15)**H**, C(18)**H**, C(22)**H**), 7.30–7.10 (m, 4H, C(16)**H**, C(19)**H**, C(20)**H**, C(21)**H**), 6.44 (d, *J* = 5.2 Hz, 1H, C(3)**H**) ppm; ^{13}C NMR (75 MHz, $CDCl_3$) δ: 161.6 (q**C**-4), 151.0 (**C**(2)H), 150.9 (q**C**-11), 149.6 (q**C**-10), 136.9 (q**C**-17), 136.0 (q**C**-12), 131.7 (**C**(13)H), 130.0 (**C**(7)H), 129.2 (**C**(15)H), 129.0 (**C**(8)H), 128.8 (2 × C, **C**(18)H, **C**(22)H), 128.2 (2 × C, **C**(19)H, **C**(21)H), 127.5 (**C**(20)H), 126.3 (**C**(14)H), 126.0 (**C**(6)H), 122.3 (**C**(16)H), 121.8 (**C**(5)H), 121.2 (q**C**-9), 104.0 (**C**(3)H) ppm; HRMS (ESI-TOF) *m/z*: $[M+H]^+$ calcd for $C_{21}H_{16}NO$: 298.1226; found: 298.1220.

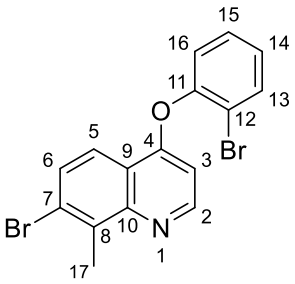
2-(Benzofuro[3,2-*c*]quinolin-3-yl)cyclohexan-1-one (103)



Compound **103** was prepared *via* the procedure described for **98** using **60** (0.038 g, 0.1 mmol, 1.0 equiv.), except that anhydrous cyclohexanone (0.5 mL) was used as solvent to yield **103** as an off-white solid (0.023 g, 73%); m.p. 204–206 °C; IR (film) ν_{max} 1697 (C=O stretch), 1640 (C=N stretch), 1501 (aromatic C=C stretch), 1342, 1286, 1052 (ether C-O stretch) cm^{-1}; ^{1}H NMR (300 MHz, $CDCl_3$) δ: 9.46 (s, 1H, C(2)**H**), 8.37 (d, *J* = 8.5 Hz, 1H, C(5)**H**), 8.16–7.95 (m, 2H, C(8)**H**, C(13)**H**), 7.74 (d, *J* = 7.9 Hz, 1H, C(16)**H**), 7.62–7.36 (m, 3H, C(6)**H**, C(14)**H**, C(15)**H**), 3.89 (dd, *J* = 12.2, 5.5 Hz, 1H, C(17)**H**), 2.70–2.34 (m, 3H, C(19)**H₂**, *one of* C(22)**H₂**), 2.32–2.01 (m, 3H, *one of* C(20)**H₂**, *one of* C(21)**H₂**, *one of* C(22)**H₂**), 2.01–1.67 (m, 2H, *one of* C(20)**H₂**, *one of* C(21)**H₂**) ppm; ^{13}C NMR (75 MHz, $CDCl_3$) δ: 209.8 (q**C**-18), 157.6 (q**C**-4), 156.0 (q**C**-11), 147.6 (q**C**-10), 144.4 (**C**(2)H), 140.5 (q**C**-7), 129.0 (**C**(8)H), 128.4 (**C**(6)H), 127.2 (**C**(15)H), 124.0 (**C**(14)H), 122.8 (q**C**-12), 120.59, 120.60 (**C**(5)H, **C**(13)H), 116.2 (q**C**-3), 116.0

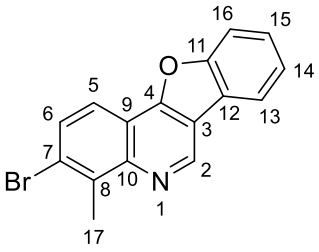
(q**C**-9), 112.1 (**C**(16)H), 57.6 (**C**(17)H), 42.3 (**C**(19)H_2), 34.9 (**C**(22)H_2), 27.8 (**C**(20)H_2), 25.3 (**C**(21)H_2) ppm; HRMS (ESI-TOF) *m/z*: $[M+H]^+$ calcd for $C_{21}H_{18}NO_2$: 316.1332; found: 316.1331.

7-Bromo-4-(2-bromophenoxy)-8-methylquinoline (104)



Compound **104** was prepared *via* the procedure described for **45** using 7-bromo-4-chloro-8-methylquinoline (0.257 g, 1.0 mmol, 1.0 equiv.) to yield **104** as an orange solid (0.211 g, 54%); m.p. 89–91 °C; IR (film) ν_{max} 1643 (C=N stretch), 1566 (aromatic C=C stretch), 1261, 1047 (ether C-O stretch), 768 (C-Br stretch) cm^{-1}; ^{1}H NMR (300 MHz, $CDCl_3$) δ: 8.69 (d, *J* = 5.1 Hz, 1H, C(2)**H**), 8.14 (d, *J* = 9.0 Hz, 1H, C(5)**H**), 7.89–7.61 (m, 2H, C(6)**H**, C(13)**H**), 7.50–7.34 (m, 1H, C(15)**H**), 7.30–7.14 (m, 2H, C(14)**H**, C(16)**H**), 6.42 (d, *J* = 5.1 Hz, 1H, C(3)**H**), 2.94 (s, 3H, C(17)**H_3**) ppm; ^{13}C NMR (75 MHz, $CDCl_3$) δ: 161.1 (q**C**-4), 151.1 (q**C**-11), 150.6 (**C**(2)H), 149.4 (q**C**-10), 136.8 (q**C**-8), 134.4 (**C**(13)H), 130.4 (**C**(6)H), 129.2 (**C**(15)H), 127.4 (**C**(14)H), 126.9 (q**C**(7)Br), 123.2 (**C**(16)H), 120.5 (**C**(5)H), 119.9 (q**C**-9), 116.3 (q**C**(12)Br), 103.7 (**C**(3)H), 18.0 (**C**(17)H_3) ppm; HRMS (ESI-TOF) *m/z*: $[M+H]^+$ calcd for $C_{16}H_{12}Br_2NO$: 391.9280; found: 391.9281.

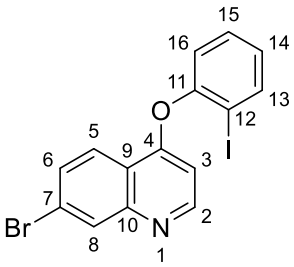
3-Bromo-4-methylbenzofuro[3,2-*c*]quinoline (105)



Compound **105** was prepared *via* the procedure described for **98** using **104** (0.038 g, 0.1 mmol, 1.0 equiv.). Purification *via* column chromatography (hexanes:DCM 90:10 to 60:40) to yield **105** as a white solid (0.014 g, 47%); m.p. 222–225 °C; ν_{max} 1607 (C=N stretch), 1566 (aromatic C=C stretch), 1376, 1218 (ether C-O stretch), 770 (C-Br stretch) cm^{-1}; ^{1}H NMR (600 MHz, $CDCl_3$) δ: 9.48 (s, 1H, C(2)**H**), 8.19–8.05 (m, 2H, C(5)**H**, C(13)**H**), 7.82 (d, *J* = 8.8 Hz, 1H, C(6)**H**), 7.74 (d, *J* = 8.2 Hz, 1H, C(16)**H**), 7.60–7.44 (m, 2H, C(14)**H**, C(15)**H**), 3.02 (s, 3H, C(17)**H_3**) ppm; ^{13}C NMR (150 MHz, $CDCl_3$) δ: 157.8 (q**C**-4), 156.1 (q**C**-11), 146.7 (q**C**-10), 143.7 (**C**(2)H), 137.7 (q**C**-8), 131.1 (**C**(6)H), 127.5 (**C**(15)H), 126.0 (q**C**(7)Br), 124.2 (**C**(14)H), 122.5 (q**C**-12), 120.8 (**C**(13)H), 119.3

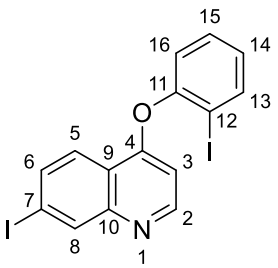
(**C**(5)H), 116.3 (q**C**-3), 116.0 (q**C**-9), 112.2 (**C**(16)H), 18.5 (**C**(17)H_3) ppm; HRMS (ESI-TOF) *m/z*: $[M+H]^+$ calcd for $C_{16}H_{11}BrNO$: 312.0019; found: 312.0015.

7-Bromo-4-(2-iodophenoxy)quinoline (106)



Compound **106** was prepared *via* the procedure described for **49** using 7-bromo-4-chloroquinoline (0.121 g, 0.5 mmol, 1.0 equiv.) and 2-iodophenol (0.330 g, 1.5 mmol, 3.0 equiv.) to yield **106** as a yellow solid (0.050 g, 24%); m.p. 89–92 °C; IR (film) ν_{max} 1613 (C=N stretch), 1561 (aromatic C=C stretch), 1215, 1096 (ether C-O stretch), 740 (C-Br stretch), 653 (C-I stretch) cm^{-1}; ^{1}H NMR (300 MHz, $CDCl_3$) δ: 8.67 (d, *J* = 3.3 Hz, 1H, C(2)**H**), 8.42–8.22 (m, 2H, C(5)**H**, C(8)**H**), 7.96 (dd, *J* = 7.9, 1.5 Hz, 1H, C(13)**H**), 7.71 (dd, *J* = 8.9, 1.6 Hz, 1H, C(6)**H**), 7.47 (ddd, *J* = 8.1, 7.4, 1.5 Hz, 1H, C(15)**H**), 7.21 (dd, *J* = 8.1, 1.5 Hz, 1H, C(16)**H**), 7.08 (ddd, *J* = 7.9, 7.5, 1.5 Hz, 1H, C(14)**H**), 6.40 (d, *J* = 5.0 Hz, 1H, C(3)**H**) ppm; ^{13}C NMR (75 MHz, $CDCl_3$) δ: 161.0 (q**C**-4), 153.8 (q**C**-11), 152.2 (**C**(2)H), 150.5 (q**C**-10), 140.5 (**C**(13)H), 131.5 (**C**(8)H), 130.4 (**C**(15)H), 130.0 (**C**(6)H), 127.9 (**C**(14)H), 124.8 (q**C**(7)Br), 123.7 (**C**(5)H), 122.5 (**C**(16)H), 120.0 (q**C**-9), 104.2 (**C**(3)H), 90.3 (q**C**(12)I) ppm; HRMS (ESI-TOF) *m/z*: $[M+H]^+$ calcd for $C_{15}H_{10}BrINO$: 425.8985; found: 425.8991.

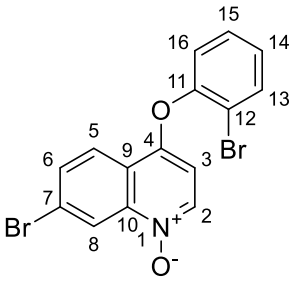
7-Iodo-4-(2-iodophenoxy)quinoline (107)



Compound **107** was prepared *via* the procedure described for **49** using **79** (0.108 g, 0.37 mmol, 1.0 equiv.) and 2-iodophenol (0.246 g, 1.12 mmol, 3.0 equiv.) to yield **107** as a beige solid (0.059 g, 36%); m.p. 87–90 °C; IR (film) ν_{max} 1610 (C=N stretch), 1557 (aromatic C=C stretch), 1215, 1094 (ether C-O stretch), 704, 631 (C-I stretch) cm^{-1}; ^{1}H NMR (300 MHz, $CDCl_3$) δ: 8.64 (d, *J* = 5.1 Hz, 1H, C(2)**H**), 8.54 (d, *J* = 1.6 Hz, 1H, C(8)**H**), 8.14 (d, *J* = 8.8 Hz, 1H, C(5)**H**), 7.95 (dd, *J* = 7.9, 1.5 Hz, 1H, C(13)**H**), 7.88 (dd, *J* = 8.8, 1.6 Hz, 1H, C(6)**H**), 7.46 (td, *J* = 8.1, 1.5 Hz, 1H, C(15)**H**), 7.20 (dd, *J* = 8.1, 1.5 Hz, 1H, C(16)**H**), 7.08 (td, *J* = 7.9, 1.5 Hz, 1H, C(14)**H**), 6.41 (d, *J* = 5.1 Hz, 1H, C(3)**H**) ppm; ^{13}C NMR (75 MHz, $CDCl_3$) δ: 160.8 (q**C**-4), 153.7 (q**C**-11), 151.9 (**C**(2)H), 150.6 (q**C**-10), 140.5 (**C**(13)H), 138.1 (**C**(8)H), 135.0 (**C**(6)H), 130.2 (**C**(15)H), 127.8 (**C**(14)H), 123.4 (**C**(5)H), 122.3 (**C**(16)H), 120.3 (q**C**-9), 104.2

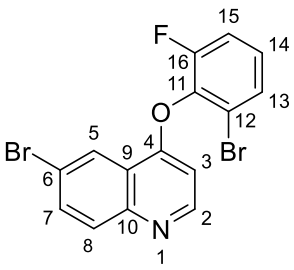
(**C**(3)H), 96.7 (q**C**(7)I), 90.2 (q**C**(12)I) ppm; HRMS (ESI-TOF) *m/z*: $[M+H]^+$ calcd for $C_{15}H_{10}I_2NO$: 473.8846; found: 473.8841.

7-Bromo-4-(2-bromophenoxy)quinoline-*N*-oxide (109)



A mixture of **60** (0.152 g, 0.4 mmol, 1.0 equiv.), *m*-CPBA (0.173 g, 1.0 mmol, 2.5 equiv.) and DCM (2 mL) was stirred in a sealed vial at r.t. for 48 h. The reaction mixture was diluted with DCM (5 mL) and washed with 10% aq. NaOH (2 × 10 mL) and H_2O (10 mL), dried over $MgSO_4$, filtered and concentrated under reduced pressure. Purification *via* column chromatography (DCM 100 to DCM:MeOH 95:5) to yield **109** as a beige solid (0.151 g, 96%); m.p. 133–136 °C; IR (film) ν_{max} 1651 (C=N stretch), 1564 (aromatic C=C stretch), 1413 (N-O stretch), 1257, 1085 (ether C-O stretch), 751, 666 (C-Br stretch) cm^{-1}; ^1H NMR (300 MHz, $CDCl_3$) δ: 9.00 (bs, 1H, C(8)**H**), 8.46–8.17 (m, 2H, C(2)**H**, C(5)**H**), 7.94–7.63 (m, 2H, C(6)**H**, C(13)**H**), 7.44 (td, *J* = 8.0, 1.5 Hz, 1H, C(15)**H**), 7.32–7.13 (m, 2H, C(14)**H**, C(16)**H**), 6.34 (d, *J* = 6.8 Hz, 1H, C(3)**H**) ppm; ^{13}C NMR (75 MHz, $CDCl_3$) δ: 152.1 (q**C**-4), 150.7 (q**C**-11), 142.1 (q**C**-10), 136.7 (**C**(2)H), 134.6 (**C**(13)H), 132.3 (**C**(6)H), 129.4 (**C**(15)H), 127.8 (**C**(14)H), 126.5 (q**C**(7)Br), 124.3 (**C**(5)H), 122.99, 122.97 (**C**(8)H, **C**(16)H), 121.2 (q**C**-9), 116.0 (q**C**(12)Br), 104.2 (**C**(3)H) ppm; HRMS (ESI-TOF) *m/z*: $[M+H]^+$ calcd for $C_{15}H_{10}Br_2NO_2$: 393.9073; found: 393.9073.

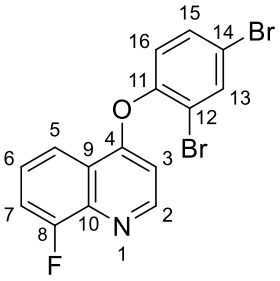
6-Bromo-4-(2-bromo-6-fluorophenoxy)quinoline (111)



Compound **111** was prepared *via* the procedure described for **49** using 6-bromo-4-chloroquinoline (0.243 g, 1.0 mmol, 1.0 equiv.) and 2-bromo-6-fluorophenol (0.287 g, 1.5 mmol, 1.5 equiv.) to yield **111** as a white solid (0.361 g, 91%); m.p. 156–159 °C; IR (film) ν_{max} 1588 (C=N stretch), 1561 (aromatic C=C stretch), 1350, 1272 (ether C-O stretch), 1095 (C-F stretch), 709, 616 (C-Br stretch) cm^{-1}; ^1H NMR (300 MHz, $CDCl_3$) δ: 8.82–8.52 (m, 2H, C(2)**H**), C(5)**H**), 7.99 (d, *J* = 9.0 Hz, 1H, C(8)**H**), 7.85 (dd, *J* = 9.0, 2.2 Hz, 1H, C(7)**H**), 7.61–7.44 (m, 1H, C(13)**H**), 7.34–7.13 (m, 2H, C(14)**H**, C(15)**H**), 6.41 (d, *J* = 5.1 Hz, $^5J_{(H,F)}$ = 1.0 Hz, 1H, C(3)**H**) ppm; ^{13}C NMR (75 MHz, $CDCl_3$) δ: 158.9 (q**C**-4), 155.5 (d, $^1J_{(C,F)}$ = 255 Hz,

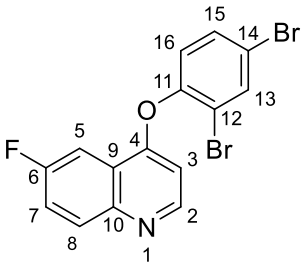
q**C**(16)F), 151.3 (**C**(2)H), 148.3 (q**C**-10), 139.0 (d, $^{2}J_{(C,F)}$ = 14 Hz, q**C**-11), 133.8 (**C**(7)H), 130.9 (**C**(8)H), 129.3 (d, $^{4}J_{(C,F)}$ = 4 Hz, **C**(13)H), 127.9 (d, $^{3}J_{(C,F)}$ = 8 Hz, **C**(14)H), 124.3 (**C**(5)H), 121.7 (q**C**-9), 120.5 (q**C**(6)Br), 118.2 (q**C**(12)Br), 116.6 (d, $^{2}J_{(C,F)}$ = 19 Hz, **C**(15)H), 103.2 (**C**(3)H) ppm; ^{19}F NMR (282 MHz, $CDCl_3$) δ: -124 ppm; HRMS (ESI-TOF) *m/z*: $[M+H]^+$ calcd for $C_{15}H_9Br_2FNO$: 395.9029; found: 395.9033.

4-(2,4-Dibromophenoxy)-8-fluoroquinoline (112)



Compound **112** was prepared *via* the procedure described for **45** using **43** (0.272 g, 1.5 mmol, 1.0 equiv.) and 2,4-dibromophenol (1.5 g, 6.0 mmol, 4.0 equiv.) to yield **112** as a white solid (0.441 g, 74%); m.p. 138–140 °C; IR (film) ν_{max} 1598 (C=N stretch), 1504 (aromatic C=C stretch), 1261 (ether C-O stretch), 1077 (C-F stretch), 1045 (ether C-O stretch), 754, 690 (C-Br stretch) cm^{-1}; ^{1}H NMR (300 MHz, $CDCl_3$) δ: 8.74 (d, *J* = 5.1 Hz, 1H, C(2)**H**), 8.16 (dd, *J* = 8.1, 1.2 Hz, 1H, C(5)**H**), 7.89 (d, *J* = 2.3 Hz, 1H, C(13)**H**), 7.63–7.42 (m, 3H, C(6)**H**, C(7)**H**, C(15)**H**), 7.13 (d, *J* = 8.6 Hz, 1H, C(16)**H**), 6.48 (d, *J* = 5.1 Hz, 1H, C(3)**H**) ppm; ^{13}C NMR (75 MHz, $CDCl_3$) δ: 160.2 (d, $^{4}J_{(C,F)}$ = 4 Hz, q**C**-4), 158.0 (d, $^{1}J_{(C,F)}$ = 256 Hz, q**C**(8)F), 151.2 (**C**(2)H), 150.2 (q**C**-11), 140.2 (d, $^{2}J_{(C,F)}$ = 13 Hz, q**C**-10), 136.7 (**C**(13)H), 132.4 (**C**(15)H), 126.2 (d, $^{3}J_{(C,F)}$ = 8 Hz, **C**(6)H), 124.4 (**C**(16)H), 122.6 (d, $^{3}J_{(C,F)}$ = 3 Hz, q**C**-9), 119.7 (q**C**(12)Br or q**C**(14)Br), 117.5 (d, $^{4}J_{(C,F)}$ = 5 Hz, **C**(5)H), 117.3 (q**C**(12)Br or q**C**(14)Br), 114.5 (d, $^{2}J_{(C,F)}$ = 19 Hz, **C**(7)H), 104.5 (**C**(3)H) ppm; ^{19}F NMR (282 MHz, $CDCl_3$) δ: -124 ppm; HRMS (ESI-TOF) *m/z*: $[M+H]^+$ calcd for $C_{15}H_9Br_2FNO$: 395.9029; found: 395.9034.

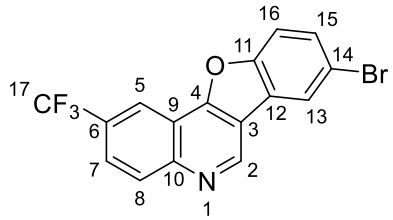
4-(2,4-Dibromophenoxy)-6-fluoroquinoline (113)



Compound **113** was prepared *via* the procedure described for **45** using 4-chloro-6-fluoroquinoline (0.182 g, 1.0 mmol, 1.0 equiv.) and 2,4-dibromophenol (1.0g, 4.0 mmol, 4.0 equiv.) to yield **113** as a white solid (0.334 g, 84%); m.p. 145–147 °C; IR (film) ν_{max} 1644 (C=N stretch), 1509 (aromatic C=C stretch), 1261 (ether C-O stretch), 1073 (C-F stretch), 1049 (ether C-O stretch), 726 (C-Br stretch) cm^{-1}; ^{1}H NMR (300 MHz, $CDCl_3$) δ: 8.65 (d, *J* = 5.1 Hz, 1H,

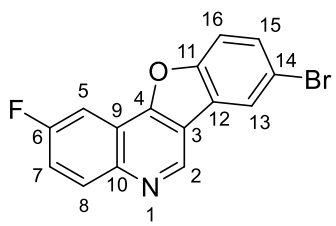
C(2)**H**), 8.12 (dd, *J* = 9.3 Hz, 1H, $^{4}J_{(H,F)}$ = 5.2 Hz, C(8)**H**), 7.97 (dd, $^{3}J_{(H,F)}$ = 9.2 Hz, *J* = 2.8 Hz, 1H, C(5)**H**), 7.88 (d, *J* = 2.3 Hz, 1H, C(13)**H**), 7.64–7.47 (m, 2H, C(7)**H**, C(15)**H**), 7.12 (d, *J* = 8.6 Hz, 1H, C(16)**H**), 6.44 (d, *J* = 5.1 Hz, 1H, C(3)**H**) ppm; ^{13}C NMR (75 MHz, $CDCl_3$) δ: 160.5 (d, $^{1}J_{(C,F)}$ = 248 Hz, q**C**(6)F), 159.9 (d, $^{4}J_{(C,F)}$ = 5 Hz, q**C**-4), 150.3 (q**C**-11), 150.1 (d, $^{6}J_{(C,F)}$ = 3 Hz, **C**(2)H), 146.9 (q**C**-10), 136.7 (**C**(13)H), 132.4 (**C**(15)H), 131.8 (d, $^{3}J_{(C,F)}$ = 9 Hz, **C**(8)H), 124.3 (**C**(16)H), 121.6 (d, $^{3}J_{(C,F)}$ = 10 Hz, q**C**-9), 120.6 (d, $^{2}J_{(C,F)}$ = 26 Hz, **C**(7)H), 119.6 (q**C**(14)Br), 117.3 (q**C**(12)Br), 105.6 (d, $^{2}J_{(C,F)}$ = 24 Hz, **C**(5)H), 104.0 (**C**(3)H) ppm; ^{19}F NMR (282 MHz, $CDCl_3$) δ: -112 ppm; HRMS (ESI-TOF) *m/z*: $[M+H]^+$ calcd $C_{15}H_9Br_2FNO$: 395.9029; found: 395.9026.

8-Bromo-2-(trifluoromethyl)benzofuro[3,2-*c*]quinoline (116)



Compound **116** was prepared *via* the procedure described for **98** using **93** (0.077 g, 0.17 mmol, 1.0 equiv.) to yield **116** as a white solid (0.022 g, 35%); m.p. 222–224 °C; IR (film) ν_{max} 1643 (C=N stretch), 1568 (aromatic C=C stretch), 1310 (ether C-O stretch), 1120 (C-F stretch), 1052 (ether C-O stretch), 678 (C-Br stretch) cm^{-1}; ^{1}H NMR (300 MHz, $CDCl_3$) δ: 9.55 (s, 1H, C(2)**H**), 8.73 (app. s, 1H, C(5)**H**), 8.39 (d, *J* = 8.9 Hz, 1H, C(8)**H**), 8.26 (d, *J* = 1.0 Hz, 1H, C(13)**H**), 7.98 (dd, *J* = 8.9, 1.8 Hz, 1H, C(7)**H**), 7.79–7.59 (m, 2H, C(15)**H**, C(16)**H**) ppm; ^{13}C NMR (150 MHz, $CDCl_3$) δ: 158.2 (q**C**-4), 154.9 (q**C**-11), 148.1 (q**C**-10), 146.2 (**C**(2)H), 131.0 (**C**(8)H), 130.9 (**C**(15)H), 129.2 (d, $^{2}J_{(C,F)}$ = 33 Hz, q**C**-6), 125.6 (q, $^{3}J_{(C,F)}$ = 3 Hz, **C**(7)H), 124.4 (q**C**-12), 123.81 (**C**(13)H), 123.82 (q, $^{1}J_{(C,F)}$ = 273 Hz, q**C**(17)F_3), 119.1 (d, $^{3}J_{(C,F)}$ = 4 Hz, **C**(5)H), 117.7 (q**C**(14)Br), 116.4 (q**C**-3), 116.2 (q**C**-9), 113.8 (**C**(16)H) ppm; ^{19}F NMR (282 MHz, $CDCl_3$) δ: -62 ppm; HRMS (ESI-TOF) *m/z*: $[M+H]^+$ calcd for $C_{16}H_8BrF_3NO$: 365.9736; found: 365.9739.

8-Bromo-2-fluorobenzofuro[3,2-*c*]quinoline (118)



Compound **118** was prepared *via* the procedure described for **98** using **113** (0.119 g, 0.3 mmol, 1.0 equiv.) to yield **118** as a white solid (0.048 g, 51%); m.p. 199–201 °C; IR (film) ν_{max} 1640 (C=N stretch), 1515 (aromatic C=C stretch), 1350, 1184 (ether C-O stretch), 1055 (C-F stretch), 710 (C-Br

stretch) cm^{-1}; ^{1}H NMR (300 MHz, $CDCl_3$) δ: 9.36 (s, 1H, C(2)**H**), 8.36–8.09 (m, 2H, C(8)**H**, C(13)**H**), 7.93 (dd, $^{3}J_{(H,F)}$ = 8.5 Hz, *J* = 2.8 Hz, 1H, C(5)**H**), 7.74–7.42 (m, 3H, C(7)**H**, C(15)**H**, C(16)**H**) ppm; ^{13}C NMR (75 MHz, $CDCl_3$) δ: 160.9 (d, $^{1}J_{(C,F)}$ = 250 Hz, q**C**(6)F), 157.6 (d, $^{4}J_{(C,F)}$ = 5 Hz, q**C**-4), 154.7 (q**C**-11), 144.6 (q**C**-10), 143.3 (d, $^{6}J_{(C,F)}$ = 3 Hz, **C**(2)H), 132.6 (d, $^{3}J_{(C,F)}$ = 9 Hz, **C**(8)H), 130.5 (**C**(15)H), 124.4 (q**C**-12), 123.7 (**C**(13)H), 119.7 (d, $^{2}J_{(C,F)}$ = 26 Hz, **C**(7)H), 117.6 (d, $^{3}J_{(C,F)}$ = 11 Hz, q**C**-9), 117.3 (q**C**(14)Br), 115.8 (q**C**-3), 113.7 (**C**(16)H), 104.8 (d, $^{2}J_{(C,F)}$ = 24 Hz, **C**(5)H) ppm; ^{19}F NMR (282 MHz, $CDCl_3$) δ: -111 ppm; HRMS (ESI-TOF) *m/z*: $[M+H]^+$ calcd for $C_{15}H_8BrFNO$: 315.9768; found: 315.9765.

References

1. Michael, J. P. *Nat. Prod. Rep.* **2008**, *25*, 166-187.
2. Taylor, R. D., MacCoss, M., Lawson, A. D. G. *J. Med. Chem.* **2014**, *57*, 5845-5859.
3. Marella, A., Tanwar, O. P., Saha, R., Ali, M. R., Srivastava, S., Akhter, M., Shaquiquzzaman, M., Alam, M. M. *Saudi Pharm. J.* **2013**, *21*, 1-12.
4. Chan, P., Shao, L., Tomlinson, B., Zhang, Y., Liu, Z.-M. *Expert Opin. Pharmacother.* **2019**, *20*, 103-113.
5. Van Deun, A., Decroo, T., Tahseen, S., Trébucq, A., Schwoebel, V., Ortuno-Gutierrez, N., de Jong, B. C., Rieder, H. L., Piubello, A., Chiang, C.-Y. *Int. J. Antimicrob. Agents* **2020**, *55*, 105822.
6. Liu, J., Cao, R., Xu, M., Wang, X., Zhang, H., Hu, H., Li, Y., Hu, Z., Zhong, W., Wang, M. *Cell Discov.* **2020**, *6*, 16.
7. Rakedzon, S., Neuberger, A., Domb, A. J., Petersiel, N., Schwartz, E. *J. Travel Med.* **2021**, *28*, taab005.
8. Gasmi, A., Peana, M., Noor, S., Lysiuk, R., Menzel, A., Gasmi Benahmed, A., Bjørklund, G. *Appl. Microbiol. Biotechnol.* **2021**, *105*, 1333-1343.
9. Jones, G. in *The Chemistry of Heterocyclic Compounds: Quinolines, Vol. 32*, John Wiley & Sons, Hoboken, NJ, **1991**, pp. 1-318.
10. Horton, D. A., Bourne, G. T., Smythe, M. L. *Chem. Rev.* **2003**, *103*, 893-930.
11. Negishi, E. *Bull. Chem. Soc. Jpn.* **2007**, *80*, 233-257.
12. King, A. O., Okukado, N., Negishi, E. *J. Chem. Soc., Chem. Comm.* **1977**, 683-684.
13. Heck, R. F., Nolley, J. P. *J. Org. Chem.* **1972**, *37*, 2320-2322.
14. Mizoroki, T., Mori, K., Ozaki, A. *Bull. Chem. Soc. Jpn.* **1971**, *44*, 581.
15. Suzuki, A. *J. Organomet.* **1999**, *576*, 147-168.
16. Stille, J. K. *Angew. Chem. Int. Ed.* **1986**, *25*, 508-524.
17. McGlacken, G. P., Bateman, L. M. *Chem. Soc. Rev.* **2009**, *38*, 2447-2464.
18. Gensch, T., Hopkinson, M. N., Glorius, F., Wencel-Delord, J. *Chem. Soc. Rev.* **2016**, *45*, 2900-2936.

19. Bryan, M. C., Dunn, P. J., Entwistle, D., Gallou, F., Koenig, S. G., Hayler, J. D., Hickey, M. R., Hughes, S., Kopach, M. E., Moine, G.*, et al. Green Chem.* **2018**, *20*, 5082-5103.
20. Xue, X.-S., Ji, P., Zhou, B., Cheng, J.-P. *Chem. Rev.* **2017**, *117*, 8622-8648.
21. Hartwig, J. F. *J. Am. Chem. Soc.* **2016**, *138*, 2-24.
22. Yang, Y., Lan, J., You, J. *Chem. Rev.* **2017**, *117*, 8787-8863.
23. Sambiagio, C., Schönbauer, D., Blieck, R., Dao-Huy, T., Pototschnig, G., Schaaf, P., Wiesinger, T., Zia, M. F., Wencel-Delord, J., Besset, T.*, et al. Chem. Soc. Rev.* **2018**, *47*, 6603-6743.
24. You, S.-L., Xia, J.-B. in *C-H Activation. Topics in Current Chemistry, Vol. 292*, Springer, Berlin, Heidelberg, **2009**, pp. 165-194.
25. Kondrashov, M., Provost, D., Wendt, O. F. *Dalton Trans.* **2016**, *45*, 525-531.
26. Wencel-Delord, J., Dröge, T., Liu, F., Glorius, F. *Chem. Soc. Rev.* **2011**, *40*, 4740-4761.
27. Prendergast, A. M., McGlacken, G. P. *Eur. J. Org. Chem.* **2018**, 6068-6082.
28. Rossi, R., Bellina, F., Lessi, M., Manzini, C. *Adv. Synth. Catal.* **2014**, *356*, 17-117.
29. Hull, K. L., Sanford, M. S. *J. Am. Chem. Soc.* **2007**, *129*, 11904-11905.
30. Yoon, W. S., Lee, S. J., Kang, S. K., Ha, D.-C., Ha, J. D. *Tetrahedron Lett.* **2009**, *50*, 4492-4494.
31. He, Y., Wu, Z., Ma, C., Zhou, X., Liu, X., Wang, X., Huang, G. *Adv. Synth. Catal.* **2016**, *358*, 375-379.
32. Gao, G.-L., Xia, W., Jain, P., Yu, J.-Q. *Org. Lett.* **2016**, *18*, 744-747.
33. Ye, M., Gao, G.-L., Edmunds, A. J. F., Worthington, P. A., Morris, J. A., Yu, J.-Q. *J. Am. Chem. Soc.* **2011**, *133*, 19090-19093.
34. Wasa, M., Worrell, B. T., Yu, J.-Q. *Angew. Chem. Int. Ed.* **2010**, *49*, 1275-1277.
35. Guo, P., Joo, J. M., Rakshit, S., Sames, D. *J. Am. Chem. Soc.* **2011**, *133*, 16338-16341.
36. Shanahan, R. M., Hickey, A., Reen, F. J., O'Gara, F., McGlacken, G. P. *Eur. J. Org. Chem.* **2018**, 6140-6149.
37. Park, H., Chekshin, N., Shen, P.-X., Yu, J.-Q. *ACS Catal.* **2018**, *8*, 9292-9297.
38. Hull, K. L., Sanford, M. S. *J. Am. Chem. Soc.* **2009**, *131*, 9651-9653.

39. Wasa, M., Chan, K. S. L., Zhang, X.-G., He, J., Miura, M., Yu, J.-Q. *J. Am. Chem. Soc.* **2012**, *134*, 18570-18572.
40. Cabrera, P. J., Lee, M., Sanford, M. S. *J. Am. Chem. Soc.* **2018**, *140*, 5599-5606.
41. Willker, W., Leibfritz, D., Kerssebaum, R., Bermel, W. *Magn. Reson. Chem.* **1993**, *31*, 287-292.
42. Pereira, M. T., Antelo, J. M., Adrio, L. A., Martínez, J., Ortigueira, J. M., López-Torres, M., Vila, J. M. *Organometallics* **2014**, *33*, 3265-3274.
43. Pazderski, L., Toušek, J., Sitkowski, J., Kozerski, L., Szłyk, E. *Magn. Reson. Chem.* **2007**, *45*, 1059-1071.
44. Pazderski, L. *Magn. Reson. Chem.* **2008**, *46*, S3-S15.
45. Pyridine and Pyridine-^{15}N priced 0.26 €/g and 1820 €/g respectively April 2022, sigmaaldrich.com/ireland.html, *accessed 20 April 2022.*
46. Marek, R., Lycka, A. *Curr. Org. Chem.* **2002**, *6*, 35-66.
47. Martin, G. E., Hadden, C. E. *J. Nat. Prod.* **2000**, *63*, 543-585.
48. Sheldon, R. A. *Chem. Commun.* **2008**, 3352-3365.
49. Vaxelaire, C., Winter, P., Christmann, M. *Angew. Chem. Int. Ed.* **2011**, *50*, 3605-3607.
50. Dobrounig, P., Trobe, M., Breinbauer, R. *Monatsh. Chem.* **2017**, *148*, 3-35.
51. Hayashi, Y. *Chem. Sci.* **2016**, *7*, 866-880.
52. Grondal, C., Jeanty, M., Enders, D. *Nat. Chem.* **2010**, *2*, 167-178.
53. Bruggink, A., Schoevaart, R., Kieboom, T. *Org. Process Res. Dev.* **2003**, *7*, 622-640.
54. Newman, S. G., Lautens, M. *J. Am. Chem. Soc.* **2010**, *132*, 11416-11417.
55. Palani, V., Perea, M. A., Sarpong, R. *Chem. Rev.* **2021**, 10.1021/acs.chemrev.1c00513.
56. Wang, J.-R., Manabe, K. *Synthesis* **2009**, *9*, 1405-1427.
57. Ouellette, R. J., Rawn, J. D. in *Organic Chemistry* 2nd ed., Academic Press, London, UK, **2018**, pp. 51-86.
58. Lautens, M., Fang, Y.-Q. *Org. Lett.* **2003**, *5*, 3679-3682.
59. Saget, T., Perez, D., Cramer, N. *Org. Lett.* **2013**, *15*, 1354-1357.
60. Shanahan, R. M. *Ph.D Thesis*, **2020**.

61. Ma, X., Gu, N., Liu, Y., Liu, P., Xie, J., Dai, B., Liu, Z. *Appl. Organomet. Chem.* **2015**, *29*, 50-56.

62. Matsumura, K., Yoshizaki, S., Maitani, M. M., Wada, Y., Ogomi, Y., Hayase, S., Kaiho, T., Fuse, S., Tanaka, H., Takahashi, T. *Chem. Eur. J.* **2015**, *21*, 9742-9747.

63. Ren, L., Chu, W., Guan, D., Hou, Y., Wang, M., Yuan, X., Sun, Z. *Appl. Organomet. Chem.* **2014**, *28*, 673-677.

64. El Akkaoui, A., Berteina-Raboin, S., Mouaddib, A., Guillaumet, G. *Eur. J. Org. Chem.* **2010**, 862-871.

65. Koubachi, J., El Kazzouli, S., Berteina-Raboin, S., Mouaddib, A., Guillaumet, G. *J. Org. Chem.* **2007**, *72*, 7650-7655.

66. Geary, L. M., Hultin, P. G. *Org. Lett.* **2009**, *11*, 5478-5481.

67. Wang, W.-Y., Feng, X., Hu, B.-L., Deng, C.-L., Zhang, X.-G. *J. Org. Chem.* **2013**, *78*, 6025-6030.

68. Chai, D. I., Lautens, M. *J. Org. Chem.* **2009**, *74*, 3054-3061.

69. Nicolaus, N., Franke, P. T., Lautens, M. *Org. Lett.* **2011**, *13*, 4236-4239.

70. Leclerc, J.-P., André, M., Fagnou, K. *J. Org. Chem.* **2006**, *71*, 1711-1714.

71. Improta, R. in *Computational Strategies for Spectroscopy: From Small Molecules to Nano Systems*, John Wiley & Sons, Hoboken, NJ, **2011**.

72. Anderson, R. J., Bendell, D. J., Groundwater, P. W. in *Organic Spectroscopic Analysis, Vol. 22*, The Royal Society of Chemistry, Cambridge, UK, **2004**, pp. 7-23.

73. Lakowicz, J. R. in *Principles of Fluorescence Spectroscopy*, 3rd ed., Springer US, Boston, MA, **2006**, pp. 1-26.

74. Worsfold, P. J., Zagatto, E. A. G. in *Encyclopedia of Analytical Science Vol. 1*, 2nd ed., Elsevier, Oxford, UK, **2005**, pp. 318-321.

75. Valeur, B., Berberan-Santos, M. N. *J. Chem. Educ.* **2011**, *88*, 731-738.

76. Acuña, A. U., Amat-Guerri, F., Morcillo, P., Liras, M., Rodríguez, B. *Org. Lett.* **2009**, *11*, 3020-3023.

77. Fu, Y., Finney, N. S. *RSC Adv.* **2018**, *8*, 29051-29061.

78. Zhao, X. J., Huang, C. Z., Huang, C. Z. *TrAC, Trends Anal. Chem.* **2010**, *29*, 354-367.

79. Hou, L., Zhang, X., Cotella, G. F., Carnicella, G., Herder, M., Schmidt, B. M., Pätzel, M., Hecht, S., Cacialli, F., Samorì, P. *Nat. Nanotechnol.* **2019**, *14*, 347-353.
80. Terai, T., Nagano, T. *Pflugers Arch - Eur. J. Physiol.* **2013**, *465*, 347-359.
81. Prodi, L., Bolletta, F., Montalti, M., Zaccheroni, N. *Coord. Chem. Rev.* **2000**, *205*, 59-83.
82. Jiang, P., Guo, Z. *Coord. Chem. Rev.* **2004**, *248*, 205-229.
83. Bronson, R. T., Montalti, M., Prodi, L., Zaccheroni, N., Lamb, R. D., Dalley, N. K., Izatt, R. M., Bradshaw, J. S., Savage, P. B. *Tetrahedron* **2004**, *60*, 11139-11144.
84. Xu, Z., Yoon, J., Spring, D. R. *Chem. Soc. Rev.* **2010**, *39*, 1996-2006.
85. Chang, Y., Fu, J., Yao, K., Li, B., Xu, K., Pang, X. *Dyes Pigm.* **2019**, *161*, 331-340.
86. Nishihara, Y., (Ed.) *Applied Cross-Coupling Reactions*, Springer, Berlin, Germany, **2013**.
87. Braga, A. A. C., Ujaque, G., Maseras, F. in *Computational Modeling for Homogeneous and Enzymatic Catalysis*, John Wiley & Sons, Weinheim, Germany, **2008**, pp. 109-130.
88. Roy, A. H., Hartwig, J. F. *J. Am. Chem. Soc.* **2001**, *123*, 1232-1233.
89. Roy, A. H., Hartwig, J. F. *J. Am. Chem. Soc.* **2003**, *125*, 13944-13945.
90. Roy, A. H., Hartwig, J. F. *Organometallics* **2004**, *23*, 1533-1541.
91. Collman, J. P., Hegedus, L. S., Norton, J. R., Finke, R. G. in *Principles and Applications of Organotransition Metal Chemistry*, 2nd ed., University Science Books, Mill Valley, CA, **1987**, pp. 279-354.
92. Fang, Y.-Q., Lautens, M. *J. Org. Chem.* **2008**, *73*, 538-549.
93. Jones, D. J., Lautens, M., McGlacken, G. P. *Nat. Catal.* **2019**, *2*, 843-851.
94. Nareddy, P., Mantilli, L., Guénée, L., Mazet, C. *Angew. Chem. Int. Ed.* **2012**, *51*, 3826-3831.
95. Newman, S. G., Lautens, M. *J. Am. Chem. Soc.* **2011**, *133*, 1778-1780.
96. Newman, S. G., Howell, J. K., Nicolaus, N., Lautens, M. *J. Am. Chem. Soc.* **2011**, *133*, 14916-14919.
97. Petrone, D. A., Malik, H. A., Clemenceau, A., Lautens, M. *Org. Lett.* **2012**, *14*, 4806-4809.

98. Petrone, D. A., Lischka, M., Lautens, M. *Angew. Chem. Int. Ed.* **2013**, *52*, 10635-10638.

99. Shank, N. I., Pham, H. H., Waggoner, A. S., Armitage, B. A. *J. Am. Chem. Soc.* **2013**, *135*, 242-251.

100. Zurro, M., Asmus, S., Beckendorf, S., Mück-Lichtenfeld, C., Mancheño, O. G. *J. Am. Chem. Soc.* **2014**, *136*, 13999-14002.

101. Khashi, M., Davoodnia, A., Chamani, J. *Phosphorus Sulfur Silicon Relat. Elem.* **2014**, *189*, 839-848.

102. Shanahan, R. M., Hickey, A., Bateman, L. M., Light, M. E., McGlacken, G. P. *J. Org. Chem.* **2020**, *85*, 2585-2596.

103. Prendergast, A. M., McGlacken, G. P. *Eur. J. Org. Chem.* **2017**, 4827-4835.

104. Prendergast, A. M. *Ph.D Thesis*, **2018**.

105. Kudo, N., Perseghini, M., Fu, G. C. *Angew. Chem. Int. Ed.* **2006**, *45*, 1282-1284.

106. Thakur, A., Zhang, K., Louie, J. *Chem. Commun.* **2012**, *48*, 203-205.

107. Widchaya, R., Niwat, P., Uthai, S. *Lett. Org. Chem.* **2013**, *10*, 640-644.

108. Klapars, A., Buchwald, S. L. *J. Am. Chem. Soc.* **2002**, *124*, 14844-14845.

109. Chen, G., Shigenari, T., Jain, P., Zhang, Z., Jin, Z., He, J., Li, S., Mapelli, C., Miller, M. M., Poss, M. A*., et al. J. Am. Chem. Soc.* **2015**, *137*, 3338-3351.

110. Navarro, M., Vásquez, F., Sánchez-Delgado, R. A., Pérez, H., Sinou, V., Schrével, J. *J. Med. Chem.* **2004**, *47*, 5204-5209.

111. Villarreal, W., Colina-Vegas, L., Rodrigues de Oliveira, C., Tenorio, J. C., Ellena, J., Gozzo, F. C., Cominetti, M. R., Ferreira, A. G., Ferreira, M. A. B., Navarro, M*., et al. Inorg. Chem.* **2015**, *54*, 11709-11720.

112. Cooper, M. A., Manatt, S. L. *J. Am. Chem. Soc.* **1970**, *92*, 4646-4652.

113. Rosar, V., Dedeic, D., Nobile, T., Fini, F., Balducci, G., Alessio, E., Carfagna, C., Milani, B. *Dalton Trans.* **2016**, *45*, 14609-14619.

114. López-Torres, M., Juanatey, P., Fernández, J. J., Fernández, A., Suárez, A., Mosteiro, R., Ortigueira, J. M., Vila, J. M. *Organometallics* **2002**, *21*, 3628-3636.

115. Schultz, T., Schmees, N., Pfaltz, A. *Appl. Organomet. Chem.* **2004**, *18*, 595-601.

116. Miyaura, N., Suzuki, A. *Chem. Rev.* **1995**, *95*, 2457-2483.

117. Rauf, W., Brown, J. M. *Chem. Commun.* **2013**, *49*, 8430-8440.

118. García-Cuadrado, D., Braga, A. A. C., Maseras, F., Echavarren, A. M. *J. Am. Chem. Soc.* **2006**, *128*, 1066-1067.

119. Gorelsky, S. I., Lapointe, D., Fagnou, K. *J. Am. Chem. Soc.* **2008**, *130*, 10848-10849.

120. Boutadla, Y., Davies, D. L., Macgregor, S. A., Poblador-Bahamonde, A. I. *Dalton Trans.* **2009**, 5820-5831.

121. Davies, D. L., Macgregor, S. A., McMullin, C. L. *Chem. Rev.* **2017**, *117*, 8649-8709.

122. Jiang, J., Yu, J.-Q., Morokuma, K. *ACS Catal.* **2015**, *5*, 3648-3661.

123. Stuart, D. R., Fagnou, K. *Science* **2007**, *316*, 1172-1175.

124. Bandara, H. M. D., Jin, D., Mantell, M. A., Field, K. D., Wang, A., Narayanan, R. P., Deskins, N. A., Emmert, M. H. *Catal. Sci. Technol.* **2016**, *6*, 5304-5310.

125. Baxter, R. D., Sale, D., Engle, K. M., Yu, J.-Q., Blackmond, D. G. *J. Am. Chem. Soc.* **2012**, *134*, 4600-4606.

126. John, L. C., Gunay, A., Wood, A. J., Emmert, M. H. *Tetrahedron* **2013**, *69*, 5758-5764.

127. Izawa, Y., Stahl, S. S. *Adv. Synth. Catal.* **2010**, *352*, 3223-3229.

128. Asseline, U., Chassignol, M., Aubert, Y., Roig, V. *Org. Biomol. Chem.* **2006**, *4*, 1949-1957.

129. Weibel, J.-M., Blanc, A., Pale, P. *Chem. Rev.* **2008**, *108*, 3149-3173.

130. Mackey, K., Jones, D. J., Pardo, L. M., McGlacken, G. P. *Eur. J. Org. Chem.* **2021**, 495-498.

131. Xu, Q., Li, N., Yan, F., Xia, X., Lu, J., Wen, X. *Eur. Polym. J.* **2008**, *44*, 1874-1880.

132. Bureš, F. *RSC Adv.* **2014**, *4*, 58826-58851.

133. Lakowicz, J. R. in *Principles of Fluorescence Spectroscopy*, 3rd ed., Springer US, Boston, MA, **2006**, pp. 277-330.

134. Shaw, P. E., Burn, P. L. *Phys. Chem. Chem. Phys.* **2017**, *19*, 29714-29730.

135. Zhang, W., Sang, J., Cheng, J., Ge, S., Yuan, S., Lo, G. V., Dou, Y. *Molecules* **2018**, *23*, 1593.

136. Sinha, S. K., Bhattacharya, T., Maiti, D. *React. Chem. Eng.* **2019**, *4*, 244-253.

137. Kim, J., Hong, S. H. *ACS Catal.* **2017**, *7*, 3336-3343.

138. Lafrance, M., Fagnou, K. *J. Am. Chem. Soc.* **2006**, *128*, 16496-16497.

139. Athira, C., Sunoj, R. B. *Org. Biomol. Chem.* **2017**, *15*, 246-255.

140. Lotz, M. D., Camasso, N. M., Canty, A. J., Sanford, M. S. *Organometallics* **2017**, *36*, 165-171.

141. Hellal, M., Singh, S., Cuny, G. D. *J. Org. Chem.* **2012**, *77*, 4123-4130.

142. Hu, X.-Q., Lichte, D., Rodstein, I., Weber, P., Seitz, A.-K., Scherpf, T., Gessner, V. H., Gooßen, L. J. *Org. Lett.* **2019**, *21*, 7558-7562.

143. MacQueen, P. M., Chisholm, A. J., Hargreaves, B. K. V., Stradiotto, M. *Chem. Eur. J.* **2015**, *21*, 11006-11009.

144. Bellina, F., Rossi, R. *Chem. Rev.* **2010**, *110*, 1082-1146.

145. He, Z.-T., Hartwig, J. F. *Nat. Commun.* **2019**, *10*, 4083.

146. Johansson, C. C. C., Colacot, T. J. *Angew. Chem. Int. Ed.* **2010**, *49*, 676-707.

147. Blokker, E., Sun, X., Poater, J., van der Schuur, J. M., Hamlin, T. A., Bickelhaupt, F. M. *Chem. Eur. J.* **2021**, *27*, 15616-15622.

148. Stambuli, J. P., Bühl, M., Hartwig, J. F. *J. Am. Chem. Soc.* **2002**, *124*, 9346-9347.

149. Stambuli, J. P., Incarvito, C. D., Bühl, M., Hartwig, J. F. *J. Am. Chem. Soc.* **2004**, *126*, 1184-1194.

150. Barrios-Landeros, F., Carrow, B. P., Hartwig, J. F. *J. Am. Chem. Soc.* **2009**, *131*, 8141-8154.

151. Sheldrick, G. M. *Acta Crystallogr. Sect. C, Struct. Chem.* **2015**, *71*, 3-8.

152. Dolomanov, O. V., Bourhis, L. J., Gildea, R. J., Howard, J. A. K., Puschmann, H. *J. Appl. Crystallogr.* **2009**, *42*, 339-341.

153. Zhou, Y., Yan, W., Cao, D., Shao, M., Li, D., Wang, F., Yang, Z., Chen, Y., He, L., Wang, T.*, et al. Eur. J. Med. Chem.* **2017**, *138*, 1114-1125.

154. Shi, L., Wu, T.-T., Wang, Z., Xue, J.-Y., Xu, Y.-G. *Eur. J. Med. Chem.* **2014**, *84*, 698-707.

155. Ressurreição, A. S., Gonçalves, D., Sitoe, A. R., Albuquerque, I. S., Gut, J., Góis, A., Gonçalves, L. M., Bronze, M. R., Hanscheid, T., Biagini, G. A.*, et al. J. Med. Chem.* **2013**, *56*, 7679-7690.

156. Ji, F., Li, X., Wu, W., Jiang, H. *J. Org. Chem.* **2014**, *79*, 11246-11253.

157. Haile, P. A., Casillas, L. N., Bury, M. J., Mehlmann, J. F., Singhaus, R., Charnley, A. K., Hughes, T. V., DeMartino, M. P., Wang, G. Z., Romano, J. J.*, et al. ACS Med. Chem. Lett.* **2018**, *9*, 1039-1044.

158. Lin, A. J., Loo, T. L. *J. Med. Chem.* **1978**, *21*, 268-272.

159. Semenov, V. P., Studenikov, A. N. *Chem. Heterocycl. Compd.* **1980**, *16*, 754-757.

160. Mehra, M. K., Tantak, M. P., Arun, V., Kumar, I., Kumar, D. *Org. Biomol. Chem.* **2017**, *15*, 4956-4961.

Chapter 3 Borylation of 6-Fluoroquinolines: Access to 6-Fluoroquinolones

"A grain of rice will tip the scale, just remember that lads!"

Páidí Ó Sé

An luibh ná faightear is í a fhóireann.

(*The herb that cannot be found is the very one which works.)*

Seanfhocal (Irish Proverb)

Introduction

In this Chapter, the C-H borylation of quinolones is explored. This transformation would allow for late-stage functionalisation of the coveted quinolone antibiotic framework, with specific intentions to functionalise the C-7 position. An overview of fluoroquinolone antibiotics and C-H borylation strategies is provided below.

3.1. Fluoroquinolone Antibiotics

As already discussed (Chapter 2), the quinoline nucleus is an essential and privileged biological scaffold. Quinolin-4-ol exists as a minor tautomer in equilibrium with quinolin-4(1*H*)-one (4-quinolone), another pivotal core structure of myriad antibiotics, autoinducers and naturally occurring compounds with medicinal properties (**Figure 3.1 (i)**).[1] As is the case with many scientific breakthroughs, the discovery of quinolone-based antibiotics was somewhat serendipitous in nature – arising from an impurity detected in the synthesis of the anti-malarial, chloroquine, in the late 1950s.[2] Although the potency of the impurity was not high enough for it to be considered as a viable antimicrobial, further developments led to the commercialisation of the first quinolone (naphthyridinone) antibiotic, nalidixic acid (**Figure 3.1 (ii)**).

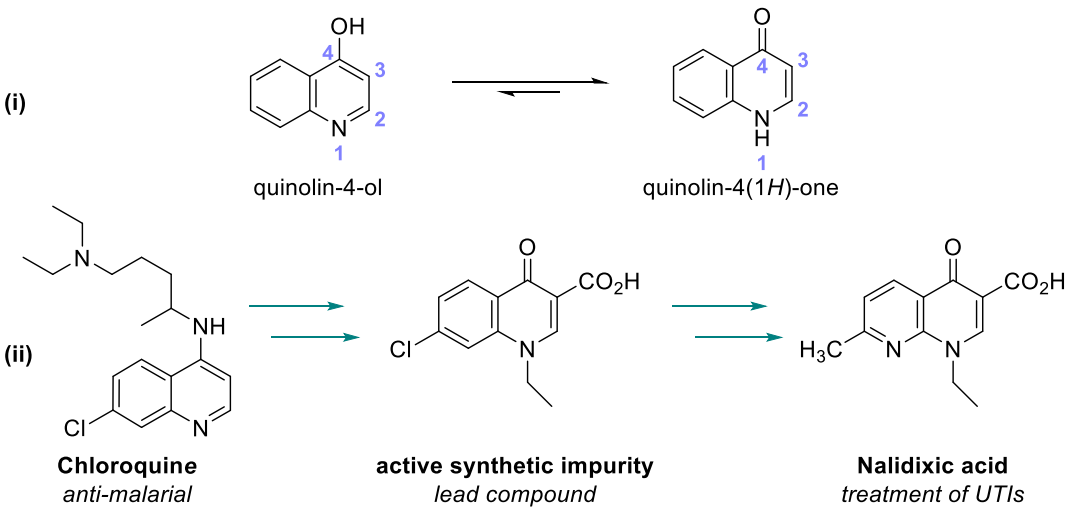


Figure 3.1 Quinoline-4-ol and 4-quinolone.

The use of nalidixic acid was limited by a narrow spectrum of activity and adverse side effects; it was originally used for the treatment of uncomplicated urinary tract

infections (UTIs) but has since been withdrawn from the market.[3] Years of trial and error, along with numerous structure-activity relationship studies, based on natural and non-natural derivatives, gave rise to a far greater understanding of the mode of action of this compound class.[1,4] Subsequent modulations of the core structure vastly altered the potency, pharmacokinetics, spectrum of activity and thus, the therapeutic utility of quinolone antibiotics. The most important addition was that of a fluorine atom at the C-6 position, giving rise to 'fluoroquinolones', which are now one of the world's most commonly prescribed classes of antimicrobials.[5-6] Two other imperative features are the 3,4-β-ketoacid and C-7 cyclic amine, and a summary of all key modifications is given below (**Figure 3.2**).[7-8]

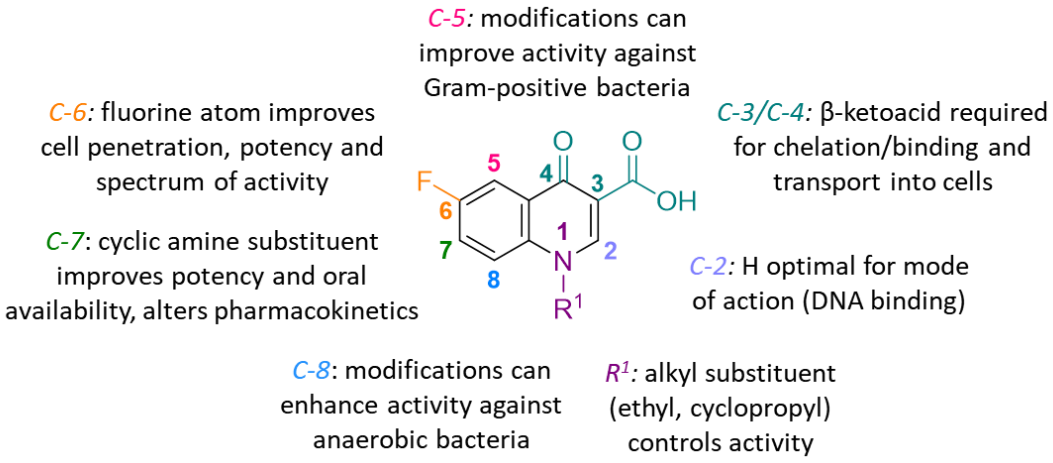


Figure 3.2 Modifications of fluoroquinolone antibiotics.[7-8]

These therapeutic discoveries have led to the development of four generations of fluoroquinolone antibiotics with an array of medicinal properties, with some contained in the World Health Organisation (WHO) Model List of Essential Medicines (**Figure 3.3**).[9] Their excellent bioavailability, broad-spectrum activity and potency profiles allow for fluoroquinolones to be utilised in the treatment of, *inter alia*, urinary tract, respiratory tract, gastrointestinal, skin and soft tissue infections.[10] The mode of action for this class of antibiotics is primarily the inhibition of bacterial DNA synthesis, by disrupting one of two stages in the DNA replication pathway. The two enzymatic targets for fluoroquinolones are both type-II bacterial topoisomerases, DNA gyrase and topoisomerase IV. DNA gyrase is responsible for the negative supercoiling of double-stranded DNA, and topoisomerase IV enables the segregation

of newly replicated chromosomes.[11] Interference with either sequence impedes DNA replication and can ultimately result in apoptosis.

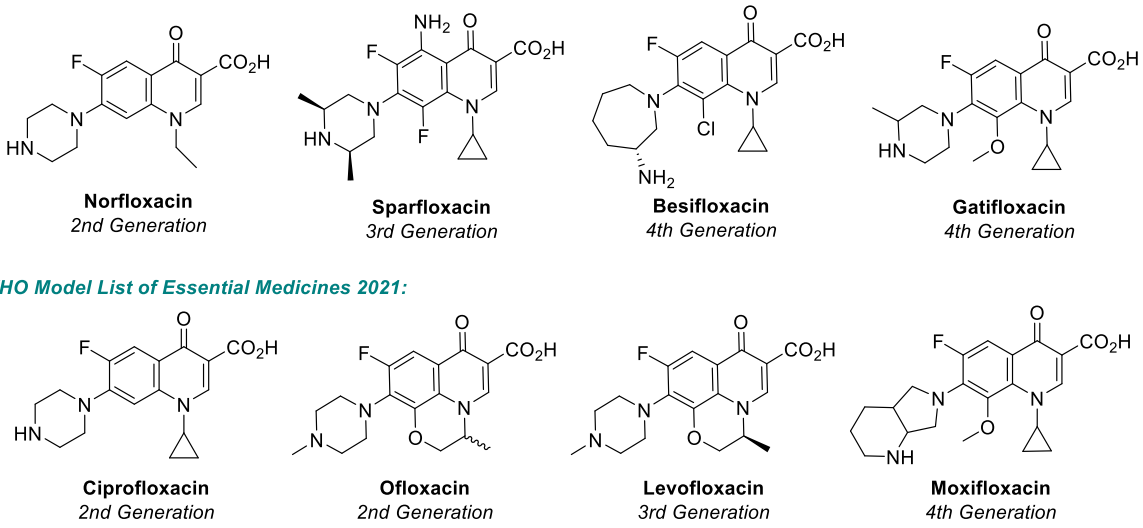
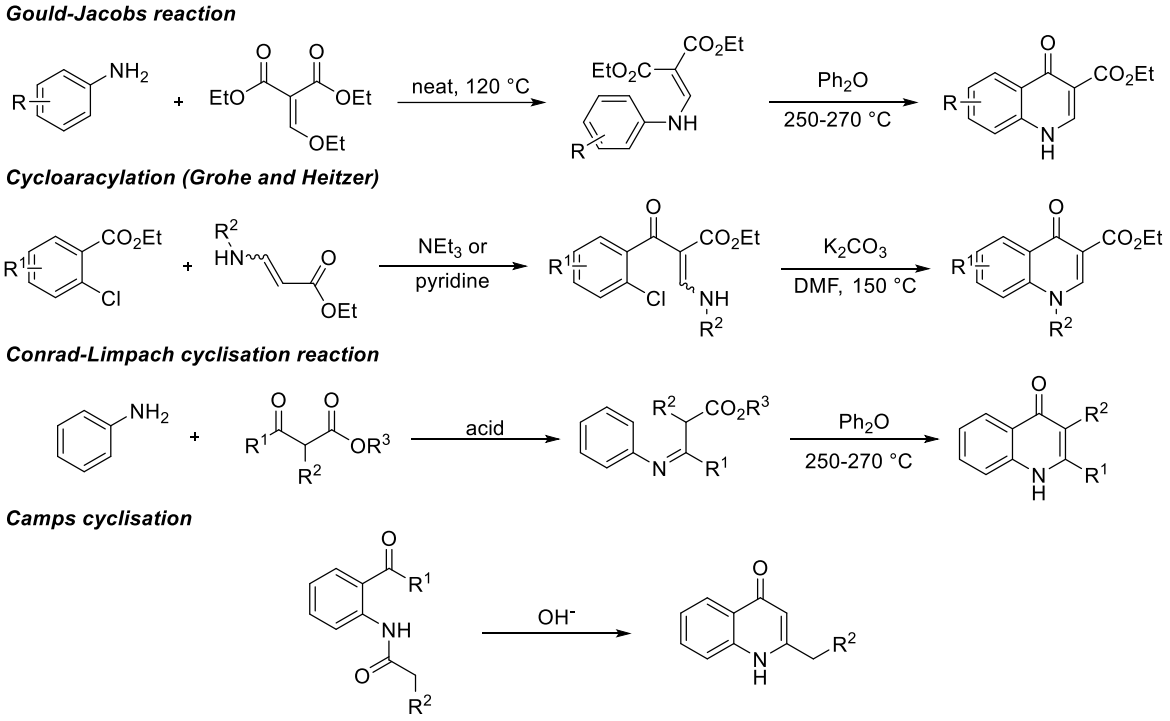


Figure 3.3 Marketed fluoroquinolone antibiotics.

3.1.1 Synthesis of Fluoroquinolones

Synthesis of quinolone analogues is normally achieved through high-temperature cyclisation processes from the corresponding substituted aniline and an unsaturated coupling partner over either one or two steps (**Scheme 3.1**).[12-14] These preparations are still widely employed, but do suffer from a small number of issues; they are dependent on the synthesis and availability of highly functionalised starting materials and, most importantly, can result in the formation of regioisomers. This problem is particularly evident in the case of C-5/C-7 modification, where a *meta*-substituted aniline can cyclise *via* either *ortho*-position.[12] Considerable strides have also been made toward catalytic processes from halogenated precursors.[15]



Scheme 3.1 Traditional syntheses of 4-quinolone structure.

3.2. C-H Activation

An introduction to C-H activation/functionalisation relative to aryl-aryl bond formation is discussed in Chapter 2.

The direct derivatisation of latent C-H bonds to myriad functional groups has rapidly become one of the most important transformations in organic chemistry. Advances in this field have been described as 'revolutionary' and have afforded functionalities and substitution patterns that were previously considered inaccessible.[16-18] These developments offer new retrosynthetic pathways to natural products and drug molecules. Disconnections which were impracticable in the past now allow for the late-stage functionalisation of complex structures with high functional group tolerance.[19-21]

3.3. Carbon-Boron Bond Formation

Aryl boronate compounds, particularly aryl boronic acids and esters, are pivotal reactive intermediates in organic synthesis, acting as a universal link to a plethora of chemical entities (**Figure 3.4**).[22-24]

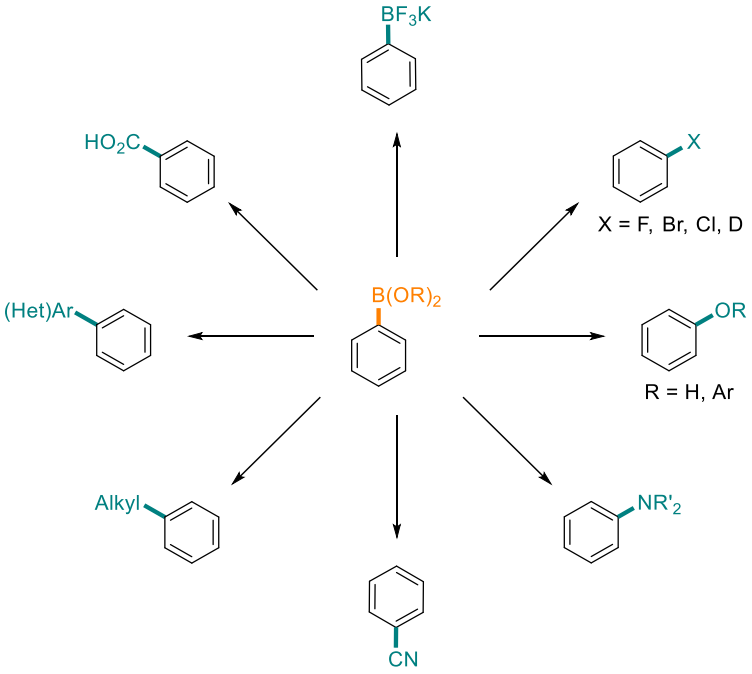
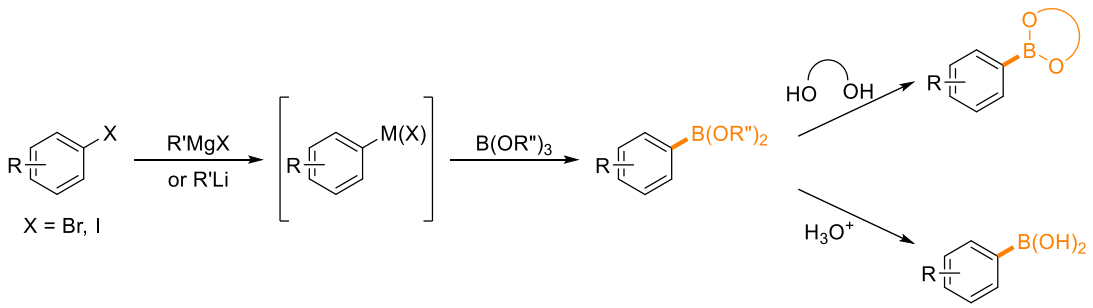


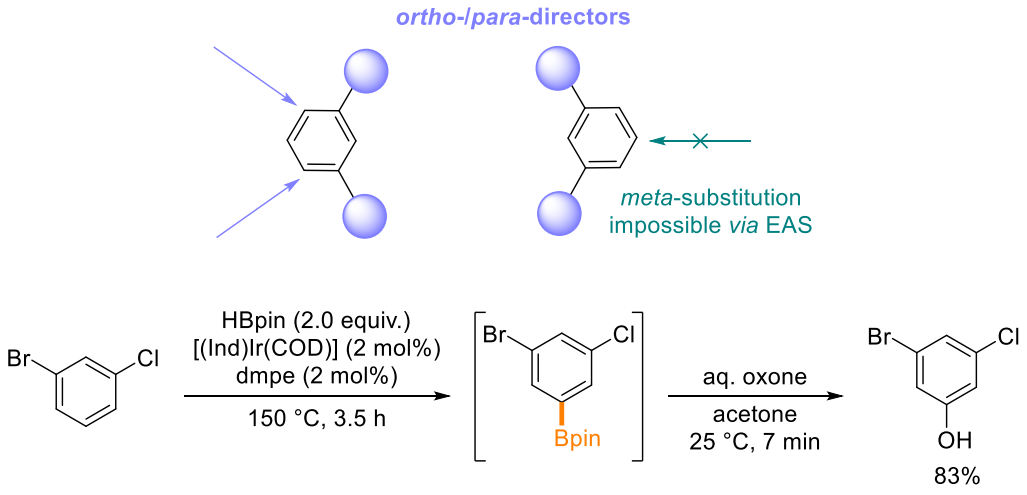
Figure 3.4 Summary of some possible boronic acid and ester transformations.

Classically, synthesis of organoboron compounds was achieved using organometallic building blocks, combining an aryl halide with either Grignard or lithium-based reagents for subsequent reaction with a trialkylborate (**Scheme 3.2**).[22,25] Although very effective for the large-scale production of simple aryl boronates, these methods possess low functional group tolerance and require the use of air- and moisture-sensitive reagents at cryogenic temperatures.[22] Other routes include the metal-catalysed coupling of aryl halides with either pinacolborane (HBpin) or bis(pinacolato)diboron (B_2pin_2)[26-27] or by use of aminoborane frustrated Lewis pairs,[28-30] neither of which will be discussed in detail here.



Scheme 3.2 Traditional synthesis of aryl boronate esters and acids.

The catalytic construction of C-B bonds through C-H activation is an area of research that has gained great interest over the last two decades.[25,31-34] These transformations are performed in a single synthetic step with high yields and regioselectivities. Thus, C-H borylation provides an attractive, step-economic route to highly reactive organoboron species, without reliance on the availability of aryl halides. This approach allows novel substitution patterns that are not achievable *via* classical methods (*vide supra*). For example, electrophilic aromatic substitution (EAS) is dependent on the electronic properties and positioning of any arene substituents; defined by either *ortho*-/*para*- or *meta*-directing effects.[35] Many electron-deficient substituents can deactivate the ring system, and regioselectivity becomes even more challenging in the case of di-/tri-substituted arenes.[36] An early and exemplary demonstration of the superior and more tuneable selectivity of metal-catalysed C-H borylation is the one-pot unified route to *meta*-substituted phenols described by Maleczka, Smith and co-workers.[37] The C-5 position of 1,3-disubstituted benzenes is typically inert in the presence of *ortho*-/*para*-directors, and formation of similar compounds is therefore impossible through EAS-type reactions (**Scheme 3.3**). Highly functionalised phenols are furnished in excellent yields over one step, while parallel routes to similar compounds are reported over 10-steps, with some starting from the highly explosive compound, TNT.[38]

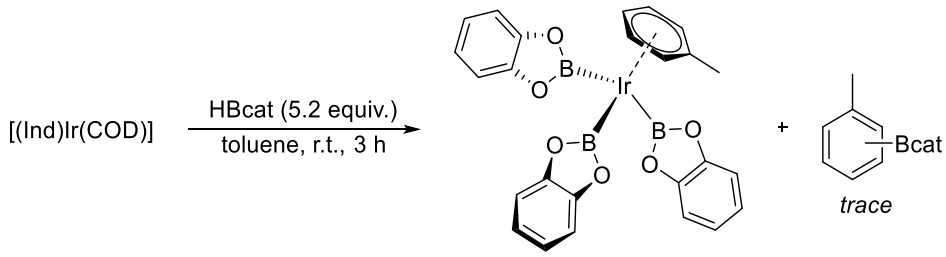


Scheme 3.3 EAS *vs* C-H activation approaches to the formation of highly functionalised phenols.[37]

3.4. Iridium-Catalysed C-H Borylation

3.4.1 Discovery and Development of Iridium-Catalysed C-H Borylation

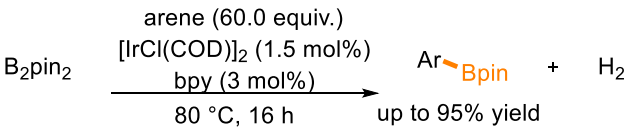
Several transition metal-based catalysts including, *inter alia*, nickel, copper, rhodium and cobalt, have been developed and applied in C-H borylation methodologies; iridium-catalysed systems are the most commonly reported and will be the focus of this introduction.[39] In 1993, Marder and co-workers reported the formation of the first iridium tris(boryl) complexes. The isolation of these complexes was achieved in solvents such as benzene and toluene, and in the supporting information, the authors note trace amounts of boron-containing by-products. The compounds were detected by GC-MS and identified as two isomers of the tolyl boronate esters; hence simultaneously publishing the first iridium-mediated C-H borylation of arenes (**Scheme 3.4**).[40]



Scheme 3.4 First observed iridium-catalysed C-H borylation.

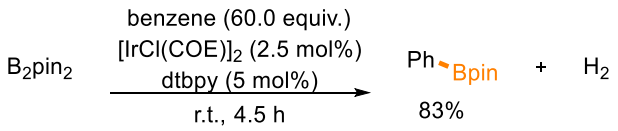
Iverson and Smith described the first catalytic C-H borylation employing an iridium catalyst in 1999.[41] Benzene-d_6 was borylated in 53% isolated yield using 17 mol% of a Cp*Ir complex with trimethylphosphine and HBpin at 150 °C. The active pre-catalyst formed in this transformation, [Cp*Ir(PMe_3)(H)(Bpin)], was then shown to effectively borylate a range of substituted aryls, with electron-deficient arenes giving the highest yields.[42] Further investigations revealed the use of electron-donating phosphine-based ligands (dppe, dmpe) in place of Cp* ligands in iridium systems could greatly improve yields.[43] Concurrently, Ishiyama, Miyaura, Hartwig and co-workers reported the borylation of arenes using strongly electron-donating bipyridine ligands with a commercially available iridium catalyst, $[Ir(Cl)COD]_2$, 2,2'-bipyridine (bpy) and B_2pin_2 at 80 °C (**Scheme 3.6**).[44] Monosubstituted aryls gave a *ca*.

2:1 mixture of *meta*-/*para*-boronate esters and no *ortho*-borylation was observed. The absence of *ortho*-substitution was credited to steric effects of the substituents, consequently, that only a single regioisomer was formed in the case of 1,2- and 1,4-disubstituted arenes.



Scheme 3.5 Iridium-catalysed C-H borylation using nitrogen-based ligand, bpy.

Careful monitoring of the reaction of benzene-d_6 and B_2pin_2 by ^1H NMR analysis, gave evidence for an induction period where the cyclooctadiene (COD) ligand was reduced to cyclooctene-d_2. This discovery led the authors to trial $[Ir(Cl)COE)]_2$ (COE = cyclooctene) as a catalyst for the reaction, in an attempt to pre-activate the catalyst. Indeed, using the modified catalyst enabled the C-H borylation to occur in excellent yield at room temperature (**Scheme 3.6**). A similar nitrogen-based ligand, 4,4'-di-*tert*-butyl-2,2'-bipyridine (dtbpy), was employed instead of bpy here to increase the solubility of the iridium pre-catalyst and prevent borylation of the ligand. The complexes formed in this case were significantly more efficient than those formed with alkylphosphine ligands, providing higher yields, substantially increased turnover numbers and, importantly, allowed for the use of milder conditions.[25]



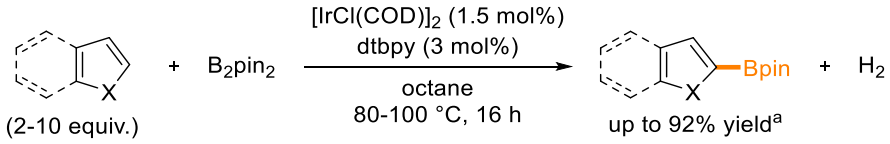
Scheme 3.6 Iridium-catalysed C-H borylation using an alternative iridium pre-catalyst and dtbpy.

An extensive, systematic study of both iridium pre-catalysts and bipyridine ligands was subsequently carried out by Ishiyama, Miyaura, Hartwig and co-workers.[45] The steric and electronic properties of the ligands were varied and their findings revealed the most proficient catalytic system comprised of $[Ir(OMe)COD]_2$ and dtbpy. This combination allowed for the high-yielding C-H borylation of arenes at room temperature in hexanes. This was the first instance where the arene substrate was

not used as solvent, a very promising development in terms of the applicability and utility of such reactions with expensive substrates.

3.4.2 Iridium-Catalysed C-H Borylation of Heteroaromatic Compounds

A few heteroaromatic substrates had been included in the scopes of the publications discussed above,[43,45] but a thorough study dedicated to heteroarenes was first published by Ishiyama, Miyaura, Hartwig and co-workers in 2002.[46] Their initial experiments employed thiophene as both substrate and solvent with $[Ir(Cl)COD]_2$, B_2pin_2 and bpy. After 16 h at 80 °C, no conversion to a borylated product was observed. The authors attributed the lack of reaction here to interference with the formation of an active iridium species, caused by the high coordinating ability of the excess thiophene. To obviate this issue, the authors utilised octane as solvent with lower equivalents of thiophene to give the desired, C-2-borylated product in 64% yield. Exchanging dtbpy for bpy improved the reactivity of catalytic species (*vide supra*) and furnished the borylated thiophene in 83% yield. The methodology was applied to a number of five-membered heteroarenes as well as benzofuran, indole, pyridine and quinoline in excellent yields with high selectivity (**Scheme 3.7**). Bis-borylation was also noted in some cases and 2,5-bisborylated products could be synthesised using an excess of B_2pin_2.



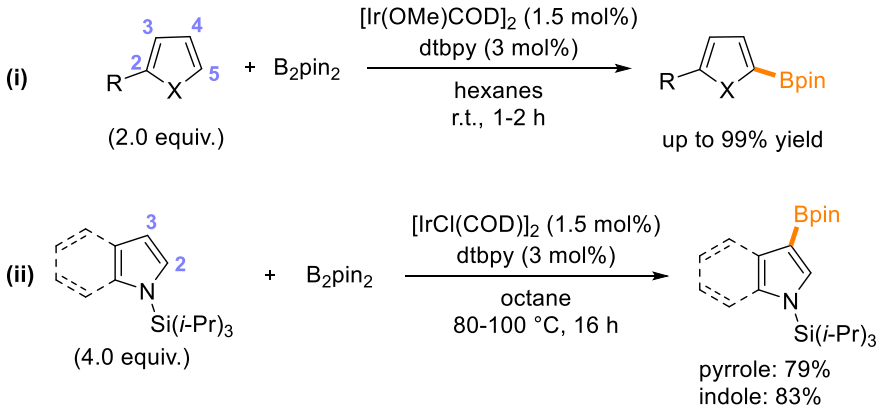
Scheme 3.7 Borylation of heteroaromatic substrates. [a]Diborylated products also produced (12-17%).[46]

Several research labs built upon this seminal publication by Ishiyama, Miyaura, Hartwig and co-workers. The same groups went on to develop a room temperature, regioselective borylation of substituted heteroarenes in hexanes using $[Ir(OMe)COD]_2$.[47] Concomitantly, the more atom-economic boron source, HBpin, was utilised by Ishiyama *et al.*,[48-49] and Beller and co-workers[50] to furnish mono-borylated heteroatomic products in very good yields. Directed o*rtho*-borylation can also be

accomplished but such transformations are outside the scope of this introduction.[51-54]

3.4.3 Regioselectivity of Iridium-Catalysed C-H Borylation Reactions

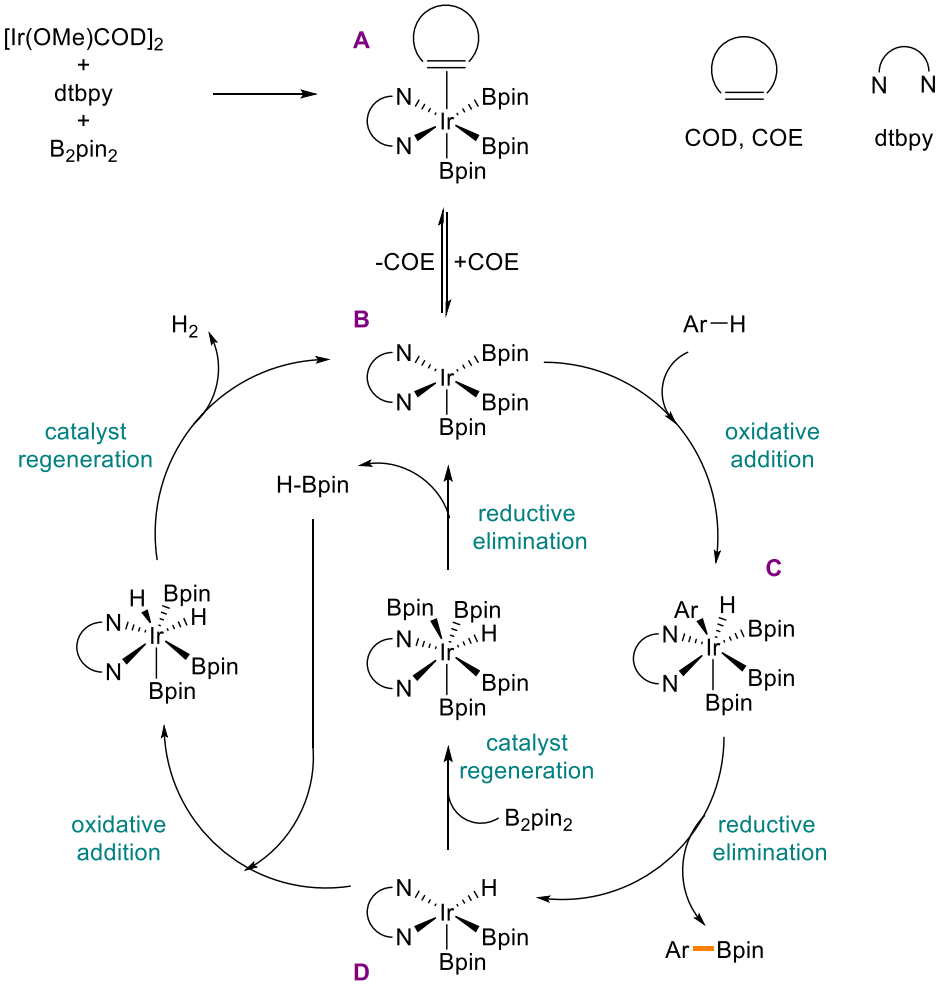
Various discoveries had been made regarding the regioselectivities related to emerging iridium-catalysed systems.[55-56] For example, five-membered heteroarenes borylate at the C-2 position and at both the C-2 and C-5 positions using an excess of the borylating agent (*vide supra*).[46,49] Many groups used these predicted reactivities to manipulate substrates and 'direct' borylation to sites that were not inherent to the unsubstituted compound.[33,57-58] Ishiyama, Miyaura, Hartwig and co-workers introduced a C-2 substituent to five-membered heteroarenes to generate mono-substituted aryls exclusively (**Scheme 3.8 (i)**),[47] and C-3 borylation of pyrrole/indole was achieved using a tri-isopropylsilyl protecting group (**Scheme 3.8 (ii)**).[46] Smith and co-workers forced the C-7 borylation of indoles through installation of a group at C-2,[59] and varied the substitution pattern of thiophenes to give a range of borylated regioisomers.[60]



Scheme 3.8 Alteration of heteroaromatic substrates to institute non-native borylation patterns.

To understand the regioselective outcomes of C-H borylations, it is important to consider the potential mechanism of reaction, and more specifically, the structures of the iridium species generated throughout the sequence (**Scheme 3.9**).[61] Initial mixing of $[Ir(OMe)COD]_2$, dtbpy and B_2pin_2 gives octahedral Ir(III) complex **A**. As

noted by Ishiyama, Miyaura, Hartwig and co-workers, a short induction period involves reduction of COD to COE, which can reversibly dissociate to form trisboryl complex **B**.[44] This unsaturated, 16e$^-$ complex reacts with an arene substrate Ar–H, *via*, for example, OA, to give Ir(V) complex **C** – the structure of which was elucidated by Sakaki and co-workers.[61] Further evidence was provided through the NMR studies performed by Boller *et al.*,[62] and was shown by Miyaura to be the turnover-limiting step.[63] Critically, regioselectivity is determined here based on the steric hinderance induced by the bidentate dtbpy ligand, as active species **C** has only one vacant coordination site. It is also worth noting a small electronic influence that will direct the addition to the most electron deficient C-H bond if the steric effects allow it.[42,64-65] Marder and co-workers observed that the dtbpy complexation is not transient – the ligand remains coordinated to the iridium centre throughout the catalytic cycle, as it too would get borylated if dissociated.[66] Ir(V) complex **C** then undergoes reductive elimination to generate the desired Ar-Bpin product and another square pyramidal Ir complex **D**. The driving force for this step lies in the formation of the B-C bond, which is thermodynamically favoured. Active catalyst **B** is then regenerated from complex **D** *via* either one of two pathways; reaction with another molecule of B_2pin_2, or reaction with the HBpin side product, to give hydrogen gas as the only by-product of the reaction.[62]



Scheme 3.9 Proposed catalytic cycle for iridium-catalysed borylation of arenes with B_2pin_2 and dtbpy.[61,67]

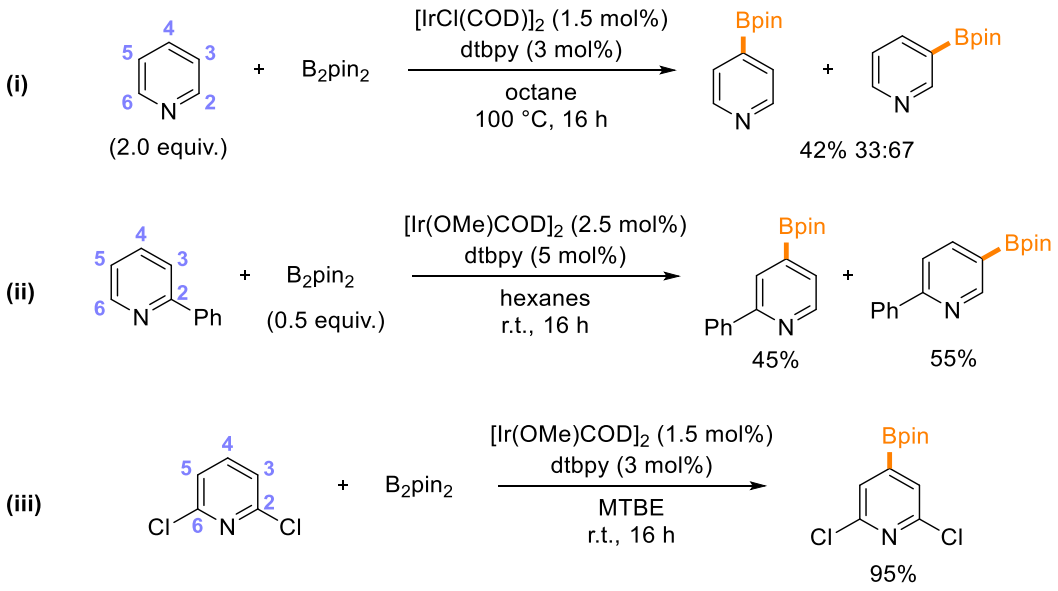
Heteroarenes display even higher reactivities towards borylation than simple aromatic compounds and this field has been extensively reviewed.[55-56,62,68] The electron-rich heteroatom-containing rings of benzofuran and indole are selectively borylated over the more sterically available, electron-poor carbocyclic rings (*vide supra*),[47] due to the acidity of the C-H bond at the α-position to the heteroatom.[65]

3.4.4 Iridium-Catalysed C-H Borylation of Pyridines and Quinolines

In the case of six-membered heterocycles, a mixture of C-3/C-4 regioisomers is observed for pyridine analogues.[46] In contrast to five-membered heterocycles, borylation is strongly disfavoured α to the azinyl nitrogen atom for these analogues.[46,55,58,68-69] This shift in reactivity could be loosely attributed to the steric encumberment of the nitrogen; but is more likely to be multifaceted. Firstly, the

nitrogen lone pair could potentially coordinate to the vacant site on the active iridium-catalyst or, cause dipolar repulsion with the C-H activation transition state were it to happen at the α-position.[46,68] Secondly, the stability of any unsubstituted, C-2 borylated pyridines/quinolines would be poor – these compounds are known to decompose through several pathways.[70]

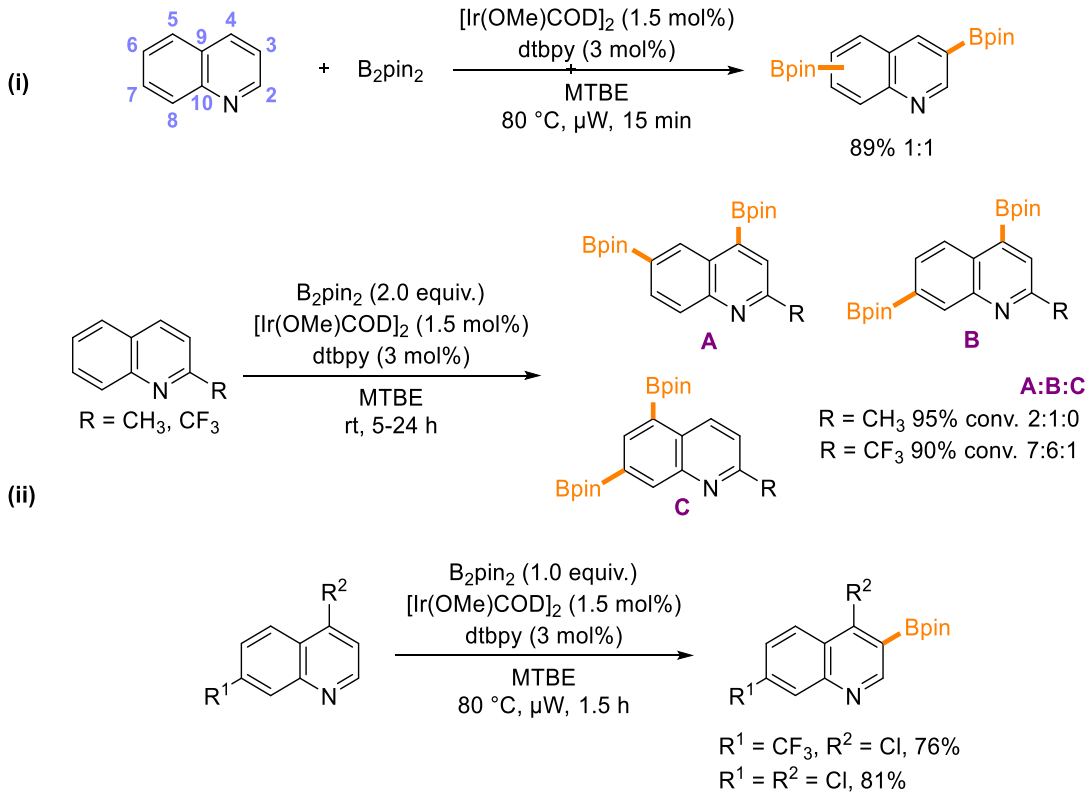
As well as forming a mixture of regioisomers, initial reactions had demonstrated the pyridine analogue to be sluggish toward C-H borylation with relatively low yields (**Scheme 3.10 (i)**).[46] Marder, Steel and co-workers performed an extensive study on the borylation of pyridines, from which the source of their poor reactivity profile was identified.[69] They established that the Lewis basic nitrogen lone pair could, in fact, bind to the vacant site of the active trisboryl Ir complex (*vide supra*), thus inhibiting the C-H activation step. Simply installing a substituent at the α-position impedes *N*-coordination, leading to improved reactivity at room temperature and higher yields (**Scheme 3.10 (ii)**). Substitution at both the C-2 and C-6 positions of pyridine gave the C-4 borylated product only (**Scheme 3.10 (iii)**).[69,71]



Scheme 3.10 Selected examples of the iridium-catalysed C-H borylation of pyridines.[46,69,71]

In the case of quinoline, the C-3 quinoline boronic ester is exclusively formed in reaction with B_2pin_2, due to the steric encumberment induced by the ring junction *ortho* to the C4-position.[46] However, Harrison *et al.* reported that the addition of an

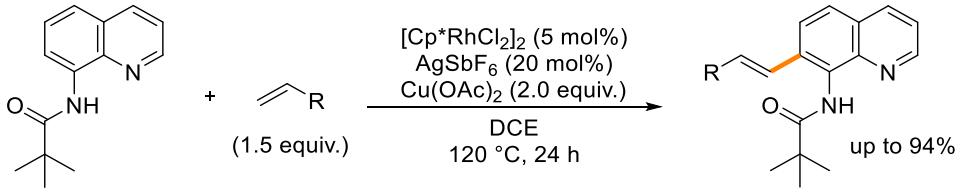
excess of the borylating reagent, introduces a second Bpin moiety to the carbocyclic ring, to give a mixture of C-3/C-6- and C-3/C-7-bisborylated quinolines (**Scheme 3.11 (i)**).[72] Following on from this, Marder, Steel and co-workers performed a salient investigation into the intriguing selectivity related to the C-H borylation of quinoline analogues.[55] The authors here wished to expand on the work of Smith and co-workers,[65] to devise a protocol that would be useful for predicting the preferred site of borylation in a given substrate. Borylation occurs preferentially at the least sterically demanding site and at the most acidic C-H bond (*vide supra*), and from this work, the authors were able to observe a strong correlation between the NMR shift patterns and the preferred borylation site. They deduced that the furthest downfield protons in the ^{1}H NMR spectrum are the most likely to undergo C-H borylation, provided that the proton is not sterically encumbered. Based on this information, they carried out borylation protocols on a number of substituted quinolines, an example of which is illustrated below (**Scheme 3.11 (ii)**).



Scheme 3.11 Selected examples of the iridium-catalysed C-H borylation of quinolines.[55,72]

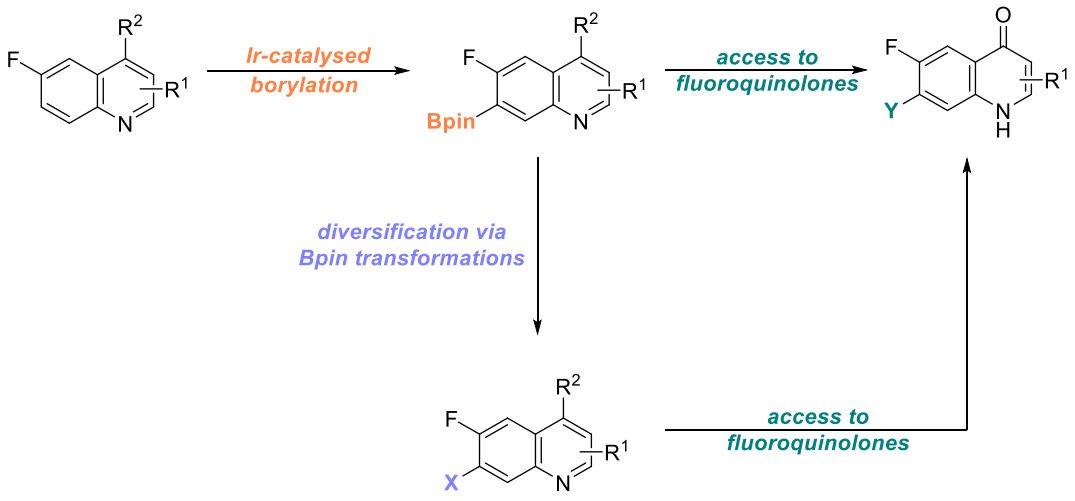
3.4.5 Access to Alternative Positions on the Quinoline Nucleus

Derivatisation of the core structure subsequent to cyclisation is possible *via* C-H activation; in many cases selectivity is governed by the presence of a directing group.[73-77] The C-2 position is the easiest to modulate due to the intrinsic reactivity of the C=N bond, and as it is proximal to the nitrogen atom, which can coordinate directly to a metal centre and guide functionalisation.[74] The quinoline *N*-oxide is often employed for this transformation, as well as the activation of the C-8 position.[78] There are also a number of examples where the C-3 (*vide supra*) and C-4 positions can be activated, whereas there are very limited reports for the C-5/C-6/C-7 positions.[73-75] To the best of our knowledge, direct access to the C-7 position has only been realised once, in a publication by Shi and co-workers.[79] The report describes the selective rhodium-catalysed C-H olefination of pyridines and quinolines using a pivaloyl amide directing group at the C-2- and C-8 positions respectively, in excellent yields (**Scheme 3.12**).



Scheme 3.12 C7-olefination of quinolines using a pivaloyl amide directing group.

As already detailed, C-H borylation of quinoline occurs preferentially at C-3, with a second equivalent of boron forming an equimolar mixture of the C-6-/C-7 isomers (**Scheme 3.11 (i)**). In Chapter 3 we seek to selectively borylate the C-7 position of 6-fluoroquinolines, with the prospect of revealing the 6-fluoroquinolone antibiotic framework for late-stage functionalisation at C-7 (**Scheme 3.13**).



Scheme 3.13 Borylation of 6-fluoroquinolines to reveal a functionalised 6-fluoroquinolone scaffold.

Results and Discussion

3.5. Objectives

Iridium-catalysed C-H borylation is an attractive route for the construction of substituted aromatic compounds.[25,31-34] It is a particularly advantageous for the late-stage modification of advanced synthetic intermediates, where certain functionalities can impede the introduction of specific moieties using other routes.[19-21] Although there are several reports pertaining to the C-H functionalisation of quinolines, the C-7 position remains an elusive target. The work in this Chapter focuses on the C-H borylation of 6-fluoroquinolines. The borylation and subsequent derivatisation of these compounds was carried out with the intention to reveal the important 6-fluoroquinolone framework.[1,5-6]

The work in this Chapter was carried out in collaboration with the group of Prof. Dr Todd B. Marder in Julius-Maximilians-Universität Würzburg, Germany who synthesised and provided the iridium pre-catalyst, $[Ir(OMe)COD]_2$.

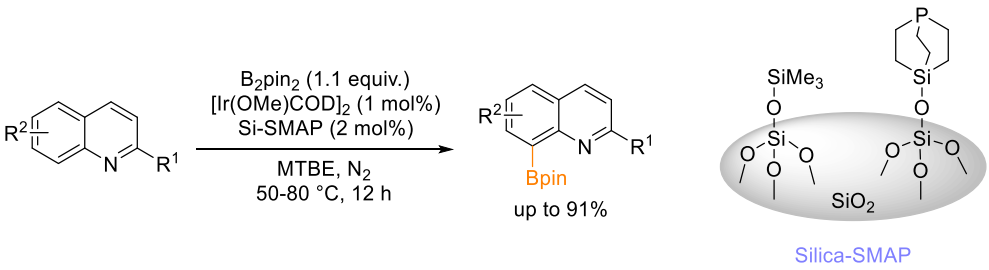
Note: All details for X-ray crystallography studies are included in **Appendix I**.

The term 'yield by NMR' is used throughout this section and is calculated from the ^1H NMR spectrum of a crude reaction mixture with 1,3,5-trimethoxybenzene as the internal standard for quantification.

3.6. Borylation of 2-Methylquinolones

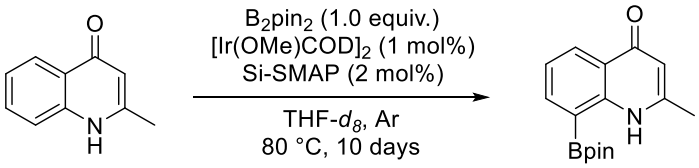
The following section describes the background and initial experiments for this project. These were carried out by Dr Julia Merz in Julius-Maximilians-Universität Würzburg, Germany as follows.[67]

As detailed in the introduction, the Marder group has published a multitude of papers in the field of C-H borylation, and more specifically, the C-H borylation of quinolines.[55] The inception of this project was inspired by a report published through collaboration of the Marder and Sawamura research groups.[80] The study utilised a silica-bound phosphine ligand developed by Sawamura and co-workers,[81] to selectively borylate the C-8 position on a number of substituted quinolines in very good yields (**Scheme 3.14**).



Scheme 3.14 Iridium-catalysed C-8 borylation of quinolines using Si-SMAP ligand.

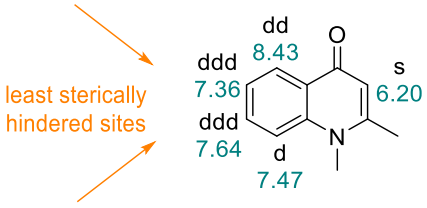
Given the experience of our group in the area of quinolone synthesis,[82-87] the Marder and McGlacken groups sought to combine their expertise on a project involving the borylation of quinolone substrates. As the above reaction suffered from concomitant reduction of the aza-ring in the absence of a C-2 substituent,[80] the primary experiment was carried out on 2-methylquinolone **121**, using the Ir/Si-SMAP system (**Scheme 3.15**).[67] After 10 days at 80 °C, 50% conversion to borylated product **122** was obtained, with no other competing isomers observed by ^{1}H NMR analysis of the crude reaction mixture. Given this promising result, the Marder group carried forward this reaction for optimisation and are in the process of performing a substantial substrate scope using quinolones synthesised by the McGlacken group. A manuscript for this work will be prepared in due course.



121 **122**, 50% conv.

Scheme 3.15 Iridium-catalysed C-8 borylation of 2-methylquinolone using Si-SMAP ligand.

Attention was then turned to the other prospective sites for borylation on the quinolone nucleus, using the Ir/dtbpy system. As the N-H bond of quinolones is labile, and would likely be the preferred site for borylation,[58,68] preliminary studies involved protecting this site using a methyl group. Based on the selectivity findings reported by Marder and others,[55,66,68-69] it was predicted that C-6 and C-7 would be the two most likely sites for borylation due to a combination of steric and electronic factors. The C-3 position is not considered aromatic and is sterically unavailable due to the neighbouring methyl group. Positions C-5/C-8 are both sterically encumbered by the adjacent ring junction and are therefore inaccessible using this system, with these deductions leaving C-6 and C-7 as possible targets. The negative mesomeric effect induced by the carbonyl group leads to enhanced selectivity at C-7, while the amine moiety possesses a positive mesomeric and a negative inductive effect. The proton at C-7 is potentially slightly more favoured than C-6 due to increased acidity, and this is also indicated by a downfield shift in the ^{1}H NMR spectrum of **123** (**Figure 3.5**).

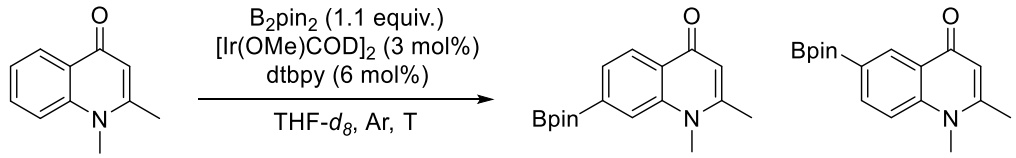


123

Figure 3.5 Predicted sites for C-H borylation of 1,2-dimethylquinolone. ^{1}H NMR shifts measured at 300 MHz in $CDCl_3$ and are reported in ppm.

These investigations aimed to exploit the inherent steric and electronic biases of the protected quinolone motif **123** to target the C-7 position for borylation. Indeed, by using dtbpy as a ligand in THF-d_8 at r.t. for 10 days, C-7 borylated quinolone **124** was

preferentially, but not exclusively, synthesised. Using this system, incomplete consumption of the quinolone starting material was observed, along with the formation of the minor C-6 isomer **125**, in a ratio of 1:0.28 (C-7:C-6) by ^{1}H NMR analysis. As the quinolone starting material is sparingly soluble in THF (and insoluble in many other common non-coordinating solvents), the temperature was then increased to encourage conversion. After 24 h at 80 °C, **123** was consumed, but the ratio C-7:C-6 was observed as 1:0.4 by ^{1}H NMR analysis (**Scheme 3.16**). The borylated products were not stable on silica and all other attempts to separate the two isomers were ineffective. Careful NMR assignments were made based on 2D-NMR experiments to identify peaks for each isomer. Interestingly, no borylation occurs in the absence of a methyl group at C-2.[67]



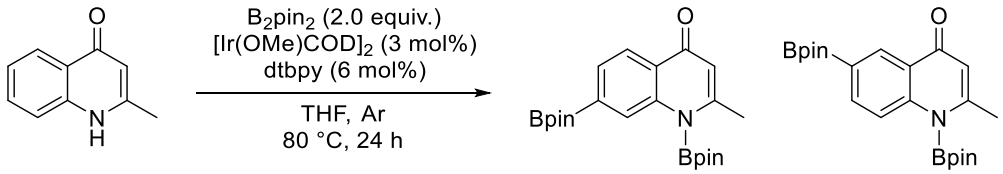
123 **124** **125**

r.t., 10 days 1:0.28

80 °C, 24 h 1:0.4

Scheme 3.16 Iridium-catalysed borylation of 1,2-dimethylquinolone **123** at r.t. and 80 °C. Ratios calculated from the characteristic peaks of each compound in the ^{1}H NMR spectrum of the crude reaction mixture.

Reaction of *N*-H quinolone **121** with one equivalent of B_2pin_2 at 80 °C furnished the predicted *N*-borylated compound; addition of excess B_2pin_2 again yielded a mixture of bis-borylated isomers, **126** and **127** (**Scheme 3.17**). The presence of a Bpin group at the nitrogen here caused a reduction in regioselectivity, with a ratio of 1:0.8 (C-7:C-6) observed by ^{1}H NMR analysis. The negative mesomeric effect of the Bpin likely withdraws electron density and increases the acidic character of the proton at C-6.[67]



121 **126** **127**

1:0.8

Scheme 3.17 Iridium-catalysed bis-borylation of 2-methylquinolone **121**.

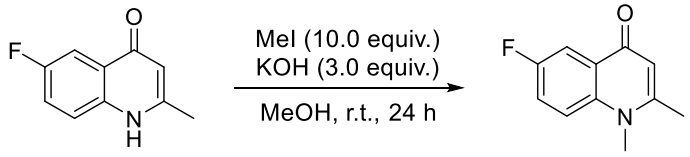
3.7. Borylation of 6-Fluoroquinolones

This project was then undertaken by the McGlacken group, all of the following sections describe work that was carried out in UCC.

During our first trials using the Ir/dtbpy system (**Scheme 3.16**) at UCC, we were unable to achieve the conversions observed by the researchers in Würzburg. Thus, a two-week visit was organised, and I was given the opportunity to work together with the Marder group to discern the cause of the irreproducibility. In Germany, we carried out the reactions under standard Schlenk techniques (outside of the glovebox) under both argon and nitrogen, giving identical results and conversion to the borylated products. In Germany, THF is dried using a solvent purification system (SPS), degassed with argon and stored over molecular sieves under argon. As is the case with many research labs, our group has moved away from using solvent stills on a regular basis for reasons of lab safety. Instead, where anhydrous solvent is necessary, we dry and store solvents (e.g. THF, toluene) over flame-dried 4 Å molecular sieves in Youngs flasks under nitrogen. This method has proved extremely effective and allows for large amounts of anhydrous solvent to be readily available with ppm water content.[88] If required, a portion would then be degassed by bubbling nitrogen into the solvent through a needle for several minutes. However, using THF that is dried/degassed in this manner, gave virtually no conversion to the desired products. Upon returning to UCC, freshly distilled THF was employed for the borylation of 1,2-dimethylquinolone **123**, allowing for the replication the original results and conversions reported by our collaborators. Going forward, THF was distilled from sodium/benzophenone under nitrogen and stored over molecular sieves under nitrogen. $[Ir(OMe)COD]_2$ was stored in a glovebox and was removed

portion-wise, as needed; the smaller portions were stored under a blanket of argon in the freezer to avoid degradation of the pre-catalyst.

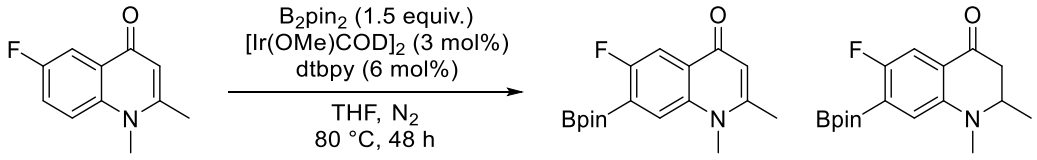
Considering the prevalence of the 6-fluoroquinolone scaffold in medicinal chemistry, and the apparent difficulties in selectively accessing the C-7 position *via* C-H functionalisation, we next decided to target 6-fluoroquinolones for borylation exclusively. For this, we synthesised 1,2-dimethyl-6-fluoroquinolone **129** by reaction of 6-fluoro-2-methyl quinolone **128** with methyl iodide (**Scheme 3.18**).



128 **129**, 40%

Scheme 3.18 *N*-methylation of 6-fluoro-2-methyl quinolone **128**.

We subjected 1,2-dimethyl-6-fluoroquinolone **129** to the Ir/dtbpy system with B_2pin_2 in THF at 80 °C. After 48 h, borylation had occurred at the desired site to yield C-7 borylated fluoroquinolone **130**, but simultaneous reduction of the C-2 to C-3 bond **131** was also observed in a ratio of 1:0.36, as determined by ^{1}H NMR analysis (**Scheme 3.19**). Efforts to isolate desired product **130** *via* column chromatography yielded only a mixture of starting material **129** and borylated, reduced product **131**.



129 **130** **131**

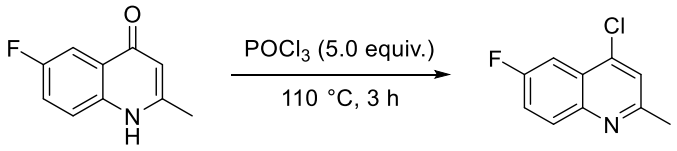
1:0.36

Scheme 3.19 Iridium-catalysed borylation of 1,2-dimethyl-6-fluoroquinolone **129**.

3.8. Alternative Strategy for Borylation of 6-Fluoroquinolones

Given the difficulties encountered, the lack of utility of the *N*-methyl group and the precedence for the borylation of quinolines, we considered using an alternative route to access the desired compounds. For this, we contemplated applying the reaction to a 4-substituted quinoline that would be converted back to the 4-quinolone form

subsequent to borylation or functionalisation. This approach would allow us to work with more soluble starting materials and, most importantly, we hoped, would negate the formation of unwanted by-products in the reaction. For this, we first installed chlorine at C-4 **132**, using the methods previously described in Chapter 2 from 6-fluoro-2-methylquinolinone **128** (**Scheme 3.20**).



128 **132**, 95%

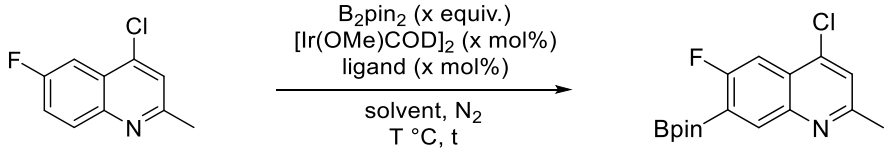
Scheme 3.20 Synthesis of 4-chloro-6-fluoro-2-methylquinoline **132**.

We also considered a handful of 'conventional' protecting groups; *tert*-butyloxycarbonyl (Boc), benzyl etc., but encountered site-selectivity issues in the attempted sythesis of *N*-protected substrates (a mixture of *N*-Me and *O*-Me isomers was also obtained in the syntheses of **123** and **129**).

Employing $[Ir(OMe)COD]_2$, dtbpy and B_2pin_2 in THF at 80 °C over 48 h, we were pleased to observe 45% yield of desired borylated product **133**, as calculated by ^1H NMR analysis, with no apparent starting material **132** remaining (**Table 3.1**, entry 1). With this promising result in hand, we sought to optimise the conditions for this transformation. Reducing the reaction time from 48 to 18 hours greatly improved the yield (entry 1). The next variable we looked at was the equivalents of B_2pin_2; using anything less than 1.1 equiv. of the borylating reagent did not give full conversion to product (entries 2–5). We then investigated an alternative ligand, 1,10-phenanthroline (phen), which, in contrast to dtbpy, required a larger excess of B_2pin_2 to garner full conversion to borylated product **133** (entries 6–8). This is likely due to the concurrent borylation of the ligand (*vide supra*).[66] Next, we looked at utilising more green solvents for this transformation. No conversion was observed in cyclopentyl methyl ether (CPME) (entry 9). Appreciable conversion was achieved using MTBE (80–95%), albeit with a small amount of starting material **132** still present in the crude reaction mixtures in all cases (entries 10–12). The loading of the iridium pre-catalyst/dtbpy ligand was lowered from 3.0/6.0 mol% to 1.5/3.0 mol% to give

100% conversion to and 93% yield of **133** by ^{1}H NMR analysis (entries 13–14). The volume of THF used in the system was then reduced from 3 mL to 1 mL (entries 15–17). The optimised conditions; 1.1 equiv. B_2pin_2, 1.5 mol% $[Ir(OMe)COD]_2$ and 3.0 mol% dtbpy in 1 mL THF, at 80 °C for 18 h, provided **133** in a 98% yield by NMR (entry 17). Three control experiments were then carried out to verify the parameters necessary for the reaction. No conversion to borylated product was observed in the absence of dtbpy (entry 18), and a trace amount of **133** was formed when undistilled, anhydrous THF was used in the system (entry 19). Finally, the reaction was performed under an atmosphere of air to give 86% yield of **133** by ^{1}H NMR analysis.

Table 3.1 Optimisation of the borylation of 4-chloro-6-fluoro-2-methylquinoline **132**.



132 **133**

entry	B_2pin_2 (equiv.)	Ir (mol%)	ligand (mol%)	solvent (mL)	temp. (°C)	time (h)	conv. (%)[a]	yield (%)[b]
1	1.5	3.0	dtbpy (6)	THF (3)	80	18–48	100	45-88
2	0.5	3.0	dtbpy (6)	THF (3)	80	24	69	61
3	0.75	3.0	dtbpy (6)	THF (3)	80	24	95	89
4	1.05	3.0	dtbpy (6)	THF (3)	80	24	95	89
5	1.1	3.0	dtbpy (6)	THF (3)	80	24	100	>99
6	1.5	3.0	phen (6)	THF (3)	80	24	100	91
7	0.5	3.0	phen (6)	THF (3)	80	24	45	–
8	1.1	3.0	phen (6)	THF (3)	80	24	80	–
9[c]	1.1	3.0	dtbpy (6)	CPME (3)	100	24	0	–
10	1.1	3.0	dtbpy (6)	MTBE (3)	60	24	80	70
11	1.1	1.5	dtbpy (3)	MTBE (1)	60	18	90	87
12	1.1	1.5	dtbpy (3)	MTBE (1)	60	24	95	95
13	1.1	2.0	dtbpy (4)	THF (3)	80	24	100	90
14	1.1	1.5	dtbpy (3)	THF (3)	80	24	100	93
15	1.1	3.0	dtbpy (6)	THF (1)	80	18	100	95
16	1.1	1.5	dtbpy (3)	THF (1)	80	12	100	90
17	**1.1**	**1.5**	**dtbpy (3)**	**THF (1)**	**80**	**18**	**100**	**98**
18	1.1	1.5	none	THF (1)	80	24	0	–
19[c]	1.1	1.5	dtbpy (3)	THF (1)	80	18	3	–
20[d]	1.1	1.5	dtbpy (3)	THF (1)	80	18	100	86

Reactions carried out on 0.2 mmol scale. [a]Conversions calculated from ^{1}H NMR analysis of the crude reaction mixture by ratio of peaks from **132** and **133**. [b]Yields calculated from the ^{1}H NMR spectrum of the crude reaction mixture using 1,3,5-trimethoxybenzene as the internal standard. [c]Solvent dried over flame-dried 4 Å molecular sieves (not distilled). [d]Reaction carried out in air.

3.9. Purification of Borylated Products

In our own experience, and that of others,[55,80] some borylated quinoline products do not withstand column chromatography on silica gel, but could be purified using column chromatography on neutral alumina, recrystallisation or Kugelrohr distillation. As part of our investigations, we also wished to optimise the purification of our borylated fluoroquinoline product **133**. As full conversion had been realised, the contaminants in our crude reaction mixture consisted of residual ligand, catalyst and B_2pin_2, along with the HBpin by-product (in some cases, the internal standard, 1,3,5-trimethoxybenzene (TMB) was also present). Generally, once the cooled mixture had been concentrated under reduced pressure, mass recovery was close to 100% and took the form of a red/brown solid. This colour is attributed to the iridium-catalyst.

Our initial purification endeavours utilised standard work-up procedures. After each manipulation, volatiles were removed under reduced pressure, any change in appearance was noted and then the mixture was again analysed by ^{1}H NMR spectroscopy to detect improvements in purity. We then dissolved the crude reaction mixture (**Table 3.1**, entry 17, 1.0 mmol scale) in DCM (12 mL) and split the solution into six equal parts, subjecting each part to a different method of purification as summarised below;

1. Filtered through a pipette of Celite with DCM: orange solid, no increase in purity was observed.
2. Filtered through a thin pad of neutral alumina using DCM, EtOAc and DCM/MeOH (9:1): pale yellow residue, a number of new species/degradation products detected.
3. Washed with H_2O (2 × 1 mL), dried over $MgSO_4$: orange solid, reduced the relative intensity of the B_2pin_2 peak.
4. Washed with sat. NH_4Cl (2 × 1 mL), dried over $MgSO_4$: orange solid, no change in purity.
5. Washed with 30% NH_4OH (2 × 1 mL), dried over $MgSO_4$: orange/red residue, slight degradation observed.
6. Treated with charcoal: beige solid, impurities still present.

As none of the methods attempted above provided analytically pure samples of **133**, we then turned our attention to the use of Kugelrohr distillation. On our first attempt (**Table 3.1**, entry 17, 0.3 mmol scale), a white solid was collected after 30 min at 125 °C (~0.5 mbar) which contained the residual B_2pin_2, HBpin by-product and the internal standard (**Figure 3.6**).

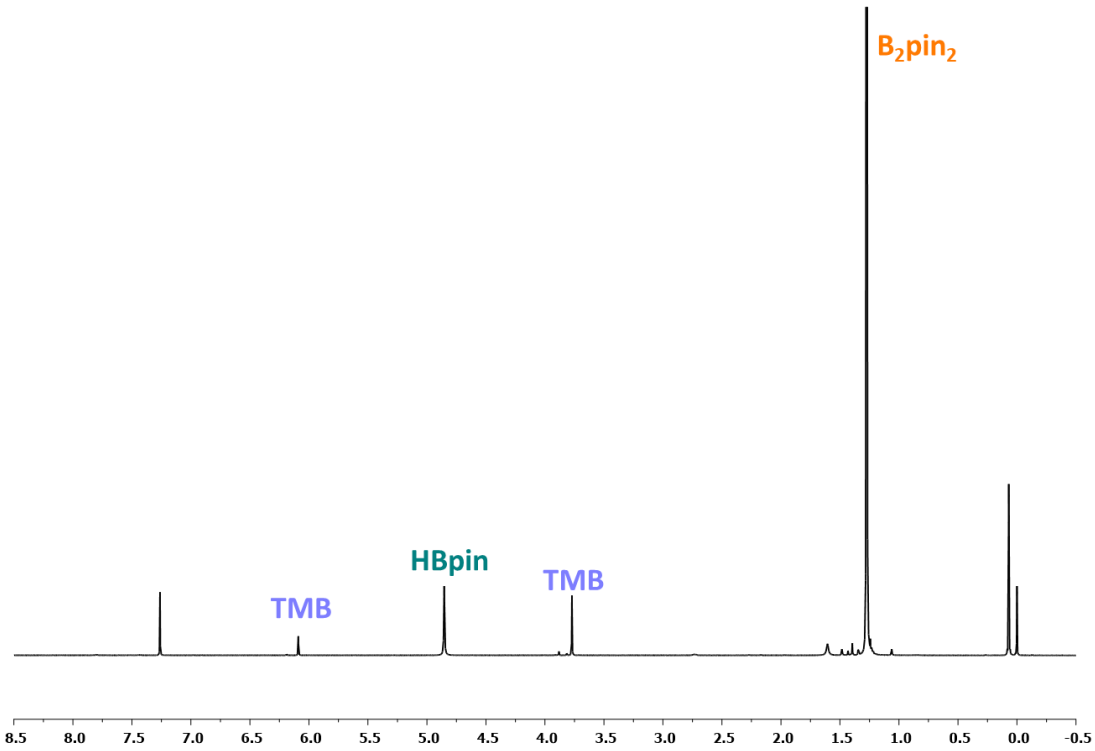


Figure 3.6 ^{1}H NMR spectrum with magnified region of first fraction from Kugelrohr distillation at 125 °C (~0.5 mbar). Spectrum recorded at 300 MHz in $CDCl_3$ at 300 K.

Heating of the remaining sample to 300°C (~0.5 mbar) did not appear to distil any further products into the collection bulb. Upon dismantling the apparatus, a bright red residue remained, along with a crystalline white solid at the neck of the load flask. Samples of both were analysed and identified as the borylated product (**Figure 3.7**).

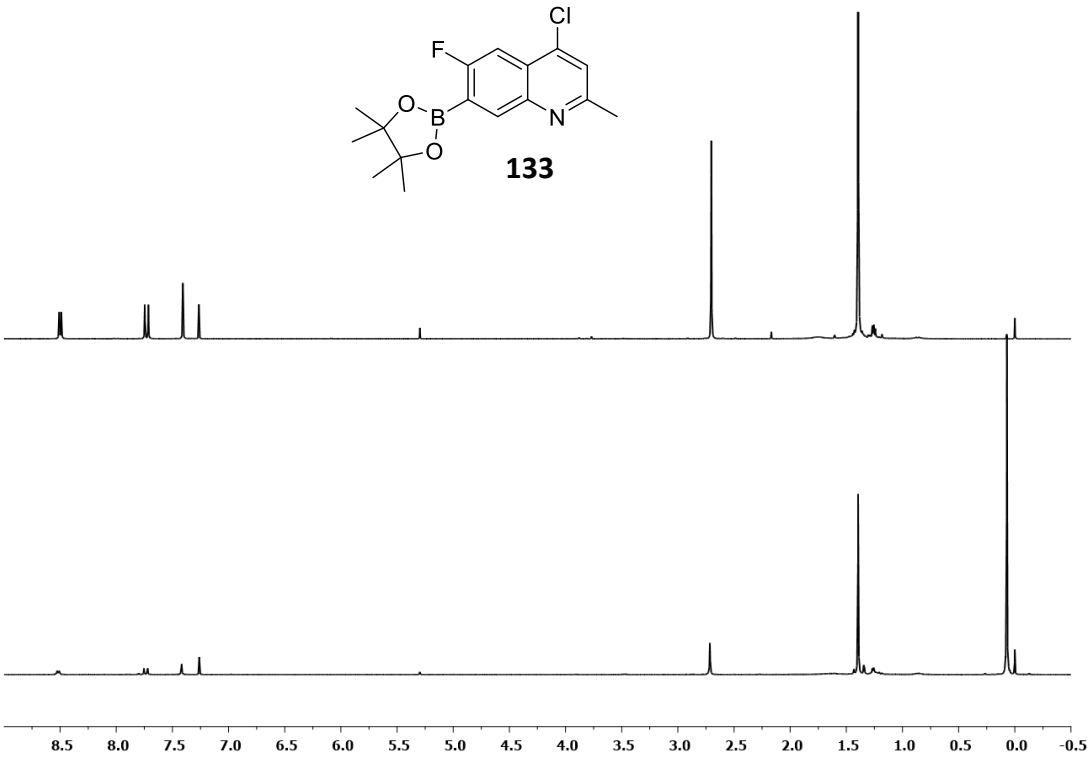


Figure 3.7 ^{1}H NMR spectra of **133**; [Bottom] white solid and [Top] red residue from Kugelrohr distillation at 300 °C (~0.5 mbar). Spectra recorded at 300 MHz in CDCl3 at 300 K.

As the distillation set-up was proving difficult, we tried to purify the mixture *via* recrystallisation from a number of different common laboratory solvents; EtOAc, Et_2O, MeOH, ACN and hexanes, as well as mixtures of those listed. The crude reaction mixture was relatively soluble in most of the solvents close to room temperature. Although solid did crystallise in some cases, residual HBpin and B_2pin_2 proved problematic to remove. To negate this issue, we looked at ways to remove the boronate contaminants prior to recrystallisation – for this, we simply diluted the crude reaction mixture (**Table 3.1**, entry 17, 2.0 mmol scale) in ~50 mL MeOH and concentrated it under reduced pressure, with the water bath at 60 °C. This manipulation forms $B(OMe)_3$ and pinacol, both of which could be fully removed by rotary evaporation from MeOH (**Figure 3.8**).[89]

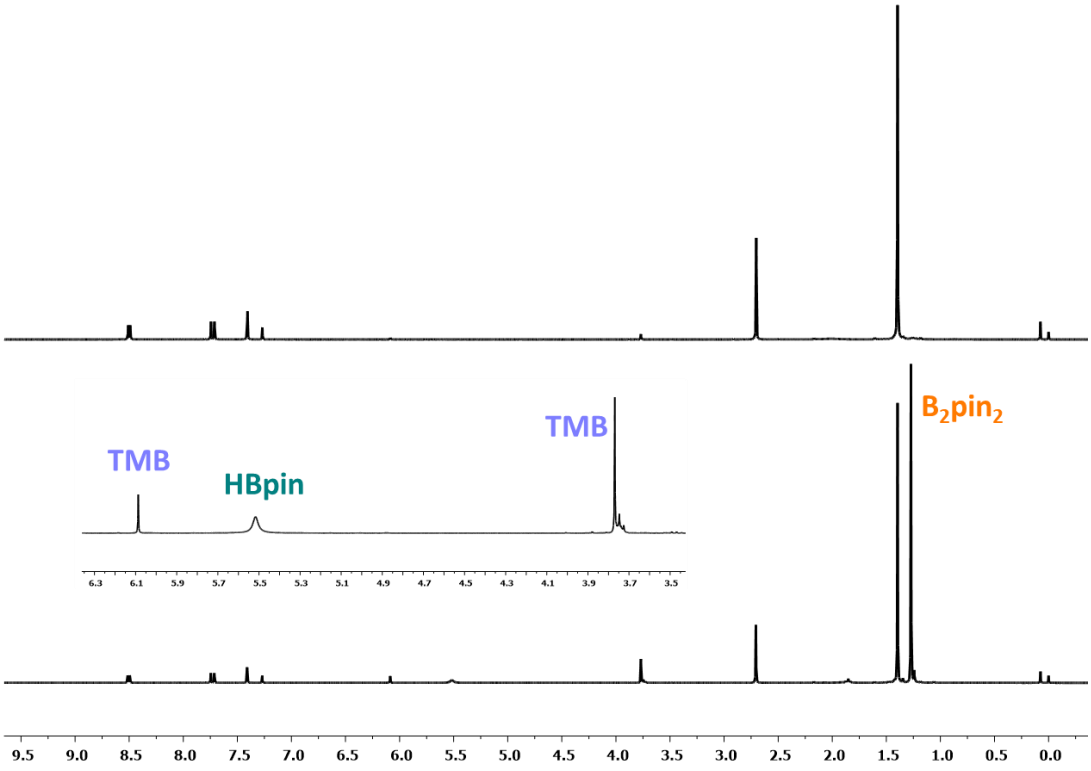


Figure 3.8 ^{1}H NMR spectra of **133**; [Bottom] crude reaction mixture and [Top] after evaporation of MeOH at 60 °C. Spectra recorded at 300 MHz in $CDCl_3$ at 300 K.

Recrystallisation of the resulting orange solid from hot MeOH gave analytically pure borylated product **133** as a white solid in 66% yield (**Figure 3.9**).

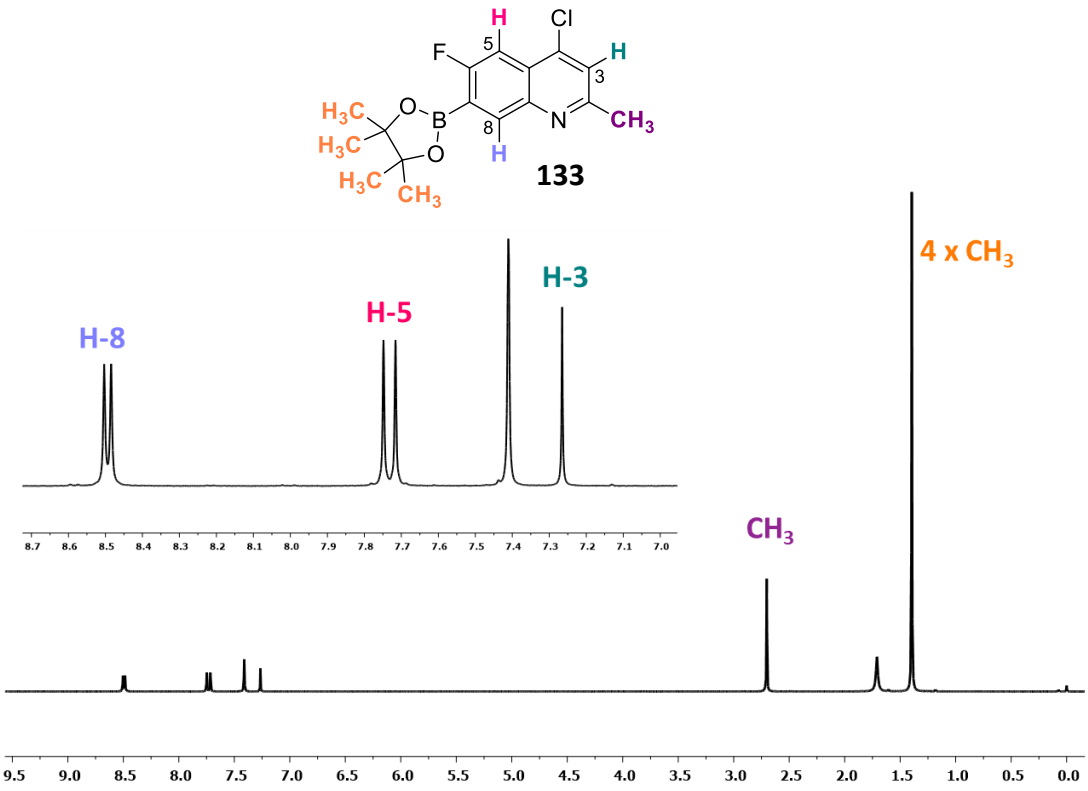


Figure 3.9 ^{1}H NMR spectrum of **133** recorded at 300 MHz in $CDCl_3$ at 300 K.

The C-7 selectivity of the C–H borylation was confirmed by X-ray diffraction analysis of single crystals of **133**, which were obtained *via* vapour diffusion (**Figure 3.10**). The crystals were grown by our colleagues in Germany from a saturated solution of DCM in Et_2O.

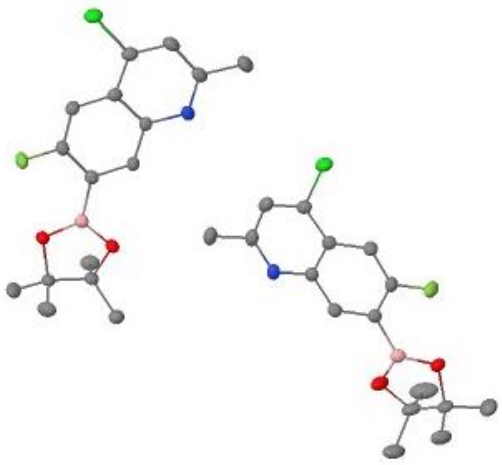
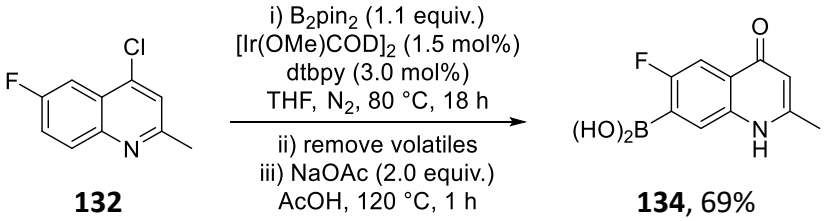


Figure 3.10 The solid-state molecular structure of **133** determined by single-crystal X-ray diffraction at 100 K. All ellipsoids are drawn at the 50% probability level. H atoms are omitted for clarity.

Finally, borylated 6-fluoroquinolone **134** was revealed through *in situ* acid hydrolysis of quinoline intermediate **133** in good yield (**Scheme 3.21**).[90] Concomitant hydrolysis of the boronate ester to the boronic acid was also observed.



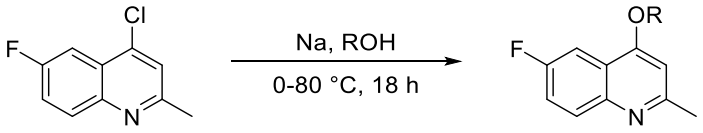
132 **134**, 69%

Scheme 3.21 Borylation and acid hydrolysis of **132**, for the construction of borylated fluoroquinolone scaffold **134**.

3.10. Synthesis of Quinoline Starting Materials

3.10.1 Alternative Groups at the C-4 Position

With these optimised conditions in hand, we looked to expand the scope of our borylation protocol to other 4-substituted 6-fluoroquinolones, with the critical quinoline to quinolone transformation in mind. Firstly, we looked at functionalising the oxygen with simple methyl and ethyl groups. Reaction of **132** with freshly prepared sodium methoxide and ethoxide gave the desired 4-alkoxy quinolines **135** and **136** in excellent yields (**Scheme 3.22**).

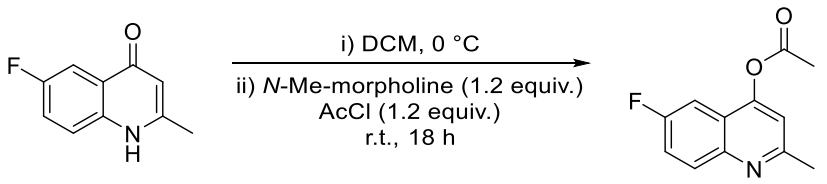


132

135, R = Me 97%
136, R = Et 89%

Scheme 3.22 Synthesis of 4-alkoxy-6-fluoro-2-methylquinolines **135** and **136**.

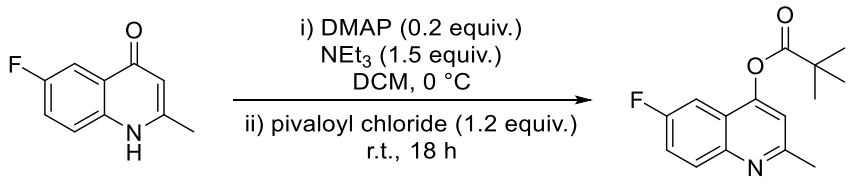
Next, we looked at using carboxylate groups at the C-4 position. An acetyl group was installed by reacting **128** with *N*-methyl morpholine and acetyl chloride in DCM to form 6-fluoro-2-methylquinolin-4-yl acetate **137** in good yield (**Scheme 3.23**).[91]



128 **137**, 82%

Scheme 3.23 Synthesis of 6-fluoro-2-methylquinolin-4-yl acetate **137**.

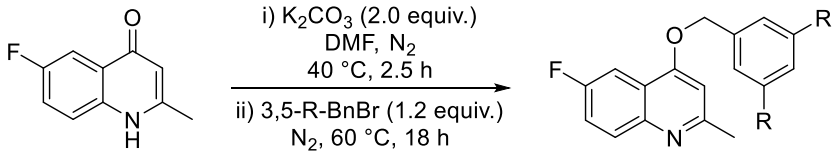
Pivaloyl-protected 6-fluoro-2-methylquinoline **138** was constructed by reacting pivaloyl chloride with **128**, employing different conditions to those detailed for the acetyl transformation above. Quinolone **128**, DMAP and NEt_3 were suspended in DCM and cooled to 0 °C. Pivaloyl chloride was added dropwise, and the resulting suspension was allowed to stir at r.t. overnight to furnish 6-fluoro-2-methylquinolin-4-yl pivalate **138** in 93% yield (**Scheme 3.24**).[92]



128 **138**, 93%

Scheme 3.24 Synthesis of 6-fluoro-2-methylquinolin-4-yl pivalate **138**.

We then installed a benzyl protecting group on the C-4-OH position of fluoroquinolone **128**. Previous studies had shown that a heterocyclic scaffold will borylate almost exclusively in systems where multiple aromatic rings are present.[66] However, we did not want to introduce any other possible sites for borylation, and therefore selected two sterically hindered benzyl bromides to furnish this particular protecting group. 6-Fluoro-2-methylquinolinone **128** was first stirred with K_2CO_3 at 40 °C. After 2.5 h, 3,5-dimethyl- or 3,5-di-*tert*-butyl-benzyl bromide was added to the mixture. The temperature was increased to 40 °C overnight to form 4-((3,5-dimethylbenzyl)oxy)-6-fluoro-2-methylquinoline **139** or 4-((3,5-di-*tert*-butyl-benzyl)-oxy)-6-fluoro-2-methylquinoline **140** respectively in very good yields (**Scheme 3.25**).[93]



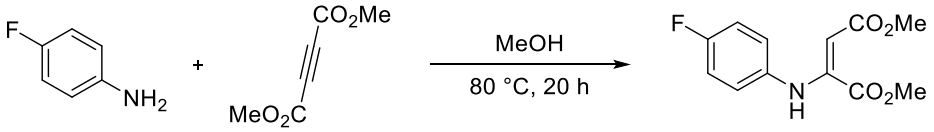
128

139, R = Me 84%
140, R = *t*-Bu 85%

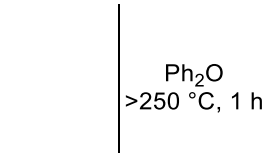
Scheme 3.25 Synthesis of 4-benzyl-6-fluoro-2-methylquinoline derivatives **139** and **140**.

3.10.2 Alternative Groups at the C-2 and C-3 positions

Although there are a small number of biologically active quinolones with a methyl group at C-2,[94-96] we were aware of the lack of utility of this group in the context of fluoroquinolone antibiotics, where hydrogen is the optimum substituent at C-2 (*vide supra*). To this end, we synthesised a C-2 quinolone carboxylate. There is literature precedence for the cleavage of this moiety through protodecarboxylation,[97-99] and we wished to harness this methodology for our borylated quinolines. For this starting material, quinolone precursor **142** was synthesised over two steps. Firstly, 4-fluoroaniline and dimethyl acetylenedicarboxylate were reacted to form intermediate **141**, which consequently underwent thermal cyclisation to form quinolone **142** in 66% yield (**Scheme 3.26**).



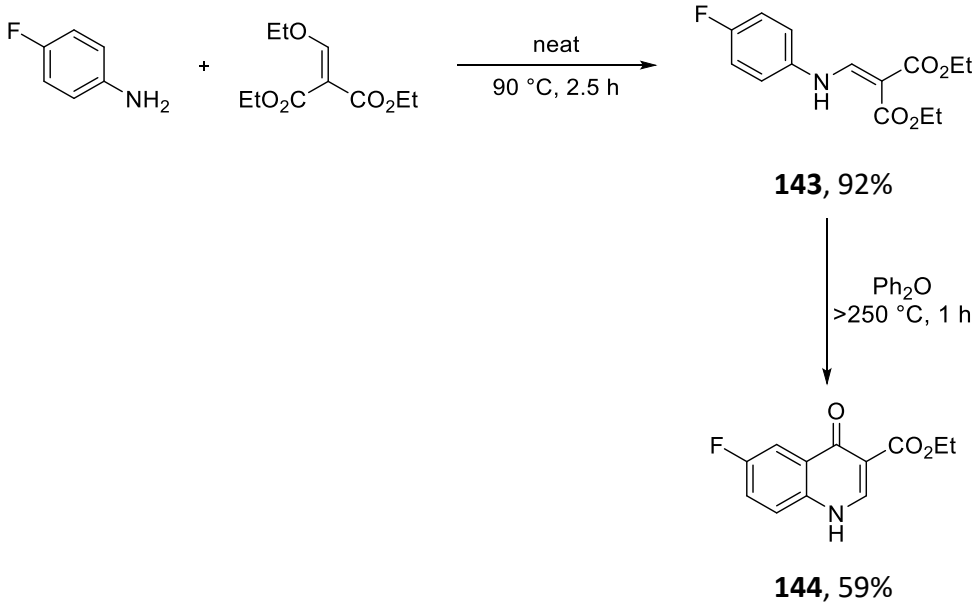
141, 92%



142, 66%

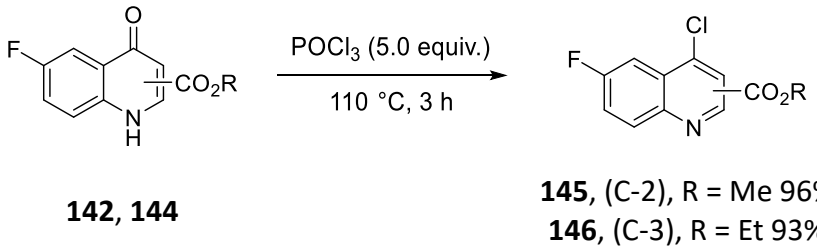
Scheme 3.26 Synthesis of methyl 6-fluoro-4-oxo-1,4-dihydroquinoline-2-carboxylate **142**.

Another key feature in fluoroquinolone antibiotics is the presence of a carboxylic acid group at the C-3 position. We were keen to include this motif (or a protected variant) to demonstrate the potential for our protocol to be employed in the late-stage modification of fluoroquinolone drug targets. Similar to the above, the C-3 quinolone carboxylate **144** was constructed in moderate yield through the cyclisation of unsaturated intermediate **143**, which was assembled in the reaction of 4-fluoroaniline with diethyl ethoxymethylenemalonate (**Scheme 3.27**).



Scheme 3.27 Synthesis of ethyl 6-fluoro-4-oxo-1,4-dihydroquinoline-3-carboxylate **144**.

Chlorination of quinolone carboxylates **142** and **144** using $POCl_3$ furnished desired C-2/C-3 quinoline carboxylate substrates **145** and **146** in excellent yields (**Scheme 3.28**).

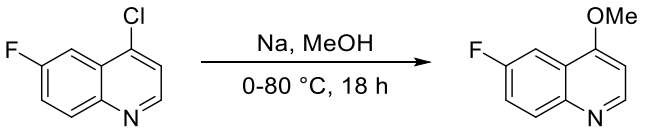


142, **144**

145, (C-2), R = Me 96%
146, (C-3), R = Et 93%

Scheme 3.28 Synthesis of 4-chloro-6-fluoro-quinoline carboxylates **145** and **146**.

Finally, 6-fluoro-4-methoxyquinoline **148** was synthesised from commercially available 4-chloro-6-fluoroquinoline **147** in 95% yield (**Scheme 3.29**).

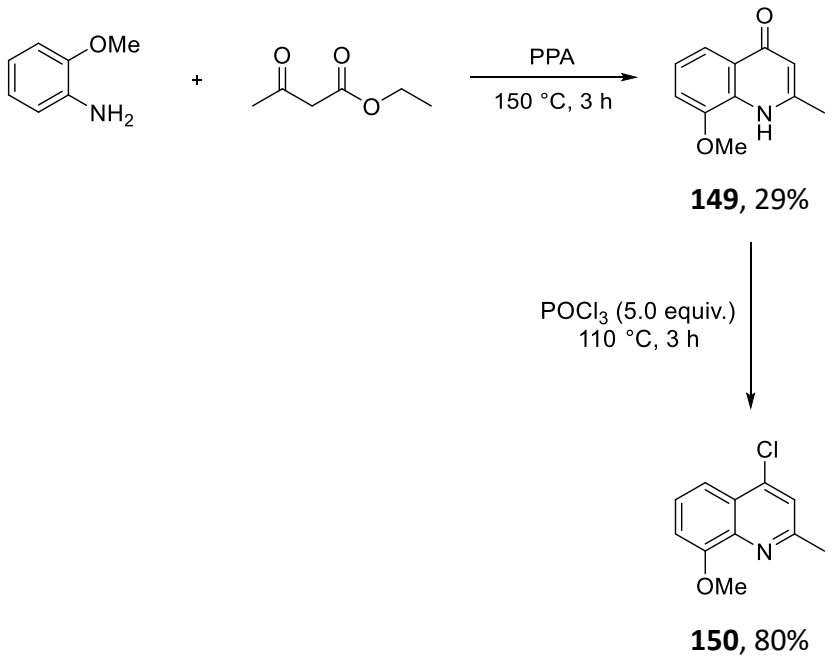


147 **148**, 95%

Scheme 3.29 Synthesis of 6-fluoro-4-methoxyquinoline **148**.

3.10.3 Sterically Encumbered Starting Material

As we had already established, substitution with a fluorine at C-6 serves to both block this competitive site for borylation, and to act as a critical functional group in the construction of antibiotic frameworks. We knew on the basis of steric and electronic factors, that C-7 would be the most likely position for borylation; and wished to test the influence of further steric encumberment proximal to the desired site. For this, we synthesised 2-methyl-8-methoxyquinolone **149** through the acid-mediated, thermal cyclisation of *o*-anisidine and ethyl acetoacetate in quite low yield. Subsequent chlorination gave desired quinoline substrate **150** in 80% yield (**Scheme 3.30**).



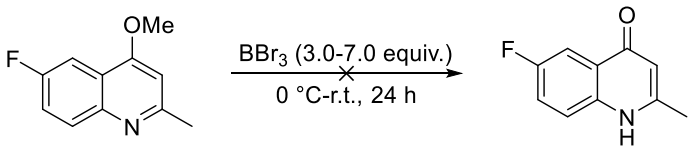
Scheme 3.30 Synthesis of sterically encumbered quinoline **150**.

3.11. Conversion of Substituted 4-Quinolines to 4-Quinolones

As the main goal of this transformation was to reveal the 4-quinolone moiety after borylation, we looked to identify suitable conditions for the conversion of our quinoline substrates to the corresponding 4-quinolones. These conditions were ascertained prior to borylation, to avoid wasting the iridium pre-catalyst and other reagents. Of course, the functionalised compounds could react differently to those with hydrogen at C-7, but we wanted to at least establish precedence for the conversion.

3.11.1 Dealkylation Strategies

Our first goal was to reveal the quinolone moiety from the alkoxy derivatives **135** and **136**. Initially, we tried removing the methyl group of 6-fluoro-4-methoxy-2-methylquinoline using of BBr_3 in DCM, a ubiquitous approach for this transformation.[100] Much to our surprise, and even employing various equivalents of BBr_3, no conversion to quinolone **128** was observed (**Scheme 3.31**). Although the demethylation of 4-quinolines and pyridines has been reported previously,[101-103] it is possible the fluorine substituent has a destabilising effect on the cation formed on the methoxy group, resulting in an unstable intermediate and thus inhibiting progress of reaction.

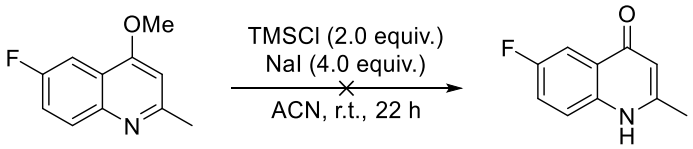


135 **128**

Scheme 3.31 Attempted demethylation of 4-methoxy quinoline **135** using BBr_3.

Another, less conventional protocol that had been utilised previously in the group for the demethylation of pyrones and coumarins was also trialled.[104] This system involved the room temperature reaction of **135** with TMS iodide, formed *in situ* from the combination of TMS chloride and sodium iodide in ACN (**Scheme 3.32**).[105] While the BBr_3 approach returned just quinoline starting material, ^{1}H NMR analysis of the

reaction mixture after aqueous work-up here, showed the presence of multiple species, none of which appeared to be the desired quinolone **128**.

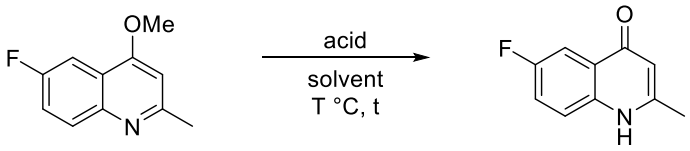


135 **128**

Scheme 3.32 Attempted demethylation of 6-fluoro-4-methoxy-2-methylquinoline **135** using TMS iodide.

As we had garnered some success with acid hydrolysis in the case of **133**, we sought to apply a similar procedure to the alkoxy substrates using reported methods (**Table 3.2**). Reaction of **135** with trifluoroacetic acid (TFA) in DCM at 50 °C gave no conversion to quinolone **128** (entry 1).[106] Various concentrations of HCl, either neat or with solvent, were employed for this transformation at 110 °C. No combination of these showed evidence of reaction by ^{1}H NMR analysis (entries 2–6).[107-109] 4-Methoxyquinoline **135** was stirred with 48% HBr in AcOH at 90 °C to give 42% conversion to the demethylated product **128** after 68 h (entry 7).[95] This was the first instance where any demethylation had occurred, and so to encourage conversion, the temperature was increased to 150 °C (entry 8). The reaction was monitored by TLC analysis and after 6 h, all starting material was consumed. The mixture was cooled, neutralised over ice using 6 M NaOH and extracted using DCM/*i*-PrOH (9:1) to give 6-fluoro-2-methylquinolone **128** in 70% isolated yield.

Table 3.2 Optimisation of the demethylation of 6-fluoro-4-methoxy-2-methylquinoline **135**.



135 **128**

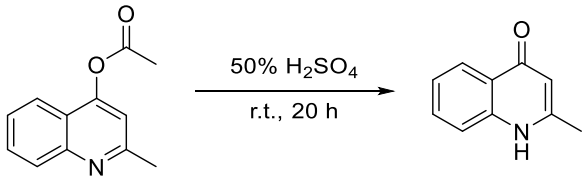
entry	acid	solvent	temp. (°C)	time (h)	conv. (%)[a]
1	TFA	DCM	50	6	0
2	10% HCl	neat	110	18	0
3	4 M HCl	neat	110	18	0
4	12 M HCl	MeOH	110	6	0
5	12 M HCl	ACN	110	14	0
6	12 M HCl	AcOH	110	14	0
7	48% HBr	AcOH	90	68	42
8	**48% HBr**	**AcOH**	**90**	**24**	**100 (70)**

Reactions carried out on 0.3 mmol scale. [a]Conversions calculated from ^{1}H NMR analysis of the crude reaction mixture by ratio of peaks from **135** and **128**. Isolated yield in parentheses.

The optimised conditions described above were then applied to 4-ethoxy-6-fluoro-2-methylquinoline **136**, but no evidence of de-ethylation was noted, and it was decided to pursue only the 4-methoxy derivative for borylation.

3.11.2 Removal of Acetyl Groups

The quinolone motif was revealed from 6-fluoro-2-methylquinolin-4-yl acetate **151** *via* a simple acid hydrolysis step, albeit in low yield (**Scheme 3.33**).[110] It was also noted that acetyl-protected quinolines **137** and **151** decomposed over a period of days to give quinolone **128** or **121** and AcOH – we were unsure about the stability of these substrates under the conditions for borylation, and did not engage in further optimisation for the cleavage of this group.



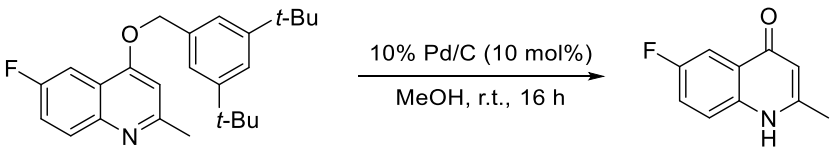
151 **121**, 30%

Scheme 3.33 Removal of acetyl group from compound **151** using H_2SO_4.

A number of reported acid- and base-mediated deprotection protocols were applied to pivaloyl derivative **138**.[109,111-113] Some deprotection was observed but none of these procedures afforded the quinolone scaffold in appreciable yield or sufficient purity.

3.11.3 Debenzylation Strategies

For the debenzylation of protected quinoline **140**, we utilised well-established reductive benzylation protocols (**Scheme 3.34**). Compound **140** was reacted with 10% palladium on carbon in MeOH under a balloon of hydrogen for 16 h, then diluted with DCM, filtered through Celite and concentrated under reduced pressure. Generally, the by-product of reductive debenzylation (toluene) can be removed by rotary evaporation; 3,5-di-*tert*-butyltoluene however, has a boiling point of 244 °C.[114] However, trituration of the crude reaction mixture from Et_2O allowed for the isolation of quinolone **128** in 88% yield.



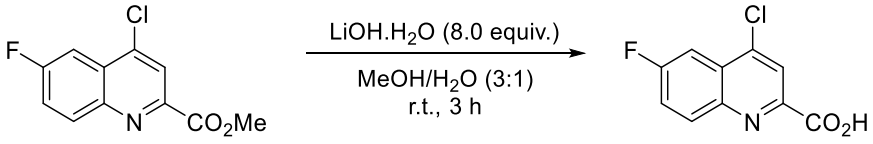
140 **128**, 88%

Scheme 3.34 Debenzylation of compound **140**.

3.11.4 Other Functional Deprotections

As we had determined routes for the conversion of our 4-substituted fluoroquinolines to the corresponding fluoroquinolones, we then turned our attention to the other functionalities on the core structure of our substrates. As already mentioned, we wished to explore the possibility of performing protodecarboxylation on the C-2 carboxylate compound **145**. The C-2 carboxylic acid

scaffold **152**, was constructed in 88% yield from the reaction of **145** with LiOH in aqueous MeOH (**Scheme 3.35**).



145 **152**, 81%

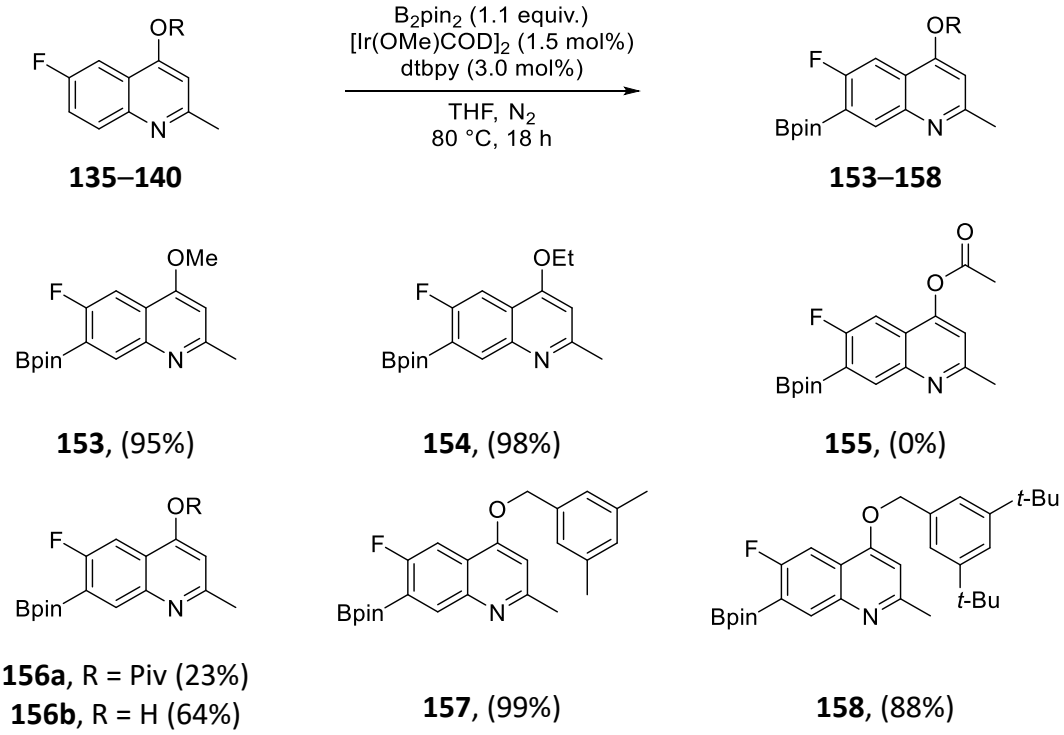
Scheme 3.35 Formation of 4-chloro-6-fluoroquinoline-2-carboxylic acid **152**.

Again, several protocols were utilised in an effort to decarboxylate **152**. Neither silver-catalysed[97-99] nor thermal[115] decarboxylation strategies gave any evidence of this transformation upon analysis of the crude reaction mixtures.

3.12. Borylation of 4-Substituted-Quinolines

3.12.1 Alternative Groups at the C-4 Position

We then subjected our library of quinoline substrates to our optimised conditions for borylation. Firstly, we looked at the application of our methodology to our various 4-substituted 6-fluoro-2-methylquinolines, furnishing the C-7-borylated quinolines in excellent yields by NMR (**Scheme 3.36**). Our alkoxy and benzyloxy substrates **135**, **136**, **139** and **140** were pleasingly all converted to borylated products **153**, **154**, **157** and **158** over 18 h at 80 °C. Full conversion from the 4-substituted quinolines was observed, with the exception of **153**, where roughly 5% of starting material **135** remained. Acetyl-protected quinoline **137** remained inert to our borylation protocol, and failed to give compound **155**. ^{1}H NMR analysis showed only quinoline **137** and deprotected quinolone **128** in a ratio of 1:0.5.



Scheme 3.36 Borylation of 4-substituted 6-fluoro-2-methylquinolines. Reactions carried out on 0.2 mmol scale. Yields in parentheses calculated from the ^{1}H NMR spectrum of the crude reaction mixture using 1,3,5-trimethoxybenzene as the internal standard.

An interesting result was obtained in the borylation of pivaloyl-protected quinoline **138**. Analysis of the crude reaction mixture indicated the presence of two borylated species in a ratio of 1:0.35, as well as a small amount of starting material **138** and quinolone **128** (~10% each by comparison of peaks from all four species, **Figure 3.11**). Borylated pivaloyl quinoline **156a** was distinguished as the minor product of the system, giving a 23% yield by NMR. The major product detected here was identified as deprotected, borylated quinolone species **156b**. It is unclear whether the deprotection and borylation steps occur simultaneously or in tandem, especially given the presence of quinolone **128**, albeit in a small amount. Upon repetition of this experiment, some reproducibility issues were encountered, whereby **156a** was appearing as the main product by ^{1}H NMR analysis. Further studies and optimisation would be required to deduce the order in which this reaction occurs, and to ultimately promote the borylation and *in situ* deprotection of this species.

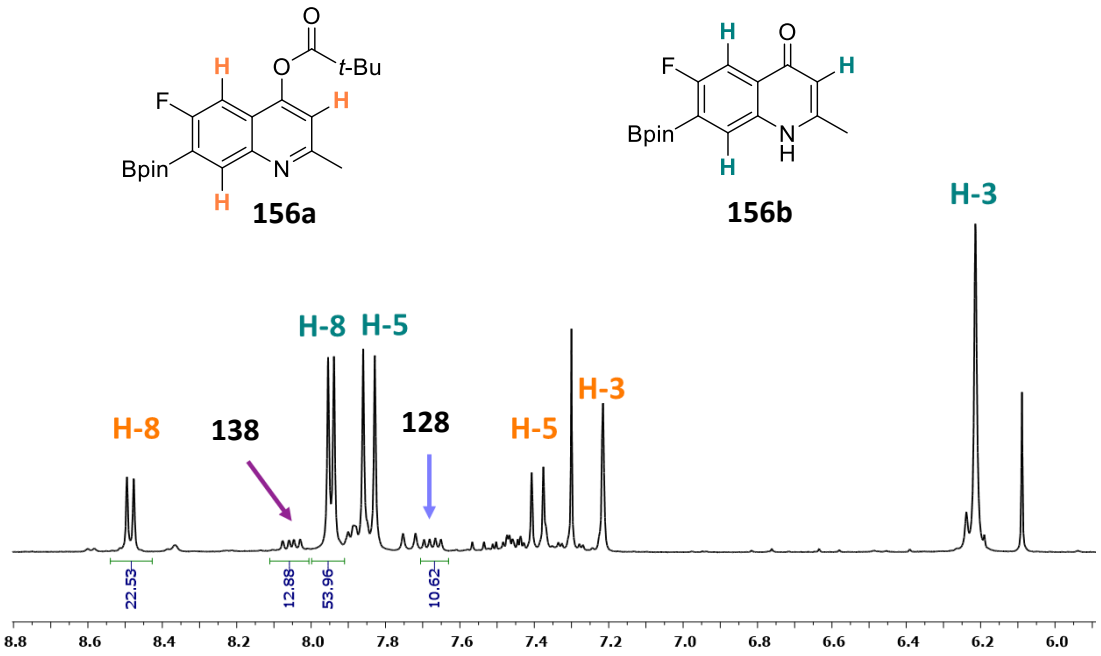
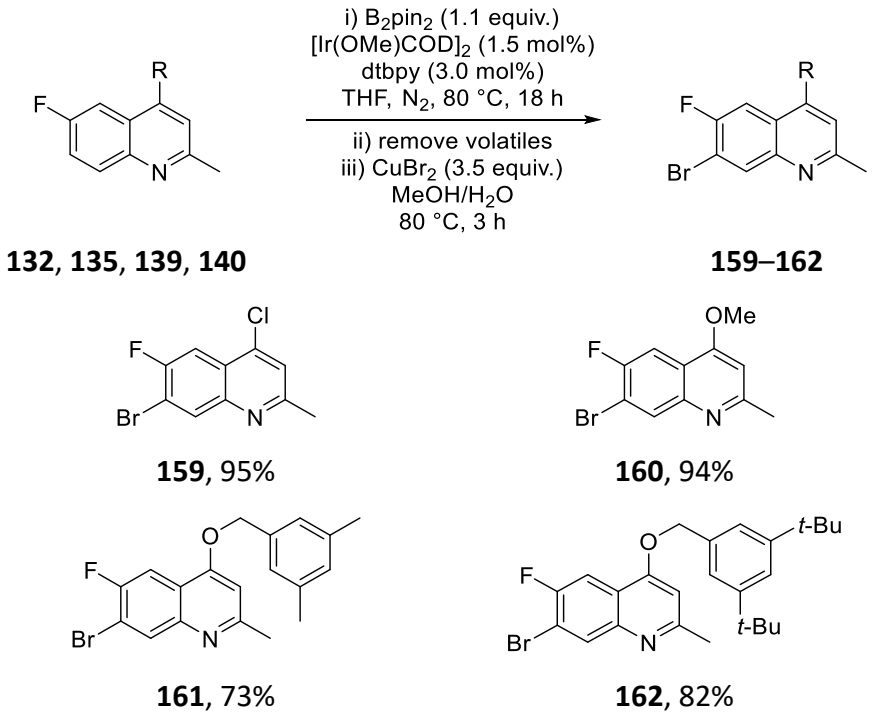


Figure 3.11 Excerpt from ^{1}H NMR spectrum for the borylation of **138**. Peaks for **156a** and **156b** are assigned in orange and green respectively, with the characteristic peaks of **128** and **138** also highlighted. Spectrum recorded at 300 MHz in $CDCl_3$ at 300 K.

Purification of borylated substrates (**153**–**158**) was not as straightforward as the recrystallisation of **133**. Other solvent systems/purification tactics were assessed, but, for ease of access, it was decided to convert the borylated products directly to the corresponding brominated derivatives for isolation and characterisation. This transformation could conveniently be carried out from the crude reaction mixtures of the borylation step using $CuBr_2$ in aqueous MeOH.[116-117] This approach furnished the C-7-bromoquinolines **159**–**162** in high yields over two steps (**Scheme 3.37**).



132, **135**, **139**, **140** **159**–**162**

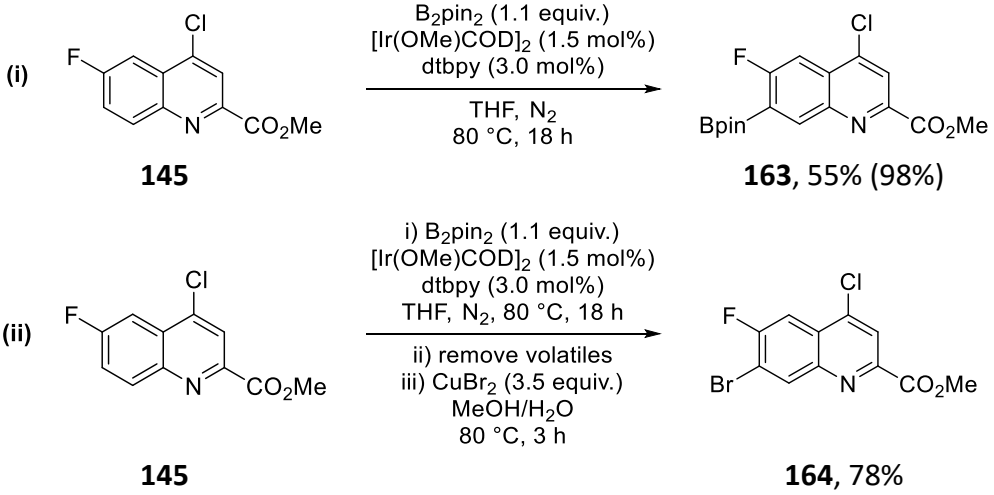
159, 95% **160**, 94%

161, 73% **162**, 82%

Scheme 3.37 Telescoped borylation and bromination of 4-substituted 6-fluoro-2-methylquinolines at the C-7 position.

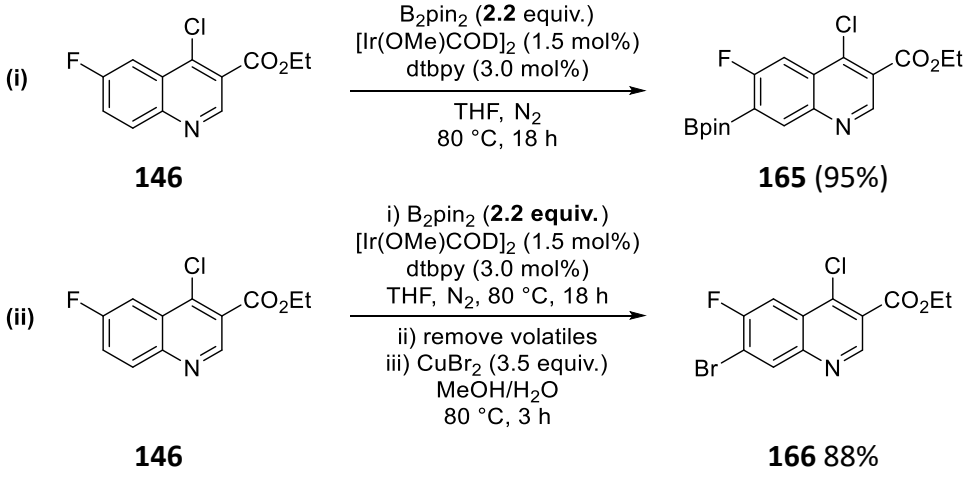
3.12.2 Alternative Groups at the C-2 and C-3 positions

Even though our decarboxylation attempts had not been efficacious, we endeavoured to borylate **145** as a demonstration of functional group tolerance (**Scheme 3.38 (i)**). In this case, analytically pure borylated product **163** was isolated by recrystallisation from MeOH in 55% yield. Substrate **145** was also subjected to the telescoped bromination process for the formation of C-7 brominated quinoline **164** in very good yield (**Scheme 3.38 (ii)**).



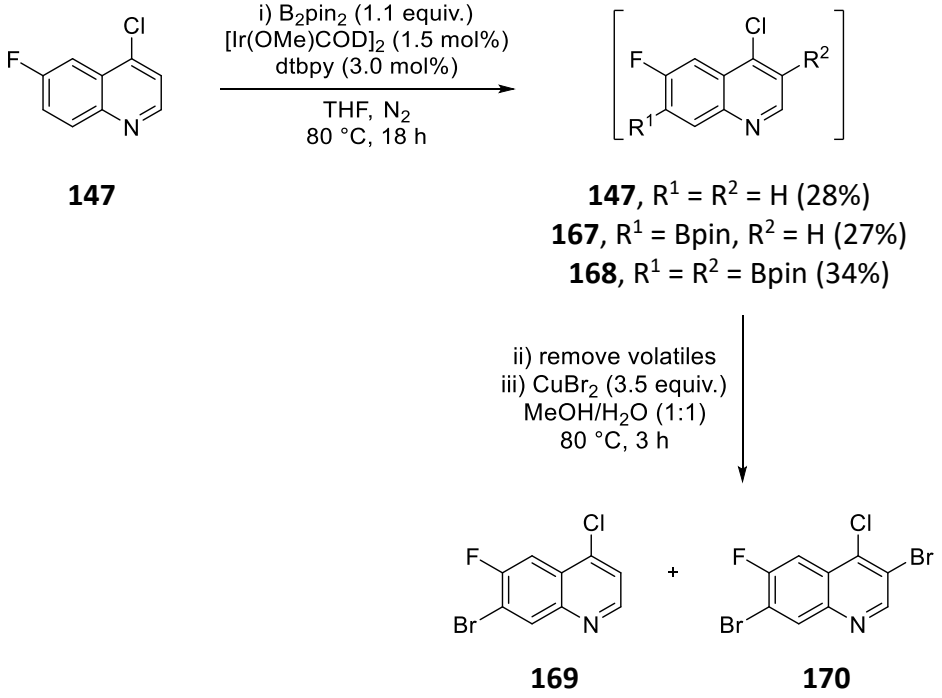
Scheme 3.38 (i) Borylation and **(ii)** telescoped borylation and bromination of quinoline 2-carboxylate **145**. Yield in parentheses calculated from the ^{1}H NMR spectrum of the crude reaction mixture using 1,3,5-trimethoxybenzene as the internal standard.

In the context of mapping onto the core antibiotic fluoroquinolone structure, initial attempts using our optimised procedure with **146**, gave only trace amounts of borylated product **165**. However, using 2.2 equiv. of B_2pin_2 allowed the borylation to **165** to occur in 95% yield by NMR (**Scheme 3.39 (i)**), and subsequent bromination gave **166** in very good yield (**Scheme 3.39 (ii)**).



Scheme 3.39 (i) Borylation and **(ii)** telescoped borylation and bromination of key antibiotic precursor **146**. Yield for **166** is isolated. Yield in parentheses calculated from the ^{1}H NMR spectrum of the crude reaction mixture using 1,3,5-trimethoxybenzene as the internal standard.

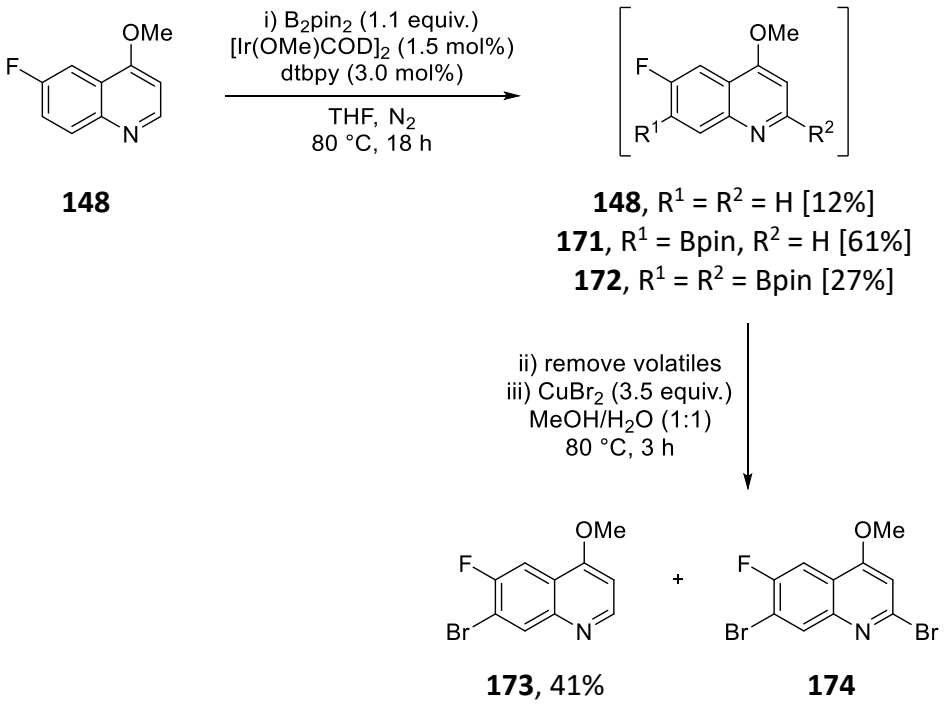
Finally, the borylations of 4-chloro-6-fluoroquinoline **147** and 6-fluoro-4-methoxyquinoline **148**, as expected, provided mixtures of isomers. These mixtures were again subjected to bromination for characterisation purposes. In the case of 4-chloro-6-fluoroquinoline **147** the borylation step did not fully consume **147**, but did yield mono- and a bis-borylated compounds **167** and **168**. Upon bromination, the 7-bromo- and 3,7-dibromo-fluoroquinolines **169** and **170** were formed and characterised (**Scheme 3.40**). Exclusion of a group at C-2 makes the C-3 position sterically available for functionalisation, albeit for the second C-H borylation in the sequence.



Scheme 3.40 Borylation and bromination of 4-chloro-6-fluoroquinoline **147**. Yields in parentheses calculated from the ^{1}H NMR spectrum of the crude reaction mixture using 1,3,5-trimethoxybenzene as the internal standard. Compounds **169** and **170** were not sufficiently pure for calculation of yield.

Similarly to **147**, borylation of **148** provided two functionalised species, **171** and **172**, along with a small portion of residual starting material **148**. Bromination in this case allowed for the isolation of 7-bromo-6-fluoro-4-methoxyquinoline **173** in 41% yield. The other compound produced using this protocol was identified as 2,7-dibromo-6-fluoroquinoline **174** (**Scheme 3.41**). Again, C-7 was the preferred and initial site for

borylation, with the C-2 position this time favoured for the second borylation. Although *meta*-directing electronic effects are at play, it is more likely this selectivity is induced by steric encumberment of the C-3 position by the *o*-methoxy substituent.[65]



148

148, $R^1 = R^2 = H$ [12%]
171, R^1 = Bpin, $R^2 = H$ [61%]
172, $R^1 = R^2$ = Bpin [27%]

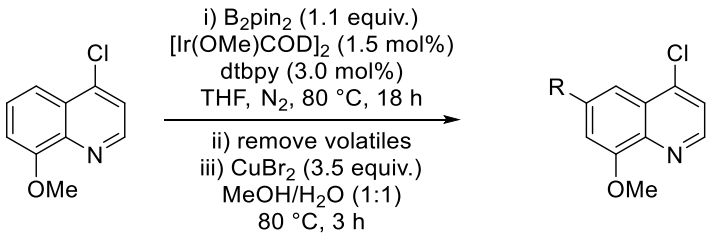
173, 41%

174

Scheme 3.41 Borylation and bromination of 4-chloro-6-fluoroquinoline **148**. Percentages in square brackets represent approximate conversions, as calculated from the ^{1}H NMR spectrum of the crude reaction mixture. Yield for **173** is isolated. Compound **174** was not sufficiently pure for calculation of yield.

3.12.3 Sterically Encumbered Starting Material

Finally, our borylation protocol was applied to compound **150**, this time functionalising C-6 exclusively, to give complete conversion to compound **175**. Subsequent bromination furnished 6-bromo-4-chloro-8-methoxy-2-methylquinoline **176** in 72% yield (**Scheme 3.42**). Analogous selectivity to that noted above (**Scheme 3.41**) was observed for this system, where the steric bulk of the C-8-methoxy group inhibits C-H activation at the C-7 position, thus directing C-H borylation to the next available site, C-6.



150

175, R = Bpin [100%]
176, R = Br 72%

Scheme 3.42 Borylation and bromination of 4-chloro-8-methoxy-2-methylquinoline **150**. Yield for **176** is isolated. Percentage in square brackets represents conversion, as calculated from the ^{1}H NMR spectrum of the crude reaction mixture.

3.13. Conversion of Functionalised 4-Substituted-Quinolines to 4-Quinolones

With our borylated intermediates in hand, we next endeavoured to exploit the lability of our chosen C-4 substituents and reveal the corresponding fluoroquinolone scaffolds. As our protocol did not yield full conversion to borylated 4-methoxyquinoline **153**, the acid-catalysed demethylation methodology (**Table 3.2**) was applied to brominated product **160**, furnishing 7-bromo-6-fluoro-2-methylquinolinone **177** in 82% yield (**Scheme 3.43**).

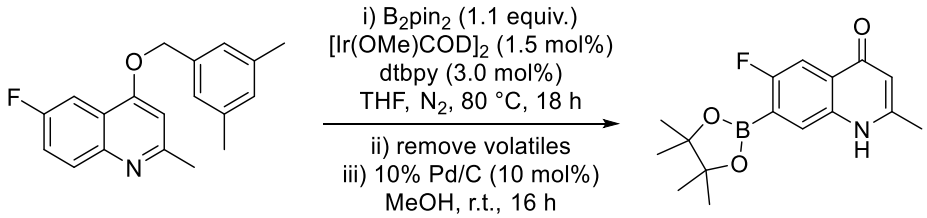


160

177, 82%

Scheme 3.43 Acid-mediated deprotection of brominated methoxyquinoline **160**.

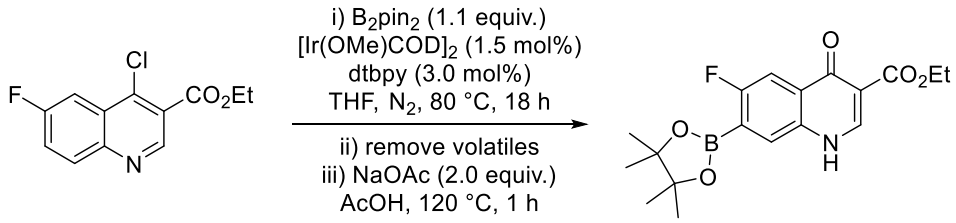
Reductive benzylation of the crude, borylated mixture from the reaction of **139**, gave quinolone boronate ester **178** in moderate yield (**Scheme 3.44**). It is worth noting that the boronate ester decomposed to the boronic acid in solution over time.



139 **178**, 53%

Scheme 3.44 Borylation of **139** and subsequent reductive benzylation for the synthesis of **178**.

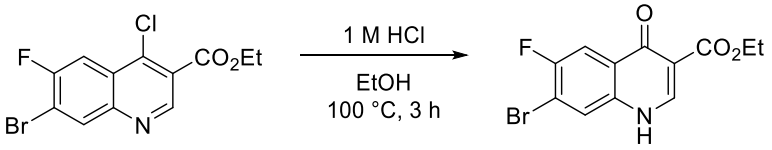
We then looked at the acid-mediated hydrolysis of our borylated antibiotic precursor (**Scheme 3.45**). The crude reaction mixture was purified by trituration of the obtained solid from MeOH/acetone (1:1) to give **179** in a yield of 53%. This compound was very insoluble and proved to be unstable in solution over a number of hours, thus a small portion (~1.5 mg) was dissolved in $(CD_3)_2SO$ with gentle heating and was then taken directly for complete NMR analysis.



146 **179**, 53%

Scheme 3.45 Borylation and acid hydrolysis of **146**, for the construction of borylated 6-fluoroquinolone antibiotic precursor **179**.

Finally, due to the instability of compound **179** in solution, we sought to convert brominated substrate **166** to the corresponding quinolone. A 1970 publication by Heindel and Fine reported the alcoholysis of electron deficient 4-chloroquinolines to the corresponding quinolones.[118] This methodology was utilised to provide brominated quinolone **180** in good yield (**Scheme 3.46**).



166 **180**, 64%

Scheme 3.46 Acid-cataysed alcoholysis of **166** for the generation of brominated quinolone **180**.

The mechanism for the above transformation is reported to proceed through a C-4 alkoxy intermediate, formed *via* the protonated, charged quinoline species. Subsequent production of the quinolone motif is thought to occur by nucleophilic attack of the alkyl group attached to the C-4 oxygen by either Cl^- or ROH to give either R_2O or RCl as by-products of the reaction (**Figure 3.12**).

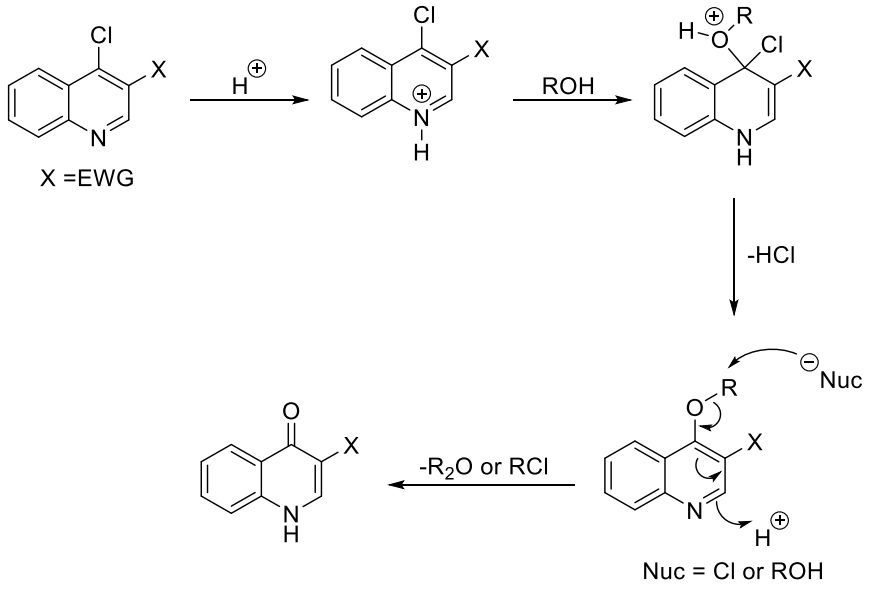


Figure 3.12 Plausible mechanism for the acid-catalysed displacement of the chloride atom in electron deficient quinolines.[118]

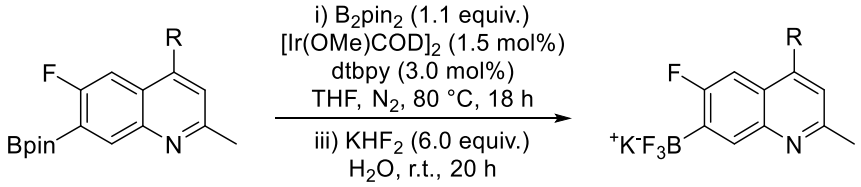
3.14. Functionalisation of 7-Borylated-4-Substituted-Quinolines

Given the commonly encountered issues associated with employing heterocycles as substrates for cross-coupling and other reactions,[119-125] it was pivotal to demonstrate that the Bpin moiety could be transformed into useful substituted quinolines. As

already demonstrated, conversion of this group to a bromide was achieved in high yields for all borylated intermediates.

3.14.1 Modulation of the Boronate Ester Group

As we had already observed concurrent hydrolysis of the boronate ester group in the synthesis of **134** (**Scheme 3.21**), we wanted to convert the Bpin into alternative, reactive boron motifs, while maintaining the core quinoline structure. The trifluoroborate salts were generated by the *in situ* reaction of borylated intermediates **133** and **153** with aqueous KHF_2 at room temperature (**Scheme 3.47**).[126] Quinoline trifluoroborate salts **181** and **182** were isolated in yields of 71% and 73% respectively.

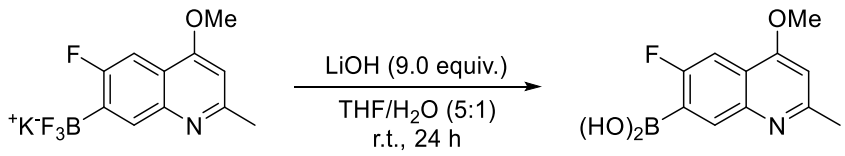


132, **135**

181, R = Cl 71%
182, R = OMe 73%

Scheme 3.47 One-pot reaction of **132** and **135** for the formation of trifluoroborate salts **181** and 182.

4-Methoxyquinoline trifluoroborate salt **182** was then converted to corresponding boronic acid **183** in very good yield using aqueous LiOH in THF (**Scheme 3.48**).[126] Application of this method to 4-chloro derivative **181** returned only starting material. It is possible interaction between the aryl chloride and hydroxide ions interferes with the progress of reaction. Some conversion to the 4-chloro-boronic acid was observed by reacting **181** with TMS chloride in aqueous ACN, but the insolubility of the product here made purification difficult and this compound was not isolated.



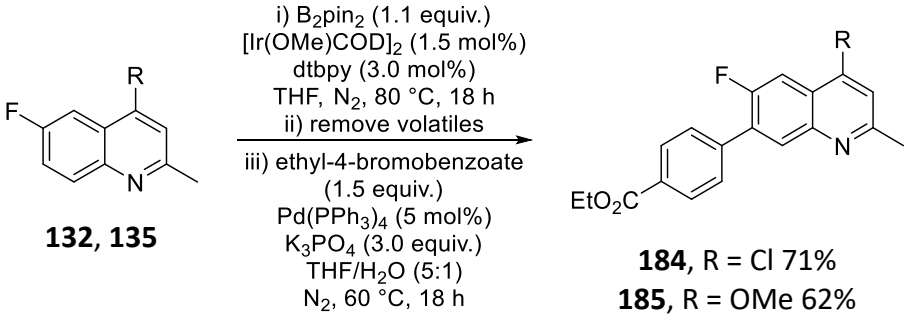
182

183, 75%

Scheme 3.48 Synthesis of quinoline boronic acid **183**.

3.14.2 Suzuki-Miyaura Cross-Coupling Reaction

Since its inception in the late 20th century, the Suzuki-Miyaura (SM) cross-coupling reaction has become a ubiquitous tool in every synthetic chemist's toolbox.[127] As such, it is the most commonly used route for the construction of carbon-carbon bonds in the pharmaceutical industry.[128] Major developments have been made towards one-pot borylation/SM reactions;[22,71-72,129-132] as discussed in Chapter 2, this type of telescoped reaction is attractive for myriad reasons. In our hands, the sequential C-H borylation/SM cross-coupling reaction reported by Sawamura, Marder and co-workers[80] afforded corresponding arylated compounds **184** and **185** in yields of 71% and 62% respectively (**Scheme 3.49**).



Scheme 3.49 Sequential C-H borylation/SM reaction of **132** and **135** for the generation of aryl quinolines **184** and **185**.

The structure of **184** was confirmed by X-ray diffraction analysis of single crystals which were obtained *via* vapour diffusion (**Figure 3.13**). The crystals were grown by our colleagues in Germany from a saturated solution of DCM in Et_2O.

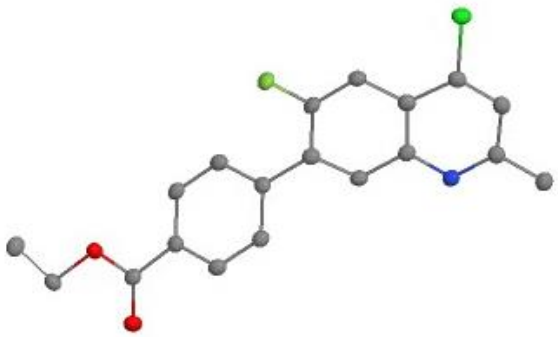
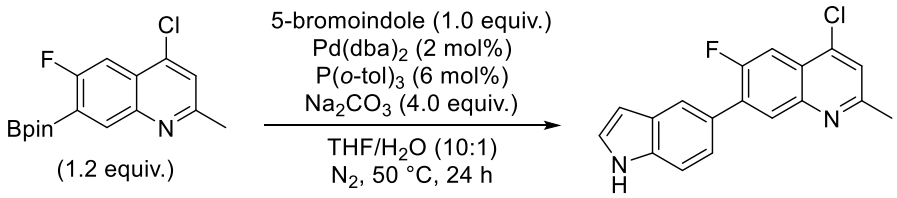


Figure 3.13 The solid-state molecular structure of **184** determined by single-crystal X-ray diffraction at 100 K. All ellipsoids are drawn at the 50% probability level. H atoms are omitted for clarity.

Preliminary attempts to perform the one-pot process developed by Hartwig and co-workers[129] for the coupling of heteroaryl-bromides with our borylated intermediates gave mixed results. Although this procedure uses the borylated intermediate in slight excess, we initially tried the reaction with an equimolar ratio of substrate and coupling partner, returning mainly protodeborylated quinoline **132** after the cross-coupling step. Using **132** in slight excess allowed for the isolation of a small amount of coupled product **186**, albeit not with sufficient purity for the calculation of yield. The reaction of purified substrate **133** with 5-bromoindole in slight excess, gave compound **186** in 39% yield. Consequently, employing 5-bromoindole as the limiting reagent furnished arylated quinoline **186** in excellent yield of 86% (**Scheme 3.50**).



133 **186**, 86%

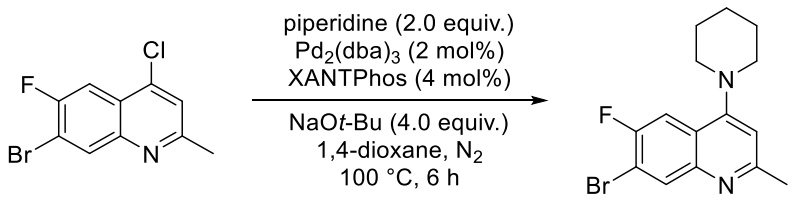
Scheme 3.50 SM reaction of **133** with heteroaromatic coupling partner, 5-bromoindole, to form **186**.

3.14.3 Amination

As highlighted in the introduction, the potency, oral availability and pharmacokinetics of 6-fluoroquinolone antibiotics is directly linked to the presence

of a cyclic amine substituent at C-7 (**Figure 3.3**). We thought it important to include this transformation in our scope. The Chan-Lam-Evans coupling of boronate esters or boronic acids with alcohols and amines allows for the synthesis of carbon-heteroatom bonds. These reactions usually require relatively facile conditions; they are generally copper-catalysed and carried out in air at room temperature.[133] However, these oxidative couplings are notoriously capricious and suffer from a number of yield-reducing side reactions.[134-137] In general, substitution *ortho* to the coupling site on the aryl substrate leads to lower yields, presumably due to steric encumberment.[135] Even though fluorine would have a negligible impact on the steric bias of any intermediates, couplings of electron-deficient boronic esters/acids are known to be sluggish.[137-138] Nonetheless, we were hopeful that this transformation could be applied to our borylated quinolines. Numerous attempts were made to transform our borylated compounds (Bpin, $B(OH)_2$ and BF_3K substrates) to the corresponding amine products, to no avail. Both stoichiometric and catalytic amounts of copper were utilised with different bases, additives, and oxidants, in various solvents, with no amination ever observed. Analysis of the crude reaction mixtures in all cases showed evidence of only starting material and protodeboronation.

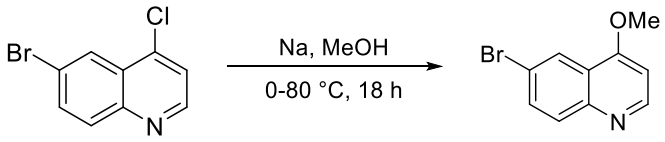
Having exhausted the possibility of a copper-catalysed coupling reaction, we then sought to utilise another salient protocol; the Hartwig-Buchwald amination reaction.[139-142] This universal palladium-catalysed carbon-nitrogen bond-forming reaction is regularly found in process development in the medicinal and agrochemical sectors.[142] We first attempted the coupling of 7-bromo-4-chloro-6-fluoro-2-methylquinoline **159** with piperidine using tris(dibenzylideneacetone)-dipalladium ($Pd_2(dba)_3$) as catalyst. Purification of the resulting mixture *via* column chromatography returned starting material **159**, along with what appeared to be an aminated product. Further analysis of this fraction confirmed the formation of 4-amino-quinoline **187**, with the C-Br bond untouched (**Scheme 3.51**). Aryl chlorides are less reactive to OA than aryl bromides (*vide supra*), and so it is possible that attack at the C-4 position is promoted by the presence of the *para* nitrogen atom.



159 **187**, 47%

Scheme 3.51 Attempted Hartwig-Buchwald amination reaction of **159**.

To obviate the occurrence of this side reaction, we employed 4-methoxy substrate **160** for further reactions. Similar conditions gave a three-component mixture, as deduced by ^{1}H NMR analysis; namely, C-7 aminated product, starting material **160** and hydrodebrominated substrate **135**. As we had identified this methodology as a viable pathway for the formation of our aminated target, we looked to apply a 'deconvolution' strategy to obtain optimal conditions. Similar to the 'design of experiment' method employed in industry; this systematic approach simultaneously tests multiple variables. Consequently, the overall number of experiments necessary for screening conditions is significantly reduced.[143-145] As compound **160** was constructed through multiple steps, we synthesised another, similar compound for use in our optimisation experiments. 6-Bromo-4-methoxyquinoline **188** was furnished from the reaction of commercially available 6-bromo-4-chloroquinoline with freshly prepared sodium methoxide in 98% yield (**Scheme 3.52**).



188, 98%

Scheme 3.52 Synthesis of 6-bromo-4-methoxyquinoline **188**.

In pursuit of a pool of suitable conditions, we limited our search to existing protocols with examples of coordinating, nitrogen-based heterocycles; the search term 'Buchwald-Hartwig' returned over 5,000 documents and close to 30,000 reactions on Reaxys! Other than specifically designed catalysts,[146] we identified $Pd_2(dba)_3$ as the most common palladium source and again narrowed our search to include this pre-catalyst only. A selection of eight common phosphine ligands (**L1**–**L8**), three bases (**B1**–**B3**) and two solvents (toluene, 1,4-dioxane) was then made for our first step

(**Figure 3.14**).[139,147] Initially, two experiments were performed in which all ligands **L1**–**L8** (10 mol% each) and bases **B1**–**B3** (2.5 equiv. each) were mixed with **188**, piperidine and $Pd_2(dba)_3$. The resulting solutions were heated to 100 °C for 24 h in toluene and 1,4-dioxane respectively (***Step 1***). The reaction in toluene garnered 63% yield by NMR of aminated product **190** and was selected as the optimal solvent going forward. Next, ligands **L1**–**L8** were split into two groups at random (**L1**–**L4** and **L5**–**L8**) and our three bases were divided into carbonate and non-carbonate groups (**B1**–**B2** and **B3**). Two experiments were conducted combining the two groups of ligands and bases, in toluene (***Step 2***). The highest yielding permutation was that of **L1**–**L4** with **B3**, NaO*t*-Bu. Finally, NaO*t*-Bu was used as the base in toluene with each of the ligands **L1**–**L4** (***Step 3***); for this step loading was reduced to 3 mol% and 6 mol% for pre-catalyst and ligand respectively. From this final deconvolution step, the most powerful catalytic system consisted of $Pd_2(dba)_3$ (3 mol%), RuPhos (**L3**, 6 mol%) and NaO*t*-Bu (**B3**, 2.5 equiv.) in toluene, and allowed for aminated quinoline **190** to be isolated in 92% yield.

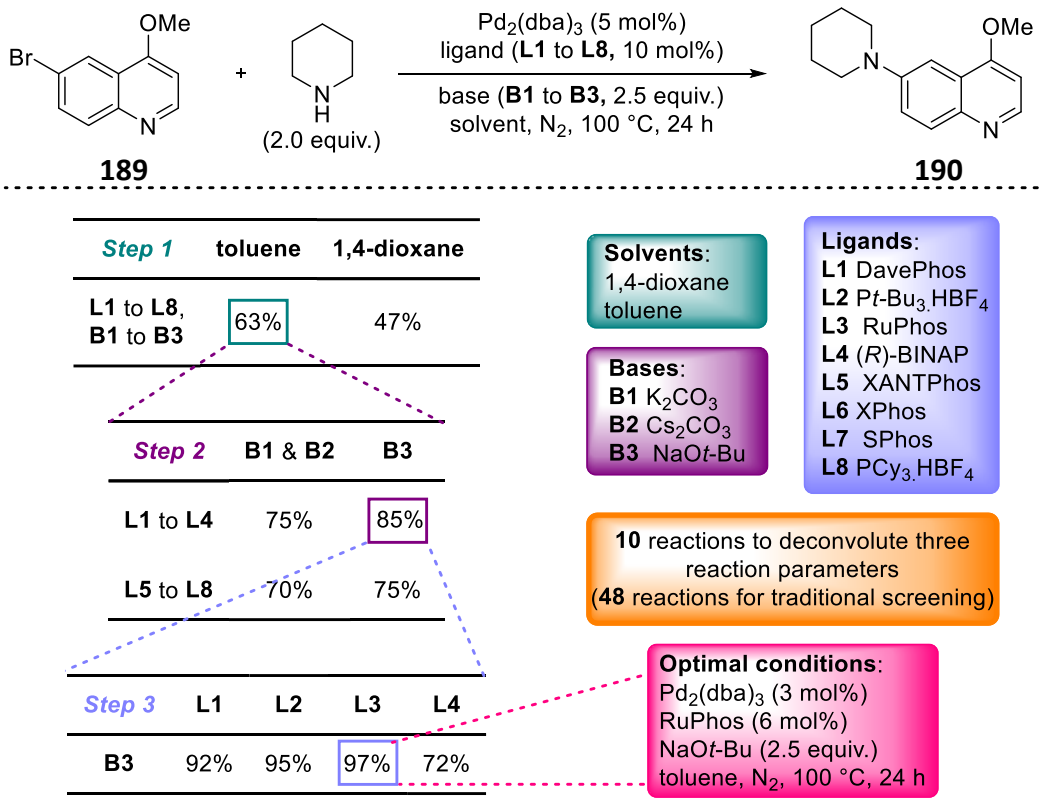
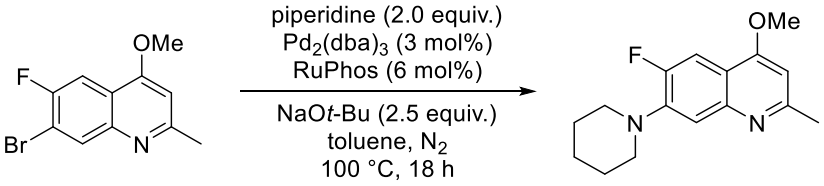


Figure 3.14 Deconvolution strategy for optimisation of Hartwig-Buchwald amination. Yields calculated from the ^{1}H NMR spectrum of the crude reaction mixture using 1,3,5-trimethoxybenzene as the internal standard.

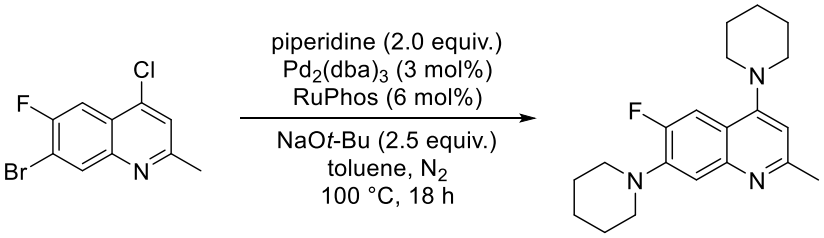
Application of our optimised conditions to **160** provided 6-fluoro-4-methoxy-2-methyl-7-(piperidin-1-yl)quinoline **191** in an excellent yield of 88% (**Scheme 3.53**).



160 **191**, 88%

Scheme 3.53 Hartwig-Buchwald amination reaction of **160**.

Interestingly, under the same conditions, chlorinated substrate **159** yielded primarily di-aminated product **192** (**Scheme 3.54**). Using an equimolar amount of piperidine and **159** gave a mixture of C-4-amino quinoline **187** and di-aminated product **192**.

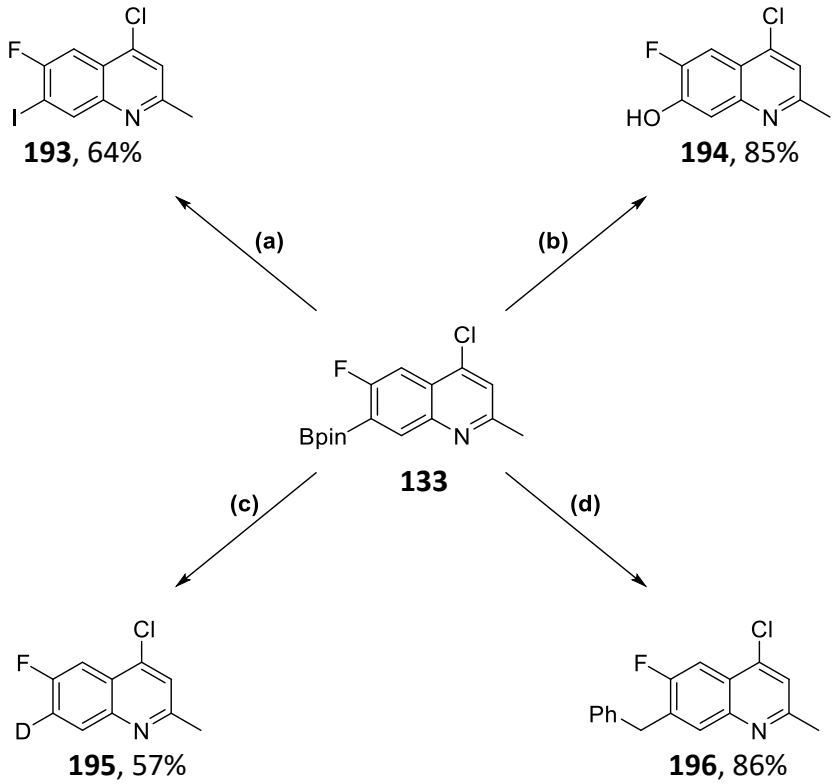


159 **192**, 80%

Scheme 3.54 Hartwig-Buchwald amination reaction of **159**.

3.14.4 Other Transformations of the Pinacol Boronate Ester Motif

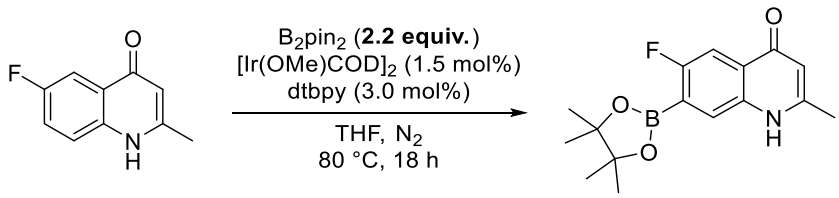
We then explored other possible transformations of the motif. Firstly, we wanted to construct the more reactive iodide species. For this, we employed a procedure developed by Yu and co-workers[119] which uses a combination of catalytic copper iodide, phenanthroline ligand and excess potassium iodide in aqueous MeOH. These conditions afforded iodinated quinoline **193** in moderate yield over two steps (**Scheme 3.55 (a)**). Hydroxylation of purified pinacol ester **133** was achieved using H_2O_2 in MeOH, providing **194** in 85% yield (**Scheme 3.55 (b)**). Next, we turned our attention to the potential deuteration of our boronate product **133**. For this, the same iridium pre-catalyst, $[Ir(OMe)COD]_2$, was employed in THF with D_2O to furnish **195** in 57% yield (**Scheme 3.55 (c)**).[148] Finally, the palladium-catalysed reaction of **133** with benzyl bromide gave C-7-benzyl quinoline **196** in excellent yield (**Scheme 3.55 (d)**).[148]



Scheme 3.55 Transformations of borylated quinoline **133**. *Conditions:* **(a)** Crude reaction mixture from borylation step, CuI (10 mol%), 1,10-phenanthroline (20 mol%), KI (1.5 equiv.), MeOH/H_2O (4:1), N_2, 80 °C, 2 h. **(b)** 30% H_2O_2 (1.2 equiv.), MeOH, 0 °C to rt, 16 h. **(c)** $[Ir(OMe)COD]_2$ (1 mol%), THF/D_2O (4:1), N_2, 80 °C, 12 h. **(d)** $Pd_2(dba)_3$ (1 mol%), PPh_3 (4 mol%), K_2CO_3 (4.0 equiv.), BnBr (1.2 equiv.), THF/H_2O (50:1), N_2, 100 °C, 24 h.

Conclusions and Future Work

Based on publications by Ya-Ming *et al*.[149] and Smith and co-workers[150] on the traceless borylation of indoles, we sought to revisit our original quinolone target, this time using 6-fluoroquinolone **128**. Using the conditions optimised for the borylation of quinoline substrates, we were surprised to observe conversion to 7-borylated product **178**, with no evidence of *N*-borylation. Increasing the amount of B_2pin_2 to 2.2. equiv. allowed for higher conversion and consequently, isolation of **178** in 63% yield (**Scheme 3.56**). As no *N*-Bpin product appears to have formed, it is possible that either the interaction is fluxional, or that the *N*-Bpin product is unstable and is cleaved before analysis can be performed.



128 **178**, 63%

Scheme 3.56 C-H borylation of 6-fluoroquinolone substrate **128** using 2.2 equiv. B_2pin_2.

In conclusion, a route to access the C-7 position of 6-fluoroquinolines was identified. The C-H borylation step occurred with excellent conversions on various 4-substituted quinolines. Depending on the choice of substituent at the C-4 position, a variety of pathways are available to reveal the corresponding functionalised 6-fluoroquinolone moiety, a pivotal intermediate in the synthesis of a plethora of antibiotics. Subsequent useful transformations of the nucleus were demonstrated, providing a range of C-7 substituted quinolines and indeed quinolones, a position which to the best of our knowledge has only been previously accessed once through a C-H functionalisation route post-cyclisation (*vide supra*).

Future work on this project will seek to obtain full conversion to borylated fluoroquinolone **178** and gain insight into the mechanistic pathway of this transformation. This more direct route would certainly allow the transformation to be considered a viable route for late-stage functionalisation of fluoroquinolone antibiotics and examples of these will be demonstrated once the process has been optimised.

Experimental

3.15. General Procedures

The catalyst precursor $[Ir(OMe)COD]_2$ was synthesised according to a literature procedure[151] and was stored in the glovebox under argon. Toluene and CPME were dried and stored over flame-dried 4 Å molecular sieves. THF was either freshly distilled from sodium/benzophenone under nitrogen and stored over molecular sieves under nitrogen (University College Cork) or dried using a solvent purification system (SPS) from Innovative Technology, degassed with argon and stored over molecular sieves under argon (Julius-Maximilians-Universität). K_2CO_3, Cs_2CO_3 and Na_2CO_3 were stored in an oven at 150 °C. All other solvents and reagents were used as obtained from commercial sources and without further purification.

Melting points were measured using a Thomas Hoover Capillary Melting Point apparatus.

Infrared spectra were measured on a Perkin-Elmer FT-IR spectrometer. Samples were dissolved in DCM and dispersed as thin films on NaCl plates and the dichloromethane allowed to evaporate before measurement of sample.

Column chromatography was carried out using 60 Å (35-70 µm) silica. TLC was carried out on pre-coated silica gel plates (Merck 60 PF254) and the developed plates were visualized under UV light.

High resolution mass spectra (HRMS) were recorded on a Waters LCT Premier Tof LC-MS instrument in electrospray ionization (ESI) mode (University College Cork) or using a Thermo Scientific Exactive Plus Orbitrap MS system with an Atmospheric Sample Analysis Probe (ASAP) (Julius-Maximilians-Universität). Samples were run using 50% acetonitrile-water containing 0.1% formic acid as eluent; and were made up at a concentration of *ca*. 1 mg mL^{-1}.

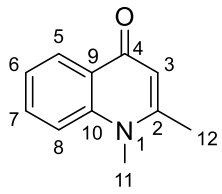
Nuclear Magnetic Resonance (NMR) spectra were run in $CDCl_3$, $(CD_3)_2SO$ or CD_3OD, as specified. ^1H NMR (600 MHz), ^1H NMR (500 MHz), ^1H NMR (400 MHz) and ^1H NMR (300 MHz) spectra were recorded on Bruker Avance 600, Bruker Avance 500, Bruker Avance 400, and Bruker Avance III 300 NMR spectrometers, respectively. ^{13}C NMR

(150 MHz), ^{13}C NMR (125 MHz) ^{13}C NMR (100 MHz) and ^{13}C NMR (75 MHz) spectra were recorded on Bruker Avance 600, Bruker Avance 500, Bruker Avance 400, and Bruker Avance III 300 NMR spectrometers, respectively, in proton decoupled mode. ^{19}F NMR (470 MHz), ^{19}F NMR (376 MHz), ^{19}F NMR (282 MHz) spectra were recorded on a Bruker Avance 500, Bruker Avance 400, and Bruker Avance III 300 NMR spectrometers, respectively, in proton decoupled mode. All NMR analyses were carried out at 300 K unless otherwise specified. Chemical shifts (δ) are expressed as parts per million (ppm), coupling constants (*J*) are expressed in Hertz (Hz), are reported as observed and their values are uncorrected. Splitting patterns in ^{1}H-NMR spectra are designated as: s (singlet), bs (broad singlet), d (doublet), dd (doublet of doublets), ddd (doublet of doublets of doublets), t (triplet), q (quartet), and m (multiplet). Compounds were numbered for ease of assignment and do not necessarily represent IUPAC nomenclature.

Single-crystal X-ray analysis was performed on a RIGAKU OXFORD DIFFRACTION XtaLAB Synergy-R diffractometer with a semiconductor HPA area detector (HyPix-Arc150) using a rotating-anode X-ray tube for X-ray generation and multi-layer mirror monochromated Cu-Kα radiation. The crystals were cooled using an Oxford Cryostreams 800 low-temperature device. Data were collected at 100 K. The images were processed and corrected for Lorentz-polarization effects and absorption as implemented in the **CrysAlisPro** software. The structure was solved using the intrinsic phasing method (**ShelXT**)[152] and Fourier expansion technique. All non-hydrogen atoms were refined in anisotropic approximation, with hydrogen atoms 'riding' on idealised positions by full-matrix least squares against F^2 of all data, using **SHELXL** software[153] and the **SHELXLE** graphical user interface.[154] Diamond[155] software was used for graphical representation.

3.16. Compounds from Preliminary Studies

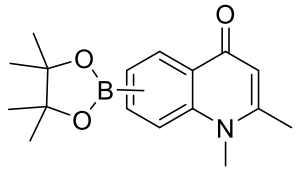
1,2-Dimethylquinolin-4(1*H*)-one (123)[156]



2-Methylquinolin-4(1*H*)-one **121** (5.0 g, 31.4 mmol, 1.0 equiv.) and KOH (5.29 g, 94.2 mmol, 3.0 equiv.) were suspended in MeOH (32 mL) and MeI (19.6 mL, 314 mmol, 10.0 equiv.) was added dropwise. The resulting mixture was stirred at r.t. for 24 h, then filtered through a pad of celite using MeOH and concentrated under reduced pressure. The residue was taken up in DCM, again filtered through a pad of celite concentrated under reduced pressure. Purification *via* column chromatography ($CHCl_3$:MeOH 99:1–95:5) to yield **123** as a beige solid (3.035 g, 56%); m.p. 169–170 °C (lit.[156] 174–175 °C); ^{1}H NMR (300 MHz, $CDCl_3$) δ: 8.43 (dd, *J* = 8.0, 1.4 Hz, 1H, C(5)**H**), 7.64 (ddd, *J* = 8.7, 7.0, 1.7 Hz, 1H, C(7)**H**), 7.47 (d, *J* = 8.6 Hz, 1H, C(8)**H**), 7.36 (ddd, *J* = 8.0, 7.0, 0.9 Hz, 1H, C(6)**H**), 6.20 (s, 1H, C(3)**H**), 3.71 (s, 3H, C(11)**H₃**), 2.45 (s, 3H, C(12)**H₃**) ppm; ^{13}C NMR (75 MHz, $CDCl_3$) δ: 177.7 (q**C**-4), 150.9 (q**C**-2), 141.7 (q**C**-10), 132.0 (**C**(7)H), 126.7 (**C**(5)H), 126.6 (q**C**-9), 123.2 (**C**(6)H), 115.1 (**C**(8)H), 111.8 (**C**(3)H), 34.2 (**C**(11)H_3), 22.2 (**C**(12)H_3) ppm; *m/z* (ES+): 174 ($(M+H)^+$ 100%).

Spectral characteristics were consistent with previously reported data.[156]

1,2-Dimethyl-6/7-(4,4,5,5-tetramethyl-1,3,2-dioxaborolan-2-yl)quinolin-4(1*H*)-one (124, 125)[67]



In an argon-filled glovebox, $[Ir(OMe)COD]_2$ (2.0 mg, 0.003 mmol, 1.5 mol%), dtbpy (1.6 mg, 0.006 mmol, 3 mol%), B_2pin_2 (0.051 g, 0.2 mmol, 1.0 equiv.), **123** (0.035 g, 0.2 mmol, 1.0 equiv.), and THF (10 mL) were added to a sealable cylindrical microwave vial. The vial was sealed with a crimptop septum cap, taken out of the glovebox and the reaction mixture was stirred at 80 °C for 24 h. The reaction was cooled to r.t. and concentrated under reduced pressure to afford the crude product. Analysis acquired from a mixture of isomers.

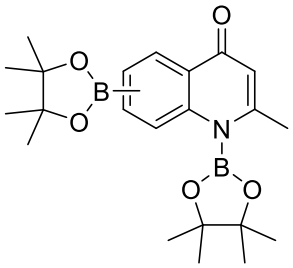
1,2-Dimethyl-7-(4,4,5,5-tetramethyl-1,3,2-dioxaborolan-2-yl)quinolin-4(1*H*)-one

^{1}H NMR (500 MHz, $CDCl_3$) δ: 8.43 (dd, *J* = 7.9 Hz, 0.5 Hz, 1H), 7.96 (s, 1H), 7.77 (dd, *J* = 7.9, 0.5 Hz, 1H), 6.29 (s, 1H), 3.81 (s, 3H), 2.50 (d, *J* = 0.5 Hz, 3H) ppm; ^{13}C NMR (125 MHz, $CDCl_3$) δ: 177.9, 151.5, 141.3, 129.2, 128.5, 126.0, 122.1, 112.2, 84.6, 34.7, 24.8, 22.5 ppm; a signal for the carbon directly attached to the boron atom was not observed; ^{11}B NMR (160 MHz $CDCl_3$) *δ* 31 ppm; HRMS (ASAP+): *m/z* calcd for $[M+H]^+$ 299.1802, found 299.1795.

1,2-Dimethyl-6-(4,4,5,5-tetramethyl-1,3,2-dioxaborolan-2-yl)quinolin-4(1*H*)-one

^{1}H NMR (500 MHz, $CDCl_3$) δ: 8.93 (dd, *J* = 1.7 Hz, 0.5 Hz, 1H), 8.03 (dd, *J* = 8.7, 1.7 Hz, 1H), 7.45 (d, *J* = 8.7, 1H), 6.27 (s, 1H), 3.74 (s, 3H), 2.48 (d, *J* = 0.5 Hz, 3H) ppm; ^{13}C NMR (125 MHz, $CDCl_3$) δ: 178.1, 151.2, 143.8, 137.9, 134.8, 125.9, 114.7, 112.6, 84.2, 34.5, 25.1, 22.4 ppm; a signal for the carbon directly attached to the boron atom was not observed; ^{11}B NMR (160 MHz $CDCl_3$) *δ* 31 ppm; HRMS (ASAP+): *m/z* calcd for $[M+H]^+$ 299.1802, found 299.1795.

2-methyl-1,6/7-bis(4,4,5,5-tetramethyl-1,3,2-dioxaborolan-2-yl)quinolin-4(1H)-one (126, 127)[67]



Mixture of isomers **126** and **127** prepared *via* the procedure described for **124** and **125**, using 2-methylquinolin-4(1*H*)-one **121** (0.035 g, 0.4 mmol, 1.0 equiv.) except that the amount of B_2pin_2 was increased (0.102 g, 0.4 mmol, 2.0 equiv.). Analysis acquired from a mixture of isomers.

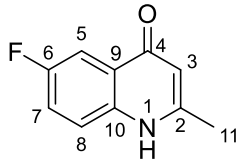
2-methyl-1,7-bis(4,4,5,5-tetramethyl-1,3,2-dioxaborolan-2-yl)quinolin-4(1H)-one

^{1}H NMR (200 MHz, $CDCl_3$) δ: 8.30 (d, *J* = 8.0 Hz, 1H), 8.03 (s, 1H), 7.67 (d, *J* = 8.0 Hz, 1H), 6.20 (s, 1H), 2.43 (s, 3H) ppm; ^{11}B NMR (160 MHz $CDCl_3$) *δ* 35 ppm; HRMS (ASAP+): *m/z* calcd for $[M+H]^+$ 410.2534, found 410.2531.

2-methyl-1,6-bis(4,4,5,5-tetramethyl-1,3,2-dioxaborolan-2-yl)quinolin-4(1H)-one

^{1}H NMR (200 MHz, $CDCl_3$) δ: 8.82 (s, 1H), 7.89 (d, *J* = 8.4 Hz, 1H), 7.59 (d, *J* = 8.4 Hz, 1H), 6.20 (s, 1H), 2.41 (s, 3H) ppm; ^{11}B NMR (160 MHz $CDCl_3$) *δ* 35 ppm; HRMS (ASAP+): *m/z* calcd for $[M+H]^+$ 410.2534, found 410.2531.

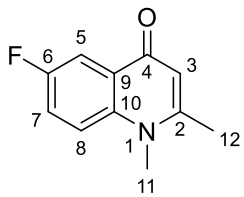
6-Fluoro-2-methylquinolin-4(1*H*)-one (128)[157]



An equimolar solution of 4-fluoroaniline (3.45 mL, 36 mmol, 1.0 equiv.) and ethyl acetoacetate (4.55 mL, 36 mmol, 1.0 equiv.) was added to polyphosphoric acid (20 g, 5% w/w) and stirred at 150 °C in a DrySyn heating block for 3 h. The reaction mixture was poured directly into ice water and neutralised using 3 M NaOH. The resulting yellow precipitate was isolated and redissolved in 5% NaOH solution, treated with charcoal, filtered, and the filtrate neutralised using 6 M HCl. The precipitate was isolated by suction filtration, washed with H_2O, and dried at 150 °C overnight to yield **128** as a white solid (2.537 g, 39%); m.p. >250 °C (lit.[157] 268–269 °C); ^{1}H NMR (300 MHz, $(CD_3)_2SO$) δ: 11.91 (bs, 1H, NH), 7.78–7.42 (m, 3H, C(5)**H**), C(7)**H**, C(8)**H**), 5.96 (s, 1H, C(3)**H**), 2.36 (s, 3H, C(11)**H₃**) ppm; ^{13}C NMR (75 MHz, $(CD_3)_2SO$) δ: 175.5 (q**C**-4), 158.1 (d, $^{1}J_{(C,F)}$ = 241 Hz, q**C**(6)F), 150.2 (q**C**-2), 136.8 (q**C**-10), 125.4 (d, $^{3}J_{(C,F)}$ = 7 Hz, q**C**-9), 120.5 (d, $^{3}J_{(C,F)}$ = 8 Hz, **C**(8)H), 120.3 (d, $^{2}J_{(C,F)}$ = 25 Hz, **C**(7)H), 108.7 (d, $^{2}J_{(C,F)}$ = 22 Hz, **C**(5)H), 107.6 (**C**(3)H), 19.4 (**C**(11)H_3) ppm; ^{19}F NMR (282 MHz, $(CD_3)_2SO$) δ: -115 ppm; *m/z* (ES+): 178 ($(M+H)^+$ 100%).

Spectral characteristics were consistent with previously reported data.[157]

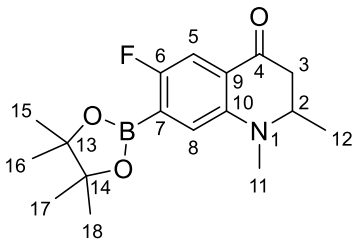
6-Fluoro-1,2-dimethylquinolin-4(1*H*)-one (129)



Compound **129** was prepared *via* the procedure described for **123**, using **128** (0.532 g, 0.4 mmol, 1.0 equiv.) to yield compound **129** as a white solid (0.233 g, 40%); m.p. 212–215 °C; IR (film) ν_{max} 1638 (C=O stretch), 1568 (alkenyl C=C stretch), 1503 (aromatic C=C stretch), 1260 (C-N stretch), 1161 (C-F stretch) cm^{-1}; ^{1}H NMR (300 MHz, CD_3OD) δ: 7.99–7.79 (m, 2H, C(8)**H**, C(5)**H**), 7.55 (ddd, *J* = 9.2, 3.1 Hz, $^{3}J_{(H,F)}$ = 7.8 Hz, 1H, C(7)**H**), 6.27 (s, 1H, C(3)**H**), 3.87 (s, 3H, C(11)**H₃**), 2.58 (s, 3H, C(12)**H₃**) ppm; ^{13}C

NMR (75 MHz, CD_3OD) δ: 177.0 (d, $^4J_{(C,F)}$ = 3 Hz, q**C**-4), 159.2 (d, $^1J_{(C,F)}$ = 245 Hz, q**C**(6)F), 154.2 (q**C**-2), 138.5 (d, $^4J_{(C,F)}$ = 2 Hz, q**C**-10), 127.1 (d, $^3J_{(C,F)}$ = 9 Hz, q**C**-9), 120.7 (d, $^2J_{(C,F)}$ = 25 Hz, **C**(7)H), 119.2 (d, $^3J_{(C,F)}$ = 8 Hz, **C**(8)H), 109.9 (**C**(3)H), 109.3 (d, $^2J_{(C,F)}$ = 23 Hz, **C**(5)H), 34.4 (**C**(12)H_3), 20.7 (**C**(11)H_3) ppm; ^{19}F NMR (282 MHz, $CDCl_3$) δ: -120 ppm; HRMS (ESI-TOF) *m/z*: $[M+H]^+$ calcd for $C_{11}H_{11}FNO$: 192.0819; found: 192.0811.

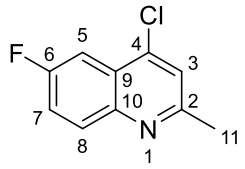
6-Fluoro-1,2-dimethyl-7-(4,4,5,5-tetramethyl-1,3,2-dioxaborolan-2-yl)-2,3-dihydroquinolin-4(1*H*)-one (131)



A 15 mL Schlenk tube was oven dried (150 °C) and cooled under vacuum. The flask was refilled with nitrogen and all reagents were added under a positive pressure of nitrogen in the order: **129** (0.057 g, 0.3 mmol, 1.0 equiv.), dtbpy (4.8 mg, 0.018 mmol, 6 mol%), B_2pin_2 (0.114 g, 0.45 mmol, 1.5 equiv.), and $[Ir(OMe)COD]_2$ (6.0 mg, 0.009 mmol, 3 mol%). The Schlenk tube was then placed under vacuum for 20 min before being refilled with nitrogen three times. THF (9 mL) was added *via* syringe through the septum, the reaction was sealed and the mixture heated to 80 °C for 48 h. The reaction mixture was then cooled to r.t. and concentrated under reduced pressure. Isolation *via* column chromatography (DCM:MeOH 98:2) to yield a portion of **131** for analysis. ^{1}H NMR (500 MHz, $CDCl_3$) δ: 7.50 (d, $^3J_{(H,F)}$ = 9.1 Hz, 1H, C(5)**H**), 6.97 (d, $^4J_{(H,F)}$ = 4.2 Hz, 1H, C(8)**H**), 3.77–3.62 (m, 1H, C(2)**H**), 3.05–2.91 (m, 4H, *one of* C(3)**H_2**, C(11)**H_3**), 2.52 (dd, *J* = 16.3, 3.3 Hz, 1H, *one of* C(3)**H_2**), 1.36 (s, 12H, C(15)**H_3**, C(16)**H_3**, C(17)**H_3**, C(18)**H_3**), 1.12 (d, *J* = 6.7 Hz, C(12)**H_3**) ppm; ^{13}C NMR (125 MHz, $CDCl_3$) δ: 193.3 (d, $^4J_{(C,F)}$ = 2 Hz, q**C**-4), 159.0 (d, $^1J_{(C,F)}$ = 241 Hz, q**C**(6)F), 146.3 (d, $^4J_{(C,F)}$ = 1 Hz, q**C**-10), 121.7 (d, $^3J_{(C,F)}$ = 6 Hz, q**C**-9), 121.4 (d, $^3J_{(C,F)}$ = 7 Hz, **C**(8)H), 112.3 (d, $^2J_{(C,F)}$ = 26 Hz, **C**(5)H), 84.4 (2 × C, q**C**-13, q**C**-14), 56.9 (**C**(2)H), 44.9 (**C**(3)H_2), 37.7 (**C**(11)H_3), 24.9 (4 × C, **C**(15)H_3, **C**(16)H_3, **C**(17)H_3, **C**(18)H_3), 14.1 (**C**(12)H_3) ppm; a signal for the carbon directly attached to the boron atom was not observed; ^{19}F NMR (470 MHz, $CDCl_3$) δ: -120 ppm; ^{11}B NMR (96 MHz, $CDCl_3$) δ: 30 ppm; HRMS (ESI-TOF) *m/z*: $[M+H]^+$ calcd for $C_{17}H_{24}BFNO_3$: 320.1828; found: 320.1830.

Note: Compound **131** was not sufficiently pure for complete analysis or calculation of yield.

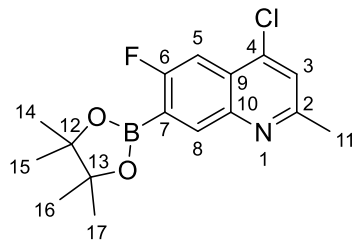
4-Chloro-6-fluoro-2-methylquinoline (132)[158]



Compound **128** (1.77 g, 10 mmol, 1.0 equiv.) was added to a Schlenk tube, dissolved in phosphoryl chloride (4.6 mL, 50 mmol, 5.0 equiv.) and the mixture was stirred at 110 °C for 3 h. The cooled reaction mixture was slowly added to iced water (30 mL) with stirring. Solid $NaHCO_3$ was then added gradually until the pH ~7 and the mixture was allowed to stir until effervescence ceased.[159] The mixture was transferred to a separating funnel and the organic layer was collected. The aq. layer was extracted with DCM (3 × 20 mL). The combined organic layers were washed with saturated $NaHCO_3$ (20 mL), H_2O (20 mL), and brine (20 mL), dried over $MgSO_4$, filtered and concentrated under reduced pressure to yield **132** as an off-white solid (1.860 g, 95%); m.p. 84–86 °C (lit.[157] 83–84 °C); ^{1}H NMR (300 MHz, $CDCl_3$) δ: 8.02 (dd, *J* = 9.2 Hz, $^4J_{(H,F)}$ = 5.3 Hz, 1H, C(8)**H**), 7.79 (dd, $^3J_{(H,F)}$ = 9.4 Hz, *J* = 2.8 Hz, 1H, C(5)**H**), 7.49 (ddd, *J* = 9.2, 2.9 Hz, $^3J_{(H,F)}$ = 8.3 Hz, 1H, C(7)**H**), 7.41 (s, 1H, C(3)**H**), 2.71 (s, 3H, C(11)**H₃**) ppm; ^{13}C NMR (75 MHz, $CDCl_3$) δ: 160.7 (d, $^1J_{(C,F)}$ = 248 Hz, q**C**(6)F), 158.2 (d, $^6J_{(C,F)}$ = 3 Hz, q**C**-2), 145.7 (q**C**-10), 141.7 (d, $^4J_{(C,F)}$ = 6 Hz, q**C**(4)Cl), 131.6 (d, $^3J_{(C,F)}$ = 9 Hz, **C**(8)H), 125.6 (d, $^3J_{(C,F)}$ = 10 Hz, q**C**-9), 122.5 (**C**(3)H), 120.5 (d, $^2J_{(C,F)}$ = 26 Hz, **C**(7)H), 107.8 (d, $^2J_{(C,F)}$ = 24 Hz, **C**(5)H), 25.0 (**C**(11)H_3) ppm; ^{19}F NMR (282 MHz, $CDCl_3$) δ: -112 ppm; *m/z* (ES+): 196 ($(M+H)^+$ 100%).

Spectral characteristics were consistent with previously reported data.[158]

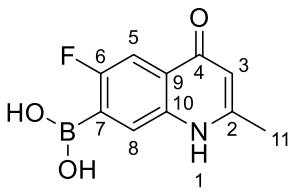
4-Chloro-6-fluoro-2-methyl-7-(4,4,5,5-tetramethyl-1,3,2-dioxaborolan-2-yl)quinoline (133)



A 15 mL Schlenk tube was oven dried (150 °C) and cooled under vacuum. The flask was refilled with nitrogen and all reagents were added under a positive pressure of nitrogen in the order: **132** (0.391 g, 2.0 mmol, 1.0 equiv.), dtbpy (0.016 g, 0.06 mmol, 3 mol%), B_2pin_2 (0.559 g, 2.2 mmol, 1.1 equiv.), and $[Ir(OMe)COD]_2$ (0.020 g, 0.03 mmol, 1.5 mol%). The Schlenk tube was then placed under vacuum for 20 min before being refilled with nitrogen three times. THF (10 mL) was added *via* syringe

through the septum, the reaction was sealed and the mixture heated to 80 °C for 18 h. The reaction mixture was then cooled to r.t., diluted with MeOH (40 mL) and concentrated under reduced pressure. Purification *via* recrystallisation from hot MeOH to yield **133** as a white solid (0.422 g, 66%); m.p. 97–100 °C; IR (film) ν_{max} 1627 (C=N stretch), 1500 (aromatic C=C stretch), 1370 (B-O stretch), 1331 (ether C-O stretch), 1261 (B-C stretch), 1147 (ether C-O stretch), 1049 (C-F stretch), 854 (C-Cl stretch) cm^{-1}; ^{1}H NMR (600 MHz, $CDCl_3$) δ: 8.56 (d, $^{4}J_{(H,F)}$ = 5.5 Hz, 1H, C(8)**H**), 7.79 (d, $^{3}J_{(H,F)}$ = 9.7 Hz, 1H, C(5)**H**), 7.47 (s, 1H, C(3)**H**), 2.77 (s, 3H, C(11)**H₃**), 1.45 (s, 12H, C(14)**H₃**, C(15)**H₃**, C(16)**H₃**, C(17)**H₃**) ppm; ^{13}C NMR (150 MHz, $CDCl_3$) δ: 164.0 (d, $^{1}J_{(C,F)}$ = 251 Hz, q**C**(6)F), 158.1 (d, $^{6}J_{(C,F)}$ = 3 Hz, q**C**-2), 145.1 (q**C**-10), 141.6 (d, $^{4}J_{(C,F)}$ = 5 Hz, q**C**(4)Cl), 139.8 (d, $^{3}J_{(C,F)}$ = 9 Hz, **C**(8)H), 127.6 (d, $^{3}J_{(C,F)}$ = 11 Hz, q**C**-9), 123.2 (**C**(3)H), 107.5 (d, $^{2}J_{(C,F)}$ = 27 Hz, **C**(5)H), 84.5 (2 × C, q**C**-12, q**C**-13), 25.0 (**C**(11)H_3), 24.9 (4 × C, **C**(14)H_3, **C**(15)H_3, **C**(16)H_3, **C**(17)H_3) ppm; a signal for the carbon directly attached to the boron atom was not observed; ^{19}F NMR (282 MHz, $CDCl_3$) δ: -105 ppm; ^{11}B NMR (96 MHz, $CDCl_3$) δ: 30 ppm; HRMS (ESI-TOF) *m/z*: $[M+H]^+$ calcd for $C_{16}H_{19}BClFNO_2$: 322.1176; found: 322.1182.

(6-Fluoro-2-methyl-4-oxo-1,4-dihydroquinolin-7-yl)boronic acid (134)

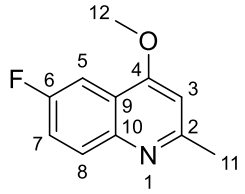


A 15 mL Schlenk tube was oven dried (150 °C) and cooled under vacuum. The flask was refilled with nitrogen and all reagents were added under a positive pressure of nitrogen in the order: **132** (0.039 g, 0.2 mmol, 1.0 equiv.), dtbpy (1.6 mg, 0.006 mmol, 3 mol%), B_2pin_2 (0.056 g, 0.22 mmol, 1.1 equiv.), and $[Ir(OMe)COD]_2$ (2.0 mg, 0.003 mmol, 1.5 mol%). The Schlenk tube was then placed under vacuum for 20 min before being refilled with nitrogen three times. THF (0.5 mL) was added *via* syringe, the reaction was sealed, and the mixture heated to 80 °C for 16 h, then cooled to r.t. and concentrated under reduced pressure. The crude reaction mixture for **133** (0.2 mmol, 1.0 equiv.) and NaOAc (32.8 mg, 0.4 mmol, 2.0 equiv.) were added to a 5 mL screw-capped vial followed by glacial acetic acid (1.25 mL). The vial was sealed and stirred at 120 °C for 1 h, then cooled to r.t., concentrated under reduced pressure, diluted with H_2O and allowed to stand for 1 h. The resulting precipitate was isolated by suction filtration, washed with H_2O and

cold Et_2O to yield **134** as a pink solid (0.030 g, 69%); m.p. 245–249 °C; IR (film) ν_{max} 1655 (C=O stretch), 1608 (C=N stretch), 1505 (aromatic C=C stretch), 1375 (B-O stretch), 1275 (B-C stretch), 1110 (C-F stretch) cm^{-1}; ^1H NMR (300 MHz, $(CD_3)_2SO$) δ: 11.68 (bs, 1H, N**H**), 8.48 (s, 2H, B(O**H**)$_2$), 7.67 (d, $^4J_{(H,F)}$ = 4.8 Hz, 1H, C(8)**H**), 7.56 (d, $^3J_{(H,F)}$ = 9.3 Hz, 1H, C(5)**H**), 5.90 (s, 1H, C(3)**H**), 2.34 (s, 3H, C(11)**H$_3$**) ppm; ^{13}C NMR (75 MHz, $(CD_3)_2SO$) δ: 176.0 (d, $^4J_{(C,F)}$ = 3 Hz, q**C**-4), 160.9 (d, $^1J_{(C,F)}$ = 241 Hz, q**C**(6)F), 149.9 (q**C**-2), 136.3 (q**C**-10), 126.4 (d, $^3J_{(C,F)}$ = 7 Hz, q**C**-9), 125.0 (d, $^3J_{(C,F)}$ = 10 Hz, **C**(8)H), 108.0 (d, $^2J_{(C,F)}$ = 26 Hz, **C**(5)H), 107.6 (**C**(3)H), 19.5 (**C**(11)H_3) ppm; a signal for the carbon directly attached to the boron atom was not observed; ^{19}F NMR (282 MHz, $(CD_3)_2SO$) δ: -111 ppm; ^{11}B NMR (96 MHz, $(CD_3)_2SO$) δ: 27 ppm; HRMS (ESI-TOF) *m/z*: $[M+H]^+$ calcd for $C_{10}H_{10}BFNO_3$: 222.0732; found: 222.0738.

3.17. Substrates for Borylation

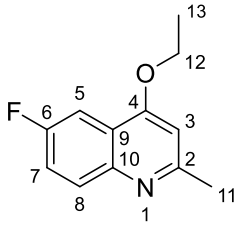
6-Fluoro-4-methoxy-2-methylquinoline (135)



A solution of **132** (0.500 g, 2.6 mmol, 1.0 equiv.) in MeOH (8 mL) was added dropwise to a freshly prepared solution of sodium (20 mmol, 8.0 equiv.) in MeOH (12 mL) over ice. The mixture was warmed to r.t. and then heated to 80 °C for 18 h, cooled to room temperature and concentrated under reduced pressure. The residue was dissolved in a mixture of EtOAc/H_2O (1:1, 20 mL) and the layers were separated. The aqueous layer was extracted with EtOAc (2 × 10 mL) and the combined organic layers were then washed with H_2O (10 mL), and brine (15 mL), dried over $MgSO_4$, filtered and concentrated under reduced pressure to yield **135** as a white solid (0.473 g, 97%); m.p. 52–54 °C; IR (film) ν_{max} 1632 (C=N stretch), 1514 (aromatic C=C stretch), 1353, 1201 (ether C-O stretch), 1180 (C-F stretch) cm^{-1}; ^1H NMR (300 MHz, $CDCl_3$) δ: 7.92 (dd, *J* = 9.2 Hz, $^4J_{(H,F)}$ = 5.2 Hz, 1H, C(8)**H**), 7.71 (dd, $^3J_{(H,F)}$ = 9.5 Hz, *J* = 2.9 Hz, 1H, C(5)**H**), 7.40 (ddd, *J* = 9.2 Hz, 2.9 Hz, $^3J_{(H,F)}$ = 8.3 Hz, 1H, C(7)**H**), 6.62 (s, 1H, C(3)**H**), 4.00 (s, 3H, C(12)**H$_3$**), 2.68 (s, 3H, C(11)**H$_3$**) ppm; ^{13}C NMR (75 MHz, $CDCl_3$) δ: 161.8 (d, $^4J_{(C,F)}$ = 5 Hz, q**C**-4), 159.7 (d, $^1J_{(C,F)}$ = 245 Hz, q**C**(6)F), 159.3 (d, $^6J_{(C,F)}$ = 2 Hz, q**C**-2), 145.7 (q**C**-10), 130.4 (d, $^3J_{(C,F)}$ = 9 Hz, **C**(8)H), 120.4 (d, $^3J_{(C,F)}$ = 9 Hz, q**C**-9), 119.5 (d, $^2J_{(C,F)}$ = 25 Hz, **C**(7)H), 105.6 (d, $^2J_{(C,F)}$ = 23 Hz, **C**(5)H), 101.0 (**C**(3)H), 55.6 (**C**(12)H_3), 25.8 (**C**(11)H_3)

ppm; ^{19}F NMR (282 MHz, $CDCl_3$) δ: -116 ppm; HRMS (ESI-TOF) *m/z*: $[M+H]^+$ calcd for $C_{11}H_{11}FNO$: 192.0819; found: 192.0817.

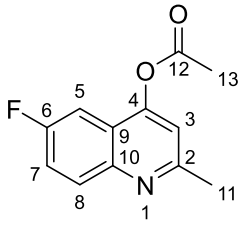
4-Ethoxy-6-fluoro-2-methylquinoline (136)



Compound **136** was prepared *via* the general procedure described for **135** using **132** (0.196 g, 1.0 mmol, 1.0 equiv.), except that EtOH was used in place of MeOH to yield **136** as a white solid (0.183 g, 89%); m.p. 82–85 °C; IR (film) ν_{max} 1603 (C=N stretch), 1514 (aromatic C=C stretch), 1350, 1192 (ether C-O stretch), 1087 (C-F stretch) cm^{-1}; ^{1}H NMR (400 MHz, $CDCl_3$) δ: 7.90 (dd, *J* = 9.2 Hz, $^4J_{(H,F)}$ = 5.2 Hz, 1H, C(8)**H**), 7.70 (dd, $^3J_{(H,F)}$ = 9.5 Hz, *J* = 2.9 Hz, 1H, C(5)**H**), 7.49–7.29 (m, 1H, C(7)**H**), 6.52 (s, 1H, C(3)**H**), 4.14 (q, *J* = 7.0 Hz, 2H, C(12)**H_2**), 2.64 (s, 3H, C(11)**H_3**), 1.51 (t, *J* = 7.0 Hz, 3H, C(13)**H_3**) ppm; ^{13}C NMR (100 MHz, $CDCl_3$) δ: 161.0 (d, $^4J_{(C,F)}$ = 5 Hz, q**C**-4), 159.5 (d, $^1J_{(C,F)}$ = 245 Hz, q**C**(6)F), 159.3 (d, $^6J_{(C,F)}$ = 2 Hz, q**C**-2), 145.7 (q**C**-10), 130.3 (d, $^3J_{(C,F)}$ = 9 Hz, **C**(8)H), 120.4 (d, $^3J_{(C,F)}$ = 10 Hz, q**C**-9), 119.3 (d, $^2J_{(C,F)}$ = 25 Hz, **C**(7)H), 105.6 (d, $^2J_{(C,F)}$ = 23 Hz, **C**(5)H), 101.4 (**C**(3)H), 64.0 (**C**(12)H_2), 25.7 (**C**(11)H_3), 14.4 (**C**(13)H_3) ppm; ^{19}F NMR (376 MHz, $CDCl_3$) δ: -116 ppm; HRMS (ESI-TOF) *m/z*: $[M+H]^+$ calcd for $C_{12}H_{13}FNO$: 206.0976; found: 206.0972.

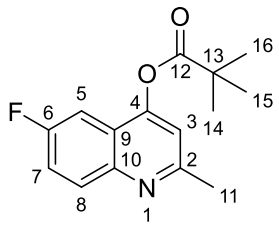
6-Fluoro-2-methylquinolin-4-yl acetate (137)

A Schlenk tube was oven dried (150 °C) and cooled under vacuum. The flask was refilled with nitrogen and **128** (0.177 g, 1.0 mmol, 1.0 equiv.) was suspended DCM (2 mL). The suspension was cooled over ice and *N*-methylmorpholine (0.13 mL, 1.2 mmol, 1.2 equiv.) was added. The resulting solution was stirred at this temperature for 10 min before the dropwise addition of acetyl chloride (0.09 mL, 1.2 mmol, 1.2 1.2 equiv.); the mixture was then allowed to stir at r.t. for 18 h.[91] The reaction was quenched with H_2O (15 mL) and extracted with DCM (3 × 10 mL). The combined organic layers were then washed with brine (15 mL), dried over $MgSO_4$, filtered and concentrated under reduced pressure to yield **137** as a pale yellow solid (0.180 g, 82%); m.p. 75–78 °C; IR (film) ν_{max} 1642 (C=O stretch), 1615 (C=N stretch), 1577 (aromatic C=C stretch), 1202, 1133 (ester C-O stretch), 1038 (C-F stretch) cm^{-1}; ^{1}H



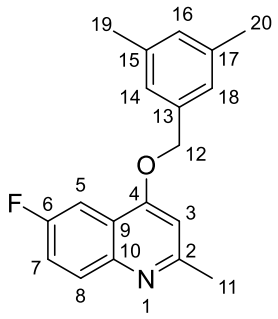
NMR (400 MHz, $CDCl_3$) δ: 8.20–7.98 (m, 1H, C(8)**H**), 7.62–7.42 (m, 2H, C(5)**H**, C(7)**H**), 7.25 (s, 1H, C(3)**H**), 2.75 (s, 3H, C(11)**H_3**), 2.48 (s, 3H, C(13)**H_3**) ppm; ^{13}C NMR (100 MHz, $CDCl_3$) δ: 168.0 (q**C**-12), 160.3 (d, $^1J_{(C,F)}$ = 246 Hz, q**C**(6)F), 159.1 (q**C**-2), 153.7 (d, $^4J_{(C,F)}$ = 5 Hz, q**C**-4), 146.3 (q**C**-10), 131.1 (d, $^3J_{(C,F)}$ = 9 Hz, **C**(8)H), 121.3 (d, $^3J_{(C,F)}$ = 10 Hz, q**C**-9), 120.3 (d, $^2J_{(C,F)}$ = 26 Hz, **C**(7)H), 114.2 (**C**(3)H), 104.9 (d, $^2J_{(C,F)}$ = 24 Hz, **C**(5)H), 25.3 (**C**(11)H_3), 21.2 (**C**(13)H_3) ppm; ^{19}F NMR (282 MHz, $CDCl_3$) δ: -113 ppm; HRMS (ESI-TOF) *m/z*: $[M\text{-}Ac]^+$ calcd for $C_{10}H_9FNO$: 178.0663; found: 178.0664.

6-Fluoro-2-methylquinolin-4-yl pivalate (138)



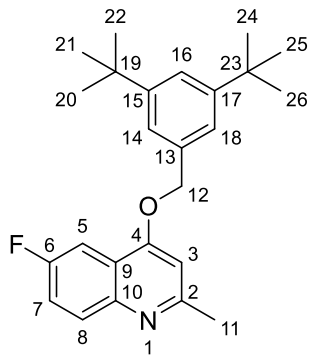
A Schlenk tube was heated under vacuum, cooled to r.t. and refilled once with nitrogen, **128** (0.354 g, 2.0 mmol, 1.0 equiv.) and DMAP (0.049 g, 0.4 mmol, 20 mol%) were added and the flask was refilled twice more with nitrogen. Dry DCM (3.6 mL) and NEt_3 (0.42 mL, 3.0 mmol, 1.5 equiv.) were added *via* syringe and the mixture cooled over ice. Pivaloyl chloride (0.29 mL, 2.4 mmol, 1.2 equiv.) was then added dropwise and the resulting mixture was stirred at 0° C for 10 min and then at r.t. for 18 h. The solution was then concentrated under reduced pressure, taken up in DCM (10 mL) and sat. NH_4Cl (10 mL) and the layers were seperated and the aqueous layer was extracted with DCM (2 × 10 mL).[92] The combined organic layers were then washed with H_2O (10 mL), and brine (15 mL), dried over $MgSO_4$, filtered and concentrated under reduced pressure to yield **138** as a beige solid (0.486 g, 93%); m.p. 74–75 °C; IR (film) ν_{max} 1760 (C=O stretch), 1614 (C=N stretch), 1564 (aromatic C=C stretch), 1231, 1102 (C-O stretches), 1026 (C-F stretch) cm^{-1}; ^{1}H NMR (400 MHz, $CDCl_3$) δ: 8.12 (dd, *J* = 8.7 Hz, $^4J_{(H,F)}$ = 5.0 Hz, 1H, C(8)**H**), 7.60–7.42 (m, 2H, C(5)**H**, C(7)**H**), 7.24 (s, 1H, C(3)**H**), 2.77 (s, 3H, C(11)**H_3**), 1.49 (s, 9H, C(14)**H_3**, C(15)**H_3**, C(16)**H_3**) ppm; ^{13}C NMR (75 MHz, $CDCl_3$) δ: 175.7 (q**C**-12), 160.2 (d, $^1J_{(C,F)}$ = 248 Hz, q**C**(6)F), 159.1 (d, $^6J_{(C,F)}$ = 3 Hz, q**C**-2), 154.0 (d, $^4J_{(C,F)}$ = 6 Hz, q**C**-4), 146.6 (q**C**-10), 131.4 (d, $^3J_{(C,F)}$ = 9 Hz, **C**(8)H), 121.6 (d, $^3J_{(C,F)}$ = 10 Hz, q**C**-9), 120.1 (d, $^2J_{(C,F)}$ = 26 Hz, **C**(7)H), 114.1 (**C**(3)H), 104.7 (d, $^2J_{(C,F)}$ = 24 Hz, **C**(5)H), 39.8 (q**C**-13), 27.2 (3 × C, **C**(14)H_3, **C**(15)H_3, **C**(16)H_3), 25.4 (**C**(11)H_3) ppm; ^{19}F NMR (282 MHz, $CDCl_3$) δ: -113 ppm; HRMS (ESI-TOF) *m/z*: $[M+H]^+$ calcd for $C_{15}H_{17}FNO_2$: 262.1238; found: 262.1242.

4-((3,5-Dimethylbenzyl)oxy)-6-fluoro-2-methylquinoline (139)



To a solution of **128** (0.266 g, 1.5 mmol, 1.0 equiv.) in DMF (30 mL) was added K_2CO_3 (0.415 g, 3.0 mmol, 2.0 equiv.). The mixture was stirred at 40 °C for 1 h before the portion-wise addition of 3,5-dimethylbenzyl bromide (0.358 g, 1.8 mmol, 1.2 equiv.), and the resulting suspension was heated to 60 °C for 16 h. The mixture was poured onto ice water and extracted with EtOAc (3 × 20 mL). The combined organic layers were washed with H_2O (2 × 20 mL), dried over $MgSO_4$, filtered and concentrated under 8:2) reduced pressure.[93] Purification *via* column chromatography (DCM 100 to DCM:EtOAc 90:10) to yield **139** as a white solid (0.373 g, 84%); m.p. 93–95 °C; IR (film) ν_{max} 1604 (C=N stretch), 1514, 1478 (aromatic C=C stretch), 1348, 1185 (ether C-O stretch), 1083 (C-F stretch) cm^{-1}; ^1H NMR (500 MHz, $CDCl_3$) δ: 7.94 (dd, *J* = 9.2 Hz, $^4J_{(H,F)}$ = 5.2 Hz, 1H, C(8)**H**), 7.79 (dd, $^3J_{(H,F)}$ = 9.5 Hz, *J* = 2.9 Hz, 1H, C(5)**H**), 7.41 (ddd, *J* = 9.2, 2.9 Hz, $^3J_{(H,F)}$ = 8.2 Hz, 1H, C(7)**H**), 7.08 (s, 2H, C(14)**H**, C(18)**H**), 7.02 (bs, 1H, C(16)**H**), 6.70 (s, 1H, C(3)**H**), 5.17 (s, 2H, C(12)$\mathbf{H_2}$), 2.68 (s, 3H, C(11)$\mathbf{H_3}$), 2.36 (s, 6H, C(19)$\mathbf{H_3}$, C(20)$\mathbf{H_3}$) ppm; ^{13}C NMR (125 MHz, $CDCl_3$) δ: 161.1 (d, $^4J_{(C,F)}$ = 5 Hz, q**C**-4), 159.7 (d, $^1J_{(C,F)}$ = 245 Hz, q**C**(6)F), 159.3 (d, $^6J_{(C,F)}$ = 2 Hz, q**C**-2), 145.8 (q**C**-10), 138.5 (2 × C, q**C**-15, q**C**-17), 135.4 (q**C**-13), 130.4 (d, $^3J_{(C,F)}$ = 9 Hz, **C**(8)H), 130.2 (**C**(16)H), 125.4 (2 × C, **C**(14)H, **C**(18)H), 120.6 (d, $^3J_{(C,F)}$ = 10 Hz, q**C**-9), 119.6 (d, $^2J_{(C,F)}$ = 25 Hz, **C**(7)H), 105.8 (d, $^2J_{(C,F)}$ = 23 Hz, **C**(5)H), 102.0 (**C**(3)H), 70.5 (**C**(12)H_2), 25.8 (**C**(11)H_3), 21.3 (2 × C, **C**(19)H_3, **C**(20)H_3) ppm; ^{19}F NMR (470 MHz, $CDCl_3$) δ: -115 ppm; HRMS (ESI-TOF) *m/z*: $[M+H]^+$ calcd for $C_{19}H_{19}FNO$: 296.1445; found: 296.1451.

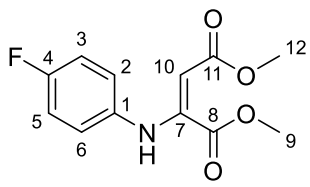
4-((3,5-Di-*tert*-butylbenzyl)oxy)-6-fluoro-2-methylquinoline (140)



Compound **140** was prepared *via* the procedure described for **139** using 3,5-di-*tert*-butyl benzyl bromide (0.340 g, 1.2 mmol, 1.2 equiv.) to yield **140** as a white solid (0.321 g, 85%); m.p. 150–153 °C; IR (film) ν_{max} 1603 (C=N stretch), 1512, 1479 (aromatic C=C stretch), 1349, 1192 (ether C-O stretch), 1088 (C-F stretch) cm^{-1}; ^1H NMR (400 MHz, $CDCl_3$) δ: 7.94 (dd, *J* = 9.2 Hz, $^4J_{(H,F)}$ = 5.2 Hz, 1H, C(8)**H**), 7.79 (dd,

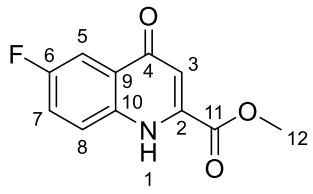
$^{3}J_{(H,F)}$ = 9.5 Hz, *J* = 2.8 Hz, 1H, C(5)**H**), 7.53–7.29 (m, 4H, C(7)**H**, C(14)**H**, C(16)**H**, C(18)**H**), 6.78 (s, 1H, C(3)**H**), 5.23 (s, 2H, C(12)**H₂**), 2.70 (s, 3H, C(11)**H₃**), 1.37 (s, 18H, C(20)**H₃**, C(21)**H₃**, C(22)**H₃**, C(24)**H₃**, C(25)**H₃**, C(26)**H₃**) ppm; ^{13}C NMR (100 MHz, $CDCl_3$) δ: 161.2 (d, $^{4}J_{(C,F)}$ = 5 Hz, q**C**-4), 159.7 (d, $^{1}J_{(C,F)}$ = 245 Hz, q**C**(6)F), 159.4 (d, $^{6}J_{(C,F)}$ = 2 Hz, q**C**-2), 151.4 (2 × C, q**C**-15, q**C**-17), 145.8 (q**C**-10), 134.6 (q**C**-13), 130.4 (d, $^{3}J_{(C,F)}$ = 9 Hz, **C**(8)H), 122.7 (**C**(16)H), 122.2 (2 × C, **C**(14)H, **C**(18)H), 120.6 (d, $^{3}J_{(C,F)}$ = 10 Hz, q**C**-9), 119.6 (d, $^{2}J_{(C,F)}$ = 25 Hz, **C**(7)H), 105.9 (d, $^{2}J_{(C,F)}$ = 23 Hz, **C**(5)H), 102.1 (**C**(3)H), 71.2 (**C**(12)H_2), 34.9 (2 × C, q**C**-19, q**C**-23), 31.5 (6 × C, **C**(20)H_3, **C**(21)H_3, **C**(22)H_3, **C**(24)H_3, **C**(25)H_3, **C**(26)H_3), 25.7 (**C**(11)H_3) ppm; ^{19}F NMR (376 MHz, $CDCl_3$) δ: -115 ppm; HRMS (ESI-TOF) *m/z*: $[M+H]^+$ calcd for $C_{25}H_{31}FNO$: 380.2384; found: 380.2375.

Dimethyl 2-((4-fluorophenyl)amino)maleate (141)



An equimolar solution of 4-fluoroaniline (0.47 mL, 5.0 mmol, 1.0 equiv.) and dimethyl acetylene dicarboxylate (0.61 mL, 5.0 mmol, 1.0 equiv.) in MeOH (18 mL) was heated to 80 °C for 20 h. The mixture was cooled to r.t. and concentrated under reduced pressure. The residue was dissolved in DCM (20 mL) and washed with 1 M HCl (10 mL) and brine (10 mL), dried over $MgSO_4$, filtered and concentrated under reduced pressure to yield **141** as a yellow oil (1.169 g, 92%); IR (film) ν_{max} 3308 (N-H stretch), 1726 (C=O stretch), 1603 (C=C stretch), 1509 (aromatic C=C stretch), 1276, 1142 (ester C-O stretches), 1028 (C-F stretch) cm^{-1}; ^{1}H NMR (300 MHz, $CDCl_3$) δ: 9.58 (bs, 1H, N**H**), 7.03–6.94 (m, 2H, C(2)**H**, C(6)**H**), 6.93–6.84 (m, 2H, C(3)**H**, C(5)**H**), 5.40 (s, 1H, C(10)**H**), 3.74 (s, 3H, C(12)**H₃**), 3.68 (s, 3H, C(9)**H₃**) ppm; ^{13}C NMR (75 MHz, $CDCl_3$) δ: 169.9 (q**C**-11), 164.5 (q**C**-8), 159.8 (d, $^{1}J_{(C,F)}$ = 244 Hz, q**C**(4)F), 148.2 (q**C**-7), 136.5 (d, $^{4}J_{(C,F)}$ = 3 Hz, q**C**-1), 122.9 (2 × C, d, $^{3}J_{(C,F)}$ = 8 Hz, **C**(2)H, **C**(6)H), 115.9 (2 × C, d, $^{2}J_{(C,F)}$ = 23 Hz, **C**(3)H, **C**(5)H), 93.4 (**C**(10)H), 52.7 (**C**(9)H_3), 51.1 (**C**(12)H_3) ppm; ^{19}F NMR (282 MHz, $CDCl_3$) δ: -118 ppm; HRMS (ESI-TOF) *m/z*: $[M+H]^+$ calcd for $C_{12}H_{13}FNO_4$: 254.0823; found: 254.0819.

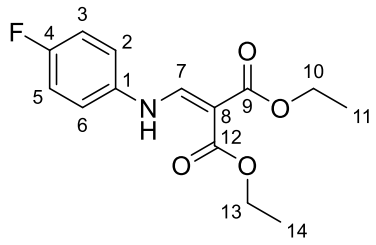
Methyl 6-fluoro-4-oxo-1,4-dihydroquinoline-2-carboxylate (142)[160]



A solution of **141** (0.702 g, 2.77 mmol, 1.0 equiv.) in Ph_2O (5 mL) was added dropwise to refluxing (>260 °C) Ph_2O (15 mL) and left to cyclise at this temperature in a DrySyn heating block for 1 h. After cooling to r.t., Et_2O (50 mL) was added. The resulting precipitate was collected by suction filtration, washed with Et_2O and hexanes to yield **142** as a beige solid (0.403 g, 66%); m.p. 250–251 °C (lit.[160] 250–251 °C); ^{1}H NMR (300 MHz, $(CD_3)_2SO$) δ: 12.22 (bs, 1H, N**H**), 8.02 (dd, *J* = 9.0 Hz, $^4J_{(H,F)}$ = 4.6 Hz, 1H, C(8)**H**), 7.85–7.48 (m, 2H, C(5)**H**), C(7)**H**), 6.61 (s, 1H, C(3)**H**), 3.97 (s, 3H, C(12)**H₃**) ppm; ^{13}C NMR (75 MHz, $(CD_3)_2SO$) δ: 176.8 (d, $^4J_{(C,F)}$ = 3 Hz, q**C**-4), 162.5 (q**C**-11), 158.8 (d, $^1J_{(C,F)}$ = 243 Hz, q**C**(6)F), 137.8 (q**C**-2), 136.7 (q**C**-10), 127.1 (d, $^3J_{(C,F)}$ = 5 Hz, q**C**-9), 122.5 (d, $^3J_{(C,F)}$ = 7 Hz, **C**(8)H), 121.6 (d, $^2J_{(C,F)}$ = 25 Hz, **C**(7)H), 109.2 (**C**(3)H), 108.6 (d, $^2J_{(C,F)}$ = 22 Hz, **C**(5)H), 53.5 (**C**(12)H_3) ppm; ^{19}F NMR (282 MHz, $(CD_3)_2SO$) δ: -117 ppm; *m/z* (ES+): 222 ($(M+H)^+$ 100%).

Spectral characteristics were consistent with previously reported data.[160]

Diethyl 2-[(4-fluorophenylamino)methylene]malonate (143)[161]

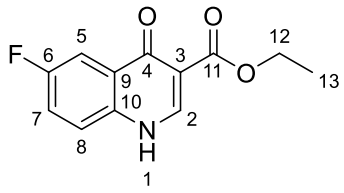


An equimolar solution of 4-fluoroaniline (1.71 mL, 18 mmol, 1.0 equiv.) and diethyl ethoxymethylenemalonate (3.64 mL, 18 mmol, 1.0 equiv.) was heated to 90 °C for 2.5 h. The mixture was cooled to r.t., concentrated under reduced pressure. The residue was dissolved in DCM (20 mL) and washed with 1 M HCl (10 mL) and brine (10 mL), dried over $MgSO_4$, filtered and concentrated under reduced pressure to yield **143** as a white crystalline solid (4.675 g, 92%); m.p. 64–65 °C (lit.[161] 69–70 °C); ^{1}H NMR (300 MHz, $CDCl_3$) δ: 11.00 (bd, *J* = 13.3 Hz, 1H, N**H**), 8.43 (d, *J* = 13.6 Hz, 1H, C(7)**H**), 7.21–6.96 (m, 4H, C(2)**H**, C(3)**H**, C(5)**H**, C(6)**H**), 4.50–4.08 (m, 4H, C(10)**H₂**, C(13)**H₂**), 1.52–1.18 (m, 6H, C(11)**H₃**, C(14)**H₃**) ppm; ^{13}C NMR (75 MHz, $CDCl_3$) δ: 169.1, 165.7 (q**C**-9, q**C**-12), 160.0 (d, $^1J_{(C,F)}$ = 245 Hz, q**C**(4)F), 152.1 (**C**(7)H), 135.6 (q**C**-1), 118.9 (2 × C, d, $^3J_{(C,F)}$ = 8 Hz, **C**(2)H, **C**(6)H), 116.6 (2 × C, d, $^2J_{(C,F)}$ = 23 Hz, **C**(3)H, **C**(5)H),

93.6 (q**C**-8), 60.4, 60.1 (**C**(10)H_2, **C**(13)H_2), 14.4, 14.3 (**C**(11)H_3, **C**(14)H_3) ppm; ^{19}F NMR (282 MHz, $CDCl_3$) δ: -118 ppm; *m/z* (ES-): 280 ($(M-H)^-$ 56%).

Spectral characteristics were consistent with previously reported data.[161]

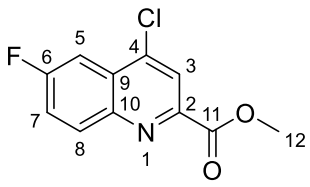
Ethyl 6-fluoro-4-oxo-1,4-dihydroquinoline-3-carboxylate (144)[161]



Compound **144** was prepared *via* the procedure described for **142** using **143** (1.41 g, 5.0 mmol, 1.0 equiv.) to yield **144** as a white solid (0.691 g, 59%); m.p. >250 °C (lit.[161] 296–298 °C); ^{1}H NMR (600 MHz, $(CD_3)_2SO$) δ: 8.59 (s, 1H, C(2)**H**), 7.80 (dd, $^3J_{(H,F)}$ = 9.3 Hz, *J* = 2.9 Hz, 1H, C(5)**H**), 7.71 (dd, *J* = 9.0 Hz, $^4J_{(H,F)}$ = 4.6 Hz, 1H, C(8)**H**), 7.62 (td, $^3J_{(H,F)}$ = 8.8 Hz, *J* = 2.9 Hz, 1H, C(7)**H**), 4.22 (q, *J* = 7.1 Hz, 2H, C(12)**H_2**), 1.28 (t, *J* = 7.1 Hz, 3H, C(13)**H_3**) ppm; ^{13}C NMR (150 MHz, $(CD_3)_2SO$) δ: 172.6 (q**C**-4), 164.9 (q**C**-11), 159.2 (d, $^1J_{(C,F)}$ = 243 Hz, q**C**(6)F), 145.3 (**C**(2)H), 136.1 (q**C**-10), 128.8 (d, $^3J_{(C,F)}$ = 7 Hz, q**C**-9), 122.0 (d, $^3J_{(C,F)}$ = 8 Hz, **C**(8)H), 121.0 (d, $^2J_{(C,F)}$ = 25 Hz, **C**(7)H), 110.0 (d, $^2J_{(C,F)}$ = 23 Hz, **C**(5)H), 109.0 (q**C**-3), 59.7 (**C**(12)H_2), 14.4 (**C**(13)H_3) ppm; ^{19}F NMR (282 MHz, $(CD_3)_2SO$) δ: -116 ppm; *m/z* (ES-): 234 ($(M-H)^-$ 100%).

Spectral characteristics were consistent with previously reported data.[161]

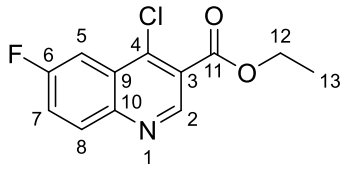
Methyl 4-chloro-6-fluoroquinoline-2-carboxylate (145)



Compound **145** was prepared *via* the procedure described for **132** using **142** (0.221 g, 1.0 mmol, 1.0 equiv.) to yield **145** as a white solid (0.230 g, 96%); m.p. 140–141 °C; IR (film) ν_{max} 1751 (C=O stretch), 1623 (C=N stretch), 1558 (aromatic C=C stretch), 1208, 1104 (ester C-O stretches), 1006 (C-F stretch), 831 (C-Cl stretch) cm^{-1}; ^{1}H NMR (300 MHz, $CDCl_3$) δ: 8.42–8.25 (m, 2H, C(3)**H**, C(8)**H**), 7.89 (dd, $^3J_{(H,F)}$ = 9.2 Hz, *J* = 2.8 Hz, 1H, C(5)**H**), 7.62 (ddd, *J* = 9.2, 2.8 Hz, $^3J_{(H,F)}$ = 8.0 Hz, 1H, C(7)**H**), 4.09 (s, 3H, C(12)**H_3**) ppm; ^{13}C NMR (75 MHz, $CDCl_3$) δ: 164.8 (q**C**-11), 162.5 (d, $^1J_{(C,F)}$ = 254 Hz, q**C**(6)F), 147.1 (d, $^6J_{(C,F)}$ = 3 Hz, q**C**-2), 145.3 (q**C**-10), 143.1 (d, $^4J_{(C,F)}$ = 6 Hz, q**C**(4)Cl), 134.0 (d, $^3J_{(C,F)}$ = 10 Hz, **C**(8)H), 128.8 (d, $^3J_{(C,F)}$ = 11 Hz, q**C**-9), 121.9 (**C**(3)H), 121.8 (d, $^2J_{(C,F)}$ = 26 Hz, **C**(7)H), 108.0 (d, $^2J_{(C,F)}$ = 25 Hz, **C**(5)H), 53.5 (**C**(12)H_3)

ppm; ^{19}F NMR (282 MHz, $CDCl_3$) δ: -107 ppm; HRMS (ESI-TOF) *m/z*: $[M+H]^+$ calcd for $C_{11}H_8ClFNO_2$: 240.0222; found: 240.0221.

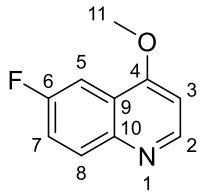
Ethyl 4-chloro-6-fluoroquinoline-3-carboxylate (146)[162]



Compound **146** was prepared *via* the procedure described for **132** using **144** (0.353 g, 1.5 mmol, 1.0 equiv.) to yield **146** as a white solid (0.352 g, 93%); m.p. 67–69 °C (lit.[163] 62–63 °C); ^{1}H NMR (600 MHz, $CDCl_3$) δ: 9.16 (s, 1H, C(2)**H**), 8.17 (dd, *J* = 9.2 Hz, $^4J_{(H,F)}$ = 5.3 Hz, 1H, C(8)**H**), 8.03 (dd, $^3J_{(H,F)}$ = 9.6 Hz, *J* = 2.7 Hz, 1H, C(5)**H**), 7.62 (ddd, *J* = 9.2, 2.8 Hz, $^3J_{(H,F)}$ = 7.9 Hz, 1H, C(7)**H**), 4.51 (q, *J* = 7.1 Hz, 2H, C(12)**H$_2$**), 1.47 (q, *J* = 7.1 Hz, 3H, C(13)**H$_3$**) ppm; ^{13}C NMR (150 MHz, $CDCl_3$) δ: 163.7 (q**C**-11), 161.1 (d, $^1J_{(C,F)}$ = 251 Hz, q**C**(6)F), 148.8 (**C**(2)H), 145.9 (q**C**-10), 142.1 (d, $^4J_{(C,F)}$ = 6 Hz, q**C**(4)Cl), 131.9 (d, $^3J_{(C,F)}$ = 9 Hz, **C**(8)H), 126.9 (d, $^3J_{(C,F)}$ = 7 Hz, q**C**-9), 123.1 (q**C**-3), 121.7 (d, $^2J_{(C,F)}$ = 26 Hz, **C**(7)H), 108.7 (d, $^2J_{(C,F)}$ = 25 Hz, **C**(5)H), 61.7 (**C**(12)H_2), 13.7 (**C**(13)H_3) ppm; ^{19}F NMR (282 MHz, $CDCl_3$) δ: -109 ppm; *m/z* (ES+): 254 ($(M+H)^+$ 100%).

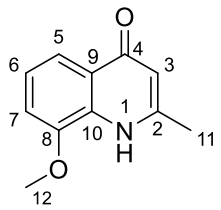
Spectral characteristics were consistent with previously reported data.[162]

6-Fluoro-4-methoxyquinoline (148)



Compound **148** was prepared *via* the general procedure described for **135** using 4-chloro-6-fluoroquinoline **147** (0.320 g, 1.76 mmol, 1.0 equiv.) to yield **148** as a white solid (0.295 g, 95%); m.p. 50–53 °C; IR (film) ν_{max} 1631 (C=N stretch), 1598 (aromatic C=C stretch), 1309, 1189 (ether C-O stretch), 1069 (C-F stretch) cm^{-1}; ^{1}H NMR (500 MHz, $CDCl_3$) δ: 8.71 (d, *J* = 5.0 Hz, 1H, C(2)**H**), 8.02 (dd, *J* = 9.2 Hz, $^4J_{(H,F)}$ = 5.3 Hz, 1H, C(8)**H**), 7.77 (dd, $^3J_{(H,F)}$ = 9.5 Hz, *J* = 2.9 Hz, 1H, C(5)**H**), 7.44 (ddd, *J* = 9.2, 2.9 Hz, $^3J_{(H,F)}$ = 8.2 Hz, 1H, C(7)**H**), 6.73 (d, *J* = 5.1 Hz, 1H, C(3)**H**), 4.02 (s, 3H, C(11)**H$_3$**) ppm; ^{13}C NMR (125 MHz, $CDCl_3$) δ: 162.0 (d, $^4J_{(C,F)}$ = 5 Hz, q**C**-4), 160.2 (d, $^1J_{(C,F)}$ = 247 Hz, q**C**(6)F), 150.7 (d, $^6J_{(C,F)}$ = 2 Hz, **C**(2)H), 146.3 (q**C**-10), 131.4 (d, $^3J_{(C,F)}$ = 9 Hz, **C**(8)H), 122.2 (d, $^3J_{(C,F)}$ = 10 Hz, q**C**-9), 119.8 (d, $^2J_{(C,F)}$ = 26 Hz, **C**(7)H), 105.8 (d, $^2J_{(C,F)}$ = 24 Hz, **C**(5)H), 100.5 (**C**(3)H), 55.8 (**C**(11)H_3) ppm; ^{19}F NMR (282 MHz, $CDCl_3$) δ: -114 ppm; HRMS (ESI-TOF) *m/z*: $[M+H]^+$ calcd for $C_{10}H_9FNO$: 178.0663; found: 178.0658.

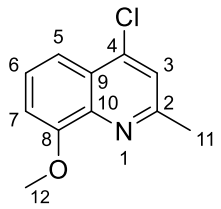
8-Methoxy-2-methylquinolin-4(1*H*)-one (149)[164]



Compound **149** was prepared *via* the procedure described for **128** using *o*-anisidine (0.90 mL, 8.0 mmol, 1.0 equiv.) to yield **149** as a white solid (0.441 g, 29%); m.p. 232–235 °C (lit.[164] 238–239 °C); ^{1}H NMR (600 MHz, $(CD_3)_2SO$) δ: 11.01 (bs, 1H, N**H**), 7.63–7.57 (m, 1H, C(5)**H**), 7.31–7.10 (m, 2H, C(6)**H**, C(7)**H**), 5.91 (s, 1H, C(3)**H**), 3.97 (s, 3H, C(12)**H₃**), 2.36 (s, 3H, C(11)**H₃**) ppm; ^{13}C NMR (150 MHz, $(CD_3)_2SO$) δ: 176.5 (q**C**-4), 149.7 (q**C**-2), 148.3 (q**C**-8), 130.9 (q**C**-10), 125.5 (q**C**-9), 122.5 (**C**(6)H), 116.1 (**C**(5)H), 111.0 (**C**(7)H), 109.1 (**C**(3)H), 56.1 (**C**(12)H_3), 19.7 (**C**(11)H_3) ppm; *m/z* (ES+): 190 ($(M+H)^+$ 100%).

Spectral characteristics were consistent with previously reported data.[164]

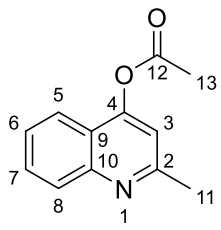
4-Chloro-8-methoxy-2-methylquinoline (150)[165]



Compound **150** was prepared *via* the procedure described for **132** using **149** (0.284 g, 1.5 mmol, 1.0 equiv.) to yield **150** as a white solid (0.249 g, 80%); m.p. 86–88 °C (lit.[165] 88–88.5°C); ^{1}H NMR (400 MHz, $CDCl_3$) δ: 7.75 (dd, *J* = 8.5, 0.9 Hz, 1H, C(5)**H**), 7.53–7.38 (m, 2H, C(3)**H**, C(6)**H**), 7.08 (d, *J* = 7.7 Hz, 1H, C(7)**H**), 4.08 (s, 3H, C(12)**H₃**), 2.77 (s, 3H, C(11)**H₃**) ppm; ^{13}C NMR (100 MHz, $CDCl_3$) δ: 157.8 (q**C**-2), 154.9 (q**C**-8), 142.5 (q**C**-4), 140.5 (q**C**-10), 126.7 (**C**(6)H), 125.8 (q**C**-9), 122.7 (**C**(3)H), 115.7 (**C**(5)H), 108.5 (**C**(7)H), 56.2 (**C**(12)H_3), 25.5 (**C**(11)H_3) ppm; *m/z* (ES+): 208 ($(M+H)^+$ 100%).

Spectral characteristics were consistent with previously reported data.[165]

2-Methylquinolin-4-yl acetate (151)[166]

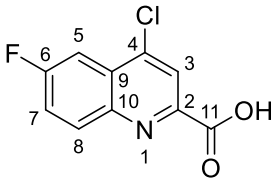


Compound **151** was prepared *via* the procedure described for **137** using **121** (0.284 g, 1.5 mmol, 1.0 equiv.) to yield **151** as an orange oil (0.169 g, 84%); ^{1}H NMR (400 MHz, $CDCl_3$) δ: 8.07 (d, *J* = 8.5 Hz, 1H, C(8)**H**), 7.89 (d, *J* = 8.3 Hz, 1H, C(5)**H**), 7.72 (ddd, *J* = 8.3, 7.0, 1.3 Hz, 1H, C(7)**H**), 7.58–7.45 (m, 1H, C(6)**H**), 7.21 (s, 1H, C(3)**H**), 2.76 (s, 3H, C(11)**H₃**), 2.48 (s, 3H, C(13)**H₃**) ppm; ^{13}C NMR (100 MHz, $CDCl_3$) δ: 168.2 (q**C**-12), 159.8 (q**C**-2), 154.2 (q**C**-4), 149.2 (q**C**-10), 130.2 (**C**(7)H), 129.5 (**C**(8)H), 126.1 (**C**(6)H), 121.0 (**C**(5)H), 120.6 (q**C**-9), 113.6 (**C**(3)H), 25.5 (**C**(11)H_3), 21.2 (**C**(13)H_3) ppm.

Note: Compound **151** proved to be unstable and only starting material **121** was observed by mass spectrometry from the cleavage of the acetyl group.

Spectral characteristics were consistent with previously reported data.[166]

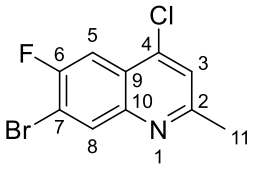
4-Chloro-6-fluoroquinoline-2-carboxylic acid (152)



To a solution of $LiOH.H_2O$ (0.168 g, 4.0 mmol, 8.0 equiv.) in H_2O (4.5 mL) was added a solution of **145** (0.112 g, 0.5 mmol, 1.0 equiv.) in MeOH (13.6 mL) and the resulting mixture was stirred at r.t. for 3 h. The reaction mixture was concentrated under reduced pressure, diluted with H_2O (10 mL) and acidified using 6 M HCl. The aqueous mixture was extracted with EtOAc (2 × 10 mL) and combined organic layers were then washed with brine (15 mL), dried over $MgSO_4$, filtered and concentrated under reduced pressure to yield **152** as a beige solid (0.091 g, 81%); m.p. 157–160 °C; IR (film) ν_{max} 2922 (O-H stretch), 1684 (C=O stretch), 1627 (C=N stretch), 1587 (aromatic C=C stretch), 1224 (acid C-O stretch), 1041 (C-F stretch), 854 (C-Cl stretch) cm^{-1}; ^1H NMR (400 MHz, $CDCl_3$) δ: 8.38 (s, 1H, C(3)**H**), 8.23 (dd, J = 9.0 Hz, $^4J_{(H,F)}$ = 5.2 Hz, 1H, C(8)**H**), 7.95 (d, $^3J_{(H,F)}$ = 9.0 Hz, 1H, C(5)**H**), 7.79–7.60 (m, 1H, C(7)**H**) ppm; ^{13}C NMR (100 MHz, $CDCl_3$) δ: 163.2 (q**C**-11), 162.8 (d, $^1J_{(C,F)}$ = 255 Hz, q**C**(6)F), 145.5 (d, $^6J_{(C,F)}$ = 3 Hz, q**C**-2), 144.7 (d, $^4J_{(C,F)}$ = 6 Hz, q**C**(4)Cl), 143.8 (q**C**-10), 132.9 (d, $^3J_{(C,F)}$ = 9 Hz, **C**(8)H), 129.4 (d, $^3J_{(C,F)}$ = 11 Hz, q**C**-9), 122.5 (d, $^2J_{(C,F)}$ = 26 Hz, **C**(7)H), 120.3 (**C**(3)H), 108.6 (d, $^2J_{(C,F)}$ = 25 Hz, **C**(5)H) ppm; ^{19}F NMR (282 MHz, $CDCl_3$) δ: -105 ppm; HRMS (ESI-TOF) *m/z*: $[M+H]^+$ calcd for $C_{10}H_6ClFNO_2$: 226.0066; found: 226.0061.

3.18. Borylation and Dervitisation of Quinoline Substrates

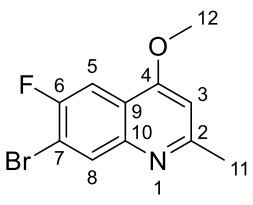
7-Bromo-4-chloro-6-fluoro-2-methylquinoline (159)



A 15 mL Schlenk tube was oven dried (150 °C) and cooled under vacuum. The flask was refilled with nitrogen and all reagents were added under a positive pressure of nitrogen in the order: **132** (0.039 g, 0.2 mmol, 1.0 equiv.), dtbpy (1.6 mg, 0.006 mmol, 3 mol%), B_2pin_2 (0.056 g, 0.22 mmol, 1.1 equiv.), and $[Ir(OMe)COD]_2$ (2.0 mg, 0.003 mmol, 1.5 mol%). The Schlenk tube was then placed under vacuum

for 20 min before being refilled with nitrogen three times. THF (0.5 mL) was added *via* syringe, the reaction was sealed, and the mixture heated to 80 °C for 16 h, then cooled to r.t. and concentrated under reduced pressure. An internal standard, 1,3,5-trimethoxybenzene (~10 mol%) was added to the residue to determine the yield of C7-borylated product **133** by ^{1}H NMR analysis. The residue was redissolved in MeOH (4 mL) and a solution of $CuBr_2$ (0.156 g, 0.7 mmol, 3.5 equiv.) in H_2O (4 mL) was added. The reaction mixture was heated to 80 °C for 3 h, cooled to r.t. diluted with 10% NH_4OH (4 mL) and then extracted with Et_2O (3 × 10 mL). The combined organic layers were washed with H_2O (10 mL) and brine (10 mL), dried over $MgSO_4$, filtered and concentrated under reduced pressure. Purification *via* column chromatography (DCM 100 to DCM:EtOAc 95:5) to yield **159** as a white solid (0.052 g, 95%); m.p. 100–101 °C; IR (film) ν_{max} 1612 (C=N stretch), 1588 (aromatic C=C stretch), 1016 (C-F stretch), 845 (C-Cl stretch), 707 (C-Br stretch) cm^{-1}; ^{1}H NMR (600 MHz, $CDCl_3$) δ: 8.27 (d, $^{4}J_{(H,F)}$ = 6.6 Hz, 1H, C(8)**H**), 7.81 (d, $^{3}J_{(H,F)}$ = 9.0 Hz, 1H, C(5)**H**), 7.40 (s, 1H, C(3)**H**), 2.70 (s, 3H, C(11)**H$_3$**) ppm; ^{13}C NMR (150 MHz, $CDCl_3$) δ: 158.8 (d, $^{6}J_{(C,F)}$ = 3 Hz, q**C**-2), 156.2 (d, $^{1}J_{(C,F)}$ = 250 Hz, q**C**(6)F), 145.2 (d, $^{4}J_{(C,F)}$ = 1 Hz, q**C**-10), 141.0 (d, $^{4}J_{(C,F)}$ = 5 Hz, q**C**(4)Cl), 133.6 (d, $^{3}J_{(C,F)}$ = 1 Hz, **C**(8)H), 124.2 (d, $^{3}J_{(C,F)}$ = 9 Hz, q**C**-9), 122.2 (**C**(3)H), 113.7 (d, $^{2}J_{(C,F)}$ = 24 Hz, q**C**(7)Br), 108.1 (d, $^{2}J_{(C,F)}$ = 26 Hz, **C**(5)H), 24.5 (**C**(11)H$_3$) ppm; ^{19}F NMR (282 MHz, $CDCl_3$) δ: -108 ppm; HRMS (ESI-TOF) *m/z*: $[M+H]^+$ calcd for $C_{10}H_7BrClFN$: 273.9429; found: 273.9424.

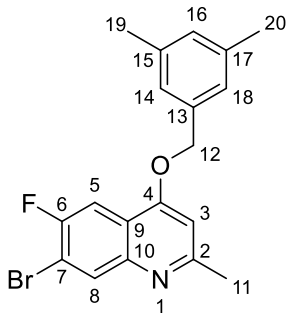
7-Bromo-6-fluoro-4-methoxy-2-methylquinoline (160)



Compound **160** was prepared *via* the procedure described for **159** using **135** (0.050 g, 0.2 mmol, 1.0 equiv.) to yield **160** as a white solid (0.051 g, 94%); m.p. 113–115 °C; IR (film) ν_{max} 1612 (C=N stretch), 1588 (aromatic C=C stretch), 1352, 1203 (ether C-O stretch), 1010 (C-F stretch), 726 (C-Br stretch) cm^{-1}; ^{1}H NMR (400 MHz, $CDCl_3$) δ: 8.23 (d, $^{4}J_{(H,F)}$ = 6.5 Hz, 1H, C(8)**H**), 7.77 (d, $^{3}J_{(H,F)}$ = 9.1 Hz, 1H, C(5)**H**), 6.64 (s, 1H, C(3)**H**), 4.03 (s, 3H, C(12)**H$_3$**), 2.69 (s, 3H, C(11)**H$_3$**) ppm; ^{13}C NMR (100 MHz, $CDCl_3$) δ: 162.0 (d, $^{4}J_{(C,F)}$ = 5 Hz, q**C**-4), 160.6 (d, $^{6}J_{(C,F)}$ = 3 Hz, q**C**-2), 155.9 (d, $^{1}J_{(C,F)}$ = 247 Hz, q**C**(6)F), 145.6 (q**C**-10), 132.9 (**C**(8)H), 119.6 (d, $^{3}J_{(C,F)}$ = 8 Hz, q**C**-9), 113.4 (d, $^{2}J_{(C,F)}$ = 24 Hz, q**C**(7)Br), 106.7 (d, $^{2}J_{(C,F)}$ = 25 Hz, **C**(5)H), 101.3 (**C**(3)H), 55.9 (**C**(12)H$_3$), 25.6

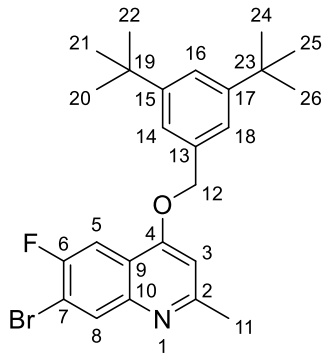
(**C**(11)H_3) ppm; ^{19}F NMR (282 MHz, $CDCl_3$) δ: -110 ppm; HRMS (ESI-TOF) *m/z*: $[M+H]^+$ calcd for $C_{11}H_{10}BrFNO$: 269.9924; found: 269.9923.

7-Bromo-4-((3,5-dimethylbenzyl)oxy)-6-fluoro-2-methylquinoline (161)



Compound **161** was prepared *via* the procedure described for **159** using **139** (0.059 g, 0.2 mmol, 1.0 equiv.) to yield **161** as a white solid (0.055 g, 73%); m.p. 138–140 °C; IR (film) ν_{max} 1601 (C=N stretch), 1561, 1500 (aromatic C=C stretch), 1347, 1193 (ether C-O stretch), 1099 (C-F stretch), 747 (C-Br stretch) cm^{-1}; ^{1}H NMR (500 MHz, $CDCl_3$) δ: 8.20 (d, $^4J_{(H,F)}$ = 6.5 Hz, 1H, C(8)**H**), 7.83 (d, $^3J_{(H,F)}$ = 9.2 Hz, 1H, C(5)**H**), 7.07 (s, 2H, C(14)**H**, C(18)**H**), 7.02 (s, 1H, C(16)**H**), 6.70 (s, 1H, C(3)**H**), 5.16 (s, 2H, C(12)$\mathbf{H_2}$), 2.66 (s, 3H, C(11)$\mathbf{H_3}$), 2.36 (s, 6H, C(19)$\mathbf{H_3}$, C(20)$\mathbf{H_3}$) ppm; ^{13}C NMR (125 MHz, $CDCl_3$) δ: 160.9 (d, $^4J_{(C,F)}$ = 5 Hz, q**C**-4), 160.6 (d, $^6J_{(C,F)}$ = 2 Hz, q**C**-2), 155.8 (d, $^1J_{(C,F)}$ = 247 Hz, q**C**(6)F), 146.1 (q**C**-10), 138.5 (2 × C, q**C**-15, q**C**-17), 135.2 (q**C**-13), 133.1 (**C**(8)H), 130.3 (**C**(16)H), 125.5 (2 × C, **C**(14)H, **C**(18)H), 119.7 (d, $^3J_{(C,F)}$ = 8 Hz, q**C**-9), 113.2 (d, $^2J_{(C,F)}$ = 24 Hz, q**C**(7)Br), 106.9 (d, $^2J_{(C,F)}$ = 25 Hz, **C**(5)H), 102.3 (**C**(3)H), 70.7 (**C**(12)H_2), 25.8 (**C**(11)H_3), 21.3 (2 × C, **C**(19)H_3, **C**(20)H_3) ppm; ^{19}F NMR (282 MHz, $CDCl_3$) δ: -111 ppm; HRMS (ESI-TOF) *m/z*: $[M+H]^+$ calcd for $C_{19}H_{18}BrFNO$: 374.0550; found: 374.0558.

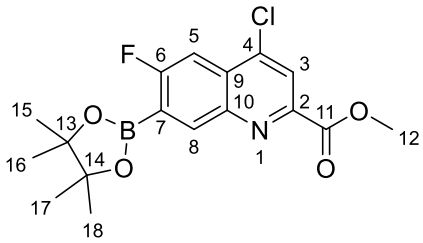
7-Bromo-4-((3,5-di-*tert*-butylbenzyl)oxy)-6-fluoro-2-methylquinoline (162)



Compound **162** was prepared *via* the procedure described for **159** using **140** (0.076 g, 0.2 mmol, 1.0 equiv.) to yield **162** as a white solid (0.075 g, 82%); m.p. 156–158 °C; IR (film) ν_{max} 1601 (C=N stretch), 1561, 1500 (aromatic C=C stretch), 1348, 1194 (ether C-O stretch), 1099 (C-F stretch), 741 (C-Br stretch) cm^{-1}; ^{1}H NMR (600 MHz, $CDCl_3$) δ: 8.21 (d, $^4J_{(H,F)}$ = 6.5 Hz, 1H, C(8)**H**), 7.84 (d, $^3J_{(H,F)}$ = 9.1 Hz, 1H, C(5)**H**), 7.52–7.45 (m, 1H, C(16)**H**), 7.33 (d, *J* = 1.3 Hz, 2H, C(14)**H**, C(18)**H**), 6.78 (s, 1H, C(3)**H**), 5.22 (s, 2H, C(12)$\mathbf{H_2}$), 2.69 (s, 3H, C(11)$\mathbf{H_3}$), 1.36 (s, 18H, C(20)$\mathbf{H_3}$, C(21)$\mathbf{H_3}$, C(22)$\mathbf{H_3}$, C(24)$\mathbf{H_3}$, C(25)$\mathbf{H_3}$, C(26)$\mathbf{H_3}$) ppm; ^{13}C NMR (150 MHz, $CDCl_3$) δ: 161.1 (d, $^4J_{(C,F)}$ = 5 Hz, q**C**-4), 160.7 (d, $^6J_{(C,F)}$ = 2 Hz, q**C**-2), 155.8 (d, $^1J_{(C,F)}$

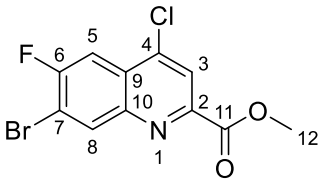
= 247 Hz, q**C**(6)F), 151.4 (2 × C, q**C**-15, q**C**-17), 146.0 (q**C**-10), 134.3 (q**C**-13), 133.1 (**C**(8)H), 122.8 (**C**(16)H), 122.3 (2 × C, **C**(14)H, **C**(18)H), 119.8 (d, $^{3}J_{(C,F)}$ = 8 Hz, q**C**-9), 113.3 (d, $^{2}J_{(C,F)}$ = 24 Hz, q**C**(7)Br), 106.9 (d, $^{2}J_{(C,F)}$ = 25 Hz, **C**(5)H), 102.4 (**C**(3)H), 71.4 (**C**(12)H_2), 34.9 (2 × C, q**C**-19, q**C**-23), 31.5 (6 × C, **C**(20)H_3, **C**(21)H_3, **C**(22)H_3, **C**(24)H_3, **C**(25)H_3, **C**(26)H_3), 25.8 (**C**(11)H_3) ppm; ^{19}F NMR (376 MHz, $CDCl_3$) δ: -111 ppm; HRMS (ESI-TOF) *m/z*: $[M+H]^+$ calcd for $C_{25}H_{30}BrFNO$: 458.1489; found: 458.1478.

Methyl 4-chloro-6-fluoro-7-(4,4,5,5-tetramethyl-1,3,2-dioxaborolan-2-yl)quinoline-2-carboxylate (163)



Compound **163** was prepared *via* the procedure described for **133** using **145** (0.048 g, 0.2 mmol, 1.0 equiv.) to yield **163** as a white solid (0.040 g, 55%); m.p. 156–158 °C; IR (film) ν_{max} 1727 (C=O stretch), 1625 (C=N stretch), 1498 (aromatic C=C stretch), 1336 (B-O stretch), 1326 (ether C-O stretch), 1230 (B-C stretch), 1118 (ether C-O stretch), 1049 (C-F stretch), 849 (C-Cl stretch) cm^{-1}; ^{1}H NMR (600 MHz, $CDCl_3$) δ: 8.84 (d, $^{4}J_{(H,F)}$ = 5.6 Hz, 1H, C(8)**H**), 8.30 (s, 1H, C(3)**H**), 7.83 (d, $^{3}J_{(H,F)}$ = 9.4 Hz, 1H, C(5)**H**), 4.09 (s, 3H, C(12)**H_3**), 1.40 (s, 12H, C(15)**H_3**, C(16)**H_3**, C(17)**H_3**, C(18)**H_3**) ppm; ^{13}C NMR (150 MHz, $CDCl_3$) δ: 165.7 (d, $^{1}J_{(C,F)}$ = 257 Hz, q**C**(6)F), 164.9 (q**C**-11), 147.1 (d, $^{6}J_{(C,F)}$ = 3 Hz, q**C**-2), 144.8 (q**C**-10), 142.8 (d, $^{4}J_{(C,F)}$ = 6 Hz, q**C**(4)Cl), 142.5 (d, $^{3}J_{(C,F)}$ = 10 Hz, **C**(8)H), 130.5 (d, $^{3}J_{(C,F)}$ = 11 Hz, q**C**-9), 122.3 (**C**(3)H), 107.7 (d, $^{2}J_{(C,F)}$ = 28 Hz, **C**(5)H), 84.6 (2 × C, q**C**-13, q**C**-14), 53.4 (**C**(12)H_3), 24.9 (4 × C, **C**(15)H_3, **C**(16)H_3, **C**(17)H_3, **C**(18)H_3) ppm; a signal for the carbon directly attached to the boron atom was not observed; ^{19}F NMR (282 MHz, $CDCl_3$) δ: -100 ppm; ^{11}B NMR (96 MHz, $CDCl_3$) δ: 30 ppm; HRMS (ESI-TOF) *m/z*: $[M+H]^+$ calcd for $C_{17}H_{19}BClFNO_4$: 366.1074; found: 366.1071.

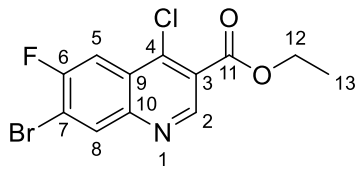
Methyl 7-bromo-4-chloro-6-fluoroquinoline-2-carboxylate (164)



Compound **164** was prepared *via* the procedure described for **159** using **145** (0.024 g, 0.1 mmol, 1.0 equiv.). Purification *via* column chromatography (DCM) to yield **164** as a white solid (0.025 g, 78%); m.p.

153–155 °C; IR (film) ν_{max} 1725 (C=O stretch), 1613 (C=N stretch), 1544 (aromatic C=C stretch), 1345, 1204 (ester C-O stretch), 1019 (C-F stretch), 787 (C-Cl stretch), 696 (C-Br stretch) cm^{-1}; ^{1}H NMR (400 MHz, $CDCl_3$) δ: 8.62 (d, $^{4}J_{(H,F)}$ = 6.6 Hz, 1H, C(8)**H**), 8.31 (s, 1H, C(3)**H**), 7.96 (d, $^{3}J_{(H,F)}$ = 8.8 Hz, 1H, C(5)**H**), 4.10 (s, 3H, C(12)$\mathbf{H_3}$) ppm; ^{13}C NMR (100 MHz, $CDCl_3$) δ: 164.6 (q**C**-11), 158.7 (d, $^{1}J_{(C,F)}$ = 255 Hz, q**C**(6)F), 148.1 (q**C**-2), 145.4 (d, $^{4}J_{(C,F)}$ = 1 Hz, q**C**-10), 143.2 (d, $^{4}J_{(C,F)}$ = 6 Hz, q**C**(4)Cl), 136.4 (d, $^{3}J_{(C,F)}$ = 2 Hz, **C**(8)H), 127.9 (d, $^{3}J_{(C,F)}$ = 9 Hz, q**C**-9), 122.1 (**C**(3)H), 115.9 (d, $^{2}J_{(C,F)}$ = 25 Hz, q**C**(7)Br), 108.8 (d, $^{2}J_{(C,F)}$ = 26 Hz, **C**(5)H), 53.6 (**C**(12)H_3) ppm; ^{19}F NMR (376 MHz, $CDCl_3$) δ: -102 ppm; HRMS (ESI-TOF) *m/z*: $[M+H]^+$ calcd for $C_{11}H_7BrClFNO_2$: 317.9327; found: 317.9328.

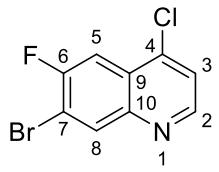
Ethyl 7-bromo-4-chloro-6-fluoroquinoline-3-carboxylate (166)



Compound **166** was prepared *via* the procedure described for **159** using **146** (0.025 g, 0.1 mmol, 1.0 equiv.), except that the amount of borylating reagent, B_2pin_2 (0.056 g, 0.22 mmol, 2.2 equiv.) was increased. Purification *via* column chromatography (hexanes:Et_2O 99:1–90:10) to yield **166** as a white solid (0.029 g, 88%); m.p. 119–120 °C; IR (film) ν_{max} 1727 (C=O stretch), 1609 (C=N stretch), 1551 (aromatic C=C stretch), 1336, 1153 (ester C-O stretch), 1037 (C-F stretch), 788 (C-Cl stretch), 689 (C-Br stretch) cm^{-1}; ^{1}H NMR (400 MHz, $CDCl_3$) δ: 9.17 (s, 1H, C(2)**H**), 8.42 (d, $^{4}J_{(H,F)}$ = 6.6 Hz, 1H, C(8)**H**), 8.08 (d, $^{3}J_{(H,F)}$ = 9.2 Hz, 1H, C(5)**H**), 4.51 (q, *J* = 7.1 Hz, 2H, C(12)$\mathbf{H_2}$), 1.47 (q, *J* = 7.1 Hz, 3H, C(13)$\mathbf{H_3}$) ppm; ^{13}C NMR (100 MHz, $CDCl_3$) δ: 164.0 (q**C**-11), 157.9 (d, $^{1}J_{(C,F)}$ = 252 Hz, q**C**(6)F), 150.5 (**C**(2)H), 142.6 (q**C**-10), 142.6 (d, $^{4}J_{(C,F)}$ = 6 Hz, q**C**(4)Cl), 135.1 (**C**(8)H), 126.6 (d, $^{3}J_{(C,F)}$ = 8 Hz, q**C**-9), 123.7 (q**C**-3), 116.6 (d, $^{2}J_{(C,F)}$ = 25 Hz, q**C**(7)Br), 110.1 (d, $^{2}J_{(C,F)}$ = 26 Hz, **C**(5)H), 62.4 (**C**(12)H_2), 14.2 (**C**(13)H_3) ppm; ^{19}F NMR (376 MHz, $CDCl_3$) δ: -104 ppm; HRMS (ESI-TOF) *m/z*: $[M+H]^+$ calcd for $C_{12}H_9BrClFNO_2$: 331.9484; found: 331.9481.

7-Bromo-4-chloro-6-fluoroquinoline (169)

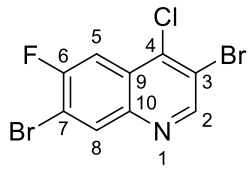
Compound **169** was prepared *via* the procedure described for **133** using **147** (0.036 g, 0.2 mmol, 1.0 equiv.) except that no recrystallisation was attempted. Isolation *via*



column chromatography (DCM:MeOH 98:2) to yield a portion of **169** for analysis. ^{1}H NMR (500 MHz, $CDCl_3$) δ: 8.76 (d, *J* = 4.7 Hz, 1H, C(2)**H**), 8.41 (d, $^{4}J_{(H,F)}$ = 6.6 Hz, 1H, C(8)**H**), 7.92 (d, $^{3}J_{(H,F)}$ = 9.0 Hz, 1H, C(5)**H**), 7.53 (d, *J* = 4.7 Hz, 1H, C(3)**H**) ppm; ^{13}C NMR (125 MHz, $CDCl_3$) δ: 157.4 (d, $^{1}J_{(C,F)}$ = 251 Hz, q**C**(6)F), 150.1 (d, $^{6}J_{(C,F)}$ = 3 Hz, **C**(2)H), 146.3 (d, $^{4}J_{(C,F)}$ = 1 Hz, q**C**-10), 141.9 (d, $^{4}J_{(C,F)}$ = 6 Hz, q**C**(4)Cl), 135.1 (d, $^{3}J_{(C,F)}$ = 1 Hz, **C**(8)H), 126.7 (d, $^{3}J_{(C,F)}$ = 9 Hz, q**C**-9), 122.0 (**C**(3)H), 114.7 (d, $^{2}J_{(C,F)}$ = 25 Hz, q**C**(7)Br), 108.8 (d, $^{2}J_{(C,F)}$ = 26 Hz, **C**(5)H) ppm; ^{19}F NMR (470 MHz, $CDCl_3$) δ: -106 ppm; HRMS (ESI-TOF) *m/z*: $[M+H]^+$ calcd for $C_9H_5BrClFN$: 259.9272; found: 259.9277.

Note: Compound **169** was not sufficiently pure for complete analysis or calculation of yield.

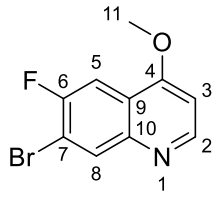
3,7-Dibromo-4-chloro-6-fluoroquinoline (170)



Compound **170** was prepared *via* the procedure described for **133** using **147** (0.036 g, 0.2 mmol, 1.0 equiv.) except that no recrystallisation was attempted. Isolation *via* column chromatography (DCM:MeOH 98:2) to yield a portion of **170** for analysis. ^{1}H NMR (500 MHz, $CDCl_3$) δ: 8.90 (s, 1H, C(2)**H**), 8.37 (d, $^{4}J_{(H,F)}$ = 6.6 Hz, 1H, C(8)**H**), 7.92 (d, $^{3}J_{(H,F)}$ = 9.1 Hz, 1H, C(5)**H**) ppm; ^{13}C NMR (125 MHz, $CDCl_3$) δ: 157.0 (d, $^{1}J_{(C,F)}$ = 252 Hz, q**C**(6)F), 151.1 (d, $^{6}J_{(C,F)}$ = 3 Hz, q**C**-2), 143.4 (d, $^{4}J_{(C,F)}$ = 2 Hz, q**C**-10), 139.7 (d, $^{4}J_{(C,F)}$ = 5 Hz, q**C**(4)Cl), 134.2 (d, $^{3}J_{(C,F)}$ = 2 Hz, **C**(8)H), 126.6 (d, $^{3}J_{(C,F)}$ = 9 Hz, q**C**-9), 118.3 (q**C**(3)Br), 113.5 (d, $^{2}J_{(C,F)}$ = 25 Hz, q**C**(7)Br), 108.3 (d, $^{2}J_{(C,F)}$ = 26 Hz, **C**(5)H) ppm; ^{19}F NMR (470 MHz, $CDCl_3$) δ: -104 ppm; HRMS (ESI-TOF) *m/z*: $[M+H]^+$ calcd for $C_9H_4Br_2ClFN$: 337.8378; found: 337.8383.

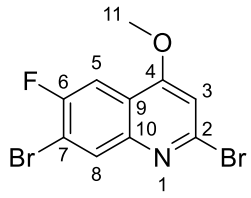
Note: Compound **170** was not sufficiently pure for complete analysis or calculation of yield.

7-Bromo-6-fluoro-4-methoxyquinoline (173)



Compound **173** was prepared *via* the procedure described for **159** using **148** (0.035 g, 0.2 mmol, 1.0 equiv.) to yield **173** as a white solid (0.021 g, 41%); m.p. 139–141 °C; IR (film) ν_{max} 1596 (C=N stretch), 1570, 1499 (aromatic C=C stretch), 1348, 1181 (ether C-O stretch), 1093 (C-F stretch), 717 (C-Br stretch) cm^{-1}; ^{1}H NMR (400 MHz, $CDCl_3$) δ: 8.72 (d, *J* = 5.2 Hz, 1H, C(2)**H**), 8.30 (d, $^{4}J_{(H,F)}$ = 6.6 Hz, 1H, C(8)**H**), 7.85 (d, $^{3}J_{(H,F)}$ = 9.2 Hz, 1H, C(5)**H**), 6.77 (d, *J* = 5.2 Hz, 1H, C(3)**H**), 4.06 (s, 3H, C(11)**H_3**) ppm; ^{13}C NMR (100 MHz, $CDCl_3$) δ: 162.0 (d, $^{4}J_{(C,F)}$ = 5 Hz, q**C**-4), 156.2 (d, $^{1}J_{(C,F)}$ = 248 Hz, q**C**(6)F), 151.6 (d, $^{6}J_{(C,F)}$ = 3 Hz, **C**(2)H), 146.3 (d, $^{4}J_{(C,F)}$ = 1 Hz, q**C**-10), 133.9 (**C**(8)H), 121.2 (d, $^{3}J_{(C,F)}$ = 8 Hz, q**C**-9), 113.6 (d, $^{2}J_{(C,F)}$ = 24 Hz, q**C**(7)Br), 106.8 (d, $^{2}J_{(C,F)}$ = 25 Hz, **C**(5)H), 100.7 (**C**(3)H), 56.0 (**C**(11)H_3) ppm; ^{19}F NMR (376 MHz, $CDCl_3$) δ: -109 ppm; HRMS (ESI-TOF) *m/z*: $[M+H]^+$ calcd for $C_{10}H_8BrFNO$: 255.9768; found: 255.9767.

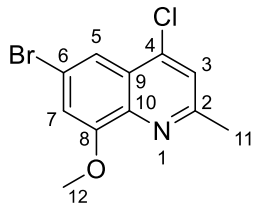
2,7-Dibromo-6-fluoro-4-methoxyquinoline (174)



Compound **174** was prepared *via* the procedure described for **159** using **148** (0.035 g, 0.2 mmol, 1.0 equiv.). A portion of **174** was isolated for analysis. ^{1}H NMR (400 MHz, $CDCl_3$) δ: 8.21 (d, $^{4}J_{(H,F)}$ = 6.4 Hz, 1H, C(8)**H**), 7.92 (d, $^{3}J_{(H,F)}$ = 9.1 Hz, 1H, C(5)**H**), 8.90 (s, 1H, C(2)**H**) ppm; ^{13}C NMR (100 MHz, $CDCl_3$) δ: 162.4 (d, $^{4}J_{(C,F)}$ = 5 Hz, q**C**-4), 156.5 (d, $^{1}J_{(C,F)}$ = 249 Hz, q**C**(6)F), 145.8 (d, $^{4}J_{(C,F)}$ = 2 Hz, q**C**-10), 142.8 (d, $^{6}J_{(C,F)}$ = 3 Hz, q**C**(2)Br), 133.3 (**C**(8)H), 120.5 (d, $^{3}J_{(C,F)}$ = 9 Hz, q**C**-9), 114.6 (d, $^{2}J_{(C,F)}$ = 24 Hz, q**C**(7)Br), 107.3 (d, $^{2}J_{(C,F)}$ = 25 Hz, **C**(5)H), 105.5 (**C**(3)H), 56.4 (**C**(11)H_3) ppm; ^{19}F NMR (376 MHz, $CDCl_3$) δ: -108 ppm; HRMS (ESI-TOF) *m/z*: $[M+H]^+$ calcd for $C_{10}H_7Br_2FNO$: 333.8873; found: 333.8870.

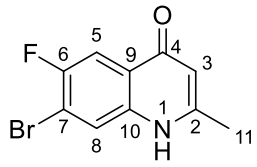
Note: Compound **174** was not sufficiently pure for complete analysis or calculation of yield.

6-Bromo-4-chloro-8-methoxy-2-methylquinoline (176)



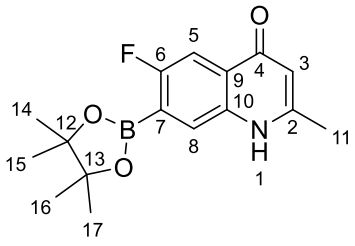
Compound **176** was prepared *via* the procedure described for **159** using **150** (0.042 g, 0.2 mmol, 1.0 equiv.) to yield **176** as a pale yellow solid (0.041 g, 72%); m.p. 138–141 °C (lit.[167] 140–142°C); IR (film) ν_{max} 1586 (C=N stretch), 1558 (aromatic C=C stretch), 1381, 1250 (ether C-O stretch), 826 (C-Cl stretch), 666 (C-Br stretch) cm^{-1}; ^{1}H NMR (400 MHz, $CDCl_3$) δ: 7.91 (d, *J* = 1.9 Hz, 1H, C(5)**H**), 7.44 (s, 1H, C(3)**H**), 7.16 (d, *J* = 1.9 Hz, 1H, C(7)**H**), 4.08 (s, 3H, C(12)$\mathbf{H_3}$), 2.75 (s, 3H, C(11)$\mathbf{H_3}$) ppm; ^{13}C NMR (100 MHz, $CDCl_3$) δ: 158.2 (q**C**-2), 155.5 (q**C**-8), 141.4 (q**C**-4), 139.5 (q**C**-10), 126.6 (q**C**-9), 123.5 (**C**(3)H), 120.7 (q**C**(6)Br), 118.1 (**C**(5)H), 112.7 (**C**(7)H), 56.6 (**C**(12)H_3), 25.5 (**C**(11)H_3) ppm; HRMS (ESI-TOF) *m/z*: $[M+H]^+$ calcd for $C_{11}H_{10}BrClNO$: 285.9629; found: 285.9623.

7-Bromo-6-fluoro-2-methylquinolin-4(1*H*)-one (177)



160 (0.027 g, 0.1 mmol, 1.0 equiv.) was added to a 5 mL screw-capped vial followed by 48% HBr solution (0.25 mL) and glacial acetic acid (0.5 mL). The vial was sealed and stirred at 150 °C for 6 h, then cooled to r.t., diluted with H_2O and neutralised using 6 M NaOH. The resulting precipitate was isolated by suction filtration and washed with H_2O and cold Et_2O to yield **177** as an off-white solid (0.021 g, 82%); m.p. >250 °C; IR (film) ν_{max} 1639 (C=O stretch), 1601 (alkenyl C=C stretch), 1558 (aromatic C=C stretch), 1272 (C-N stretch), 1021 (C-F stretch), 751 (C-Br stretch) cm^{-1}; ^{1}H NMR (600 MHz, $(CD_3)_2SO$) δ: 11.73 (bs, 1H, N**H**), 8.00–7.62 (m, 2H, C(5)**H**), C(8)**H**), 5.95 (s, 1H, C(3)**H**), 2.36 (s, 3H, C(11)$\mathbf{H_3}$) ppm; ^{13}C NMR (150 MHz, $(CD_3)_2SO$) δ: 175.4 (q**C**-4), 154.2 (d, $^{1}J_{(C,F)}$ = 242 Hz, q**C**(6)F), 150.5 (q**C**-2), 137.3 (q**C**-10), 125.0 (d, $^{3}J_{(C,F)}$ = 5 Hz, q**C**-9), 122.8 (**C**(8)H), 113.0 (d, $^{2}J_{(C,F)}$ = 24 Hz, q**C**(7)Br), 110.4 (d, $^{2}J_{(C,F)}$ = 23 Hz, **C**(5)H), 108.1 (**C**(3)H), 19.5 (**C**(11)H_3) ppm; ^{19}F NMR (282 MHz, $(CD_3)_2SO$) δ: -115 ppm; HRMS (ESI-TOF) *m/z*: $[M+H]^+$ calcd for $C_{10}H_8BrFNO$: 255.9768; found: 255.9772.

6-Fluoro-2-methyl-7-(4,4,5,5-tetramethyl-1,3,2-dioxaborolan-2-yl)quinolin-4(1*H*)-one (178)



A 15 mL Schlenk tube was oven dried (150 °C) and cooled under vacuum. The flask was refilled with nitrogen and all reagents were added under a positive pressure of nitrogen in the order: **139** (0.059 g, 0.2 mmol, 1.0 equiv.), dtbpy (1.6 mg, 0.006 mmol, 3 mol%), B_2pin_2 (0.056 g, 0.22 mmol, 1.1 equiv.), and $[Ir(OMe)COD]_2$ (2.0 mg, 0.003 mmol, 1.5 mol%). The Schlenk tube was then placed under vacuum for 20 min before being refilled with nitrogen three times. THF (0.5 mL) was added *via* syringe, the reaction was sealed, and the mixture heated to 80 °C for 24 h, then cooled to r.t. and concentrated under reduced pressure. The crude reaction mixture for **157** (0.2 mmol, 1.0 equiv.) was dissolved in MeOH (2 mL) and added to a Schlenk tube, followed by 10% Pd/C (2.0 mg, 0.02 mmol, 10 mol%). The resulting suspension was purged with H_2 and then stirred under a balloon of H_2 at 50 °C for 16 h. The mixture was cooled to r.t., diluted with DCM and filtered through a short plug of Celite and concentrated under reduced pressure. Purification *via* trituration from DCM/Et_2O (1:1) to yield **178** as a beige solid (0.032 g, 53%); m.p. >250 °C; IR (film) ν_{max} 1643 (C=O stretch), 1561 (aromatic C=C stretch), 1373 (B-O stretch), 1340 (ether C-O stretch), 1265 (B-C stretch), 1142 (ether C-O stretch), 1035 (C-F stretch) cm^{-1}; ^1H NMR (600 MHz, $(CD_3)_2SO$) δ: 11.71 (bs, 1H, N**H**), 7.92 (d, $^4J_{(H,F)}$ = 4.8 Hz, 1H, C(8)**H**), 7.60 (d, $^3J_{(H,F)}$ = 9.5 Hz, 1H, C(5)**H**), 5.93 (s, 1H, C(3)**H**), 2.34 (s, 3H, C(11)$\mathbf{H_3}$), 1.34 (s, 12H, C(14)$\mathbf{H_3}$, C(15)$\mathbf{H_3}$, C(16)$\mathbf{H_3}$, C(17)$\mathbf{H_3}$) ppm; ^{13}C NMR (150 MHz, $(CD_3)_2SO$) δ: 175.7 (q**C**-4), 161.4 (d, $^1J_{(C,F)}$ = 246 Hz, q**C**(6)F), 150.2 (q**C**-2), 136.2 (q**C**-10), 127.9 (d, $^3J_{(C,F)}$ = 7 Hz, q**C**-9), 127.4 (d, $^3J_{(C,F)}$ = 8 Hz, **C**(8)H), 108.7 (d, $^2J_{(C,F)}$ = 25 Hz, **C**(5)H), 107.9 (**C**(3)H), 84.2 (2 × C, q**C**-12, q**C**-13), 24.7 (4 × C, **C**(14)H_3, **C**(15)H_3, **C**(16)H_3, **C**(17)H_3), 19.5 (**C**(11)H_3) ppm; a signal for the carbon directly attached to the boron atom was not observed; ^{19}F NMR (282 MHz, $(CD_3)_2SO$) δ: -110 ppm; ^{11}B NMR (96 MHz, $(CD_3)_2SO$) δ: 30 ppm; HRMS (ESI-TOF) *m/z*: $[M+H]^+$ calcd for $C_{16}H_{20}BFNO_3$: 304.1515; found: 304.1515.

Ethyl 6-fluoro-4-oxo-7-(4,4,5,5-tetramethyl-1,3,2-dioxaborolan-2-yl)-1,4-dihydroquinoline-3-carboxylate (179)

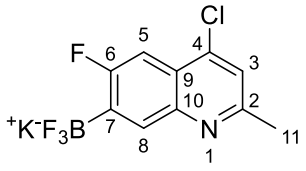
Compound **179** was prepared *via* the procedure described for **134** using **146** (0.051 g, 0.2 mmol, 1.0 equiv.), except that the amount of borylating reagent, B_2pin_2 (0.112 g, 0.44 mmol, 2.2 equiv.) was increased. Purification *via* trituration from a mixture of hot acetone/MeOH to yield **179** as a white solid (0.039 g, 53%); m.p. >250 °C; IR (film) ν_{max} 1694, 1613 (C=O stretches), 1534 (aromatic C=C stretch), 1401 (B-O stretch), 1334 (ether C-O stretch), 1265 (B-C stretch), 1143 (ether C-O stretch), 1043 (C-F stretch) cm^{-1}; ^1H NMR (600 MHz, $(CD_3)_2SO$) δ: 8.60 (s, 1H, C(3)**H**), 8.01 (d, $^4J_{(H,F)}$ = 4.8 Hz, 1H, C(8)**H**), 7.71 (d, $^3J_{(H,F)}$ = 9.4 Hz, 1H, C(5)**H**), 4.21 (q, *J* = 7.1 Hz, 2H, C(12)$\mathbf{H_2}$), 1.39–1.18 (m, 15H, C(13)$\mathbf{H_3}$, C(16)$\mathbf{H_3}$, C(17)$\mathbf{H_3}$, C(18)$\mathbf{H_3}$, C(19)$\mathbf{H_3}$) ppm; ^{13}C NMR (150 MHz, $(CD_3)_2SO$) δ: 172.5 (q**C**-4), 164.8 (q**C**-11), 162.5 (d, $^1J_{(C,F)}$ = 248 Hz, q**C**(6)F), 145.5 (**C**(2)H), 135.6 (q**C**-10), 131.0 (d, $^3J_{(C,F)}$ = 6 Hz, q**C**-9), 128.6 (**C**(8)H), 109.8 (d, $^2J_{(C,F)}$ = 25 Hz, **C**(5)H), 109.1 (q**C**-3), 84.2 (2 × C, q**C**-14, q**C**-15), 59.6 (**C**(12)H_2), 26.7 (4 × C, **C**(16)H_3, **C**(17)H_3, **C**(18)H_3, **C**(19)H_3), 14.3 (**C**(13)H_3) ppm; a signal for the carbon directly attached to the boron atom was not observed; ^{19}F NMR (282 MHz, $(CD_3)_2SO$) δ: -108 ppm; ^{11}B NMR (96 MHz, $(CD_3)_2SO$) δ: 30 ppm; HRMS (ESI-TOF) *m/z*: $[M+H]^+$ calcd for $C_{18}H_{22}BFNO_5$: 362.1570; found: 362.1577.

Ethyl 7-bromo-6-fluoro-4-oxo-1,4-dihydroquinoline-3-carboxylate (180)

166 (0.030 g, 0.09 mmol, 1.0 equiv.) was dissolved in EtOH (2.5 mL) and 1 M HCl (0.5 mL) was added. The mixture was stirred at 100 °C for 3 h. Upon cooling, a white precipitate formed which was isolated *via* suction filtration and rinsed with H_2O, cold EtOH and Et_2O to yield **180** as a white solid (0.018 g, 64%); m.p. >250 °C; IR (film) ν_{max} 1694 (C=O stretch), 1549 (alkenyl C=C stretch), 1507 (aromatic C=C stretch), 1358 (ester C-O stretch), 1250 (C-N stretch), 1192 (ether C-O stretch), 1103 (C-F stretch) cm^{-1}; ^1H NMR (600 MHz, 313 K, $(CD_3)_2SO$) δ: 8.59 (s, 1H, C(2)**H**), 7.98 (d, $^4J_{(H,F)}$ = 5.8 Hz, 1H, C(8)**H**), 7.91 (d, $^3J_{(H,F)}$ = 9.1 Hz, 1H, C(5)**H**), 4.22 (q, *J* = 7.1 Hz, 2H, C(12)$\mathbf{H_2}$), 1.28 (q, *J* = 7.1 Hz, 3H, C(13)$\mathbf{H_3}$) ppm; ^{13}C NMR (150 MHz,

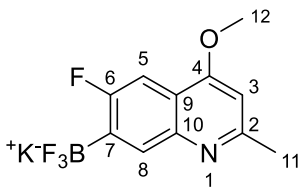
313 K, $(CD_3)_2SO$) δ: 172.2 (q**C**-4), 164.8 (q**C**-11), 155.2 (d, $^1J_{(C,F)}$ = 244 Hz, q**C**(6)F), 146.3 (d, $^6J_{(C,F)}$ = 2 Hz, **C**(2)H), 137.3 (d, $^4J_{(C,F)}$ = 3 Hz, q**C**-10), 128.2 (d, $^3J_{(C,F)}$ = 6 Hz, q**C**-9), 124.8 (**C**(8)H), 113.7 (d, $^2J_{(C,F)}$ = 25 Hz, q**C**(7)Br), 111.3 (d, $^2J_{(C,F)}$ = 23 Hz, **C**(5)H), 109.4 (q**C**-3), 59.7 (**C**(12)H_2), 14.3 (**C**(13)H_3) ppm; ^{19}F NMR (282 MHz, $(CD_3)_2SO$) δ: -113 ppm; HRMS (ESI-TOF) *m/z*: $[M+H]^+$ calcd for $C_{12}H_{10}BrFNO_3$: 313.9823; found: 313.9826.

(4-Chloro-6-fluoro-2-methylquinolin-7-yl)trifluoroborate potassium salt (181)



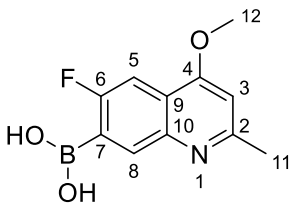
A 15 mL Schlenk tube was oven dried (150 °C) and cooled under vacuum. The flask was refilled with nitrogen and all reagents were added under a positive pressure of nitrogen in the order: **132** (0.196 g, 1.0 mmol, 1.0 equiv.), dtbpy (8.1 mg, 0.03 mmol, 3 mol%), B_2pin_2 (0.0.279 g, 0.22 mmol, 1.1 equiv.), and $[Ir(OMe)COD]_2$ (9.9 mg, 0.015 mmol, 1.5 mol%). The Schlenk tube was then placed under vacuum for 20 min before being refilled with nitrogen three times. THF (5 mL) was added *via* syringe, the reaction was sealed, and the mixture heated to 80 °C for 18 h. The solution was cooled, H_2O (3 mL) and KHF_2 (0.469 g, 6.0 mmol, 6.0 equiv.) were added and the mixture allowed to stir for a further 24 h before being diluted with acetone/H_2O (1:1, 15 mL). Volatiles were removed under reduced pressure and the resulting precipitate was isolated by suction filtration and washed with H_2O (15 mL) and cold hexane (15 mL)[126] to give **181** as a beige solid (0.215 g, 71%); m.p. >250 °C; IR (film) ν_{max} 1640 (C=N stretch), 1583 (aromatic C=C stretch), 1120 (B-C stretch), 1033 (C-F stretch), 799 (C-Cl stretch) cm^{-1}; ^{1}H NMR (600 MHz, $(CD_3)_2SO$) δ: 7.93 (d, $^4J_{(H,F)}$ = 5.6 Hz, 1H, C(8)**H**), 7.56 (s, 1H, C(3)**H**), 7.45 (d, $^3J_{(H,F)}$ = 9.2 Hz, 1H, C(5)**H**), 2.61 (s, 3H, C(11)**H_3**) ppm; ^{13}C NMR (150 MHz, $(CD_3)_2SO$) δ: 164.8 (d, $^1J_{(C,F)}$ = 245 Hz, q**C**(6)F), 156.7 (d, $^6J_{(C,F)}$ = 2 Hz, q**C**-2), 145.2 (q**C**-10), 139.8 (q**C**(4)Cl), 134.3 (d, $^3J_{(C,F)}$ = 15 Hz, **C**(8)H), 123.5 (d, $^3J_{(C,F)}$ = 11 Hz, q**C**-9), 121.1 (**C**(3)H), 104.8 (d, $^2J_{(C,F)}$ = 30 Hz, **C**(5)H), 24.4 (**C**(11)H_3) ppm; a signal for the carbon directly attached to the boron atom was not observed; ^{19}F NMR (282 MHz, $(CD_3)_2SO$) δ: -105 (qC(6)**F**), -138 (B**F_3**K) ppm; ^{11}B NMR (96 MHz, $(CD_3)_2SO$) δ: 2 ppm; HRMS (ESI-TOF) *m/z*: $[M+H]^+$ calcd for $C_{10}H_7BClF_3N$: 244.0307; found: 244.0311.

6-Fluoro-4-methoxy-2-methylquinolin-7-yl)trifluoroborate potassium salt (182)



Compound **182** was prepared *via* the procedure described for **181** using **135** (0.153 g, 0.8 mmol, 1.0 equiv.) to yield **182** as a brown solid (0.174 g, 73%); m.p. >250 °C; IR (film) ν_{max} 1645 (C=N stretch), 1592 (aromatic C=C stretch), 1146 (B-C stretch), 1017 (C-F stretch), 834 (C-Cl stretch) cm^{-1}; ^{1}H NMR (600 MHz, $(CD_3)_2SO$) δ: 8.01 (d, $^{4}J_{(H,F)}$ = 4.6 Hz, 1H, C(8)**H**), 7.59 (d, $^{3}J_{(H,F)}$ = 8.4 Hz, 1H, C(5)**H**), 7.38 (s, 1H, C(3)**H**), 4.21 (s, 3H, C(12)**H₃**), 2.80 (s, 3H, C(11)**H₃**) ppm; ^{13}C NMR (150 MHz, $(CD_3)_2SO$) δ: 166.9 (d, $^{4}J_{(C,F)}$ = 5 Hz, q**C**-4), 164.6 (d, $^{1}J_{(C,F)}$ = 247 Hz, q**C**(6)F), 156.8 (q**C**-2), 135.4 (q**C**-10), 125.1 (d, $^{3}J_{(C,F)}$ = 14 Hz, **C**(8)H), 118.7 (d, $^{3}J_{(C,F)}$ = 10 Hz, q**C**-9), 104.7 (d, $^{2}J_{(C,F)}$ = 30 Hz, **C**(5)H), 102.4 (**C**(3)H), 58.2 (**C**(12)H_3), 20.7 (**C**(11)H_3) ppm; a signal for the carbon directly attached to the boron atom was not observed; ^{19}F NMR (282 MHz, $(CD_3)_2SO$) δ: -103 (qC(6)**F**), -139 (B**F₃**K) ppm; ^{11}B NMR (96 MHz, $(CD_3)_2SO$) δ: 2 ppm; HRMS (ESI-TOF) *m/z*: $[M+H]^+$ calcd for $C_{11}H_{10}BF_3NO$: 240.0802; found: 240.0807.

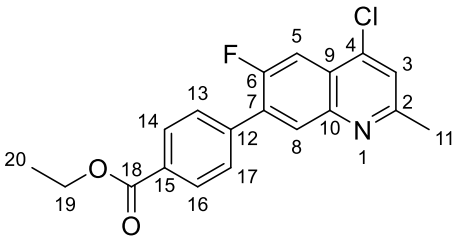
(6-Fluoro-4-methoxy-2-methylquinolin-7-yl)boronic acid (183)



182 (0.098 g, 0.33 mmol, 1.0 equiv.) was suspended in THF (11.1 mL) and a solution of $LiOH.H_2O$ (0.125 mg, 2.97 mmol, 9.0 equiv.) in H_2O (2.2 mL) was added. The resulting mixture was stirred at r.t. for 24 h. THF was removed under reduced pressure and the mixture was acidified to pH~5 using saturated NH_4Cl (~4 mL) and 1 M HCl (~2 mL). The resulting precipitate was collected by suction filtration, then redissolved in 1 M HCl and extracted once with Et_2O. The aqueous portion was then neutralised using solid $NaHCO_3$ and extracted with DCM/iPrOH (9:1, 3 × 10 mL). The organic layers were dried over $MgSO_4$, filtered and concentrated under reduced pressure to yield **183** as a white solid (0.058 g, 75%); m.p. >250 °C; IR (film) ν_{max} 1646 (C=N stretch), 1504 (aromatic C=C stretch), 1362 (B-O stretch), 1250 (C-O stretch), 1202 (B-C stretch), 1091 (C-F stretch) cm^{-1}; ^{1}H NMR (600 MHz, $(CD_3)_2SO$) δ: 8.52 (s, 2H, B(O**H**)$_2$), 8.04 (d, $^{4}J_{(H,F)}$ = 5.7 Hz, 1H, C(8)**H**), 7.56 (d, $^{3}J_{(H,F)}$ = 9.6 Hz, 1H, C(5)**H**), 6.95 (s, 1H, C(3)**H**), 4.01 (s, 3H, C(12)**H₃**), 2.59 (s, 3H, C(11)**H₃**) ppm; ^{13}C NMR (150 MHz, $(CD_3)_2SO$) δ: 161.8 (d, $^{1}J_{(C,F)}$ = 243 Hz, q**C**(6)F), 160.9 (d, $^{4}J_{(C,F)}$ = 5 Hz, q**C**-4), 159.2 (d, $^{6}J_{(C,F)}$ = 2 Hz, q**C**-2), 144.9 (q**C**-10), 136.1 (d, $^{3}J_{(C,F)}$ = 10 Hz, **C**(8)H), 120.6 (d, $^{3}J_{(C,F)}$ = 10

Hz, q**C**-9), 104.3 (d, $^{2}J_{(C,F)}$ = 27 Hz, **C**(5)H), 101.9 (**C**(3)H), 56.1 (**C**(12)H_3), 25.4 (**C**(11)H_3) ppm; a signal for the carbon directly attached to the boron atom was not observed; ^{19}F NMR (282 MHz, $(CD_3)_2SO$) δ: -108 ppm; ^{11}B NMR (96 MHz, $(CD_3)_2SO$) δ: 27 ppm; HRMS (ESI-TOF) *m/z*: $[M+H]^+$ calcd for $C_{11}H_{12}BFNO_3$: 236.0889; found: 236.0894.

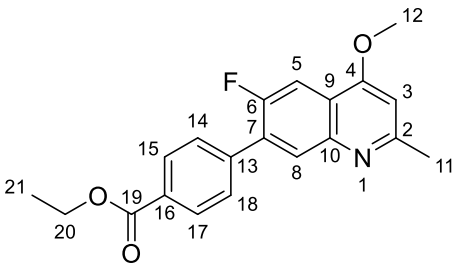
Ethyl 4-(4-chloro-6-fluoro-2-methylquinolin-7-yl)benzoate (184)



A 15 mL Schlenk tube was oven dried (150 °C) and cooled under vacuum. The flask was refilled with nitrogen and all reagents were added under a positive pressure of nitrogen in the order: **132** (0.039 g, 0.2 mmol, 1.0 equiv.), dtbpy (1.6 mg, 0.006 mmol, 3 mol%), B_2pin_2 (0.056 g, 0.22 mmol, 1.1 equiv.), and $[Ir(OMe)COD]_2$ (2.0 mg, 0.003 mmol, 1.5 mol%). The Schlenk tube was then placed under vacuum for 20 min before being refilled with nitrogen three times. THF (0.5 mL) was added *via* syringe, the reaction was sealed, and the mixture heated to 80 °C for 16 h, then cooled to r.t. and concentrated under reduced pressure. An internal standard, 1,3,5-trimethoxybenzene (~10 mol%) was added to the residue to determine the yield of C7-borylated product **133** by ^{1}H NMR analysis. A 15 mL Schlenk was heated under vacuum, cooled to r.t. and refilled with nitrogen. The crude reaction mixture for **133** (0.2 mmol, 1.0 equiv.), $Pd(PPh_3)_4$ (11.6 mg, 0.01 mmol, 5.0 mol%), and K_3PO_4 (0.127 g, 0.6 mmol, 3.0 equiv.) were added and the flask was evacuated and backfilled with nitrogen three times. Ethyl-4-bromobenzoate (0.05 mL, 0.3 mmol, 1.5 equiv.), THF (2 mL) and H_2O (0.4 mL) were added, the vessel sealed, and the mixture heated to 60 °C for 18 h.[80] The solution was cooled to r.t., diluted with H_2O and extracted with Et_2O (3 × 10 mL). The combined organic layers were washed with brine (10 mL), dried over $MgSO_4$, filtered and concentrated under reduced pressure. Purification *via* column chromatography (DCM 100 to DCM:Et_2O 90:10) to yield **184** as a white solid (0.052 g, 76%); m.p. 120–122 °C; IR (film) ν_{max} 1710 (C=O stretch), 1610 (C=N stretch), 1598 (aromatic C=C stretch), 1383, 1291 (ester C-O stretch), 1027 (C-F stretch), 857 (C-Cl stretch) cm^{-1}; ^{1}H NMR (300 MHz, $CDCl_3$) δ: 8.25–8.09 (m, 3H, C(8)**H**, C(14)**H**, C(16)**H**), 7.89 (d, $^{3}J_{(H,F)}$ = 11.2 Hz, 1H, C(5)**H**), 7.81–7.67 (m, 2H, C(13)**H**, C(17)**H**), 7.42 (s, 1H, C(3)**H**), 4.42 (q, *J* = 7.1 Hz, 2H, C(19)$\mathbf{H_2}$),

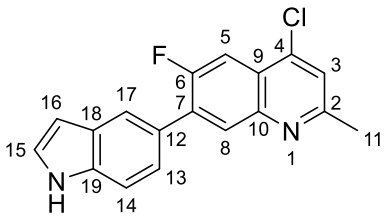
2.73 (s, 3H, C(11)**H₃**), 1.43 (t, *J* = 7.1 Hz, 3H, C(20)**H₃**) ppm; ^{13}C NMR (75 MHz, $CDCl_3$) δ: 166.2 (q**C**-18), 158.9 (d, $^{6}J_{(C,F)}$ = 2 Hz, q**C**-2), 158.1 (d, $^{1}J_{(C,F)}$ = 251 Hz, q**C**(6)F), 145.6 (q**C**-10), 141.5 (d, $^{4}J_{(C,F)}$ = 6 Hz, q**C**(4)Cl), 139.1 (d, $^{3}J_{(C,F)}$ = 2 Hz, q**C**-12), 133.1 (d, $^{2}J_{(C,F)}$ = 18 Hz, q**C**-7), 131.3 (d, $^{3}J_{(C,F)}$ = 4 Hz, **C**(8)H), 130.4 (q**C**-15), 129.8 (2 × C, **C**(14)H, **C**(16)H), 129.2 (2 × C, d, $^{4}J_{(C,F)}$ = 3 Hz, **C**(13)H, **C**(17)H), 125.3 (d, $^{3}J_{(C,F)}$ = 10 Hz, q**C**-9), 122.6 (**C**(3)H), 108.9 (d, $^{2}J_{(C,F)}$ = 26 Hz, **C**(5)H), 61.1 (**C**(19)H_2), 25.1 (**C**(11)H_3), 14.4 (**C**(20)H_3) ppm; ^{19}F NMR (282 MHz, $CDCl_3$) δ: -116 ppm; HRMS (ESI-TOF) *m/z*: $[M+H]^+$ calcd for $C_{19}H_{16}ClFNO_2$: 344.0848; found: 344.0839.

Ethyl 4-(6-fluoro-4-methoxy-2-methylquinolin-7-yl)benzoate (185)



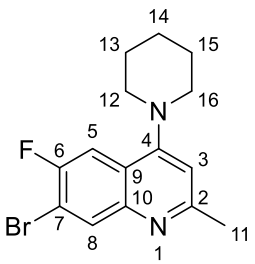
Compound **185** was prepared *via* the procedure described for **184** using **135** (0.057 g, 0.3 mmol, 1.0 equiv.) to yield **185** as a white solid (0.063 g, 62%); m.p. 93–95 °C; IR (film) ν_{max} 1712 (C=O stretch), 1608 (C=N stretch), 1556 (aromatic C=C stretch), 1348, 1280, 1201, 1107 (C-O stretches), 1024 (C-F stretch) cm^{-1}; ^{1}H NMR (300 MHz, $CDCl_3$) δ: 8.19–8.11 (m, 2H, C(15)**H**, C(17)**H**), 8.06 (d, $^{4}J_{(H,F)}$ = 7.3 Hz, 1H, C(8)**H**), 7.84 (d, $^{3}J_{(H,F)}$ = 11.4 Hz, 1H, C(5)**H**), 7.79–7.69 (m, 2H, C(14)**H**, C(18)**H**), 6.66 (s, 1H, C(3)**H**), 4.42 (q, *J* = 7.1 Hz, 2H, C(20)**H₂**), 4.05 (s, 3H, C(12)**H₃**), 2.71 (s, 3H, C(11)**H₃**), 1.42 (t, *J* = 7.1 Hz, 3H, C(21)**H₃**) ppm; ^{13}C NMR (75 MHz, $CDCl_3$) δ: 166.4 (q**C**-19), 161.7 (d, $^{4}J_{(C,F)}$ = 5 Hz, q**C**-4), 160.1 (d, $^{6}J_{(C,F)}$ = 2 Hz, q**C**-2), 157.1 (d, $^{1}J_{(C,F)}$ = 248 Hz, q**C**(6)F), 145.8 (q**C**-10), 139.9 (q**C**-13), 132.0 (d, $^{2}J_{(C,F)}$ = 17 Hz, q**C**-7), 130.4 (d, $^{3}J_{(C,F)}$ = 4 Hz, **C**(8)H), 130.0 (q**C**-16), 129.7 (2 × C, **C**(15)H, **C**(17)H), 129.2 (2 × C, d, $^{4}J_{(C,F)}$ = 3 Hz, **C**(14)H, **C**(18)H), 120.2 (d, $^{3}J_{(C,F)}$ = 10 Hz, q**C**-9), 106.8 (d, $^{2}J_{(C,F)}$ = 25 Hz, **C**(5)H), 101.2 (**C**(3)H), 61.1 (**C**(20)H_2), 55.7 (**C**(12)H_3), 25.9 (**C**(11)H_3), 14.4 (**C**(21)H_3) ppm; ^{19}F NMR (282 MHz, $CDCl_3$) δ: -120 ppm; HRMS (ESI-TOF) *m/z*: $[M+H]^+$ calcd for $C_{20}H_{19}FNO_3$: 340.1343; found: 340.1336.

4-Chloro-6-fluoro-7-(1H-indol-5-yl)-2-methylquinoline (186)



A 15 mL Schlenk flask was oven dried (150 °C), cooled to r.t. under vacuum and refilled with nitrogen. 5-Bromoindole (0.024 g, 0.12 mmol, 1.0 equiv.), **133** (0.048 g, 0.15 mmol, 1.25 equiv.), $Pd(dba)_2$ (1.4 mg, 0.0024 mmol, 2.0 mol%), P(*o*-tol)$_3$ (2.2 mg, 0.0072 mmol, 6.0 mol%) and Na_2CO_3 (0.051 g, 0.48 mmol, 4.0 equiv.) were added and the Schlenk flask was evacuated and backfilled with nitrogen three times. THF (0.45 mL) and H_2O (0.05 mL) were added, the vessel sealed and the mixture heated to 50 °C for 24 h.[129] The mixture was cooled to r.t., filtered through a short plug of Celite with DCM and concentrated under reduced pressure. Purification *via* column chromatography (DCM 100 to DCM:EtOAc 98:2) to yield **186** as a bright yellow solid (0.032 g, 86%); m.p. 160–162 °C; IR (film) ν_{max} 3415 (N-H stretch), 1626 (C=N stretch), 1596, 1545 (aromatic C=C stretch), 1011 (C-F stretch), 867 (C-Cl stretch) cm^{-1}; ^{1}H NMR (400 MHz, $(CD_3)_2SO$) δ: 11.30 (bs, 1H, N**H**), 8.06 (d, $^4J_{(H,F)}$ = 7.5 Hz, 1H, C(8)**H**), 7.97–7.77 (m, 2H, C(5)**H**, C(17)**H**), 7.66 (s, 1H, C(3)**H**), 7.55 (d, *J* = 8.4 Hz, 1H, C(14)**H**), 7.51–7.32 (m, 2H, C(13)**H**, C(15)**H**), 6.54 (bs, 1H, C(16)**H**), 2.64 (s, 3H, C(11)**H$_3$**) ppm; ^{13}C NMR (100 MHz, $(CD_3)_2SO$) δ: 158.9 (d, $^6J_{(C,F)}$ = 2 Hz, q**C**-2), 158.0 (d, $^1J_{(C,F)}$ = 249 Hz, q**C**(6)F), 145.2 (q**C**-10), 140.1 (d, $^4J_{(C,F)}$ = 5 Hz, q**C**(4)Cl), 135.9 (q**C**-19), 135.1 (d, $^2J_{(C,F)}$ = 18 Hz, q**C**-7), 130.4 (d, $^3J_{(C,F)}$ = 3 Hz, **C**(8)H), 128.0 (q**C**-18), 126.4 (**C**(15)H), 124.7 (d, $^3J_{(C,F)}$ = 1 Hz, q**C**-12), 123.4 (d, $^3J_{(C,F)}$ = 11 Hz, q**C**-9), 122.27, 122.24 (**C**(3)H, **C**(13)H), 121.1 (d, $^4J_{(C,F)}$ = 3 Hz, **C**(17)H), 111.8 (**C**(14)H), 108.0 (d, $^2J_{(C,F)}$ = 26 Hz, **C**(5)H), 101.8 (**C**(16)H), 24.5 (**C**(11)H$_3$) ppm; ^{19}F NMR (282 MHz, $(CD_3)_2SO$) δ: -116 ppm; HRMS (ESI-TOF) *m/z*: $[M+H]^+$ calcd for $C_{18}H_{13}ClFN_2$: 311.0746; found: 311.0741.

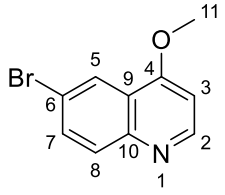
7-Bromo-6-fluoro-2-methyl-4-(piperidin-1-yl)quinoline (187)



A 15 mL Schlenk flask was dried under vacuum, cooled to r.t. and refilled with nitrogen. **159** (0.082 mg, 0.3 mmol, 1.0 equiv.), $Pd_2(dba)_3$ (5.5 mg, 0.006 mmol, 2.0 mol%), XANTPhos (6.9 mg, 0.012 mmol, 4.0 mol%) and NaO*t*-Bu (0.043 g, 0.45 mmol, 1.5 equiv.) were added and the flask was evacuated and backfilled with nitrogen three times. Piperidine (0.06 mL, 0.6 mmol,

2.0 equiv.) and toluene (1.5 mL) were added, the was vessel sealed and the suspension heated to 100 °C for 6 h. The product was purified *via* column chromatography (DCM 100 to DCM:EtOAc 90:10 with 1% NEt_3 as modifier) to yield **187** as a brown solid (0.046 g, 47%); m.p. 120–123 °C; IR (film) ν_{max} 1641 (C=N stretch), 1591 (aromatic C=C stretch), 1195 (C-N stretch), 1021 (C-F stretch), 717 (C-Br stretch) cm^{-1}; ^1H NMR (600 MHz, $CDCl_3$) δ: 8.19 (d, $^4J_{(H,F)}$ = 6.8 Hz, 1H, C(8)**H**), 7.60 (d, $^3J_{(H,F)}$ = 9.8 Hz, 1H, C(5)**H**), 6.73 (s, 1H, C(3)**H**), 3.24–2.97 (m, 4H, C(12)$\mathbf{H_2}$, C(16)$\mathbf{H_2}$), 2.64 (s, 3H, C(11)$\mathbf{H_3}$), 1.93–1.58 (m, 6H, C(13)$\mathbf{H_2}$, C(14)$\mathbf{H_2}$, C(15)$\mathbf{H_2}$) ppm; ^{13}C NMR (150 MHz, $CDCl_3$) δ: 159.9 (d, $^6J_{(C,F)}$ = 2 Hz, q**C**-2), 157.7 (d, $^4J_{(C,F)}$ = 5 Hz, q**C**-4), 155.4 (d, $^1J_{(C,F)}$ = 246 Hz, q**C**(6)F), 146.5 (q**C**-10), 133.9 (**C**(8)H), 122.2 (d, $^3J_{(C,F)}$ = 8 Hz, q**C**-9), 112.0 (d, $^2J_{(C,F)}$ = 24 Hz, q**C**(7)Br), 110.3 (**C**(3)H), 108.5 (d, $^2J_{(C,F)}$ = 24 Hz, **C**(5)H), 53.5 (2 × C, **C**(12)H_2, **C**(16)H_2), 26.1 (2 × C, **C**(13)H_2, **C**(15)H_2), 25.5 (**C**(11)H_3), 24.4 (**C**(14)H_2) ppm; ^{19}F NMR (282 MHz, $CDCl_3$) δ: -111 ppm; HRMS (ESI-TOF) *m/z*: $[M+H]^+$ calcd for $C_{15}H_{17}BrFN_2$: 323.0554; found: 323.0551.

6-Bromo-4-methoxyquinoline (188)[168]



Compound **188** was prepared *via* the general procedure described for **135** using 6-bromo-4-chloroquinoline (0.364 g, 1.5 mmol, 1.0 equiv.) to yield **188** as an off-white solid (0.355 g, 98%); m.p. 85–87 °C; ^1H NMR (400 MHz, $CDCl_3$) δ: 8.74 (d, *J* = 5.2 Hz, 1H, C(2)**H**), 8.34 (d, *J* = 2.1 Hz, 1H, C(5)**H**), 7.90 (d, *J* = 8.9 Hz, 1H, C(8)**H**), 7.75 (dd, *J* = 9.0, 2.2 Hz, 1H, C(7)**H**), 6.74 (d, *J* = 5.2 Hz, 1H, C(3)**H**), 4.03 (s, 3H, C(11)$\mathbf{H_3}$) ppm; ^{13}C NMR (100 MHz, $CDCl_3$) δ: 161.4 (q**C**-4), 151.6 (**C**(2)H), 147.6 (q**C**-10), 133.2 (**C**(7)H), 130.6 (**C**(8)H), 124.4 (**C**(5)H), 122.5 (q**C**-9), 119.6 (q**C**(6)Br), 100.7 (**C**(3)H), 55.9 (**C**(11)H_3) ppm; *m/z* (ES+): 238 ($(M+H)^+$ 100%).

Spectral characteristics were consistent with previously reported data.[168]

Deconvolution experiments:

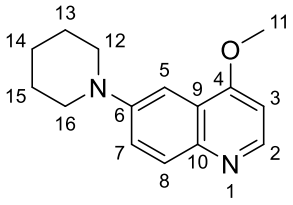
Step 1: Two Schlenk flasks were dried under vacuum, cooled to r.t. and refilled with nitrogen. **188** (0.024 g, 0.1 mmol, 1.0 equiv.), **L1**–**L8** (0.01 mmol, 10 mol% each) and **B1**–**B3** (0.25 mmol, 2.5 equiv. each) were added and the flasks was evacuated and backfilled with nitrogen three times. Piperidine (0.02 mL, 0.2 mmol, 2.0 equiv.) and

either toluene or 1,4-dioxane (5 mL) were added, and the mixtures were degassed with nitrogen for 5 min. $Pd_2(dba)_3$ (4.6 mg, 0.005 mmol, 5.0 mol%) was then added, the vessels sealed and the suspensions heated to 100 °C for 24 h. An internal standard, 1,3,5-trimethoxybenzene (~10 mol%) was added to the residue to determine the yield of **190** by ^{1}H NMR analysis.

Step 2: Two Schlenk flasks were dried under vacuum, cooled to r.t. and refilled with nitrogen. **188** (0.024 g, 0.1 mmol, 1.0 equiv.), the corresponding ligands **L1**–**L8** (0.01 mmol, 10 mol% each) and corresponding bases **B1**–**B3** (0.25 mmol, 2.5 equiv. each) were added and the flasks were evacuated and backfilled with nitrogen three times. Piperidine (0.02 mL, 0.2 mmol, 2.0 equiv.) and toluene (2.5 mL) were added, and the mixtures were degassed with nitrogen for 5 min. $Pd_2(dba)_3$ (4.6 mg, 0.005 mmol, 5.0 mol%) was then added, the vessels sealed and the suspensions heated to 100 °C for 20 h. An internal standard, 1,3,5-trimethoxybenzene (~10 mol%) was added to the residue to determine the yield of **190** by ^{1}H NMR analysis.

Step 3: Four 15 mL Schlenk flasks were dried under vacuum, cooled to r.t. and refilled with nitrogen. **188** (0.024 g, 0.1 mmol, 1.0 equiv.), the corresponding ligands **L1**–**L4** (0.006 mmol, 6.0 mol% each) and **B3** NaO*t*-Bu (0.024 g, 0.25 mmol, 2.5 equiv. each) were added and the flasks were evacuated and backfilled with nitrogen three times. Piperidine (0.02 mL, 0.2 mmol, 2.0 equiv.) and toluene (1 mL) were added, and the mixtures were degassed with nitrogen for 5 min. $Pd_2(dba)_3$ (2.7 mg, 0.003 mmol, 2.0 mol%) was then added, the vessels sealed and the suspensions heated to 100 °C for 20 h. An internal standard, 1,3,5-trimethoxybenzene (~10 mol%) was added to the residue to determine the yield of **190** by ^{1}H NMR analysis.

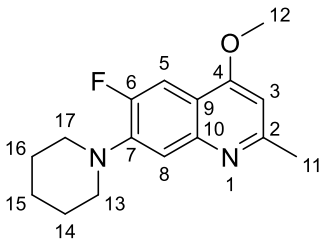
4-Methoxy-6-(piperidin-1-yl)quinoline (190)



A 15 mL Schlenk flask was dried under vacuum, cooled to r.t. and refilled with nitrogen. **188** (0.024 g, 0.1 mmol, 1.0 equiv.), RuPhos (2.8 mg, 0.006 mmol, 6.0 mol%) and NaO*t*-Bu (0.024 g, 0.25 mmol, 2.5 equiv.) were added and the flask was evacuated and backfilled with nitrogen three times. Piperidine (0.02 mL, 0.2 mmol, 2.0 equiv.) and toluene (1 mL) were added, and the mixture was

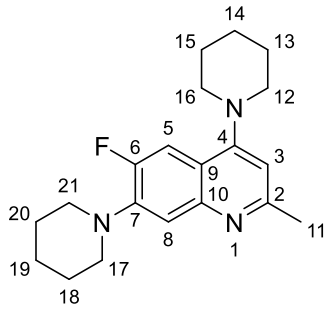
degassed with nitrogen for 5 min. $Pd_2(dba)_3$ (2.7 mg, 0.003 mmol, 3.0 mol%) was then added, the vessel sealed and the suspension heated to 100 °C for 16 h. The product was purified *via* column chromatography (DCM 100 to DCM:MeOH 98:2 with 1% NEt_3 as modifier) to yield **190** as a yellow oil (0.022 g, 92%); IR (film) ν_{max} 1621 (C=N stretch), 1507 (aromatic C=C stretch), 1373 (C-N stretch), 1305 (ether C-O stretch), 1236 (C-N stretch), 1105 (ether C-O stretch), 1026 (C-F stretch) cm^{-1}; ^1H NMR (500 MHz, $CDCl_3$) δ: 8.54 (d, *J* = 5.2 Hz, 1H, C(2)**H**), 7.91 (d, *J* = 9.2 Hz, 1H, C(8)**H**), 7.47 (dd, *J* = 9.2, 2.8 Hz, 1H, C(7)**H**), 7.40 (d, *J* = 2.7 Hz, 1H, C(5)**H**), 6.66 (d, *J* = 5.2 Hz, 1H, C(3)**H**), 4.02 (s, 3H, C(11)$\mathbf{H}_3$), 3.40–3.14 (m, 4H, C(12)$\mathbf{H}_2$, C(16)$\mathbf{H}_2$), 1.86–1.51 (m, 6H, C(13)$\mathbf{H}_2$, C(14)$\mathbf{H}_2$, C(15)$\mathbf{H}_2$) ppm; ^{13}C NMR (125 MHz, $CDCl_3$) δ: 161.3 (q**C**-4), 149.8 (q**C**-10), 147.8 (**C**(2)H), 143.9 (q**C**-10), 129.2 (**C**(8)H), 123.3 (**C**(7)H), 122.2 (q**C**-9), 103.4 (**C**(5)H), 100.1 (**C**(3)H), 55.6 (**C**(11)H_3) 50.7 (2 × C, **C**(12)H_2, **C**(16)H_2), 25.8 (2 × C, **C**(13)H_2, **C**(15)H_2), 24.3 (**C**(14)H_2) ppm; HRMS (ESI-TOF) *m/z*: $[M+H]^+$ calcd for $C_{15}H_{19}N_2O$: 243.1492; found: 243.1497.

6-Fluoro-4-methoxy-2-methyl-7-(piperidin-1-yl)quinoline (191)



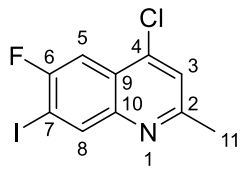
Compound **191** was prepared *via* the procedure described for **190** using **160** (0.027 g, 0.1 mmol, 1.0 equiv.) to yield **191** as a yellow oil (0.024 g, 88%); IR (film) ν_{max} 1605 (C=N stretch), 1514 (aromatic C=C stretch), 1381 (C-N stretch), 1350 (ether C-O stretch), 1241 (C-N stretch), 1131 (ether C-O stretch), 1019 (C-F stretch) cm^{-1}; ^1H NMR (500 MHz, $CDCl_3$) δ: 7.64 (d, $^2J_{(H,F)}$ = 13.5 Hz, 1H, C(5)**H**), 7.39 (d, $^3J_{(H,F)}$ = 8.3 Hz, 1H, C(8)**H**), 6.50 (s, 1H, C(3)**H**), 3.98 (s, 3H, C(12)$\mathbf{H_3}$), 3.22–3.09 (m, 4H, C(13)$\mathbf{H_2}$, C(17)$\mathbf{H_2}$), 2.65 (s, 3H, C(11)$\mathbf{H_3}$), 1.86–1.70 (m, 4H, C(14)$\mathbf{H_2}$, C(16)$\mathbf{H_2}$), 1.67–1.56 (m, 2H, C(15)$\mathbf{H_2}$) ppm; ^{13}C NMR (125 MHz, $CDCl_3$) δ: 162.0 (d, $^4J_{(C,F)}$ = 5 Hz, q**C**-4), 159.4 (d, $^6J_{(C,F)}$ = 2 Hz, q**C**-2), 154.7 (d, $^1J_{(C,F)}$ = 248 Hz, q**C**(6)F), 147.0 (q**C**-10), 144.9 (d, $^2J_{(C,F)}$ = 12 Hz, q**C**-7), 115.9 (d, $^3J_{(C,F)}$ = 3 Hz, **C**(8)H), 114.5 (d, $^3J_{(C,F)}$ = 10 Hz, q**C**-9), 106.5 (d, $^2J_{(C,F)}$ = 24 Hz, **C**(5)H), 99.5 (**C**(3)H), 55.6 (**C**(12)H_3), 52.1 (2 × C, d, $^4J_{(C,F)}$ = 4 Hz, **C**(13)H_2, **C**(17)H_2), 26.2 (2 × C, **C**(14)H_2, **C**(16)H_2), 25.8 (**C**(11)H_3), 24.4 (**C**(15)H_2) ppm; ^{19}F NMR (376 MHz, $CDCl_3$) δ: -123 ppm; HRMS (ESI-TOF) *m/z*: $[M+H]^+$ calcd for $C_{16}H_{20}FN_2O$: 275.1554; found: 275.1555.

6-Fluoro-2-methyl-4,7-di(piperidin-1-yl)quinoline (192)



Compound **192** was prepared *via* the procedure described for **190** using **159** (0.028 g, 0.1 mmol, 1.0 equiv.) except that the amount of coupling partner piperidine (0.02 mL, 0.2 mmol, 2.0 equiv.) was doubled to yield **192** as a yellow oil (0.026 g, 80%); IR (film) ν_{max} 1625 (C=N stretch), 1589 (aromatic C=C stretch), 1381, 1275, 1239 (C-N stretches), 1026 (C-F stretch) cm^{-1}; ^{1}H NMR (500 MHz, $CDCl_3$) δ: 7.47 (d, $^{2}J_{(H,F)}$ = 14.2 Hz, 1H, C(5)**H**), 7.41 (d, $^{4}J_{(H,F)}$ = 8.6 Hz, 1H, C(8)**H**), 6.60 (s, 1H, C(3)**H**), 3.29–2.93 (m, 8H, C(12)$\mathbf{H_2}$, C(16)$\mathbf{H_2}$, C(17)$\mathbf{H_2}$, C(21)$\mathbf{H_2}$), 2.62 (s, 3H, C(11)$\mathbf{H_3}$), 1.89–1.73 (m, 8H, C(13)$\mathbf{H_2}$, C(15)$\mathbf{H_2}$, C(18)$\mathbf{H_2}$, C(20)$\mathbf{H_2}$), 1.72–1.56 (m, 4H, C(14)$\mathbf{H_2}$, C(19)$\mathbf{H_2}$) ppm; ^{13}C NMR (125 MHz, $CDCl_3$) δ: 158.5 (d, $^{6}J_{(C,F)}$ = 2 Hz, q**C**-2), 157.6 (d, $^{4}J_{(C,F)}$ = 5 Hz, q**C**-4), 154.2 (d, $^{1}J_{(C,F)}$ = 248 Hz, q**C**(6)F), 147.1 (q**C**-10), 144.0 (d, $^{2}J_{(C,F)}$ = 12 Hz, q**C**-7), 117.0 (d, $^{3}J_{(C,F)}$ = 9 Hz, q**C**-9), 116.4 (d, $^{3}J_{(C,F)}$ = 3 Hz, **C**(8)H), 108.3 (d, $^{2}J_{(C,F)}$ = 24 Hz, **C**(5)H), 108.1 (**C**(3)H), 53.4 (2 × C, **C**(12)H_2, **C**(16)H_2), 52.0 (2 × C, d, $^{4}J_{(C,F)}$ = 4 Hz, **C**(17)H_2, **C**(21)H_2), 26.1 (2 × C, **C**(18)H_2, **C**(20)H_2), 26.0 (2 × C, **C**(13)H_2, **C**(15)H_2), 25.3 (**C**(11)H_3), 24.5 (**C**(19)H_2), 24.2 (**C**(14)H_2) ppm; ^{19}F NMR (470 MHz, $CDCl_3$) δ: -123 ppm; HRMS (ESI-TOF) *m/z*: $[M+H]^+$ calcd for $C_{20}H_{27}FN_3$: 328.2184; found: 328.2190.

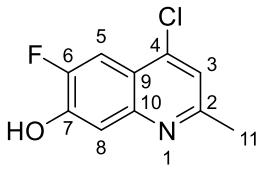
4-Chloro-6-fluoro-7-iodo-2-methylquinoline (193)



A 15 mL Schlenk tube was oven dried (150 °C) and cooled under vacuum. The flask was refilled with nitrogen and all reagents were added under a positive pressure of nitrogen in the order: **132** (0.039 g, 0.2 mmol, 1.0 equiv.), dtbpy (1.6 mg, 0.006 mmol, 3 mol%), B_2pin_2 (0.056 g, 0.22 mmol, 1.1 equiv.), and $[Ir(OMe)COD]_2$ (2.0 mg, 0.003 mmol, 1.5 mol%). The Schlenk tube was then placed under vacuum for 20 min before being refilled with nitrogen three times. THF (0.5 mL) was added *via* syringe, the reaction was sealed, and the mixture heated to 80 °C for 16 h, then cooled to r.t. and concentrated under reduced pressure. The crude reaction mixture for **133** (0.2 mmol, 1.0 equiv.) was dissolved in MeOH (1.6 mL) and added to a 5 mL screw-capped vial containing CuI (3.8 mg, 0.02 mmol, 10 mol%), 1,10-phenanthroline (7.2 mg, 0.04 mmol, 0.2 equiv.) and KI (49.8 mg, 0.3 mmol, 1.5 equiv.). The mixture was stirred at

r.t. for 5 min, H_2O (0.4 mL) was then added, the vial sealed and heated to 80 °C for 2 h.[119] The solution was cooled to r.t., diluted with DCM and H_2O and the layers were separated. The aqueous portion was extracted with DCM (2 × 5 mL) and the combined organic layers were then washed with brine (10 mL), dried over $MgSO_4$, filtered and concentrated under reduced pressure. Purification *via* column chromatography (DCM 100 to DCM:EtOAc 95:5) to yield **193** as a white solid (0.038 g, 64%); m.p. 108–111 °C; IR (film) ν_{max} 1594 (C=N stretch), 1538 (aromatic C=C stretch), 1097 (C-F stretch), 704 (C-Cl stretch), 628 (C-Br stretch) cm^{-1}; ^1H NMR (300 MHz, $CDCl_3$) δ: 8.52 (d, $^4J_{(H,F)}$ = 6.0 Hz, 1H, C(8)**H**), 7.76 (d, $^3J_{(H,F)}$ = 8.4 Hz, 1H, C(5)**H**), 7.41 (s, 1H, C(3)**H**), 2.70 (s, 3H, C(11)**H₃**) ppm; ^{13}C NMR (75 MHz, $CDCl_3$) δ: 159.1 (d, $^6J_{(C,F)}$ = 3 Hz, q**C**-2), 159.0 (d, $^1J_{(C,F)}$ = 247 Hz, q**C**(6)F), 146.1 (q**C**-10), 141.7 (d, $^4J_{(C,F)}$ = 5 Hz, q**C**(4)Cl), 140.8 (d, $^3J_{(C,F)}$ = 3 Hz, **C**(8)H), 125.6 (d, $^3J_{(C,F)}$ = 9 Hz, q**C**-9), 122.9 (**C**(3)H), 107.5 (d, $^2J_{(C,F)}$ = 27 Hz, **C**(5)H), 87.2 (d, $^2J_{(C,F)}$ = 29 Hz, q**C**(7)I), 25.0 (**C**(11)H_3) ppm; ^{19}F NMR (282 MHz, $CDCl_3$) δ: -95 ppm; HRMS (ESI-TOF) *m/z*: $[M+H]^+$ calcd for $C_{10}H_7ClFIN$: 321.9290; found: 321.9286.

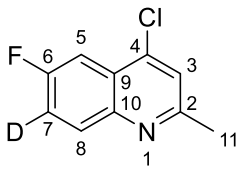
4-Chloro-6-fluoro-2-methylquinolin-7-ol (194)



A solution of **133** (0.064 g, 0.2 mmol, 1.0 equiv.) in MeOH (0.5 mL) in a 5 mL screw-capped vial was cooled over ice. 30% H_2O_2 solution (0.02 mL, 0.24 mmol, 1.18 equiv.) was gradually added. The mixture was allowed warm slowly to r.t. and stirred at this temperature for 16 h. The reaction mixture was then diluted with MeOH, quenched using saturated $Na_2S_2O_3$ solution (~1 mL) and MeOH was removed under reduced pressure. The mixture was then extracted with EtOAc (3 × 10 mL), dried over $MgSO_4$, filtered and concentrated under reduced pressure. to yield **194** as a white solid (0.036 g, 85%); m.p. 192–195 °C; IR (film) ν_{max} 1629 (C=N stretch), 1539 (aromatic C=C stretch), 1261 (C-O stretch), 1032 (C-F stretch), 797 (C-Cl stretch) cm^{-1}; ^1H NMR (600 MHz, $(CD_3)_2SO$) δ: 11.09 (bs, 1H, O**H**), 7.78 (d, $^3J_{(H,F)}$ = 11.7 Hz, 1H, C(5)**H**), 7.49 (s, 1H, C(3)**H**), 7.40 (d, $^4J_{(H,F)}$ = 8.5 Hz, 1H, C(8)**H**), 2.58 (s, 3H, C(11)**H₃**) ppm; ^{13}C NMR (150 MHz, $(CD_3)_2SO$) δ: 158.7 (d, $^6J_{(C,F)}$ = 2 Hz, q**C**-2), 152.1 (d, $^1J_{(C,F)}$ = 249 Hz, q**C**(6)F), 149.2 (d, $^2J_{(C,F)}$ = 15 Hz, q**C**-7), 146.5 (q**C**-10), 140.0 (d, $^4J_{(C,F)}$ = 5 Hz, q**C**(4)Cl), 119.8 (**C**(3)H), 117.8 (d, $^3J_{(C,F)}$ = 9 Hz, q**C**-9), 113.1 (d, $^3J_{(C,F)}$ = 3 Hz, **C**(8)H),

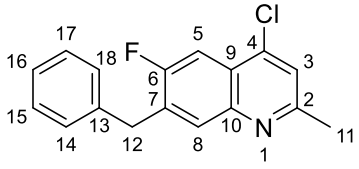
108.1 (d, $^{2}J_{(C,F)}$ = 21 Hz, **C**(5)H), 24.5 (**C**(11)H_3) ppm; ^{19}F NMR (282 MHz, $(CD_3)_2SO$) δ: -131 ppm; HRMS (ESI-TOF) *m/z*: $[M+H]^+$ calcd for $C_{10}H_8ClFNO$: 212.0273; found: 212.0269.

4-Chloro-6-fluoro-2-methylquinoline-7-*d* (195)



A 15 mL Schlenk flask was flame dried and cooled under vacuum. The Schlenk flask was refilled with nitrogen and **133** (0.064 g, 0.2 mmol, 1.0 equiv.) and $[Ir(OMe)COD]_2$ (1.3 mg, 0.002 mmol, 1.0 mol%) were added and the Schlenk flask was evacuated and backfilled with nitrogen three times. THF (0.8 mL) and D_2O (0.2 mL) were added, the vessel sealed, and the mixture heated to 80 °C for 12 h. The solution was cooled to r.t. and extracted with Et_2O (2 × 5 mL).[148] The combined organic layers were washed with brine (10 mL), dried over $MgSO_4$, filtered and concentrated under reduced pressure. Purification *via* column chromatography (DCM 100 to DCM:EtOAc 90:10) to yield **195** as a colourless crystalline solid (0.021 g, 57%); m.p. 85–86 °C; IR (film) ν_{max} 1617 (C=N stretch), 1555 (aromatic C=C stretch), 1025 (C-F stretch), 830 (C-Cl stretch) cm^{-1}; ^{1}H NMR (400 MHz, $CDCl_3$) δ: 8.02 (d, $^{4}J_{(H,F)}$ = 5.2 Hz, 1H, C(8)**H**), 7.79 (d, $^{3}J_{(H,F)}$ = 9.4 Hz, 1H, C(5)**H**), 7.41 (s, 1H, C(3)**H**), 2.71 (s, 3H, C(11)$\mathbf{H_3}$) ppm; ^{13}C NMR (100 MHz, $CDCl_3$) δ: 160.8 (d, $^{1}J_{(C,F)}$ = 249 Hz, q**C**(6)F), 158.3 (d, $^{6}J_{(C,F)}$ = 3 Hz, q**C**-2), 145.6 (q**C**-10), 142.1 (d, $^{4}J_{(C,F)}$ = 5 Hz, q**C**(4)Cl), 131.5 (d, $^{3}J_{(C,F)}$ = 9 Hz, **C**(8)H), 125.8 (d, $^{3}J_{(C,F)}$ = 11 Hz, q**C**-9), 122.7 (**C**(3)H), 121.0–120.0 (m, q**C**(7)D), 107.9 (d, $^{2}J_{(C,F)}$ = 24 Hz, **C**(5)H), 25.0 (**C**(11)H_3) ppm; ^{19}F NMR (282 MHz, $CDCl_3$) δ: -113 ppm; HRMS (ESI-TOF) *m/z*: $[M+H]^+$ calcd for $C_{10}H_7DClFN$: 197.0387; found: 197.0380.

7-Benzyl-4-chloro-6-fluoro-2-methylquinoline (196)



A 15 mL Schlenk flask was dried under vacuum, cooled to r.t. and refilled with nitrogen. **133** (0.064 g, 0.2 mmol, 1.0 equiv.), $Pd_2(dba)_3$ (1.8 mg, 0.002 mmol, 1.0 mol%), PPh_3 (2.1 mg, 0.008 mmol, 4.0 mol%) and K_2CO_3 (0.111 g, 0.8 mmol, 4.0 equiv.) were added and the flask was evacuated and backfilled with nitrogen three times. Benzyl bromide (0.03 mL, 0.24 mmol, 1.2 equiv.), THF (1 mL) and H_2O (0.02 mL) were added, the vessel sealed and the

mixture heated to 100 °C for 24 h.[148] The solution was cooled to r.t., diluted with H_2O and extracted with EtOAc (3 × 10 mL). The combined organic layers were washed with brine (10 mL), dried over $MgSO_4$, filtered and concentrated under reduced pressure. Purification *via* column chromatography (DCM) to yield **196** as an off-white solid (0.049 g, 86%); m.p. 94–96 °C; IR (film) ν_{max} 1635 (C=N stretch), 1598, 1551 (aromatic C=C stretch), 1027 (C-F stretch), 871 (C-Cl stretch) cm^{-1}; ^1H NMR (400 MHz, $CDCl_3$) δ: 7.88–7.66 (m, 2H, C(5)**H**, C(8)**H**), 7.39–7.14 (m, 6H, C(3)**H**, C(14)**H**, C(15)**H**, C(16)**H**, C(17)**H**, C(18)**H**), 4.16 (s, 2H, C(12)$\mathbf{H_2}$), 2.66 (s, 3H, C(11)$\mathbf{H_3}$) ppm; ^{13}C NMR (100 MHz, $CDCl_3$) δ: 159.7 (d, $^1J_{(C,F)}$ = 250 Hz, q**C**(6)F), 158.1 (d, $^6J_{(C,F)}$ = 2 Hz, q**C**-2), 145.6 (q**C**-10), 141.6 (d, $^4J_{(C,F)}$ = 5 Hz, q**C**(4)Cl), 138.5 (q**C**-13), 134.3 (d, $^2J_{(C,F)}$ = 20 Hz, q**C**-7), 131.0 (d, $^3J_{(C,F)}$ = 6 Hz, **C**(8)H), 129.1 (2 × C, **C**(14)H, **C**(18)H), 128.7 (2 × C, **C**(15)H, **C**(17)H), 126.6 (**C**(16)H), 124.4 (d, $^3J_{(C,F)}$ = 10 Hz, q**C**-9), 121.9 (**C**(3)H), 107.7 (d, $^2J_{(C,F)}$ = 26 Hz, **C**(5)H), 35.5 (d, $^3J_{(C,F)}$ = 3 Hz, **C**(12)H_2), 24.9 (**C**(11)H_3) ppm; ^{19}F NMR (376 MHz, $CDCl_3$) δ: -117 ppm; HRMS (ESI-TOF) *m/z*: $[M+H]^+$ calcd for $C_{17}H_{14}ClFN$: 286.0793; found: 286.0785.

References

1. Heeb, S., Fletcher, M. P., Chhabra, S. R., Diggle, S. P., Williams, P., Cámara, M. *FEMS Microbiol. Rev.* **2011**, *35*, 247-274.
2. Bisacchi, G. S. *J. Med. Chem.* **2015**, *58*, 4874-4882.
3. Emmerson, A. M., Jones, A. M. *J. Antimicrob. Chemother.* **2003**, *51*, 13-20.
4. Bryskier, A., Chantot, J. F. *Drugs* **1995**, *49*, 16-28.
5. Suda, K. J., Hicks, L. A., Roberts, R. M., Hunkler, R. J., Matusiak, L. M., Schumock, G. T. *Clin. Infect. Dis.* **2017**, *66*, 185-190.
6. Almalki, Z. S., Yue, X., Xia, Y., Wigle, P. R., Guo, J. J. *PharmacoEconomics - Open* **2017**, *1*, 123-131.
7. Zhanel, G. G., Walkty, A., Vercaigne, L., Karlowsky, J. A., Embil, J., Gin, A. S., Hoban, D. J. *Can. J. Infect. Dis.* **1999**, *10*, 207-238.
8. Zhanel, G. G., Ennis, K., Vercaigne, L., Walkty, A., Gin, A. S., Embil, J., Smith, H., Hoban, D. J. *Drugs* **2002**, *62*, 13-59.
9. *World Health Organization Model List of Essential Medicines – 22nd List*, (Geneva: World Health Organization), **2021**.
10. Mitscher, L. A. *Chem. Rev.* **2005**, *105*, 559-592.
11. Drlica, K., Zhao, X. *Microbiol Mol Biol Rev* **1997**, *61*, 377-392.
12. Grohe, K. in *Quinolone Antibacterials*, Springer, Berlin, Heidelberg, **1998**, pp. 13-62.
13. Li, J. J. *Name Reactions: A Collection of Detailed Mechanisms and Synthetic Applications Fifth Edition*, Springer International Publishing, Cham, **2014**.
14. Ghosh, P., Das, S. *Eur. J. Org. Chem.* **2019**, *2019*, 4466-4516.
15. Shen, C., Wang, A., Xu, J., An, Z., Loh, K. Y., Zhang, P., Liu, X. *Chem* **2019**, *5*, 1059-1107.
16. Bergman, R. G. *Nature* **2007**, *446*, 391-393.
17. Wencel-Delord, J., Dröge, T., Liu, F., Glorius, F. *Chem. Soc. Rev.* **2011**, *40*, 4740-4761.
18. Wencel-Delord, J., Glorius, F. *Nat. Chem.* **2013**, *5*, 369-375.
19. Guillemard, L., Kaplaneris, N., Ackermann, L., Johansson, M. J. *Nat. Rev. Chem.* **2021**, *5*, 522-545.

20. Lam, N. Y. S., Wu, K., Yu, J.-Q. *Angew. Chem. Int. Ed.* **2021**, *60*, 15767-15790.
21. Godula, K., Sames, D. *Science* **2006**, *312*, 67-72.
22. Hall, D. G. in *Boronic Acids*, John Wiley & Sons, Weinheim, Germany, **2011**, pp. 1-133.
23. Fernández, E., Whiting, A., (Eds) *Synthesis and Application of Organoboron Compounds*, Springer, Cham, Switzerland, **2015**.
24. Suzuki, A. *Angew. Chem. Int. Ed.* **2011**, *50*, 6722-6737.
25. Mkhalid, I. A. I., Barnard, J. H., Marder, T. B., Murphy, J. M., Hartwig, J. F. *Chem. Rev.* **2010**, *110*, 890-931.
26. Chow, W. K., Yuen, O. Y., Choy, P. Y., So, C. M., Lau, C. P., Wong, W. T., Kwong, F. Y. *RSC Adv.* **2013**, *3*, 12518-12539.
27. Wang, M., Shi, Z. *Chem. Rev.* **2020**, *120*, 7348-7398.
28. Légaré, M.-A., Courtemanche, M.-A., Rochette, É., Fontaine, F.-G. *Science* **2015**, *349*, 513-516.
29. Fontaine, F.-G., Desrosiers, V. *Synthesis* **2021**, *53*, 4599-4613.
30. Del Grosso, A., Singleton, P. J., Muryn, C. A., Ingleson, M. J. *Angew. Chem. Int. Ed.* **2011**, *50*, 2102-2106.
31. Hartwig, J. F. *Acc. Chem. Res.* **2012**, *45*, 864-873.
32. Fyfe, J. W. B., Watson, A. J. B. *Chem* **2017**, *3*, 31-55.
33. Ros, A., Fernández, R., Lassaletta, J. M. *Chem. Soc. Rev.* **2014**, *43*, 3229-3243.
34. Bose, S. K., Mao, L., Kuehn, L., Radius, U., Nekvinda, J., Santos, W. L., Westcott, S. A., Steel, P. G., Marder, T. B. *Chem. Rev.* **2021**, *121*, 13238-13341.
35. Nelson, K. L. *J. Org. Chem.* **1956**, *21*, 145-155.
36. Klumpp, D. A. in *Arene Chemistry: Reaction Mechanisms and Methods for Aromatic Compounds*, John Wiley & Sons, Hoboken, New Jersey, **2015**, pp. 1-31.
37. Maleczka, R. E., Shi, F., Holmes, D., Smith, M. R. *J. Am. Chem. Soc.* **2003**, *125*, 7792-7793.
38. Hodgson, H. H., Wignall, J. S. *J. Chem. Soc.* **1926**, *129*, 2077-2079.
39. Xu, L., Wang, G., Zhang, S., Wang, H., Wang, L., Liu, L., Jiao, J., Li, P. *Tetrahedron* **2017**, *73*, 7123-7157.

40. Nguyen, P., Blom, H. P., Westcott, S. A., Taylor, N. J., Marder, T. B. *J. Am. Chem. Soc.* **1993**, *115*, 9329-9330.
41. Iverson, C. N., Smith, M. R. *J. Am. Chem. Soc.* **1999**, *121*, 7696-7697.
42. Cho, J.-Y., Iverson, C. N., Smith, M. R. *J. Am. Chem. Soc.* **2000**, *122*, 12868-12869.
43. Cho, J.-Y., Tse, M. K., Holmes, D., Maleczka, R. E., Smith, M. R. *Science* **2002**, *295*, 305-308.
44. Ishiyama, T., Takagi, J., Ishida, K., Miyaura, N., Anastasi, N. R., Hartwig, J. F. *J. Am. Chem. Soc.* **2002**, *124*, 390-391.
45. Ishiyama, T., Takagi, J., Hartwig, J. F., Miyaura, N. *Angew. Chem. Int. Ed.* **2002**, *41*, 3056-3058.
46. Takagi, J., Sato, K., Hartwig, J. F., Ishiyama, T., Miyaura, N. *Tetrahedron Lett.* **2002**, *43*, 5649-5651.
47. Ishiyama, T., Takagi, J., Yonekawa, Y., Hartwig, J. F., Miyaura, N. *Adv. Synth. Catal.* **2003**, *345*, 1103-1106.
48. Ishiyama, T., Miyaura, N. *Pure Appl. Chem.* **2006**, *78*, 1369-1375.
49. Ishiyama, T., Nobuta, Y., Hartwig, J. F., Miyaura, N. *Chem. Commun.* **2003**, 2924-2925.
50. Mertins, K., Zapf, A., Beller, M. *J. Mol. Catal. A Chem.* **2004**, *207*, 21-25.
51. Kawamorita, S., Ohmiya, H., Hara, K., Fukuoka, A., Sawamura, M. *J. Am. Chem. Soc.* **2009**, *131*, 5058-5059.
52. Xu, F., Duke, O. M., Rojas, D., Eichelberger, H. M., Kim, R. S., Clark, T. B., Watson, D. A. *J. Am. Chem. Soc.* **2020**, *142*, 11988-11992.
53. Bai, S.-T., Bheeter, C. B., Reek, J. N. H. *Angew. Chem. Int. Ed.* **2019**, *58*, 13039-13043.
54. Boebel, T. A., Hartwig, J. F. *J. Am. Chem. Soc.* **2008**, *130*, 7534-7535.
55. Tajuddin, H., Harrisson, P., Bitterlich, B., Collings, J. C., Sim, N., Batsanov, A. S., Cheung, M. S., Kawamorita, S., Maxwell, A. C., Shukla, L.*, et al. Chem. Sci.* **2012**, *3*, 3505-3515.
56. Wright, J. S., Scott, P. J. H., Steel, P. G. *Angew. Chem. Int. Ed.* **2021**, *60*, 2796-2821.
57. Robbins, D. W., Hartwig, J. F. *Angew. Chem. Int. Ed.* **2013**, *52*, 933-937.

58. Sadler, S. A., Hones, A. C., Roberts, B., Blakemore, D., Marder, T. B., Steel, P. G. *J. Org. Chem.* **2015**, *80*, 5308-5314.

59. Paul, S., Chotana, G. A., Holmes, D., Reichle, R. C., Maleczka, R. E., Smith, M. R. *J. Am. Chem. Soc.* **2006**, *128*, 15552-15553.

60. Chotana, G. A., Kallepalli, V. A., Maleczka, R. E., Smith, M. R. *Tetrahedron* **2008**, *64*, 6103-6114.

61. Tamura, H., Yamazaki, H., Sato, H., Sakaki, S. *J. Am. Chem. Soc.* **2003**, *125*, 16114-16126.

62. Boller, T. M., Murphy, J. M., Hapke, M., Ishiyama, T., Miyaura, N., Hartwig, J. F. *J. Am. Chem. Soc.* **2005**, *127*, 14263-14278.

63. Miyaura, N. *Bull. Chem. Soc. Jpn.* **2008**, *81*, 1535-1553.

64. Chotana, G. A., Rak, M. A., Smith, M. R. *J. Am. Chem. Soc.* **2005**, *127*, 10539-10544.

65. Vanchura, I. I. B. A., Preshlock, S. M., Roosen, P. C., Kallepalli, V. A., Staples, R. J., Maleczka, J. R. E., Singleton, D. A., Smith, I. I. I. M. R. *Chem. Commun.* **2010**, *46*, 7724-7726.

66. Mkhalid, I. A. I., Coventry, D. N., Albesa-Jove, D., Batsanov, A. S., Howard, J. A. K., Perutz, R. N., Marder, T. B. *Angew. Chem. Int. Ed.* **2006**, *45*, 489-491.

67. Merz, J. M. *Ph.D Thesis*, **2019**.

68. Larsen, M. A., Hartwig, J. F. *J. Am. Chem. Soc.* **2014**, *136*, 4287-4299.

69. Sadler, S. A., Tajuddin, H., Mkhalid, I. A. I., Batsanov, A. S., Albesa-Jove, D., Cheung, M. S., Maxwell, A. C., Shukla, L., Roberts, B., Blakemore, D. C., *et al. Org. Biomol. Chem.* **2014**, *12*, 7318-7327.

70. Cox, P. A., Leach, A. G., Campbell, A. D., Lloyd-Jones, G. C. *J. Am. Chem. Soc.* **2016**, *138*, 9145-9157.

71. Harrisson, P., Morris, J., Steel, P. G., Marder, T. B. *Synlett* **2009**, *2009*, 147-150.

72. Harrisson, P., Morris, J., Marder, T. B., Steel, P. G. *Org. Lett.* **2009**, *11*, 3586-3589.

73. Corio, A., Gravier-Pelletier, C., Busca, P. *Molecules* **2021**, *26*, 5467.

74. Iwai, T., Sawamura, M. *ACS Catal.* **2015**, *5*, 5031-5040.

75. Stephens, D. E., Larionov, O. V. *Tetrahedron* **2015**, *71*, 8683-8716.

76. Sharma, R., Thakur, K., Kumar, R., Kumar, I., Sharma, U. *Catal. Rev.* **2015**, *57*, 345-405.

77. Das, R., Kapur, M. *Asian J. Org. Chem.* **2018**, *7*, 1217-1235.

78. Wang, D., Désaubry, L., Li, G., Huang, M., Zheng, S. *Adv. Synth. Catal.* **2021**, *363*, 2-39.

79. Zhou, J., Li, B., Hu, F., Shi, B.-F. *Org. Lett.* **2013**, *15*, 3460-3463.

80. Konishi, S., Kawamorita, S., Iwai, T., Steel, P. G., Marder, T. B., Sawamura, M. *Chem. Asian J.* **2014**, *9*, 434-438.

81. Hamasaka, G., Kawamorita, S., Ochida, A., Akiyama, R., Hara, K., Fukuoka, A., Asakura, K., Chun, W. J., Ohmiya, H., Sawamura, M. *Organometallics* **2008**, *27*, 6495-6506.

82. Reen, F. J., Shanahan, R., Cano, R., O'Gara, F., McGlacken, G. P. *Org. Biomol. Chem.* **2015**, *13*, 5537-5541.

83. Reen, F. J., Phelan, J. P., Woods, D. F., Shanahan, R., Cano, R., Clarke, S., McGlacken, G. P., O'Gara, F. *Front. Microbiol.* **2016**, *7*, 2074.

84. Reen, F. J., Phelan, J. P., Gallagher, L., Woods, D. F., Shanahan, R. M., Cano, R., Ó Muimhneacháin, E., McGlacken, G. P., O'Gara, F. *Antimicrob. Agents Chemother.* **2016**, *60*, 5894-5905.

85. Shanahan, R., Reen, F. J., Cano, R., O'Gara, F., McGlacken, G. P. *Org. Biomol. Chem.* **2017**, *15*, 306-310.

86. Ramos, A. F., Woods, D. F., Shanahan, R., Cano, R., McGlacken, G. P., Serra, C., O'Gara, F., Reen, F. J. *Microbiology* **2020**, *166*, 169-179.

87. Torres-Fuentes, C., Pastor-Cavada, E., Cano, R., Kandil, D., Shanahan, R., Juan, R., Shaban, H., McGlacken, G. P., Schellekens, H. *Int. J. Mol. Sci.* **2018**, *19*, 1605.

88. Williams, D. B. G., Lawton, M. *J. Org. Chem.* **2010**, *75*, 8351-8354.

89. Murphy, J. M., Tzschucke, C. C., Hartwig, J. F. *Org. Lett.* **2007**, *9*, 757-760.

90. Bannen, L. C., Bui, M., Jiang, F., Wang, Y., Xu, W., *Compounds for the Treatment of Kinase-Dependent Disorders*, (Exelixis, Inc. US), WO2019/148043, **2019**.

91. Vasdev, N., Rotstein, B. H., Liang, H. S., *Method Of Fluorination Using Iodonium Ylides*, (The General Hospital Corporation Boston), US10259800B2, **2019**.

92. Iqbal, S. A., Cid, J., Procter, R. J., Uzelac, M., Yuan, K., Ingleson, M. J. *Angew. Chem. Int. Ed.* **2019**, *58*, 15381-15385.

93. Szamosvári, D., Prothiwa, M., Dieterich, C. L., Böttcher, T. *Chem. Commun.* **2020**, *56*, 6328-6331.

94. Nilsen, A., Miley, G. P., Forquer, I. P., Mather, M. W., Katneni, K., Li, Y., Pou, S., Pershing, A. M., Stickles, A. M., Ryan, E.*, et al. J. Med. Chem.* **2014**, *57*, 3818-3834.

95. Pou, S., Dodean, R. A., Frueh, L., Liebman, K. M., Gallagher, R. T., Jin, H., Jacobs, R. T., Nilsen, A., Stuart, D. R., Doggett, J. S.*, et al. Org. Process Res. Dev.* **2021**, *25*, 1841-1852.

96. Doggett, J. S., Schultz, T., Miller, A. J., Bruzual, I., Pou, S., Winter, R., Dodean, R., Zakharov, L. N., Nilsen, A., Riscoe, M. K.*, et al. Antimicrob. Agents Chemother.* **2020**, *64*, e00535-00520.

97. Grainger, R., Nikmal, A., Cornella, J., Larrosa, I. *Org. Biomol. Chem.* **2012**, *10*, 3172-3174.

98. Rudzki, M., Alcalde-Aragonés, A., Dzik, W. I., Rodríguez, N., Gooßen, L. J. *Synthesis* **2012**, *44*, 184-193.

99. Lu, P., Sanchez, C., Cornella, J., Larrosa, I. *Org. Lett.* **2009**, *11*, 5710-5713.

100. McOmie, J. F. W., Watts, M. L., West, D. E. *Tetrahedron* **1968**, *24*, 2289-2292.

101. Weiss, M. M., Dineen, T. A., Marx, I. E., Altmann, S., Boezio, A., Bregman, H., Chu-Moyer, M., DiMauro, E. F., Feric Bojic, E., Foti, R. S.*, et al. J. Med. Chem.* **2017**, *60*, 5969-5989.

102. Bui, M., Hao, X., Shin, Y., Cardozo, M., He, X., Henne, K., Suchomel, J., McCarter, J., McGee, L. R., San Miguel, T.*, et al. Bioorg. Med. Chem. Lett.* **2015**, *25*, 1104-1109.

103. Bretéché, A., Marchand, P., Nourrisson, M.-R., De Nanteuil, G., Duflos, M. *Tetrahedron* **2010**, *66*, 4490-4494.

104. Prendergast, A. M., McGlacken, G. P. *Eur. J. Org. Chem.* **2017**, 4827-4835.

105. Olah, G. A., Narang, S. C., Gupta, B. G. B., Malhotra, R. *J. Org. Chem.* **1979**, *44*, 1247-1251.

106. Wu, H., Lin, J., Li, Y., Wei, C., Chen, S., Long, C., Chen, X., Liu, Z., Chen, L., *Quinoline derivatives as smo inhibitors*, (Guangdong Zhongsheng Pharmaceutical Co. Ltd), EP3124482A1, **2017**.

107. Santana, L., Uriarte, E., Fall, Y., Teijeira, M., Terán, C., García-Martínez, E., Tolf, B.-R. *Eur. J. Med. Chem.* **2002**, *37*, 503-510.

108. Wu, S., Xu, C., Xia, K., Lin, Y., Tian, S., Ma, H., Ji, Y., Zhu, F., He, S., Zhang, X. *Eur. J. Med. Chem.* **2021**, *217*, 113327.

109. Rádl, S., Rezková, H., Obadalová, I., Srbek, J., Břicháč, J., Pekárek, T. *Synthesis* **2014**, *46*, 899-908.

110. Shubin, Y., Jianjun, M., Feifei, Z., Guangyu, F., Zeyu, W., Hongyun, Y., Liying, W., Xuewei, W., *Indole-glucoside substrate and preparation method and application thereof in detection of aerobe vaginitis*, (Autobio Diagnostics Co. Ltd), CN108409815 (A), **2018**.

111. Schroeder, G. M., Chen, X.-T., Williams, D. K., Nirschl, D. S., Cai, Z.-W., Wei, D., Tokarski, J. S., An, Y., Sack, J., Chen, Z.*, et al. Bioorg. Med. Chem. Lett.* **2008**, *18*, 1945-1951.

112. Hocke, H., Uozumi, Y. *Tetrahedron* **2003**, *59*, 619-630.

113. Recsei, C., McErlean, C. S. P. *Tetrahedron* **2012**, *68*, 464-480.

114. McCaulay, D. A., Lien, A. P., Launer, P. J. *J. Am. Chem. Soc.* **1954**, *76*, 2354-2357.

115. Thinnes, C. C., Tumber, A., Yapp, C., Scozzafava, G., Yeh, T., Chan, M. C., Tran, T. A., Hsu, K., Tarhonskaya, H., Walport, L. J.*, et al. Chem. Commun.* **2015**, *51*, 15458-15461.

116. Thompson, A. L. S., Kabalka, G. W., Akula, M. R., Huffman, J. W. *Synthesis* **2005**, *2005*, 547-550.

117. Murphy, J. M., Liao, X., Hartwig, J. F. *J. Am. Chem. Soc.* **2007**, *129*, 15434-15435.

118. Heindel, N. D., Fine, S. A. *J. Org. Chem.* **1970**, *35*, 796-798.

119. Chen, G., Shigenari, T., Jain, P., Zhang, Z., Jin, Z., He, J., Li, S., Mapelli, C., Miller, M. M., Poss, M. A.*, et al. J. Am. Chem. Soc.* **2015**, *137*, 3338-3351.

120. Ji, Y., Brueckl, T., Baxter, R. D., Fujiwara, Y., Seiple, I. B., Su, S., Blackmond, D. G., Baran, P. S. *Proc. Natl. Acad. Sci. U.S.A.* **2011**, *108*, 14411-14415.

121. Fujiwara, Y., Dixon, J. A., O'Hara, F., Funder, E. D., Dixon, D. D., Rodriguez, R. A., Baxter, R. D., Herlé, B., Sach, N., Collins, M. R.*, et al. Nature* **2012**, *492*, 95-99.

122. Fujiwara, Y., Domingo, V., Seiple, I. B., Gianatassio, R., Del Bel, M., Baran, P. S. *J. Am. Chem. Soc.* **2011**, *133*, 3292-3295.

123. Schröter, S., Stock, C., Bach, T. *Tetrahedron* **2005**, *61*, 2245-2267.

124. Düfert, M. A., Billingsley, K. L., Buchwald, S. L. *J. Am. Chem. Soc.* **2013**, *135*, 12877-12885.

125. Rossi, R., Bellina, F., Lessi, M., Manzini, C. *Adv. Synth. Catal.* **2014**, *356*, 17-117.

126. Crawford, A. G., Liu, Z., Mkhalid, I. A. I., Thibault, M.-H., Schwarz, N., Alcaraz, G., Steffen, A., Collings, J. C., Batsanov, A. S., Howard, J. A. K.*, et al. Chem. Eur. J.* **2012**, *18*, 5022-5035.

127. Miyaura, N., Suzuki, A. *Chem. Rev.* **1995**, *95*, 2457-2483.

128. Blakemore, D. in *Synthetic Methods in Drug Discovery, Vol. 1*, The Royal Society of Chemistry, **2016**, pp. 1-69.

129. Robbins, D. W., Hartwig, J. F. *Org. Lett.* **2012**, *14*, 4266-4269.

130. Ji, H., Cai, J., Gan, N., Wang, Z., Wu, L., Li, G., Yi, T. *Chem. Cent. J.* **2018**, *12*, 136.

131. Ji, H., Wu, L.-Y., Cai, J.-H., Li, G.-R., Gan, N.-N., Wang, Z.-H. *RSC Adv.* **2018**, *8*, 13643-13648.

132. Ramírez, J., Lillo, V., Segarra, A. M., Fernández, E. *Curr. Org. Chem.* **2008**, *12*, 405-423.

133. Chen, J.-Q., Li, J.-H., Dong, Z.-B. *Adv. Synth. Catal.* **2020**, *362*, 3311-3331.

134. Vantourout, J. C., Law, R. P., Isidro-Llobet, A., Atkinson, S. J., Watson, A. J. B. *J. Org. Chem.* **2016**, *81*, 3942-3950.

135. Vantourout, J. C., Miras, H. N., Isidro-Llobet, A., Sproules, S., Watson, A. J. B. *J. Am. Chem. Soc.* **2017**, *139*, 4769-4779.

136. West, M. J., Fyfe, J. W. B., Vantourout, J. C., Watson, A. J. B. *Chem. Rev.* **2019**, *119*, 12491-12523.

137. Hardouin Duparc, V., Bano, G. L., Schaper, F. *ACS Catal.* **2018**, *8*, 7308-7325.
138. Grimes, K. D., Gupte, A., Aldrich, C. C. *Synthesis* **2010**, *2010*, 1441-1448.
139. Surry, D. S., Buchwald, S. L. *Chem. Sci.* **2011**, *2*, 27-50.
140. Ruiz-Castillo, P., Buchwald, S. L. *Chem. Rev.* **2016**, *116*, 12564-12649.
141. Paradies, J. in *Metal-Catalyzed Cross-Coupling Reactions and More*, **2014**, pp. 995-1066.
142. Forero-Cortés, P. A., Haydl, A. M. *Org. Process Res. Dev.* **2019**, *23*, 1478-1483.
143. Troshin, K., Hartwig, J. F. *Science* **2017**, *357*, 175-181.
144. Gramage-Doria, R., Roisnel, T. *Eur. J. Org. Chem.* **2018**, *2018*, 6083-6087.
145. Collins, K. D., Gensch, T., Glorius, F. *Nat. Chem.* **2014**, *6*, 859-871.
146. Bruno, N. C., Tudge, M. T., Buchwald, S. L. *Chem. Sci.* **2013**, *4*, 916-920.
147. Surry, D. S., Buchwald, S. L. *Angew. Chem. Int. Ed.* **2008**, *47*, 6338-6361.
148. Chaturvedi, J., Haldar, C., Bisht, R., Pandey, G., Chattopadhyay, B. *J. Am. Chem. Soc.* **2021**, *143*, 7604-7611.
149. Tian, Y.-M., Guo, X.-N., Wu, Z., Friedrich, A., Westcott, S. A., Braunschweig, H., Radius, U., Marder, T. B. *J. Am. Chem. Soc.* **2020**, *142*, 13136-13144.
150. Preshlock, S. M., Plattner, D. L., Maligres, P. E., Krska, S. W., Maleczka Jr, R. E., Smith Iii, M. R. *Angew. Chem. Int. Ed.* **2013**, *52*, 12915-12919.
151. Uson, R., Oro, L. A., Cabeza, J. A., Bryndza, H. E., Stepro, M. P. in *Inorganic Syntheses*, John Wiley & Sons, New York, NY, **1985**, pp. 126-130.
152. Sheldrick, G. *Acta Crystallogr. Sect. A, Found. Crystallogr.* **2015**, *71*, 3-8.
153. Sheldrick, G. M. *Acta Crystallogr. Sect. C, Struct. Chem.* **2015**, *71*, 3-8.
154. Hübschle, C. B., Sheldrick, G. M., Dittrich, B. *J. Appl. Crystallogr.* **2011**, *44*, 1281-1284.
155. Diamond (version 4.6.7), Crystal and Molecular Structure Visualization, Crystal Impact GbR, Putz, H., Brandenburg, K., **2022**.
156. Gale, D., Wilshire, J. *Aust. J. Chem.* **1974**, *27*, 1295-1308.
157. Nayak, N., Ramprasad, J., Dalimba, U. *J. Fluor. Chem.* **2016**, *183*, 59-68.
158. Sellam, Z., Brandam, G., Blanc, R., Mouad, A., Hamze, A., Provot, O., Khélifi, I., *New Targeted Cytotoxic Isocombretaquinoline Derivatives And Conjugates Thereof*, (Avicenna Oncology GMBH; Centre National De La Recherche Scientifique (CNRS); Universite Paris-Sud), WO2018/178277, **2018**.

159. Shank, N. I., Pham, H. H., Waggoner, A. S., Armitage, B. A. *J. Am. Chem. Soc.* **2013**, *135*, 242-251.

160. Kurasawa, Y., Yoshida, K., Yamazaki, N., Iwamoto, K., Hamamoto, Y., Kaji, E., Sasaki, K., Zamami, Y. *J. Heterocycl. Chem.* **2012**, *49*, 1323-1331.

161. Niedermeier, S., Singethan, K., Rohrer, S. G., Matz, M., Kossner, M., Diederich, S., Maisner, A., Schmitz, J., Hiltensperger, G., Baumann, K.*, et al. J. Med. Chem.* **2009**, *52*, 4257-4265.

162. Goncalves, V., Brannigan, J. A., Whalley, D., Ansell, K. H., Saxty, B., Holder, A. A., Wilkinson, A. J., Tate, E. W., Leatherbarrow, R. J. *J. Med. Chem.* **2012**, *55*, 3578-3582.

163. Takada, S., Shindo, H., Sasatani, T., Chomei, N., Matsushita, A., Eigyo, M., Kawasaki, K., Murata, S., Takahara, Y., Shintaku, H. *J. Med. Chem.* **1988**, *31*, 1738-1745.

164. Chang, F.-S., Chen, W., Wang, C., Tzeng, C.-C., Chen, Y.-L. *Bioorg. Med. Chem.* **2010**, *18*, 124-133.

165. Rassias, G., Leonardi, S., Rigopoulou, D., Vachlioti, E., Afratis, K., Piperigkou, Z., Koutsakis, C., Karamanos, N. K., Gavras, H., Papaioannou, D. *Eur. J. Med. Chem.* **2021**, *210*, 112948.

166. Li, W., Gao, J. J., Zhang, Y., Tang, W., Lee, H., Fandrick, K. R., Lu, B., Senanayake, C. H. *Adv. Synth. Catal.* **2011**, *353*, 1671-1675.

167. Davis, S. E., Rauckman, B. S., Chan, J. H., Roth, B. *J. Med. Chem.* **1989**, *32*, 1936-1942.

168. Scheufler, C., Möbitz, H., Gaul, C., Ragot, C., Be, C., Fernández, C., Beyer, K. S., Tiedt, R., Stauffer, F. *ACS Med. Chem. Lett.* **2016**, *7*, 730-734.

Appendix I

Supplementary Material

1.1. X-Ray Crystallography Methods for Chapter 2

Single crystals were obtained from a saturated solution of toluene by vapour diffusion with hexane. A suitable crystal was selected and mounted on a MITIGEN holder with silicon oil on a Rigaku AFC12 FRE-HF diffractometer equipped with an Oxford Cryosystems low-temperature device. The crystals were kept at a steady T = 100(2) K during data collection. The structures were solved with the ShelXT[1] structure solution program using the Intrinsic Phasing solution method and by using Olex2[2] as the graphical interface. The models were refined with version 2016/6 of ShelXL[1] using Least Squares minimisation.

Data were measured using profile data from ω-scans of 1.0 ° per frame using MoK_α radiation (Rotating-anode X-ray tube, 45.0 kV, 55.0 mA). The total number of runs and images was based on the strategy calculation from the program CrysAlisPro (Rigaku, V1.171.40.37a, 2019).

Cell parameters were retrieved using the CrysAlisPro (Rigaku, V1.171.40.37a, 2019) software and refined using CrysAlisPro (Rigaku, V1.171.40.37a, 2019). Data reduction was performed using the CrysAlisPro (Rigaku, V1.171.40.37a, 2019) software that corrects for Lorentz polarisation. The final completeness is 99.80% out to their respective values in Θ.

A multi-scan absorption correction was performed using CrysAlisPro 1.171.40.37a[3] using spherical harmonics as implemented in SCALE3 ABSPACK. The absorption coefficient μ of these materials are obtained at λ = 0.711Å.

The structures were solved in space groups by Intrinsic Phasing using the ShelXT[4] structure solution program and refined by Least Squares using version 2016/6 of ShelXL.[1] All non-hydrogen atoms were refined anisotropically. Hydrogen atom positions were calculated geometrically and refined using the riding model.

_exptl_absorpt_process_details: CrysAlisPro 1.171.40.37a[3] using spherical harmonics as implemented in SCALE3 ABSPACK.

Crystal Data

Compound **68** There is a single molecule in the asymmetric unit, which is represented by the reported sum formula. In other words: Z is 2 and Z' is 1.

Compound **83** The value of Z' is 0.5. This means that only half of the formula unit is present in the asymmetric unit, with the other half consisting of symmetry equivalent atoms.

85 The value of Z' is 0.5. This means that only half of the formula unit is present in the asymmetric unit, with the other half consisting of symmetry equivalent atoms.

Table 1 X-ray diffraction collection data and refinement details for **68**, **83** and **85**.

Compound	**68**	**83**	**85**
Formula	$C_{22}H_{19}NO_3$	$C_{34}H_{26}Br_2N_2O_6$ Pd, 1.33(H_2O)	$C_{34}H_{28}N_2O_6Pd$
$D_{calc.}$/g cm^{-3}	1.348	1.758	1.362
μ/mm^{-1}	0.090	3.124	0.615
Formula Weight	345.38	848.80	666.98
Colour	clear colourless	clear yellow	clear dark yellow
Shape	prism	block	block
Size/mm^3	0.16×0.11×0.03	0.11×0.08×0.06	0.54×0.36×0.12
T/K	100(2)	100(2)	100(2)
Crystal System	triclinic	monoclinic	orthorhombic
Flack Parameter	-	-	-
Hooft Parameter	-	-	-
Space Group	*P*-1	*C*2/*c*	*Pbcn*
a/Å	5.6018(2)	19.9231(3)	18.3076(3)
b/Å	10.0673(5)	10.1765(2)	7.82700(10)
c/Å	16.0613(8)	15.8477(4)	22.6989(4)
α/°	106.886(4)	90	90
β/°	91.313(4)	93.433(2)	90
γ/°	99.947(4)	90	90
V/Å^3	851.12(7)	3207.31(11)	3252.61(9)
Z	2	4	4
Z'	1	0.5	0.5
Wavelength/Å	0.71073	0.71073	0.71073
Radiation type	MoKα	MoKα	MoKα
Θ_{min}/°	2.848	3.194	2.969
Θ_{max}/°	28.500	28.498	28.495
Measured Refl.	13102	20357	25683
Independent Refl.	4317	4057	4132
Reflections with I>2(I)	3942	3566	3937
R_{int}	0.0397	0.0463	0.0299
Parameters	238	223	197
Restraints	0	1	0
Largest Peak	0.402	0.791	0.423
Deepest Hole	-0.290	-0.556	-0.367
GooF	1.314	1.127	1.251
wR_2 (all data)	0.1697	0.0963	0.0996
wR_2	0.1650	0.0924	0.0984
R_1 (all data)	0.1071	0.0512	0.0586
R_1	0.0953	0.0413	0.0561

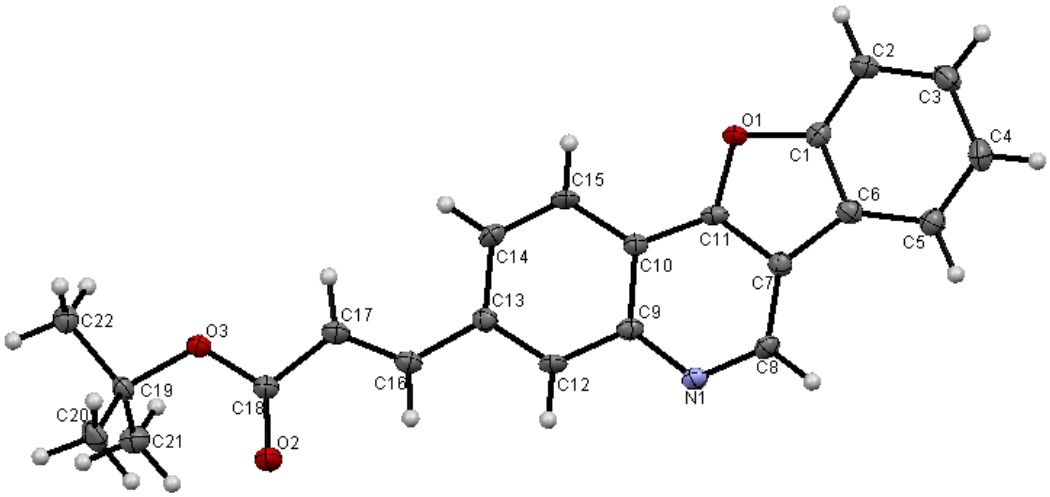


Figure 1 Thermal ellipsoids of **68** drawn at the 50% probability level.

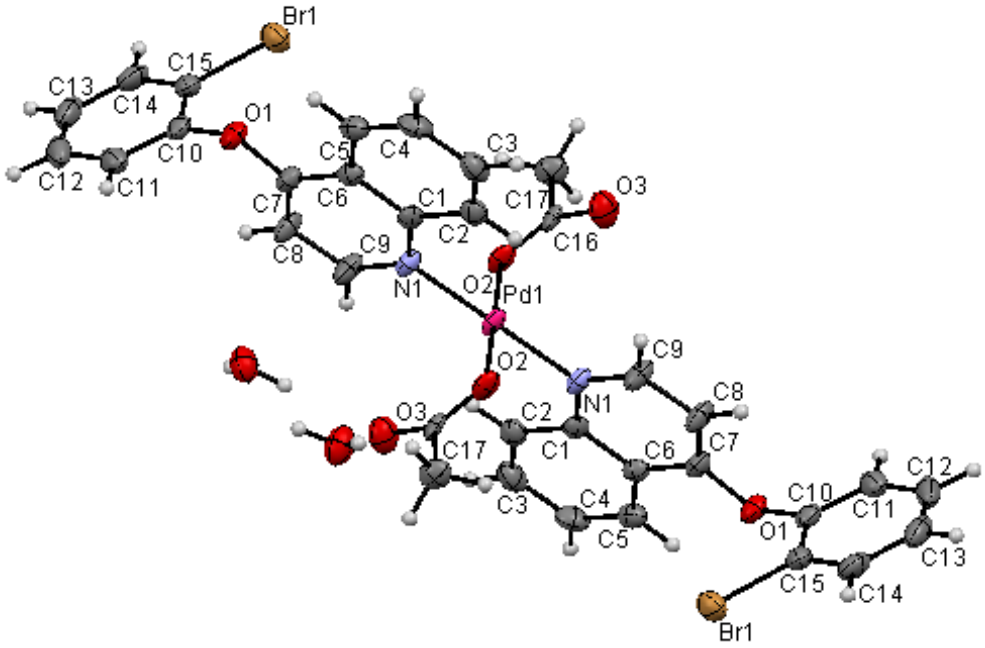


Figure 2 Thermal ellipsoids of **83** drawn at the 50% probability level.

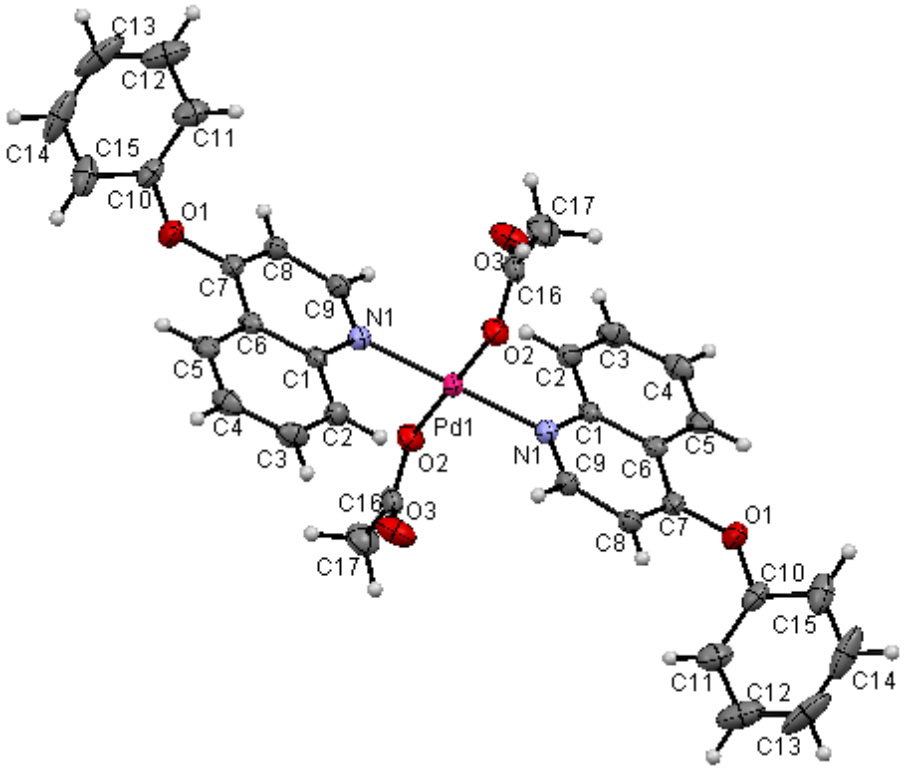


Figure 3 Thermal ellipsoids of **85** drawn at the 50% probability level. Disordered solvent (methanol) treated using solvent masking techniques.

1.2. X-Ray Crystallography Methods for Chapter 3

The crystals of compounds **133** and **184** were grown by vapor diffusion by dissolving the compound in CH_2Cl_2 in a small vial and placing that vial in a larger vial containing Et_2O. Crystals suitable for single-crystal X-ray diffraction were selected, coated in perfluoropolyether oil, and mounted on a polyimide microloop. Diffraction data of **133** and **184** were collected on a RIGAKU OXFORD DIFFRACTION XTALAB SYNERGY-R diffractometer with a semiconductor HPA area detector (HyPix-Arc150) using a rotating-anode X-ray tube for X-ray generation and multi-layer mirror monochromated Cu-K_α radiation. The crystals were cooled using an Oxford Cryostreams 800 low-temperature device. Data were collected at 100 K. The images were processed and corrected for Lorentz-polarization effects and absorption as implemented in the CrysAlis^{Pro} software. The structure was solved using the intrinsic phasing method (SHELXT)[4] and Fourier expansion technique. All non-hydrogen atoms were refined in anisotropic approximation, with hydrogen atoms 'riding' on idealised positions by full-matrix least squares against F^2 of all data, using SHELXL software[1] and the SHELXLE graphical user interface.[5]

Crystal Data

The crystal structure of **133** was refined as an inversion twin and the twin fraction refined to 47.2%. The unit cell of **133** contains disordered diethyl ether solvent molecules which have been treated as a diffuse contribution to the overall scattering without specific atom positions by SQUEEZE/PLATON.[6] Diamond[7] software was used for graphical representation. Crystal data and experimental details are listed in ; full structural information has been deposited with Cambridge Crystallographic Data Centre. CCDC-2159956 (**133**) and 2159957 (**184**).

Table 2 X-ray diffraction collection data and refinement details for **133** and **184**.

Compound	**133**	**184**
Empirical formula	$C_{16}H_{18}BClFNO_2$ [+ Et_2O]	$C_{19}H_{15}ClFNO_2$
Formula weight/g·mol^{-1}	321.57	343.77
T/K	100(2)	100(2)
Radiation, λ/Å	Cu-K_α 1.54184	Cu-K_α 1.54184
Crystal size/mm³	0.179×0.083×0.027	0.432×0.055×0.042
Crystal color, habit	colorless plate	colorless needle
μ/mm^{-1}	2.102	2.351
Crystal system	orthorhombic	monoclinic
Space group	$P2_12_12_1$	$P2_1/n$
a/Å	7.1800(1)	3.81971(14)
b/Å	16.3318(1)	21.4427(10)
c/Å	29.2511(3)	19.2195(6)
α/°	90	90
β/°	90	93.267(3)
γ/°	90	90
Volume/Å^3	3430.05(6)	1571.61(11)
Z	8	4
ρ_{calc}/g·cm^{-3}	1.245	1.453
F(000)	1344	712
θ range/°	3.021 – 74.486	3.091 – 74.492
Reflections collected	45414	15732
Unique reflections	6984	3181
Parameters	408	219
GooF on F^2	1.036	1.092
R_1 [I>2σ(I)]	0.0303	0.0409
wR_2 (all data)	0.0799	0.1162
Max. / min. residual electron density / e·Å^{-3}	0.211 / –0.231	0.336 / –0.437

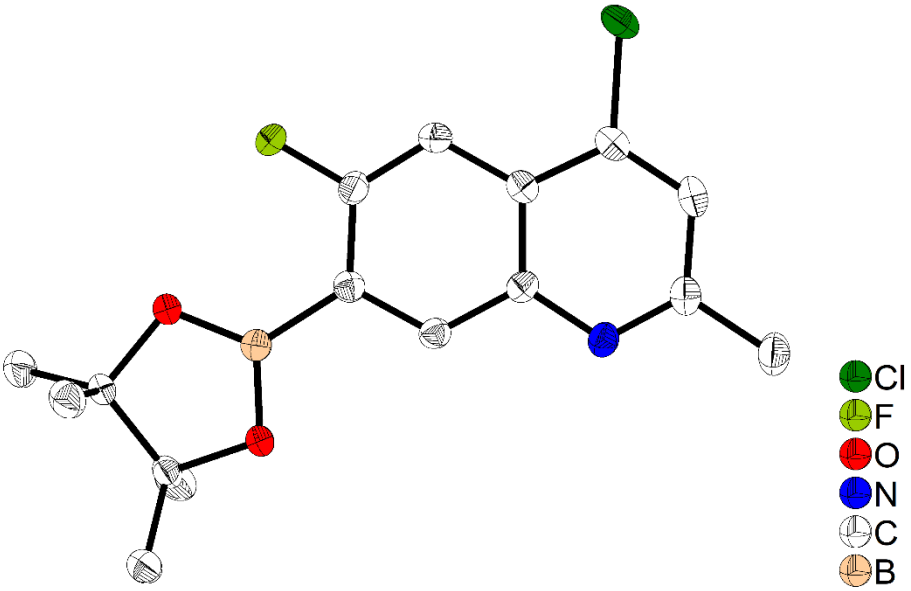


Figure 4 The solid-state molecular structure of **133** determined by single-crystal X-ray diffraction at 100 K. All ellipsoids are drawn at the 50% probability level. H atoms are omitted for clarity. Only one of two symmetrically independent molecules is shown here.

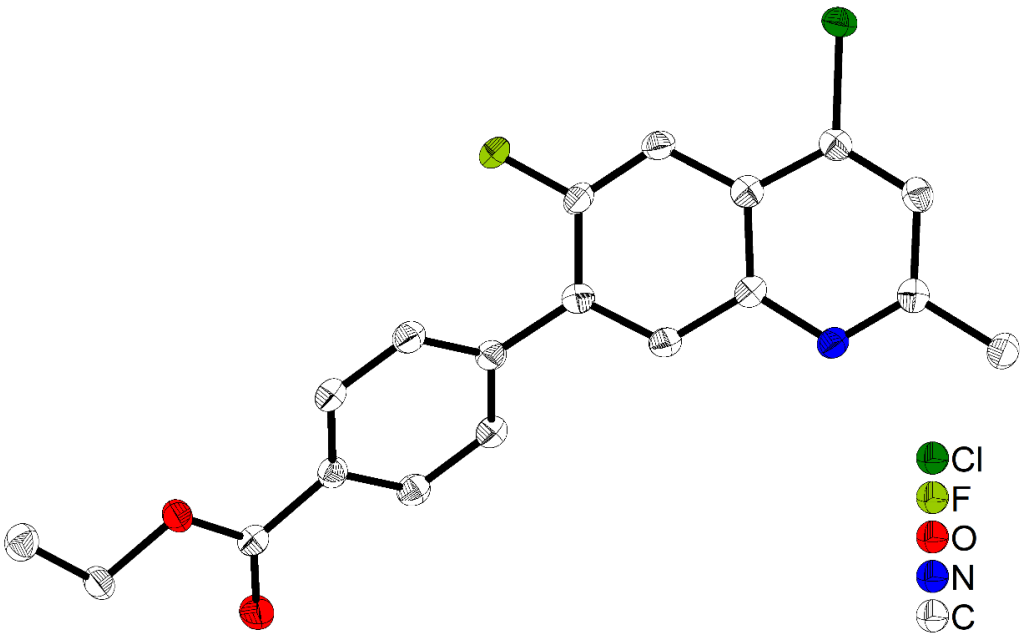
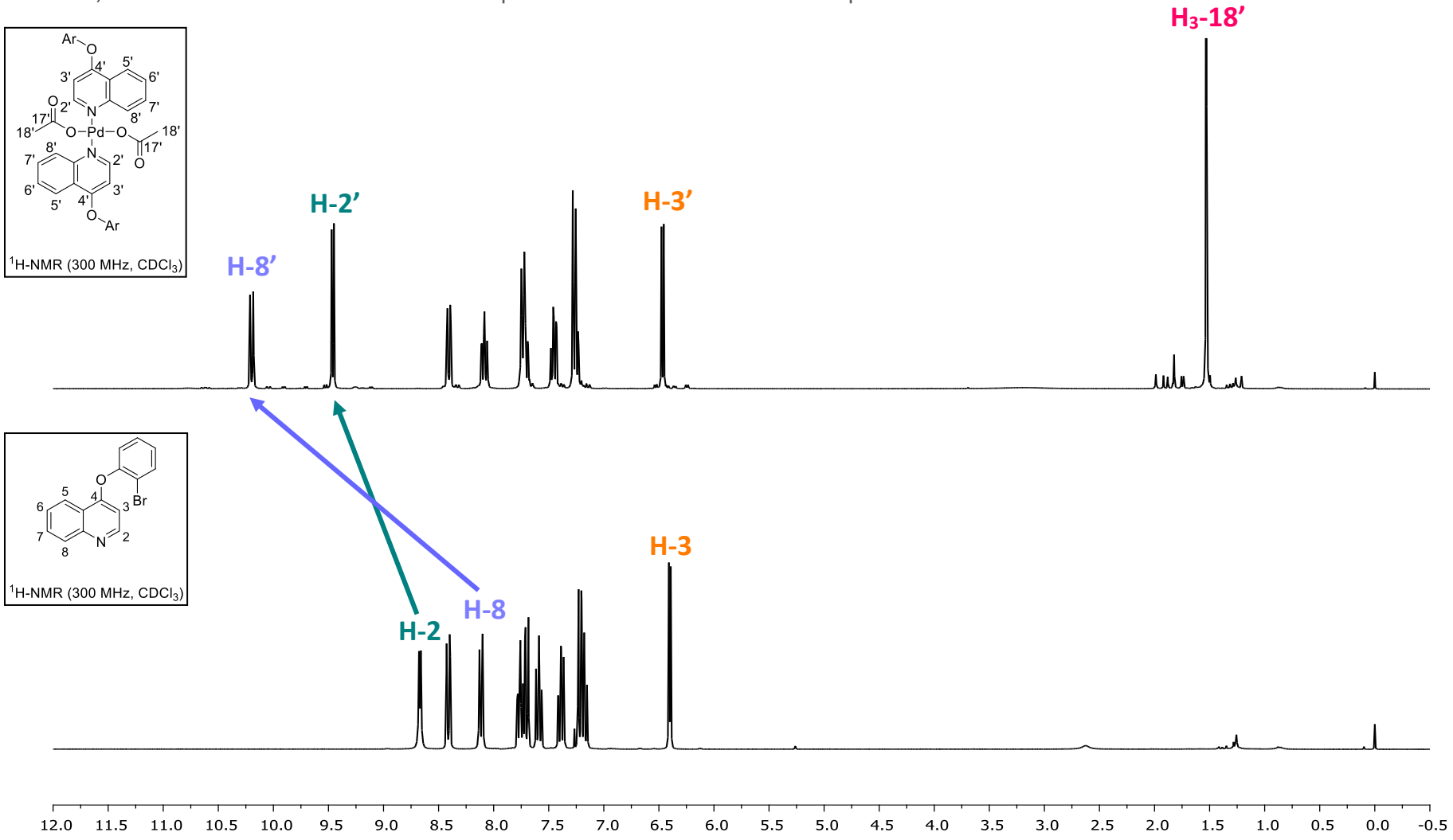


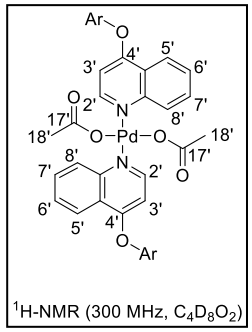
Figure 5 The solid-state molecular structure of **184** determined by single-crystal X-ray diffraction at 100 K. All ellipsoids are drawn at the 50% probability level. H atoms are omitted for clarity.

References

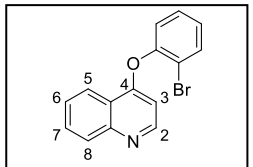
1. Sheldrick, G. M. *Acta Crystallogr. Sect. C, Struct. Chem.* **2015**, *71*, 3-8.
2. Dolomanov, O. V., Bourhis, L. J., Gildea, R. J., Howard, J. A. K., Puschmann, H. *J. Appl. Crystallogr.* **2009**, *42*, 339-341.
3. CrysAlisPro Software System, Rigaku Oxford Diffraction, **2019**.
4. Sheldrick, G. *Acta Crystallogr. Sect. A, Found. Crystallogr.* **2015**, *71*, 3-8.
5. Hübschle, C. B., Sheldrick, G. M., Dittrich, B. *J. Appl. Crystallogr.* **2011**, *44*, 1281-1284.
6. Spek, A. L. *Acta Crystallogr. Sect. C, Struct. Chem.* **2015**, *71*, 9-18.
7. Diamond (version 4.6.7), Crystal and Molecular Structure Visualization, Crystal Impact GbR, Putz, H., Brandenburg, K., **2022**.

1.3. ^{1}H, ^{13}C and ^{1}H-^{15}N HMBC NMR Spectra for Palladium Complexes





^{1}H-NMR (300 MHz, $C_4D_8O_2$)



^{1}H-NMR (300 MHz, $C_4D_8O_2$)

H-8’

H-2’

H-3’

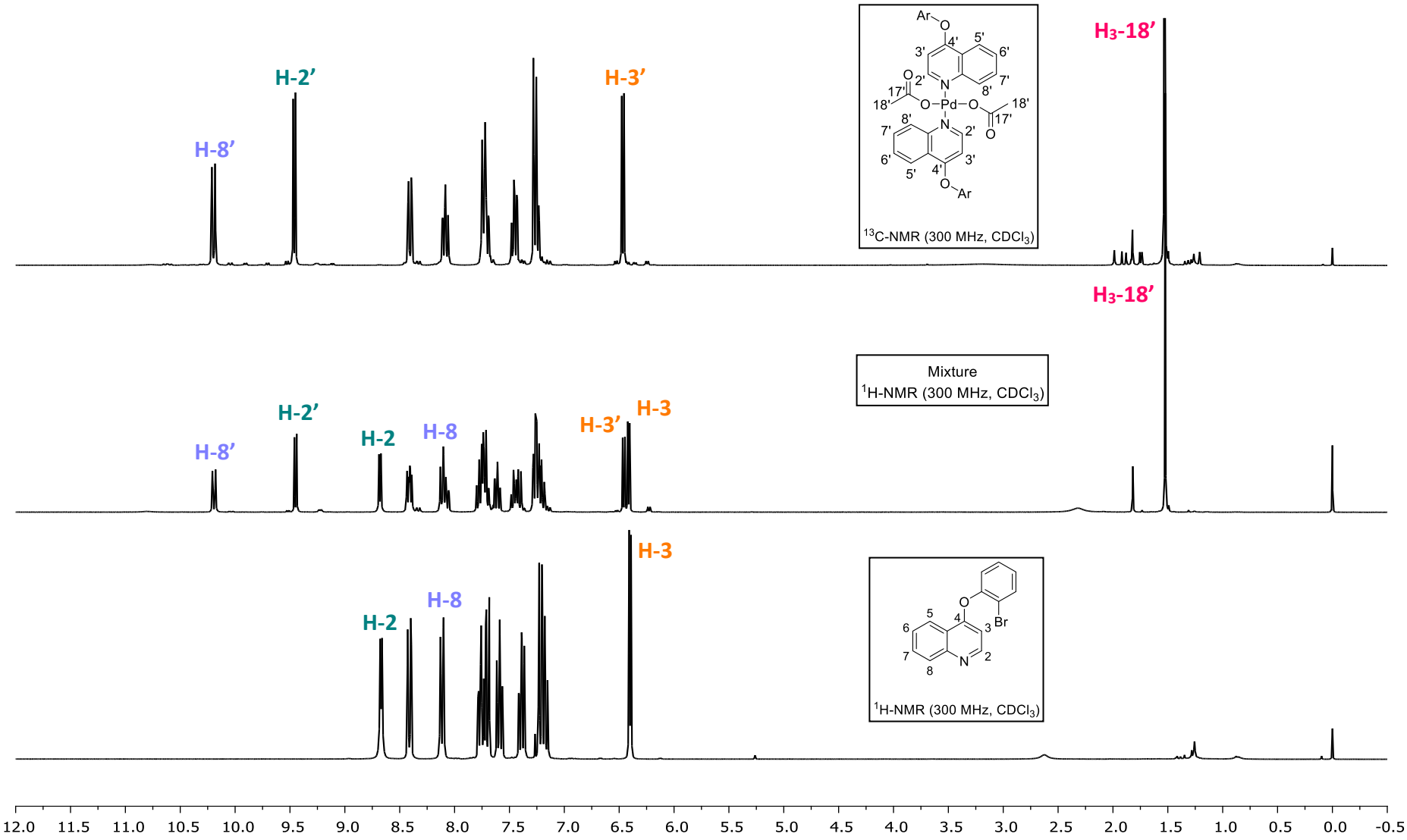
H_3-18’

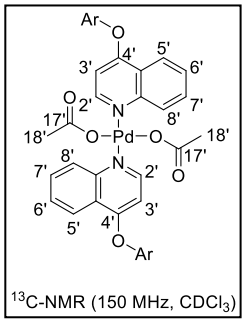
H-2

H-8

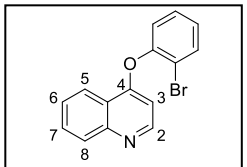
H-3

12.0 11.5 11.0 10.5 10.0 9.5 9.0 8.5 8.0 7.5 7.0 6.5 6.0 5.5 5.0 4.5 4.0 3.5 3.0 2.5 2.0 1.5 1.0 0.5 0.0 -0.5


H-8’
H-2’
H-3’
H3-18’
13C-NMR (300 MHz, CDCl3)
H3-18’
Mixture
1H-NMR (300 MHz, CDCl3)
H-8’
H-2’
H-2
H-8
H-3’
H-3
H-3
H-2
H-8
1H-NMR (300 MHz, CDCl3)
12.0 11.5 11.0 10.5 10.0 9.5 9.0 8.5 8.0 7.5 7.0 6.5 6.0 5.5 5.0 4.5 4.0 3.5 3.0 2.5 2.0 1.5 1.0 0.5 0.0 -0.5



^{13}C-NMR (150 MHz, $CDCl_3$)



^{13}C-NMR (150 MHz, $CDCl_3$)

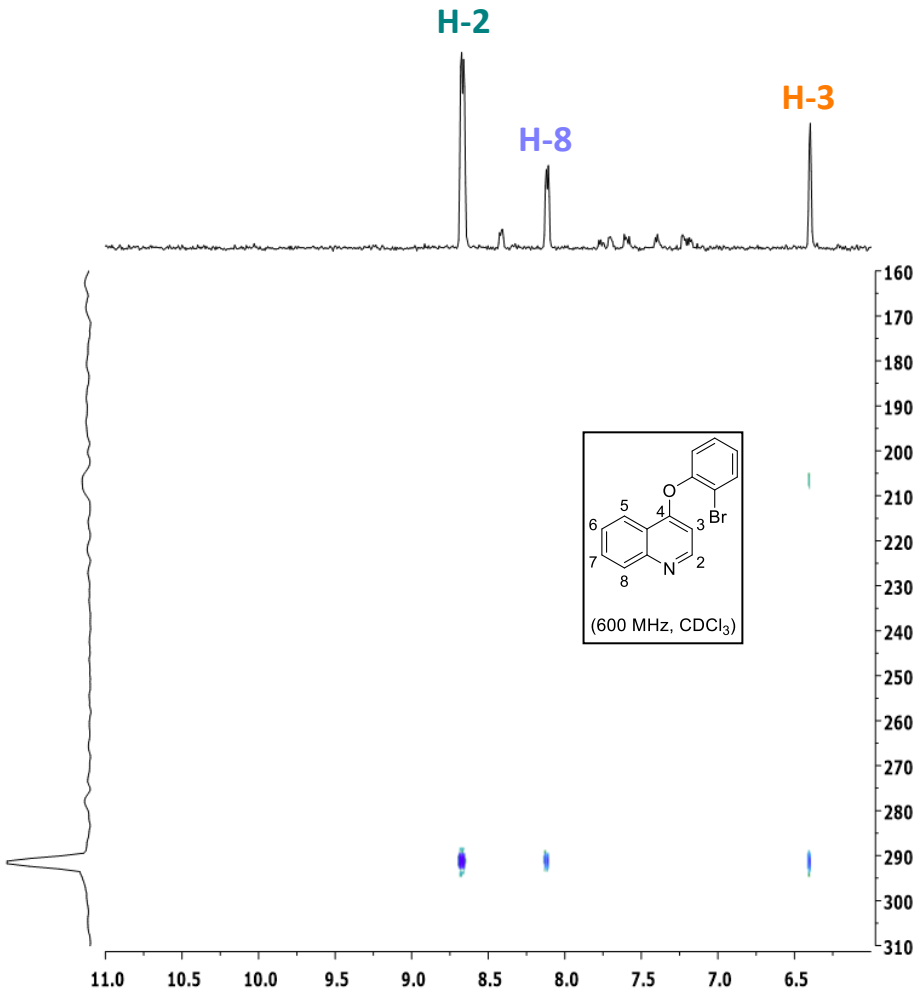
qC-17’

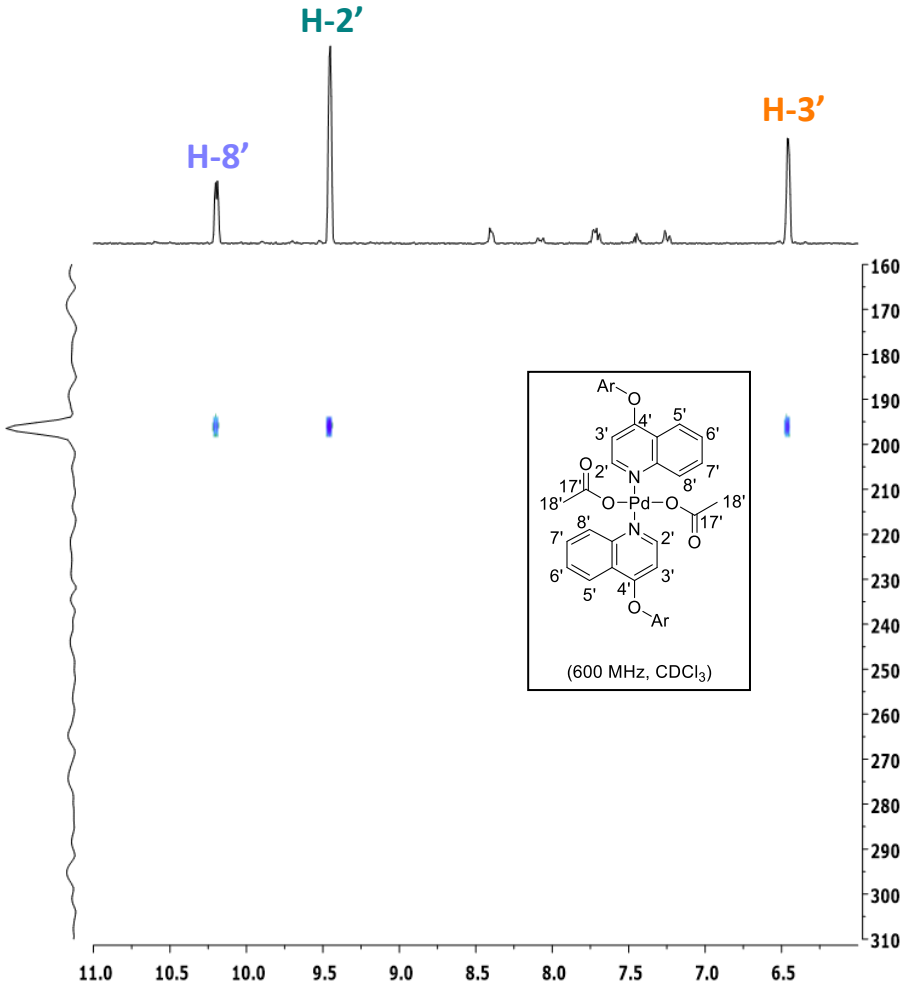
C-2’

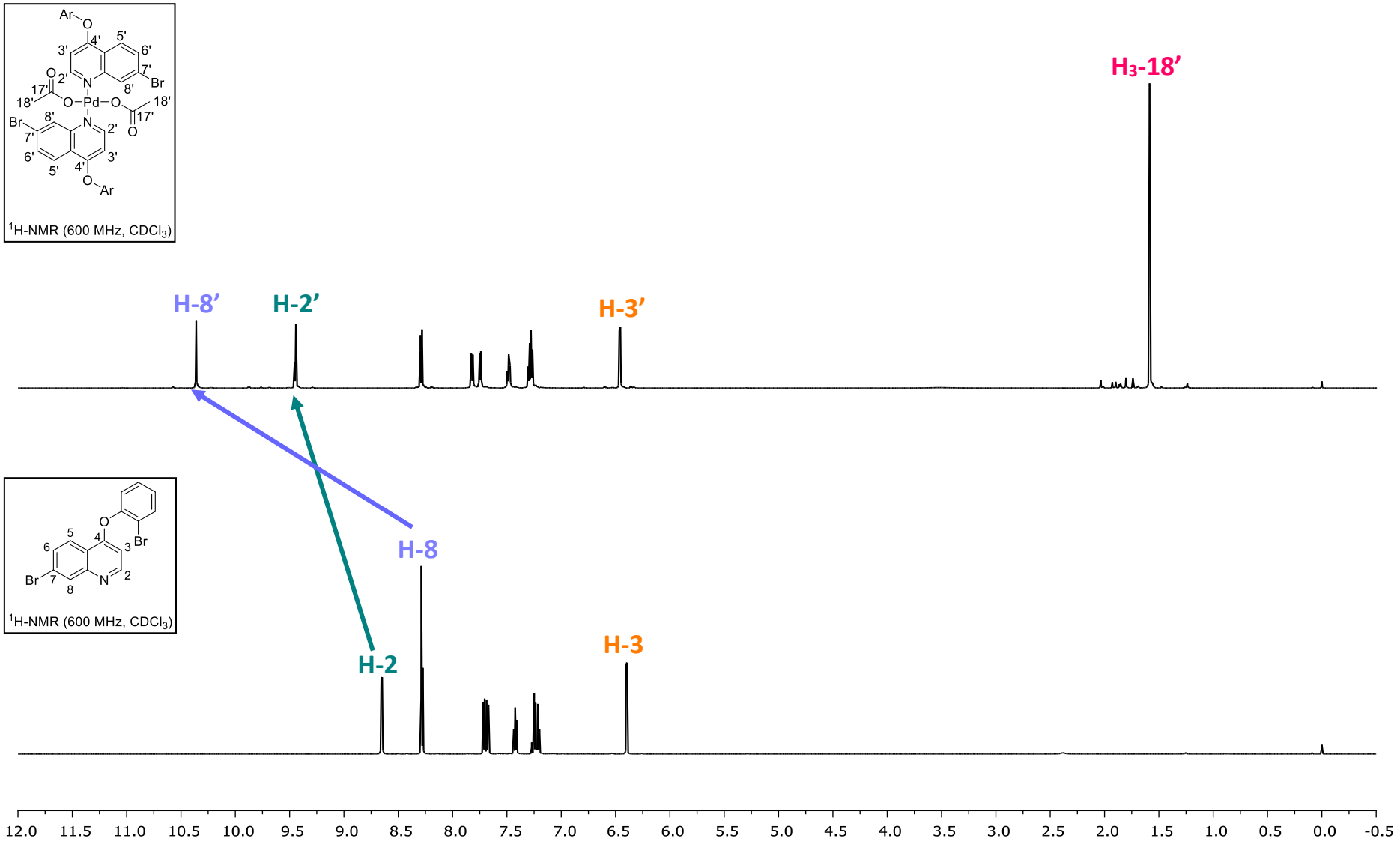
C-2

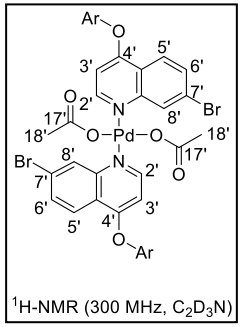
CH_3-18’

200 190 180 170 160 150 140 130 120 110 100 90 80 70 60 50 40 30 20 10 0

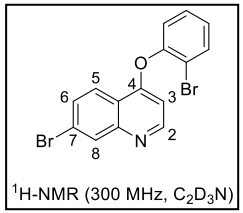

H-2
H-8
H-3
(600 MHz, CDCl3)
11.0
10.5
10.0
9.5
9.0
8.5
8.0
7.5
7.0
6.5


H-2’
H-8’
H-3’
(600 MHz, CDCl3)
11.0
10.5
10.0
9.5
9.0
8.5
8.0
7.5
7.0
6.5


H-8’
H-2’
H-3’
H3-18’
H-8
H-2
H-3
1H-NMR (600 MHz, CDCl3)
1H-NMR (600 MHz, CDCl3)
12.0 11.5 11.0 10.5 10.0 9.5 9.0 8.5 8.0 7.5 7.0 6.5 6.0 5.5 5.0 4.5 4.0 3.5 3.0 2.5 2.0 1.5 1.0 0.5 0.0 -0.5



^{1}H-NMR (300 MHz, C_2D_3N)



^{1}H-NMR (300 MHz, C_2D_3N)

H-8’

H-2’

H-3’

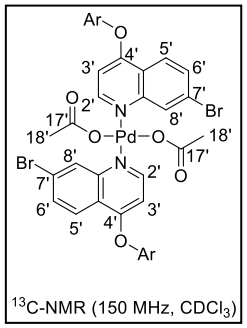
H_3-18’

H-2

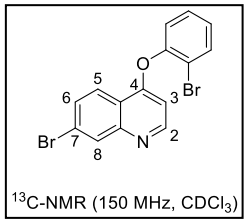
H-8

H-3

12.0 11.5 11.0 10.5 10.0 9.5 9.0 8.5 8.0 7.5 7.0 6.5 6.0 5.5 5.0 4.5 4.0 3.5 3.0 2.5 2.0 1.5 1.0 0.5 0.0 -0.5



^{13}C-NMR (150 MHz, $CDCl_3$)



^{13}C-NMR (150 MHz, $CDCl_3$)

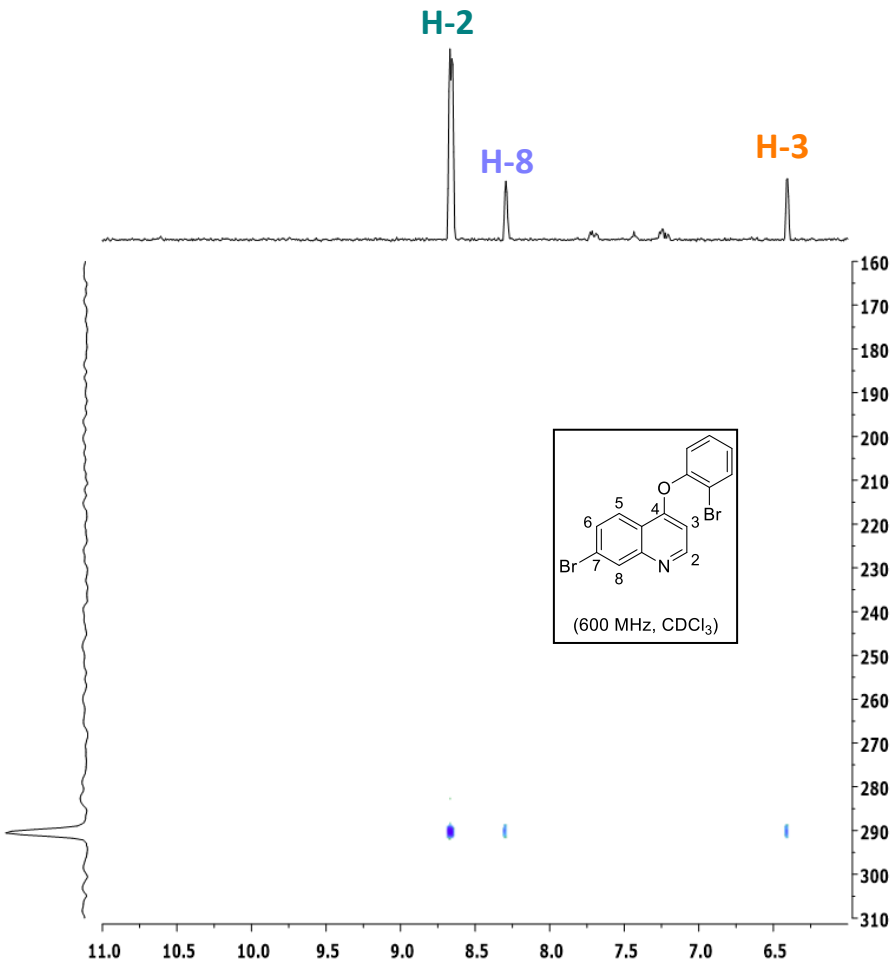
qC-17’

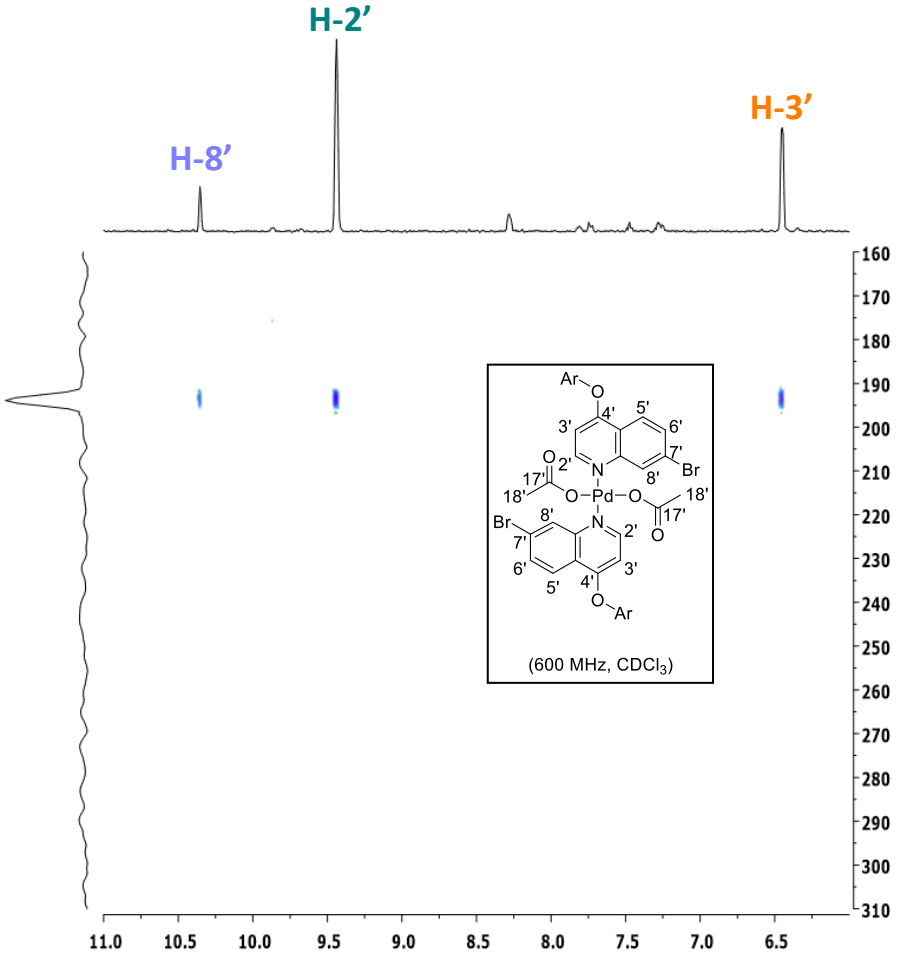
C-2’

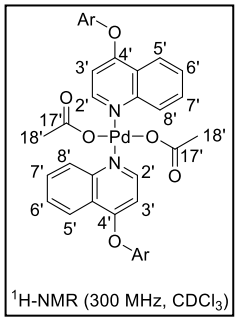
CH_3-18’

C-2

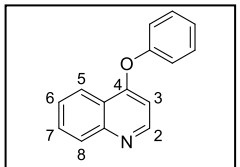
200 190 180 170 160 150 140 130 120 110 100 90 80 70 60 50 40 30 20 10 0


H-2
H-8
H-3
(600 MHz, CDCl3)

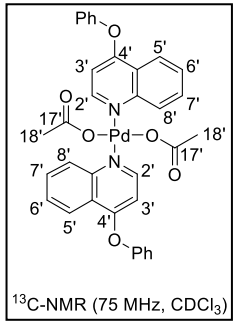

H-2’
H-8’
H-3’
(600 MHz, CDCl3)



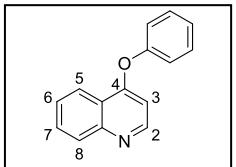
^{1}H-NMR (300 MHz, $CDCl_3$)



^{1}H-NMR (300 MHz, $CDCl_3$)



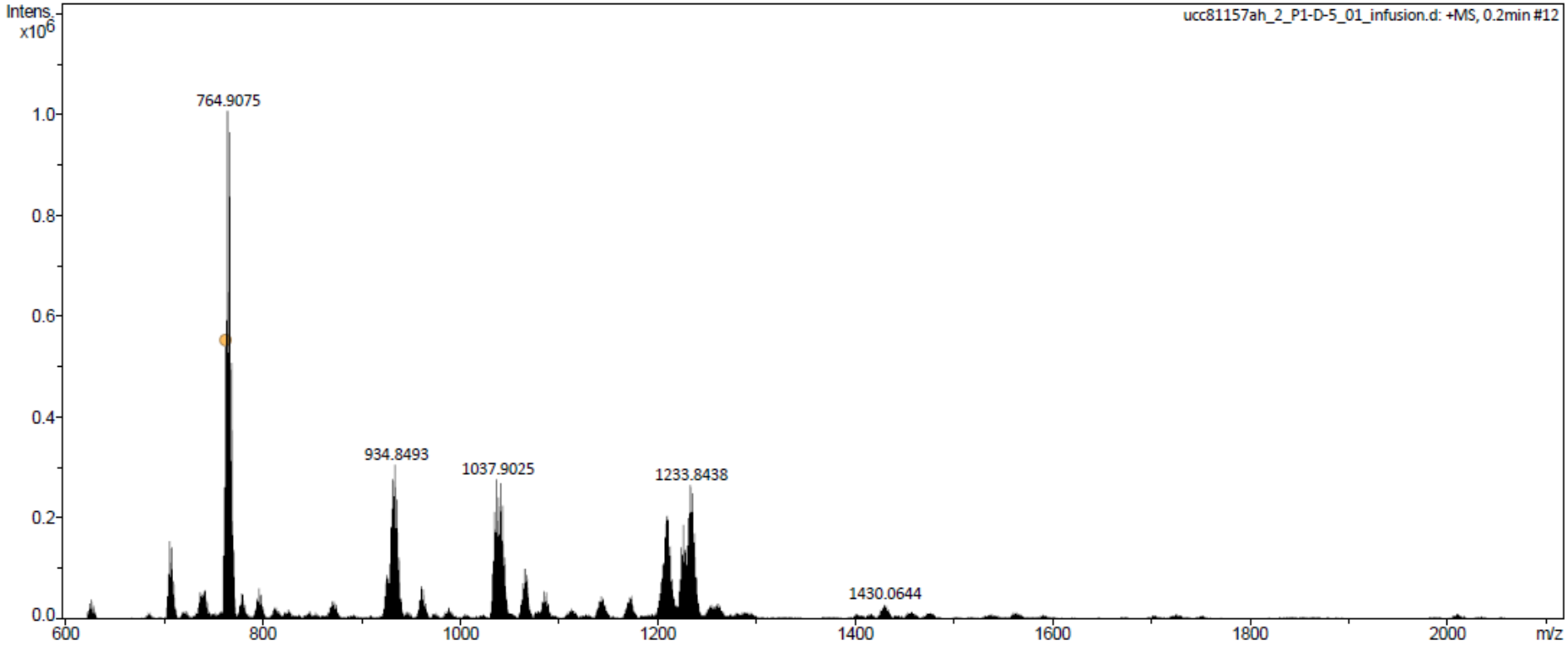
^{13}C-NMR (75 MHz, $CDCl_3$)



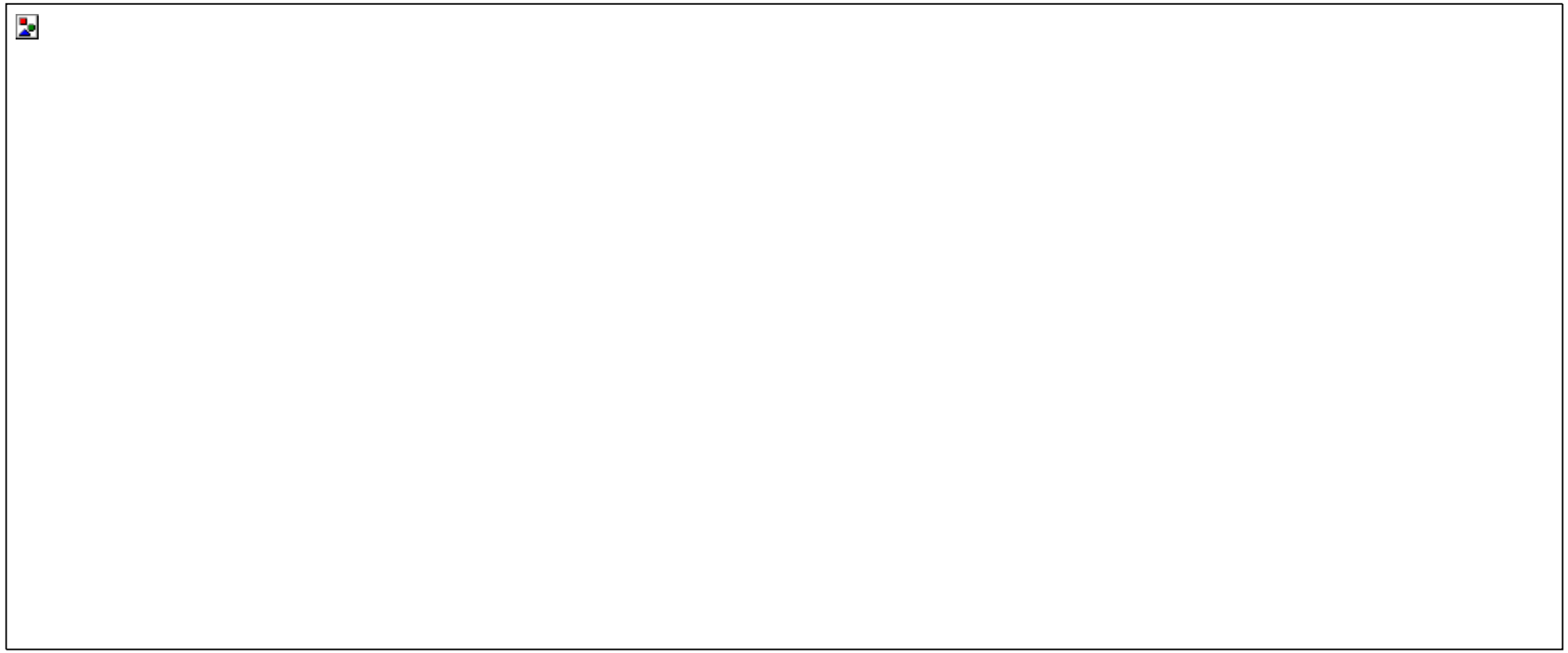
^{13}C-NMR (75 MHz, $CDCl_3$)

1.4. Measured & Simulated HRMS Data for Palladium Complexes

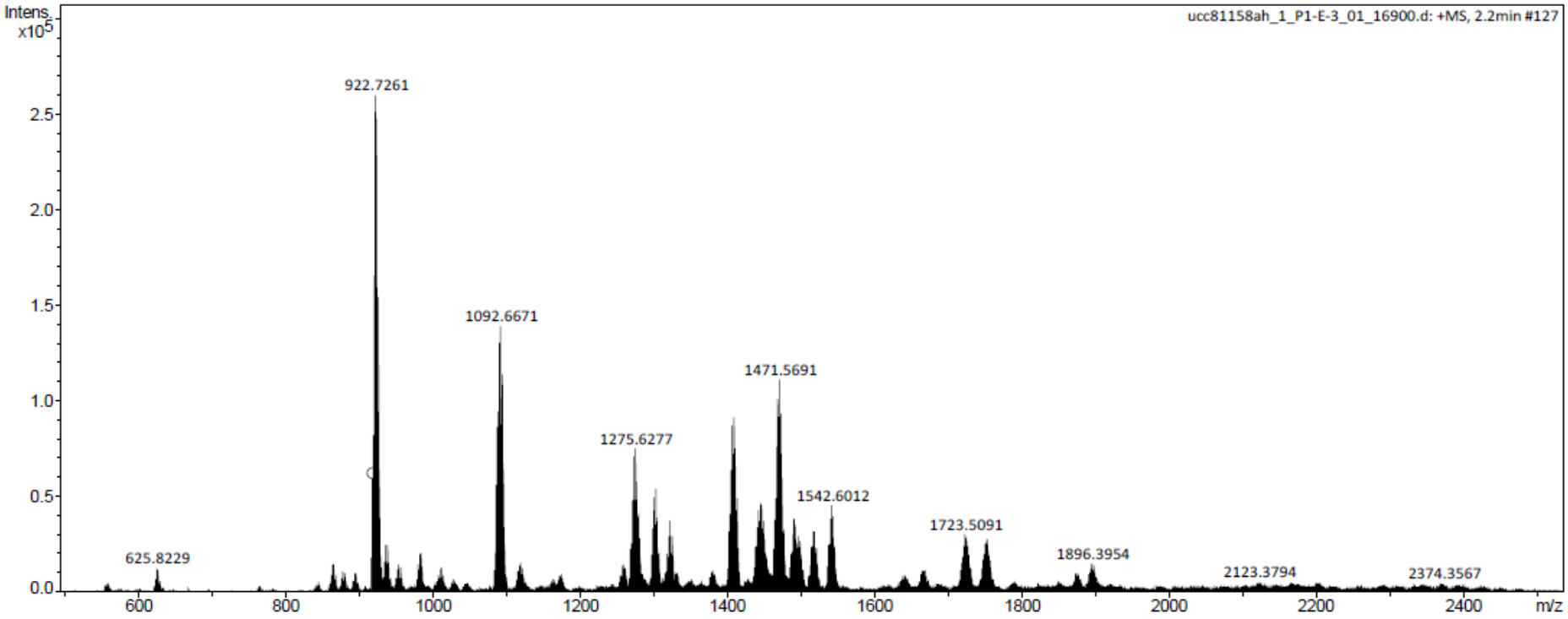
HRMS data for complex **83**.



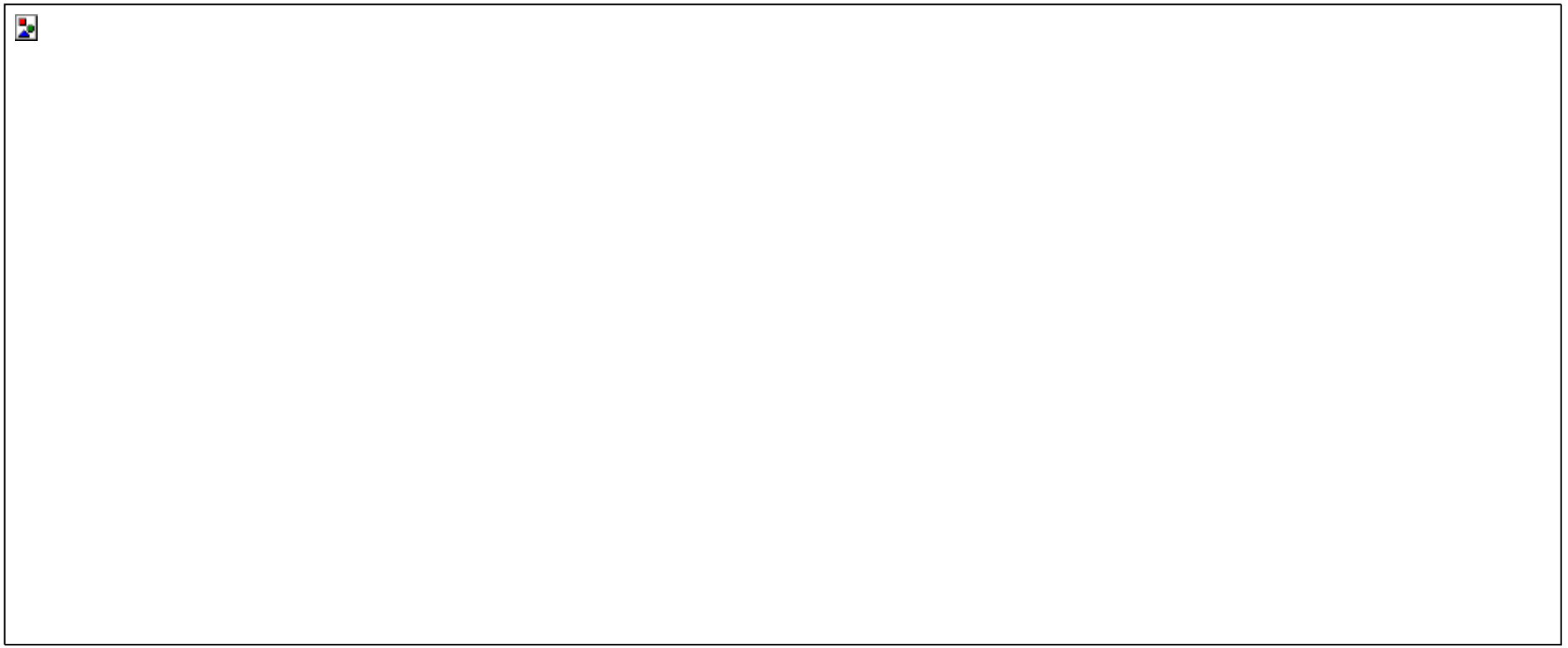
Meas. m/z	#	Ion Formula	m/z	err [ppm]	err [mDa]	mSigma	Mean err [ppm]
762.9081	1	C32H23Br2N2O4Pd	762.9054	-3.4	-2.6	7.2	-2.9



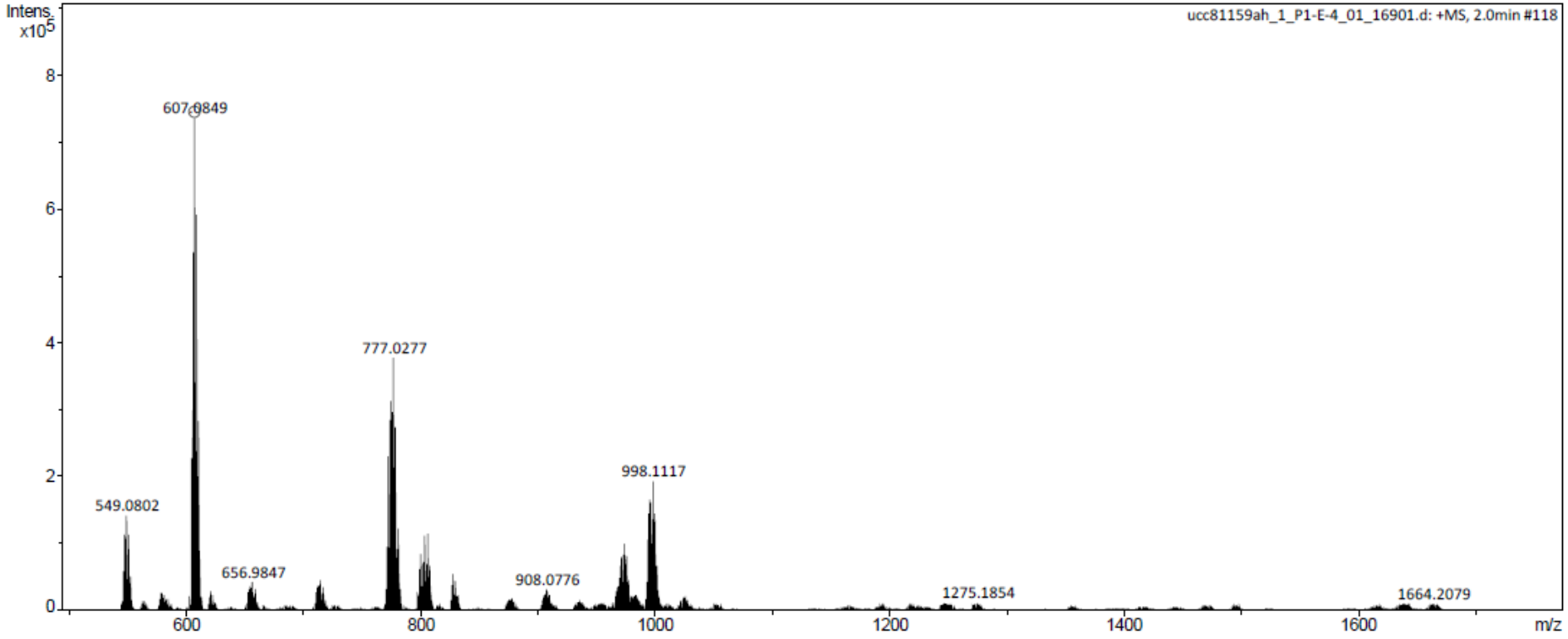
HRMS data for complex **84**.



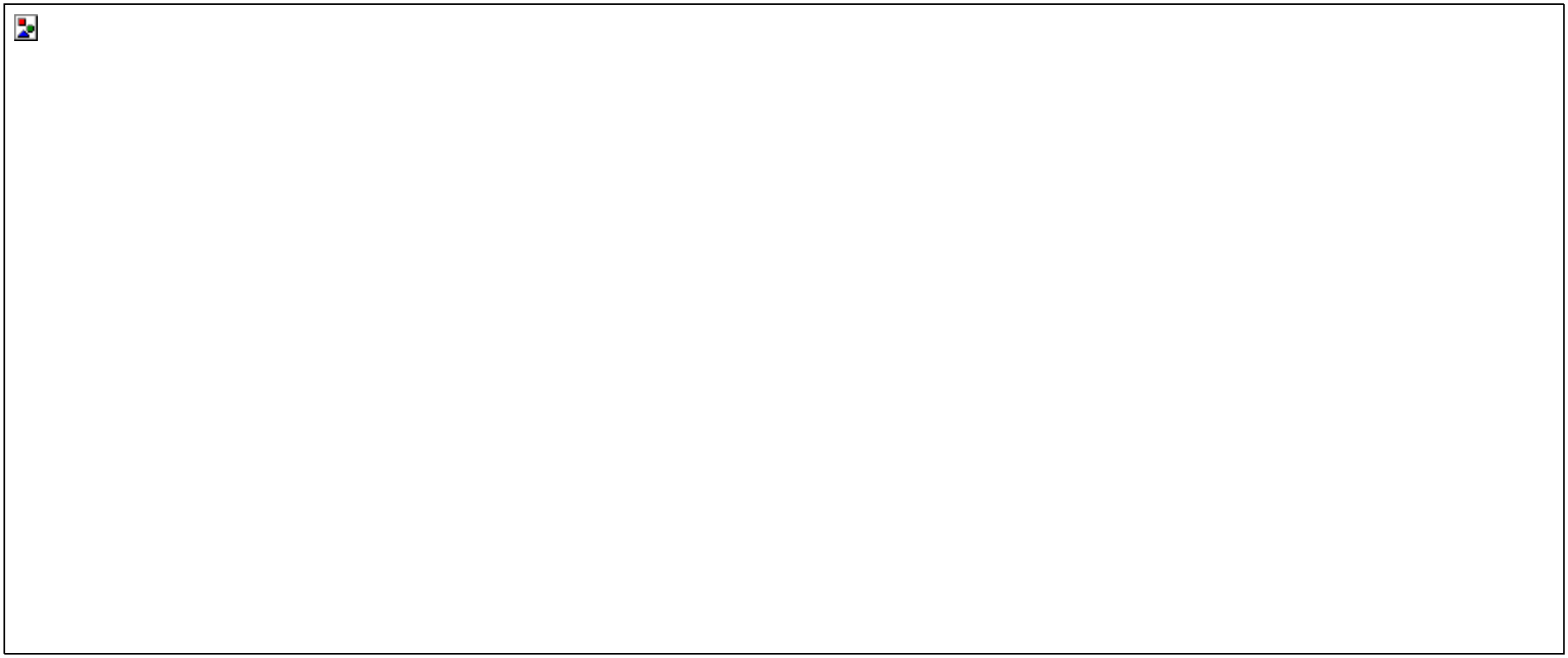
Meas. m/z	#	Ion Formula	m/z	err [ppm]	err [mDa]	mSigma	Mean err [ppm]
918.7284	1	C32H21Br4N2O4Pd	918.7264	-2.6	-2.3	6.0	-2.4



HRMS data for complex **85**.

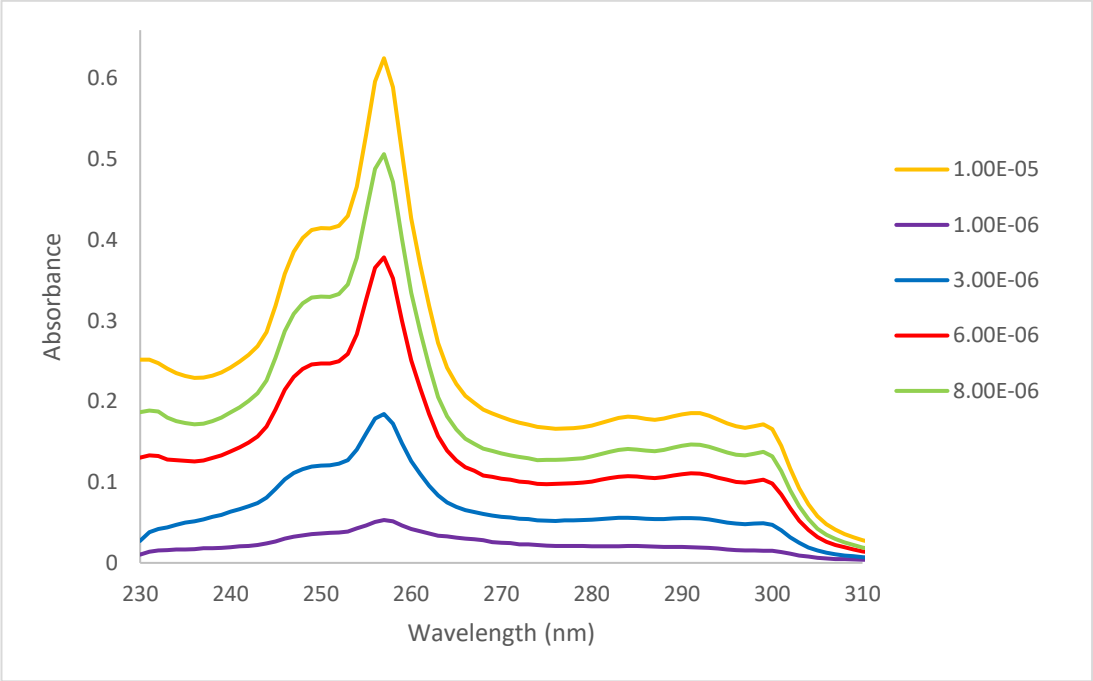


Meas. m/z	#	Ion Formula	m/z	err [ppm]	err [mDa]	mSigma	Mean err [ppm]
607.0849	1	C32H25N2O4Pd	607.0844	1.2	0.7	4.7	1.9

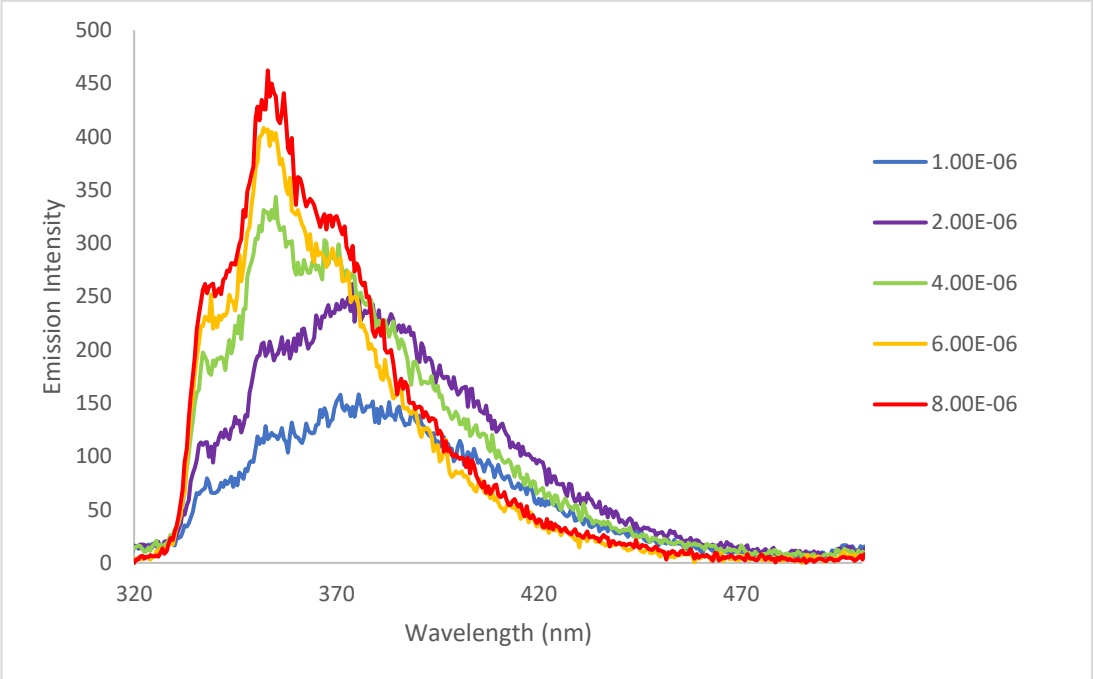


1.5. UV-Visible and Fluorescence Spectroscopy Data

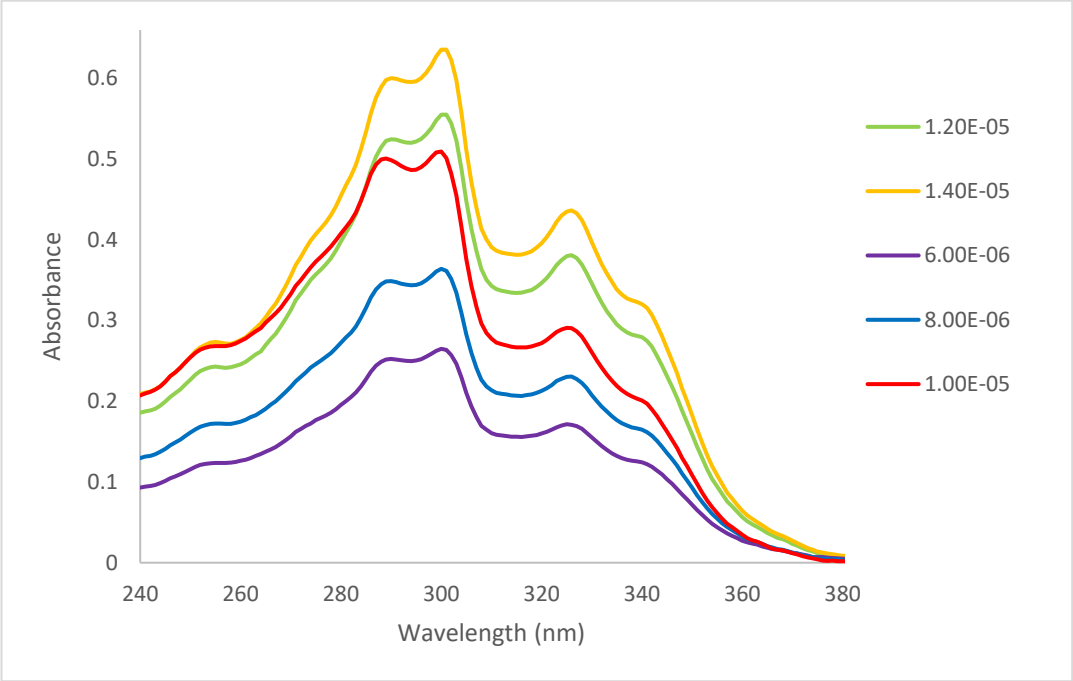
1.1 UV-Visible spectroscopic analysis of compound **86** (concentration range in the figure key, in mol dm^{-3})



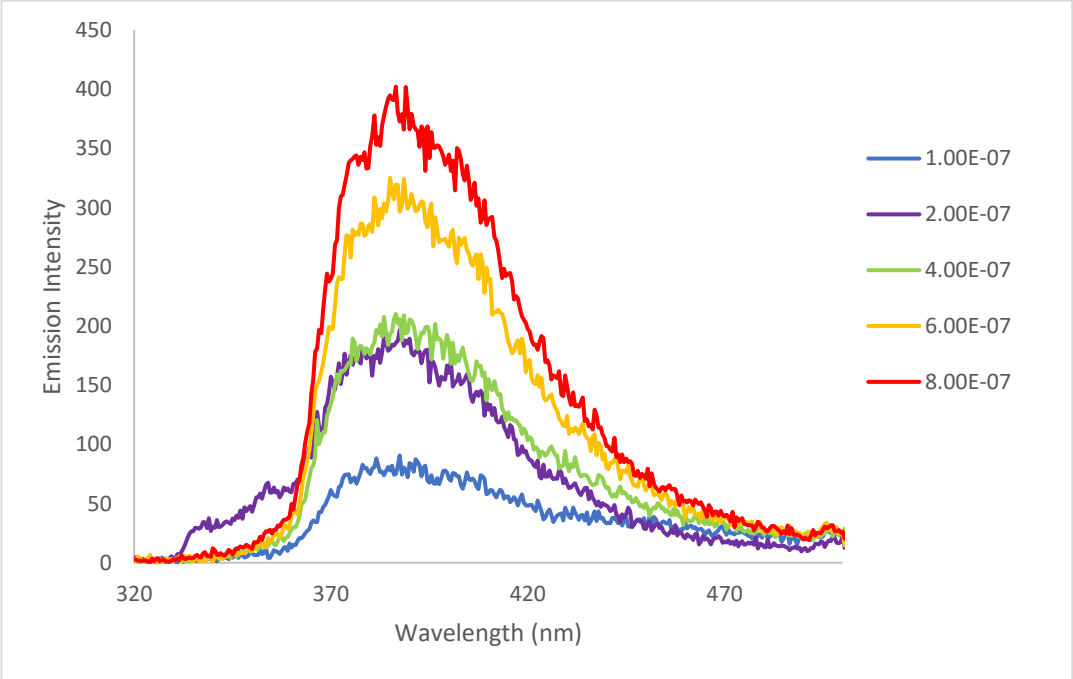
1.2 Fluorescence spectroscopic analysis of compound **86** (concentration range in the figure key, in mol dm^{-3})



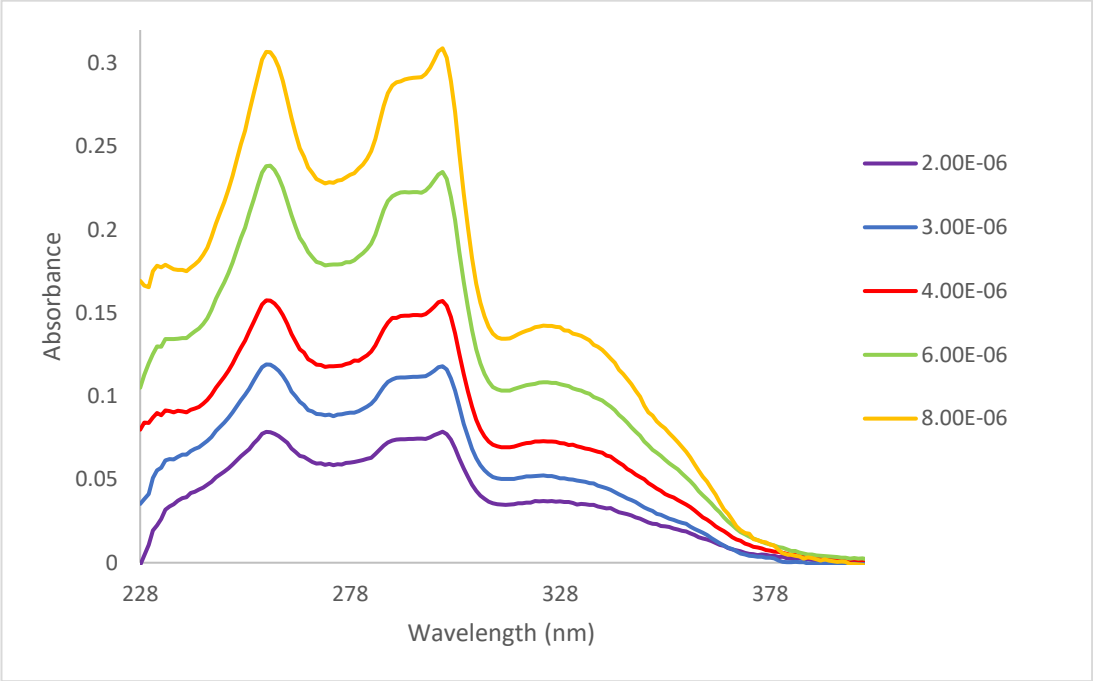
1.3 UV-Visible spectroscopic analysis of compound **65** (concentration range in the figure key, in mol dm^{-3})



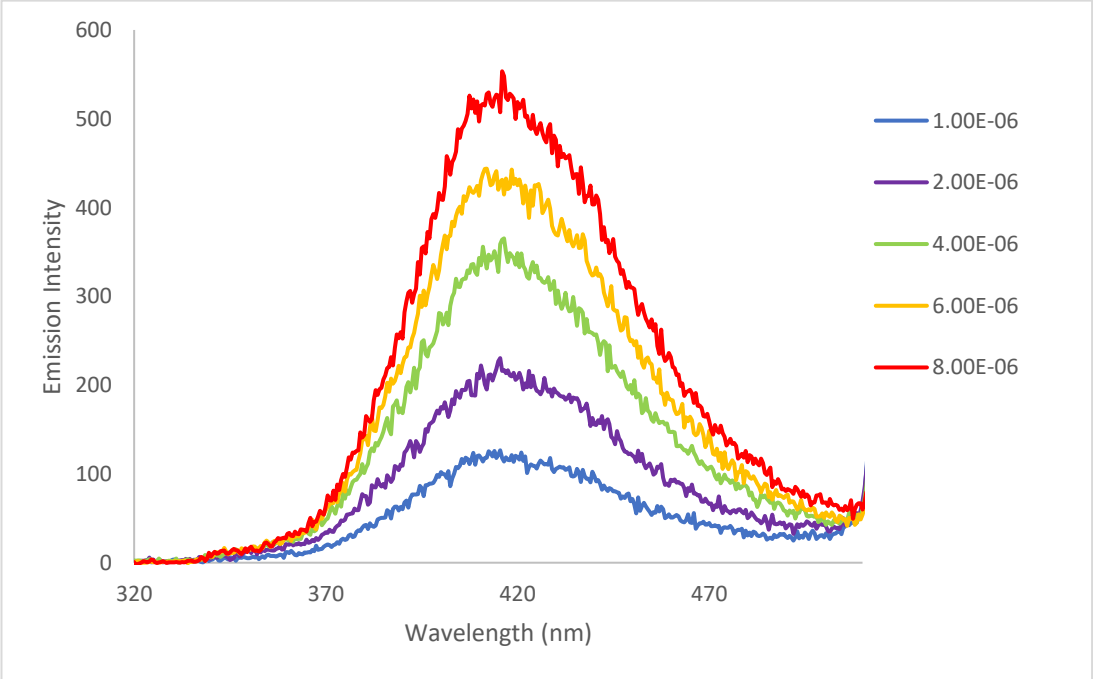
1.4 Fluorescence spectroscopic analysis of compound **65** (concentration range in the figure key, in mol dm^{-3})



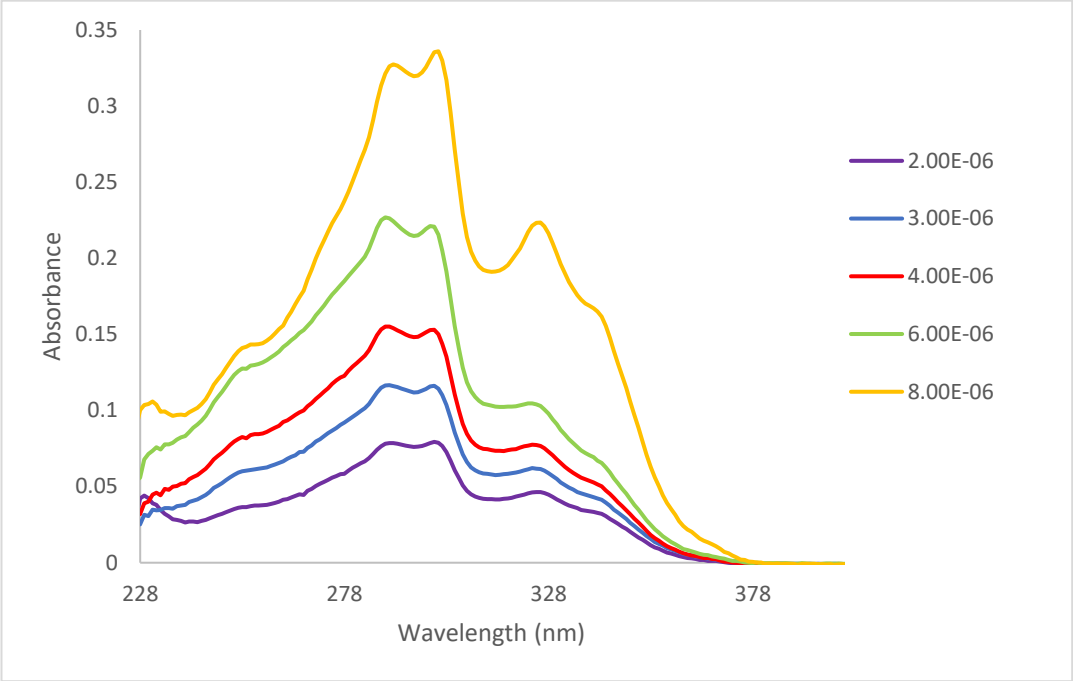
1.5 UV-Visible spectroscopic analysis of compound **66** (concentration range in the figure key, in mol dm^{-3})



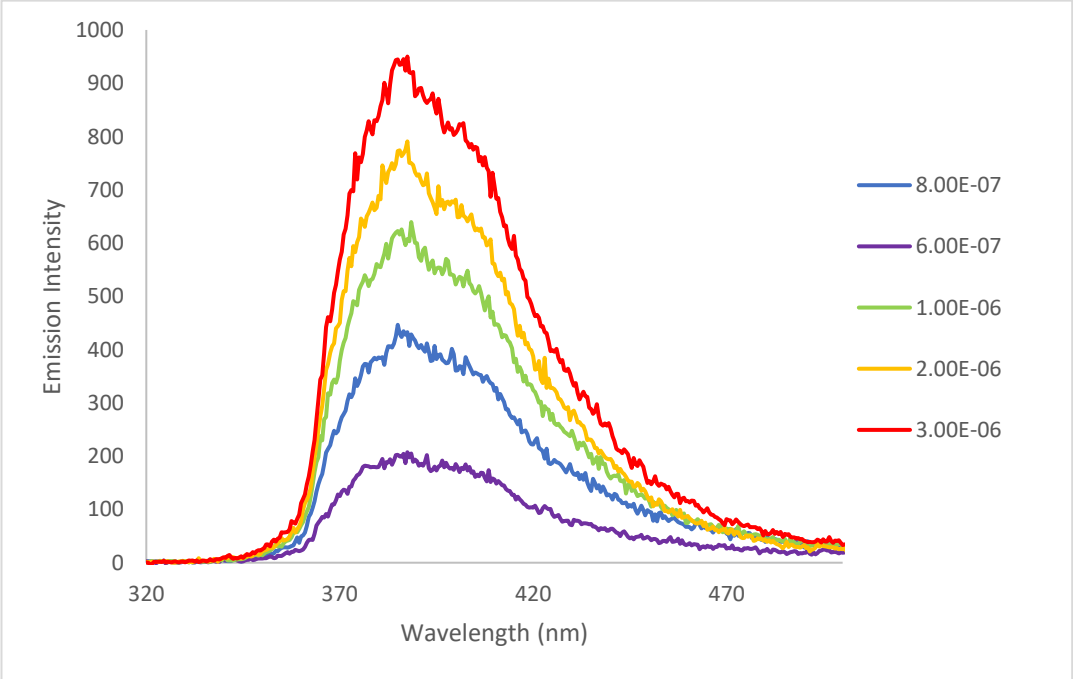
1.6 Fluorescence spectroscopic analysis of compound **66** (concentration range in the figure key, in mol dm^{-3})



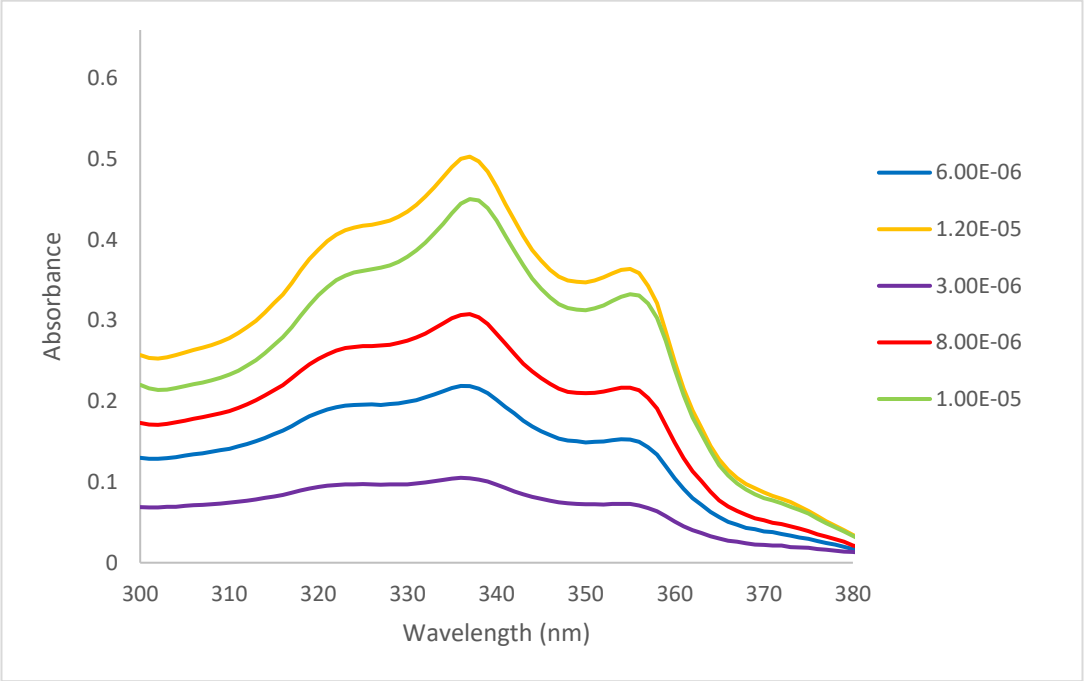
1.7 UV-Visible spectroscopic analysis of compound **67** (concentration range in the figure key, in mol dm^{-3})



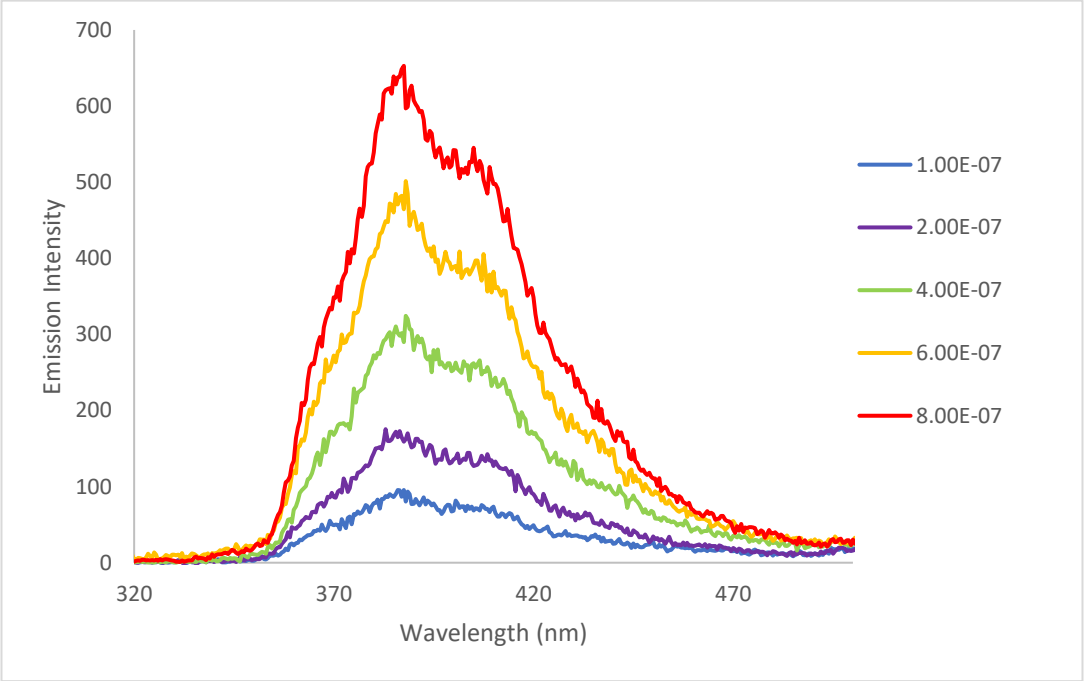
1.8 Fluorescence spectroscopic analysis of compound **67** (concentration range in the figure key, in mol dm^{-3})



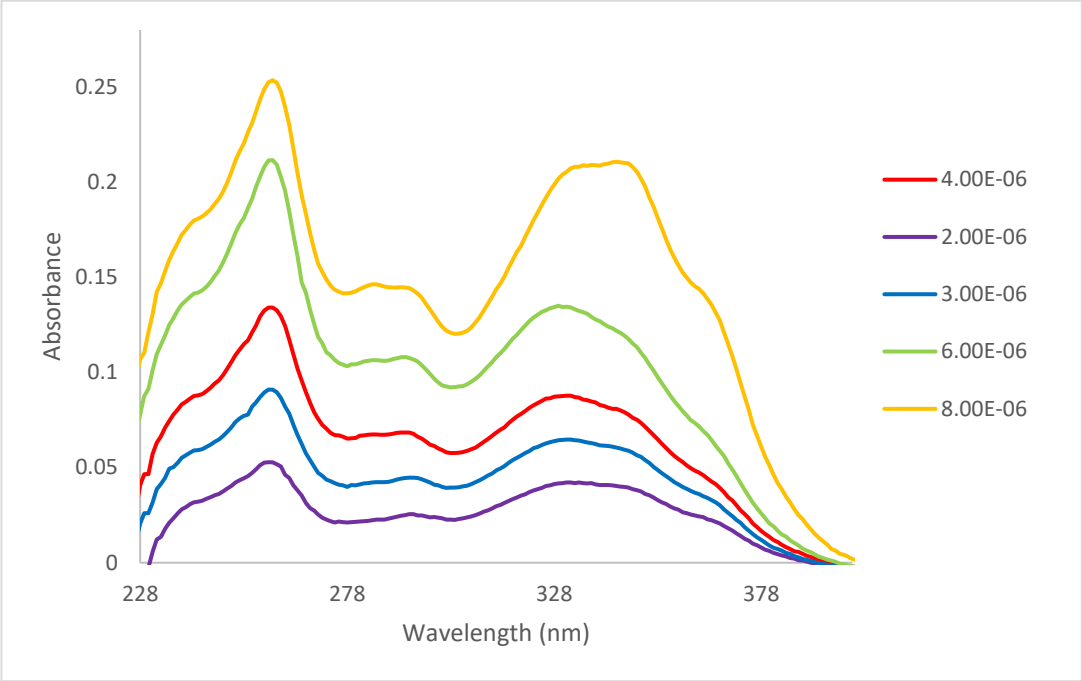
1.9 UV-Visible spectroscopic analysis of compound **69** (concentration range in the figure key, in mol dm^{-3})



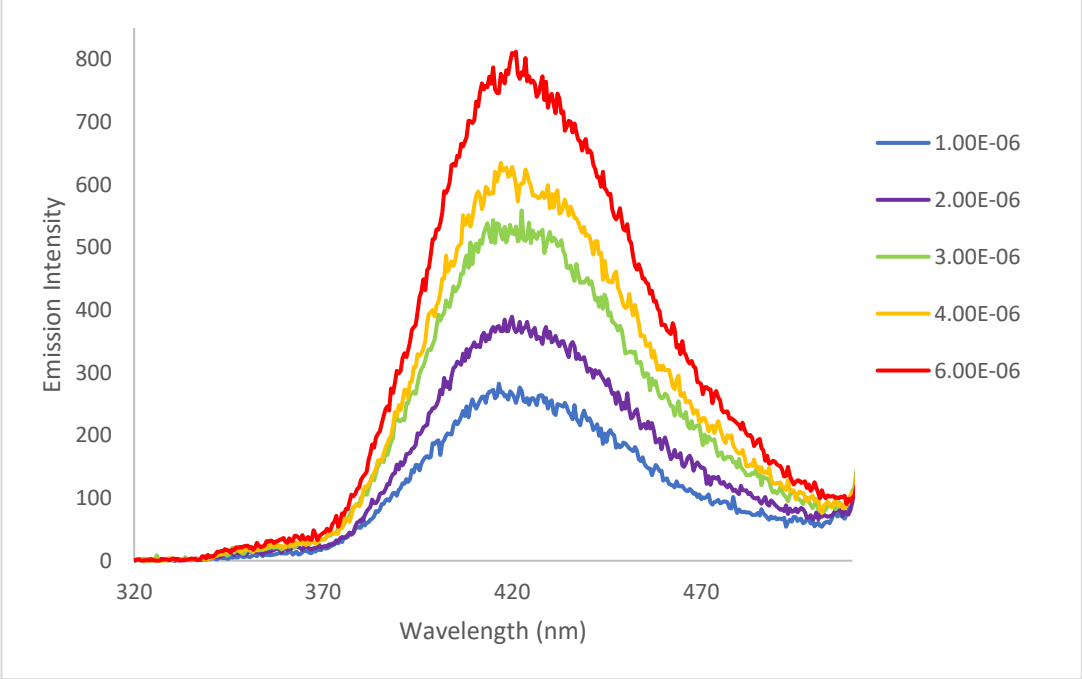
1.10 Fluorescence spectroscopic analysis of compound **69** (concentration range in the figure key, in mol dm^{-3})



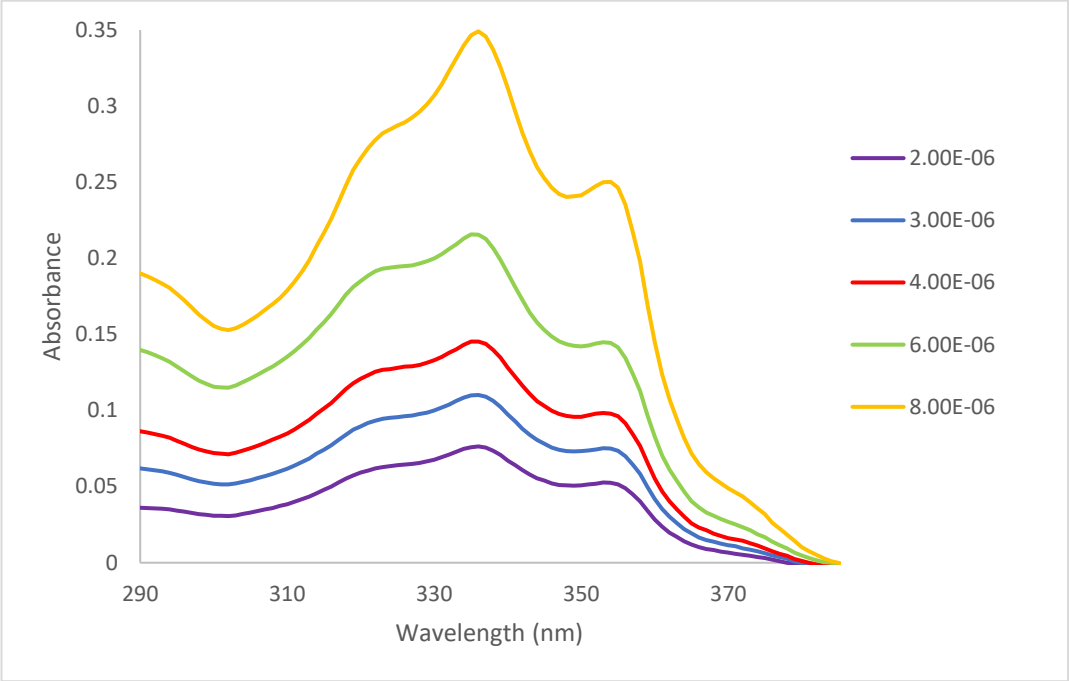
1.11 UV-Visible spectroscopic analysis of compound **70** (concentration range in the figure key, in mol dm^{-3})



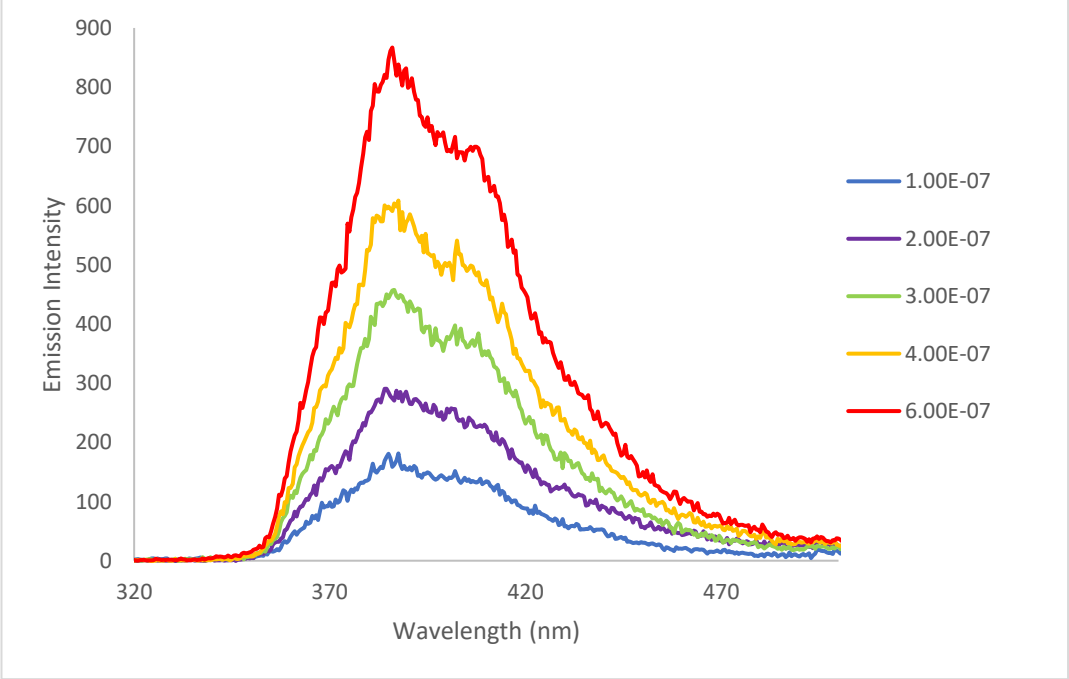
1.12 Fluorescence spectroscopic analysis of compound **70** (concentration range in the figure key, in mol dm^{-3})



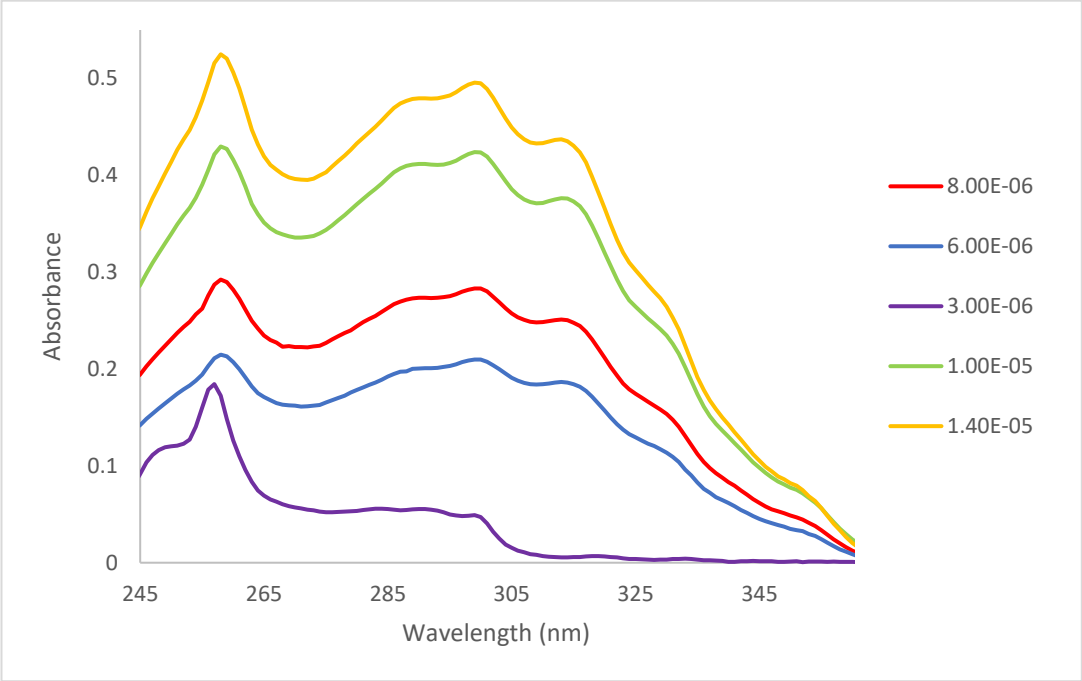
1.13 UV-Visible spectroscopic analysis of compound **71** (concentration range in the figure key, in mol dm^{-3})



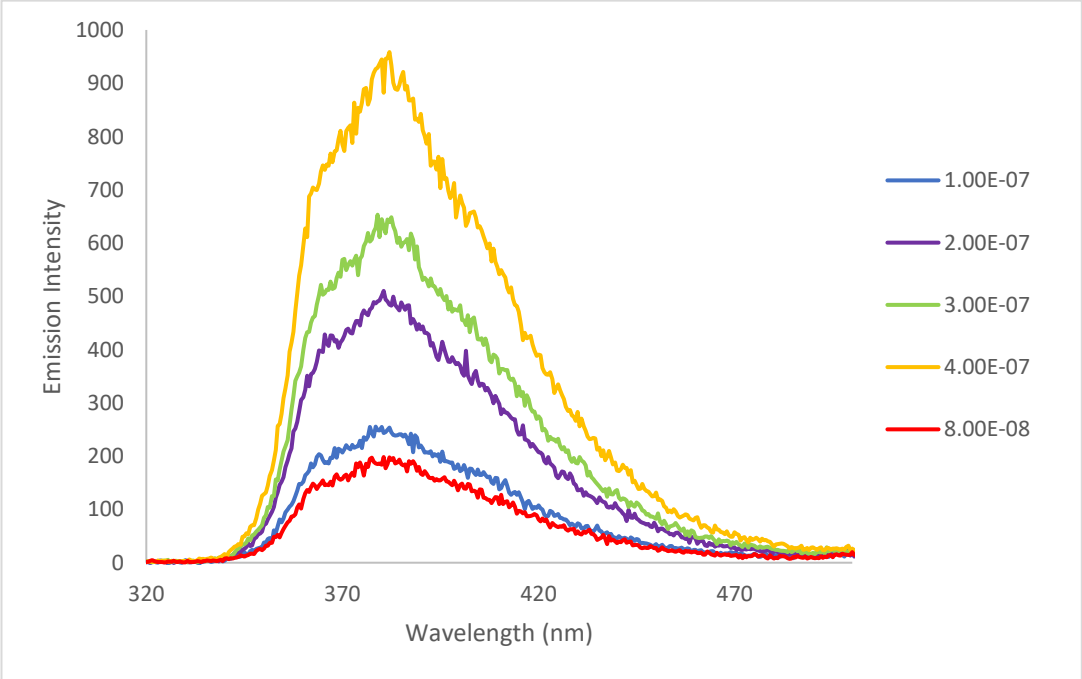
1.14 Fluorescence spectroscopic analysis of compound **71** (concentration range in the figure key, in mol dm^{-3})



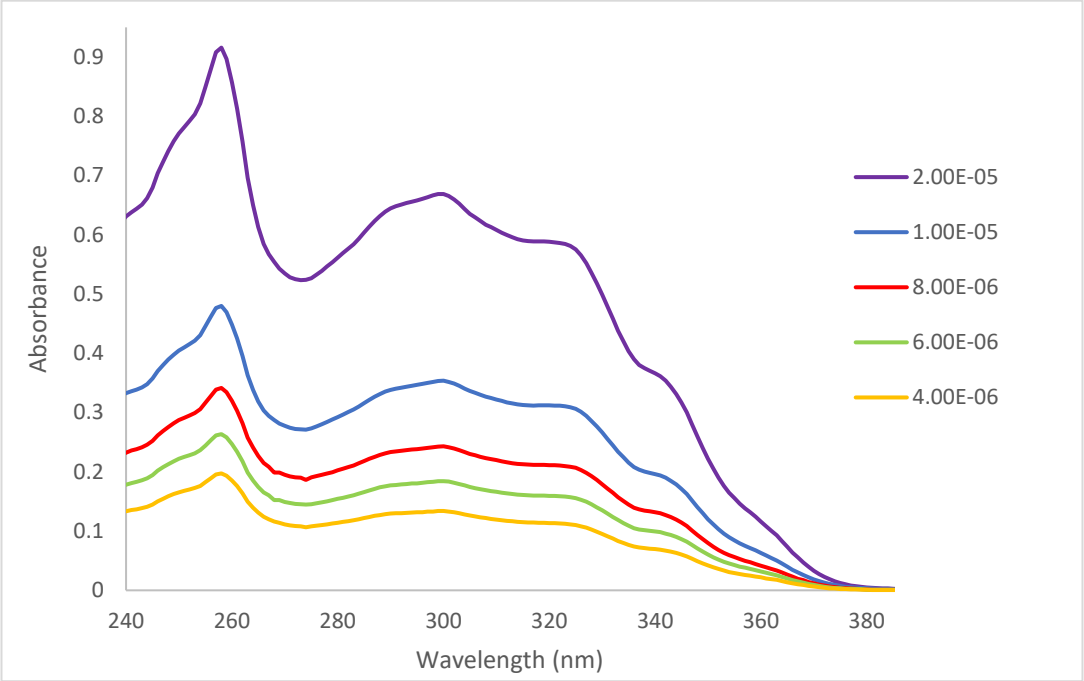
1.15 UV-Visible spectroscopic analysis of compound **73** (concentration range in the figure key, in mol dm^{-3})



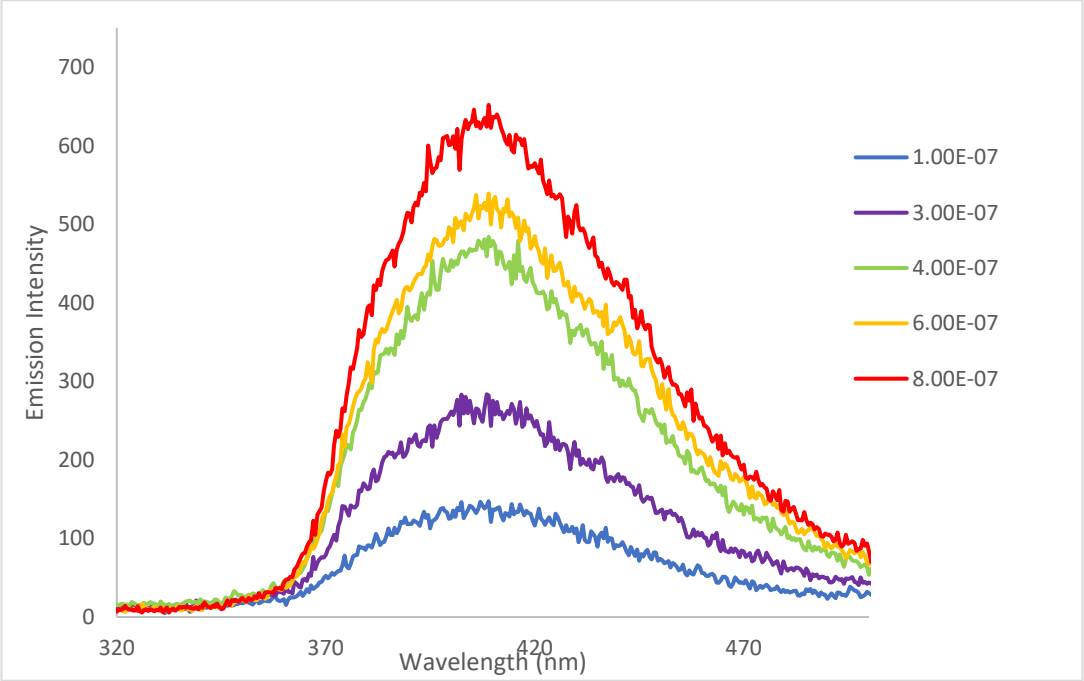
1.16 Fluorescence spectroscopic analysis of compound **73** (concentration range in the figure key, in mol dm^{-3})



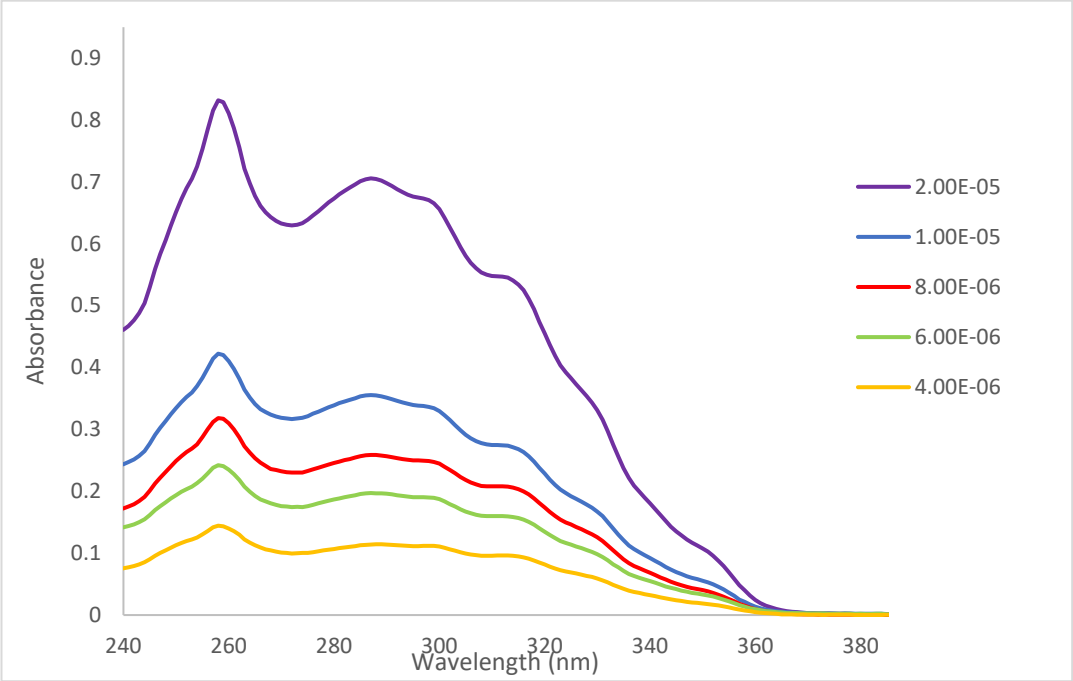
1.17 UV-Visible spectroscopic analysis of compound **74** (concentration range in the figure key, in mol dm^{-3})



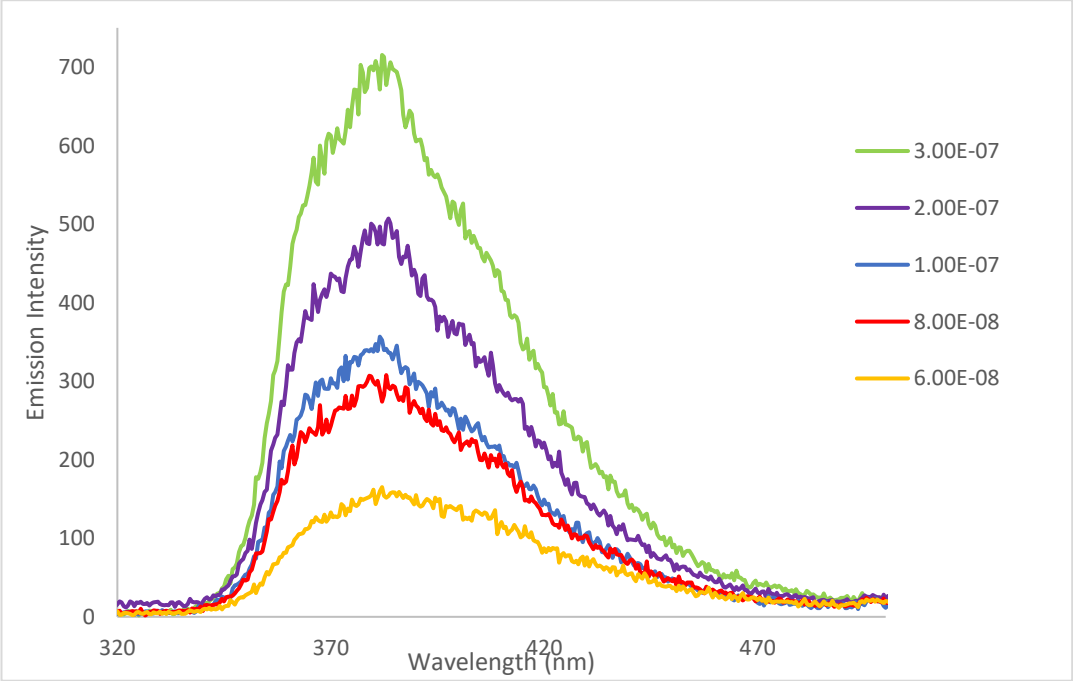
1.18 Fluorescence spectroscopic analysis of compound **74** (concentration range in the figure key, in mol dm^{-3})



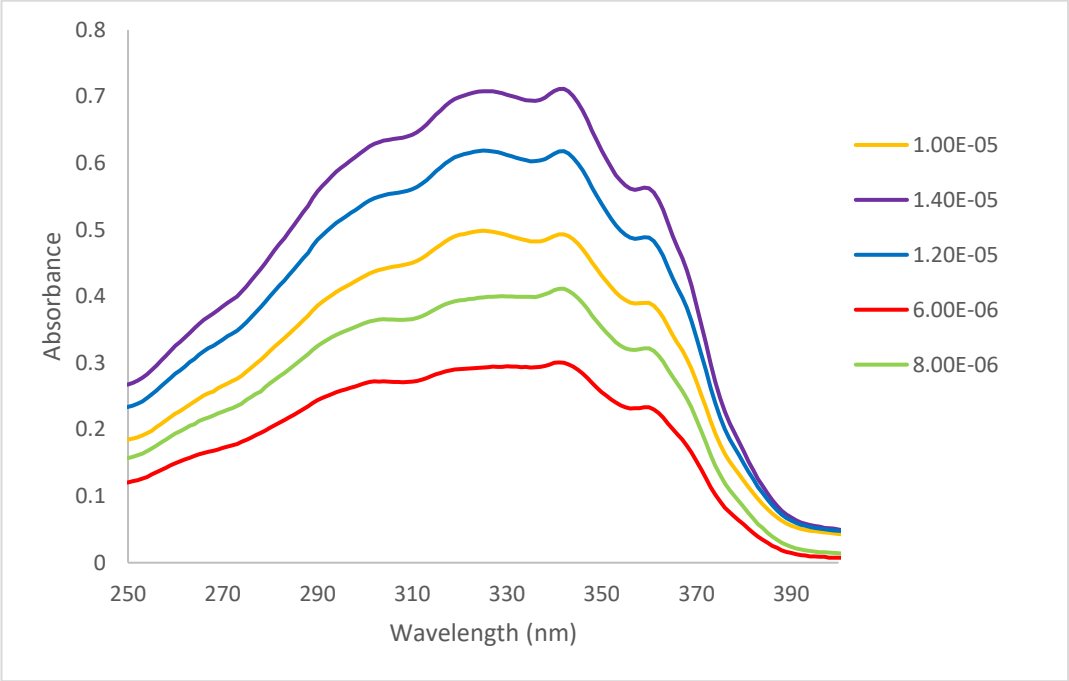
1.19 UV-Visible spectroscopic analysis of compound **75** (concentration range in the figure key, in mol dm^{-3})



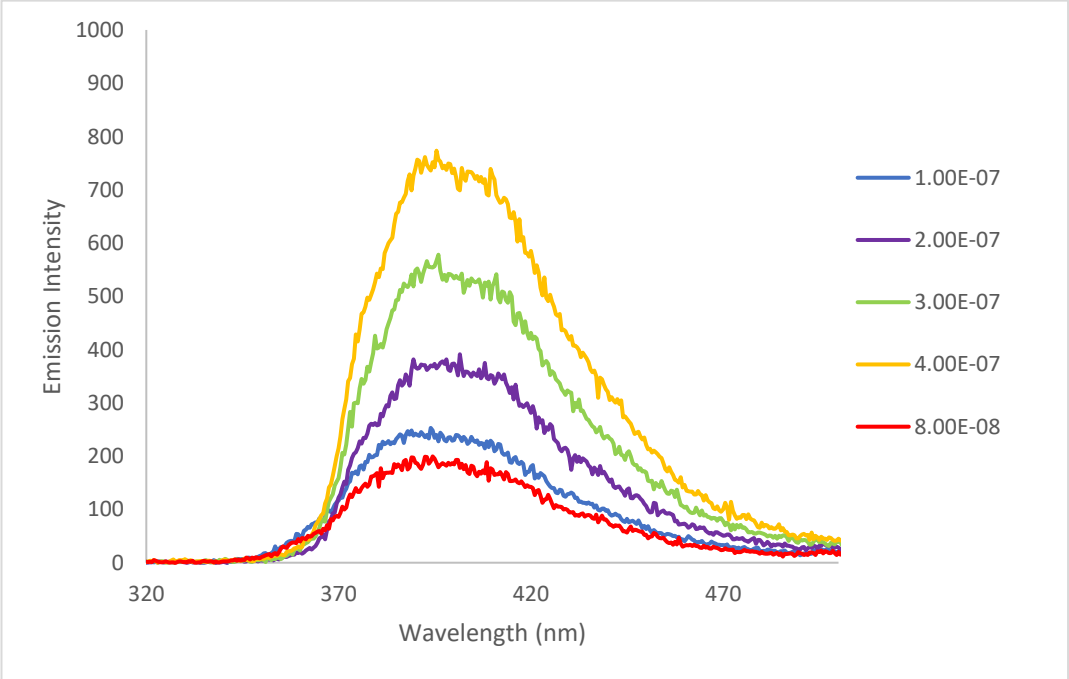
1.20 Fluorescence spectroscopic analysis of compound **75** (concentration range in the figure key, in mol dm^{-3})



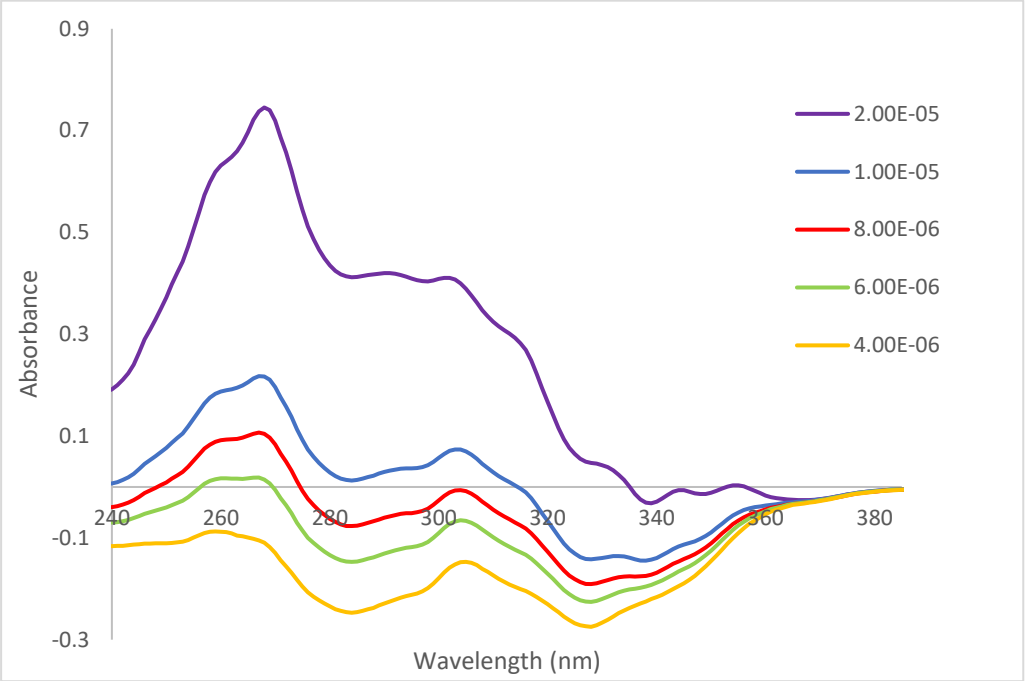
1.21 UV-Visible spectroscopic analysis of compound **77** (concentration range in the figure key, in mol dm^{-3})



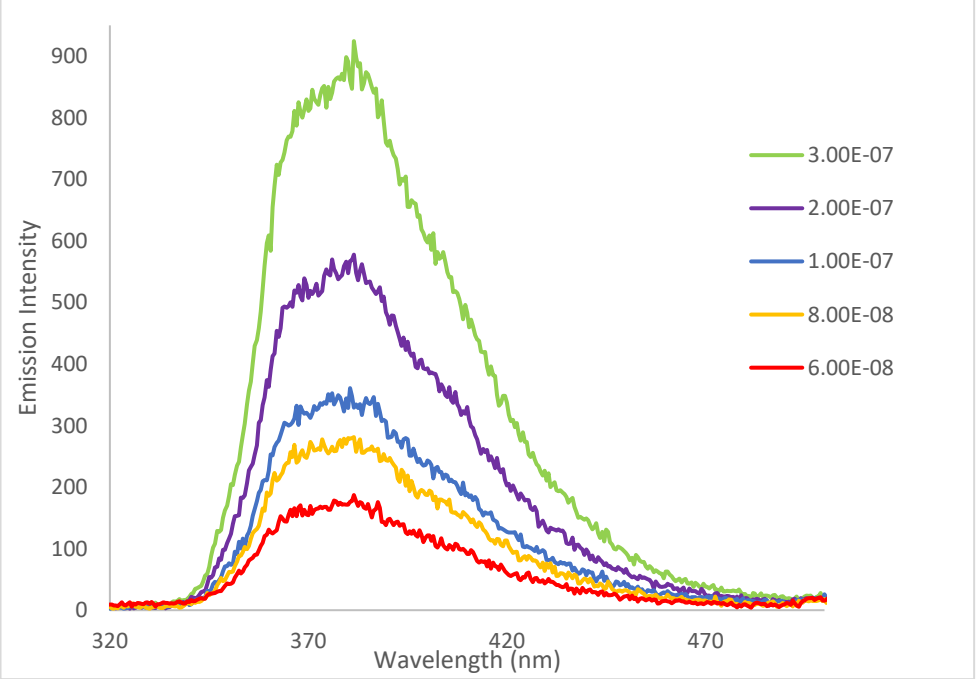
1.22 Fluorescence spectroscopic analysis of compound **77** (concentration range in the figure key, in mol dm^{-3})



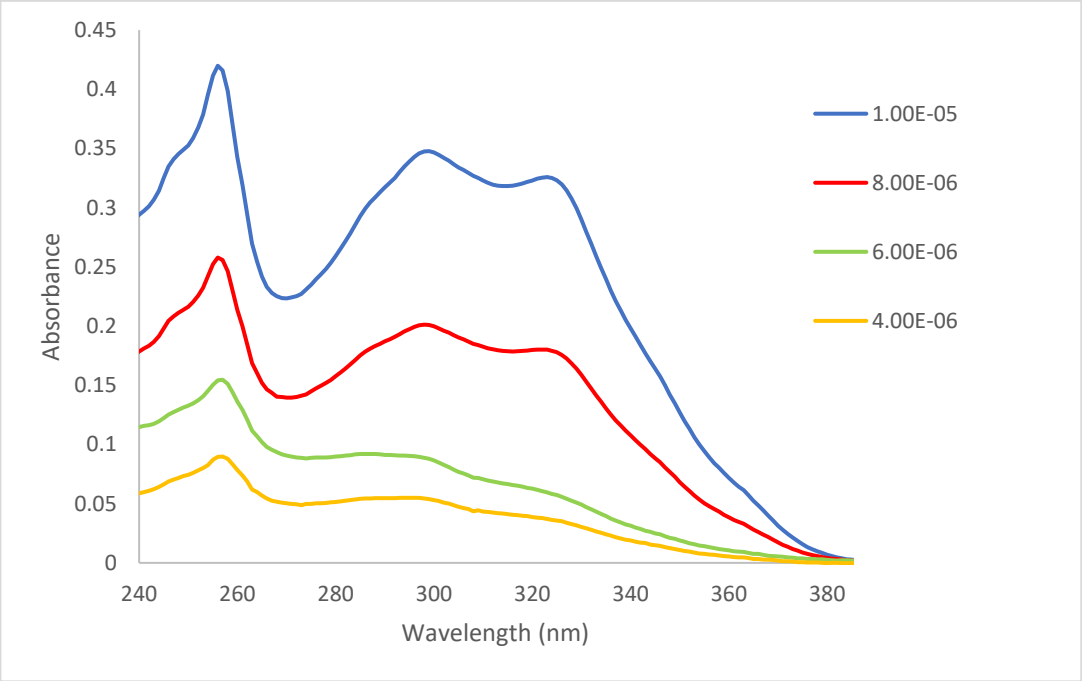
1.23 UV-Visible spectroscopic analysis of compound **95** (concentration range in the figure key, in mol dm^{-3})



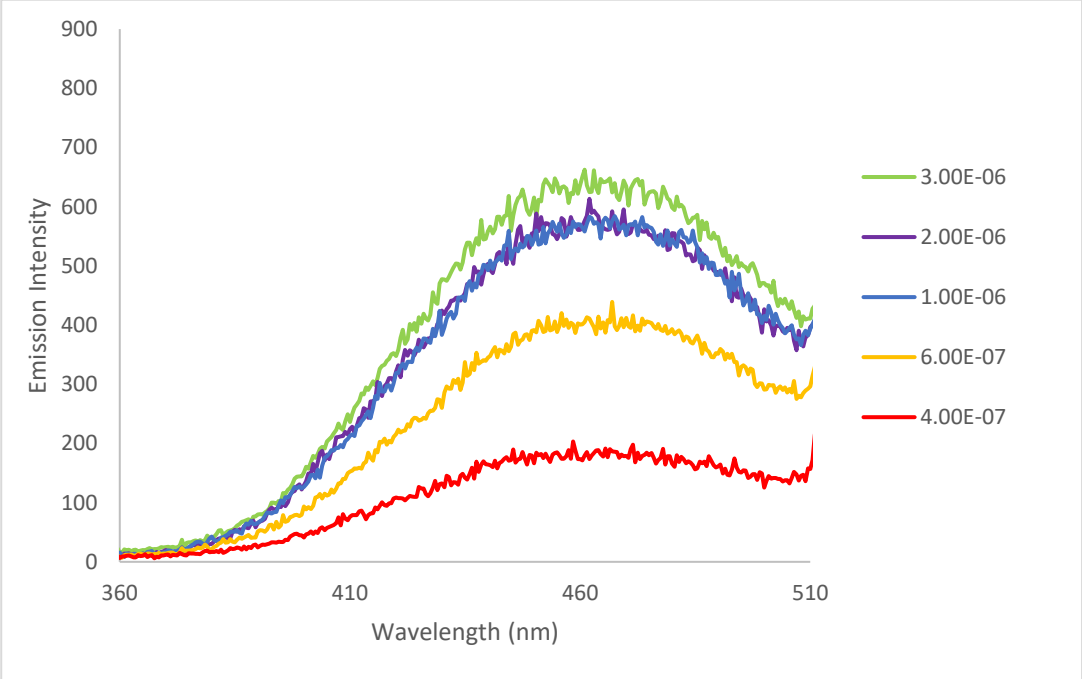
1.24 Fluorescence spectroscopic analysis of compound **95** (concentration range in the figure key, in mol dm^{-3})



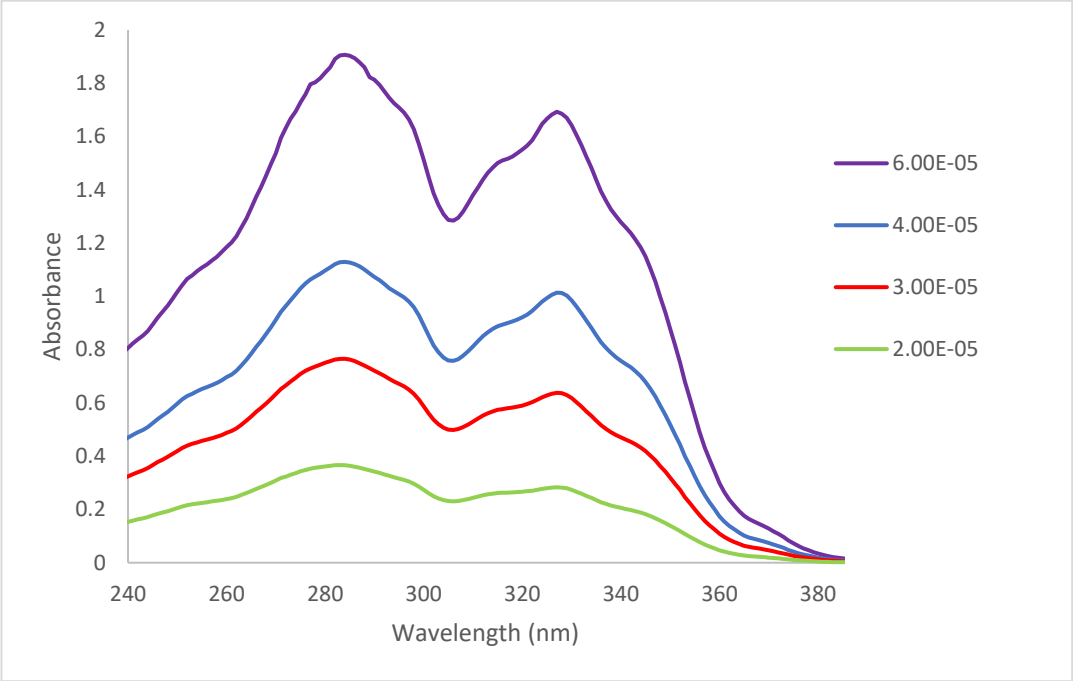
1.25 UV-Visible spectroscopic analysis of compound **96** (concentration range in the figure key, in mol dm^{-3})



1.26 Fluorescence spectroscopic analysis of compound **96** (concentration range in the figure key, in mol dm^{-3})



1.27 UV-Visible spectroscopic analysis of compound **97** (concentration range in the figure key, in mol dm^{-3})



Appendix II

Publications

How do tiny organisms like bacteria communicate?

Updated / Thursday, 13 Aug 2020 15:58



Hey bud, two metres please

Opinion: interrupting how bacteria communicates could scupper infection and slow down the development of bacterial resistance

By Aobha Hickey, Jerry Reen, Fergal O'Gara and Gerard McGlacken, UCC

Communication is the very foundation upon which our society is built. From how we form connections, to the spread of knowledge and international relations, we adopt assorted dialects even within the scope of our own languages. We also know that humans are not alone in our need to communicate. Group hunters like lions and wolves coordinate their attacks through different cues and signals. Their potential prey can equally employ auditory warning signals to alert other vulnerable creatures to the imminent danger. The languages used between these various animals are studied and reported in depth.

But what about tiny organisms like bacteria – how do they communicate? Bacteria are tiny, single-cell microorganisms, about 1,000 times smaller than the tip of a pencil. They can inhabit virtually any ecosystem on the planet and can survive in the most extreme conditions, even space.

They live on and around us and are generally not harmful. The quantity of bacteria on and in our bodies is so great that we have more bacterial genes than human ones. They mostly aid digestion in the gut, but also help prevent infection in the nose and mouth. These microbes are the good guys but, as is the case with most stories, some bacteria fall into the bad guys category. Some common illnesses caused by harmful bacteria include urinary tract infections and food poisoning.

Estimated to have appeared nearly four billion years ago, bacteria are the ancestors to nearly every plant and animal on our planet. During their extended stay, some of these archaic beings have developed the ability to communicate with one-another and co-ordinate their activities. In fact, multiple bacteria can work together to accomplish tasks that would be non-productive for a single bacterium.

One of the most intriguing cooperative behaviours is bioluminescence (the release of light). This form of co-operation was first discovered in the 1970s through the study of a marine bacteria called *Aliivibrio fischeri*. These bacteria adopt a remarkable relationship with the Hawaiian bobtail squid *Euprymna scolopes*.

Each day at dusk, the squid attracts the bacteria into its light organ where the bacteria receive sustenance and shelter, and happily multiply. When the bacterial colony becomes sufficiently large, bioluminescence is initiated. The brightness of the light emitted from the organ is controlled by the squid in response to the light of the moon. As a result, the squid does not cast a shadow on the seabed, effectively camouflaging itself from its predators at night. Millions of bacteria emit light in unison, creating camouflage that is conceivably more effective than light from a single, microscopic cell.

But how do the bacteria know when to co-ordinate this behaviour? The language used by many bacteria consists of small chemical signals, or molecules, instead of words. A bacterium makes the small molecule and releases it into its environment, as a way of saying "I'm here and we need to do X, Y or Z" to other bacteria.

Other bacteria in the colony 'listen out' for the signals while also releasing their own. The denser the population becomes, the louder the signal. Once the signal reaches a certain level, the bacteria alter their actions to behave as a multicellular unit and execute the coordinated action.

Bacteria use this communicative network to perform all sorts of auspicious tasks like cell multiplication, motility and the production of various proteins. They use chemical communication to coordinate their behaviour to survive, often to the detriment of the host, which is sometimes us humans.

One such example is the bacteria *Pseudomonas aeruginosa* which infects the lungs of immunocompromised patients, particularly those with Cystic fibrosis. In this case, bacteria communicate with each other to create a protective biofilm which covers the entire population of bacteria. This group behaviour is a major problem in the clinical treatment of pseudomonas infections. The protective layer in which biofilms are encased is very difficult to penetrate, making the infection increasingly challenging to treat using traditional antibiotics, effectually promoting antibiotic resistance.

The emergence of resistant species has led researchers to return to the drawing board in an effort to discern new therapeutic routes. If bacteria communicate to protect themselves against our immune system and antibiotics, could we interrupt this social network as a new route to tackle infection? By making small molecules similar to those produced natively, we could confuse the bacteria. Research has been promising, as *Pseudomonas aeruginosa* struggles to create the proper biofilm architecture when chemical 'words' are introduced to their environment.

What is unusual and counterintuitive about interrupting bacterial communication is that we interfere with their disease-causing attributes without killing the bacterial cells. So why is this a good thing? Well think about how bacteria become resistant to antibiotics. Antibiotic resistance occurs when a bacterial cell replicates and one of the offspring experiences a random genetic change (or mutation). By chance, this new genetic coding allows the offspring to be less susceptible to antibiotics. This bacterium thus survives antibiotic treatment and passes its favourable genes onto the next generation. The prevailing survival of the mutant is dependent on the destruction of the others. If we do not kill the colony, then the mutant has no genetic advantage.

Research in UCC is bringing together the collaborative expertise of microbiologists and synthetic chemists to understand the complex networks employed by bacteria and design new molecules to disrupt their group behaviours. Some signalling molecules of certain species are known, but others need to be discovered. Current experiments work with millions of bacteria at a time, introducing novel small chemical alterations, so that the bacteria struggle to communicate and work in unison. For *Pseudomonas*, this means no protective biofilm, allowing for more successful treatment in combination with antibiotics.

However, it can get a little more complicated. We have shown that communication can transpire between different species of bacteria and even fungi. Many of these pathogens co-inhabit natural ecosystems and a variety of microbes can also live within an infected site. This can often cause a more severe illness, that demands a unique therapeutic approach.

Our research continues to try and learn the language of bacteria and study the communicative pathways they use to perform tasks which benefit their colony. We synthesise confusing words in an attempt to prevent bacteria from enacting cooperative behaviour both within and outside of their own colonies. Overall, this approach could scupper bacterial infection and slow down the development of bacterial resistance.

Aobha Hickey is a PhD researcher with the School of Chemistry at UCC. She is an Irish Research Council awardee. Dr Jerry Reen is a Lecturer in Molecular Microbial Ecology in the School of Microbiology at UCC and funded through the Health Research Board. Professor Fergal O'Gara is Professor Emeritus of Microbiology at UCC and a funded investigator with SSPC, the SFI Research Centre for Pharmaceuticals. He is a former Irish Research Council awardee. Dr Gerard McGlacken is a Senior Lecturer at UCC and funded through SSPC.

The views expressed here are those of the author and do not represent or reflect the views of RTÉ

Article printed from RTE.ie

ACS OMEGA

http://pubs.acs.org/journal/acsodf

Article

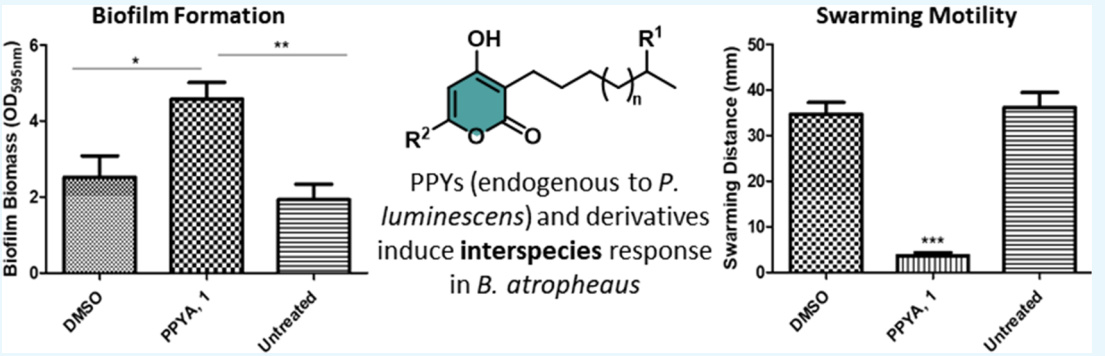
Pyrones Identified as LuxR Signal Molecules in *Photorhabdus* and Their Synthetic Analogues Can Alter Multicellular Phenotypic Behavior of *Bacillus atropheaus*

Aobha Hickey, Leticia M. Pardo, F. Jerry Reen,* and Gerard P. McGlacken*

Cite This: *ACS Omega* 2021, 6, 33141−33148

Read Online

ACCESS | Metrics & More | Article Recommendations | Supporting Information



ABSTRACT: Individual bacteria communicate by the release and interpretation of small molecules, a phenomenon known as quorum sensing (QS). We hypothesized that QS compounds extruded by *Photorhabdus* could be interpreted by *Bacillus*—a form of interspecies communication. We interrogate the structure−activity relationship within the recently discovered pyrone QS network and reveal the exquisite structural features required for targeted phenotypic behavior. The interruption of QS is an exciting, nonbiocidal approach to tackling infection, and understanding its nuances can only be achieved by studies such as this.

Downloaded via 78.17.114.107 on January 7, 2022 at 10:05:54 (UTC).
See https://pubs.acs.org/sharingguidelines for options on how to legitimately share published articles.

INTRODUCTION

Bacteria can coordinate their collective behavior through an elaborate communication network.[1] This remarkable realization has offered new insights into the complexity of microbial infections.[1] Cooperation of/within microbial consortia is governed by the extrusion and perception of small-molecule signals (called autoinducers—AIs), a phenomenon known as quorum sensing (QS). Thus, bacteria monitor their external environment and can significantly alter gene expression to act as a single multicellular organism if required.[2,3] These interactions yield the capacity to accomplish tasks that are futile when performed by an individual bacterium[4]—typically bioluminescence, secondary metabolite synthesis, and perhaps, most importantly, biofilm formation and virulence factor production.[5−8] Through this ability to coordinate behavior and form biofilms, QS allows bacteria to become more potent pathogens, less susceptible to antibiotic treatments, and often facilitates the evolution of antibiotic resistance.[9,10]

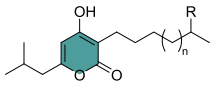
The prototypical QS model in Gram-negative bacteria is comprised of a LuxI-type AI synthase and a LuxR-type receptor, with *N*-acyl homoserine lactones (AHLs) being the most predominant class of AIs generated and received by these proteins.[11] Although not fully understood, systems lacking any LuxI-like AHL synthase can still encompass proteins with homology to LuxR-type receptors, namely LuxR orphans or solos.[12,13] Seminal reports by Heermann and co-workers explicitly target the concept that non-AHL producing bacteria can employ these receptors in the detection of other endogenously synthesized compounds and operate a QS signaling pathway.[14,15] Critically, this group unearthed "photopyrones" (PPYs) participating in the QS network of the Gram-negative pathogen *Photorhabdus luminescens* through an orphan LuxR receptor. The quorum in this case activates a signaling cascade that transcribes the operon responsible for the *Photorhabdus* clumping factor (Pcf)—a biofilm-like phenotype that plays a vital role in the pathogenicity of these bacteria.[14,16,17] These findings encompass the first demonstration of 2-pyrones, specifically 3-alkyl-4-hydroxy-6-isobutyl-2*H*-pyran-2-ones (Figure 1), acting as signaling molecules in any bacterial strain.[14]

Received: October 4, 2021
Accepted: November 10, 2021
Published: November 22, 2021



ACS Publications

© 2021 The Authors. Published by American Chemical Society



PPY	R	*n*
A	H	1
B	CH_3	1
C	H	3
D	CH_3	3
E	H	5
F	CH_3	5
G	H	7
H	CH_3	7

Figure 1. Photopyrones (PPYs) A−H isolated from Photorhabdus luminescens.

Although the findings specified the detection of endogenously produced PPY signals, it is also known that orphan receptors can be used to respond to exogenous signals, produced by coinhabiting microorganisms, for example.[15,18,19] Following on from our work describing the interspecies and interkingdom activity of the alkyl hydroxyquinolone signals 2-heptyl-4-quinolone (HHQ) and *Pseudomonas* quinolone signal (PQS) produced by *Pseudomonas aeruginosa*,[20−26] this report describes interspecies behavioral control exerted by the *P. luminescens* pyrone signals on a model organism, *Bacillus atropheaus* subtilis var. niger (globigii) termed *B. atropheaus* hereafter. Importantly, this Gram-positive, aerobic bacterium utilizes QS in the formation of biofilms,[27] making it a suitable model for analysis of signal-based interference with cell−cell communication. Entomopathogenic *Photorhabdus* and *Bacillus* species have demonstrated a close inter-relationship, working synergistically in some infections[28,29] and exchanging toxin systems in others.[30] The emerging interspecies and interkingdom role in cell−cell communication signals and the close relationship between *Photorhabdus* and *Bacillus* species led us to investigate the possibility that 2-pyrones, similar to those produced by the former, could exert behavioral control over the latter.

A bacterial biofilm is a polymeric matrix structure that can grow on living or inert surfaces.[31] Its formation involves a complex multistage process, underpinned by a signaling-based communication system that spans from the initial attachment phase through to maturation and dispersion. This lifestyle is adopted by up to 80% of infections in humans,[32] frequently allowing the bacterial colony to circumvent the host immune system and increase resistance to antibacterial agents.[10] Swarming is also governed by a complex QS-based communication system, which directs multiple aspects of behavior, including head to tail connections between individual bacterial cells in this and other *Bacillus* species.[33] Both of these essential phenotypes, which are linked to persistence, virulence, and antibiotic resistance in bacteria, were investigated using *B. atropheaus*.[34,35]

RESULTS AND DISCUSSION

The simplest of the natural signals, isolated from *Photorhabdus*, **PPYA**, (**1**) was initially synthesized and tested for biofilm and swarming motility altering activity.[36,37] Addition of **PPYA 1** (50 μM) to media prior to inoculation with *B. atropheaus* cultures led to a dramatic increase in attached biofilm biomass when compared with dimethyl sulfoxide (DMSO) and untreated controls (Figure 2a). We reasoned that a low micromolar concentration would be in the physiological range and consistent with previous studies investigating the interspecies role of other quorum sensing molecules.[20,38,39] In contrast, swarming motility was significantly repressed in the presence of **PPYA**, pyrone **1** (Figure 2b). This was independent of any growth-related effects, as determined by visual analysis of the biofilm formed, indicating a shift toward stronger pellicle formation at the liquid−air interface (SI, Figure S1). The addition of a reduced concentration of compound **1** (10 μM) did not elicit a response from *B. atropheaus* at the same cell seeding density, indicating dose-dependency to the effects observed (SI, Figure S1). The influence of **1** on biofilm formation and swarming motility in *B. atropheaus* has extensive potential implications. This suggests that **1** has the propensity to induce interspecies activity beyond its inherent role in the signal-producing *Photorhabdus* species.

Following on from these promising results, we looked at preparing a suite of analogues (known and novel) to probe the structure−activity relationship. Diversification at C3 and C6 was targeted, along with some modification of the pyrone core (Scheme 1).[36,37] We then investigated the impact of these analogues on biofilm and swarming properties in *B. atropheaus*.

Based on the trend toward enhanced biofilm formation observed with the native pyrone signal **PPYA 1**, we examined the impact of our 2-pyrone derivatives on the ability of *B.*

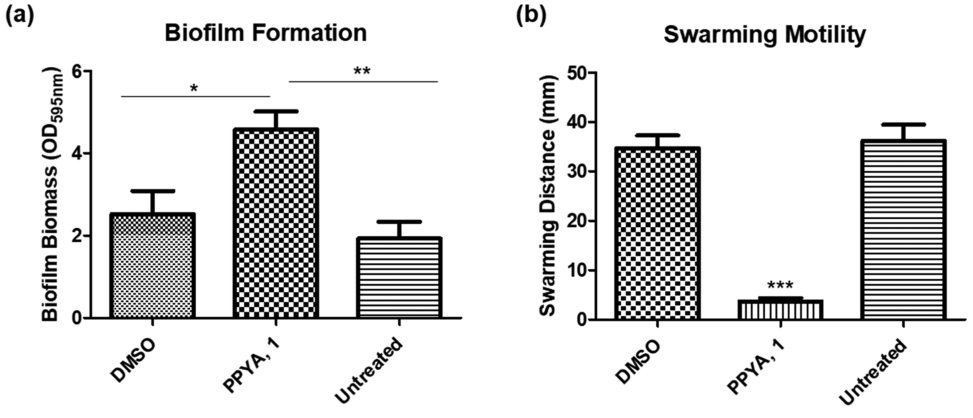
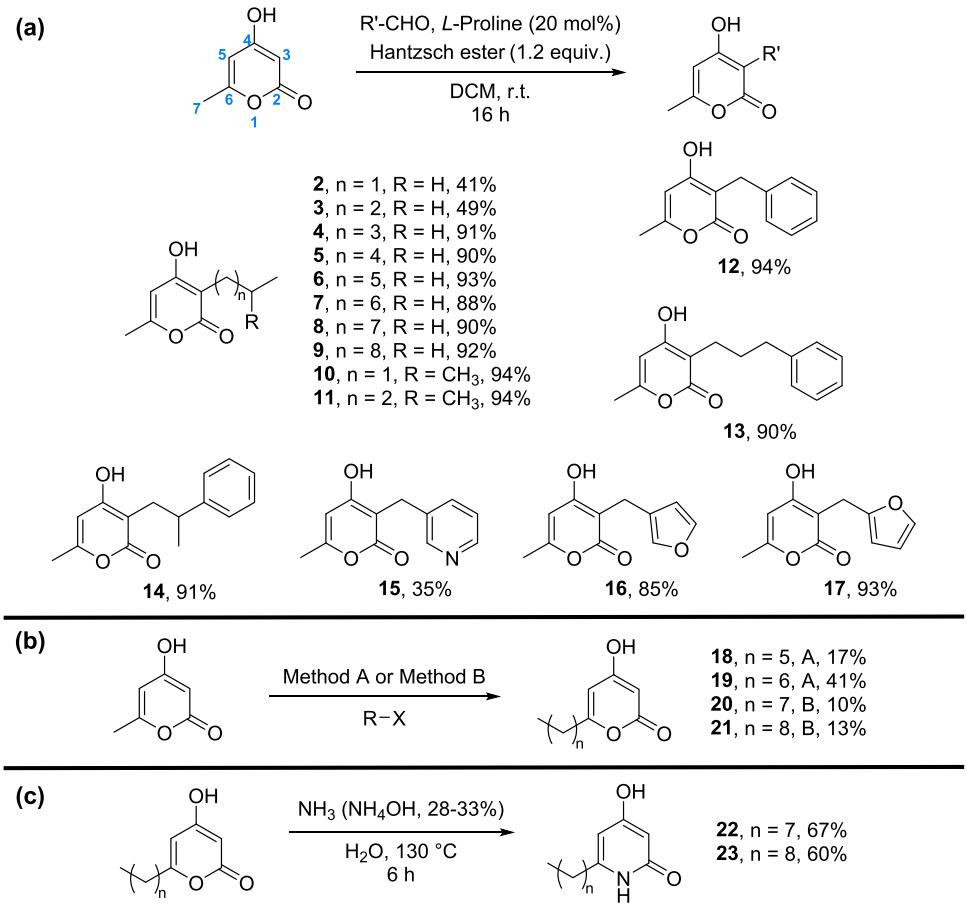


Figure 2. (a) Biofilm formation in *B. atropheaus* in the presence **PPYA** at 50 μM in DMSO presented as Abs_{595nm} following crystal violet staining. (b) Swarming motility of *B. atropheaus* with **PPYA** or carrier control. Data presented are the average (±standard error of the mean (SEM)) of three independent biological replicates. Statistical analysis was performed by one-way analysis of variance (ANOVA) with Bonferroni post hoc corrective testing (*$p \leq 0.05$; **$p \leq 0.005$; ***$p \leq 0.001$).

https://doi.org/10.1021/acsomega.1c05508
ACS Omega 2021, 6, 33141−33148

Scheme 1. (a–c) 2-Pyrone and 2-Pyridinone Derivatives Synthesized[a]



[a]The Hantzsch ester used here is 1,4-dihydro-2,6-dimethyl-3,5-pyridinedicarboxylate. Method A: (i) hexamethyldisilazane (HMDS) (3 mL/mmol), N_2, 80 °C, 1 h and (ii) tetrahydrofuran (THF), *n*-BuLi (1.25 equiv), alkyl bromide (2.3 equiv), −78 °C–rt, 16 h. Method B: (i) *N*,*N*,*N*′,*N*′-tetramethylethylenediamine (TMEDA) (1.0 equiv), THF/hexamethylphosphoramide (HMPA) (5:1), *n*-BuLi (2.4 equiv), 0 °C, N_2 and (ii) alkyl iodide (1.8 equiv), 0 °C–rt, 16 h (see the SI for details).

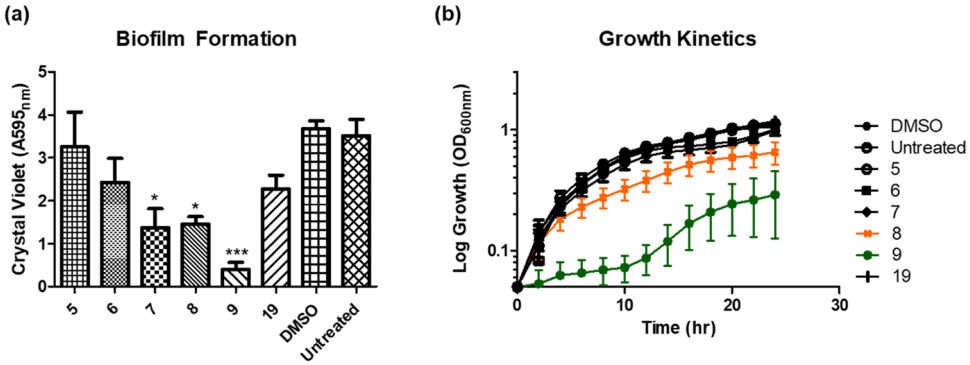


Figure 3. (a) Antibiofilm activity of pyrone derivative compounds at 50 μM in DMSO presented as Abs_{595nm} following crystal violet staining. Assays were performed in 24-well plates. (b) Growth curve analysis of *B. atropheaus* in the presence of pyrone derivatives (see the SI for details). All data presented are the average (±SEM) of at least three independent biological replicates. Statistical analysis was performed by one-way ANOVA with Bonferroni multiple comparison post hoc corrective testing (*$p \leq 0.05$; ***$p \leq 0.001$).

atropheaus to form biofilms and attach to the surface of multiwell plates. We started with analogues bearing a methyl group at C6 (**2**–**17**), which are relatively easy to synthesize. When tested at 50 μM, the following compounds exhibited antibiofilm activity: **7**, **8**, and **9**—in direct contrast to the activity of the natural pyrone signal **1** (SI, Figure S2). Although **6** led to a reduction in biofilm formation, this was not statistically significant when tested in 24-well plates (Figure 3a). It should be noted that all compounds exhibiting antibiofilm activity, contain a long alkyl chain at C3 (C_7–C_{10}). Subsequent validation analysis of lead derivatives through dose–response studies at 10, 30, and 50 μM confirmed the biofilm limiting activity of these compounds (SI, Figure S3).

To determine whether the influence on biofilm was simply a reflection of growth inhibition, *B. atropheaus* was grown in the presence of each compound and investigated temporally. In

https://doi.org/10.1021/acsomega.1c05508
ACS Omega 2021, 6, 33141−33148

terms of growth kinetics profiling, while compounds **8** and **9** had a growth-limiting effect on *B. atropheaus*, growth was not comparably affected in the presence of pyrones **6** and **7** (Figure 3b). This clearly delineates the biofilm formation and growth, at least in compounds **6** and **7**. We, therefore, propose these compounds as lead compounds for antibiofilm activity, potentially working through interference with signaling mechanisms. None of the other compounds, with shorter or longer (linear, branched alkyl chains, aryl, heterocyclic) groups at C3 showed considerable antibiofilm activity. For the activity of all 17 analogues, see the SI.

The ability of specific pyrone analogues to interfere with biofilm formation in *B. atropheaus* led us to examine the impact on swarming motility. These phenotypes (biofilm formation and swarming motility) are linked, with both requiring coordinated communication between cells and the latter is critical in the initiation of the former.[40] Interference with this highly complex behavior would result in a less competitive organism at the community level. Pyrones **8** and **9** abolished swarming activity in *B. atropheaus* on semisolid agar, while pyrones **1** and **7** also strongly suppressed swarming motility, although not to the same extent (Figure 4). Based on the

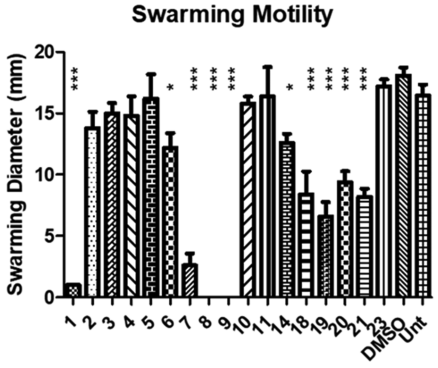
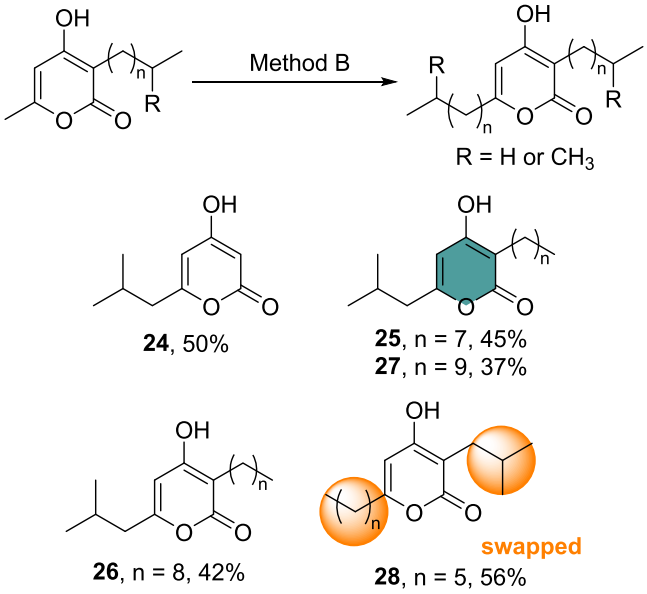


Figure 4. Swarming motility of B. atropheaus with 50 μM compound or carrier control (see the SI for details). All data presented are the average (±SEM) of at least three independent biological replicates. Statistical analysis was performed by one-way ANOVA with Bonferroni post hoc corrective testing ($*p \leq 0.05$, $***p \leq 0.001$).

kinetic growth profiles, the absence of swarming motility in the presence of **9** could simply be attributed to growth antagonism rather than specific interference with the multicellular behavior. However, the absence of swarming activity in the presence of other pyrone compounds indicates a more behavioral mechanism. The trend here is similar to that in the antibiofilm test, i.e., pyrones with long alkyl chains at C3 suppress swarming. However, in this case, the naturally occurring **PPYA** (**1**) trended with the analogues.

In terms of biofilm formation, the simpler synthetic pyrones discussed so far, possessing a methyl group at C6, showed contrasting effects on biofilm formation, relative to the naturally occurring **PPYA** signal (with an *i*-Bu group at C6). Even compound **5**, which is otherwise identical, gave a dramatically different phenotype. Thus, we needed to ascertain the importance of the C6 group. First, we synthesized the C6-*i*-Bu compound **24**, without any alkyl group at C3, to examine the properties of this analogue (Scheme 2). We then took the best performing C3-alkylated derivatives, **7**, **8**, and **9**, and reacted them with 2-iodopropane to give compounds **25** (native, **PPYC**), **26** (non-native), and **27** (native, **PPYE**).

Scheme 2. 2-Pyrone Derivatives Synthesized for Further Structure−Activity Relationship Studies[a]



[a]Method B: (i) TMEDA (1.0 equiv), THF/HMPA (5:1), *n*-BuLi (2.4 equiv), 0 °C, N_2 and (ii) alkyl iodide (1.8 equiv), 0 °C−rt, 16 h (see the SI for details).

Finally, we reversed the positions of the alkyl chains present in **PPYA**, placing the *i*-Bu group at C3 and the *n*-hexyl group at C6 (**28**). The compounds were then tested for their impact on biofilm formation and growth of *B. atropheaus* as described above.

While **1** again led to a notable increase in biofilm formation in *B. atropheaus*, none of the derivative compounds retained this activity (Figure 5a). Swarming motility was suppressed in the presence of **26** to the same extent as with **1** but was unaffected in the presence of **27**, which only differs by a CH_2 group (Figure 5b). This is also consistent with the growth kinetics data, and thus, of the pyrone signals and derivative compounds tested, **26** was the only one that achieved swarming suppression activity comparable to **1**. However, it should be noted that the growth kinetics of *B. atropheaus* was affected in the presence of **26**, with the organism failing to reach the growth rate or final biomass achieved in the presence of the DMSO control. Compounds **24**, **25**, and **28** led to the abolition of growth on the plate, there was no evidence of colony initiation from the point of inoculation (Figure 5c). Remarkably, the bioactivity of compound **1** toward *B. atropheaus* appears to be entirely specific to the exact structural arrangement. The activity of the naturally occurring compounds **25** and **27** with respect to cell-clumping in *Photorhabdus* is as yet unknown.[14] The data presented here suggest that they may play a distinct signaling role from the other native pyrones.

CONCLUSIONS

In conclusion, some 25 natural[41] and unnatural pyrones were synthesized.[42−44] The naturally (in *P. luminescens*) occurring **PPYA** compound **1** was shown to enhance biofilm formation in *B. atropheaus*. In direct contrast, replacement of the isobutyl group at the C6 position with a simple methyl group gave compounds that induced antibiofilm activity. Indeed, antibiofilm activity was also noted for all other compounds, even

https://doi.org/10.1021/acsomega.1c05508
ACS Omega 2021, 6, 33141−33148

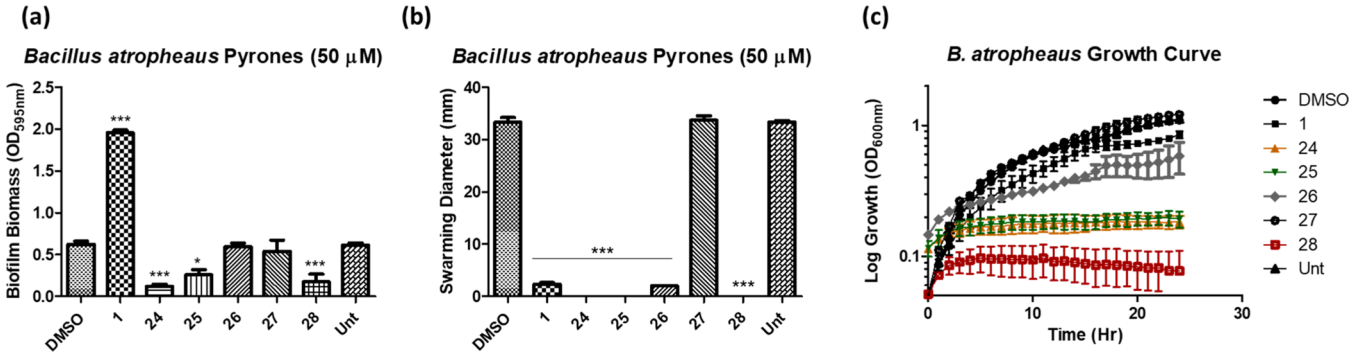


Figure 5. (a) Biofilm formation of B. atropheaus in the presence of derivative compounds **24**–**28**. (b) Swarming motility of B. atropheaus in the presence of derivative compounds **24**–**28**. (c) Growth curve analysis of B. atropheaus in the presence of derivative compounds **24**–**28** (see the SI for details). All data presented are the average (±SEM) of at least three independent biological replicates. Statistical analysis was performed by one-way ANOVA with Bonferroni post hoc corrective testing (*$p \leq 0.05$, ***$p \leq 0.001$).

those with an isobutyl group at C6 and differing from **1** by $\pm CH_2$ in the alkyl chain. Swarming inhibition activity appeared to require less structural specificity compared to the biofilm activity, although a requirement for specific chain length at C3 did emerge as critical for inhibition.

The mechanistic basis of the behavioral changes identified in response to the pyrone signals and their derivatives remains to be elucidated. A LuxR-type receptor–ligand interaction would be complex and likely multifaceted, considering the varied impacts of the PPY derivatives synthesized when compared to the native **PPYA** signal.

QS plays a role in biofilm development and swarming motility in *B. subtilis*,[33,45,46] with AI-2 signaling recently reported eliciting a biofilm-dependent response through the LuxS receptor under specific environmental conditions.[47] A LuxR-type receptor–ligand interaction, such as that described for the pyrones in *Photorhabdus*, would equally be complex and likely multifaceted. The activity and specificity of the natural pyrone signal **1** suggest that pyrones may have an interspecies communication role similar to that seen for the alkyl hydroxyquinolone signal molecules, HHQ and PQS, in *P. aeruginosa*, which also display similar specific structure–activity relationships.[20,21,26] It is also worth noting that both HHQ and PQS modulate the behavior of a broad range of co-colonizing pathogens, yet the MvfR/PqsR receptor for these two QS molecules has not yet been identified outside of *P. aeruginosa*. The pyrone signal and derivatives presented in this report showed interspecies activity in the low micromolar range, eliciting a dose-dependent phenotypic response at 50 μM, in contrast to the nM range of endogenous signal activity observed in *P. luminescens*.[14] This is consistent with the activity range of the HHQ and PQS signals, which are active in the nM range against their native receptor (PqsR) in *P. aeruginosa*,[23] yet require concentrations in the 10–100 μM range to elicit an interspecies response.[20,21,26] An important consideration here is the degree to which these compounds are naturally soluble in assays or indeed within the particular microbial community or ecosystem within which they are found. As an analogy, the solubility of both HHQ and PQS is significantly enhanced by endogenous biosurfactants called rhamnolipids, which are produced by *P. aeruginosa*.[48] It is unclear as yet whether a similar phenomenon underpins the biological activity of photopyrones at the interspecies level as reported here, or indeed their interaction with solo LuxR receptor proteins.

Deciphering the breadth of signal-mediated interactions that underpins microbial communication is an important endeavor as we attempt to understand the "community networks" that sustain microbiomes in health and disease.[49] The pyrone derivative described here may have applications against other pathogenic bacteria, which possess a LuxR solo protein, and this will be the focus of further studies. When this is the case, an extensive investigation of pyrone production in microbial communities would be warranted, particularly in light of the network of orphan LuxR proteins that exist in pathogenic organisms. The key finding of this study, the capacity for pyrones to elicit behavioral changes in a Gram-positive organism at a low micromolar concentration, points to the role of this new class of molecular signal in the interspecies interactome. Elucidating that role, and the extent to which it governs virulence and pathogenesis in competing organisms will require an interdisciplinary approach.

EXPERIMENTAL SECTION

Biology. *Biofilm Formation Assays.* *B. atropheaus* was inoculated from −80 °C stock onto tryptic soy agar (TSA) and incubated at 30 °C overnight. A colony was inoculated into 5 mL of tryptic soy broth (TSB) and incubated with shaking overnight at 30 °C. The culture was transferred to fresh TSB media with a starting OD_{600nm} of 0.05, combined with either a pyrone compound or DMSO control, and added to multiwell plates (200 μL into 96-well plates, 1 mL into 24-well plates). The plates were incubated static overnight at 30 °C and developed using the crystal violet assay as described previously.[22]

Swarming Motility Assays. Motility agar plates consisting of TSB with 0.3% w/v agar were allowed to air dry in a laminar flow for 30 min, after which time a fresh colony of *B. atropheaus* grown on TSA was spotted onto the center of the motility plate using a pipette tip. The plates were incubated statically at 30 °C and the zonal swarming diameter was measured. To facilitate screening of a large number of compounds, 6-well plates (Sarstedt), with each well containing 4 mL of motility agar, were used. Carrier and untreated controls were included in all experiments.

Growth Kinetics Assays. *B. atropheaus* was prepared for growth analysis following the protocol described for biofilm formation (vide supra). Once transferred into fresh TSB at a starting OD_{600nm} of 0.05, 200 μL was inoculated into a honeycomb plate and placed on the BioScreen C reader.

https://doi.org/10.1021/acsomega.1c05508
ACS Omega 2021, 6, 33141−33148

Measurements (OD_{600nm}) were taken every 30 min, with shaking for 10 s prior to data capture. DMSO and carrier controls were included in each experiment.

Chemistry. *General Considerations.* Solvents and reagents were used as obtained from commercial sources and without purification, with the exception of THF, which was freshly distilled from sodium/benzophenone under nitrogen. All syntheses and spectra were run at the University College Cork. Melting points were measured in the Thomas Hoover Capillary Melting Point apparatus. Infrared spectra were recorded on a PerkinElmer Fourier transform infrared (FT-IR) spectrometer as thin films in dichloromethane (DCM). Column chromatography was carried out using 60 Å (35−70 μm) silica. Thin-layer chromatography (TLC) was carried out on precoated silica gel plates (Merck 60 PF254) and the developed plates were visualized under UV light. High-resolution precise mass spectra (HRMS) were recorded on a Waters LCT Premier time-of-flight liquid chromatography−mass spectrometry (TOF LC−MS) instrument in University College Cork. Samples were run in the electrospray ionization (ESI) mode using 50% acetonitrile−water containing 0.1% formic acid as the eluent; the samples were made up to a concentration of ca. 1 mg/mL. Nuclear magnetic resonance (NMR) samples were run in deuterated chloroform ($CDCl_3$), deuterated dimethyl sulfoxide ($(CD_3)_2SO$), or deuterated methanol (CD_3OD), as specified. ^{1}H-NMR (500 MHz) and ^{1}H-NMR (300 MHz) spectra were recorded on Bruker Avance 500 and Bruker Avance III 300 NMR spectrometers, respectively, in the proton coupled mode using tetramethylsilane (TMS) as the internal standard. ^{13}C-NMR (125 MHz) and ^{13}C-NMR (75 MHz) spectra were recorded on Bruker Avance 500 and Bruker Avance III 300 NMR spectrometers, respectively, in proton decoupled mode at 300 K using TMS as the internal standard. Chemical shifts (δ) are expressed as parts per million (ppm), positive shift being downfield from TMS; coupling constants (J) are expressed in hertz (Hz). Splitting patterns in ^{1}H-NMR spectra are designated as s (singlet), bs (broad singlet), d (doublet), dd (doublet of doublets), dt (doublet of triplets), t (triplet), and m (multiplet). Elemental analysis was performed at the Microanalysis Laboratory, National University of Ireland, Cork, using PerkinElmer 240 and Exeter Analytical CE440 elemental analyzers.

Representative Procedure for Reductive Alkylation at C3 of 2-Pyrones. To a round bottom flask in open air was added 2-pyrone (1.0 equiv), the corresponding aldehyde (3.0 equiv), diethyl 1,4-dihydro-2,6-dimethyl-3,5-pyridinedicarboxylate (1.2 equiv), and DCM (15 mL/mmol). L-Proline (20 mol %) was then added and the sides of the flask were rinsed again with DCM. The resulting reaction mixture was allowed to stir vigorously for 16 h at rt. The reaction mixture was then concentrated under reduced pressure. The crude product was purified by column chromatography (hexane/EtOAc: 9:1 to 7:3).[36]

Representative Procedure for Electrophilic Substitution at C7 of 6-Alkyl-4-hydroxy-2H-pyran-2-ones. Method A. A Schlenk tube was heated under vacuum and refilled with N_2 three times. 2-Pyrone (1.0 equiv) and HMDS (3 mL/mmol) were added, and the resulting reaction mixture was heated to 80 °C under N_2 for 1 h. The solution was allowed to cool and HMDS was removed under reduced pressure. THF (3 mL/mmol) was then added, and the solution was cooled to −78 °C. *n*-BuLi (1.25 equiv) was added carefully over 15 min, and the solution was stirred for 1 h. Alkyl bromide (2.3 equiv) was then added over 10 min and the solution was allowed to warm gradually to rt, and then stirred for 16 h. The reaction was then quenched with 6 M HCl until pH ∼ 2 and the solvent was concentrated under reduced pressure. The residual mass was dissolved in ethyl acetate (10 mL) and washed with brine (2 × 10 mL). The combined organic extracts were dried over $MgSO_4$, filtered, and concentrated under reduced pressure. The crude product was purified by column chromatography (hexane/EtOAc: 1:1).[50]

Method B. A Schlenk tube was heated under vacuum and refilled with N_2 three times. 2-Pyrone (1.0 equiv) was added, followed by THF (2.77 mL/mmol), and the resulting white suspension was stirred at rt for 5 min. TMEDA (1.0 mmol, 1.0 equiv) and HMPA (0.55 mL/mmol) were added, and the resulting pale-yellow reaction mixture was cooled to 0 °C for 30 min. *n*-BuLi (2.4 equiv) was added dropwise for over 10 min giving a deep red reaction mixture that was stirred further for 1 h at 0 °C, followed by the dropwise addition of the corresponding alkyl iodide (1.8 equiv). The orange reaction mixture was warmed to rt and stirred under N_2 for 16 h. The reaction was acidified with 4 M HCl until pH ∼ 2−3 and was then extracted with Et_2O (3 × 10 mL). The combined organic layers were washed with H_2O (3 × 10 mL) and brine (10 mL), dried over $MgSO_4$, filtered, and concentrated under reduced pressure. The crude product was purified by column chromatography (hexane/EtOAc: 7:3).[36]

Representative Procedure for the Synthesis of 6-Alkyl-4-hydroxy-pyridin-2(1H)-ones. The corresponding pyrone (1.0 equiv), ammonia (5 mL/mmol), and water (2 mL/mmol) were heated at 130 °C for 6 h. The reaction was cooled to rt and diluted with water (4 mL/mmol). The mixture was acidified to pH ∼ 1 with 0.5 M HCl and the resulting precipitate was filtered and dried under vacuum.[51]

■ ASSOCIATED CONTENT

Supporting Information

The Supporting Information is available free of charge at https://pubs.acs.org/doi/10.1021/acsomega.1c05508.

Characterization data of all compounds, supplementary figures and tables and copies of NMR spectra (PDF)

■ AUTHOR INFORMATION

Corresponding Authors

F. Jerry Reen − *School of Microbiology and Synthesis and Solid State Pharmaceutical Centre, University College Cork, Cork T12 YN60, Ireland*; Email: j.reen@ucc.ie

Gerard P. McGlacken − *School of Chemistry, Analytical and Biological Chemistry Research Facility and Synthesis and Solid State Pharmaceutical Centre, University College Cork, Cork T12 YN60, Ireland*; orcid.org/0000-0002-7821-0804; Email: g.mcglacken@ucc.ie

Authors

Aobha Hickey − *School of Chemistry, Analytical and Biological Chemistry Research Facility, University College Cork, Cork T12 YN60, Ireland*

Leticia M. Pardo − *School of Chemistry, Analytical and Biological Chemistry Research Facility, University College Cork, Cork T12 YN60, Ireland*

Complete contact information is available at: https://pubs.acs.org/10.1021/acsomega.1c05508

https://doi.org/10.1021/acsomega.1c05508
ACS Omega 2021, 6, 33141−33148

Author Contributions

A.H. and L.P. synthesized and characterized all compounds. F.J.R. performed all biological assays. The manuscript was prepared with contributions from all authors.

Funding

F.J.R. acknowledges funding from the Health Research Board/Irish Thoracic Society (MRCG-2018-16 and HRB-ILP-POR-2019-004) and from Science Foundation Ireland (SSPC3-Pharm5 12/RC/2275_P2). G.P.M. thanks the Irish Research Council (IRC) and Science Foundation Ireland (SFI) (grant number SFI/12/IP/1315) and the Synthesis and Solid State Pharmaceutical Centre (SSPC) (SFI/12/RC/2275 and SFI/12/RC/2275_P2).

Notes

The authors declare no competing financial interest.

REFERENCES

(1) Mukherjee, S.; Bassler, B. L. Bacterial quorum sensing in complex and dynamically changing environments. *Nat. Rev. Microbiol.* **2019**, *17*, 371−382.

(2) Rutherford, S. T.; Bassler, B. L. Bacterial quorum sensing: its role in virulence and possibilities for its control. *Cold Spring Harbor Perspect. Med.* **2012**, *2*, No. a012427.

(3) Bassler, B. L.; Losick, R. Bacterially Speaking. *Cell* **2006**, *125*, 237−246.

(4) Papenfort, K.; Bassler, B. L. Quorum sensing signal-response systems in Gram-negative bacteria. *Nat. Rev. Microbiol.* **2016**, *14*, 576−588.

(5) Engebrecht, J.; Nealson, K.; Silverman, M. Bacterial bioluminescence: Isolation and genetic analysis of functions from *Vibrio fischeri*. *Cell* **1983**, *32*, 773−781.

(6) Barnard, A. M. L.; Bowden, S. D.; Burr, T.; Coulthurst, S. J.; Monson, R. E.; Salmond, G. P. C. Quorum sensing, virulence and secondary metabolite production in plant soft-rotting bacteria. *Philos. Trans. R. Soc., B* **2007**, *362*, 1165−1183.

(7) Miller, M. B.; Bassler, B. L. Quorum Sensing in Bacteria. *Annu. Rev. Microbiol.* **2001**, *55*, 165−199.

(8) de Kievit, T. R.; Iglewski, B. H. Bacterial quorum sensing in pathogenic relationships. *Infect. Immun.* **2000**, *68*, 4839−4849.

(9) Billings, N.; Ramirez Millan, M.; Caldara, M.; Rusconi, R.; Tarasova, Y.; Stocker, R.; Ribbeck, K. The Extracellular Matrix Component Psl Provides Fast-Acting Antibiotic Defense in *Pseudomonas aeruginosa* Biofilms. *PLoS Pathog.* **2013**, *9*, No. e1003526.

(10) Davies, D. Understanding biofilm resistance to antibacterial agents. *Nat. Rev. Drug Discovery* **2003**, *2*, 114−122.

(11) Case, R. J.; Labbate, M.; Kjelleberg, S. AHL-driven quorum-sensing circuits: their frequency and function among the Proteobacteria. *ISME J.* **2008**, *2*, 345−349.

(12) Patankar, A. V.; González, J. E. Orphan LuxR regulators of quorum sensing. *FEMS Microbiol. Rev.* **2009**, *33*, 739−756.

(13) Subramoni, S.; Venturi, V. LuxR-family "solos": bachelor sensors/regulators of signalling molecules. *Microbiology* **2009**, *155*, 1377−1385.

(14) Brachmann, A. O.; Brameyer, S.; Kresovic, D.; Hitkova, I.; Kopp, Y.; Manske, C.; Schubert, K.; Bode, H. B.; Heermann, R. Pyrones as bacterial signaling molecules. *Nat. Chem. Biol.* **2013**, *9*, 573−578.

(15) Brameyer, S.; Kresovic, D.; Bode, H. B.; Heermann, R. Dialkylresorcinols as bacterial signaling molecules. *Proc. Natl. Acad. Sci. U.S.A.* **2015**, *112*, 572−577.

(16) Heinrich, A. K.; Hirschmann, M.; Neubacher, N.; Bode, H. B. LuxS-dependent AI-2 production is not involved in global regulation of natural product biosynthesis in Photorhabdus and Xenorhabdus. *PeerJ* **2017**, *5*, No. e3471.

(17) Krin, E.; Chakroun, N.; Turlin, E.; Givaudan, A.; Gaboriau, F.; Bonne, I.; Rousselle, J.-C.; Frangeul, L.; Lacroix, C.; Hullo, M.-F.; Marisa, L.; Danchin, A.; Derzelle, S. Pleiotropic role of quorum-sensing autoinducer 2 in *Photorhabdus luminescens*. *Appl. Environ. Microbiol.* **2006**, *72*, 6439−6451.

(18) Whiteley, M.; Diggle, S. P.; Greenberg, E. P. Progress in and promise of bacterial quorum sensing research. *Nature* **2017**, *551*, 313−320.

(19) Ahmer, B. M. Cell-to-cell signalling in *Escherichia coli* and *Salmonella enterica*. *Mol. Microbiol.* **2004**, *52*, 933−945.

(20) Reen, F. J.; Mooij, M. J.; Holcombe, L. J.; McSweeney, C. M.; McGlacken, G. P.; Morrissey, J. P.; O'Gara, F. The Pseudomonas quinolone signal (PQS), and its precursor HHQ, modulate interspecies and interkingdom behaviour. *FEMS Microbiol. Ecol.* **2011**, *77*, 413−428.

(21) Reen, F. J.; Phelan, J. P.; Gallagher, L.; Woods, D. F.; Shanahan, R. M.; Cano, R.; Ó Muimhneacháin, E.; McGlacken, G. P.; O'Gara, F. Exploiting Interkingdom Interactions for Development of Small-Molecule Inhibitors of Candida albicans Biofilm Formation. *Antimicrob. Agents Chemother.* **2016**, *60*, 5894−5905.

(22) Reen, F. J.; Shanahan, R.; Cano, R.; O'Gara, F.; McGlacken, G. P. A structure activity-relationship study of the bacterial signal molecule HHQ reveals swarming motility inhibition in *Bacillus atrophaeus*. *Org. Biomol. Chem.* **2015**, *13*, 5537−5541.

(23) Shanahan, R.; Reen, F. J.; Cano, R.; O'Gara, F.; McGlacken, G. P. The requirements at the C-3 position of alkylquinolones for signalling in *Pseudomonas aeruginosa*. *Org. Biomol. Chem.* **2017**, *15*, 306−310.

(24) Ramos, A. F.; Woods, D. F.; Shanahan, R.; Cano, R.; McGlacken, G. P.; Serra, C.; O'Gara, F.; Reen, F. J. A structure-function analysis of interspecies antagonism by the 2-heptyl-4-alkyl-quinolone signal molecule from *Pseudomonas aeruginosa*. *Microbiology* **2020**, *166*, 169−179.

(25) Legendre, C.; Reen, F. J.; Mooij, M. J.; McGlacken, G. P.; Adams, C.; O'Gara, F. *Pseudomonas aeruginosa* Alkyl Quinolones Repress Hypoxia-Inducible Factor 1 (HIF-1) Signaling through HIF-1α Degradation. *Infect. Immun.* **2012**, *80*, 3985−3992.

(26) Reen, F. J.; Phelan, J. P.; Woods, D. F.; Shanahan, R.; Cano, R.; Clarke, S.; McGlacken, G. P.; O'Gara, F. Harnessing Bacterial Signals for Suppression of Biofilm Formation in the Nosocomial Fungal Pathogen *Aspergillus fumigatus*. *Front. Microbiol.* **2016**, *7*, No. 2074.

(27) Burke, S. A.; Wright, J. D.; Robinson, M. K.; Bronk, B. V.; Warren, R. L. Detection of molecular diversity in *Bacillus atrophaeus* by amplified fragment length polymorphism analysis. *Appl. Environ. Microbiol.* **2004**, *70*, 2786−2790.

(28) Jung, S.; Kim, Y. Synergistic Effect of Entomopathogenic Bacteria (Xenorhabdus sp. and *Photorhabdus temperata* ssp. temperata) on the Pathogenicity of *Bacillus thuringiensis* ssp. aizawai Against *Spodoptera exigua* (Lepidoptera: Noctuidae). *Environ. Entomol.* **2006**, *35*, 1584−1589.

(29) Benfarhat-Touzri, D.; Amira, A. B.; Khedher, S. B.; Givaudan, A.; Jaoua, S.; Tounsi, S. Combinatorial effect of *Bacillus thuringiensis* kurstaki and *Photorhabdus luminescens* against *Spodoptera littoralis* (Lepidoptera: Noctuidae). *J. Basic Microbiol.* **2014**, *54*, 1160−1165.

(30) Blackburn, M. B.; Martin, P. A. W.; Kuhar, D.; Farrar, R. R., Jr.; Gundersen-Rindal, D. E. The occurrence of photorhabdus-like toxin complexes in *Bacillus thuringiensis*. *PLoS One* **2011**, *6*, No. e18122.

(31) Donlan, R. M. Biofilms: microbial life on surfaces. *Emerg. Infect. Dis.* **2002**, *8*, 881−890.

(32) CDC. *Issues in Healthcare Settings: CDC's Seven Healthcare Safety Challenges*; United States Department of Health and Human Services: Atlanta, GA, 2001.

(33) Hamze, K.; Autret, S.; Hinc, K.; Laalami, S.; Julkowska, D.; Briandet, R.; Renault, M.; Absalon, C.; Holland, I. B.; Putzer, H.; Séror, S. J. Single-cell analysis in situ in a *Bacillus subtilis* swarming community identifies distinct spatially separated subpopulations differentially expressing hag (flagellin), including specialized swarmers. *Microbiology* **2011**, *157*, 2456−2469.

(34) Butler, M. T.; Wang, Q.; Harshey, R. M. Cell density and mobility protect swarming bacteria against antibiotics. *Proc. Natl. Acad. Sci. U.S.A.* **2010**, *107*, 3776−3781.

https://doi.org/10.1021/acsomega.1c05508
ACS Omega 2021, 6, 33141−33148

(35) García, C. F.; Kretschmer, M.; Lozano-Andrade, C. N.; Schönleitner, M.; Dragoŝ, A.; Kovács, Á. T.; Lieleg, O. Metal ions weaken the hydrophobicity and antibiotic resistance of *Bacillus subtilis* NCIB 3610 biofilms. *npj Biofilms Microbiomes* **2020**, *6*, No. 1.
(36) Kraus, G. A.; Basemann, K.; Guney, T. Selective pyrone functionalization: reductive alkylation of triacetic acid lactone. *Tetrahedron Lett.* **2015**, *56*, 3494−3496.
(37) Zhang, X.; McLaughlin, M.; Muñoz, R. L. P.; Hsung, R. P.; Wang, J.; Swidorski, J. Syntheses of 2-Pyrones via Electrophilic Substitutions at C7 of 4-Hydroxy-6-methyl-2-pyrone through Mono- or Dianion Formation. *Synthesis* **2007**, 749−753.
(38) Zhang, L.; Li, S.; Liu, X.; Wang, Z.; Jiang, M.; Wang, R.; Xie, L.; Liu, Q.; Xie, X.; Shang, D.; Li, M.; Wei, Z.; Wang, Y.; Fan, C.; Luo, Z.-Q.; Shen, X. Sensing of autoinducer-2 by functionally distinct receptors in prokaryotes. *Nat. Commun.* **2020**, *11*, No. 5371.
(39) Atkinson, S.; Williams, P. Quorum sensing and social networking in the microbial world. *J. R. Soc. Interface* **2009**, *6*, 959−978.
(40) Bindel Connelly, M.; Young, G. M.; Sloma, A. Extracellular Proteolytic Activity Plays a Central Role in Swarming Motility in *Bacillus subtilis*. *J. Bacteriol.* **2004**, *186*, 4159−4167.
(41) McGlacken, G. P.; Fairlamb, I. J. S. 2-Pyrone natural products and mimetics: isolation, characterisation and biological activity. *Nat. Prod. Rep.* **2005**, *22*, 369−385.
(42) Nolan, M.-T.; Bray, J. T. W.; Eccles, K.; Cheung, M. S.; Lin, Z.; Lawrence, S. E.; Whitwood, A. C.; Fairlamb, I. J. S.; McGlacken, G. P. Pd-catalysed intramolecular regioselective arylation of 2-pyrones, pyridones, coumarins and quinolones by C−H bond functionalization. *Tetrahedron* **2014**, *70*, 7120−7127.
(43) Clarke, S. L.; McGlacken, G. P. Access to trifluoromethylated 4-alkoxy-2-pyrones, pyridones and quinolones. *Tetrahedron* **2015**, *71*, 2906−2913.
(44) Prendergast, A. M.; McGlacken, G. P. Transition Metal Mediated C−H Activation of 2-Pyrones, 2-Pyridones, 2-Coumarins and 2-Quinolones. *Eur. J. Org. Chem.* **2018**, *2018*, 6068−6082.
(45) Kalamara, M.; Spacapan, M.; Mandic-Mulec, I.; Stanley-Wall, N. R. Social behaviours by *Bacillus subtilis*: quorum sensing, kin discrimination and beyond. *Mol. Microbiol.* **2018**, *110*, 863−878.
(46) Verdugo-Fuentes, A.; Gastélum, G.; Rocha, J.; de la Torre, M. dl.; Margolin, W. Multiple and Overlapping Functions of Quorum Sensing Proteins for Cell Specialization in Bacillus Species. *J. Bacteriol.* **2020**, *202*, No. e00721-19.
(47) Duanis-Assaf, D.; Steinberg, D.; Chai, Y.; Shemesh, M. The LuxS Based Quorum Sensing Governs Lactose Induced Biofilm Formation by *Bacillus subtilis*. *Front. Microbiol.* **2016**, *6*, No. 1517.
(48) Kim, K.; Kim, Y. U.; Koh, B. H.; Hwang, S. S.; Kim, S.-H.; Lépine, F.; Cho, Y.-H.; Lee, G. R. HHQ and PQS, two *Pseudomonas aeruginosa* quorum-sensing molecules, down-regulate the innate immune responses through the nuclear factor-kappaB pathway. *Immunology* **2010**, *129*, 578−588.
(49) García-Contreras, R.; Maeda, T.; Wood, T. K. Can resistance against quorum-sensing interference be selected? *ISME J.* **2016**, *10*, 4−10.
(50) Swidorski, J. J.; Wang, J.; Hsung, R. P. A Concise Total Synthesis of (−)-Cylindricine C through a Stereoselective Intramolecular Aza-[3 + 3] Annulation Strategy. *Org. Lett.* **2006**, *8*, 777−780.
(51) Demuner, A. J.; Valente, V. M. M.; Barbosa, L. C. A.; Rathi, A. H.; Donohoe, T. J.; Thompson, A. L. Synthesis and phytotoxic activity of new pyridones derived from 4-hydroxy-6-methylpyridin-2(1*H*)-one. *Molecules* **2009**, *14*, 4973−4986.

https://doi.org/10.1021/acsomega.1c05508
ACS Omega 2021, 6, 33141−33148

ChemPubSoc Europe

DOI: 10.1002/ejoc.201800923

EurJOC European Journal of Organic Chemistry

Full Paper

Check for updates



Direct Arylation

SPECIAL ISSUE

Synthesis of Benzofuroquinolines via Phosphine-Free Direct Arylation of 4-Phenoxyquinolines in Air

Rachel M. Shanahan,[a] Aobha Hickey,[a] F. Jerry Reen,[b] Fergal O'Gara,[c,d] and Gerard P. McGlacken*[a]

Abstract: A palladium-catalysed, phosphine-free, direct arylation of 4-phenoxyquinolines, in air is described. Using an intramolecular approach, the ring-closed products are formed in yields of up to 95 %. This approach allows access to a range of benzofuroquinolines. An array of functional groups on both the quinoline and phenoxy rings are tolerated.

Introduction

The quinoline nucleus occurs in many natural and synthetic pharmacologically active compounds,[1] and is ranked 22nd in the top 100 most frequently used ring systems present in FDA approved drugs.[2] Thus, the quinoline motif is considered a privileged biological scaffold, utilised by synthetic chemists to build molecular complexity, and ultimately improve biological activity. As a versatile heterocycle, it displays reactivity similar to that of other aromatic (pyridine/benzene) analogues, and thus can undergo a wide range of synthetic transformations.[3,4]

One of the most important transformations in organic synthesis remains the linking of two (hetero)aryl groups via a new carbon–carbon bond.[5] Traditionally, the most reliable class of C–C bond forming reactions involves the palladium-catalysed coupling of an aryl or vinyl halide with an organometallic reagent.[6–9] Examples include the Suzuki–Miyaura coupling,[10] Stille coupling,[11] and Negishi coupling.[12] An alternative is the use of direct arylation protocols, which are less reliant on the installation of a reactive functionality prior to cross-coupling.[13–15]

Direct arylation of simple arenes has been increasingly utilised in organic synthesis to access complex polycyclic ring systems.[16–20] By comparison, similar reactions involving heterocycles tend to require specialised catalyst/ligand systems and are therefore less prevalent in the literature.[21] One of the earliest relevant examples of an intramolecular direct arylation of a heteroarene was reported in 1984 by Ames and Opalko.[22] As a recent example, Ha et al. reported a palladium-catalysed synthesis of benzofuropyridines in moderate to excellent yields.[23]

Herein we report a palladium-catalysed direct arylation of 4-phenoxyquinolines as a route to benzofuro[3,2-*c*]quinolines (Figure 1). Access to these products will aid exploration of their untapped biological potential, given that similar quinoline-based compounds exhibit anticancer,[24] antimalarial[25] and antibacterial[26] effects.

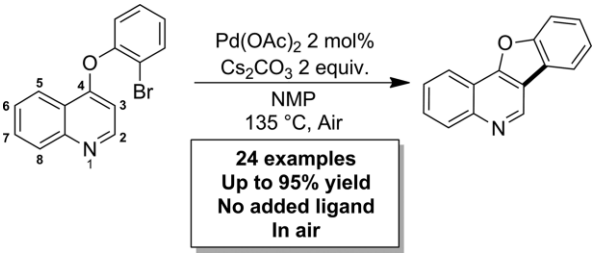


Figure 1. Intramolecular direct arylation of 4-phenoxyquinolines.

Previous syntheses of some of these substrates via direct arylation have relied upon positioning the activated carbon-halide on the C-3 position of the quinoline coupling partner[27,28] which limits the accessibility and versatility of products

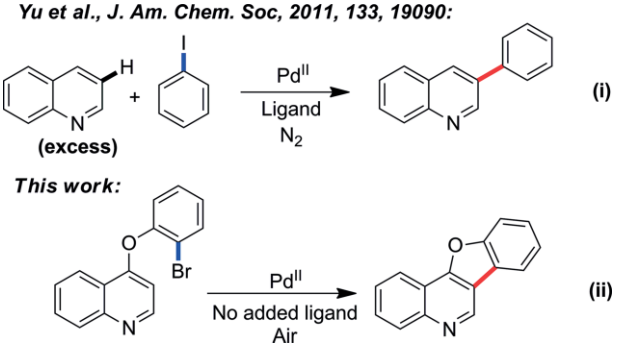


Figure 2. Palladium-catalysed direct arylation at the C-3 position of quinolines.

[a] *Analytical and Biological Research Facility (ABCRF) & School of Chemistry, University College Cork, Cork, Ireland*
E-mail: g.mcglacken@ucc.ie
http://research.ucc.ie/profiles/D004/gmcglacken
[b] *School of Microbiology, University College Cork, Cork, Ireland*
[c] *BIOMERIT Research Centre, School of Microbiology, University College Cork, Cork, Ireland*
[d] *School of Biomedical Sciences, Curtin Health Innovation Research Institute, Curtin University, Perth, WA 6102, Australia*

Supporting information and ORCID(s) from the author(s) for this article are available on the WWW under https://doi.org/10.1002/ejoc.201800923.

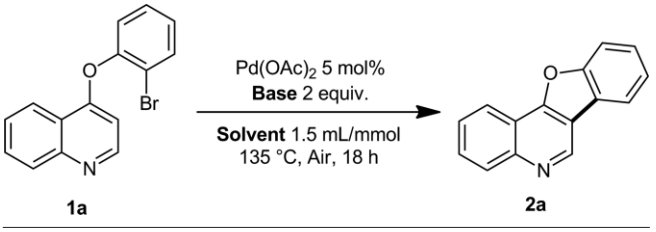
© 2018 Wiley-VCH Verlag GmbH & Co. KGaA, Weinheim

formed. The first example of non-directed direct arylation/C–H activation of the C-3 position of pyridines and quinolines was reported by Yu and co-workers (Figure 2(i)), using phenanthroline ligands under inert reaction conditions.[29] This method also relies upon the use of a large excess of the quinoline or pyridine substrate, which is only applicable to an intermolecular system. Herein we describe a system that requires no added ligand for arylation of the C-3 position of the quinoline ring, via intramolecular direct arylation, in air [Figure 2 (ii)].

Results and Discussion

Initially, 4-(2-bromophenoxy)quinoline **1a** was chosen as a model substrate, which was readily accessible from reaction of 4-chloroquinoline and 2-bromophenol. Our initial coupling conditions allowed formation of the fused product **2a** in 57 % isolated yield in air (Table 1 entry 1). Next, a variety of reaction parameters were assessed (Table 1). A solvent screen indicated that high-boiling point amide solvents were necessary for good conversion (entries 1–3). Other organic solvents gave little or no conversion to product (entries 4–8). Changing the base from Na_2CO_3 to K_2CO_3 or Cs_2CO_3 allowed the reaction to reach 100 % conversion (entry 9 and 10), while use of a stronger butoxide base resulted in partial decomposition of the starting material (entry 11). A further reduction in catalyst loading to 2 mol-% was also achieved (entry 12), at which point the desired product **2a** could be obtained in 95 % isolated yield under the optimised conditions.

Table 1. Optimisation of reaction conditions.



1a **2a**

Entry	Base	Solvent	Yield by NMR [%][a]	Isolated Yield [%]
1	Na_2CO_3	DMA	–	57
2	Na_2CO_3	DMF	67	–
3	Na_2CO_3	NMP	70	72
4	Na_2CO_3	DMSO	0	–
5[b]	Na_2CO_3	1,4-dioxane	0	–
6[b]	Na_2CO_3	EtOH	0	–
7[b]	Na_2CO_3	1,2-DCE	0	–
8[b]	Na_2CO_3	MeCN	0	–
9	K_2CO_3	NMP	72	–
10	Cs_2CO_3	NMP	83	–
11	NaO*t*Bu	NMP	39[c]	–
12[d]	Cs_2CO_3	NMP	99	95
13[e]	Cs_2CO_3	NMP	33	–

[a] Yields determined by ^{1}H NMR analysis of the crude reaction mixture using 1,3,5-trimethoxybenzene as internal standard. [b] Reaction carried out at the reflux temperature of solvent. [c] Decomposition of starting material observed. [d] 2 mol-% $Pd(OAc)_2$ used. [e] 1 mol-% $Pd(OAc)_2$ used.

With optimised conditions in hand, the substrate scope of the reaction was evaluated (Figure 3). Overall, it was observed that the reaction could tolerate a variety of functional groups on both the phenoxy and quinoline coupling partners. Substrates bearing weakly electron-withdrawing substituents (**2b–f**) on the phenoxy ring were well tolerated. Additionally, the chlorides in **2e** and **2f** were retained as a synthetic handle for further cross-coupling. The more strongly electron-withdrawing substituents on **2g** and **2h** led to cyclisation in excellent yields of 88 % and 90 %, respectively. Moderate yields were observed in the case of the nitro (**2i**) and ester (**2j**) analogues.

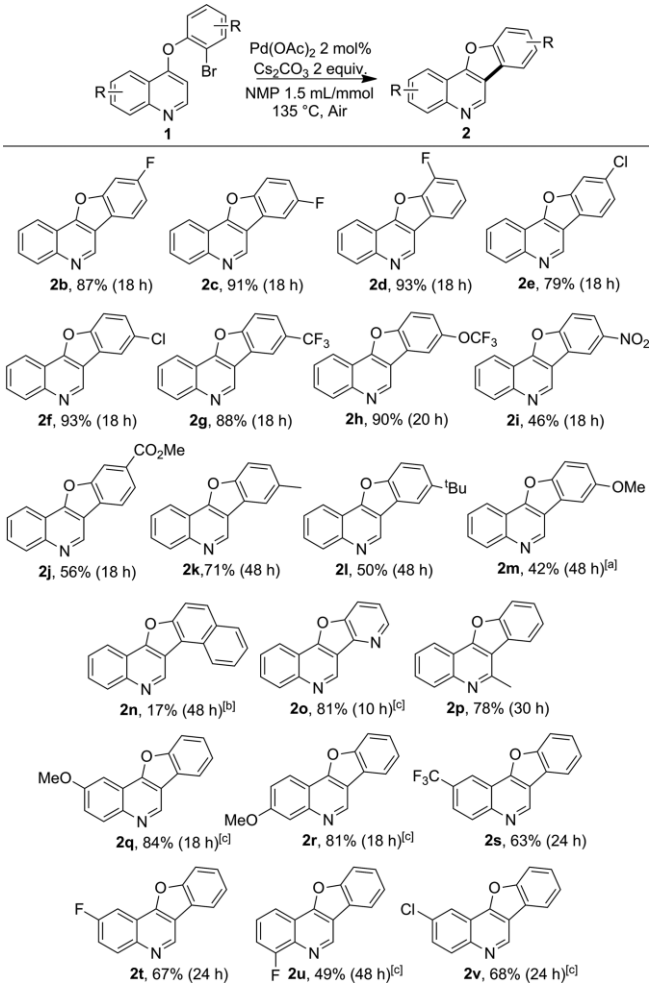


Figure 3. Substrate scope. All yields are isolated yields. [a] The yield of this product could be improved to 60 % when using the following conditions: 5 mol-% $Pd(OAc)_2$, 10 mol-% PCy_3·HBF_4, 2 equiv. Cs_2CO_3 under N_2 at 135 °C for 18 h. [b] The yield of this product could be improved to 66 % when using the same conditions described in [a]. [c] 5 mol-% $Pd(OAc)_2$ used.

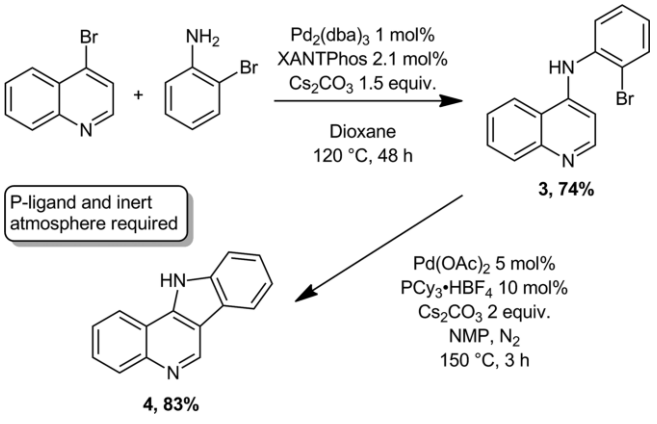
Longer reaction times were required in the case of electron-rich phenoxy substrates (**2k–m**). In the case of the naphthyl analogue **2n**, the desired product could only be obtained in 17 % isolated yield, with the majority of the remaining material attributed to unreacted starting material. This may be due to the steric bulk of the naphthyl group hindering access to the coupling site. Pleasingly, compound **2o** bearing a pyridine moiety instead of an aryl was obtained in an excellent yield of 81 %.

The scope of the reaction with respect to the quinoline was also examined. A methyl group at the C-2 position was well tolerated (**2p**). On the aryl backbone, both electron donating -OMe substituents (**2q** and **2r**) and electron withdrawing -CF_3,

© 2018 Wiley-VCH Verlag GmbH & Co. KGaA, Weinheim

-F and -Cl substituents (**2s–v**) also led to very good yields of product. The reaction conditions were also applicable to a 4-phenoxy pyridine substrate.[30] A few quinoline analogues (*p*-pyridinyl, aldehydic, and those with an S-linker) failed to cyclise under these conditions.[31]

Compounds containing fused indolquinoline rings are known to possess antimalarial,[32] antiproliferative and anticancer activity.[33] Thus, we hoped to access similar compounds by including this functionality in our substrate scope. A Hartwig–Buchwald coupling gave the precursor **3** in 74 % isolated yield (Scheme 1). However, when this compound was subjected to the previously optimised direct arylation conditions given above, no product was observed. Even when using the protected (*N*-Boc) substrate, coupling could not be achieved under these conditions.[34] We reasoned at this point that inhibitive N-ligation to palladium could be avoided by the addition of competitive phosphine ligands.[35] Indeed, when a new catalytic system of 5 mol-% $Pd(OAc)_2$ and 10 mol-% $PCy_3{\bullet}HBF_4$ was employed, the fused product could be obtained in 83 % isolated yield after 3 h. An inert atmosphere was required (Scheme 1).[36]



Scheme 1. Synthesis and direct arylation of 4-anilinoquinoline substrate.

The mechanism probably proceeds via an initial oxidative addition followed by a rate-determining C–H activation via a concerted metalation deprotonation (CMD).[29,37–40] A CMD mechanism is often characterised by the acidity of the key C–H bond. To probe this, a number of competition experiments were carried out using a basic quinoline substrate **1a** and those substituted with an electron-withdrawing (**1s**) and an electron-donating (**1q**) group (Figure 4 and SI). In all cases the experiment revealed that the electron-poor substrate outpaced the electron-rich substrate.

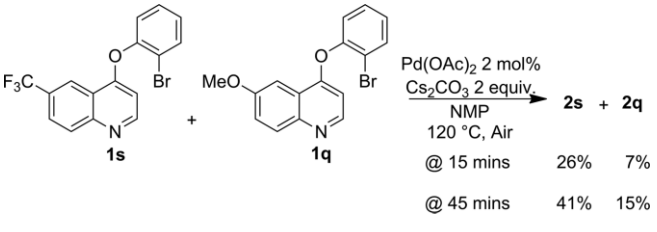


Figure 4. Competition experiment between **1s** and **1q**.

We then wished to apply the methodology to a more challenging quinoline of potential biological importance. Many species of bacteria use a sophisticated communication system termed "quorum sensing" (QS).[41] This coordinated behaviour allows for the construction of protective biofilms and the production of virulence factors, ultimately for the benefit of the entire colony. In contrast to antibiotic treatment, disrupting QS, termed "quorum quenching", is non-biocidal and thus as a strategy, is less likely to promote bacterial resistance by reducing the level of mutant dominance.[42] *Pseudomonas aeruginosa* uses quinolones such as 4-hydroxy-2-heptylquinoline (HHQ) and its 3-OH analogue Pseudomonas quinolone signal (PQS) to modulate quorum sensing (Figure 5). Thus analogues of these molecules could be used as competitive binders, disrupting numerous downstream processes.

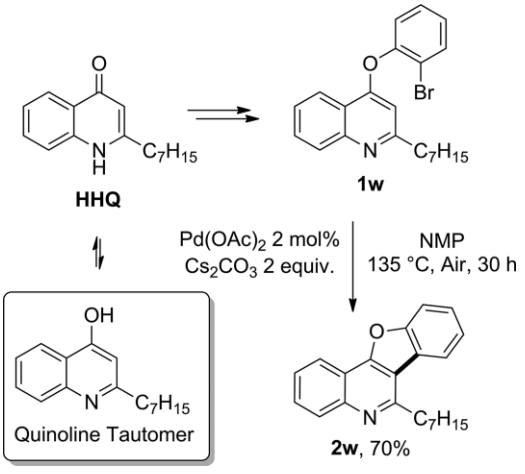


Figure 5. HHQ-like substrate blocked at C-3.

Following on from our continuing investigation of quinolone and quinoline analogues of HHQ and PQS,[43–49] using molecules which are "blocked" at the C-3 position, we chose to apply our intramolecular arylation methodology to a HHQ/PQS analogue (Figure 5). Substitution of C-3 is often crucial as it prevents hydroxylation of HHQ at this position by PqsH. Analogues with a hydroxyl group at C-3 can lead to unwanted agonistic behaviour.[50,51]

Thus HHQ was converted into the phenoxy precursor, which cyclised well, considering the steric encumbrance of the heptyl chain (the heptyl chain is critical for most biological activity). The impact of compound **2w** on quinolone signalling (more specifically PqsR signalling) was then investigated. HHQ (and PQS) are known to act as co-inducer signals of the PqsR LysR-type transcriptional regulator, leading to transcriptional activation of the *pqsA* promoter. Thus, the *pqsA* promoter itself acts as a proxy for activation of PqsR signalling. A *pqsA* fusion plasmid reporter (pLP0996) contains the *pqsA* promoter sequence upstream of the *lacZ* encoding gene and thus was ultimately used as indicator.[52] Wild-type *P. aeruginosa* produces endogenous HHQ, and thus any interference with activation of the plasmid encoded *pqsA*-promoter would likely infer antagonism of natural co-inducer binding. However, no such interference was observed and levels of *pqsA* transcriptional activation were comparable in carrier and cells treated with cyclised quinoline **2w** (Figure 6). Activation of the pLP0996 encoded *pqsA* promoter in a *pqsA* mutant lacking endogenous HHQ and PQS can only

© 2018 Wiley-VCH Verlag GmbH & Co. KGaA, Weinheim

occur upon addition of exogenous signal. In this case, while HHQ activated promoter activity, addition of quinoline **2w** had no effect beyond baseline. Thus quinoline **2w** displayed neither agonist nor antagonist behaviour with respect to PqsR signalling. This was further evident from the lack of inhibition of pyocyanin production in a wild-type strain and the lack of pyocyanin restoration in the *pqsA* mutant.

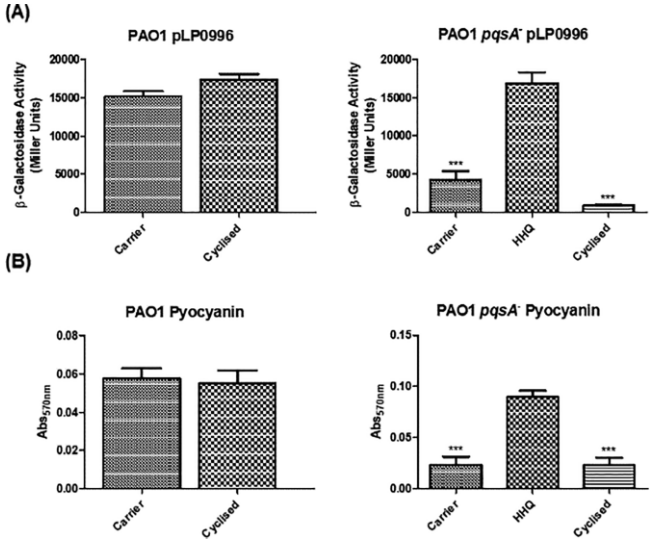


Figure 6. **(A)** Transcriptional activation of the *pqsA* promoter was unaffected in wild-type (PAO1 pMP0996) and mutant (PAO1 *pqsA*⁻ pLP0996) cells upon addition of **2w**. This suggests that the compound is neither an antagonist nor an agonist of PqsR signalling under conditions tested. **(B)** Pyocyanin production followed a similar pattern, i.e. unaffected in the presence of **2w** in either the wild-type or mutant cells. All data presented is the mean (+/– SEM) of three independent biological replicates. Statistical analysis was performed by Students t-test and one way ANOVA with Bonferroni post-hoc testing (*** $p < 0.001$).

The production of HHQ-like compounds which do not and cannot be hydroxylated in vivo at C-3[51] and thus do not exhibit any strong agonistic or antagonist behaviour, make for an excellent molecular framework for further modification and structure-activity studies. Further details of the biological activity will be published in due course.

Conclusions

In summary, the application of direct arylation methodology towards the synthesis of fused benzofuroquinoline products has been demonstrated. Placement of the halide on the phenoxy component of the coupling precursor allows for easy access to cyclised products. No added phosphine is required and the reactions can be carried out in air. Modification of the methodology allows for the inclusion of 4-anilinoquinoline substrates, without the requirement for *N*-protection. Finally, electron-poor quinolines appear to work best as evidenced by competition experiments. Application to a sterically hindered (C-2 = *n*-heptyl) HHQ mimic proceeds well.

Experimental Section

General Methods: Solvents and reagents were used as obtained from commercial sources and without purification. Melting points were measured in a Thomas Hoover Capillary Melting Point apparatus. Infrared spectra were measured on a Perkin–Elmer FT-IR spectrometer. Nuclear Magnetic Resonance (NMR) samples were run in deuterated chloroform ($CDCl_3$) or deuterated dimethylsulfoxide ($[D_6]$DMSO) as specified. ^{1}H NMR (600 MHz), ^{1}H NMR (500 MHz), ^{1}H NMR (400 MHz), and ^{1}H NMR (300 MHz) spectra were recorded on Bruker Avance 600, Bruker Avance 500, Bruker Avance 400 and Bruker Avance 300 NMR spectrometers, respectively, in proton coupled mode using tetramethysilane (TMS) as the internal standard. ^{13}C NMR (150 MHz), ^{13}C NMR (125 MHz), ^{13}C NMR (100 MHz), and ^{13}C NMR (75 MHz) spectra were recorded on Bruker Avance 600, Bruker Avance 500, Bruker Avance 400 and Bruker Avance 300 NMR spectrometers, respectively, in proton decoupled mode at 20 °C using tetramethysilane (TMS) as the internal standard. ^{19}F NMR (282 MHz) spectra were recorded on a Bruker Avance 300 NMR spectrometer in proton decoupled mode at 20 °C. All spectra were run at University College Cork. Chemical shifts (δ) are expressed as parts per million (ppm), positive shift being downfield from TMS; coupling constants (J) are expressed in Hertz [Hz]. Splitting patterns in ^{1}H NMR spectra are designated as: s (singlet), bs (broad singlet), d (doublet), dd (doublet of doublets), ddd (doublet of doublets of doublets), t (triplet), td (triplet of doublets), q (quartet), quin (quintet) and m (multiplet). High resolution precise mass spectra (HRMS) were recorded on a Waters LCT Premier Tof LC-MS instrument in electrospray ionisation (ESI) mode using 50 % acetonitrile/water containing 0.1 % formic acid as eluent; samples were made up in acetonitrile at a concentration of ca. 1 mg/mL. Column chromatography was carried out using 60 Å (35–70 μm) silica. TLC was carried out on pre-coated silica gel plates (Merck 60 PF254). The developed plates were visualized under UV light.

Palladium-catalysed intramolecular direct arylation reactions were carried out in sealed reaction tubes which were placed in a solid multi-reaction heating plate.

General Procedures for Synthesis of 4-(2-Bromophenoxy)quinoline Substrates 1a–1w

Method (a): Compounds 1a–1c, 1f, 1i, 1k, 1l, 1o–1w: A mixture of the 4-chloroquinoline substrate (1 equiv.), the substituted 2-bromophenol (5 equiv.) and sodium hydroxide (crushed pellets) (1.5 equiv.) was stirred at 120 °C until reaction was completed (2–6 h) as evident by thin layer chromatography (hexane/ethyl acetate, 8:2). The cooled reaction mixture was diluted with 10 % aq. NaOH (5 mL) and stirred at room temperature for 1 h. The aqueous phase was extracted with DCM (3 × 20 mL). The combined organic layers were washed with 6 M NaOH (3 × 10 mL), water (10 mL) and brine (10 mL), dried with $MgSO_4$, filtered and concentrated in vacuo. The crude mixture was purified by column chromatography over silica gel using hexane/ethyl acetate (8:2) as eluent.

Method (b): Compounds 1d, 1e, 1g, 1h, 1j, 1m, 1n: A mixture of 4-chloroquinoline (1 equiv.), the substituted 2-bromophenol (1.5 equiv.) and 4-dimethylaminopyridine (3 equiv.) in toluene (1.5 mL/mmol) was stirred at 130 °C until the reaction was completed as evident by thin layer chromatography (hexane/ethyl acetate, 8:2). The cooled reaction mixture was diluted with 10 % aq. NaOH (5 mL) and stirred at room temperature for 1 h. The aqueous phase was extracted with DCM (3 × 20 mL). The combined organic layers were washed with 3 M NaOH (3 × 10 mL), 1 M HCl (2 × 10 mL), water (10 mL) and brine (10 mL), dried with $MgSO_4$, filtered and concentrated in vacuo. The crude mixture was purified by column chromatography over silica gel using hexane/ethyl acetate (8:2) as eluent.

4-(2-Bromophenoxy)quinoline (1a): Method (a) – white solid (2.89 g, 78 %); m.p. 62–64 °C. IR (film): $\tilde{\nu}_{max}$ = 3434, 1596, 1305,

© 2018 Wiley-VCH Verlag GmbH & Co. KGaA, Weinheim

1223, 659 cm^{-1}. ^1H NMR (300 MHz, $CDCl_3$): δ = 6.41 (d, J = 5.1 Hz, 1 H), 7.18–7.27 (m, 2 H), 7.43 (ddd, J = 8.1, 7.3, 1.6 Hz, 1 H), 7.61 (ddd, J = 8.2, 6.9, 1.1 Hz, 1 H), 7.70–7.82 (m, 2 H), 8.12 (d, J = 8.2 Hz, 1 H), 8.42 (dd, J = 8.3, 0.9 Hz, 1 H), 8.68 (d, J = 5.1 Hz, 1 H) ppm. ^{13}C NMR (75 MHz, $CDCl_3$): δ = 103.7, 116.4, 121.1, 121.9, 123.2, 126.3, 127.3, 129.1, 129.2, 130.2, 134.3, 149.8, 151.0, 151.2, 160.7 ppm. HRMS (ESI-TOF) m/z: $[M + H]^+$ calcd. for $C_{15}H_{11}BrNO$: 300.0024, found 300.0016.

4-(2-Bromo-5-fluorophenoxy)quinoline (1b): Method (a) – pale yellow solid (0.891 g, 91 %); m.p. 77–78 °C. IR (film): $\tilde{\nu}_{max}$ = 3066, 1476, 1305, 1252, 1159, 601 cm^{-1}. ^1H NMR (300 MHz, $CDCl_3$): δ = 6.49 (d, J = 5.1 Hz, 1 H), 6.94–7.01 (m, 1 H), 6.99 (d, J = 8.1 Hz, 1 H), 7.57–7.74 (m, 2 H), 7.80 (ddd, J = 8.4, 6.9, 1.4 Hz, 1 H), 8.13 (d, J = 8.5 Hz, 1 H), 8.37 (dd, J = 8.4, 1.0 Hz, 1 H), 8.73 (d, J = 5.1 Hz, 1 H) ppm. ^{13}C NMR (75 MHz, $CDCl_3$): δ = 104.1, 110.7, 110.9 [d, ^2J(C,F) = 25 Hz], 114.5 [d, ^2J(C,F) = 22 Hz], 120.9, 121.7, 126.5, 129.2, 130.4, 134.7 [d, ^3J(C,F) = 9 Hz], 149.9, 151.0, 152.0 [d, ^3J(C,F) = 11 Hz], 160.1, 162.4 [d, ^1J(C,F) = 250 Hz] ppm. ^{19}F NMR (282 MHz, $CDCl_3$): δ = –111 ppm. HRMS (ESI-TOF) m/z: $[M + H]^+$ calcd. for $C_{15}H_{10}BrFNO$: 317.9930, found 317.9936.

4-(2-Bromo-4-fluorophenoxy)quinoline (1c): Method (a) – pale yellow solid (0.188 g, 38 %); m.p. 100–103 °C. IR (film): $\tilde{\nu}_{max}$ = 3065, 1480, 1305, 1248, 1183, 765 cm^{-1}. ^1H NMR (300 MHz, $CDCl_3$): δ = 6.39 (d, J = 5.1 Hz, 1 H), 7.10–7.29 (m, 2 H), 7.48 (dd, J = 7.7, 2.8 Hz, 1 H), 7.62 (ddd, J = 8.2, 5.5, 1.2 Hz, 1 H), 7.79 (ddd, J = 8.5, 6.9, 1.5 Hz, 1 H), 8.12 (d, J = 8.5 Hz, 1 H), 8.40 (dd, J = 8.3, 0.9 Hz, 1 H), 8.69 (d, J = 5.1 Hz, 1 H) ppm. ^{13}C NMR (75 MHz, $CDCl_3$): δ = 103.4, 116.1 [d, ^2J(C,F) = 23 Hz], 116.9 [d, ^3J(C,F) = 10 Hz], 120.9, 121.3 [d, ^2J(C,F) = 26 Hz], 121.8, 124.3 [d, ^3J(C,F) = 9 Hz], 126.4, 129.2, 130.3, 147.4, 149.8, 151.0, 159.9 [d, ^1J(C,F) = 250 Hz], 160.7 ppm. ^{19}F NMR (282 MHz, $CDCl_3$): δ = –114 ppm. HRMS (ESI-TOF) m/z: $[M + H]^+$ calcd. for $C_{15}H_{10}BrFNO$: 317.9930, found 317.9935.

4-(2-Bromo-6-fluorophenoxy)quinoline (1d): Method (b) – pale yellow solid (0.318 g, 72 %); m.p. 118–119 °C. IR (film): $\tilde{\nu}_{max}$ = 3064, 1502, 1471, 1305, 1271, 1042, 665 cm^{-1}. ^1H NMR (300 MHz, $CDCl_3$): δ = 6.39 (d, J = 5.1 Hz, 1 H), 7.15–7.30 (m, 2 H), 7.47–7.54 (m, 1 H), 7.63 (ddd, J = 8.1, 7.0, 1.1 Hz, 1 H), 7.79 (ddd, J = 8.4, 6.9, 1.5 Hz, 1 H), 8.13 (d, J = 8.5 Hz, 1 H), 8.46 (dd, J = 8.3, 1.1 Hz, 1 H), 8.69 (d, J = 5.0 Hz, 1 H) ppm. ^{13}C NMR (75 MHz, $CDCl_3$): δ = 102.5, 116.5 [d, ^2J(C,F) = 19 Hz], 118.3, 120.6, 121.9, 126.4, 127.7 [d, ^3J(C,F) = 8 Hz], 129.10, 129.16, 130.2, 139.3 [d, ^2J(C,F) = 14 Hz], 149.8, 150.9, 155.6 [d, ^1J(C,F) = 255 Hz], 159.8 ppm. ^{19}F NMR (282 MHz, $CDCl_3$): δ = –124 ppm. HRMS (ESI-TOF) m/z: $[M + H]^+$ calcd. for $C_{15}H_{10}BrFNO$: 317.9930, found 317.9921.

4-(2-Bromo-5-chlorophenoxy)quinoline (1e): Method (b) – white solid (0.290 g, 89 %); m.p. 79–81 °C. IR (film): $\tilde{\nu}_{max}$ = 3370, 1562, 1464, 1305, 1252, 765, 665 cm^{-1}. ^1H NMR (300 MHz, $CDCl_3$): δ = 6.48 (d, J = 5.1 Hz, 1 H), 7.16–7.29 (m, 2 H), 7.57–7.69 (m, 2 H), 7.79 (ddd, J = 8.5, 6.9, 1.5 Hz, 1 H), 8.13 (d, J = 8.6 Hz, 1 H), 8.36 (dd, J = 8.4, 0.9 Hz, 1 H), 8.72 (d, J = 5.1 Hz, 1 H) ppm. ^{13}C NMR (75 MHz, $CDCl_3$): δ = 104.1, 114.4, 120.9, 121.7, 123.3, 126.5, 127.4, 129.2, 130.4, 134.5, 134.8, 149.9, 151.0, 151.9, 160.1 ppm. HRMS (ESI-TOF) m/z: $[M + H]^+$ calcd. for $C_{15}H_{10}BrClNO$: 333.9634, found 333.9622.

4-(2-Bromo-4-chlorophenoxy)quinoline (1f): Method (a) – off-white solid (1.97 g, 96 %); m.p. 112–115 °C. IR (film): $\tilde{\nu}_{max}$ = 3403, 1596, 1465, 1392, 1257, 824, 765 cm^{-1}. ^1H NMR (300 MHz, $CDCl_3$): δ = 6.42 (d, J = 5.1 Hz, 1 H), 7.17 (d, J = 8.6 Hz, 1 H), 7.40 (dd, J = 8.7, 2.5 Hz, 1 H), 7.61 (ddd, J = 8.2, 6.9, 1.2 Hz, 1 H), 7.70–7.84 (m, 2 H), 8.12 (d, J = 8.5 Hz, 1 H), 8.38 (dd, J = 8.4, 0.9 Hz, 1 H), 8.70 (d, J = 5.1 Hz, 1 H) ppm. ^{13}C NMR (75 MHz, $CDCl_3$): δ = 103.7, 117.0, 120.9, 121.7, 123.8, 126.4, 129.2, 129.3, 130.3, 132.0, 133.9, 149.9, 150.0, 151.0, 160.4 ppm. HRMS (ESI-TOF) m/z: $[M + H]^+$ calcd. for $C_{15}H_{10}BrClNO$: 333.9634, found 333.9629.

4-[2-Bromo-4-(trifluoromethyl)phenoxy]quinoline (1g): Method (b) – sticky colourless oil (0.0731 g, 20 %). IR (film): $\tilde{\nu}_{max}$ = 1623, 1569, 1320, 1263, 1231, 1130, 588 cm^{-1}. ^1H NMR (300 MHz, $CDCl_3$): δ = 6.50 (d, J = 5.1 Hz, 1 H), 7.28 (d, J = 8.5 Hz, 1 H), 7.54–7.70 (m, 2 H), 7.79 (ddd, J = 8.4, 6.9, 1.4 Hz, 1 H), 8.00 (d, J = 1.7 Hz, 1 H), 8.14 (d, J = 8.5 Hz, 1 H), 8.34 (dd, J = 8.4, 0.9 Hz, 1 H), 8.73 (d, J = 4.9 Hz, 1 H) ppm. ^{13}C NMR (75 MHz, $CDCl_3$): δ = 104.7, 116.5, 121.0, 121.7, 122.6, 122.9 [q, ^1J(C,F) = 272 Hz], 126.4 [q, ^3J(C,F) = 4 Hz], 126.7, 129.2 [q, ^2J(C,F) = 34 Hz], 129.3, 130.5, 131.7 [q, ^3J(C,F) = 4 Hz], 150.0, 150.9, 154.4, 159.8 ppm. ^{19}F NMR (282 MHz, $CDCl_3$): δ = –62 ppm. HRMS (ESI-TOF) m/z: $[M + H]^+$ calcd. for $C_{16}H_{10}BrF_3NO$: 367.9898, found 367.9886.

4-[2-Bromo-4-(trifluoromethoxy)phenoxy]quinoline (1h): Method (b) – pale yellow solid (0.3015 g, 78 %); m.p. 50–52 °C. IR (film): $\tilde{\nu}_{max}$ = 1640, 1597, 1306, 1253, 1218, 1187, 567 cm^{-1}. ^1H NMR (300 MHz, $CDCl_3$): δ = 6.44 (d, J = 5.1 Hz, 1 H), 7.22–7.35 (m, 2 H), 7.55–7.69 (m, 2 H), 7.79 (ddd, J = 8.5, 6.9, 1.5 Hz, 1 H), 8.13 (d, J = 8.4 Hz, 1 H), 8.38 (dd, J = 8.4, 0.9 Hz, 1 H), 8.71 (d, J = 5.1 Hz, 1 H) ppm. ^{13}C NMR (75 MHz, $CDCl_3$): δ = 103.8, 116.9, 120.4 [q, ^1J(C,F) = 259 Hz], 120.9, 121.7, 121.8, 123.7, 126.5, 127.0, 129.2, 130.4, 146.6, 149.9, 150.0, 151.0, 160.3 ppm. ^{19}F NMR (282 MHz, $CDCl_3$): δ = –58 ppm. HRMS (ESI-TOF) m/z: $[M + H]^+$ calcd. for $C_{16}H_{10}BrF_3NO_2$: 383.9847, found 383.9843.

4-(2-Bromo-4-nitrophenoxy)quinoline (1i): Method (a) – pale yellow solid (0.192 g, 80 %); m.p. 151–152 °C. IR (film): $\tilde{\nu}_{max}$ = 3376, 1523, 1346, 1305, 1257, 665 cm^{-1}. ^1H NMR (300 MHz, $CDCl_3$): δ = 6.65 (d, J = 5.0 Hz, 1 H), 7.23 (d, J = 8.9 Hz, 1 H), 7.64 (ddd, J = 8.1, 7.1, 0.7 Hz, 1 H), 7.83 (ddd, J = 8.4, 7.0, 1.3 Hz, 1 H), 8.17 (d, J = 8.5 Hz, 1 H), 8.25 (d, J = 8.8 Hz, 1 H), 8.27 (dd, J = 8.9, 2.7 Hz, 1 H), 8.65 (d, J = 2.6 Hz, 1 H), 8.80 (d, J = 5.0 Hz, 1 H) ppm. ^{13}C NMR (75 MHz, $CDCl_3$): δ = 106.0, 115.9, 121.1, 121.2, 121.5, 124.6, 127.1, 129.5, 129.9, 130.7, 144.9, 150.2, 151.0, 157.2, 159.1 ppm. HRMS (ESI-TOF) m/z: $[M + H]^+$ calcd. for $C_{15}H_{10}BrN_2O_3$: 344.9875, found 344.9865.

Methyl 4-Bromo-3-(quinolin-4-yloxy)benzoate (1j): Method (b) – off white solid (0.258 g, 62 %); m.p. 87–89 °C. IR (film): $\tilde{\nu}_{max}$ = 3586, 2950, 1724, 1565, 1502, 1392, 1294, 1241, 765 cm^{-1}. ^1H NMR (300 MHz, $CDCl_3$): δ = 3.92 (s, 3 H), 6.43 (d, J = 5.1 Hz, 1 H), 7.63 (ddd, J = 8.2, 6.9, 1.1 Hz, 1 H), 7.76–7.90 (m, 4 H), 8.13 (d, J = 8.5 Hz, 1 H), 8.40 (dd, J = 8.3, 0.9 Hz, 1 H), 8.70 (d, J = 5.1 Hz, 1 H) ppm. ^{13}C NMR (75 MHz, $CDCl_3$): δ = 52.6, 103.9, 121.0, 121.7, 122.0, 123.9, 126.5, 128.0, 129.2, 130.4, 131.6, 134.5, 149.9, 151.0, 151.4, 160.3, 165.4 ppm. HRMS (ESI-TOF) m/z: $[M + H]^+$ calcd. for $C_{17}H_{13}BrNO_3$: 358.0079, found 358.0089.

4-(2-Bromo-4-methylphenoxy)quinoline (1k): Method (a) – orange solid (0.242 g, 84 %); m.p. 122–125 °C. IR (film): $\tilde{\nu}_{max}$ = 3064, 1568, 1485, 1392, 1255, 765 cm^{-1}. ^1H NMR (300 MHz, $CDCl_3$): δ = 2.41 (s, 3 H), 6.40 (d, J = 5.2 Hz, 1 H), 7.13 (d, J = 8.2 Hz, 1 H), 7.22 (dd, J = 8.2, 1.5 Hz, 1 H), 7.54 (d, J = 1.4 Hz, 1 H), 7.61 (ddd, J = 8.1, 6.9, 1.1 Hz, 1 H), 7.78 (ddd, J = 8.4, 6.9, 1.4 Hz, 1 H), 8.11 (d, J = 8.5 Hz, 1 H), 8.43 (dd, J = 8.3, 1.0 Hz, 1 H), 8.67 (d, J = 5.1 Hz, 1 H) ppm. ^{13}C NMR (75 MHz, $CDCl_3$): δ = 20.7, 103.5, 115.9, 121.1, 121.9, 122.9, 126.2, 129.1, 129.8, 130.1, 134.5, 137.5, 148.8, 149.8, 151.0, 161.0 ppm. HRMS (ESI-TOF) m/z: $[M + H]^+$ calcd. for $C_{16}H_{13}Br$ NO: 314.0181, found 314.0169.

4-[2-Bromo-4-(*tert*-butyl)phenoxy]quinoline (1l): Method (a) – pale yellow solid (0.073 g, 56 %); m.p. 68–70 °C. IR (film): $\tilde{\nu}_{max}$ = 2963, 1568, 1488, 1391, 1306, 1263, 766 cm^{-1}. ^1H NMR (300 MHz, $CDCl_3$): δ = 1.36 (s, 9 H), 6.43 (d, J = 5.1 Hz, 1 H), 7.16 (d, J = 8.5 Hz,

© 2018 Wiley-VCH Verlag GmbH & Co. KGaA, Weinheim

1 H), 7.41 (dd, *J* = 8.5, 2.2 Hz, 1 H), 7.60 (t, *J* = 7.6 Hz, 1 H), 7.65–7.83 (m, 2 H), 8.11 (d, *J* = 8.5 Hz, 1 H), 8.42 (d, *J* = 8.3 Hz, 1 H), 8.67 (d, *J* = 5.0 Hz, 1 H) ppm. ^{13}C NMR (75 MHz, $CDCl_3$): δ = 31.3, 34.7, 103.6, 115.8, 121.1, 121.9, 122.6, 126.2, 126.3, 129.0, 130.2, 131.2, 148.5, 149.7, 150.9, 151.1, 160.9 ppm. HRMS (ESI-TOF) *m/z*: $[M + H]^+$ calcd. for $C_{19}H_{19}BrNO$: 356.0650, found 356.0642.

4-(2-Bromo-4-methoxyphenoxy)quinoline (1m): Method (b) – beige solid (0.304 g, 56 %); m.p. 184–185 °C. IR (film): $\tilde{\nu}_{max}$ = 3062, 2835, 1595, 1487, 1392, 1212, 765 cm^{-1}. ^{1}H NMR (300 MHz, $CDCl_3$): δ = 3.86 (s, 3 H), 6.38 (d, *J* = 5.2 Hz, 1 H), 6.96 (dd, *J* = 8.9, 2.9 Hz, 1 H), 7.17 (d, *J* = 8.9 Hz, 1 H), 7.24 (d, *J* = 2.9 Hz, 1 H), 7.60 (ddd, *J* = 8.1, 6.9, 1.1 Hz, 1 H), 7.77 (ddd, *J* = 8.5, 6.9, 1.5 Hz, 1 H), 8.11 (d, *J* = 8.5 Hz, 1 H), 8.43 (dd, *J* = 8.3, 0.9 Hz, 1 H), 8.67 (d, *J* = 5.0 Hz, 1 H) ppm. ^{13}C NMR (75 MHz, $CDCl_3$): δ = 55.9, 103.3, 114.9, 116.7, 118.9, 121.0, 121.9, 123.7, 126.2, 129.0, 130.1, 144.5, 149.7, 151.0, 157.9, 161.3 ppm. HRMS (ESI-TOF) *m/z*: $[M + H]^+$ calcd. for $C_{16}H_{13}BrNO_2$: 330.0130, found 330.0125.

4-[(1-Bromonaphthalen-2-yl)oxy]quinoline (1n): Method (a) – off-white solid (0.318 g, 61 %); m.p. 197–200 °C. IR (film): $\tilde{\nu}_{max}$ = 3062, 1594, 1568, 1499, 1392, 1253, 764 cm^{-1}. ^{1}H NMR (300 MHz, $CDCl_3$): δ = 6.42 (d, *J* = 5.1 Hz, 1 H), 7.36 (d, *J* = 8.8 Hz, 1 H), 7.55–7.72 (m, 3 H), 7.80 (ddd, *J* = 8.5, 6.9, 1.5 Hz, 1 H), 7.92 (d, *J* = 8.1 Hz, 1 H), 7.93 (d, *J* = 8.8 Hz, 1 H), 8.14 (d, *J* = 8.5 Hz, 1 H), 8.33 (d, *J* = 8.5 Hz, 1 H), 8.51 (dd, *J* = 8.3, 1.0 Hz, 1 H), 8.56 (d, *J* = 5.1 Hz, 1 H) ppm. ^{13}C NMR (75 MHz, $CDCl_3$): δ = 103.9, 115.2, 121.1, 121.3, 122.0, 126.3, 126.6, 127.1, 128.2, 128.4, 129.1, 129.8, 130.3, 132.4, 133.2, 149.0, 149.8, 151.1, 160.8 ppm. HRMS (ESI-TOF) *m/z*: $[M + H]^+$ calcd. for $C_{19}H_{13}BrNO$: 350.0181, found 350.0178.

4-[(2-Bromopyridin-3-yl)oxy]quinoline (1o): Method (a) – pale pink solid (0.2378 g, 79 %); m.p. 170–173 °C. IR (film): $\tilde{\nu}_{max}$ = 1639, 1503, 1305, 1268, 666 cm^{-1}. ^{1}H NMR (300 MHz, $CDCl_3$): δ = 6.45 (d, *J* = 5.1 Hz, 1 H), 7.38 (dd, *J* = 8.0, 4.6 Hz, 1 H), 7.47–7.70 (m, 2 H), 7.79 (ddd, *J* = 8.4, 7.0, 1.4 Hz, 1 H), 8.13 (d, *J* = 8.5 Hz, 1 H), 8.28–8.47 (m, 2 H), 8.72 (d, *J* = 5.1 Hz, 1 H) ppm. ^{13}C NMR (75 MHz, $CDCl_3$): δ = 104.1, 121.0, 121.7, 124.0, 126.7, 129.2, 130.5, 130.5, 136.6, 147.0, 148.7, 149.9, 150.8, 159.9 ppm. HRMS (ESI-TOF) *m/z*: $[M + H]^+$ calcd. for $C_{14}H_{10}BrN_2O$: 300.9976, found 300.9986.

4-(2-Bromophenoxy)-2-methylquinoline (1p): Method (a) – pale pink solid (0.331 g, 93 %); m.p. 98–101 °C. IR (film): $\tilde{\nu}_{max}$ = 2923, 1599, 1470, 1342, 1235, 754 cm^{-1}. ^{1}H NMR (300 MHz, $CDCl_3$): δ = 2.60 (s, 3 H), 6.29 (s, 1 H), 7.15–7.29 (m, 2 H), 7.42 (ddd, *J* = 8.6, 7.3, 1.6 Hz, 1 H), 7.54 (ddd, *J* = 8.2, 6.9, 1.2 Hz, 1 H), 7.68–7.79 (m, 2 H), 8.02 (d, *J* = 8.4 Hz, 1 H), 8.35 (dd, *J* = 8.4, 1.0 Hz, 1 H) ppm. ^{13}C NMR (75 MHz, $CDCl_3$): δ = 25.8, 104.2, 116.3, 119.5, 121.7, 123.2, 125.4, 127.1, 128.3, 129.1, 130.2, 134.3, 149.4, 151.3, 159.9, 160.8 ppm. HRMS (ESI-TOF) *m/z*: $[M + H]^+$ calcd. for $C_{16}H_{13}BrNO$: 314.0181, found 314.0179.

4-(2-Bromophenoxy)-6-methoxyquinoline (1q): Method (a) – yellow sticky oil (0.599 g, 70 %). IR (film): $\tilde{\nu}_{max}$ = 3392, 1596, 1467, 1365, 1262, 1223, 778 cm^{-1}. ^{1}H NMR (300 MHz, $CDCl_3$): δ = 3.98 (s, 3 H), 6.40 (d, *J* = 5.1 Hz, 1 H), 7.16–7.29 (m, 2 H), 7.37–7.47 (m, 2 H), 7.64 (d, *J* = 2.8 Hz, 1 H), 7.73 (dd, *J* = 8.0, 1.5 Hz, 1 H), 8.01 (d, *J* = 9.2 Hz, 1 H), 8.54 (d, *J* = 5.1 Hz, 1 H) ppm. ^{13}C NMR (75 MHz, $CDCl_3$): δ = 55.7, 99.4, 104.2, 116.4, 121.8, 122.9, 123.2, 127.2, 129.2, 130.7, 134.3, 145.9, 148.4, 151.3, 157.8, 159.7 ppm. HRMS (ESI-TOF) *m/z*: $[M + H]^+$ calcd. for $C_{16}H_{13}BrNO_2$: 330.0130, found 330.0130.

4-(2-Bromophenoxy)-7-methoxyquinoline (1r): Method (a) – pale yellow solid (0.380 g, 74 %); m.p. 99–100 °C. IR (film): $\tilde{\nu}_{max}$ = 3388, 1622, 1428, 1315, 1227, 665 cm^{-1}. ^{1}H NMR (300 MHz, $CDCl_3$): δ = 3.98 (s, 3 H), 6.30 (d, *J* = 5.2 Hz, 1 H), 7.15–7.29 (m, 3 H), 7.36–7.47 (m, 2 H), 7.72 (dd, *J* = 7.9, 1.5 Hz, 1 H), 8.29 (d, *J* = 9.2 Hz, 1 H), 8.59 (d, *J* = 5.2 Hz, 1 H) ppm. ^{13}C NMR (75 MHz, $CDCl_3$): δ = 55.5, 102.4, 107.3, 115.8, 116.3, 119.2, 123.1, 123.2, 127.1, 129.1, 134.2, 151.2, 151.5, 151.8, 160.7, 161.3 ppm. HRMS (ESI-TOF) *m/z*: $[M + H]^+$ calcd. for $C_{16}H_{12}BrNO_2$: 330.0130, found 330.0128.

4-(2-Bromophenoxy)-6-(trifluoromethyl)quinoline (1s): Method (a) – off-white solid (0.254 g, 80 %); m.p. 67–69 °C. IR (film): $\tilde{\nu}_{max}$ = 3069, 1570, 1467, 1316, 1224, 1126, 739 cm^{-1}. ^{1}H NMR (300 MHz, $CDCl_3$): δ = 6.47 (d, *J* = 5.2 Hz, 1 H), 7.21–7.32 (m, 2 H), 7.46 (ddd, *J* = 8.1, 7.3, 1.6 Hz, 1 H), 7.75 (dd, *J* = 7.9, 1.3 Hz, 1 H), 7.95 (dd, *J* = 8.9, 2.1 Hz, 1 H), 8.22 (d, *J* = 8.9 Hz, 1 H), 8.76 (s, 1 H), 8.77 (d, *J* = 5.2 Hz, 1 H) ppm. ^{13}C NMR (125 MHz, $CDCl_3$): δ = 104.4, 116.4, 120.2, 120.3 [q, ^3J(C,F) = 5 Hz], 123.4, 124.1 [q, ^1J(C,F) = 272 Hz], 126.0 [q, ^3J(C,F) = 3 Hz], 127.8, 128.2 [q, ^2J(C,F) = 33 Hz], 129.4, 130.3, 134.5, 150.6, 150.7, 153.2, 161.3 ppm. ^{19}F NMR (282 MHz, $CDCl_3$): δ = –62 ppm. HRMS (ESI-TOF) *m/z*: $[M + H]^+$ calcd. for $C_{16}H_{10}BrF_3NO$: 367.9898, found 367.9894.

4-(2-Bromophenoxy)-6-fluoroquinoline (1t): Method (a) – pale yellow solid (0.344 g, 65 %); m.p. 75–79 °C. IR (film): $\tilde{\nu}_{max}$ = 3422, 1630, 1262, 1222, 1177, 657 cm^{-1}. ^{1}H NMR (300 MHz, $CDCl_3$): δ = 6.43 (d, *J* = 5.1 Hz, 1 H), 7.19–7.24 (m, 1 H), 7.25 (d, *J* = 8.7 Hz, 1 H), 7.44 (t, *J* = 7.4 Hz, 1 H), 7.54 (td, *J* = 8.7, 2.8 Hz, 1 H), 7.73 (d, *J* = 9.9 Hz, 1 H), 8.02 (dd, *J* = 9.3, 2.8 Hz, 1 H), 8.12 (dd, *J* = 9.2, 5.2 Hz, 1 H), 8.64 (d, *J* = 5.1 Hz, 1 H) ppm. ^{13}C NMR (75 MHz, $CDCl_3$): δ = 104.0, 105.7 [d, ^2J(C,F) = 24 Hz], 116.3, 120.4 [d, ^2J(C,F) = 26 Hz], 121.7 [d, ^3J(C,F) = 10 Hz], 123.3, 127.5, 129.3, 131.7 [d, ^3J(C,F) = 10 Hz], 134.4, 146.9, 150.3 [d, ^6J(C,F) = 3 Hz], 150.8, 160.3 [d, ^4J(C,F) = 5 Hz], 160.4 [d, ^1J(C,F) = 248 Hz] ppm. ^{19}F NMR (282 MHz, $CDCl_3$): δ = –113 ppm. HRMS (ESI-TOF) *m/z*: $[M + H]^+$ calcd. for $C_{15}H_{10}BrFNO$: 317.9930, found 317.9917.

4-(2-Bromophenoxy)-8-fluoroquinoline (1u): Method (a) – pale yellow crystalline solid (0.2519 g, 53 %); m.p. 87–90 °C. IR (film): $\tilde{\nu}_{max}$ = 1631, 1597, 1264, 1224, 949, 612 cm^{-1}. ^{1}H NMR (300 MHz, $CDCl_3$): δ = 6.45 (d, *J* = 5.1 Hz, 1 H), 7.12–7.29 (m, 2 H), 7.34–7.58 (m, 3 H), 7.70 (dd, *J* = 8.0, 1.4 Hz, 1 H), 8.19 (d, *J* = 8.0 Hz, 1 H), 8.71 (d, *J* = 5.1 Hz, 1 H) ppm. ^{13}C NMR (75 MHz, $CDCl_3$): δ = 104.4, 114.3 [d, ^4J(C,F) = 19 Hz], 116.2, 117.7 [d, ^4J(C,F) = 5 Hz], 122.7 [d, ^3J(C,F) = 3 Hz], 123.2, 126.0 [d, ^3J(C,F) = 8 Hz], 127.55, 129.3, 134.3, 140.0 [d, ^2J(C,F) = 13 Hz], 150.7, 151.2, 157.9 [d, ^1J(C,F) = 256 Hz], 160.6 [d, ^4J(C,F) = 4 Hz] ppm. ^{19}F NMR (282 MHz, $CDCl_3$): δ = –125 ppm. HRMS (ESI-TOF) *m/z*: $[M + H]^+$ calcd. for $C_{15}H_{10}BrFNO$: 317.9930, found 317.9918.

4-(2-Bromophenoxy)-6-chloroquinoline (1v): Method (a) – off-white solid (0.4525 g, 90 %); m.p. 89–90 °C. IR (film): $\tilde{\nu}_{max}$ = 1642, 1563, 1262, 1222, 666, 643 cm^{-1}. ^{1}H NMR (300 MHz, $CDCl_3$): δ = 6.41 (d, *J* = 5.2 Hz, 1 H), 7.17–7.30 (m, 2 H), 7.44 (ddd, *J* = 8.2, 7.3, 1.6 Hz, 1 H), 7.65–7.69 (m, 2 H), 8.04 (d, *J* = 9.0 Hz, 1 H), 8.40 (d, *J* = 2.3 Hz, 1 H), 8.66 (d, *J* = 5.2 Hz, 1 H) ppm. ^{13}C NMR (75 MHz, $CDCl_3$): δ = 104.2, 116.3, 121.0, 121.6, 123.2, 127.5, 129.3, 130.8, 131.1, 132.2, 134.3, 148.1, 150.7, 151.2, 160.0 ppm. HRMS (ESI-TOF) *m/z*: $[M + H]^+$ calcd. for $C_{15}H_{10}BrClNO$: 333.9634, found 333.9628.

4-(2-Bromophenoxy)-2-heptylquinoline (1w): Method (a) – off-white solid (0.205 g, 90 %); m.p. 75–77 °C. IR (film): $\tilde{\nu}_{max}$ = 2926, 2855, 1600, 1470, 1359, 1234, 763 cm^{-1}. ^{1}H NMR (300 MHz, $CDCl_3$): δ = 0.85 (t, *J* = 6.7 Hz, 3 H), 1.14–1.42 (m, 8 H), 1.68 (m, 2 H), 2.80 (t, *J* = 8.1 Hz, 2 H), 6.30 (s, 1 H), 7.17–7.25 (m, 2 H), 7.42 (ddd, *J* = 8.5, 7.2, 1.5 Hz, 1 H), 7.53 (ddd, *J* = 8.1, 7.0, 1.1 Hz, 1 H), 7.63–7.81 (m, 2 H), 8.05 (d, *J* = 8.4 Hz, 1 H), 8.34 (dd, *J* = 8.3, 0.9 Hz, 1 H) ppm. ^{13}C NMR (75 MHz, $CDCl_3$): δ = 14.1, 22.6, 29.2, 29.4, 30.0, 31.8, 39.7, 103.8, 116.3, 119.7, 121.7, 123.1, 125.4, 127.1, 128.5, 129.2, 130.1, 134.3, 149.5, 151.4, 160.7, 164.2 ppm. HRMS (ESI-TOF) *m/z*: $[M + H]^+$ calcd. for $C_{22}H_{25}BrNO$: 398.1120, found 398.1135.

© 2018 Wiley-VCH Verlag GmbH & Co. KGaA, Weinheim

General Procedure for Palladium-Catalysed Intramolecular Direct Arylation Reactions for the Preparation of Compounds 2a–2w: A mixture of the 4-(2-bromophenoxy)quinoline substrate **1** (1 equiv.), $Pd(OAc)_2$ (2–5 mol-%), and anhydrous caesium carbonate (2 equiv.) in anhydrous *N*-methylpyrrolidone (1.5 mL/mmol) was stirred at 135 °C in a sealed reaction tube until the reaction was completed as evident by ^1H NMR analysis. The cooled reaction mixture was diluted with DCM, filtered through a short plug of Celite and concentrated in vacuo. The crude mixture was purified by column chromatography over silica gel using DCM/EtOAc (99:1–95:5) as eluent.

Benzofuro[3,2-*c*]quinoline (2a):[27] White solid (0.068 g, 95 %); m.p. 132–135 °C (lit.[27] 135–138 °C). IR (film): $\tilde{\nu}_{max}$ = 3369, 1566, 1510, 1399, 1190 cm^{-1}. ^1H NMR (300 MHz, $CDCl_3$): δ = 7.44–7.58 (m, 2 H), 7.65–7.83 (m, 3 H), 8.12 (dd, *J* = 7.2, 0.9 Hz, 1 H), 8.28 (d, *J* = 8.4 Hz, 1 H), 8.44 (dd, *J* = 8.1, 1.0 Hz, 1 H), 9.51 (s, 1 H) ppm. ^{13}C NMR (75 MHz, $CDCl_3$): δ = 112.1, 116.3, 117.2, 120.6, 120.8, 122.7, 124.1, 127.0, 127.2, 129.3, 129.9, 144.4, 147.4, 156.0, 157.5 ppm. HRMS (ESI-TOF) *m/z*: $[M + H]^+$ calcd. for $C_{15}H_{10}NO$: 220.0762, found 220.0755.

9-Fluorobenzofuro[3,2-*c*]quinoline (2b):[53] White solid (0.064 g, 88 %); m.p. 149–150 °C (lit.[53] 148–150 °C). IR (film): $\tilde{\nu}_{max}$ = 3052, 1564, 1512, 1396, 1254, 1134 cm^{-1}. ^1H NMR (300 MHz, $CDCl_3$): δ = 7.22 (ddd, *J* = 8.9, 6.9, 2.2 Hz, 1 H), 7.45 (dd, *J* = 8.6, 2.2 Hz, 1 H), 7.63–7.85 (m, 2 H), 8.00 (dd, *J* = 8.6, 5.3 Hz, 1 H), 8.25 (d, *J* = 8.3 Hz, 1 H), 8.36 (dd, *J* = 8.1, 1.1 Hz, 1 H), 9.43 (s, 1 H) ppm. ^{13}C NMR (75 MHz, $CDCl_3$): δ = 100.3 [d, ^2J(C,F) = 27 Hz], 112.3 [d, ^2J(C,F) = 24 Hz], 115.8, 117.0, 118.9 [d, ^4J(C,F) = 2 Hz], 120.6, 121.2 [d, ^3J(C,F) = 10 Hz], 127.2, 129.4, 129.8, 143.9, 147.1, 156.1 [d, ^3J(C,F) = 14 Hz], 158.1 [d, ^5J(C,F) = 3 Hz], 162.2 [d, ^1J(C,F) = 247 Hz] ppm. ^{19}F NMR (282 MHz, $CDCl_3$): δ = –112 ppm. HRMS (ESI-TOF) *m/z*: $[M + H]^+$ calcd. for $C_{15}H_9FNO$: 238.0668, found 238.0668.

8-Fluorobenzofuro[3,2-*c*]quinoline (2c):[27] White solid (0.087 g, 91 %); m.p. 163–164 °C (lit.[27] 162–163 °C). IR (film): $\tilde{\nu}_{max}$ = 3368, 1565, 1479, 1319, 1247, 1146 cm^{-1}. ^1H NMR (300 MHz, $CDCl_3$): δ = 7.21–7.33 (m, 1 H), 7.65–7.87 (m, 4 H), 8.28 (d, *J* = 8.4 Hz, 1 H), 8.41 (dd, *J* = 8.1, 1.0 Hz, 1 H), 9.45 (s, 1 H) ppm. ^{13}C NMR (75 MHz, $CDCl_3$): δ = 106.7 [d, ^2J(C,F) = 26 Hz], 112.9 [d, ^3J(C,F) = 9 Hz], 114.7 [d, ^2J(C,F) = 26 Hz], 116.1 [d, ^4J(C,F) = 4 Hz], 117.0, 120.8, 123.6 [d, ^3J(C,F) = 11 Hz], 127.2, 129.6, 129.9, 144.2, 147.5, 151.9, 158.6, 159.7 [d, ^1J(C,F) = 241 Hz] ppm. ^{19}F NMR (282 MHz, $CDCl_3$): δ = –118 ppm. HRMS (ESI-TOF) *m/z*: $[M + H]^+$ calcd. for $C_{15}H_9FNO$: 238.0668, found 238.0659.

10-Fluorobenzofuro[3,2-*c*]quinoline (2d):[27] White solid (0.104 g, 93 %); m.p. 156–157 °C (lit.[27] 157–158 °C). IR (film): $\tilde{\nu}_{max}$ = 3368, 1564, 1496, 1347, 1200, 1189 cm^{-1}. ^1H NMR (300 MHz, $CDCl_3$): δ = 7.27–7.35 (m, 1 H), 7.42 (td, *J* = 8.0, 4.4 Hz, 1 H), 7.73 (ddd, *J* = 8.1, 7.0, 1.2 Hz, 1 H), 7.79–7.92 (m, 2 H), 8.29 (d, *J* = 8.2 Hz, 1 H), 8.49 (dd, *J* = 8.1, 0.9 Hz, 1 H), 9.50 (s, 1 H) ppm. ^{13}C NMR (75 MHz, $CDCl_3$): δ = 113.7 [d, ^2J(C,F) = 16 Hz], 116.0, 116.1 [d, ^4J(C,F) = 4 Hz], 117.0, 120.8, 124.8 [d, ^3J(C,F) = 6 Hz], 126.2 [d, ^3J(C,F) = 3 Hz], 127.3, 129.7, 129.8, 142.7 [d, ^2J(C,F) = 11 Hz], 144.3, 147.7, 148.3 [d, ^1J(C,F) = 251 Hz], 157.8 ppm. ^{19}F NMR (282 MHz, $CDCl_3$): δ = –135 ppm. HRMS (ESI-TOF) *m/z*: $[M + H]^+$ calcd. for $C_{15}H_9FNO$: 238.0668, found 238.0662.

9-Chlorobenzofuro[3,2-*c*]quinoline (2e): White solid (0.086 g, 79 %); m.p. 198–199 °C. IR (film): $\tilde{\nu}_{max}$ = 3047, 1562, 1508, 1338, 1049, 755 cm^{-1}. ^1H NMR (300 MHz, $CDCl_3$): δ = 7.47 (dd, *J* = 8.3, 1.8 Hz, 1 H), 7.66–7.87 (m, 3 H), 8.00 (d, *J* = 8.3 Hz, 1 H), 8.27 (d, *J* = 8.4 Hz, 1 H), 8.40 (d, *J* = 8.0 Hz, 1 H), 9.46 (s, 1 H) ppm. ^{13}C NMR (75 MHz, $CDCl_3$): δ = 112.8, 115.7, 117.0, 120.7, 121.1, 121.4, 124.8, 127.2, 129.6, 129.9, 132.9, 144.1, 147.5, 156.0, 157.8 ppm. HRMS (ESI-TOF) *m/z*: $[M + H]^+$ calcd. for $C_{15}H_9ClNO$: 254.0373, found 254.0363.

8-Chlorobenzofuro[3,2-*c*]quinoline (2f):[27] White solid (0.071 g, 93 %); m.p. 187–189 °C (lit.[27] 189–190 °C). IR (film): $\tilde{\nu}_{max}$ = 2917, 1564, 1511, 1395, 1194, 871 cm^{-1}. ^1H NMR (300 MHz, $CDCl_3$): δ = 7.51 (dd, *J* = 8.8, 2.2 Hz, 1 H), 7.69 (dd, *J* = 8.8, 0.4 Hz, 1 H), 7.72 (ddd, *J* = 8.1, 7.0, 1.2 Hz, 1 H), 7.82 (ddd, *J* = 8.5, 7.0, 1.5 Hz, 1 H), 8.08 (dd, *J* = 2.2, 0.4 Hz, 1 H), 8.28 (d, *J* = 8.2 Hz, 1 H), 8.41 (dd, *J* = 8.2, 0.9 Hz, 1 H), 9.46 (s, 1 H) ppm. ^{13}C NMR (100 MHz, $CDCl_3$): δ = 113.1, 115.5, 117.0, 120.5, 120.8, 124.1, 127.28, 127.34, 129.75, 129.78, 130.0, 144.2, 147.6, 154.2, 158.2 ppm. HRMS (ESI-TOF) *m/z*: $[M + H]^+$ calcd. for $C_{15}H_9ClNO$: 254.0373, found 254.0370.

8-(Trifluoromethyl)benzofuro[3,2-*c*]quinoline (2g): White crystalline solid (0.0533 g, 88 %); m.p. 170–173 °C. IR (film): $\tilde{\nu}_{max}$ = 1627, 1567, 1333, 1310, 1151, 1110 cm^{-1}. ^1H NMR (400 MHz, $CDCl_3$): δ = 7.65–7.91 (m, 4 H), 8.29 (d, *J* = 8.5 Hz, 1 H), 8.35–8.48 (m, 2 H), 9.52 (s, 1 H) ppm. ^{13}C NMR (75 MHz, $CDCl_3$): δ = 112.5, 115.4, 116.8, 118.3 [q, ^3J(C,F) = 4 Hz], 120.7, 123.0, 124.3 [q, ^3J(C,F) = 4 Hz], 124.3 [q, ^1J(C,F) = 272 Hz], 126.8 [q, ^2J(C,F) = 33 Hz], 127.4, 129.9, 130.0, 144.1, 147.8, 157.2, 158.4 ppm. ^{19}F NMR (282 MHz, $CDCl_3$): δ = –61 ppm. HRMS (ESI-TOF) *m/z*: $[M + H]^+$ calcd. for $C_{16}H_9F_3NO$: 288.0636, found 288.0629.

8-(Trifluoromethoxy)benzofuro[3,2-*c*]quinoline (2h): White crystalline solid (0.1367 g, 90 %); m.p. 124–126 °C. IR (film): $\tilde{\nu}_{max}$ = 1641, 1512, 1280, 1247, 1206, 1141, 1156 cm^{-1}. ^1H NMR (300 MHz, $CDCl_3$): δ = 7.41 (ddd, *J* = 8.9, 2.4, 0.8 Hz, 1 H), 7.64–7.88 (m, 3 H), 7.95 (d, *J* = 1.1 Hz, 1 H), 8.28 (d, *J* = 8.4 Hz, 1 H), 8.41 (dd, *J* = 8.1, 1.0 Hz, 1 H), 9.47 (s, 1 H) ppm. ^{13}C NMR (75 MHz, $CDCl_3$): δ = 113.0, 113.6, 115.9, 117.0, 120.6 [q, ^1J(C,F) = 257 Hz], 120.7, 120.8, 123.8, 127.4, 129.9, 130.0, 144.2, 145.8, 147.8, 153.9, 158.7 ppm. ^{19}F NMR (282 MHz, $CDCl_3$): δ = –58 ppm. HRMS (ESI-TOF) *m/z*: $[M + H]^+$ calcd. for $C_{16}H_9F_3NO_2$: 304.0585, found 304.0574.

8-Nitrobenzofuro[3,2-*c*]quinoline (2i): Orange solid (0.028 g, 46 %); m.p. > 250 °C. IR (film): $\tilde{\nu}_{max}$ = 3030, 1528, 1397, 1344, 1200 cm^{-1}. ^1H NMR (300 MHz, $CDCl_3$): δ = 7.77 (ddd, *J* = 8.1, 7.2, 1.0 Hz, 1 H), 7.84–7.91 (m, 2 H), 8.32 (d, *J* = 8.5 Hz, 1 H), 8.41–8.52 (m, 2 H), 9.02 (d, *J* = 2.3 Hz, 1 H), 9.56 (s, 1 H) ppm. ^{13}C NMR (100 MHz, $CDCl_3$): δ = 112.6, 115.4, 116.8, 117.1, 120.8, 123.0, 123.6, 127.8, 130.1, 130.5, 144.1, 144.9, 148.1, 158.6, 159.3 ppm. HRMS (ESI-TOF) *m/z*: $[M + H]^+$ calcd. for $C_{15}H_9N_2O_3$: 265.0613, found 265.0611.

Methyl Benzofuro[3,2-*c*]quinoline-9-carboxylate (2j): Beige solid (0.043 g, 56 %); m.p. 192–193 °C. IR (film): $\tilde{\nu}_{max}$ = 3402, 1717, 1565, 1434, 1397, 1281, 1234 cm^{-1}. ^1H NMR (300 MHz, $CDCl_3$): δ = 4.00 (s, 3 H), 7.70 (m, 1 H), 7.81 (ddd, *J* = 8.5, 7.0, 1.5 Hz, 1 H), 8.09 (d, *J* = 7.8 Hz, 1 H), 8.16 (dd, *J* = 8.2, 1.3 Hz, 1 H), 8.26 (d, *J* = 8.4 Hz, 1 H), 8.36–8.43 (m, 2 H), 9.46 (s, 1 H) ppm. ^{13}C NMR (75 MHz, $CDCl_3$): δ = 52.5, 113.6, 115.5, 116.9, 120.2, 121.0, 125.5, 126.8, 127.3, 129.0, 129.9, 130.0, 144.5, 147.8, 155.4, 159.0, 166.6 ppm. HRMS (ESI-TOF) *m/z*: $[M + H]^+$ calcd. for $C_{17}H_{12}NO_3$: 278.0817, found 278.0811.

8-Methylbenzofuro[3,2-*c*]quinoline (2k):[27] White solid (0.062 g, 71 %); m.p. 145–148 °C (lit.[27] 149–150 °C). IR (film): $\tilde{\nu}_{max}$ = 2917, 1564, 1510, 1321, 1192 cm^{-1}. ^1H NMR (300 MHz, $CDCl_3$): δ = 2.57 (s, 3 H), 7.35 (ddd, *J* = 8.5, 1.8, 0.5 Hz, 1 H), 7.61–7.73 (m, 2 H), 7.78 (ddd, *J* = 8.5, 6.9, 1.6 Hz, 1 H), 7.89–7.92 (m, 1 H), 8.26 (d, *J* = 8.5 Hz, 1 H), 8.41 (dd, *J* = 8.1, 0.9 Hz, 1 H), 9.47 (s, 1 H) ppm. ^{13}C NMR (75 MHz, $CDCl_3$): δ = 21.4, 111.5, 116.2, 117.2, 120.5, 120.8, 122.6, 126.8, 128.3, 129.1, 129.8, 133.7, 144.3, 147.3, 154.3, 157.6 ppm. HRMS (ESI-TOF) *m/z*: $[M + H]^+$ calcd. for $C_{16}H_{12}NO$: 234.0919, found 234.0921.

8-(*tert*-Butyl)benzofuro[3,2-*c*]quinoline (2l):[27] Pale yellow solid (0.025 g, 50 %); m.p. 97–100 °C (lit.[27] 99–100 °C). IR (film): $\tilde{\nu}_{max}$ =

© 2018 Wiley-VCH Verlag GmbH & Co. KGaA, Weinheim

2962, 1567, 1488, 1392, 1201 cm^{-1}. ^1H NMR (600 MHz, $CDCl_3$): δ = 1.47 (s, 9 H), 7.61 (dd, J = 8.7, 2.0 Hz, 1 H), 7.67–7.72 (m, 2 H), 7.79 (ddd, J = 8.4, 6.9, 1.5 Hz, 1 H), 8.10 (d, J = 1.7 Hz, 1 H), 8.27 (d, J = 8.4 Hz, 1 H), 8.42 (dd, J = 8.2, 1.0 Hz, 1 H), 9.52 (s, 1 H) ppm. ^{13}C NMR (150 MHz, $CDCl_3$): δ = 31.9, 35.0, 111.4, 116.7, 116.9, 117.3, 120.8, 122.3, 125.1, 126.9, 129.2, 129.8, 144.4, 147.3, 147.4, 154.2, 157.8 ppm. HRMS (ESI-TOF) *m/z*: $[M + H]^+$ calcd. for $C_{19}H_{18}NO$: 276.1388, found 276.1377.

8-Methoxybenzofuro[3,2-*c*]quinoline (2m):[28] Off-white solid (0.032 g, 42 %); m.p. 165–167 °C (lit.[28] 160–162 °C). IR (film): $\tilde{\nu}_{max}$ = 3350, 1570, 1486, 1330, 1186, 1164 cm^{-1}. ^1H NMR (300 MHz, $CDCl_3$): δ = 3.96 (s, 3 H), 7.13 (dd, J = 9.0, 2.6 Hz, 1 H), 7.54 (d, J = 2.6 Hz, 1 H), 7.59–7.85 (m, 3 H), 8.26 (d, J = 8.4 Hz, 1 H), 8.40 (dd, J = 8.1, 1.0 Hz, 1 H), 9.46 (s, 1 H) ppm. ^{13}C NMR (75 MHz, $CDCl_3$): δ = 56.1, 103.3, 112.6, 115.5, 116.6, 117.3, 120.8, 123.3, 127.0, 129.3, 129.8, 144.4, 147.3, 150.7, 156.9, 158.1 ppm. HRMS (ESI-TOF) *m/z*: $[M + H]^+$ calcd. for $C_{16}H_{12}NO_2$: 250.0868, found 250.0858.

Naphtho[1′,2′:4,5]furo[3,2-*c*]quinoline (2n): Off-white solid (0.014 g, 17 %); m.p. 203–205 °C. IR (film): $\tilde{\nu}_{max}$ = 2919, 1562, 1507, 1310, 1223 cm^{-1}. ^1H NMR (600 MHz, $CDCl_3$): δ = 7.64 (ddd, J = 8.0, 6.9, 1.1 Hz, 1 H), 7.75 (ddd, J = 8.0, 6.9, 1.1 Hz, 1 H), 7.79–7.85 (m, 2 H), 7.94 (d, J = 8.9 Hz, 1 H), 8.02 (d, J = 8.9 Hz, 1 H), 8.09 (d, J = 8.2 Hz, 1 H), 8.33 (d, J = 8.4 Hz, 1 H), 8.51 (dd, J = 8.4, 1.1 Hz, 1 H), 8.69 (d, J = 8.2 Hz, 1 H), 9.97 (s, 1 H) ppm. ^{13}C NMR (150 MHz, $CDCl_3$): δ = 112.7, 117.0, 117.3, 117.7, 120.7, 124.2, 125.3, 127.2, 127.7, 128.5, 128.8, 129.2, 129.4, 129.8, 131.0, 145.1, 146.4, 154.1, 157.0 ppm. HRMS (ESI-TOF) *m/z*: $[M + H]^+$ calcd. for $C_{19}H_{12}NO$: 270.0919, found 270.0916.

Pyrido[2′,3′:4,5]furo[3,2-*c*]quinoline (2o): Pale yellow solid (0.0896 g, 81 %); m.p. 174–175 °C. IR (film): $\tilde{\nu}_{max}$ = 1637, 1570, 1306, 1264 cm^{-1}. ^1H NMR (300 MHz, $CDCl_3$): δ = 7.42 (dd, J = 8.4, 4.8 Hz, 1 H), 7.60–7.86 (m, 2 H), 7.96 (dd, J = 8.4, 1.3 Hz, 1 H), 8.17–8.43 (m, 2 H), 8.71 (dd, J = 4.8, 1.2 Hz, 1 H), 9.66 (s, 1 H) ppm. ^{13}C NMR (75 MHz, $CDCl_3$): δ = 115.3, 116.9, 119.0, 120.6, 121.3, 127.3, 130.0, 130.2, 142.8, 144.4, 146.6, 148.2, 149.2, 159.1 ppm. HRMS (ESI-TOF) *m/z*: $[M + H]^+$ calcd. for $C_{14}H_9N_2O$: 221.0715, found 221.0710.

6-Methylbenzofuro[3,2-*c*]quinoline (2p):[27] Pale yellow solid (0.029 g, 78 %); m.p. 132–134 °C (lit.[27] 132–133 °C). IR (film): $\tilde{\nu}_{max}$ = 3380, 1563, 1509, 1364, 1084 cm^{-1}. ^1H NMR (300 MHz, $CDCl_3$): δ = 3.16 (s, 3 H), 7.41–7.69 (m, 3 H), 7.72–7.79 (m, 2 H), 8.10 (dd, J = 7.6, 2.1 Hz, 1 H), 8.18 (d, J = 8.4 Hz, 1 H), 8.38 (dd, J = 8.1, 2.1 Hz, 1 H) ppm. ^{13}C NMR (75 MHz, $CDCl_3$): δ = 24.3, 112.1, 115.5, 116.2, 120.7, 121.8, 123.5, 124.0, 126.1, 126.7, 128.9, 129.4, 146.9, 154.8, 155.9, 157.5 ppm. HRMS (ESI-TOF) *m/z*: $[M + H]^+$ calcd. for $C_{16}H_{12}NO$: 234.0919, found 234.0915.

2-Methoxybenzofuro[3,2-*c*]quinoline (2q):[27] Off-white solid (0.095 g, 84 %); m.p. 150–152 °C (lit.[27] 150–153 °C). IR (film): $\tilde{\nu}_{max}$ = 2954, 1350, 1514, 1468, 1228, 1191, 1031 cm^{-1}. ^1H NMR (300 MHz, $CDCl_3$): δ = 3.96 (s, 3 H), 7.28–7.53 (m, 4 H), 7.64 (d, J = 8.1 Hz, 1 H), 7.97 (dd, J = 7.4, 0.8 Hz, 1 H), 8.08 (d, J = 9.2 Hz, 1 H), 9.23 (s, 1 H) ppm. ^{13}C NMR (75 MHz, $CDCl_3$): δ = 55.6, 98.5, 111.9, 116.4, 117.7, 120.6, 121.7, 122.8, 123.9, 127.1, 131.3, 141.5, 143.3, 155.8, 156.7, 158.2 ppm. HRMS (ESI-TOF) *m/z*: $[M + H]^+$ calcd. for $C_{16}H_{12}NO_2$: 250.0868, found 250.0858.

3-Methoxybenzofuro[3,2-*c*]quinoline (2r): Off-white solid (0.091 g, 81 %); m.p. 146–147 °C. IR (film): $\tilde{\nu}_{max}$ = 3022, 1639, 1452, 1345, 1324, 1242, 1168 cm^{-1}. ^1H NMR (300 MHz, $CDCl_3$): δ = 3.97 (s, 3 H), 7.31 (dd, J = 9.0, 2.3 Hz, 1 H), 7.36–7.54 (m, 2 H), 7.58 (d, J = 2.3 Hz, 1 H), 7.68 (d, J = 8.0 Hz, 1 H), 7.99 (d, J = 7.1 Hz, 1 H), 8.25 (d, J = 9.0 Hz, 1 H), 9.37 (s, 1 H) ppm. ^{13}C NMR (75 MHz, $CDCl_3$): δ = 55.5, 108.4, 111.7, 112.0, 115.0, 119.7, 120.3, 121.9, 122.8, 123.9, 126.7, 144.6, 149.3, 155.8, 157.8, 160.7 ppm. HRMS (ESI-TOF) *m/z*: $[M + H]^+$ calcd. for $C_{16}H_{12}NO_2$: 250.0868, found 250.0865.

2-(Trifluoromethyl)benzofuro[3,2-*c*]quinoline (2s): Yellow solid (0.049 g, 63 %); m.p. 141–143 °C. IR (film): $\tilde{\nu}_{max}$ = 2917, 1567, 1443, 1348, 1167, 1111 cm^{-1}. ^1H NMR (300 MHz, $CDCl_3$): δ = 7.43–7.67 (m, 2 H), 7.80 (d, J = 8.2 Hz, 1 H), 7.96 (dd, J = 9.0, 2.0 Hz, 1 H), 8.13 (d, J = 8.4 Hz, 1 H), 8.38 (d, J = 8.9 Hz, 1 H), 8.75 (s, 1 H), 9.60 (s, 1 H) ppm. ^{13}C NMR (100 MHz, $CDCl_3$): δ = 112.3, 116.3, 117.3, 119.1 [q, ^3J(C,F) = 5 Hz], 120.8, 122.1, 124.3 [q, ^1J(C,F) = 270 Hz], 124.5, 124.9 [q, ^3J(C,F) = 3 Hz], 127.9, 128.8 [q, ^2J(C,F) = 33 Hz], 131.0, 146.4, 148.0, 156.1, 157.5 ppm. ^{19}F NMR (282 MHz, $CDCl_3$): δ = –62 ppm. HRMS (ESI-TOF) *m/z*: $[M + H]^+$ calcd. for $C_{16}H_9F_3NO$: 288.0636, found 288.0634.

2-Fluorobenzofuro[3,2-*c*]quinoline (2t):[53] White solid (0.025 g, 67 %); m.p. 146–148 °C (lit.[53] 148–149 °C). IR (film): $\tilde{\nu}_{max}$ = 3399, 1515, 1462, 1364, 1195, 1175 cm^{-1}. ^1H NMR (300 MHz, $CDCl_3$): δ = 7.45–7.61 (m, 3 H), 7.76 (d, J = 8.1 Hz, 1 H), 8.00 (dd, J = 8.6, 2.8 Hz, 1 H), 8.10 (dd, J = 7.6, 0.8 Hz, 1 H), 8.26 (dd, J = 9.3, 5.2 Hz, 1 H), 9.45 (s, 1 H) ppm. ^{13}C NMR (75 MHz, $CDCl_3$): δ = 104.7 [d, ^2J(C,F) = 24 Hz], 112.2, 116.8, 117.8 [d, ^3J(C,F) = 11 Hz], 119.3 [d, ^2J(C,F) = 26 Hz], 120.8, 122.5, 124.2, 127.6, 132.5 [d, ^3J(C,F) = 9 Hz], 143.6 [d, ^6J(C,F) = 3 Hz], 144.4, 156.1, 157.1 [d, ^4J(C,F) = 5 Hz], 160.8 [d, ^1J(C,F) = 249 Hz] ppm. ^{19}F NMR (282 MHz, $CDCl_3$): δ = –111 ppm. HRMS (ESI-TOF) *m/z*: $[M + H]^+$ calcd. for $C_{15}H_9FNO$: 238.0668, found 238.0659.

4-Fluorobenzofuro[3,2-*c*]quinoline (2u): White crystalline solid (0.0405 g, 49 %); m.p. 153–155 °C. IR (film): $\tilde{\nu}_{max}$ = 1640, 1596, 1300, 1249, 949 cm^{-1}. ^1H NMR (300 MHz, $CDCl_3$): δ = 7.40–7.68 (m, 4 H), 7.75 (d, J = 8.1 Hz, 1 H), 7.99–8.27 (m, 2 H), 9.53 (s, 1 H) ppm. ^{13}C NMR (100 MHz, $CDCl_3$): δ = 112.2, 113.7 [d, ^2J(C,F) = 19 Hz], 116.6 [d, ^2J(C,F) = 19 Hz], 117.3, 118.9 [d, ^3J(C,F) = 3 Hz], 120.9, 122.4, 124.3, 127.1 [d, ^3J(C,F) = 8 Hz], 127.7, 137.3 [d, ^2J(C,F) = 12 Hz], 144.6, 156.0, 157.0 [d, ^4J(C,F) = 5 Hz], 158.6 [d, ^1J(C,F) = 257 Hz] ppm. ^{19}F NMR (282 MHz, $CDCl_3$): δ = –122 ppm. HRMS (ESI-TOF) *m/z*: $[M + H]^+$ calcd. For $C_{15}H_9FNO$: 238.0668, found 238.0661.

2-Chlorobenzofuro[3,2-*c*]quinoline (2v):[53] White crystalline solid (0.0865 g, 68 %); m.p. 141–142 °C (lit.[53] 139–141 °C). ^1H NMR (300 MHz, $CDCl_3$): δ = 7.38–7.58 (m, 2 H), 7.59–7.76 (m, 2 H), 8.02 (dd, J = 7.6, 0.6 Hz, 1 H), 8.12 (d, J = 9.0 Hz, 1 H), 8.27 (d, J = 2.3 Hz, 1 H), 9.38 (s, 1 H) ppm. ^{13}C NMR (75 MHz, $CDCl_3$): δ = 112.2 116.9, 117.7, 119.8, 120.7, 122.3, 124.2, 127.6, 130.0, 131.4, 132.9, 144.4, 145.5, 156.0, 156.3 ppm. HRMS (ESI-TOF) *m/z*: $[M + H]^+$ calcd. for $C_{15}H_9ClNO$: 254.0373, found 254.0368.

6-Heptylbenzofuro[3,2-*c*]quinoline (2w): White solid (0.056 g, 70 %); m.p. 90–92 °C. IR (film): $\tilde{\nu}_{max}$ = 2917, 1559, 1445, 1363, 1202 cm^{-1}. ^1H NMR (300 MHz, $CDCl_3$): δ = 0.88 (t, J = 6.7 Hz, 3 H), 1.22–1.64 (m, 8 H), 1.95 (dt, J = 15.7, 7.7 Hz, 2 H), 3.40 (t, J = 8.0 Hz, 2 H), 7.40–7.67 (m, 3 H), 7.69–7.79 (m, 2 H), 8.00 (d, J = 7.3 Hz, 1 H), 8.19 (d, J = 8.4 Hz, 1 H), 8.35 (d, J = 8.1 Hz, 1 H) ppm. ^{13}C NMR (75 MHz, $CDCl_3$): δ = 14.1, 22.7, 28.6, 29.2, 29.9, 31.8, 38.0, 112.1, 114.8, 116.2, 120.7, 121.8, 123.1, 124.0, 126.0, 126.6, 129.1, 129.3, 146.9, 155.9, 157.7, 159.0 ppm. HRMS (ESI-TOF) *m/z*: $[M + H]^+$ calcd. for $C_{22}H_{24}NO$: 318.1858, found 318.1845.

Synthesis of *N*-(2-Bromophenyl)quinolin-4-amine (3): To a degassed solution of $Pd_2(dba)_3$ (2 mol-%) and XantPhos (4 mol-%) in anhydrous 1,4-dioxane (4 mL/mmol) were added caesium carbonate (1.4 equiv.), 4-bromoquinoline (1 equiv.) and 2-bromoaniline (1.1 equiv.) under a nitrogen atmosphere. The reaction mixture was stirred at 120 °C under nitrogen for 24 h. The cooled reaction mixture was diluted with DCM, filtered through Celite and concentrated in vacuo. The crude mixture was purified by column chromatogra-

© 2018 Wiley-VCH Verlag GmbH & Co. KGaA, Weinheim

phy over silica gel using DCM/EtOAc (3:1) as eluent to yield the product as a yellow solid (0.322 g, 74 %); m.p. 238–241 °C. IR (film): $\tilde{\nu}_{max}$ = 3360, 3061, 1572, 1526, 1335, 747 cm^{1} cm^{-1}. ^{1}H NMR (300 MHz, $CDCl_3$): δ = 6.88 (br. s, 1 H), 7.02 (td, J = 8.0, 1.5 Hz, 1 H), 7.08 (d, J = 5.2 Hz, 1 H), 7.31–7.38 (m, 1 H), 7.51–7.61 (m, 2 H), 7.65–7.78 (m, 2 H), 8.01 (d, J = 8.3 Hz, 1 H), 8.09 (d, J = 8.0 Hz, 1 H), 8.66 (d, J = 5.2 Hz, 1 H) ppm. ^{13}C NMR (75 MHz, $CDCl_3$): δ = 103.4, 116.9, 120.0, 120.3, 122.2, 125.0, 125.8, 128.4, 129.6, 130.1, 133.5, 138.3, 146.2, 149.2, 150.8 ppm. HRMS (ESI-TOF) m/z: $[M + H]^+$ calcd. for $C_{15}H_{12}BrN_2$: 299.0184, found 299.0187.

Synthesis of 11*H*-Indolo[3,2-*c*]quinoline (4):[54] *N*-(2-bromophenyl)quinolin-4-amine **3** (1 equiv.), $Pd(OAc)_2$ (5 mol-%), $PCy_3{\cdot}HBF_4$ (10 mol-%) and caesium carbonate (2 equiv.) were added to degassed *N*-methylpyrrolidone (1.5 mL/mmol) under Schlenk conditions under a nitrogen atmosphere. The reaction mixture was stirred at 150 °C (sand bath) for 3 h. The cooled reaction mixture was diluted with DCM and filtered through Celite. The mixture was washed with water (3 × 10 mL) and brine (15 mL), dried with $MgSO_4$, filtered and concentrated in vacuo. The crude mixture was purified by column chromatography over silica gel using DCM/EtOAc (7:3) as eluent to yield the product as an off-white solid (0.030 g, 83 %); m.p. > 250 °C (lit.[54] 340–341 °C). IR (film): $\tilde{\nu}_{max}$ = 3355, 2916, 2849, 1567, 1512, 1459, 1236 cm^{-1}. ^{1}H NMR (300 MHz, [D_6]DMSO): δ = 7.35 (t, J = 7.5 Hz, 1 H), 7.51 (t, J = 7.6 Hz, 1 H), 7.63–7.81 (m, 3 H), 8.15 (dd, J = 8.2, 1.3 Hz, 1 H), 8.33 (d, J = 7.8 Hz, 1 H), 8.53 (dd, J = 8.0, 1.4 Hz, 1 H), 9.60 (s, 1 H), 12.72 (s, 1 H) ppm. ^{13}C NMR (75 MHz, [D_6]DMSO): δ = 112.3, 114.8, 117.6, 120.6, 121.1, 122.4, 122.6, 126.0, 126.1, 128.5, 130.0, 139.3, 140.2, 145.3, 145.9 ppm. HRMS (ESI-TOF) m/z: $[M + H]^+$ calcd. for $C_{15}H_{11}N_2$: 219.0922, found 219.0911.

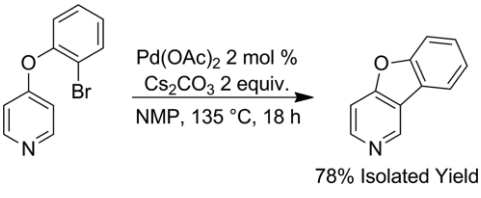
Supporting Information (see footnote on the first page of this article): Additional competition experiments, as well as ^{1}H, ^{13}C and ^{19}F NMR spectra of all new compounds, key intermediates and final products.

Acknowledgments

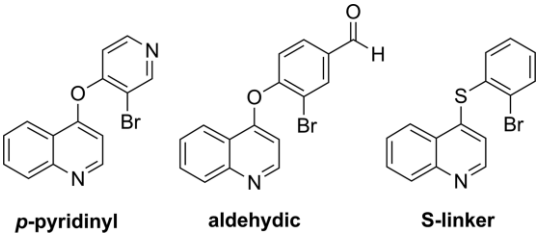
Our research is supported by Science Foundation Ireland (grant number SFI/12/IP/1315) and the Synthesis and Solid State Pharmaceutical Centre (SSPC) (SFI/12/RC/2275). The Authors thank the European Cooperation in Science and Technology COST initiative for funding CA15106, C-H Activation in Organic Synthesis (CHAOS). FJR, GMG, and FOG acknowledge support from Enterprise Ireland (CF-2017-0757-P).

Keywords: Quinoline · Direct arylation · CH activation · Ring closure

[1] J. P. Michael, *Nat. Prod. Rep.* **2008**, *25*, 166–187.
[2] R. D. Taylor, M. MacCoss, A. D. G. Lawson, *J. Med. Chem.* **2014**, *57*, 5845–5859.
[3] G. Jones The Chemistry of Heterocyclic Compounds - Quinolines, Vol. 104, Wiley, **2009**.
[4] M. J. Mphahlele, L. G. Lesenyeho, *J. Heterocycl. Chem.* **2013**, *50*, 1–16.
[5] Y. Nishihara *Applied cross-coupling reactions, Vol. 80*, Springer Science & Business Media, **2012**.
[6] J. Stille, *Angew. Chem. Int. Ed.* **1986**, *25*, 508–524; *Angew. Chem.* **1986**, *98*, 504–519.
[7] S. L. Buchwald, K. Fugami, T. Hiyama, M. Kosugi, M. Miura, N. Miyaura, A. Muci, M. Nomura, E. Shirakawa, K. Tamao *Cross-coupling reactions: a practical guide, Vol. 219*, Springer, **2003**.
[8] T.-Y. Luh, M.-k. Leung, K.-T. Wong, *Chem. Rev.* **2000**, *100*, 3187–3204.
[9] J. Hassan, M. Sévignon, C. Gozzi, E. Schulz, M. Lemaire, *Chem. Rev.* **2002**, *102*, 1359–1470.
[10] N. Miyaura, A. Suzuki, *Chem. Rev.* **1995**, *95*, 2457–2483.
[11] D. Milstein, J. Stille, *J. Am. Chem. Soc.* **1978**, *100*, 3636–3638.
[12] E.-I. Negishi, *Acc. Chem. Res.* **1982**, *15*, 340–348.
[13] D. Alberico, M. E. Scott, M. Lautens, *Chem. Rev.* **2007**, *107*, 174–238.
[14] G. P. McGlacken, L. M. Bateman, *Chem. Soc. Rev.* **2009**, *38*, 2447–2464.
[15] L. Ackermann, R. Vicente, A. R. Kapdi, *Angew. Chem. Int. Ed.* **2009**, *48*, 9792–9826; *Angew. Chem.* **2009**, *121*, 9976.
[16] L.-C. Campeau, M. Parisien, M. Leblanc, K. Fagnou, *J. Am. Chem. Soc.* **2004**, *126*, 9186–9187.
[17] K. Mackey, L. M. Pardo, A. M. Prendergast, M.-T. Nolan, L. M. Bateman, G. P. McGlacken, *Org. Lett.* **2016**, *18*, 2540–2543.
[18] M.-T. Nolan, L. M. Pardo, A. M. Prendergast, G. P. McGlacken, *J. Org. Chem.* **2015**, *80*, 10904–10913.
[19] M.-T. Nolan, J. T. W. Bray, K. Eccles, M. S. Cheung, Z. Lin, S. E. Lawrence, A. C. Whitwood, I. J. S. Fairlamb, G. P. McGlacken, *Tetrahedron* **2014**, *70*, 7120–7127.
[20] Y. Yang, J. Lan, J. You, *Chem. Rev.* **2017**, *117*, 8787–8863.
[21] R. Rossi, F. Bellina, M. Lessi, C. Manzini, *Adv. Synth. Catal.* **2014**, *356*, 17–117.
[22] D. Ames, A. Opalko, *Tetrahedron* **1984**, *40*, 1919–1925.
[23] W. S. Yoon, S. J. Lee, S. K. Kang, D.-C. Ha, J. Du Ha, *Tetrahedron Lett.* **2009**, *50*, 4492–4494.
[24] Y.-L. Chen, C.-H. Chung, I. L. Chen, P.-H. Chen, H.-Y. Jeng, *Bioorg. Med. Chem.* **2002**, *10*, 2705–2712.
[25] Z. Xiao, N. C. Waters, C. L. Woodard, Z. Li, P.-K. Li, *Bioorg. Med. Chem. Lett.* **2001**, *11*, 2875–2878.
[26] M. Zhao, T. Kamada, A. Takeuchi, H. Nishioka, T. Kuroda, Y. Takeuchi, *Bioorg. Med. Chem. Lett.* **2015**, *25*, 5551–5554.
[27] F. Hong, Y. Chen, B. Lu, J. Cheng, *Adv. Synth. Catal.* **2016**, *358*, 353–357.
[28] M. K. Mehra, M. P. Tantak, I. Kumar, D. Kumar, *Synlett* **2016**, *27*, 604–610.
[29] M. Ye, G.-L. Gao, A. J. F. Edmunds, P. A. Worthington, J. A. Morris, J.-Q. Yu, *J. Am. Chem. Soc.* **2011**, *133*, 19090–19093.
[30] The authors wish to thank the reviewers for the suggestion to try the following reaction:



[31] Substrates that failed to undergo clean coupling under the optimised conditions:



[32] L. R. Whittell, K. T. Batty, R. P. Wong, E. M. Bolitho, S. A. Fox, T. M. Davis, P. E. Murray, *Bioorg. Med. Chem.* **2011**, *19*, 7519–7525.
[33] N. Wang, M. Świtalska, M.-Y. Wu, K. Imai, T. A. Ngoc, C.-Q. Pang, L. Wang, J. Wietrzyk, T. Inokuchi, *Eur. J. Med. Chem.* **2014**, *78*, 314–323.
[34] When the Boc-protected substrate was subjected to the optimized conditions, deprotected starting material (**3**) was recovered exclusively.
[35] J. P. Heiskanen, A. E. Tolkki, H. J. Lemmetyinen, O. E. O. Hormi, *J. Mater. Chem.* **2011**, *21*, 14766–14775.
[36] Under aerobic conditions the reaction proceeded sluggishly. Decomposition of starting material was evident by analysis of the ^{1}H NMR spectra of the reaction mixture.
[37] A. M. Prendergast, G. P. McGlacken, *Eur. J. Org. Chem.* **2018**, *2018*.
[38] M. Lafrance, K. Fagnou, *J. Am. Chem. Soc.* **2006**, *128*, 16496–16497.

© 2018 Wiley-VCH Verlag GmbH & Co. KGaA, Weinheim

[39] D. García-Cuadrado, A. A. Braga, F. Maseras, A. M. Echavarren, *J. Am. Chem. Soc.* **2006**, *128*, 1066–1067.
[40] D. García-Cuadrado, P. de Mendoza, A. A. Braga, F. Maseras, A. M. Echavarren, *J. Am. Chem. Soc.* **2007**, *129*, 6880–6886.
[41] M. Whiteley, S. P. Diggle, E. P. Greenberg, *Nature* **2017**, *551*, 313.
[42] F. J. Reen, G. P. McGlacken, F. O'Gara, *FEMS Microbiol. Lett.* **2018**, *365*, fny076.
[43] G. P. McGlacken, C. M. McSweeney, T. O'Brien, S. E. Lawrence, C. J. Elcoate, F. J. Reen, F. O'Gara, *Tetrahedron Lett.* **2010**, *51*, 5919–5921.
[44] F. J. Reen, S. L. Clarke, C. Legendre, C. M. McSweeney, K. S. Eccles, S. E. Lawrence, F. O'Gara, G. P. McGlacken, *Org. Biomol. Chem.* **2012**, *10*, 8903–8910.
[45] F. J. Reen, M. J. Mooij, L. J. Holcombe, C. M. McSweeney, G. P. McGlacken, J. P. Morrissey, F. O'Gara, *FEMS Microbiol. Ecol.* **2011**, *77*, 413–428.
[46] F. J. Reen, J. P. Phelan, L. Gallagher, D. F. Woods, R. M. Shanahan, R. Cano, E. Ó. Muimhneacháin, G. P. McGlacken, F. O'Gara, *Antimicrob. Agents Chemother.* **2016**, *60*, 5894–5905.
[47] F. J. Reen, J. P. Phelan, D. F. Woods, R. Shanahan, R. Cano, S. Clarke, G. P. McGlacken, F. O'Gara, *Front. Microbiol.* **2016**, *7*, 2074.
[48] F. J. Reen, R. Shanahan, R. Cano, F. O'Gara, G. P. McGlacken, *Org. Biomol. Chem.* **2015**, *13*, 5537–5541.
[49] R. Shanahan, F. J. Reen, R. Cano, F. O'Gara, G. P. McGlacken, *Org. Biomol. Chem.* **2017**, *15*, 306–310.
[50] C. Lu, B. Kirsch, C. Zimmer, J. C. de Jong, C. Henn, C. K. Maurer, M. Müsken, S. Häussler, A. Steinbach, R. W. Hartmann, *Chem. Biol.* **2012**, *19*, 381–390.
[51] C. Lu, C. K. Maurer, B. Kirsch, A. Steinbach, R. W. Hartmann, *Angew. Chem. Int. Ed.* **2014**, *53*, 1109–1112; *Angew. Chem.* **2014**, *126*, 1127.
[52] S. McGrath, D. S. Wade, E. C. Pesci, *FEMS Microbiol. Lett.* **2004**, *230*, 27–34.
[53] F. Ji, X. Li, W. Wu, H. Jiang, *J. Org. Chem.* **2014**, *79*, 11246–11253.
[54] A. V. Aksenov, D. A. Aksenov, N. A. Orazova, N. A. Aksenov, G. D. Griaznov, A. De Carvalho, R. Kiss, V. Mathieu, A. Kornienko, M. Rubin, *J. Org. Chem.* **2017**, *82*, 3011–3018

Received: June 13, 2018

 © 2018 Wiley-VCH Verlag GmbH & Co. KGaA, Weinheim

JOC The Journal of Organic Chemistry

pubs.acs.org/joc Article

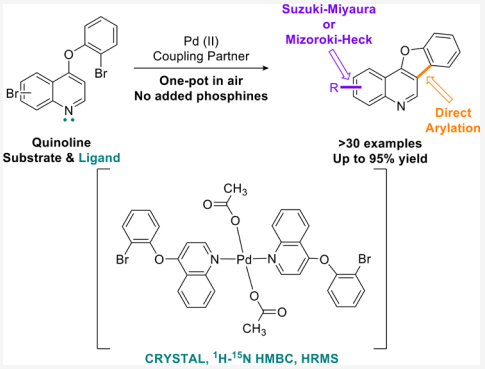
One-Pot Cross-Coupling/C−H Functionalization Reactions: Quinoline as a Substrate and Ligand through N−Pd Interaction

Rachel M. Shanahan,[⊥] Aobha Hickey,[⊥] Lorraine M. Bateman, Mark E. Light, and Gerard P. McGlacken*

Cite This: J. Org. Chem. 2020, 85, 2585−2596 Read Online

ACCESS | Metrics & More | Article Recommendations | Supporting Information

ABSTRACT: Herein, we report a one-pot process that marries mechanistically distinct, traditional cross-coupling reactions with C−H functionalization using the same precatalyst. The reactions proceed in yields of up to 95%, in air, and require no extraneous ligand. The reactions are thought to be facilitated by harnessing the substrate quinoline as an *N*-ligand, and evidence of the palladium−quinoline interaction is provided by ^{1}H-^{15}N HMBC NMR spectroscopy and X-ray crystallographic structures. Application of the methodology is demonstrated by the quick formation of fluorescent, π-extended frameworks.



Downloaded via UNIV COLG CORK on March 25, 2021 at 10:42:49 (UTC).
See https://pubs.acs.org/sharingguidelines for options on how to legitimately share published articles.

INTRODUCTION

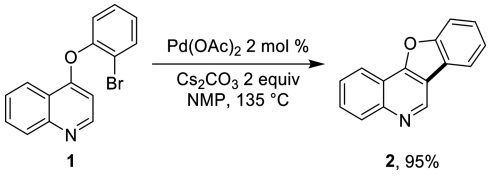
The formation of multiple carbon−carbon bonds in a telescoped, one-pot procedure is an efficient and environmentally friendly approach to the construction of new chemical entities.[1] However, carrying out two or more chemical reactions in a single vessel places significant demands on the methodologies involved, specifically in terms of reagent, catalyst, and substrate compatibility.[2] Additionally, avoiding secondary manipulation during a reaction is highly preferable if the procedures are to be applied industrially.

Pyridine, quinoline, and furan moieties are prominent in synthetic and naturally occurring pharmacologically active compounds.[3] In drugs, they represent the 2nd, 22nd, and 25th most common ring systems, respectively.[4] We recently reported a palladium-catalyzed intramolecular direct arylation (DA) protocol that gives a variety of benzofuro[3,2-*c*]quinolines **2** from 4-(2-bromophenoxy)quinolines **1** in excellent yields (Scheme 1).[5]

Chemoselectivity and regioselectivity proved to be very predictable in these mono-halogenated systems. Conversely, cross-coupling reactions involving substrates bearing more than one halogen are far less predictable.[2,6] The selective functionalization of substrates with two different halogens usually relies upon the marked difference in the rates of oxidative addition (OA) at the C−X bonds. Using halogens of the same type is considerably more difficult as significant rate differences in the oxidation step (I vs Br or Br vs Cl) are not easily harnessed.[7] A limited number of one-pot reactions combining C−H functionalization with a Suzuki−Miyaura reaction have been reported.[8] However, we are aware of very few protocols that do not require perturbation of the reaction setup by the addition of secondary reactants, reagents, or catalysts subsequent to reaction initiation.[9] In all cases, added phosphine ligand is required. The use of phosphine ligands adds significantly to the cost of any catalytic process; in fact, they are often the most expensive component of a catalytic system.[10]

This report describes a selection of one-pot tandem Suzuki−Miyaura/direct arylation (SM/DA) and Mizoroki−Heck/direct arylation (MH/DA) reactions with di- and tribromoquinolines. Once the reaction is initiated, no further manipulation is required, and no subsequent addition of solvents, reagents, reactants, or catalysts is needed. Overall, the reaction proceeds using 2 mol % $Pd(OAc)_2$, in air, and without recourse to extraneous ligands. Through further development to a one-pot Mizoroki−Heck/direct arylation protocol, π-extended quinolines, with structural features of interest to

Scheme 1. Intramolecular Direct Arylation of 1



Received: December 10, 2019
Published: January 23, 2020

ACS Publications © 2020 American Chemical Society

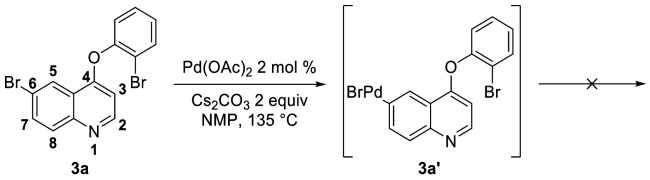
https://dx.doi.org/10.1021/acs.joc.9b03321
J. Org. Chem. 2020, 85, 2585−2596

medicinal[11] and materials[12] chemists, were prepared. These entities are challenging to synthesize by traditional, stepwise cross-coupling techniques.[13] We provide structural characterization of initially formed palladium−quinoline (Pd−Q) complexes using cystallography, mass spectrometry, and heteronuclear multiple bond correlation (HMBC) NMR spectroscopy.

RESULTS AND DISCUSSION

Our initial aim was to test the chemoselectivity of **3a** and perhaps exploit entropic factors to carry out the intramolecular DA reaction while leaving the bromide on the quinoline backbone untouched. Using the reaction conditions that had so efficiently furnished **2** from **1**, no DA was observed (Scheme 2). We doubted that the bromine on the quinoline ring would affect the electronics of the C-3 position to such an extent that C−H functionalization would be prevented. Thus, we rationalized that OA at the quinoline-Br was favored over the phenoxy-Br. In the absence of a suitable coupling partner, the OA product **3a′** was a catalytic dead end, with the palladium trapped at a nonproductive site.

Scheme 2. Failed Intramolecular DA of Dibromoquinoline 3a



3a **3a'**

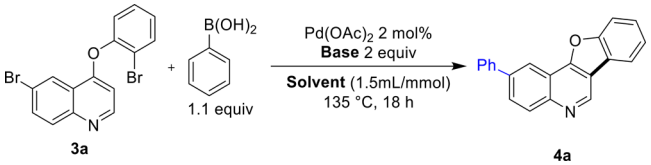
Catalytic Dead-End

In an effort to liberate the palladium, phenylboronic acid was introduced into the reaction mixture. Indeed, after optimization, the Suzuki−Miyaura reaction occurred, along with the direct arylation, giving 2-phenyl-benzofuro[3,2-*c*]quinoline **4a** in 83% isolated yield (Table 1).

A broad range of substituted phenylboronic acids underwent one-pot tandem SM/DA coupling, allowing access to novel benzofuroquinolines in good to excellent yields. Both electron-releasing (**4b** and **4c**) and electron-withdrawing (**4d**−**4k**) groups were well tolerated. The chloride on **4f** and **4l** was retained as a synthetic handle. Considering the prevalence of the pyridine moiety in biologically active compounds,[14] we also applied the SM/DA reaction conditions to this substrate and were pleased to furnish the benzofuropyridine **4m** in good yield. The Suzuki−Miyaura coupling was also conducive to positioning the bromine at C-7 (**4n**−**4r**) (Figure 1a).

We were then keen to expand the scope of our one-pot process to include Mizoroki−Heck transformations. Using either *tert*-butyl acrylate or styrene derivatives, the one-pot tandem MH/DA products were obtained in very good yields (**5a**−**5h**) (Figure 1b). Both transformations also worked efficiently when the second bromine was placed on the phenoxy ring (**6a**−**6c**) (Figure 1c). Given the apparent versatility of our methodology, a three-component tandem process was devised using tribrominated substrates and two equivalents of either coupling partner (**7a**−**7c**) (Figure 1d). The structures of **4a**, **4n**, and **5b** were confirmed by X-ray diffraction analysis of single crystals (Figure 2 and see Supporting Information S3−S6).

Table 1. Solvent and Base Screen for Tandem SM/DA Reaction of 3a



3a **4a**

entry	base	solvent	conv. (%)	yield[a] (%)
1	Cs_2CO_3	NMP	100	73 (75)
2[b]	Cs_2CO_3	1,4-dioxane	90	68
3[c]	Cs_2CO_3	toluene	25	
4[c]	Cs_2CO_3	xylene	16	
5[c]	Cs_2CO_3	cyclohexanone	85	61
6[c]	Cs_2CO_3	*i*-PrOAc	25	
7[c]	Cs_2CO_3	*n*-BuOAc	20	
8	Na_2CO_3	NMP	100	80
9	K_2CO_3	NMP	100	86 (83)
10	KOH	NMP	30	20
11	NaOH	NMP	65	44
12	NaO*t*-Bu	NMP	0[d]	

[a]Yields determined by ^{1}H NMR analysis of the crude reaction mixture using 1,3,5-trimethoxybenzene as an internal standard; values in parentheses represent isolated yields. [b]Reaction carried out at 125 °C. [c]Reaction carried out at 110 °C. [d]Complete decomposition of **3a** was observed.

Incorporating heteroatomic substrates in cross-coupling reactions usually necessitates the employment of an added ligand and inert atmosphere,[15] and in the reported C−H functionalization of pyridines and quinolines,[16] ancillary ligands are also required. Considering that pyridines,[17] and indeed quinolines,[18] possess the propensity to act as ligands for palladium, we suspected that our methodology might be underpinned by Pd−Q coordination. In order to determine any Pd−Q interaction, we undertook ^{1}H-^{15}N HMBC NMR spectroscopy. Inherent in this powerful technique are gradient-enhanced pulse sequences, which allow for suppression of t_1 noise facilitating the observation of the relatively weak long-range ^{1}H-^{15}N correlations.[19] Overall, the low natural abundance and low gyromagnetic ratio are overcome. Using this technique, structures **8a** and **8b** were elucidated. Initially, 0.5 equiv of $Pd(OAc)_2$ was added to **1** and **3b** in $CDCl_3$ (Scheme 3), and the ^{1}H, ^{13}C, and ^{1}H-^{15}N HMBC NMR spectra were recorded (see Supporting Information S14).

Complete consumption of both substrates was observed, accompanied by upfield shifts in the ^{1}H signals of the C-2, C-3, and C-8 protons and a dramatic upfield shift in the ^{15}N nucleus resonance (for example, from 291.7 ppm **1** to 196.7 ppm **8a**) in the respective ^{1}H-^{15}N HMBC spectra (Figure 3 and Supporting Information S14−S25). The significant shielding of the nitrogen atom and the considerable accompanying shift in both the C-2 and C-8 protons are indicative of direct Pd−N coordination.[20] Upon addition of $Pd(OAc)_2$ to **3h**, ^{1}H and ^{13}C NMR shifts analogous to those in **8a** and **8b** were observed. Similar downfield shifts were also discerned in the ^{1}H NMR spectra of **8a** in dioxane-d_8 and ACN-d_3 (Supporting Information S16 and S20). Crystal structures for complexes **8a** and **8c** were obtained (Figure 4), and the compositions of **8a**−**8c** were also verified by HRMS data (Supporting Information S8−S13).

https://dx.doi.org/10.1021/acs.joc.9b03321
J. Org. Chem. 2020, 85, 2585−2596

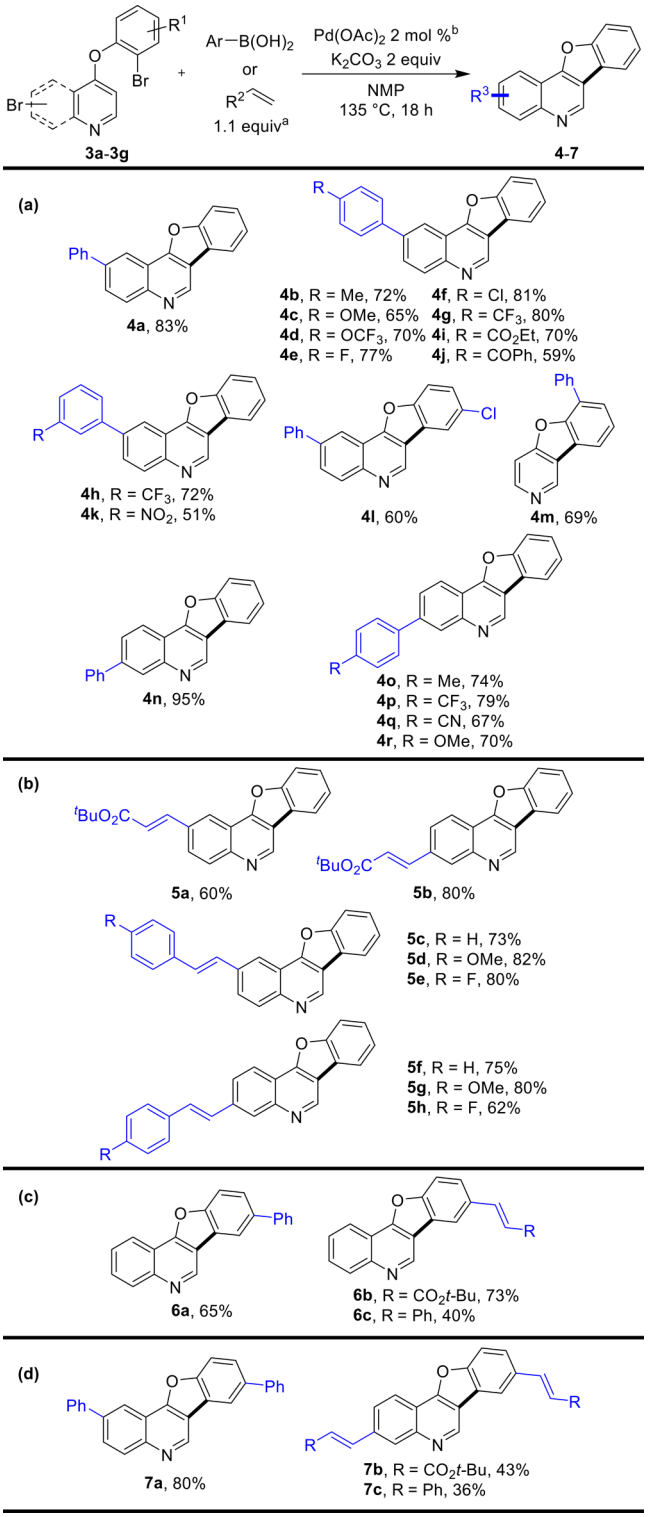


Figure 1. One-pot tandem SM/DA and MH/DA substrate scope. All yields are isolated. [a]2.2 equiv. of coupling partner employed in the synthesis of **7a**–**7c**. [b]5 mol % $Pd(OAc)_2$ used for all styrene-based derivatives.

We consider the Suzuki–Miyaura reaction to be the initial transformation in the sequence (Supporting Information Schemes S1 and S2), progressing via the typical Pd(II)/Pd(0) mechanistic cycle. For the DA step, we postulate two plausible mechanisms: first, OA at C–Br followed by C–H activation via, for example, concerted metalation–deprotona-

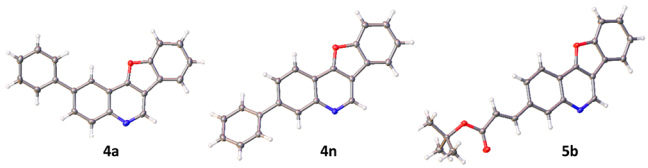
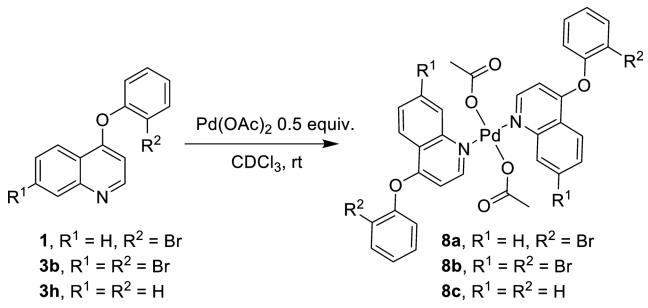


Figure 2. Crystal structures of **4a**, **4n**, and **5b** drawn at the 50% probability level. Second molecule in the asymmetric unit of **4a** omitted for clarity (see Supporting Information S4 for further information).

Scheme 3. Precatalyst Formation and Structure



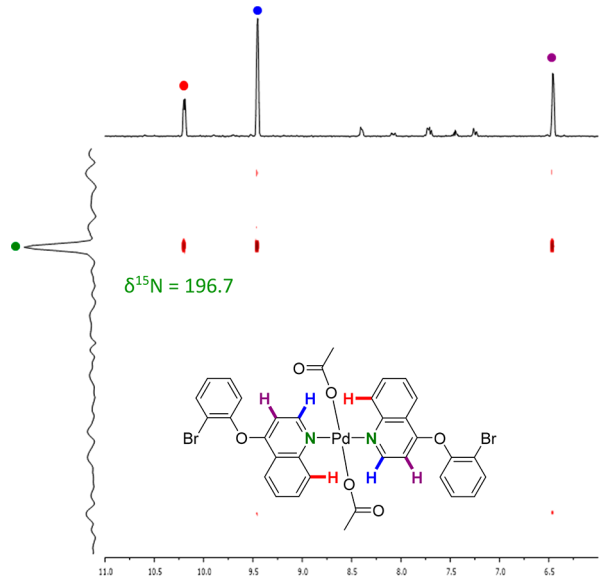


Figure 3. ^{1}H-^{15}N HMBC NMR spectrum of **8a** in $CDCl_3$ at 300 K as recorded at 600 MHz (^{1}H) and 60 MHz (^{15}N). All chemical shifts δ reported in ppm.

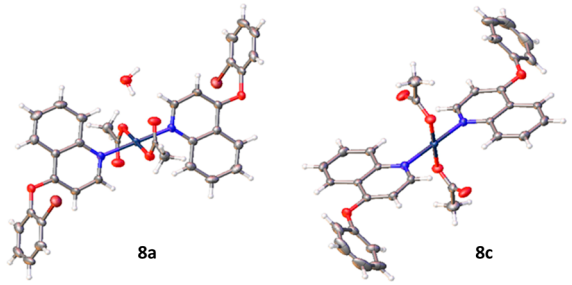
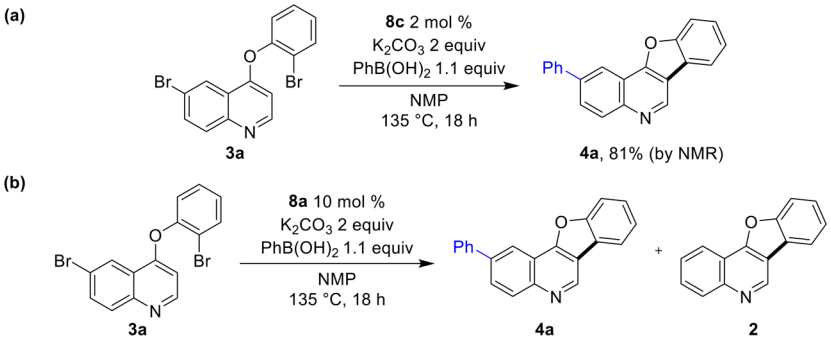


Figure 4. Crystal structures of **8a** and **8c** drawn at the 50% probability level. Disordered solvent (methanol) treated using solvent masking techniques for structure **8c** (see Supporting Information S4–S7 for further information).

https://dx.doi.org/10.1021/acs.joc.9b03321
J. Org. Chem. 2020, 85, 2585–2596

Scheme 4. Preformed 8c/8a as Competent Precatalysts for the SM/DA Reaction



tion (CMD),[21] and second, a Pd(II)/Pd(IV) route is also plausible, as proposed by Yu and Morokuma.[16a,22]

Albeit undefined at this stage, we envisage these complexes playing an important role as precatalysts, with the quinoline aiding precatalyst-to-catalyst transformation, although it is difficult to rule out an additional role of the quinoline in preventing catalyst decomposition.[23] Importantly, **8c** was deemed a competent precatalyst for the SM/DA reaction (Scheme 4a). A further experiment using mono-bromo-Pd complex **8a** as the sole catalytic-source for the SM/DA reaction yielded both **2** and **4a**, proving that the Pd−Q interaction is fluxional and ruling out a spectator-only role for the quinoline ligands (analogous to phosphine ligands for example) in the initially formed complexes **8a** and **8b** (Scheme 4b).[24]

Many small, conjugated organic molecules have the ability to emit fluorescent light and can be exploited for a variety of applications, such as in selective probes for ion detection[12,25] and optoelectronic devices[26] and as dyes or tags in bioimaging.[27] We were intrigued to investigate if our π-extended MH/DA products displayed any useful photophysical characteristics. Thus, UV−Visible absorption data for the styrene-functionalized compounds **2**, **5c**−**5h**, **6c**, and **7c** was obtained, and their fluorescent properties were investigated. The standard benzofuro[3,2-*c*]quinoline framework **2** is given for comparison (Table 2).

All compounds exhibit their maximum absorption band (λ_{max}) in the UV or near-UV region and yield large molar absorption coefficients (ε) in the range of 10^4 dm^3 mol^{-1} cm^{-1}. The addition of further auxochromes to the substituted frameworks resulted in notable shifts in λ_{max}. For example, the introduction of an electron releasing methoxy group (**5d** and **5g**) induced a hypsochromic shift relative to the parent styrene compounds **5c** and **5f**. In contrast, the more electronically poor quinoline frameworks (**5e** and **5h**) were blueshifted by a single nanometer. A significant bathochromic shift and increased intensity are displayed in the emission spectra for all compounds with respect to **2**. The addition of electron-poor/rich groups to our molecular framework gives rise to tunable differences in emission intensity and wavelength.

Table 2. UV−Vis Data, Fluorescence Emission (em.) Data, and Molar Absorption Coefficients (ε) for Compounds 2, 5c−5h, 6c, and 7c (See Supporting Information S125−S133 for More Information)

compd	abs. λ_{max} (nm)	em. λ_{em} (nm)	ε^a (dm^3 mol^{-1} cm^{-1})
2	257	353	63,300
5c	301	389	45,188
5d	259	416	38,338
5e	300	388	42,000
5f	337	387	38,500
5g	260	421	31,700
5h	336	386	43,638
6c	258	382	36,538
7c	342	346	51,438

[a] ε calculated at 8×10^{-6} mol dm^{-3}.

In summary, we report the occurrence of two mechanistically distinct reactions in one pot using the same precatalyst and without a requisite for an added ligand. The reactions work well in air, furnishing substituted benzofuroquinolines, which represent an interesting molecular framework for biological investigations. Direct evidence that the substrate quinoline forms a precatalytic species with palladium is provided, and excellent characterization data is furnished. The π-extended products also display interesting and potentially useful florescence properties.

EXPERIMENTAL SECTION

Materials and Methods. Solvents and reagents were used as obtained from commercial sources and without purification.

Melting points were measured in a Thomas Hoover Capillary Melting Point apparatus.

Infrared spectra were measured on a Perkin-Elmer FT-IR spectrometer as thin films in dichloromethane (DCM).

Column chromatography was carried out using 60 Å (35−70 μm) silica. Thin-layer chromatography (TLC) was carried out on precoated silica gel plates (Merck 60 PF254). The developed plates were visualized under UV light.

High-resolution precise mass spectra (HRMS) were recorded on a Waters LCT Premier Tof LC-MS instrument in University College Cork. Samples were run in electrospray ionization (ESI) mode using 50% acetonitrile/water containing 0.1% formic acid as an eluent; samples were made up at a concentration of ca. 1 mg mL^{-1}. HRMS of metal-containing complexes were recorded on a Bruker compact TOF-MS in the University of York. Samples were run in electrospray ionization (ESI) mode using 50% MeOH/water as eluent; samples were made up at a concentration of ca. 1 mg mL^{-1}. Acquisitions were internally calibrated using sodium formate clusters.

Nuclear magnetic resonance (NMR) samples were run in deuterated chloroform ($CDCl_3$), deuterated dimethyl sulfoxide ($(CD_3)_2SO$), deuterated dioxane ($C_4D_8O_2$), or deuterated acetonitrile (C_2D_3N) as specified. ^{1}H NMR (600 MHz) and ^{1}H NMR (300 MHz) spectra were recorded on Bruker Avance III 600 and Bruker Avance III 300 NMR spectrometers, respectively, in proton-coupled mode using tetramethysilane (TMS) as the internal standard. ^{13}C NMR (150 MHz), ^{13}C NMR (100 MHz), and ^{13}C NMR (75 MHz) spectra were recorded on Bruker Avance III 600, Bruker Avance 400, and Bruker Avance III 300 NMR spectrometers, respectively, in

https://dx.doi.org/10.1021/acs.joc.9b03321
J. Org. Chem. 2020, 85, 2585−2596

proton-decoupled mode at 300 K using TMS as the internal standard. ^{19}F NMR (282 MHz) spectra were recorded on a Bruker Avance III 300 NMR spectrometer in proton-decoupled mode at 300 K. ^{1}H-^{15}N HMBC spectra were recorded on a Bruker Avance III 600 NMR spectrometer [600 MHz (^{1}H) and 60 MHz (^{15}N)] equipped with Bruker BBFO cryoprobe. All spectra recorded at 300 K and referenced externally to nitromethane at 380.2 ppm, and the value of which was uncorrected. ^{1}H-^{15}N HMBC spectra were acquired using the Bruker HMBC pulse program (2D H-1/X correlation via heteronuclear zero and double quantum coherence optimized on long-range couplings) with four scans and a spectral width of 600−650 ppm. All spectra were run at University College Cork. Chemical shifts (δ) are expressed as parts per million (ppm), positive shift being downfield from TMS; coupling constants (J) are expressed in hertz (Hz). Splitting patterns in ^{1}H NMR spectra are designated as follows: s (singlet), bs (broad singlet), d (doublet), dd (doublet of doublets), ddd (doublet of doublets of doublets), t (triplet), td (triplet of doublets), q (quartet), quin (quintet), and m (multiplet).

Single-crystal X-ray analysis was performed on a Rigaku AFC12 FRE-HF diffractometer equipped with an Oxford Cryosystems low-temperature device. The crystals were kept at a steady T = 100(2) K during data collection. The structures were solved with the ShelXT[28] structure solution program using the Intrinsic Phasing solution method and by using Olex2[29] as the graphical interface. The models were refined with version 2016/6 of ShelXL[28] using least-squares minimization. Cell parameters were retrieved and refined using the CrysAlisPro (Rigaku, V1.171.40.37a, 2019). All nonhydrogen atoms were refined anisotropically. Hydrogen atom positions were calculated geometrically and refined using the riding model. Further information is available in the Supporting Information.

UV−Visible absorption was measured on a Thermo Scientific Evolution 60S UV−Visible spectrophotometer. All solutions were made up in DCM, and measurements were performed in high-precision quartz cells of 10 mm in path length. A baseline in DCM was recorded by an internal reference detector. Molar absorption values were calculated using Beer's law at a concentration of 8×10^{-6} mol dm^{-3}. Fluorescence intensities were measured on a PerkinElmer Fluorescence Spectrometer LS 55. All solutions were made up in DCM, and measurements were performed in high-precision quartz cells of 10 × 10 mm in path length. Spectra were recorded in the range of 200−700 nm, and compounds were excited at 257 nm.

General Procedure for the Synthesis of 4-Phenoxyquinoline Substrates. A mixture of the 4-chloroquinoline substrate (1 equiv), the phenol (5 equiv), and NaOH (crushed pellets) (1.5 equiv) was stirred at 120 °C in an aluminum heating mantle until the reaction was complete (2−6 h) as evidenced by TLC (Hex/EtOAc 8:2). The cooled reaction mixture was diluted with 10% aqueous NaOH (5 mL) and stirred at room temperature for 1 h. The aqueous phase was extracted with DCM (3 × 20 mL). The combined organic layers were washed with 6 M NaOH (3 × 10 mL), water (10 mL), and brine (10 mL), dried over $MgSO_4$, filtered, and concentrated in vacuo. The crude mixture was purified by column chromatography over silica gel using Hex/EtOAc (8:2) as an eluent unless otherwise specified.

*6-Bromo-4-(2-bromophenoxy)quinoline (**3a**).* 6-Bromo-4-chloroquinoline (0.970 g, 4.0 mmol), 2-bromophenol (2.32 mL, 20 mmol), and NaOH (0.240 g, 6.0 mmol) were reacted according to the general procedure for the synthesis of 4-phenoxyquinolines above to give the title product as a pale yellow solid; yield: 1.406 g (93%); m.p. 97−98 °C; IR (NaCl): ν 3399, 1590, 1491, 1350, 1221, 665 cm^{-1}; ^{1}H NMR (300 MHz, $CDCl_3$) δ: 6.41 (d, J = 5.2 Hz, 1H), 7.19−7.28 (m, 2H), 7.39−7.47 (m, 1H), 7.73 (dd, J = 8.3, 1.5 Hz, 1H), 7.84 (dd, J = 9.0, 2.2 Hz, 1H), 7.98 (d, J = 9.0 Hz, 1H), 8.58 (d, J = 2.2 Hz, 1H), 8.67 (d, J = 5.2 Hz, 1H) ppm; ^{13}C{^{1}H} NMR (75 MHz, $CDCl_3$) δ: 104.2, 116.4, 120.3, 122.2, 123.3, 124.3, 127.6, 129.3, 130.9, 133.7, 134.4, 148.4, 150.8, 151.4, 159.8 ppm; HRMS (ESI-TOF) m/z: [M + H]$^+$ calcd for $C_{15}H_{10}Br_2NO$ 377.9129; found: 377.9132.

*7-Bromo-4-(2-bromophenoxy)quinoline (**3b**).* 7-Bromo-4-chloroquinoline (0.970 g, 4.0 mmol), 2-bromophenol (2.32 mL, 20.0 mmol), and NaOH (0.240 g, 6.0 mmol) were reacted according to the general procedure for the synthesis of 4-phenoxyquinolines above to give the title product as a pale yellow solid; yield: 1.397 g (92%); m.p. 73−74 °C; IR (NaCl): ν 3064, 1561, 1468, 1301, 1220, 657 cm^{-1}; ^{1}H NMR (300 MHz, $CDCl_3$) δ: 6.41 (d, J = 5.2 Hz, 1H), 7.19−7.30 (m, 2H), 7.39−7.48 (m, 1H), 7.66−7.76 (m, 2H), 8.25−8.33 (m, 2H), 8.66 (d, J = 5.2 Hz, 1H) ppm; ^{13}C{^{1}H} NMR (75 MHz, $CDCl_3$) δ: 103.9, 116.3, 119.7, 123.3, 123.5, 124.6, 127.6, 129.3, 129.8, 131.4, 134.4, 150.5, 150.8, 152.1, 160.8 ppm; HRMS (ESI-TOF) m/z: [M + H]$^+$ calcd for $C_{15}H_{10}Br_2NO$ 377.9129; found: 377.9119.

*6-Bromo-4-(2-bromo-4-chlorophenoxy)quinoline (**3c**).* 6-Bromo-4-chloroquinoline (0.500 g, 2.06 mmol), 2-bromo-4-chlorophenol (2.140 g, 10.31 mmol), and NaOH (0.126 g, 3.14 mmol) were reacted according to the general procedure for the synthesis of 4-phenoxyquinolines above to give the title product as a pale pink solid; yield: 531 mg (77%); m.p. 157−159 °C; IR (NaCl): ν 3392, 1590, 1467, 1349, 1256, 729, 667 cm^{-1}; ^{1}H NMR (300 MHz, $CDCl_3$) δ: 6.41 (d, J = 5.1 Hz, 1H), 7.18 (d, J = 8.6 Hz, 1H), 7.42 (dd, J = 8.6, 2.5 Hz, 1H), 7.74 (d, J = 2.4 Hz, 1H), 7.84 (dd, J = 9.0, 2.2 Hz, 1H), 7.98 (d, J = 9.0 Hz, 1H), 8.55 (d, J = 2.2 Hz, 1H), 8.68 (d, J = 5.1 Hz, 1H) ppm; ^{13}C{^{1}H} NMR (75 MHz, $CDCl_3$) δ: 104.1, 117.0, 120.5, 122.0, 124.0, 124.2, 129.4, 131.0, 132.4, 133.9, 134.0, 148.4, 149.6, 151.3, 159.5 ppm; HRMS (ESI-TOF) m/z: [M + H]$^+$ calcd for $C_{15}H_9Br_2ClNO$ 411.8739; found: 411.8730.

*4-(2,6-Dibromophenoxy)pyridine (**3d**).* A neat mixture of 4-chloropyridine (0.250 g, 1.66 mmol) and 2,6-dibromophenol (0.630 g, 2.50 mmol) was stirred at 120 °C in an aluminum heating mantle until the reaction was complete (16 h) as evidenced by TLC (Hex/EtOAc 8:2). The cooled reaction mixture was diluted with 10% aqueous NaOH (5 mL) and stirred at room temperature for 1 h. The aqueous phase was extracted with DCM (3 × 20 mL). The combined organic layers were washed with 6 M NaOH (3 × 10 mL), water (10 mL), and brine (10 mL), dried over $MgSO_4$, filtered, and concentrated in vacuo. The crude mixture was purified by recrystallization from cyclohexane to give the title product as an off-white solid; yield: 365 mg (66%); m.p. 91−93 °C; IR (NaCl): ν 3393, 1590, 1434, 1261, 1200, 665 cm^{-1}; ^{1}H NMR (300 MHz, $CDCl_3$) δ: 6.75 (d, J = 5.0 Hz, 2H), 7.07 (t, J = 8.1 Hz, 1H), 7.63 (dd, J = 8.1, 1.9 Hz, 2H), 8.49 (d, J = 5.2 Hz, 2H) ppm; ^{13}C{^{1}H} NMR (75 MHz, $CDCl_3$) δ: 110.8, 118.3, 128.3, 133.1, 147.7, 151.5, 162.5 ppm; HRMS (ESI-TOF) m/z: [M + H]$^+$ calcd for $C_{11}H_8Br_2NO$ 327.8973; found: 327.8961.

*4-(2,4-Dibromophenoxy)quinoline (**3e**).* 4-Chloroquinoline (0.260 g, 1.60 mmol), 2,4-dibromophenol (2.00 g, 7.90 mmol), and NaOH (0.095 g, 2.40 mmol) were reacted according to the general procedure for the synthesis of 4-phenoxyquinolines above to give the title product as a pale yellow solid; yield: 517 mg (85%); m.p. 125−126 °C; IR (NaCl): ν 3394, 1596, 1464, 1305, 1224, 667 cm^{-1}; ^{1}H NMR (300 MHz, $CDCl_3$) δ: 6.43 (d, J = 5.1 Hz, 1H), 7.13 (d, J = 8.6 Hz, 1H), 7.50−7.68 (m, 2H), 7.79 (ddd, J = 8.5, 6.9, 1.4 Hz, 1H), 7.88 (d, J = 2.3 Hz, 1H), 8.12 (d, J = 8.4 Hz, 1H), 8.38 (dd, J = 8.4, 0.9 Hz, 1H), 8.70 (d, J = 5.1 Hz, 1H) ppm; ^{13}C{^{1}H} NMR (75 MHz, $CDCl_3$) δ: 103.8, 117.4, 119.3, 120.9, 121.8, 124.3, 126.5, 129.2, 130.4, 132.3, 136.6, 149.8, 150.5, 151.0, 160.3 ppm; HRMS (ESI-TOF) m/z: [M + H]$^+$ calcd for $C_{15}H_{10}Br_2NO$ 377.9129; found: 377.9114.

*6-Bromo-4-(2,4-dibromophenoxy)quinoline (**3f**).* 6-Bromo-4-chloroquinoline (0.240 g, 0.99 mmol), 2,4-dibromophenol (1.247 g, 4.95 mmol), and NaOH (0.059 g, 1.5 mmol) were reacted according to the general procedure for the synthesis of 4-phenoxyquinolines above to give the title product as a pale yellow solid; yield: 268 mg (59%); m.p. 162−163 °C; IR (NaCl): ν 3370, 1590, 1449, 1349, 1255, 665 cm^{-1}; ^{1}H NMR (300 MHz, $CDCl_3$) δ: 6.42 (d, J = 5.1 Hz, 1H), 7.12 (d, J = 8.6 Hz, 1H), 7.56 (dd, J = 8.6, 2.3 Hz, 1H), 7.80−7.91 (m, 2H), 7.98 (d, J = 9.0 Hz, 1H), 8.54 (d, J = 2.2 Hz, 1H), 8.68 (d, J = 5.1 Hz, 1H) ppm; ^{13}C{^{1}H} NMR (75 MHz, $CDCl_3$) δ: 104.2, 117.4, 119.7, 120.5, 122.0, 124.2, 124.4, 131.0, 132.4, 133.9, 136.7, 148.4, 150.1, 151.3, 159.4 ppm; HRMS (ESI-TOF) m/z: [M + H]$^+$ calcd for $C_{15}H_9Br_3NO$ 455.8234; found: 455.8233.

*7-Bromo-4-(2,4-dibromophenoxy)quinoline (**3g**).* 7-Bromo-4-chloroquinoline (0.243 g, 1.0 mmol), 2,4-dibromophenol (1.26 g,

https://dx.doi.org/10.1021/acs.joc.9b03321
J. Org. Chem. 2020, 85, 2585−2596

5.0 mmol), and NaOH (0.06 g, 1.5 mmol) were reacted according to the general procedure for the synthesis of 4-phenoxyquinolines above to give the title product as a white solid; yield: 398 mg (87%); m.p. 140−142 °C; IR (NaCl) ν 3583, 1615, 1559, 1302, 1096, 666 cm^{-1}; ^1H NMR (300 MHz, $CDCl_3$) δ: 6.42 (d, J = 5.2 Hz, 1H), 7.13 (d, J = 8.6 Hz, 1H), 7.56 (dd, J = 8.6, 2.3 Hz, 1H), 7.70 (dd, J = 8.9, 1.9 Hz, 1H), 7.88 (d, J = 2.3 Hz, 1H), 8.18−8.36 (m, 2H), 8.68 (d, J = 5.2 Hz, 1H) ppm; $^{13}C\{^1H\}$ NMR (75 MHz, $CDCl_3$) δ: 103.9, 117.4, 119.6, 119.7, 123.3, 124.4, 124.7, 130.0, 131.5, 132.4, 136.7, 150.2, 150.5, 152.1, 160.5 ppm; HRMS (ESI-TOF) m/z: $[M + H]^+$ calcd for $C_{15}H_9Br_3NO$ 455.8229; found: 455.8233.

*4-Phenoxyquinoline (**3h**).*[30] 4-Chloroquinoline (0.164 g, 1.0 mmol), phenol (0.471 g, 5.0 mmol), and NaOH (0.06 g, 1.5 mmol) were reacted according to the general procedure for the synthesis of 4-phenoxyquinolines above to give the title product as a yellow oil; yield: 192 mg (87%); ^1H NMR (300 MHz, $CDCl_3$) δ: 6.54 (d, J = 5.2 Hz, 1H), 7.13−7.22 (m, 2H), 7.23−7.33 (m, 1H), 7.39−7.50 (m, 2H), 7.56 (ddd, J = 8.2, 6.9, 1.1 Hz, 1H), 7.74 (ddd, J = 8.5, 6.9, 1.5 Hz, 1H), 8.10 (d, J = 8.3 Hz, 1H), 8.36 (dd, J = 8.4, 1.1 Hz, 1H), 8.66 (d, J = 5.1 Hz, 1H) ppm; $^{13}C\{^1H\}$ NMR (75 MHz, $CDCl_3$) δ: 104.4, 121.1, 121.5, 121.8, 125.6, 126.1, 129.1, 130.1, 130.3, 149.8, 151.1, 154.4, 161.9 ppm; HRMS (ESI-TOF) m/z: $[M + H]^+$ calcd for $C_{15}H_{12}NO$ 222.0913; found: 222.0913.

*6-Bromo-4-phenoxyquinoline (**3i**).* 6-Bromo-4-chloroquinoline (0.500 g, 2.1 mmol), phenol (0.970 g, 10.31 mmol), and NaOH (0.126 g, 3.14 mmol) were reacted according to the general procedure for the synthesis of 4-phenoxyquinolines above to give the title product as a pale yellow solid; yield: 517 mg (83%); m.p. 84−86 °C; IR (NaCl): ν 3401, 1561, 1487, 1351, 1213, 667 cm^{-1}; ^1H NMR (300 MHz, $CDCl_3$) δ: 6.54 (d, J = 5.2 Hz, 1H), 7.13−7.22 (m, 2H), 7.25−7.36 (m, 1H), 7.41−7.53 (m, 2H), 7.80 (dd, J = 9.0, 2.2 Hz, 1H), 7.95 (d, J = 9.0 Hz, 1H), 8.53 (d, J = 2.2 Hz, 1H), 8.65 (d, J = 5.2 Hz, 1H) ppm; $^{13}C\{^1H\}$ NMR (75 MHz, $CDCl_3$) δ: 104.7, 120.2, 121.1, 122.6, 124.3, 125.9, 130.4, 130.9, 133.6, 148.3, 151.5, 154.0, 161.0 ppm; HRMS (ESI-TOF) m/z: $[M + H]^+$ calcd for $C_{15}H_{11}BrNO$ 300.0024; found: 300.0013.

General Procedure for Palladium-Catalyzed One-Pot Suzuki−Miyaura and Intramolecular Direct Arylation Reactions. A mixture of the 4-(2-bromophenoxy)quinoline substrate (1 equiv), $PhB(OH)_2$ (1.1 equiv), $Pd(OAc)_2$ (2 mol %), and anhydrous K_2CO_3 (2 equiv) in anhydrous NMP (1.5 mL $mmol^{-1}$) was stirred at 135 °C in a sealed reaction tube in an aluminum multireaction heating mantle until the reaction was complete as evidenced by ^1H NMR analysis. The cooled reaction mixture was diluted with DCM, filtered through a short plug of Celite, and concentrated in vacuo. The crude mixture was purified by column chromatography over silica gel using DCM/EtOAc (99:1−95:5) as an eluent unless otherwise specified.

*2-Phenylbenzofuro[3,2-c]quinoline (**4a**).* A mixture of substrate **3a** (0.100 g, 0.26 mmol), phenylboronic acid (0.035 g, 0.29 mmol), $Pd(OAc)_2$ (1.2 mg, 2 mol %), and anhydrous K_2CO_3 (0.073 g, 0.53 mmol) in anhydrous NMP (0.4 mL, 1.5 mL $mmol^{-1}$) was reacted according to the general one-pot SM/DA procedure above to give the title product as a pale yellow solid; X-ray quality crystals were obtained via vapor diffusion from a saturated solution of toluene in hexane, the CCDC number is 1967876; yield: 63 mg (83%); m.p. 169−171 °C; IR (NaCl): ν 3450, 1559, 1460, 1359, 1193 cm^{-1}; ^1H NMR (300 MHz, $CDCl_3$) δ: 7.39−7.61 (m, 5H), 7.74−7.87 (m, 3H), 8.02−8.15 (m, 2H), 8.33 (d, J = 8.8 Hz, 1H), 8.62 (d, J = 1.7 Hz, 1H), 9.49 (s, 1H) ppm; $^{13}C\{^1H\}$ NMR (75 MHz, $CDCl_3$) δ: 112.1, 116.6, 117.3, 118.4, 120.6, 122.7, 124.1, 127.3, 127.5, 127.9, 128.8, 129.0, 130.2, 139.7, 140.1, 144.2, 146.7, 156.0, 157.6 ppm; HRMS (ESI-TOF) m/z: $[M + H]^+$ calcd for $C_{21}H_{14}NO$ 296.1075; found: 296.1062.

*2-(p-Tolyl)benzofuro[3,2-c]quinoline (**4b**).* A mixture of substrate **3a** (0.150 g, 0.396 mmol), *o*-tolylboronic acid (0.059 g, 0.435 mmol), $Pd(OAc)_2$ (1.8 mg, 2 mol %), and anhydrous K_2CO_3 (0.109 g, 0.79 mmol) in anhydrous NMP (0.6 mL, 1.5 mL $mmol^{-1}$) was reacted according to the general one-pot SM/DA procedure above to give the title product as a white solid; yield: 89 mg (72%); m.p. 183−185 °C; IR (NaCl): ν 3583, 3401, 1505, 1460, 1358, 1190 cm^{-1}; ^1H NMR (300 MHz, $CDCl_3$) δ: 2.45 (s, 3H), 7.35 (d, J = 7.9 Hz, 2H), 7.44−7.62 (m, 2H), 7.69−7.82 (m, 3H), 8.02−8.16 (m, 2H), 8.33 (d, J = 8.8 Hz, 1H), 8.61 (d, J = 1.9 Hz, 1H), 9.49 (s, 1H) ppm; $^{13}C\{^1H\}$ NMR (75 MHz, $CDCl_3$) δ: 21.2, 112.1, 116.5, 117.4, 118.0, 120.7, 122.7, 124.1, 127.27, 127.34, 128.8, 129.8, 130.2, 137.2, 137.9, 139.6, 144.0, 146.6, 156.0, 157.6 ppm; HRMS (ESI-TOF) m/z: $[M + H]^+$ calcd for $C_{22}H_{16}NO$ 310.1232; found: 310.1222.

*2-(4-Methoxyphenyl)benzofuro[3,2-c]quinoline (**4c**).* A mixture of substrate **3a** (0.150 g, 0.396 mmol), 4-methoxyphenylboronic acid (0.066 g, 0.435 mmol), $Pd(OAc)_2$ (4.5 mg, 5 mol %), and anhydrous K_2CO_3 (0.109 g, 0.79 mmol) in anhydrous NMP (0.6 mL, 1.5 mL $mmol^{-1}$) was reacted according to the general one-pot SM/DA procedure above to give the title product as a white solid; yield: 84 mg (65%); m.p. 189−191 °C; IR (NaCl): ν 3320, 1505, 1460, 1359, 1246, 1190 cm^{-1}; ^1H NMR (300 MHz, $CDCl_3$) δ: 3.90 (s, 3H), 7.01−7.12 (m, 2H), 7.43−7.60 (m, 2H), 7.71−7.81 (m, 3H), 8.01 (dd, J = 8.8, 2.1 Hz, 1H), 8.10 (dd, J = 7.6, 0.9 Hz, 1H), 8.30 (d, J = 8.8 Hz, 1H), 8.55 (d, J = 1.9 Hz, 1H), 9.46 (s, 1H) ppm; $^{13}C\{^1H\}$ NMR (75 MHz, $CDCl_3$) δ: 55.4, 112.1, 114.5, 116.5, 117.4, 117.5, 120.6, 122.7, 124.1, 127.2, 128.56, 128.61, 130.2, 132.6, 139.3, 143.9, 146.4, 156.0, 157.5, 159.7 ppm; HRMS (ESI-TOF) m/z: $[M + H]^+$ calcd for $C_{22}H_{16}NO_2$ 326.1181; found: 326.1185.

*2-(4-(Trifluoromethoxy)phenyl)benzofuro[3,2-c]quinoline (**4d**).* A mixture of substrate **3a** (0.150 g, 0.396 mmol), (4-(trifluoromethoxy)-phenyl)boronic acid (0.090 g, 0.435 mmol), $Pd(OAc)_2$ (1.8 mg, 2 mol %), and anhydrous K_2CO_3 (0.109 g, 0.79 mmol) in anhydrous NMP (0.6 mL, 1.5 mL $mmol^{-1}$) was reacted according to the general one-pot SM/DA procedure above to give the title product as a yellow solid; yield: 105 mg (70%); m.p. 148−150 °C; IR (NaCl): ν 3583, 1504, 1459, 1283, 1210, 1191, 1165 cm^{-1}; ^1H NMR (300 MHz, $CDCl_3$) δ: 7.37 (dd, J = 8.8, 0.9 Hz, 2H), 7.43−7.62 (m, 2H), 7.72−7.86 (m, 3H), 7.97 (dd, J = 8.8, 2.1 Hz, 1H), 8.09 (dd, J = 7.6, 0.8 Hz, 1H), 8.31 (d, J = 8.8 Hz, 1H), 8.54 (d, J = 2.0 Hz, 1H), 9.47 (s, 1H) ppm; $^{13}C\{^1H\}$ NMR (75 MHz, $CDCl_3$) δ: 112.1, 116.8, 117.4, 118.6, 120.5 (q, $^1J_{(C,F)}$ = 257 Hz), 120.7, 121.4, 122.6, 124.2, 127.4, 128.5, 128.9, 130.5, 138.3, 138.9, 144.5, 146.7, 149.2 (q, $^3J_{(C,F)}$ = 2 Hz), 156.0, 157.5 ppm; $^{19}F\{^1H\}$ NMR (282 MHz, $CDCl_3$) δ: −58 ppm; HRMS (ESI-TOF) m/z: $[M + H]^+$ calcd for $C_{22}H_{13}F_3NO_2$ 380.0898; found: 380.0889.

*2-(4-Fluorophenyl)benzofuro[3,2-c]quinoline (**4e**).* A mixture of substrate **3a** (0.150 g, 0.396 mmol), 4-fluorophenylboronic acid (0.061 g, 0.435 mmol), $Pd(OAc)_2$ (1.8 mg, 2 mol %), and anhydrous K_2CO_3 (0.109 g, 0.79 mmol) in anhydrous NMP (0.6 mL, 1.5 mL $mmol^{-1}$) was reacted according to the general one-pot SM/DA procedure above to give the title product as a pale yellow solid; yield: 95 mg (77%); m.p. 185−186 °C; IR (NaCl): ν 3391, 1561, 1460, 1334, 1192, 1123 cm^{-1}; ^1H NMR (300 MHz, $CDCl_3$) δ: 7.16−7.29 (m, 2H), 7.46−7.62 (m, 2H), 7.72−7.83 (m, 3H), 8.00 (dd, J = 8.8, 2.1 Hz, 1H), 8.13 (dd, J = 7.2, 1.3 Hz, 1H), 8.33 (d, J = 8.8 Hz, 1H), 8.57 (d, J = 2.0 Hz, 1H), 9.50 (s, 1H) ppm; $^{13}C\{^1H\}$ NMR (75 MHz, $CDCl_3$) δ: 112.1, 115.9 (d, $^2J_{(C,F)}$ = 22 Hz), 116.7, 117.4, 118.2, 120.7, 122.7, 124.1, 127.3, 128.6, 129.1 (d, $^3J_{(C,F)}$ = 8 Hz), 130.4, 136.2, 138.7, 144.3, 146.6, 156.0, 157.5, 162.9 (d, $^1J_{(C,F)}$ = 247 Hz) ppm; $^{19}F\{^1H\}$ NMR (282 MHz, $CDCl_3$) δ: −115 ppm; HRMS (ESI-TOF) m/z: $[M + H]^+$ calcd for $C_{21}H_{13}FNO$ 314.0981; found: 314.0971.

*2-(4-Chlorophenyl)benzofuro[3,2-c]quinoline (**4f**).* A mixture of substrate **3a** (0.150 g, 0.396 mmol), 4-chlorophenylboronic acid (0.068 g, 0.435 mmol), $Pd(OAc)_2$ (1.8 mg, 2 mol %), and anhydrous K_2CO_3 (0.109 g, 0.79 mmol) in anhydrous NMP (0.6 mL, 1.5 mL $mmol^{-1}$) was reacted according to the general one-pot SM/DA procedure above to give the title product as a pale yellow solid; yield: 106 mg (81%); m.p. 191−192 °C; IR (NaCl): ν 3389, 1556, 1458, 1356, 1191, 821 cm^{-1}; ^1H NMR (300 MHz, $CDCl_3$) δ: 7.38−7.57 (m, 4H), 7.61−7.75 (m, 3H), 7.89 (dd, J = 8.8, 2.1 Hz, 1H), 8.02 (dd, J = 7.6, 0.8 Hz, 1H), 8.24 (d, J = 8.8 Hz, 1H), 8.43 (d, J = 2.0 Hz, 1H), 9.39 (s, 1H) ppm; $^{13}C\{^1H\}$ NMR (75 MHz, $CDCl_3$) δ: 112.1, 116.7, 117.3, 118.2, 120.7, 122.6, 124.1, 127.3, 128.3, 128.6, 129.1, 130.4, 134.1, 138.3, 138.5, 144.4, 146.7, 155.9, 157.4 ppm; HRMS

https://dx.doi.org/10.1021/acs.joc.9b03321
J. Org. Chem. 2020, 85, 2585−2596

(ESI-TOF) m/z: $[M + H]^+$ calcd for $C_{21}H_{13}ClNO$ 330.0680; found: 330.0676.

*2-(4-(Trifluoromethyl)phenyl)benzofuro[3,2-c]quinoline (**4g**).* A mixture of substrate **3a** (0.150 g, 0.396 mmol), (4-(trifluoromethyl)-phenyl)boronic acid (0.083 g, 0.435 mmol), $Pd(OAc)_2$ (1.8 mg, 2 mol %), and anhydrous K_2CO_3 (0.109 g, 0.79 mmol) in anhydrous NMP (0.6 mL, 1.5 mL $mmol^{-1}$) was reacted according to the general one-pot SM/DA procedure above to give the title product as a pale yellow solid; yield: 114 mg (80%); m.p. 194−195 °C; IR (NaCl): ν 3384, 1614, 1460, 1331, 1189, 1116 cm^{-1}; ^1H NMR (300 MHz, $CDCl_3$) δ: 7.46−7.63 (m, 2H), 7.74−7.85 (m, 3H), 7.93 (d, J = 8.2 Hz, 2H), 8.04 (dd, J = 8.8, 2.1 Hz, 1H), 8.13 (d, J = 7.4 Hz, 1H), 8.37 (d, J = 8.8 Hz, 1H), 8.65 (d, J = 1.9 Hz, 1H), 9.53 (s, 1H) ppm; $^{13}C\{^1H\}$ NMR (75 MHz, $CDCl_3$) δ: 112.1, 116.8, 117.3, 119.0, 120.7, 122.6, 124.22, 124.23 (q, $^1J_{(C,F)}$ = 270 Hz), 125.9 (q, $^3J_{(C,F)}$ = 4 Hz), 127.5, 127.7, 128.4, 130.0 (q, $^2J_{(C,F)}$ = 33 Hz), 130.6, 138.1, 143.6, 144.8, 146.9, 156.0, 157.5 ppm; $^{19}F\{^1H\}$ NMR (282 MHz, $CDCl_3$) δ: −62 ppm; HRMS (ESI-TOF) m/z: $[M + H]^+$ calcd for $C_{22}H_{13}F_3NO$ 364.0949; found: 364.0938.

*2-(3-(Trifluoromethyl)phenyl)benzofuro[3,2-c]quinoline (**4h**).* A mixture of substrate **3a** (0.150 g, 0.396 mmol), (3-(trifluoromethyl)-phenyl)boronic acid (0.083 g, 0.435 mmol), $Pd(OAc)_2$ (1.8 mg, 2 mol %), and anhydrous K_2CO_3 (0.109 g, 0.79 mmol) in anhydrous NMP (0.6 mL, 1.5 mL $mmol^{-1}$) was reacted according to the general one-pot SM/DA procedure above to give the title product as a pale yellow solid; yield: 104 mg (72%); m.p. 171−173 °C; IR (NaCl): ν 3391, 1561, 1446, 1334, 1166, 1123 cm^{-1}; ^1H NMR (300 MHz, $CDCl_3$) δ: 7.45−7.73 (m, 4H), 7.79 (d, J = 7.9 Hz, 1H), 7.95−8.09 (m, 3H), 8.13 (dd, J = 7.6, 0.8 Hz, 1H), 8.37 (d, J = 8.8 Hz, 1H), 8.63 (d, J = 2.0 Hz, 1H), 9.52 (s, 1H) ppm; $^{13}C\{^1H\}$ NMR (75 MHz, $CDCl_3$) δ: 112.1, 116.8, 117.3, 118.7, 120.7, 122.6, 124.19, 124.20 (q, $^1J_{(C,F)}$ = 273 Hz), 124.3 (q, $^3J_{(C,F)}$ = 4 Hz), 124.6 (q, $^3J_{(C,F)}$ = 4 Hz), 127.5, 128.4, 129.5, 130.6, 130.7, 131.5 (q, $^2J_{(C,F)}$ = 32 Hz), 138.1, 140.9, 144.7, 146.8, 156.0, 157.5 ppm; $^{19}F\{^1H\}$ NMR (282 MHz, $CDCl_3$) δ: −62 ppm; HRMS (ESI-TOF) m/z: $[M + H]^+$ calcd for $C_{22}H_{13}F_3NO$ 364.0944; found: 364.0947.

*Ethyl 4-(Benzofuro[3,2-c]quinolin-2-yl)benzoate (**4i**).* A mixture of substrate **3a** (0.150 g, 0.396 mmol), 4-ethoxycarbonylphenylboronic acid (0.084 g, 0.435 mmol), $Pd(OAc)_2$ (1.8 mg, 2 mol %), and anhydrous K_2CO_3 (0.109 g, 0.79 mmol) in anhydrous NMP (0.6 mL, 1.5 mL $mmol^{-1}$) was reacted according to the general one-pot SM/DA procedure above to give the title product as a beige solid; yield: 105 mg (70%); m.p. 160−161 °C; IR (NaCl): ν 2922, 1715, 1607, 1460, 1357, 1278, 1190 cm^{-1}; ^1H NMR (300 MHz, $CDCl_3$) δ: 1.45 (t, J = 7.1 Hz, 3H), 4.44 (q, J = 7.1 Hz, 2H), 7.43−7.63 (m, 2H), 7.79 (d, J = 7.9 Hz, 1H), 7.84−7.95 (m, 2H), 8.02−8.28 (m, 4H), 8.36 (d, J = 8.8 Hz, 1H), 8.67 (d, J = 1.7 Hz, 1H), 9.52 (s, 1H) ppm; $^{13}C\{^1H\}$ NMR (75 MHz, $CDCl_3$) δ: 14.4, 61.1, 112.1, 116.7, 117.2, 118.8, 120.7, 122.5, 124.1, 127.3, 127.4, 128.8, 129.8, 130.2, 130.5, 138.3, 144.2, 144.6, 146.9, 155.9, 157.4, 166.4 ppm; HRMS (ESI-TOF) m/z: $[M + H]^+$ calcd for $C_{24}H_{18}NO_3$: 368.1281; found: 368.1282.

*(4-(Benzofuro[3,2-c]quinolin-2-yl)phenyl)(phenyl)methanone (**4j**).* A mixture of substrate **3a** (0.150 g, 0.396 mmol), (4-benzoylphenyl)boronic acid (0.098 g, 0.435 mmol), $Pd(OAc)_2$ (1.8 mg, 2 mol %), and anhydrous K_2CO_3 (0.109 g, 0.79 mmol) in anhydrous NMP (0.6 mL, 1.5 mL $mmol^{-1}$) was reacted according to the general one-pot SM/DA procedure above to give the title product as a pale yellow solid; yield: 94 mg (59%); m.p. 184−187 °C; IR (NaCl): ν 3401, 1652, 1602, 1460, 1357, 1190 cm^{-1}; ^1H NMR (300 MHz, $CDCl_3$) δ: 7.46−7.70 (m, 5H), 7.79 (d, J = 8.3 Hz, 1H), 7.84−8.04 (m, 6H), 8.05−8.20 (m, 2H), 8.38 (d, J = 8.8 Hz, 1H), 8.71 (d, J = 1.9 Hz, 1H), 9.53 (s, 1H) ppm; $^{13}C\{^1H\}$ NMR (75 MHz, $CDCl_3$) δ: 112.1, 116.8, 117.4, 119.0, 120.7, 122.6, 124.2, 127.3, 127.5, 128.4, 128.5, 130.0, 130.6, 130.9, 132.5, 136.8, 137.6, 138.4, 144.0, 144.7, 146.9, 156.0, 157.5, 196.2 ppm; HRMS (ESI-TOF) m/z: $[M + H]^+$ calcd for $C_{28}H_{18}NO_2$ 400.1332; found: 400.1331.

*2-(3-Nitrophenyl)benzofuro[3,2-c]quinoline (**4k**).* A mixture of substrate **3a** (0.150 g, 0.396 mmol), 3-nitrophenylboronic acid (0.072 g, 0.435 mmol), $Pd(OAc)_2$ (1.8 mg, 2 mol %), and anhydrous K_2CO_3 (0.109 g, 0.79 mmol) in anhydrous NMP (0.6 mL, 1.5 mL $mmol^{-1}$) was reacted according to the general one-pot SM/DA procedure above to give the title product as a yellow solid; yield: 69 mg (51%); m.p. 227−228 °C; IR (NaCl): ν 3392, 1529, 1460, 1348, 1321, 1191 cm^{-1}; ^1H NMR (300 MHz, $CDCl_3$) δ: 7.47−7.64 (m, 2H), 7.72 (t, J = 8.0 Hz, 1H), 7.80 (d, J = 8.0 Hz, 1H), 8.06 (dd, J = 8.8, 2.2 Hz, 1H), 8.10−8.19 (m, 2H), 8.30 (ddd, J = 8.2, 2.2, 1.0 Hz, 1H), 8.40 (d, J = 8.8 Hz, 1H), 8.65−8.73 (m, 2H), 9.55 (s, 1H) ppm; $^{13}C\{^1H\}$ NMR (75 MHz, $CDCl_3$) δ: 112.2, 117.0, 117.4, 119.1, 120.8, 122.3, 122.5, 122.6, 124.3, 127.6, 128.2, 130.0, 131.0, 133.3, 137.1, 141.9, 145.1, 147.0, 148.9, 156.1, 157.5 ppm; HRMS (ESI-TOF) m/z: $[M + H]^+$ calcd for $C_{21}H_{13}N_2O_3$: 341.0921; found: 341.0919.

*8-Chloro-2-phenylbenzofuro[3,2-c]quinoline (**4l**).* A mixture of substrate **3c** (0.200 g, 0.60 mmol), phenylboronic acid (0.080 g, 0.658 mmol), $Pd(OAc)_2$ (2.7 mg, 2 mol %), and anhydrous K_2CO_3 (0.165 g, 1.20 mmol) in anhydrous NMP (0.9 mL, 1.5 mL $mmol^{-1}$) was reacted according to the general one-pot SM/DA procedure above to give the title product as a pale yellow solid; yield: 118 mg (60%); m.p. 213−214 °C; IR (NaCl): ν 3583, 1461, 1359, 1192, 665 cm^{-1}; ^1H NMR (300 MHz, $CDCl_3$) δ: 7.38−7.60 (m, 4H), 7.66 (d, J = 8.8 Hz, 1H), 7.75−7.87 (m, 2H), 7.99−8.12 (m, 2H), 8.31 (d, J = 8.8 Hz, 1H), 8.55 (d, J = 1.8 Hz, 1H), 9.41 (s, 1H) ppm; $^{13}C\{^1H\}$ NMR (75 MHz, $CDCl_3$) δ: 113.1, 115.8, 117.2, 118.4, 120.5, 124.2, 127.4, 127.5, 128.1, 129.1, 129.3, 129.9, 130.4, 140.0, 140.1, 144.0, 147.0, 154.3, 158.4 ppm; HRMS (ESI-TOF) m/z: $[M + H]^+$ calcd for $C_{21}H_{13}ClNO$ 330.0681; found: 330.0684.

*6-Phenylbenzofuro[3,2-c]pyridine (**4m**).* A mixture of substrate **3d** (0.150 g, 0.456 mmol), phenylboronic acid (0.061 g, 0.50 mmol), $Pd(OAc)_2$ (2.0 mg, 2 mol %), and anhydrous K_2CO_3 (0.126 g, 0.912 mmol) in anhydrous NMP (0.7 mL, 1.5 mL $mmol^{-1}$) was reacted according to the general one-pot SM/DA procedure above and purified via column chromatography using 100% Et_2O as an eluent to give the title product as a pale yellow solid; yield: 77 mg (69%); m.p. 66−68 °C; IR (NaCl): ν 3402, 3032, 1577, 1450, 1332, 1168 cm^{-1}; ^1H NMR (300 MHz, $CDCl_3$) δ: 7.35−7.63 (m, 5H), 7.67 (dd, J = 7.6, 1.3 Hz, 1H), 7.83−7.92 (m, 2H), 8.01 (dd, J = 7.7, 1.3 Hz, 1H), 8.67 (d, J = 5.7 Hz, 1H), 9.30 (s, 1H) ppm; $^{13}C\{^1H\}$ NMR (75 MHz, $CDCl_3$) δ: 107.6, 120.1, 121.6, 122.4, 124.4, 126.4, 128.07, 128.13, 128.77, 128.80, 135.8, 143.7, 147.5, 153.1, 160.9 ppm; HRMS (ESI-TOF) m/z: $[M + H]^+$ calcd for $C_{17}H_{12}NO$ 246.0913; found: 246.0914. Note: Here, a second Suzuki−Miyaura reaction occurred in competition with the direct arylation. These products were separable by careful column chromatography.

*3-Phenylbenzofuro[3,2-c]quinoline (**4n**).* A mixture of substrate **3b** (0.200 g, 0.528 mmol), phenylboronic acid (0.071 g, 0.58 mmol), $Pd(OAc)_2$ (2.4 mg, 2 mol %), and anhydrous K_2CO_3 (0.146 g, 1.06 mmol) in anhydrous NMP (0.8 mL, 1.5 mL $mmol^{-1}$) was reacted according to the general one-pot SM/DA procedure above to give the title product as a pale yellow solid; X-ray quality crystals were obtained via vapor diffusion from a saturated solution of toluene in hexane, the CCDC number is 1967484; yield: 146 mg (95%); m.p. 172−173 °C; IR (NaCl): ν 3275, 1559, 1452, 1379, 1188 cm^{-1}; ^1H NMR (300 MHz, $CDCl_3$) δ: 7.37−7.64 (m, 5H), 7.72−7.88 (m, 3H), 7.98 (dd, J = 8.5, 1.7 Hz, 1H), 8.12 (dd, J = 7.5, 1.0 Hz, 1H), 8.42−8.59 (m, 2H), 9.54 (s, 1H) ppm; $^{13}C\{^1H\}$ NMR (75 MHz, $CDCl_3$) δ: 112.2, 116.1, 116.4, 120.6, 121.3, 122.8, 124.1, 126.6, 127.3, 127.5, 127.6, 128.0, 129.1, 140.2, 142.2, 144.9, 147.8, 156.1, 157.5 ppm; HRMS (ESI-TOF) m/z: $[M + H]^+$ calcd for $C_{21}H_{14}NO$ 296.1070; found: 296.1072.

*3-(p-Tolyl)benzofuro[3,2-c]quinoline (**4o**).* A mixture of substrate **3b** (0.150 g, 0.396 mmol), o-tolylboronic acid (0.059 g, 0.435 mmol), $Pd(OAc)_2$ (1.8 mg, 2 mol %), and anhydrous K_2CO_3 (0.109 g, 0.79 mmol) in anhydrous NMP (0.6 mL, 1.5 mL $mmol^{-1}$) was reacted according to the general one-pot SM/DA procedure above to give the title product as a white solid; yield: 90 mg (74%); m.p. 200−202 °C; IR (NaCl): ν 3150, 1554, 1450, 1379, 1190 cm^{-1}; ^1H NMR (300 MHz, $CDCl_3$) δ: 2.45 (s, 3H), 7.34 (d, J = 7.9 Hz, 2H), 7.44−7.60 (m, 2H), 7.66−7.81 (m, 3H), 7.97 (dd, J = 8.5, 1.5 Hz, 1H), 8.11 (dd, J = 7.6, 0.9 Hz, 1H), 8.42−8.52 (m, 2H), 9.51 (s, 1H) ppm; $^{13}C\{^1H\}$ NMR (75 MHz, $CDCl_3$) δ: 21.2, 112.1, 115.9, 116.2, 120.5, 121.1, 122.7, 124.0, 126.4, 127.1, 127.2, 127.3, 129.8, 137.3, 137.9, 142.0,

https://dx.doi.org/10.1021/acs.joc.9b03321
J. Org. Chem. 2020, 85, 2585−2596

144.7, 147.9, 156.0, 157.4 ppm; HRMS (ESI-TOF) m/z: $[M + H]^+$ calcd for $C_{22}H_{16}NO$ 310.1232; found: 310.1244.

*3-(4-(Trifluoromethyl)phenyl)benzofuro[3,2-c]quinoline (**4p**).* A mixture of substrate **3b** (0.150 g, 0.396 mmol), (4-(trifluoromethyl)-phenyl)boronic acid (0.083 g, 0.435 mmol), $Pd(OAc)_2$ (1.8 mg, 2 mol %), and anhydrous K_2CO_3 (0.109 g, 0.79 mmol) in anhydrous NMP (0.6 mL, 1.5 mL $mmol^{-1}$) was reacted according to the general one-pot SM/DA procedure above to give the title product as a yellow solid; yield: 114 mg (79%); m.p. 205−208 °C; IR (NaCl): ν 3251, 1559, 1450, 1329, 1188, 1110 cm^{-1}; ^1H NMR (300 MHz, $CDCl_3$) δ: 7.46−7.63 (m, 2H), 7.76−7.82 (m, 3H), 7.86−8.02 (m, 3H), 8.13 (dd, J = 7.6, 0.9 Hz, 1H), 8.49−8.57 (m, 2H), 9.55 (s, 1H) ppm; $^{13}C\{^1H\}$ NMR (75 MHz, $CDCl_3$) δ: 112.2, 116.7, 120.7, 121.6, 122.6, 124.21, 124.22 (q, $^1J_{(C,F)}$ = 270 Hz), 126.0 (q, $^3J_{(C,F)}$ = 4 Hz), 126.2, 127.5, 127.7, 128.2, 129.9 (q, $^2J_{(C,F)}$ = 32 Hz), 140.4, 143.7, 145.1, 147.6, 156.1, 157.3 ppm; $^{19}F\{^1H\}$ NMR (282 MHz, $CDCl_3$) δ: −62 ppm; HRMS (ESI-TOF) m/z: $[M + H]^+$ calcd for $C_{22}H_{13}F_3NO$ 364.0949; found: 364.0951. Note: ^{13}C NMR shift at 116.7 ppm represents two individual carbon signals as confirmed by 2D NMR experiments.

*4-(Benzofuro[3,2-c]quinolin-3-yl)benzonitrile (**4q**).* A mixture of substrate **3b** (0.150 g, 0.396 mmol), 4-cyanophenylboronic acid (0.065 g, 0.435 mmol), $Pd(OAc)_2$ (4.4 mg, 5 mol %), and anhydrous K_2CO_3 (0.109 g, 0.79 mmol) in anhydrous NMP (0.6 mL, 1.5 mL $mmol^{-1}$) was reacted according to the general one-pot SM/DA procedure above to give the title product as a white solid; yield: 85 mg (67%); m.p. >250 °C; IR (NaCl): ν 3348, 2223, 1553, 1447, 1344, 1184 cm^{-1}; ^1H NMR (300 MHz, $CDCl_3$) δ: 7.45−7.64 (m, 2H), 7.73−7.80 (m, 6H), 8.13 (dd, J = 7.6, 0.8 Hz, 1H), 8.45−8.60 (m, 2H), 9.55 (s, 1H) ppm; $^{13}C\{^1H\}$ NMR (75 MHz, $CDCl_3$) δ: 111.7, 112.3, 116.9, 117.0, 118.8, 120.8, 121.9, 122.6, 124.3, 126.0, 127.6, 128.1, 128.4, 132.9, 139.9, 144.7, 145.3, 147.5, 156.2, 157.2 ppm; HRMS (ESI-TOF) m/z: $[M + H]^+$ calcd for $C_{22}H_{13}N_2O$: 321.1028; found: 321.1033.

*3-(4-Methoxyphenyl)benzofuro[3,2-c]quinoline (**4r**).* A mixture of substrate **3b** (0.150 g, 0.396 mmol), 4-methoxyphenylboronic acid (0.066 g, 0.435 mmol), $Pd(OAc)_2$ (1.8 mg, 2 mol %), and anhydrous K_2CO_3 (0.109 g, 0.79 mmol) in anhydrous NMP (0.6 mL, 1.5 mL $mmol^{-1}$) was reacted according to the general one-pot SM/DA procedure above to give the title product as a white solid; yield: 88 mg (70%); m.p. 157−158 °C; IR (NaCl): ν 3369, 2998, 1607, 1450, 1303, 1245, 1188 cm^{-1}; ^1H NMR (300 MHz, $CDCl_3$) δ: 3.88 (s, 3H), 6.99−7.10 (m, 2H), 7.41−7.57 (m, 2H), 7.68−7.77 (m, 3H), 7.91 (dd, J = 8.6, 1.7 Hz, 1H), 8.07 (dd, J = 7.5, 1.5 Hz, 1H), 8.37−8.45 (m, 2H), 9.47 (s, 1H) ppm; $^{13}C\{^1H\}$ NMR (75 MHz, $CDCl_3$) δ: 55.4, 112.1, 114.5, 115.7, 116.1, 120.5, 121.2, 122.8, 124.1, 126.3, 126.8, 127.1, 128.5, 132.7, 141.7, 144.8, 148.0, 156.0, 157.5, 159.8 ppm; HRMS (ESI-TOF) m/z: $[M + H]^+$ calcd for $C_{22}H_{16}NO_2$ 326.1176; found: 326.1173.

General Procedure for Palladium-Catalyzed One-Pot Mizoroki−Heck and Intramolecular Direct Arylation Reactions. A mixture of the 4-(2-bromophenoxy)quinoline substrate (1 equiv), Heck coupling partner (1.1 equiv), $Pd(OAc)_2$ (2 mol % for *tert*-butyl acrylate or 5 mol % for styrene derivatives), and anhydrous K_2CO_3 (2 equiv) in anhydrous NMP (1.5 mL $mmol^{-1}$) was stirred at 135 °C in a sealed reaction tube in an aluminum multireaction heating mantle until the reaction was completed as evidenced by ^1H NMR analysis (18−24 h). The cooled reaction mixture was diluted with DCM, filtered through a short plug of Celite, and concentrated in vacuo. The crude mixture was purified by column chromatography over silica gel using DCM/EtOAc (99:1−95:5) as an eluent.

*tert-Butyl (E)-3-(Benzofuro[3,2-c]quinolin-2-yl)acrylate (**5a**).* A mixture of substrate **3a** (0.050 g, 0.132 mmol), *tert*-butyl acrylate (21 μL, 0.145 mmol), $Pd(OAc)_2$ (0.6 mg, 2 mol %), and anhydrous K_2CO_3 (0.036 g, 0.264 mmol) in anhydrous NMP (0.2 mL, 1.5 mL $mmol^{-1}$) was reacted according to the general one-pot MH/DA procedure above to give the title product as a white solid; yield: 27 mg (60%); m.p. 169−170 °C; IR (NaCl): ν 3393, 2976, 1701, 1560, 1460, 1366, 1238, 1151 cm^{-1}; ^1H NMR (300 MHz, $CDCl_3$) δ: 1.58 (s, 9H), 6.60 (d, J = 16.0 Hz, 1H), 7.44−7.65 (m, 2H), 7.73−7.89 (m, 2H), 7.94 (dd, J = 8.9, 2.0 Hz, 1H), 8.11 (dd, J = 7.6, 0.8 Hz, 1H), 8.24 (d, J = 8.8 Hz, 1H), 8.51 (d, J = 1.9 Hz, 1H), 9.49 (s, 1H) ppm; $^{13}C\{^1H\}$ NMR (100 MHz, $CDCl_3$) δ: 28.2, 80.9, 112.3, 117.0, 117.3, 120.8, 121.6, 122.0, 122.5, 124.3, 127.4, 127.6, 130.5, 133.4, 142.5, 145.1, 147.9, 156.1, 157.5, 166.1 ppm; HRMS (ESI-TOF) m/z: $[M + H]^+$ calcd for $C_{22}H_{20}NO_3$: 346.1438; found: 346.1434.

*tert-Butyl (E)-3-(Benzofuro[3,2-c]quinolin-3-yl)acrylate (**5b**).* A mixture of substrate **3b** (0.050 g, 0.132 mmol), *tert*-butyl acrylate (21 μL, 0.145 mmol), $Pd(OAc)_2$ (0.6 mg, 2 mol %), and anhydrous K_2CO_3 (0.036 g, 0.264 mmol) in anhydrous NMP (0.2 mL, 1.5 mL $mmol^{-1}$) was reacted according to the general one-pot MH/DA procedure above to give the title product as a pale yellow solid; X-ray quality crystals were obtained via vapor diffusion from a saturated solution of toluene in hexane, the CCDC number is 1967537; yield: 36 mg (80%); m.p. 160−162 °C; IR (NaCl): ν 3393, 2976, 1703, 1560, 1452, 1366, 1285, 1149 cm^{-1}; ^1H NMR (300 MHz, $CDCl_3$) δ: 1.58 (s, 9H), 6.59 (d, J = 16.0 Hz, 1H), 7.44−7.63 (m, 2H), 7.71−7.92 (m, 3H), 8.11 (dd, J = 7.6, 0.8 Hz, 1H), 8.30−8.46 (m, 2H), 9.51 (s, 1H) ppm; $^{13}C\{^1H\}$ NMR (75 MHz, $CDCl_3$) δ: 28.2, 80.8, 112.2, 117.1, 117.7, 120.8, 121.4, 122.0, 122.5, 124.3, 125.1, 127.6, 130.7, 135.6, 142.8, 145.2, 147.4, 156.2, 157.1, 166.0 ppm; HRMS (ESI-TOF) m/z: $[M + H]^+$ calcd for $C_{22}H_{20}NO_3$: 346.1438; found: 346.1432.

*(E)-2-Styrylbenzofuro[3,2-c]quinoline (**5c**).* A mixture of substrate **3a** (0.114 g, 0.30 mmol), styrene (38 μL, 0.33 mmol), $Pd(OAc)_2$ (3.4 mg, 5 mol %), and anhydrous K_2CO_3 (0.083 g, 0.60 mmol) in anhydrous NMP (0.5 mL, 1.5 mL $mmol^{-1}$) was reacted according to the general one-pot MH/DA procedure above to give the title product as a white solid; yield: 70 mg (73%); m.p. 201−202 °C; IR (NaCl) ν 3379, 1662, 1561, 1377, 1188 cm^{-1}; ^1H NMR (300 MHz, $CDCl_3$) δ: 7.22−7.66 (m, 9H), 7.76 (d, J = 8.1 Hz, 1H), 7.98 (dd, J = 8.9, 2.0 Hz, 1H), 8.07 (dd, J = 7.6, 0.8 Hz, 1H), 8.22 (d, J = 8.9 Hz, 1H), 8.39 (d, J = 1.8 Hz, 1H), 9.41 (s, 1H) ppm; $^{13}C\{^1H\}$ NMR (75 MHz, $CDCl_3$) δ: 112.1, 116.7, 117.4, 118.6, 120.7, 122.7, 124.1, 126.8, 127.2, 127.3, 127.8, 128.1, 128.8, 130.1, 130.6, 136.1, 137.0, 143.9, 147.0, 156.0, 157.4 ppm; HRMS (ESI-TOF) m/z: $[M + H]^+$ calcd for $C_{23}H_{16}NO$ 322.1226; found: 322.1223.

*(E)-2-(4-Methoxystyryl)benzofuro[3,2-c]quinoline (**5d**).* A mixture of substrate **3a** (0.114 g, 0.30 mmol), 4-methoxystyrene (44 μL, 0.33 mmol), $Pd(OAc)_2$ (3.4 mg, 5 mol %), and anhydrous K_2CO_3 (0.083 g, 0.60 mmol) in anhydrous NMP (0.5 mL, 1.5 mL $mmol^{-1}$) was reacted according to the general one-pot MH/DA procedure above to give the title product as a white solid; yield: 86 mg (82%); m.p. 190−192 °C; IR (NaCl) ν 3388, 1656, 1602, 1562, 1346, 1250, 1110 cm^{-1}; ^1H NMR (300 MHz, $CDCl_3$) δ: 3.86 (s, 3H), 6.84−7.04 (m, 2H), 7.12−7.38 (m, 2H), 7.40−7.65 (m, 4H), 7.76 (d, J = 8.1 Hz, 1H), 7.97 (dd, J = 8.9, 1.8 Hz, 1H), 8.09 (d, J = 7.4 Hz, 1H), 8.21 (d, J = 8.9 Hz, 1H), 8.38 (d, J = 1.7 Hz, 1H), 9.41 (s, 1H) ppm; $^{13}C\{^1H\}$ NMR (75 MHz, $CDCl_3$) δ: 55.4, 112.1, 114.3, 116.7, 117.5, 118.1, 120.7, 122.8, 124.1, 125.7, 127.2, 127.3, 128.0, 129.8, 130.1, 130.2, 136.5, 143.7, 146.9, 156.0, 157.4, 159.7 ppm; HRMS (ESI-TOF) m/z: $[M + H]^+$ calcd for $C_{24}H_{18}NO_2$ 352.1332; found: 352.1328.

*(E)-2-(4-Fluorostyryl)benzofuro[3,2-c]quinoline (**5e**).* A mixture of substrate **3a** (0.114 g, 0.30 mmol), 4-fluorostyrene (39 μL, 0.33 mmol), $Pd(OAc)_2$ (3.4 mg, 5 mol %), and anhydrous K_2CO_3 (0.083 g, 0.60 mmol) in anhydrous NMP (0.5 mL, 1.5 mL $mmol^{-1}$) was reacted according to the general one-pot MH/DA procedure above to give the title product as a yellow solid; yield: 82 mg (80%); m.p. 189−191 °C; IR (NaCl) ν 3404, 1676, 1598, 1559, 1346, 1234, 1096 cm^{-1}; ^1H NMR (300 MHz, $CDCl_3$) δ: 7.00−7.15 (m, 2H), 7.17−7.34 (m, 2H), 7.41−7.63 (m, 4H), 7.75 (d, J = 8.1 Hz, 1H), 7.95 (dd, J = 8.9, 2.0 Hz, 1H), 8.07 (d, J = 7.5 Hz, 1H), 8.21 (d, J = 8.9 Hz, 1H), 8.37 (d, J = 1.8 Hz, 1H), 9.41 (s, 1H) ppm; $^{13}C\{^1H\}$ NMR (75 MHz, $CDCl_3$) δ: 112.1, 115.8 (d, $^2J_{(C,F)}$ = 22 Hz), 116.7, 117.4, 118.6, 120.7, 122.7, 124.1, 127.1, 127.3, 127.6 (d, $^6J_{(C,F)}$ = 2 Hz), 128.3 (d, $^3J_{(C,F)}$ = 8 Hz), 129.4, 130.2, 133.2 (d, $^4J_{(C,F)}$ = 3 Hz), 135.9, 144.0, 147.0, 156.0, 157.4, 162.6 (d, $^1J_{(C,F)}$ = 248 Hz) ppm; $^{19}F\{^1H\}$ NMR (282 MHz, $CDCl_3$) δ: −113 ppm; HRMS (ESI-TOF) m/z: $[M + H]^+$ calcd for $C_{23}H_{15}FNO$ 340.1132; found: 340.1135.

https://dx.doi.org/10.1021/acs.joc.9b03321
J. Org. Chem. 2020, 85, 2585−2596

*(E)-3-Styrylbenzofuro[3,2-c]quinoline (**5f**).* A mixture of substrate **3b** (0.114 g, 0.30 mmol), styrene (38 μL, 0.33 mmol), $Pd(OAc)_2$ (3.4 mg, 5 mol %), and anhydrous K_2CO_3 (0.083 g, 0.60 mmol) in anhydrous NMP (0.5 mL, 1.5 mL $mmol^{-1}$) was reacted according to the general one-pot MH/DA procedure above to give the title product as a yellow solid; yield: 72 mg (75%); m.p. 179−182 °C; IR (NaCl) ν 3583, 1656, 1632, 1561, 1348, 1190 cm^{-1}; ^1H NMR (300 MHz, $CDCl_3$) δ: 7.20−7.65 (m, 9H), 7.74 (d, J = 7.9 Hz, 1H), 7.91 (dd, J = 8.6, 1.5 Hz, 1H), 8.07 (dd, J = 7.5, 0.9 Hz, 1H), 8.27 (d, J = 1.3 Hz, 1H), 8.36 (d, J = 8.6 Hz, 1H), 9.46 (s, 1H) ppm; $^{13}C\{^1H\}$ NMR (75 MHz, $CDCl_3$) δ: 112.1, 116.3, 120.6, 121.1, 122.7, 124.1, 124.9, 126.8, 127.2, 128.0, 128.1, 128.8, 130.7, 137.0, 138.5, 144.8, 147.9, 156.1, 157.4 ppm; HRMS (ESI-TOF) m/z: $[M + H]^+$ calcd for $C_{23}H_{16}NO$ 322.1226; found: 322.1227. Note: ^{13}C NMR shifts at 116.3 and 128.1 ppm represent two individual carbon signals as confirmed by 2D NMR experiments.

*(E)-3-(4-Methoxystyryl)benzofuro[3,2-c]quinoline (**5g**).* A mixture of substrate **3b** (0.114 g, 0.30 mmol), 4-methoxystyrene (44 μL, 0.33 mmol), $Pd(OAc)_2$ (3.4 mg, 5 mol %), and anhydrous K_2CO_3 (0.083 g, 0.60 mmol) in anhydrous NMP (0.5 mL, 1.5 mL $mmol^{-1}$) was reacted according to the general one-pot MH/DA procedure above to give the title product as a yellow solid; yield: 84 mg (80%); m.p. 168−170 °C; IR (NaCl) ν 3379, 1687, 1603, 1560, 1347, 1176, 1033 cm^{-1}; ^1H NMR (300 MHz, $CDCl_3$) δ: 3.86 (s, 3H), 6.89−7.00 (m, 2H), 7.13−7.39 (m, 2H), 7.42−7.65 (m, 4H), 7.75 (d, J = 7.8 Hz, 1H), 7.92 (dd, J = 8.6, 1.5 Hz, 1H), 8.09 (dd, J = 7.2, 1.3 Hz, 1H), 8.27 (d, J = 1.2 Hz, 1H), 8.38 (d, J = 8.6 Hz, 1H), 9.47 (s, 1H) ppm; $^{13}C\{^1H\}$ NMR (75 MHz, $CDCl_3$) δ: 55.4, 112.1, 114.3, 116.0, 116.2, 120.5, 121.0, 122.8, 124.1, 124.8, 126.0, 127.1, 127.5, 128.1, 129.8, 130.3, 138.9, 144.7, 148.0, 156.0, 157.4, 159.7 ppm; HRMS (ESI-TOF) m/z: $[M + H]^+$ calcd for $C_{24}H_{18}NO_2$ 352.1332; found: 352.1333.

*(E)-3-(4-Fluorostyryl)benzofuro[3,2-c]quinoline (**5h**).* A mixture of substrate **3b** (0.114 g, 0.30 mmol), 4-fluorostyrene (39 μL, 0.33 mmol), $Pd(OAc)_2$ (3.4 mg, 5 mol %), and anhydrous K_2CO_3 (0.083 g, 0.60 mmol) in anhydrous NMP (0.5 mL, 1.5 mL $mmol^{-1}$) was reacted according to the general one-pot MH/DA procedure above to give the title product as a yellow solid; yield: 63 mg (62%); m.p. 209−211 °C; IR (NaCl) ν 3049, 1682, 1637, 1508, 1347, 1228, 1012 cm^{-1}; ^1H NMR (300 MHz, $CDCl_3$) δ: 7.02−7.16 (m, 2H), 7.20−7.38 (m, 2H), 7.42−7.64 (m, 4H), 7.76 (dd, J = 7.6, 0.7 Hz, 1H), 7.91 (dd, J = 8.6, 1.6 Hz, 1H), 8.04−8.15 (m, 1H), 8.28 (d, J = 1.4 Hz, 1H), 8.39 (d, J = 8.6 Hz, 1H), 9.48 (s, 1H), ppm; $^{13}C\{^1H\}$ NMR (75 MHz, $CDCl_3$) δ: 112.1, 115.8 (d, $^2J_{(C,F)}$ = 22 Hz), 116.31, 116.34, 120.6, 121.1, 122.7, 124.1, 124.8, 127.3, 127.86, 127.89, 128.3 (d, $^3J_{(C,F)}$ = 8 Hz), 129.4, 133.2 (d, $^4J_{(C,F)}$ = 3 Hz), 138.3, 144.8, 147.9, 156.0, 157.4, 162.6 (d, $^1J_{(C,F)}$ = 248 Hz) ppm; $^{19}F\{^1H\}$ NMR (282 MHz, $CDCl_3$) δ: −113 ppm; HRMS (ESI-TOF) m/z: $[M + H]^+$ calcd for $C_{23}H_{15}FNO$ 340.1132; found: 340.1135.

General Procedure for the Synthesis of Phenoxy-Substituted SM/DA and MH/DA Products. The same procedures and purification methods outlined for the SM/DA and MH/DA reactions were employed here using 4-(2,4-dibromphenoxy)quinoline **3e** (1 equiv) as the substrate.

*8-Phenylbenzofuro[3,2-c]quinoline (**6a**).* A mixture of substrate **3e** (0.200 g, 0.528 mmol), phenylboronic acid (0.071 g, 0.58 mmol), $Pd(OAc)_2$ (2.4 mg, 2 mol %), and anhydrous K_2CO_3 (0.146 g, 1.06 mmol) in anhydrous NMP (0.8 mL, 1.5 mL $mmol^{-1}$) was reacted according to the general one-pot SM/DA procedure above to give the title product as a yellow solid; yield: 103 mg (65%); m.p. 153−155 °C; IR (NaCl): ν 2922, 1567, 1460, 1325, 1202 cm^{-1}; ^1H NMR (300 MHz, $CDCl_3$) δ: 7.36−7.45 (m, 1H), 7.46−7.56 (m, 2H), 7.67−7.86 (m, 6H), 8.24−8.35 (m, 2H), 8.45 (dd, J = 8.1, 1.6 Hz, 1H), 9.55 (s, 1H) ppm; $^{13}C\{^1H\}$ NMR (75 MHz, $CDCl_3$) δ: 112.2, 116.4, 117.2, 119.1, 120.8, 123.3, 126.7, 127.1, 127.4, 127.5, 128.9, 129.4, 129.9, 137.9, 140.9, 144.4, 147.5, 155.5, 158.0 ppm; HRMS (ESI-TOF) m/z: $[M + H]^+$ calcd for $C_{21}H_{14}NO$ 296.1070; found: 296.1072.

*tert-Butyl (E)-3-(Benzofuro[3,2-c]quinolin-8-yl)acrylate (**6b**).* A mixture of substrate **3e** (0.076 g, 0.20 mmol), *tert*-butyl acrylate (32 μL, 0.22 mmol), $Pd(OAc)_2$ (0.9 mg, 2 mol %), and anhydrous K_2CO_3 (0.055 g, 0.40 mmol) in anhydrous NMP (0.3 mL, 1.5 mL $mmol^{-1}$) was reacted according to the general one-pot MH/DA procedure above to give the title product as a white solid; yield: 50 mg (73%); m.p. 157−158 °C; IR (NaCl) ν 3434, 1703, 1638, 1594, 1566, 1367, 1203, 1151 cm^{-1}; ^1H NMR (300 MHz, $CDCl_3$) δ: 1.58 (s, 9H), 6.47 (d, J = 15.9 Hz, 1H), 7.50−7.89 (m, 5H), 8.09−8.30 (m, 2H), 8.36 (dd, J = 8.1, 1.1 Hz, 1H), 9.45 (s, 1H) ppm; $^{13}C\{^1H\}$ NMR (75 MHz, $CDCl_3$) δ: 28.3, 80.7, 112.5, 115.9, 117.1, 120.2, 120.4, 120.8, 123.5, 127.22, 127.24, 129.6, 130.0, 131.2, 143.0, 144.3, 147.7, 156.7, 158.2, 166.2 ppm; HRMS (ESI-TOF) m/z: $[M + H]^+$ $C_{22}H_{20}NO_3$: 346.1438; found: 346.1430.

*(E)-8-Styrylbenzofuro[3,2-c]quinoline (**6c**).* A mixture of substrate **3e** (0.076 g, 0.20 mmol), styrene (25 μL, 0.22 mmol), $Pd(OAc)_2$ (2.5 mg, 5 mol %), and anhydrous K_2CO_3 (0.055 g, 0.40 mmol) in anhydrous NMP (0.3 mL, 1.5 mL $mmol^{-1}$) was reacted according to the general one-pot MH/DA procedure above to give the title product as a yellow solid; yield: 25 mg (40%); m.p. 200−203 °C; IR (NaCl) ν 3583, 1650, 1598, 1567, 1324, 1195 cm^{-1}; ^1H NMR (300 MHz, $CDCl_3$) δ: 7.11−7.47 (m, 5H), 7.55−7.61 (m, 2H), 7.63−7.87 (m, 4H), 8.11−8.32 (m, 2H), 8.39 (dd, J = 8.1, 1.3 Hz, 1H), 9.50 (s, 1H) ppm; $^{13}C\{^1H\}$ NMR (75 MHz, $CDCl_3$) δ: 112.2, 116.2, 117.2, 118.2, 120.8, 123.3, 126.0, 126.5, 127.1, 127.8, 128.1, 128.8, 128.9, 129.4, 129.9, 133.9, 137.2, 144.4, 147.5, 155.6, 158.0 ppm; HRMS (ESI-TOF) m/z: $[M + H]^+$ calcd for $C_{23}H_{16}NO$ 322.1226; found: 322.1223.

General Procedure for the Synthesis of Three-Component SM/DA and MH/DA Products. The same procedures and purification methods outlined for the SM/DA and MH/DA reactions were employed here using bromo-4-(2,4-dibromphenoxy)quinoline (1 equiv) as the substrate and double the equivalent of coupling partner (2.2 equiv).

*2,8-Diphenylbenzofuro[3,2-c]quinoline (**7a**).* A mixture of substrate **3f** (0.200 g, 0.437 mmol), phenylboronic acid (0.117 g, 0.96 mmol), $Pd(OAc)_2$ (2.0 mg, 2 mol %), and anhydrous K_2CO_3 (0.121 g, 0.873 mmol) in anhydrous NMP (0.7 mL, 1.5 mL $mmol^{-1}$) was reacted according to the general one-pot SM/DA procedure above to give the title product as a pale yellow solid; yield: 129 mg (80%); m.p. 206−207 °C; IR (NaCl): ν 3054, 2920, 1682, 1560, 1460, 1358, 1200 cm^{-1}; ^1H NMR (300 MHz, $CDCl_3$) δ: 7.37−7.60 (m, 6H), 7.68−7.88 (m, 6H), 8.07 (dd, J = 8.8, 2.1 Hz, 1H), 8.28−8.40 (m, 2H), 8.64 (d, J = 1.7 Hz, 1H), 9.54 (s, 1H) ppm; $^{13}C\{^1H\}$ NMR (75 MHz, $CDCl_3$) δ: 112.2, 116.6, 117.4, 118.4, 119.1, 123.3, 126.8, 127.4, 127.50, 127.54, 128.0, 128.9, 129.0, 130.3, 137.9, 139.8, 140.1, 140.9, 144.2, 146.8, 155.5, 158.1 ppm; HRMS (ESI-TOF) m/z: $[M + H]^+$ calcd for $C_{27}H_{18}NO$ 372.1388; found: 372.1384. Note: ^{13}C NMR shift at 128.9 ppm represents two individual carbon signals as confirmed by 2D NMR experiments.

*Di-tert-butyl 3,3′-(Benzofuro[3,2-c]quinoline-3,8-diyl)(2E,2′E)-diacrylate (**7b**).* A mixture of substrate **3g** (0.050 g, 0.11 mmol), *tert*-butyl acrylate (35 μL, 0.242 mmol), $Pd(OAc)_2$ (0.5 mg, 2 mol %), and anhydrous K_2CO_3 (0.030 g, 0.22 mmol) in anhydrous NMP (0.3 mL, 1.5 mL $mmol^{-1}$) was reacted according to the general one-pot MH/DA procedure above to give the title product as a white solid; yield: 23 mg (43%); m.p. 217−219 °C; IR (NaCl) ν 3402, 1703, 1638, 1559, 1512, 1368, 1201, 1148 cm^{-1}; ^1H NMR (300 MHz, $CDCl_3$) δ: 1.50−1.61 (m, 18H), 6.40−6.67 (m, 2H), 7.66−7.94 (m, 5H), 8.23 (d, J = 0.8 Hz, 1H), 8.29−8.44 (m, 2H), 9.49 (s, 1H) ppm; $^{13}C\{^1H\}$ NMR (75 MHz, $CDCl_3$) δ: 28.22, 28.24, 80.7, 80.9, 112.6, 116.6, 117.6, 120.3, 120.5, 121.4, 122.3, 123.3, 125.3, 127.5, 130.7, 131.4, 136.0, 142.7, 142.8, 145.0, 147.7, 156.9, 157.8, 166.0, 166.1 ppm; HRMS (ESI-TOF) m/z: $[M + H]^+$ calcd for $C_{29}H_{30}NO_5$: 472.2118; found: 472.2117.

*3,8-Di((E)-styryl)benzofuro[3,2-c]quinoline (**7c**).* A mixture of substrate **3g** (0.115 g, 0.25 mmol), styrene (63 μL, 0.55 mmol), $Pd(OAc)_2$ (2.8 mg, 5 mol %), and anhydrous K_2CO_3 (0.069 g, 0.50 mmol) in anhydrous NMP (0.4 mL, 1.5 mL $mmol^{-1}$) was reacted according to the general one-pot MH/DA procedure above to give the title product as a white solid; yield: 76 mg (36%); m.p. >250 °C; IR (NaCl) ν 3387, 1691, 1594, 1560, 1326, 1044 cm^{-1}; ^1H NMR (600 MHz, $(CD_3)_2SO$) δ: 7.20−7.54 (m, 9H), 7.59 (app. s, 2H), 7.63−7.75 (m, 4H), 7.87 (dd, J = 8.6, 1.6 Hz, 1H), 7.94 (d, J = 8.5

https://dx.doi.org/10.1021/acs.joc.9b03321
J. Org. Chem. 2020, 85, 2585−2596

Hz, 1H), 8.17 (dd, J = 8.7, 1.4 Hz, 1H), 8.35 (d, J = 1.3 Hz, 1H), 8.41 (d, J = 8.5 Hz, 1H), 8.61 (d, J = 1.5 Hz, 1H), 9.69 (s, 1H) ppm; $^{13}C\{^1H\}$ NMR (150 MHz, $(CD_3)_2SO$) δ: 112.8, 115.9, 116.4, 119.1, 121.4, 123.2, 127.0, 127.2, 127.3, 128.29, 128.33, 128.6, 129.0, 129.3, 131.2, 134.3, 137.3, 137.5, 139.0, 146.0, 148.1, 155.5, 157.4 ppm; HRMS (ESI-TOF) m/z: $[M + H]^+$ calcd for $C_{31}H_{22}NO$ 424.1696; found: 424.1690. Note: This compound was highly insoluble, spectra were acquired on <3 mg of this compound after heating in $(CD_3)_2SO$, and it was difficult to directly assign. As with other compounds, some ^{13}C shifts from this spectrum represent more than one signal as confirmed by 2D NMR experiments.

Isolation of Suzuki−Miyaura Only Products. To further probe the hypothesis that the Suzuki−Miyaura reaction was occurring at the C-6 position before direct arylation at the C-3 position, substrate **3i** was synthesized. This substrate could only undergo the Suzuki−Miyaura reaction and proceeded as anticipated (Supporting Information Scheme S1).

*4-Phenoxy-6-phenylquinoline (**4s**).* A mixture of substrate **3i** (0.200 g, 0.666 mmol, 1 equiv), phenylboronic acid (0.081 g, 0.666 mmol, 1 equiv), $Pd(OAc)_2$ (3.0 mg, 2 mol %), and anhydrous K_2CO_3 (0.184 g, 1.333 mmol, 2 equiv) in anhydrous NMP (1.0 mL, 1.5 mL $mmol^{-1}$) was stirred at 135 °C in a sealed reaction tube in an aluminum multireaction heating mantle until the reaction was completed as evidenced by ^1H NMR analysis (4 h). The cooled reaction mixture was diluted with DCM, filtered through a short plug of Celite, and concentrated in vacuo. The crude mixture was purified by column chromatography over silica gel using Hex/EtOAc (7:3−6:4) as an eluent to give the title product as a pale yellow solid; yield: 168 mg (84%); m.p. 78−80 °C; IR (NaCl): ν 3058, 1562, 1487, 1460, 1360, 1203 cm^{-1}; ^1H NMR (300 MHz, $CDCl_3$) δ: 6.58 (d, J = 5.1 Hz, 1H), 7.16−7.57 (m, 8H), 7.72−7.74 (m, 2H), 8.03 (dd, J = 8.8, 2.1 Hz, 1H), 8.17 (d, J = 8.8 Hz, 1H), 8.58 (d, J = 2.0 Hz, 1H), 8.67 (d, J = 4.9 Hz, 1H) ppm; $^{13}C\{^1H\}$ NMR (75 MHz, $CDCl_3$) δ: 104.6, 119.6, 121.2, 121.7, 125.7, 127.5, 127.7, 129.0, 129.6, 129.8, 130.3, 139.0, 140.5, 149.1, 151.1, 154.4, 162.1 ppm; HRMS (ESI-TOF) m/z: $[M + H]^+$ calcd for $C_{21}H_{16}NO$ 298.1226; found: 298.1228.

The tandem reaction was carried out on **3a** at a lower temperature to see if the Suzuki−Miyaura only product could be isolated and prove that it was happening prior to the direct arylation reaction. At this temperature, the major product was the uncyclized Suzuki−Miyaura product **4t**, although some of the tandem product **4a** and starting material **3a** were also isolated (Supporting Information Scheme S2).

*4-(2-Bromophenoxy)-6-phenylquinoline (**4t**).* A mixture of substrate **3a** (0.150 g, 0.396 mmol), phenylboronic acid (0.048 g, 0.396 mmol), $Pd(OAc)_2$ (1.8 mg, 2 mol %), and anhydrous K_2CO_3 (0.109 g, 0.79 mmol) in anhydrous NMP (0.6 mL, 1.5 mL $mmol^{-1}$) was stirred at 100 °C in a sealed reaction tube in an aluminum multireaction heating mantle for 24 h. The cooled reaction mixture was diluted with DCM, filtered through a short plug of Celite, and concentrated in vacuo. The crude mixture was purified by column chromatography over silica gel using Hex/EtOAc (8:2−7:3) as an eluent to give the title product as a pale yellow solid; yield: 73 mg (49%); m.p. 85−87 °C; IR (NaCl): ν 3059, 1564, 1460, 1361, 1222, 667 cm^{-1}; ^1H NMR (300 MHz, $CDCl_3$) δ: 6.43 (d, J = 5.2 Hz, 1H), 7.16−7.32 (m, 2H), 7.34−7.57 (m, 4H), 7.70−7.84 (m, 3H), 8.05 (dd, J = 8.8, 2.1 Hz, 1H), 8.20 (d, J = 8.7 Hz, 1H), 8.62 (d, J = 2.0 Hz, 1H), 8.69 (d, J = 5.3 Hz, 1H) ppm; $^{13}C\{^1H\}$ NMR (75 MHz, $CDCl_3$) δ: 103.9, 116.4, 119.6, 121.3, 123.3, 127.6, 127.9, 129.0, 129.3, 130.2, 134.4, 139.4, 140.3, 148.2, 150.5, 151.0, 161.5 ppm; HRMS (ESI-TOF) m/z: $[M + H]^+$ calcd for $C_{21}H_{15}BrNO$ 376.0332; found: 376.0331. Note: ^{13}C NMR shifts at 127.6 and 129.0 ppm each represent two individual carbon signals as confirmed by 2D NMR experiments.

The Synthesis of Palladium−Quinoline Complexes. *4-(2-Bromophenoxy)quinoline Palladium Diacetate Dimer (**8a**).* To an NMR tube were added **1** (61.5 mg, 0.204 mmol, 1.0 equiv), $Pd(OAc)_2$ (22.9 mg, 0.102 mmol, 0.5 equiv), and $CDCl_3$ (0.6 mL); X-ray quality crystals were obtained via vapor diffusion from a saturated solution of toluene/methanol in hexane, the CCDC number is 1970630; decomposition >150 °C; IR (NaCl) ν 3436, 1615, 1589, 1573, 1303, 1217, 1075, 695 cm^{-1}; ^1H NMR (300 MHz, $CDCl_3$) δ: 1.53 (s, 6H), 6.47 (d, J = 6.2 Hz, 2H), 7.11−7.34 (m, 4H), 7.37−7.54 (m, 2H), 7.59−7.84 (m, 4H), 8.08 (ddd, J = 8.6, 7.0, 1.4 Hz, 2H), 8.41 (dd, J = 8.1, 0.9 Hz, 2H), 9.46 (d, J = 6.2 Hz, 2H), 10.20 (d, J = 8.6 Hz, 2H) ppm; $^{13}C\{^1H\}$ NMR (150 MHz, $CDCl_3$) δ: 22.6, 103.9, 116.2, 121.3, 122.0, 123.4, 127.4, 128.1, 129.0, 129.4, 132.1, 134.5, 147.9, 150.2, 156.1, 162.6, 178.3 ppm; HRMS (ESI-TOF) m/z: $[M - OAc]^+$ calcd for $C_{32}H_{23}Br_2N_2O_4Pd$ 762.9054; found: 762.9081.

*7-Bromo-4-(2-bromophenoxy)quinoline Palladium Diacetate Dimer (**8b**).* To an NMR tube were added **3b** (60.8 mg, 0.160 mmol, 1.0 equiv), $Pd(OAc)_2$ (18.0 mg, 0.080 mmol, 0.5 equiv), and $CDCl_3$ (0.6 mL). Decomposition >190 °C; IR (NaCl) ν 3419, 1623, 1590, 1511, 1306, 1219, 1063, 733, 693 cm^{-1}; ^1H NMR (600 MHz, $CDCl_3$) δ: 1.59 (s, 6H), 6.46 (d, J = 6.2 Hz, 2H), 7.16−7.37 (m, 4H), 7.41−7.57 (m, 2H), 7.66−7.93 (m, 4H), 8.29 (d, J = 8.8 Hz, 2H), 9.43 (d, J = 6.2 Hz, 2H), 10.36 (d, J = 1.7 Hz, 2H) ppm; $^{13}C\{^1H\}$ NMR (150 MHz, $CDCl_3$) δ: 22.7, 104.2, 116.1, 120.1, 123.3, 123.5, 127.0, 128.4, 129.6, 131.2, 134.6, 148.4, 149.9, 157.4, 162.8, 178.4 ppm; HRMS (ESI-TOF) m/z: $[M - OAc]^+$ calcd for $C_{32}H_{21}Br_4N_2O_4Pd$ 918.7264; found: 918.7284. Note: ^{13}C NMR shift at 131.2 ppm represents two individual carbon signals as confirmed by 2D NMR experiments.

*4-Phenoxyquinoline Palladium Diacetate Dimer (**8c**).* To 25 mL of RBF were added **3h** (55.0 mg, 0.249 mmol, 1.0 equiv), $Pd(OAc)_2$ (27.9 mg, 0.124 mmol, 0.5 equiv), and $CDCl_3$ (2 mL); X-ray quality crystals were obtained via vapor diffusion from a saturated solution of toluene/methanol in hexane, the CCDC number is 1970507; decomposition >150 °C; IR (NaCl) ν 3413, 1621, 1595, 1305, 1512, 1203, 1063 cm^{-1}; ^1H NMR (300 MHz, $CDCl_3$) δ: 1.53 (s, 6H), 6.50 (d, J = 6.2 Hz, 2H), 7.03−7.21 (m, 4H), 7.23−7.51 (m, 6H), 7.61 (ddd, J = 8.2, 7.0, 1.0 Hz, 2H), 7.99 (ddd, J = 8.6, 7.0, 1.4 Hz, 2H), 8.28 (dd, J = 8.4, 1.0 Hz, 2H), 9.34 (d, J = 6.2 Hz, 2H), 10.08 (d, J = 8.6 Hz, 2H) ppm; $^{13}C\{^1H\}$ NMR (75 MHz, $CDCl_3$) δ: 22.7, 104.3, 121.4, 121.8, 122.0, 126.7, 127.3, 129.1, 130.7, 132.0, 148.0, 153.4, 156.1, 163.9, 178.3 ppm; HRMS (ESI-TOF) m/z: $[M - OAc]^+$ calcd for $C_{32}H_{25}N_2O_4Pd$ 607.0844; found: 607.0849.

Experiments To Prove Viability of Palladium−Quinoline Complexes. 1. A 0.062 M stock solution of **8c** in $CDCl_3$ was prepared, and 0.1 mL (4.1 mg, 2 mol %) was transferred to a reaction tube and concentrated in vacuo to give a yellow residue. To the tube containing this residue were added substrate **3a** (0.118 g, 0.310 mmol, 1 equiv), phenylboronic acid (0.042 g, 0.341 mmol, 1.1 equiv), anhydrous K_2CO_3 (0.086 g, 0.62 mmol), and NMP (0.5 mL, 1.5 mL $mmol^{-1}$). The resulting mixture was stirred at 135 °C in the sealed reaction tube in an aluminum multireaction heating mantle until the reaction was complete as evidenced by ^1H NMR analysis (20 h). The cooled reaction mixture was diluted with DCM, filtered through a short plug of Celite, and concentrated in vacuo. A yield of 81% **4a** was determined by ^1H NMR analysis of the crude reaction mixture using 1,3,5-trimethoxybenzene as an internal standard (Scheme 4a).

2. A 0.062 M stock solution of **8c** in $CDCl_3$ was prepared, and 0.1 mL (4.1 mg, 2 mol %) was transferred to a reaction tube and concentrated in vacuo to give a yellow residue. To the tube containing this residue were added substrate **1** (0.093 g, 0.310 mmol, 1 equiv), anhydrous K_2CO_3 (0.086 g, 0.62 mmol), and NMP (0.5 mL, 1.5 mL $mmol^{-1}$). The resulting mixture was stirred at 135 °C in the sealed reaction tube in an aluminum multireaction heating mantle until the reaction was complete as evidenced by ^1H NMR analysis (20 h). The cooled reaction mixture was diluted with DCM, filtered through a short plug of Celite, and concentrated in vacuo. A 99% yield of **2** was determined by ^1H NMR analysis of the crude reaction mixture using 1,3,5-trimethoxybenzene as an internal standard (Supporting Information Scheme S3).

3. A 0.10 M stock solution of **8a** in $CHCl_3$ was prepared, and 0.2 mL (16.5 mg, 10 mol %) was transferred to a reaction tube and concentrated in vacuo to give a yellow residue. To the tube containing this residue were added substrate **3a** (0.076 g, 0.20 mmol, 1 equiv), phenylboronic acid (0.027 g, 0.22 mmol, 1.1 equiv), anhydrous

https://dx.doi.org/10.1021/acs.joc.9b03321
J. Org. Chem. 2020, 85, 2585−2596

K_2CO_3 (0.055 g, 0.40 mmol), and NMP (0.3 mL, 1.5 mL $mmol^{-1}$). The resulting mixture was stirred at 135 °C in the sealed reaction tube in an aluminum multi-reaction heating mantle until the reaction was complete as evidenced by ^1H NMR analysis (18 h). The cooled reaction mixture was diluted with DCM, filtered through a short plug of Celite, and concentrated in vacuo. Upon analysis of the crude reaction mixture, no starting material remained, and the peaks for both products **4a** and **2** were present. The signals for **4a** and **2** were too close to obtain accurate NMR yields and were nonseparable by column chromatography (Scheme 4b).

■ ASSOCIATED CONTENT

Supporting Information

The Supporting Information is available free of charge at https://pubs.acs.org/doi/10.1021/acs.joc.9b03321.

Copies of the ^1H, ^{13}C, and ^1H-^{15}N HMBC NMR spectra, additional experiments, X-ray crystallography data, HRMS data for metal-containing complexes, fluorescence emission, and UV−Vis absorption data (PDF)

X-ray crystallography data for **4a**, **4n**, **5b**, **8a**, and **8c** (CIF)

■ AUTHOR INFORMATION

Corresponding Author

Gerard P. McGlacken − *School of Chemistry, Analytical and Biological Chemistry Research Facility (ABCRF) and Synthesis and Solid State Pharmaceutical Centre (SSPC), University College Cork, Cork T12 YN60, Ireland;* orcid.org/0000-0002-7821-0804; Email: g.mcglacken@ucc.ie

Authors

Rachel M. Shanahan − *School of Chemistry, Analytical and Biological Chemistry Research Facility (ABCRF), University College Cork, Cork T12 YN60, Ireland*

Aobha Hickey − *School of Chemistry, Analytical and Biological Chemistry Research Facility (ABCRF), University College Cork, Cork T12 YN60, Ireland*

Lorraine M. Bateman − *School of Chemistry, Analytical and Biological Chemistry Research Facility (ABCRF), Synthesis and Solid State Pharmaceutical Centre (SSPC), and School of Pharmacy, University College Cork, Cork T12 YN60, Ireland*

Mark E. Light − *Department of Chemistry, University of Southampton, Southampton SO17 1BJ, United Kingdom*

Complete contact information is available at: https://pubs.acs.org/10.1021/acs.joc.9b03321

Author Contributions

⊥R.M.S. and A.H. contributed equally.

Notes

The authors declare no competing financial interest.

■ ACKNOWLEDGMENTS

The authors would like to thank Dr. Trevor Carey, Prof John Sodeau, Dr. Peter Byrne, and Dr. Leticia Pardo for useful discussion. The authors acknowledge the Irish Research Council (IRC) and Science Foundation Ireland (SFI) (grant number SFI/12/IP/1315) and the Synthesis and Solid State Pharmaceutical Centre (SSPC) (SFI/12/RC/2275 and SFI/12/RC/2275_P2). The authors thank the European Cooperation in Science and Technology COST initiative for funding CA15106, C-H Activation in Organic Synthesis (CHAOS). This publication has emanated from research conducted with the financial support of SFI through a research infrastructure award for process flow spectroscopy (Prospect) under the grant number 15/RI/3221.

■ REFERENCES

(1) (a) Hayashi, Y. Pot economy and one-pot synthesis. *Chem. Sci.* **2016**, *7*, 866−880. (b) Vaxelaire, C.; Winter, P.; Christmann, M. One-Pot Reactions Accelerate the Synthesis of Active Pharmaceutical Ingredients. *Angew. Chem., Int. Ed.* **2011**, *50*, 3605−3607.

(2) Dobrounig, P.; Trobe, M.; Breinbauer, R. Sequential and iterative Pd-catalyzed cross-coupling reactions in organic synthesis. *Monatsh. Chem.* **2017**, *148*, 3−35.

(3) Majumdar, K. C.; Chattopadhyay, S. K. *Heterocycles in Natural Product Synthesis*; John Wiley & Sons: Weinheim, Germany, 2011.

(4) Taylor, R. D.; MacCoss, M.; Lawson, A. D. G. Rings in Drugs. *J. Med. Chem.* **2014**, *57*, 5845−5859.

(5) Shanahan, R. M.; Hickey, A.; Reen, F. J.; O'Gara, F.; McGlacken, G. P. Synthesis of Benzofuroquinolines via Phosphine-Free Direct Arylation of 4-Phenoxyquinolines in Air. *Eur. J. Org. Chem.* **2018**, *2018*, 6140−6149.

(6) Newman, S. G.; Lautens, M. The role of reversible oxidative addition in selective palladium (0)-catalyzed intramolecular cross-couplings of polyhalogenated substrates: synthesis of brominated indoles. *J. Am. Chem. Soc.* **2010**, *132*, 11416−11417.

(7) Wang, J.-R.; Manabe, K. Transition-Metal-Catalyzed Site-Selective Cross-Coupling of Di- and Polyhalogenated Compounds. *Synthesis* **2009**, *2009*, 1405−1427.

(8) (a) Ma, X.; Gu, N.; Liu, Y.; Liu, P.; Xie, J.; Dai, B.; Liu, Z. One-pot synthesis of polyfluoroterphenyls via palladium-catalyzed Suzuki-Miyaura coupling of chlorobromobenzene and C-H bond functionalization of perfluoroarenes. *Appl. Organomet. Chem.* **2015**, *29*, 50−56. (b) Matsumura, K.; Yoshizaki, S.; Maitani, M. M.; Wada, Y.; Ogomi, Y.; Hayase, S.; Kaiho, T.; Fuse, S.; Tanaka, H.; Takahashi, T. Rapid Synthesis of Thiophene-Based, Organic Dyes for Dye-Sensitized Solar Cells (DSSCs) by a One-Pot, Four-Component Coupling Approach. *Chem. − Eur. J.* **2015**, *21*, 9742−9747. (c) Ren, L.; Chu, W.; Guan, D.; Hou, Y.; Wang, M.; Yuan, X.; Sun, Z. Chemoselective one-pot synthesis of terphenyl derivatives by sequential directed C-H functionalization-Suzuki coupling. *Appl. Organomet. Chem.* **2014**, *28*, 673−677. (d) El Akkaoui, A.; Berteina-Raboin, S.; Mouaddib, A.; Guillaumet, G. Direct Arylation of Imidazo[1,2-b]pyridazines: Microwave-Assisted One-Pot Suzuki Coupling/Pd-Catalysed Arylation. *Eur. J. Org. Chem.* **2010**, *2010*, 862−871. (e) Koubachi, J.; El Kazzouli, S.; Berteina-Raboin, S.; Mouaddib, A.; Guillaumet, G. Synthesis of polysubstituted imidazo[1,2-*a*]pyridines via microwave-assisted one-pot cyclization/Suzuki coupling/palladium-catalyzed heteroarylation. *J. Org. Chem.* **2007**, *72*, 7650−7655.

(9) (a) Geary, L. M.; Hultin, P. G. Modular Construction of 2-Substituted Benzo[b]furans from 1,2-Dichlorovinyl Ethers. *Org. Lett.* **2009**, *11*, 5478−5481. (b) Wang, W.-Y.; Feng, X.; Hu, B.-L.; Deng, C.-L.; Zhang, X.-G. Synthesis of 6-(Trifluoromethyl) Phenanthridines via Palladium-Catalyzed Tandem Suzuki/C-H Arylation Reactions. *J. Org. Chem.* **2013**, *78*, 6025−6030. (c) Chai, D. I.; Lautens, M. Tandem Pd-Catalyzed Double C-C Bond Formation: Effect of Water. *J. Org. Chem.* **2009**, *74*, 3054−3061. (d) Nicolaus, N.; Franke, P. T.; Lautens, M. Modular Synthesis of Naphthothiophenes by Pd-Catalyzed Tandem Direct Arylation/Suzuki Coupling. *Org. Lett.* **2011**, *13*, 4236−4239. (e) Leclerc, J.-P.; André, M.; Fagnou, K. Heck, Direct Arylation, and Hydrogenation: Two or Three Sequential Reactions from a Single Catalyst. *J. Org. Chem.* **2006**, *71*, 1711−1714.

(10) Friedman, D.; Masiangioli, T.; Olson, S. *The Role of the Chemical Sciences in Finding Alternatives to Critical Resources: A Workshop Summary*; National Academies Press: Washington, DC, 2012.

(11) (a) Zhao, M.; Kamada, T.; Takeuchi, A.; Nishioka, H.; Kuroda, T.; Takeuchi, Y. Structure−activity relationship of indoloquinoline analogs anti-MRSA. *Bioorg. Med. Chem. Lett.* **2015**, *25*, 5551−5554. (b) Chen, Y.-L.; Chung, C.-H.; Chen, I. L.; Chen, P.-H.; Jeng, H.-Y.

Synthesis and cytotoxic activity evaluation of indolo-, pyrrolo-, and benzofuro-quinolin-2(1H)-ones and 6-anilinoindoloquinoline derivatives. *Bioorg. Med. Chem.* **2002**, *10*, 2705−2712.
(12) Chang, Y.; Fu, J.; Yao, K.; Li, B.; Xu, K.; Pang, X. Novel fluorescent probes for sequential detection of Cu2+ and citrate anion and application in living cell imaging. *Dyes Pigm.* **2019**, *161*, 331−340.
(13) Although conventional EAS would not be useful here, it is worth noting that C−H borylation could be considered a viable route, as demonstrated in the following reports: (a) Mkhalid, I. A. I.; Coventry, D. N.; Albesa-Jove, D.; Batsanov, A. S.; Howard, J. A. K.; Perutz, R. N.; Marder, T. B. Ir-Catalyzed Borylation of C-H Bonds in N-Containing Heterocycles: Regioselectivity in the Synthesis of Heteroaryl Boronate Esters. *Angew. Chem., Int. Ed.* **2006**, *45*, 489−491. (b) Tajuddin, H.; Harrisson, P.; Bitterlich, B.; Collings, J. C.; Sim, N.; Batsanov, A. S.; Cheung, M. S.; Kawamorita, S.; Maxwell, A. C.; Shukla, L.; Morris, J.; Lin, Z.; Marder, T. B.; Steel, P. G. Iridium-catalyzed C-H borylation of quinolines and unsymmetrical 1,2-disubstituted benzenes: insights into steric and electronic effects on selectivity. *Chem. Sci.* **2012**, *3*, 3505−3515.
(14) Altaf, A. A.; Shahzad, A.; Gul, Z.; Rasool, N.; Badshah, A.; Lal, B.; Khan, E. A review on the medicinal importance of pyridine derivatives. *J. Drug Des. Med. Chem.* **2015**, *1*, 1−11.
(15) Yang, Y.; Lan, J.; You, J. Oxidative C-H/C-H Coupling Reactions between Two (Hetero)arenes. *Chem. Rev.* **2017**, *117*, 8787−8863.
(16) (a) Ye, M.; Gao, G.-L.; Edmunds, A. J. F.; Worthington, P. A.; Morris, J. A.; Yu, J.-Q. Ligand-Promoted C3-Selective Arylation of Pyridines with Pd Catalysts: Gram-Scale Synthesis of (±)-Preclamol. *J. Am. Chem. Soc.* **2011**, *133*, 19090−19093. (b) Iwai, T.; Sawamura, M. Transition-Metal-Catalyzed Site-Selective C-H Functionalization of Quinolines beyond C2 Selectivity. *ACS Catal.* **2015**, *5*, 5031−5040. (c) Hilton, M. C.; Dolewski, R. D.; McNally, A. Selective Functionalization of Pyridines via Heterocyclic Phosphonium Salts. *J. Am. Chem. Soc.* **2016**, *138*, 13806−13809. (d) Konishi, S.; Kawamorita, S.; Iwai, T.; Steel, P. G.; Marder, T. B.; Sawamura, M. Site-Selective C-H Borylation of Quinolines at the C8 Position Catalyzed by a Silica-Supported Phosphane-Iridium System. *Chem. − Asian J.* **2014**, *9*, 434−438.
(17) Park, H.; Chekshin, N.; Shen, P.-X.; Yu, J.-Q. Ligand-Enabled, Palladium-Catalyzed β-C(sp3)-H Arylation of Weinreb Amides. *ACS Catal.* **2018**, *8*, 9292−9297.
(18) (a) Wasa, M.; Chan, K. S. L.; Zhang, X.-G.; He, J.; Miura, M.; Yu, J.-Q. Ligand-Enabled Methylene C(sp3)-H Bond Activation with a Pd(II) Catalyst. *J. Am. Chem. Soc.* **2012**, *134*, 18570−18572. (b) He, Y.; Wu, Z.; Ma, C.; Zhou, X.; Liu, X.; Wang, X.; Huang, G. Palladium-Catalyzed Selective C-H Activation: A Simple Method to Synthesize C-3 Site Arylated Quinoline Derivatives. *Adv. Synth. Catal.* **2016**, *358*, 375−379.
(19) Martin, G. E.; Hadden, C. E. Long-Range1H-15N Heteronuclear Shift Correlation at Natural Abundance. *J. Nat. Prod.* **2000**, *63*, 543−585.
(20) (a) Rosar, V.; Dedeic, D.; Nobile, T.; Fini, F.; Balducci, G.; Alessio, E.; Carfagna, C.; Milani, B. Palladium complexes with simple iminopyridines as catalysts for polyketone synthesis. *Dalton Trans.* **2016**, *45*, 14609−14619. (b) Pereira, M. T.; Antelo, J. M.; Adrio, L. A.; Martínez, J.; Ortigueira, J. M.; López-Torres, M.; Vila, J. M. Novel Bidentate [N,S] Palladacycle Metalloligands. 1H-15N HMBC as a Decisive NMR Technique for the Structural Characterization of Palladium-Rhodium and Palladium-Palladium Bimetallic Complexes. *Organometallics* **2014**, *33*, 3265−3274. (c) Villarreal, W.; Colina-Vegas, L.; Rodrigues de Oliveira, C.; Tenorio, J. C.; Ellena, J.; Gozzo, F. C.; Cominetti, M. R.; Ferreira, A. G.; Ferreira, M. A. B.; Navarro, M.; Batista, A. A. Chiral Platinum(II) Complexes Featuring Phosphine and Chloroquine Ligands as Cytotoxic and Monofunctional DNA-Binding Agents. *Inorg. Chem.* **2015**, *54*, 11709−11720.
(21) (a) García-Cuadrado, D.; Braga, A. A. C.; Maseras, F.; Echavarren, A. M. Proton Abstraction Mechanism for the Palladium-Catalyzed Intramolecular Arylation. *J. Am. Chem. Soc.* **2006**, *128*, 1066−1067. (b) Gorelsky, S. I.; Lapointe, D.; Fagnou, K. Analysis of the Concerted Metalation-Deprotonation Mechanism in Palladium-Catalyzed Direct Arylation Across a Broad Range of Aromatic Substrates. *J. Am. Chem. Soc.* **2008**, *130*, 10848−10849. (c) Boutadla, Y.; Davies, D. L.; Macgregor, S. A.; Poblador-Bahamonde, A. I. Mechanisms of C-H bond activation: rich synergy between computation and experiment. *Dalton Trans.* **2009**, *2009*, 5820−5831.
(22) Jiang, J.; Yu, J.-Q.; Morokuma, K. Mechanism and Stereoselectivity of Directed C(sp3)-H Activation and Arylation Catalyzed by Pd(II) with Pyridine Ligand and Trifluoroacetate: A Computational Study. *ACS Catal.* **2015**, *5*, 3648−3661.
(23) Cabrera, P. J.; Lee, M.; Sanford, M. S. Second-Generation Palladium Catalyst System for Transannular C−H Functionalization of Azabicycloalkanes. *J. Am. Chem. Soc.* **2018**, *140*, 5599−5606.
(24) While it is difficult to rule out a role for NMP-stabilized Pd nanoparticles, it is noted that these reactions work in dioxane. Also, the addition of quinoline ligands to the DA reaction of non-coordinating substrates increases turnover significantly; these reactions will be published in due course.
(25) Zhao, X. J.; Huang, C. Z.; Huang, C. Z. Small organic molecules as fluorescent probes for nucleotides and their derivatives. *TrAC, Trends Anal. Chem.* **2010**, *29*, 354−367.
(26) Hou, L.; Zhang, X.; Cotella, G. F.; Carnicella, G.; Herder, M.; Schmidt, B. M.; Pätzel, M.; Hecht, S.; Cacialli, F.; Samorì, P. Optically switchable organic light-emitting transistors. *Nat. Nanotechnol.* **2019**, *14*, 347−353.
(27) Terai, T.; Nagano, T. Small-molecule fluorophores and fluorescent probes for bioimaging. *Pflugers Arch - Eur. J. Physiol.* **2013**, *465*, 347−359.
(28) Sheldrick, G. M. Crystal Structure Refinement with SHELXL. *Acta Crystallogr. Sect. C, Struct. Chem.* **2015**, *71*, 3−8.
(29) Dolomanov, O. V.; Bourhis, L. J.; Gildea, R. J.; Howard, J. A. K.; Puschmann, H. OLEX2: A Complete Structure Solution, Refinement and Analysis Program. *J. Appl. Crystallogr.* **2009**, *42*, 339−341.
(30) Mehra, M. K.; Tantak, M. P.; Arun, V.; Kumar, I.; Kumar, D. Metal-free regioselective formation of C-N and C-O bonds with the utilization of diaryliodonium salts in water: facile synthesis of N-arylquinolones and aryloxyquinolines. *Org. Biomol. Chem.* **2017**, *15*, 4956−4961.

https://dx.doi.org/10.1021/acs.joc.9b03321
J. Org. Chem. 2020, 85, 2585−2596

JOC The Journal of Organic Chemistry

pubs.acs.org/joc Article

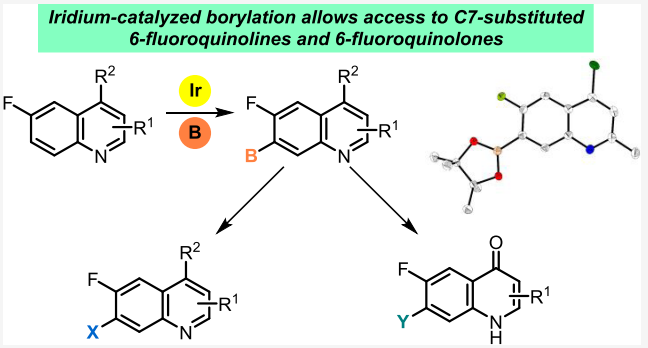
Iridium-Catalyzed Borylation of 6-Fluoroquinolines: Access to 6-Fluoroquinolones

Aobha Hickey, Julia Merz, Hamad H. Al Mamari, Alexandra Friedrich, Todd B. Marder, and Gerard P. McGlacken*

Cite This: J. Org. Chem. 2022, 87, 9977−9987 Read Online

ACCESS | Metrics & More | Article Recommendations | Supporting Information

ABSTRACT: The Ir-catalyzed C−H borylation of fluoroquinolines has been realized. The quinoline boronic ester formed undergoes a range of important transformations of relevance to medicinal chemistry. Judicious choice of the substituent at C4 on the quinoline facilitated the unmasking of a fluoroquinolone—the core structure of many antibiotics.



Downloaded via 78.16.32.36 on August 24, 2022 at 17:21:22 (UTC).
See https://pubs.acs.org/sharingguidelines for options on how to legitimately share published articles.

INTRODUCTION

The C−H bond functionalization of heteroarenes has emerged as an important synthetic methodology,[1] considering the roles that heteroarenes play in pharmaceuticals, agrochemical products, and electronic materials.[2] Iridium-catalyzed C−H borylation has proven to be a useful method for the functionalization of heteroarenes because of its ability to produce highly versatile aryl organoboronate ester intermediates without the need for reactive groups, such as halides or sulfonates (Scheme 1a).[3] In particular, the use of [Ir(OMe)-COD]$_2$ with bidentate ligands such as 4,4′-di-*tert*-butyl-2,2′-dipyridyl (dtbpy) has emerged as a powerful methodology for the borylation of arenes using both bis(pinacolato)diboron (B_2pin_2) and pinacolborane (HBpin).[3,4] Given its role as a key scaffold in a plethora of synthetic and naturally occurring pharmacologically active compounds,[5] the quinoline-nucleus has been used in a number of borylation-based methodologies. However, expansion of quinoline C−H borylation strategies requires additional developments regarding the regioselectivity control (Scheme 1b).[3l,n,6]

Fluoroquinolone antibiotics are one of the world's most commonly prescribed classes of antimicrobials[7] and are among the World Health Organization (WHO) Model List of Essential Medicines (Figure 1).[8] Their bioavailability, broad-spectrum activity, and potency profiles have established 6-fluoroquinolones as the treatment of choice for a variety of infections, including urinary tract, soft tissue, and gastrointestinal infections.[9] Synthesis of the core quinolone structure (and various analogues) is normally achieved through cyclization processes, carried out at elevated temperatures from the corresponding (substituted) aniline and an unsaturated coupling partner.[10] These preparations are still widely employed but do suffer from a number of issues. The processes are dependent on the availability of highly functionalized starting materials and thus are not amenable to late-stage derivatization.[11] In addition, the cyclization process can result in the formation of regioisomers. This problem is particularly evident in the case of C-5/C-7 substitution of the quinolone, where the *meta*-substituted starting aniline can cyclize at either *ortho*-position.[10a] However, considerable strides have also been made toward catalytic processes using halogenated precursors.[12]

Herein, we describe the C7−H borylation of 6-fluoroquinolines. We hoped that the fluorine atom would serve to guide the borylation to the C7 position[13] and also act as a critical functional group, especially if a quinoline to quinolone transformation could be developed (Scheme 2).[9d,14]

RESULTS AND DISCUSSION

We initiated our optimization experiments using fluoroquinoline **1a** with [Ir(OMe)COD]$_2$, dtbpy, and B_2pin_2 (Table 1, see the Supporting Information (SI) for more detail). Although tetrahydrofuran (THF) proved to be the most effective solvent, it is worth noting the very good conversion achieved

Received: April 25, 2022
Published: July 15, 2022



© 2022 The Authors. Published by American Chemical Society

Scheme 1. Iridium-Catalyzed Borylation of Quinolines

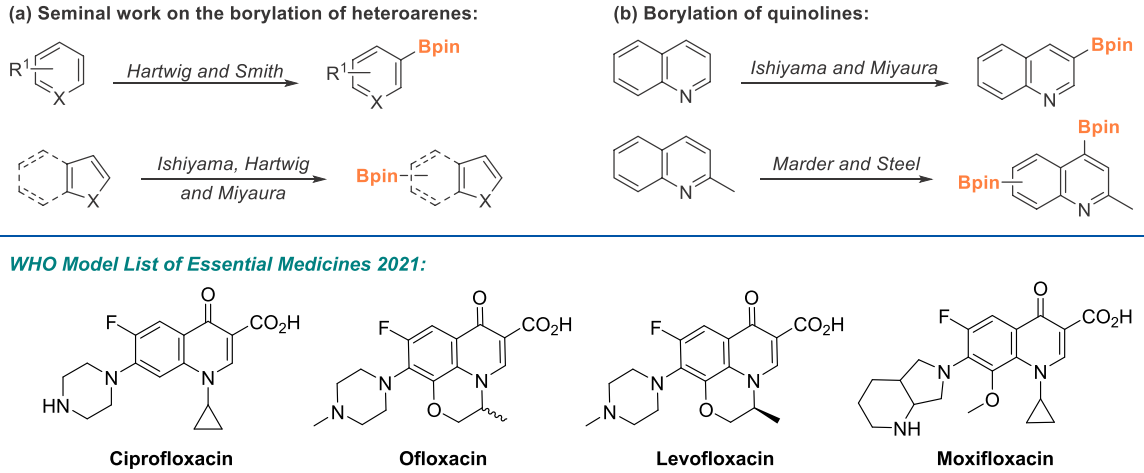


Figure 1. Fluoroquinolone antibiotics contained on the WHO Model List of Essential Medicines 2021.

Scheme 2. Iridium-Catalyzed Borylation of Substituted Quinolines and Subsequent Access to 6-Fluoroquinolones

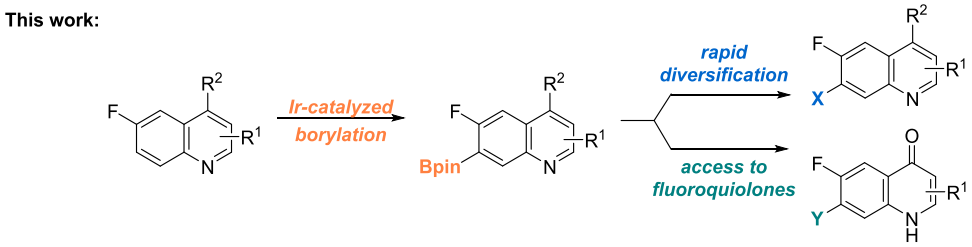


Table 1. Optimization of the Borylation of 1a

entry	B_2pin_2 (equiv)	Ir cat. (mol %)	ligand (mol %)	solvent[a] (mL)	yield (%)[b]
1	1.1	3.0	dtbpy 6.0	CPME 3	0
2	1.1	3.0	dtbpy 6.0	MTBE 3	70
3	1.1.	1.5	dtbpy 3.0	MTBE 1	95
4	1.5	3.0	dtbpy 6.0	THF 3	88
5	1.1	3.0	phen 6.0	THF 3	80
6	1.5	3.0	phen 6.0	THF 3	91
7	1.1	3.0	dtbpy 6.0	THF 3	>99
8	0.75	3.0	dtbpy 6.0	THF 1	89
9	1.1	1.5	dtbpy 3.0	THF 1	98

[a]Reactions carried out on the 0.2 mmol scale. Reaction temperatures are as follows: CPME 100 °C; MTBE 60 °C; THF 80 °C. [b]Yields calculated from ^{1}H NMR analysis of the crude reaction mixture using 1,3,5-trimethoxybenzene as an internal standard.

using methyl *tert*-butyl ether (MTBE), an easy to handle, relatively nonperoxidizable ether, which is already widely used in the industry, as the solvent (entries 2 and 3). No conversion to the borylated product was observed in cyclopentyl methyl ether (CPME) (entry 1). As a ligand, 1,10-phenanthroline (phen) also proved useful for this transformation (entries 5 and 6), but the superior reactivity profile of dtbpy is clearly demonstrated under otherwise identical conditions (entry 7). Optimized conditions allowed the formation of **2a** in a 98% yield (by ^{1}H NMR analysis, entry 9).

Substrates for borylation were then selected with varying groups at C4 and either an H, Me, or ester group at C2 (Scheme 3). In our choice of groups at C4, we were conscious that a quinoline to quinolone transformation would be very valuable as this methodology could provide an excellent route to substituted fluoroquinolones. We anticipated that compounds **2a**, **2b**, **2d**, and **2e** could undergo acid-hydrolysis to provide the corresponding 4-quinolone,[15] while orthogonally, **2c** could be deprotected using palladium-catalyzed hydrogenation (*vide infra*).[16]

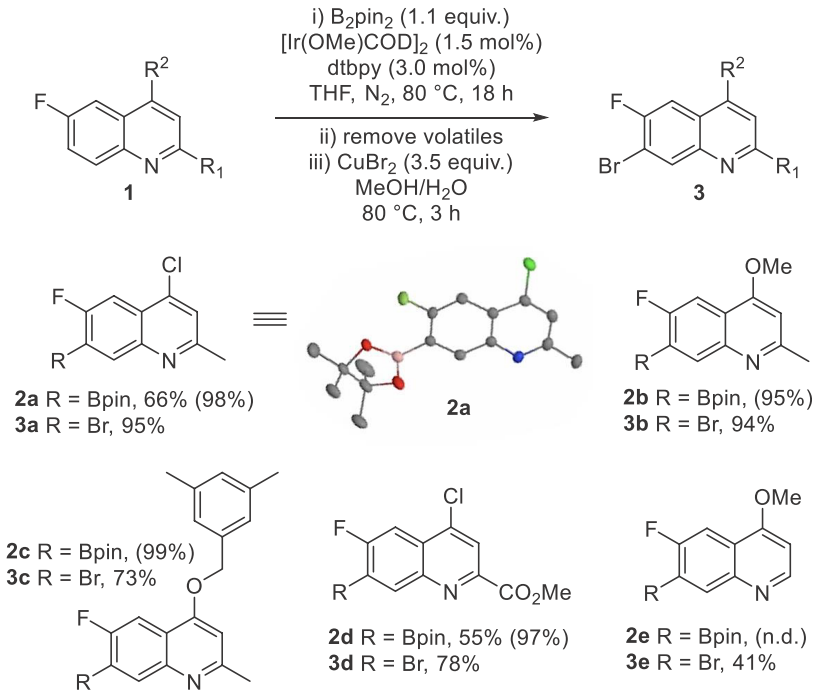
The borylated quinolines were unstable on silica gel and proved difficult to purify.[3l] However, we were able to isolate compounds **2a** and **2d** in good yields by recrystallization from methanol. Generally, the intermediate borylation steps gave very good yields (by ^{1}H NMR analysis, using an internal standard), with the exception of **2e**; here, the reduction in yield is attributed to **1e** having a competitive site for borylation (see the SI). In any case, and conveniently, the crude material could be converted to the C7-brominated products,[17] which were purified and characterized (Scheme 3). The C7 selectivity of the C−H borylation was confirmed by the molecular structure of **2a** obtained by single-crystal X-ray diffraction.

In our experience and that of others,[18] quinolones tend to suffer from solubility issues, especially those lacking pendant organic groups. Here, however, the apparently increased solubility of the quinoline motif meant that the borylated quinoline compounds could undergo a range of synthetically valuable transformations (Scheme 4). Given the commonly encountered issues associated with employing heterocycles as substrates for cross-coupling and other reactions,[19] it was critically important to demonstrate that the Bpin moiety could be transformed into useful substituted quinolines.

The *in situ* borylated quinolines **2** were converted to the bromo-quinoline analogues in excellent yields over two steps using copper bromide (a). The iodinated compound was accessed in a moderate yield using copper iodide (b), again

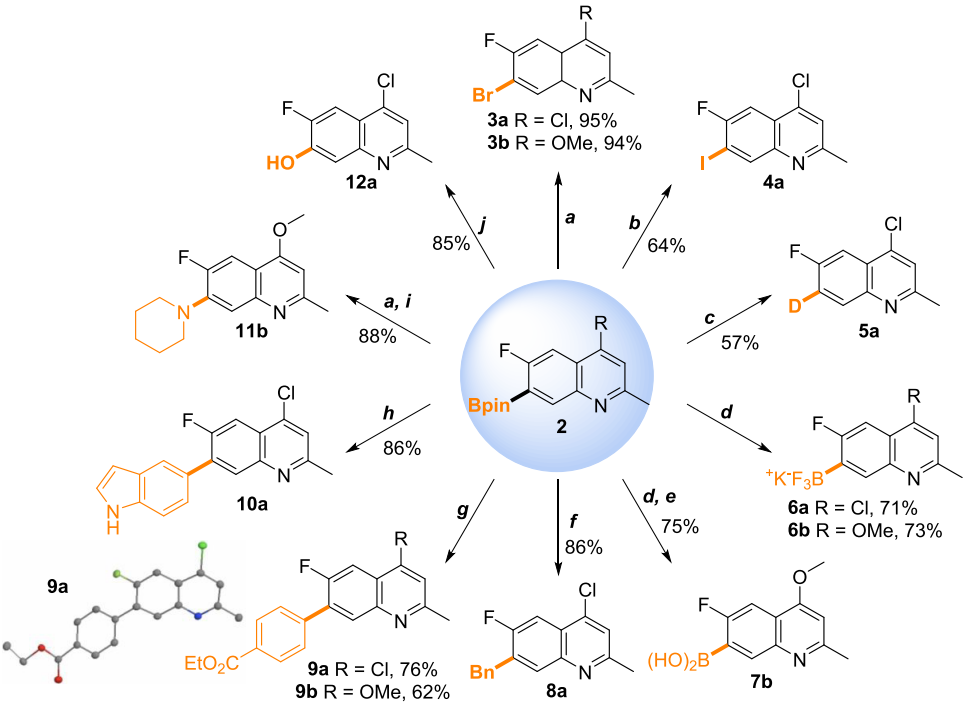
https://doi.org/10.1021/acs.joc.2c00973
J. Org. Chem. 2022, 87, 9977−9987

Scheme 3. Borylated and Brominated Quinoline Substrates[a,b]



[a]Yields are isolated. Yields in parentheses calculated from ^{1}H NMR analysis of the crude reaction mixture using 1,3,5-trimethoxybenzene as an internal standard. [b]n.d. = not determined, see the SI for more information.

Scheme 4. Synthetic Transformations of C7-Borylated Quinolines[a]



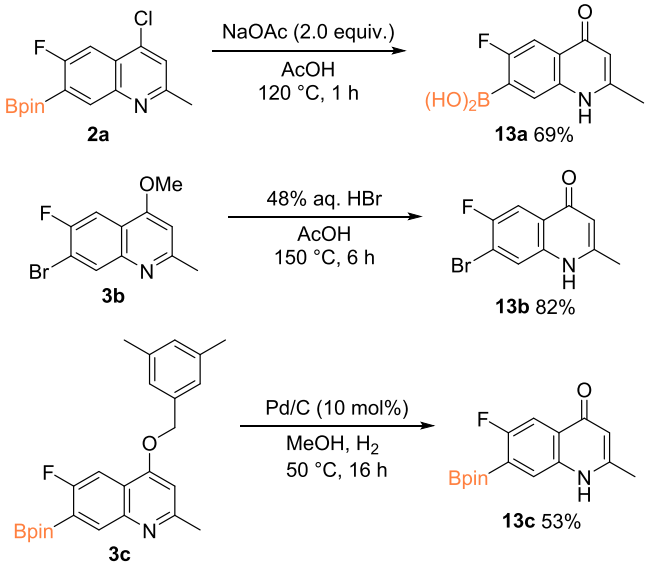
[a]**Conditions**: (a) $CuBr_2$ (3.5 equiv), MeOH/H_2O (1:1 v/v), 80 °C, 3 h. (b) CuI (10 mol %), 1,10-phenanthroline (20 mol %), KI (1.5 equiv), MeOH/H_2O (4:1 v/v), N_2, 80 °C, 2 h. (c) $[Ir(OMe)COD]_2$ (1 mol %), THF/D_2O (4:1 v/v), N_2, 80 °C, 12 h. (d) KHF_2 (6.0 equiv), THF/H_2O (3:1 v/v), rt, 16 h. (e) LiOH·H_2O (9.0 equiv), THF/H_2O (5:1 v/v), rt, 24 h. (f) $Pd_2(dba)_3$ (1 mol %), PPh_3 (4 mol %), K_2CO_3 (4.0 equiv), BnBr (1.2 equiv), THF/H_2O (50:1 v/v), N_2, 100 °C, 24 h. (g) $Pd(PPh_3)_4$ (5 mol %), K_3PO_4 (3.0 equiv), ethyl-4-bromobenzoate (1.5 equiv), THF/H_2O (5:1 v/v), N_2, 60 °C, 18 h. (h) $Pd(dba)_2$ (2 mol %), P(o-tol)3 (6 mol %), Na_2CO_3 (4.0 equiv), 5-bromoindole (0.8 equiv), THF/H_2O (10:1 v/v), N_2, 50 °C, 24 h. (i) $Pd_2(dba)_3$ (3 mol %), RuPhos (6 mol %), NaOtBu (2.5 equiv), Piperidine (2.0 equiv), Toluene, N_2, 80 °C, 16 h. (j) 30% H_2O_2 (1.2 equiv), MeOH, 0 °C to rt, 16 h.

https://doi.org/10.1021/acs.joc.2c00973
J. Org. Chem. 2022, 87, 9977−9987

over two steps. The purified C7-borylated product was converted to the deuterio and hydroxy analogues in good yields (c, j). The useful and more reactive trifluoroborate salt was obtained using potassium bifluoride in aqueous THF (d), and the boronic acid motif was subsequently accessed after reaction of the salt with lithium hydroxide in aqueous THF (e). The borylated quinoline substrate **2a** was coupled with a number of brominated substrates in high-yielding, palladium-catalyzed Suzuki–Miyaura reactions (f, g, h). Finally, amination of the C7 position was achieved *via* a Hartwig–Buchwald coupling reaction of the brominated substrate **3b** with piperidine (i).

While this borylation protocol provides excellent access to a number of substituted quinolines, underpinning our choices for the moiety at C4 was the potential to furnish the quinolone scaffold, thus gaining access to some fluoroquinolones. Indeed, 4-Cl borylated quinoline **2a** and 4-OMe brominated quinoline **3b** were converted to the corresponding quinolones **13a** and **13b** in 68 and 82% yields, respectively. In the case of **2a**, concurrent hydrolysis to the boronic acid **13a** was observed. Debenzylation of compound **3c** was achieved *via* palladium-catalyzed hydrogenolysis in methanol (Scheme 5).

Scheme 5. Access to Substituted Fluoroquinolones

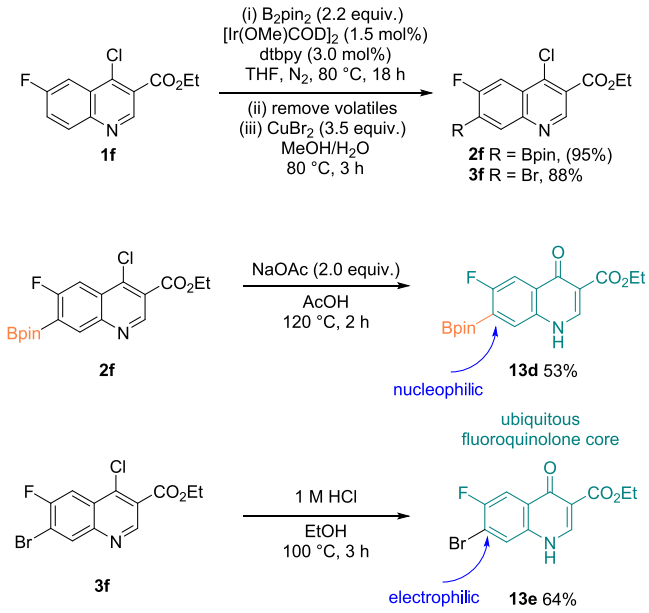


Finally, in the context of mapping onto the core antibiotic fluoroquinolone structure, initial attempts using our optimized conditions (Table 1) with **1f** gave only trace amounts of the borylated product. However, using 2.2 equiv of B_2pin_2 allowed the borylation to **2f** to occur in a very good yield, and subsequent bromination gave **3f** in a yield of 88% (Scheme 6). Finally, the key fluoroquinolone framework was furnished by acid-catalyzed hydrolysis of **2f** to give the boronate ester **13d** (C7 = nucleophilic) in a 53% yield. The complementary brominated fluoroquinolone moiety (C7 = electrophilic) was also accessible by alcoholysis of **3f** to give **13e** in a 64% yield.

CONCLUSIONS

In summary, we have developed an efficient protocol for the C–H functionalization/borylation of quinolines incorporating useful and useable substituents. Importantly, borylation is selective for C7, avoiding, for example, C3. Extensive diversification at C7 is demonstrated in the presence of the basic quinoline group. Finally, the ubiquitous fluoroquinolone moiety can be generated in a simple hydrolysis step.

Scheme 6. Synthesis of the 6-Fluoroquinolone Antibiotic Framework[a]



[a]Yields are isolated. Yields in parentheses calculated from ^{1}H NMR analysis of the crude reaction mixture using 1,3,5-trimethoxybenzene as an internal standard.

EXPERIMENTAL SECTION

General Considerations. The catalyst precursor [Ir(OMe)-COD]$_2$ was synthesized according to a literature procedure[20] and was stored in a glovebox under an argon atmosphere. Toluene and CPME were dried and stored over flame-dried 4 Å molecular sieves. THF was either freshly distilled from sodium/benzophenone under a nitrogen atmosphere and stored over molecular sieves under the nitrogen atmosphere (University College Cork) or dried using a solvent purification system (SPS) from Innovative Technology, degassed with argon, and stored over molecular sieves under the argon atmosphere (Julius-Maximilians-Universität Würzburg). K_2CO_3 and Na_2CO_3 were stored in an oven at 150 °C. All other solvents and reagents were used as obtained from commercial sources and without further purification. Melting points were measured using a Thomas Hoover Capillary Melting Point apparatus. Infrared spectra were measured on a PerkinElmer FT-IR spectrometer as thin films in DCM. Column chromatography was carried out using 60 Å (35–70 μm) silica. TLC was carried out on precoated silica gel plates (Merck 60 PF254), and the developed plates were visualized under UV light. High-resolution mass spectra (HRMS) were recorded on a Waters LCT Premier Tof LC-MS instrument in electrospray ionization (ESI) mode (University College Cork) or using a Thermo Scientific Exactive Plus Orbitrap MS system with an Atmospheric Sample Analysis Probe (ASAP) (Julius-Maximilians-Universität Würzburg). Samples were run using 50% acetonitrile–water containing 0.1% formic acid as the eluent and were prepared at a concentration of *ca.* 1 mg mL^{-1}. Nuclear magnetic resonance (NMR) spectra were recorded in $CDCl_3$, $(CD_3)_2SO$, or CD_3OD, as specified. ^{1}H NMR (600 MHz), ^{1}H NMR (500 MHz), ^{1}H NMR (400 MHz), and ^{1}H NMR (300 MHz) spectra were recorded on Bruker Avance 600, Bruker Avance 500, Bruker Avance 400, and Bruker Avance III 300 NMR spectrometers, respectively. ^{13}C NMR (150 MHz), ^{13}C NMR (125 MHz), ^{13}C NMR (100 MHz), and ^{13}C NMR (75 MHz) spectra were recorded on Bruker Avance 600, Bruker Avance 500, Bruker Avance 400, and Bruker Avance III 300 NMR spectrometers, respectively, in proton decoupled mode. ^{19}F NMR (470 MHz), ^{19}F NMR (376

https://doi.org/10.1021/acs.joc.2c00973
J. Org. Chem. 2022, 87, 9977–9987

MHz), and ^{19}F NMR (282 MHz) spectra were recorded on Bruker Avance 500, Bruker Avance 400, and Bruker Avance III 300 NMR spectrometers, respectively, in proton decoupled mode. All NMR analyses were carried out at 300 K unless otherwise specified. Chemical shifts (δ) are expressed as parts per million (ppm) and coupling constants (J) are expressed in Hertz (Hz).

Synthesis of Quinoline Starting Materials. *4-Chloro-6-fluoro-2-methylquinoline (**1a**).*[21] 6-Fluoro-2-methylquinolin-4(1*H*)-one (1.77 g, 10 mmol, 1.0 equiv) was added to a Schlenk flask, dissolved in $POCl_3$ (4.6 mL, 50 mmol, 5.0 equiv), and the mixture was stirred in an oil bath at 110 °C for 3 h. The cooled reaction mixture was slowly added to iced water (20 mL) with stirring. Solid $NaHCO_3$ was then added gradually until the pH reached ca.∼ 7, and the mixture was allowed to stir until effervescence ceased. The mixture was transferred to a separating funnel, and the organic layer was collected. The aq. layer was extracted with DCM (3 × 20 mL). The combined organic layers were washed with saturated $NaHCO_3$ (20 mL), H_2O (20 mL), and brine (20 mL), dried over $MgSO_4$, filtered, and concentrated under reduced pressure. White solid (1.860 g, 95%); m.p. 84−86 °C (lit.[22] 83−84 °C); ^{1}H NMR (300 MHz, $CDCl_3$) δ: 8.02 (dd, J = 9.2, 5.3 Hz, 1H), 7.79 (dd, J = 9.4, 2.8 Hz, 1H), 7.49 (ddd, J = 9.2, 8.3, 2.9 Hz, 1H), 7.41 (s, 1H), 2.71 (s, 3H) ppm; ^{13}C{^{1}H} NMR (75 MHz, $CDCl_3$) δ: 160.7 (d, J = 248 Hz), 158.2 (d, J = 3 Hz), 145.7, 141.7 (d, J = 6 Hz), 131.6 (d, J = 9 Hz), 125.6 (d, J = 10 Hz), 122.5, 120.5 (d, J = 26 Hz), 107.8 (d, J = 24 Hz), 25.0 ppm; ^{19}F NMR (282 MHz, $CDCl_3$) δ: −112 ppm; m/z (ES+): 196 ((M + H)$^+$ 100%).

*6-Fluoro-4-methoxy-2-methylquinoline (**1b**).* 4-Chloro-6-fluoro-2-methylquinoline **1a** (500 mg, 2.6 mmol, 1.0 equiv) in MeOH (8 mL) was added dropwise to a freshly prepared solution of sodium (20 mmol, 8.0 equiv) in MeOH (12 mL) over ice. The mixture was warmed to r.t. and then heated to 80 °C in an oil bath for 18 h, cooled to room temperature, and concentrated under reduced pressure. The residue was dissolved in a mixture of EtOAc/H_2O (1:1, 20 mL), and the layers were separated. The aqueous layer was extracted with EtOAc (2 × 10 mL), and the combined organic layers were then washed with H_2O (10 mL) and brine (15 mL), dried over $MgSO_4$, filtered, and concentrated under reduced pressure. Beige solid (0.473 g, 97%); m.p. 52−54 °C; IR (film) ν_{max} 1632, 1514, 1353, 1201, 1180 cm^{-1}; ^{1}H NMR (300 MHz, $CDCl_3$) δ: 7.92 (dd, J = 9.2, 5.2 Hz, 1H), 7.71 (dd, J = 9.5, 2.9 Hz, 1H), 7.40 (ddd, J = 9.2, 8.3, 2.9 Hz, 1H), 6.62 (s, 1H), 4.00 (s, 3H), 2.68 (s, 3H) ppm; ^{13}C{^{1}H} NMR (75 MHz, $CDCl_3$) δ: 161.8 (d, J = 5 Hz), 159.7 (d, J = 245 Hz), 159.3 (d, J = 2 Hz), 145.7, 130.4 (d, J = 9 Hz), 120.4 (d, J = 9 Hz), 119.5 (d, J = 25 Hz), 105.6 (d, J = 23 Hz), 101.0, 55.6, 25.8 ppm; ^{19}F NMR (282 MHz, $CDCl_3$) δ: −116 ppm; HRMS (ESI-TOF) m/z: [M + H]$^+$ calcd for $C_{11}H_{11}FNO$: 192.0819; found: 192.0817.

*4-((3,5-Dimethylbenzyl)oxy)-6-fluoro-2-methylquinoline (**1c**).* To a solution of 6-fluoro-2-methylquinolin-4(1*H*)-one (265.8 mg, 1.5 mmol, 1.0 equiv) in DMF (30 mL) was added K_2CO_3 (414.6 mg, 3.0 mmol, 2.0 equiv). The mixture was stirred at 40 °C for 1 h before the portion-wise addition of 3,5-dimethylbenzyl bromide (358.4 mg, 1.8 mmol, 1.2 equiv), and the resulting suspension was heated to 60 °C in an oil bath for 16 h. The mixture was poured onto ice water and extracted with EtOAc (3 × 20 mL). The combined organic layers were washed with water (2 × 20 mL), dried over $MgSO_4$, filtered, and concentrated under reduced pressure. The product was purified *via* column chromatography (DCM/EtOAc, 90:10). White solid (0.373 g, 84%); m.p. 93−95 °C; IR (film) ν_{max} 1604, 1514, 1478, 1348, 1185, 1083 cm^{-1}; ^{1}H NMR (500 MHz, $CDCl_3$) δ: 7.94 (dd, J = 9.2, 5.2 Hz, 1H), 7.79 (dd, J = 9.5, 2.9 Hz, 1H), 7.41 (ddd, J = 9.2, 8.2, 2.9 Hz, 1H), 7.08 (s, 2H), 7.02 (bs, 1H), 6.70 (s, 1H), 5.17 (s, 2H), 2.68 (s, 3H), 2.36 (s, 6H) ppm; ^{13}C{^{1}H} NMR (125 MHz, $CDCl_3$) δ: 161.1 (d, J = 5 Hz), 159.7 (d, J = 245 Hz), 159.3 (d, J = 2 Hz), 145.8, 138.5, 135.4, 130.4 (d, J = 9 Hz), 130.2, 125.4, 120.6 (d, J = 10 Hz), 119.6 (d, J = 25 Hz), 105.8 (d, J = 23 Hz), 102.0, 70.5, 25.8, 21.3 ppm; ^{19}F NMR (470 MHz, $CDCl_3$) δ: −115 ppm; HRMS (ESI-TOF) m/z: [M + H]$^+$ calcd for $C_{19}H_{19}FNO$: 296.1445; found: 296.1451.

*Methyl 4-chloro-6-fluoroquinoline-2-carboxylate (**1d**).* Prepared *via* the method described for compound **1a** using methyl 6-fluoro-4-oxo-1,4-dihydroquinoline-2-carboxylate (221.2 mg, 1.0 mmol, 1.0 equiv). White solid (0.230 g, 96%); m.p. 140−141 °C; IR (film) ν_{max} 1751, 1623, 1558, 1208, 1104, 1006, 831 cm^{-1}; ^{1}H NMR (300 MHz, $CDCl_3$) δ: 8.42−8.25 (m, 2H), 7.89 (dd, J = 9.2, 2.8 Hz, 1H), 7.62 (ddd, J = 9.2, 8.0, 2.8 Hz, 1H), 4.09 (s, 3H) ppm; ^{13}C{^{1}H} NMR (75 MHz, $CDCl_3$) δ: 164.8, 162.5 (d, J = 254 Hz), 147.1 (d, J = 3 Hz), 145.3, 143.1 (d, J = 6 Hz), 134.0 (d, J = 10 Hz), 128.8 (d, J = 11 Hz), 121.9, 121.8 (d, J = 26 Hz), 108.0 (d, J = 25 Hz), 53.5 ppm; ^{19}F NMR (282 MHz, $CDCl_3$) δ: −107 ppm; HRMS (ESI-TOF) m/z: [M + H]$^+$ calcd for $C_{11}H_8ClFNO_2$: 240.0222; found: 240.0221.

*6-Fluoro-4-methoxyquinoline (**1e**).* Prepared *via* the method described for compound **1b** using 4-chloro-6-fluoroquinoline (320 mg, 1.76 mmol, 1.0 equiv). White solid (0.295 g, 95%); m.p. 50−53 °C; IR (film) ν_{max} 1631, 1598, 1309, 1189, 1069 cm^{-1}; ^{1}H NMR (500 MHz, $CDCl_3$) δ: 8.71 (d, J = 5.0 Hz, 1H), 8.02 (dd, J = 9.2, 5.3 Hz, 1H), 7.77 (dd, J = 9.5, 2.9 Hz, 1H), 7.44 (ddd, J = 9.2, 8.2, 2.9 Hz, 1H), 6.73 (d, J = 5.1 Hz, 1H), 4.02 (s, 3H) ppm; ^{13}C{^{1}H} NMR (125 MHz, $CDCl_3$) δ: 162.0 (d, J = 5 Hz), 160.2 (d, J = 247 Hz), 150.7 (d, J = 2 Hz), 146.3, 131.4 (d, J = 9 Hz), 122.2 (d, J = 10 Hz), 119.8 (d, J = 26 Hz), 105.8 (d, J = 24 Hz), 100.5, 55.8 ppm; ^{19}F NMR (282 MHz, $CDCl_3$) δ: −114 ppm; HRMS (ESI-TOF) m/z: [M + H]$^+$ calcd for $C_{10}H_9FNO$: 178.0663; found: 178.0658.

*Ethyl-4-chloro-6-fluoroquinoline-3-carboxylate (**1f**).*[23] Prepared *via* the method described for compound **1a** using ethyl 6-fluoro-4-oxo-1,4-dihydroquinoline-3-carboxylate (352.8 mg, 1.5 mmol, 1.0 equiv). White solid (0.352 g, 93%); m.p. 67−69 °C (lit.[24] 62−63 °C); ^{1}H NMR (600 MHz, $CDCl_3$) δ: 9.16 (s, 1H), 8.17 (dd, J = 9.2, 5.3 Hz, 1H), 8.03 (dd, J = 9.6, 2.7 Hz, 1H), 7.62 (ddd, J = 9.2, 7.9, 2.8 Hz, 1H), 4.51 (q, J = 7.1 Hz, 2H), 1.47 (q, J = 7.1 Hz, 3H) ppm; ^{13}C{^{1}H} NMR (150 MHz, $CDCl_3$) δ: 163.7, 161.1 (d, J = 251 Hz), 148.8, 145.9, 142.1 (d, J = 6 Hz), 131.9 (d, J = 9 Hz), 126.9 (d, J = 7 Hz), 123.1, 121.7 (d, J = 26 Hz), 108.7 (d, J = 25 Hz), 61.7, 13.7 ppm; ^{19}F NMR (282 MHz, $CDCl_3$) δ: −109 ppm; m/z (ES+): 254 ((M + H)$^+$ 100%).

Borylation of 6-Fluoroquinolines. *General Procedure for the Borylation of 6-Fluoroquinolines.* A 15 mL Schlenk flask was oven-dried (150 °C) and cooled under vacuum. The Schlenk flask was refilled with nitrogen, and all reagents were added under a positive pressure of nitrogen in the order: quinoline (1.0 equiv), dtbpy (3 mol %), B_2pin_2 (1.1 equiv), and [Ir(OMe)COD]$_2$ (1.5 mol %). The Schlenk flask was then placed under vacuum for 20 min before being refilled with nitrogen 3 times. THF (2.5 mL/mmol) was added *via* a syringe through the septum, the reaction was sealed, and the mixture was heated to 80 °C in an aluminum heating block for 12−18 h. The reaction mixture was then cooled to r.t., diluted with MeOH (20 mL/mmol), and concentrated under reduced pressure. The product was purified *via* recrystallization from hot MeOH.

*4-Chloro-6-fluoro-2-methyl-7-(4,4,5,5-tetramethyl-1,3,2-dioxaborolan-2-yl)quinoline (**2a**).* Prepared *via* the general procedure using **1a** (391.2 mg, 2.0 mmol, 1.0 equiv); X-ray quality crystals were obtained *via* vapor diffusion from a saturated solution of DCM in Et_2O; and the CCDC number is 2159956. White solid (0.422 g, 66%); m.p. 97−100 °C; IR (film) ν_{max} 1627, 1500, 1370, 1331, 1261, 1147, 1049, 854 cm^{-1}; ^{1}H NMR (600 MHz, $CDCl_3$) δ: 8.56 (d, J = 5.5 Hz, 1H), 7.79 (d, J = 9.7 Hz, 1H), 7.47 (s, 1H), 2.77 (s, 3H), 1.45 (s, 12H) ppm; ^{13}C{^{1}H} NMR (150 MHz, $CDCl_3$) δ: 164.0 (d, J = 251 Hz), 158.1 (d, J = 3 Hz), 145.1, 141.6 (d, J = 5 Hz), 139.8 (d, J = 9 Hz), 127.6 (d, J = 11 Hz), 123.2, 107.5 (d, J = 27 Hz), 84.5, 25.0, 24.9 ppm; a signal for the carbon directly attached to the boron atom was not observed; ^{19}F NMR (282 MHz, $CDCl_3$) δ: −105 ppm; ^{11}B NMR (96 MHz, $CDCl_3$) δ: 30 ppm; HRMS (ESI-TOF) m/z: [M + H]$^+$ calcd for $C_{16}H_{19}BClFNO_2$: 322.1176; found: 322.1182.

*Methyl 4-chloro-6-fluoro-7-(4,4,5,5-tetramethyl-1,3,2-dioxaborolan-2-yl)quinoline-2-carboxylate (**2d**).* Prepared *via* the general procedure using **1d** (47.9 mg, 0.2 mmol, 1.0 equiv). White solid (0.040 g, 55%); m.p. 156−158 °C; IR (film) ν_{max} 1727, 1625, 1498, 1336, 1326, 1230, 1118, 1049, 849 cm^{-1}; ^{1}H NMR (600 MHz, $CDCl_3$) δ: 8.84 (d, J = 5.6 Hz, 1H), 8.30 (s, 1H), 7.83 (d, J = 9.4 Hz, 1H), 4.09 (s, 3H), 1.40 (s, 12H) ppm; ^{13}C{^{1}H} NMR (150 MHz, $CDCl_3$) δ: 165.7 (d, J = 257 Hz), 164.9, 147.1 (d, J = 3 Hz), 144.8, 142.8 (d, J = 6 Hz), 142.5 (d, J = 10 Hz), 130.5 (d, J = 11 Hz), 122.3,

https://doi.org/10.1021/acs.joc.2c00973
J. Org. Chem. 2022, 87, 9977−9987

107.7 (d, J = 28 Hz), 84.6, 53.4, 24.9 ppm; a signal for the carbon directly attached to the boron atom was not observed; ^{19}F NMR (282 MHz, $CDCl_3$) δ: −100 ppm; ^{11}B NMR (96 MHz, $CDCl_3$) δ: 30 ppm; HRMS (ESI-TOF) m/z: $[M + H]^+$ calcd for $C_{17}H_{19}BClFNO_4$: 366.1074; found: 366.1071.

General Procedure for the Borylation and Subsequent Bromination of 6-Fluoroquinolines. A 15 mL Schlenk was oven-dried (150 °C) and cooled under vacuum. The Schlenk flask was refilled with nitrogen, and all reagents were added under a positive pressure of nitrogen in the order: quinoline (1.0 equiv), dtbpy (3 mol %), B_2pin_2 (1.1 equiv), and $[Ir(OMe)COD]_2$ (1.5 mol %). The Schlenk flask was then placed under vacuum for 20 min before being refilled with nitrogen 3 times. THF (2.5 mL/mmol) was added *via* a syringe through the septum, the reaction was sealed, and the mixture was heated to 80 °C in an aluminum heating block for 12−18 h. The reaction mixture was then cooled to r.t., diluted with Et_2O, and concentrated under reduced pressure. An internal standard 1,3,5-trimethoxybenzene (∼10 mol %) was added to the residue to determine the yield of the C7-borylated product **2a**−**2e** by ^{1}H NMR analysis. The residue was redissolved in MeOH (20 mL/mmol), and a solution of $CuBr_2$ (3.5 equiv) in H_2O (20 mL/mmol) was added. The reaction mixture was heated to 80 °C in an oil bath for 3 h, cooled to r.t. diluted with 10% NH_4OH (40 mL/mmol), and then extracted with Et_2O (3 × 10 mL/mmol). The combined organic layers were washed with H_2O (10 mL/mmol) and brine (10 mL/mmol), dried over $MgSO_4$, filtered, and concentrated under reduced pressure. The product was purified *via* column chromatography (DCM/EtOAc gradient, unless otherwise specified).

*7-Bromo-4-chloro-6-fluoro-2-methylquinoline (**3a**).* Prepared *via* the general procedure using **1a** (39.1 mg, 0.2 mmol, 1.0 equiv). White solid (0.052 g, 95%); m.p. 100−101 °C; IR (film) ν_{max} 1612, 1588, 1016, 845, 707 cm^{-1}; ^{1}H NMR (600 MHz, $CDCl_3$) δ: 8.27 (d, J = 6.6 Hz, 1H), 7.81 (d, J = 9.0 Hz, 1H), 7.40 (s, 1H), 2.70 (s, 3H) ppm; $^{13}C\{^1H\}$ NMR (150 MHz, $CDCl_3$) δ: 158.8 (d, J = 3 Hz), 156.2 (d, J = 250 Hz), 145.2 (d, J = 1 Hz), 141.0 (d, J = 5 Hz), 133.6 (d, J = 1 Hz), 124.2 (d, J = 9 Hz), 122.2, 113.7 (d, J = 24 Hz), 108.1 (d, J = 26 Hz), 24.5 ppm; ^{19}F NMR (282 MHz, $CDCl_3$) δ: −108 ppm; HRMS (ESI-TOF) m/z: $[M + H]^+$ calcd for $C_{10}H_7BrClFN$: 273.9429; found: 273.9424.

*7-Bromo-6-fluoro-4-methoxy-2-methylquinoline (**3b**).* Prepared *via* the general procedure using **1b** (49.8 mg, 0.2 mmol, 1.0 equiv). 95% yield **2b** by ^{1}H NMR analysis using 1,3,5-trimethoxybenzene as an internal standard. White solid (0.051 g, 94%); m.p. 113−115 °C; IR (film) ν_{max} 1612, 1588, 1352, 1203, 1010, 726 cm^{-1}; ^{1}H NMR (400 MHz, $CDCl_3$) δ: 8.23 (d, J = 6.5 Hz, 1H), 7.77 (d, J = 9.1 Hz, 1H), 6.64 (s, 1H), 4.03 (s, 3H), 2.69 (s, 3H) ppm; $^{13}C\{^1H\}$ NMR (100 MHz, $CDCl_3$) δ: 162.0 (d, J = 5 Hz), 160.6 (d, J = 3 Hz), 155.9 (d, J = 247 Hz), 145.6, 132.9, 119.6 (d, J = 8 Hz), 113.4 (d, J = 24 Hz), 106.7 (d, J = 25 Hz), 101.3, 55.9, 25.6 ppm; ^{19}F NMR (282 MHz, $CDCl_3$) δ: −110 ppm; HRMS (ESI-TOF) m/z: $[M + H]^+$ calcd for $C_{11}H_{10}BrFNO$: 269.9924; found: 269.9923.

*7-Bromo-4-((3,5-dimethylbenzyl)oxy)-6-fluoro-2-methylquinoline (**3c**).* Prepared *via* the general procedure using **1c** (59.1 mg, 0.2 mmol, 1.0 equiv). 99% yield **2c** by ^{1}H NMR analysis using 1,3,5-trimethoxybenzene as an internal standard. White solid (0.055 g, 73%); m.p. 138−140 °C; IR (film) ν_{max} 1601, 1561, 1500, 1347, 1193, 1099, 747 cm^{-1}; ^{1}H NMR (500 MHz, $CDCl_3$) δ: 8.20 (d, J = 6.5 Hz, 1H), 7.83 (d, J = 9.2 Hz, 1H), 7.07 (s, 2H), 7.02 (s, 1H), 6.70 (s, 1H), 5.16 (s, 2H), 2.66 (s, 3H), 2.36 (s, 6H) ppm; $^{13}C\{^1H\}$ NMR (125 MHz, $CDCl_3$) δ: 160.9 (d, J = 5 Hz), 160.6 (d, J = 2 Hz), 155.8 (d, J = 247 Hz), 146.1, 138.5, 135.2, 133.1, 130.3, 125.5, 119.7 (d, J = 8 Hz), 113.2 (d, J = 24 Hz), 106.9 (d, J = 25 Hz), 102.3, 70.7, 25.8, 21.3 ppm; ^{19}F NMR (282 MHz, $CDCl_3$) δ: −111 ppm; HRMS (ESI-TOF) m/z: $[M + H]^+$ calcd for $C_{19}H_{18}BrFNO$: 374.0550; found: 374.0558.

*Methyl 7-bromo-4-chloro-6-fluoroquinoline-2-carboxylate (**3d**).* Prepared *via* the general procedure using **1d** (24.0 mg, 0.1 mmol, 1.0 equiv) and purified *via* column chromatography (DCM). 97% yield **2d** by ^{1}H NMR analysis using 1,3,5-trimethoxybenzene as an internal standard. White solid (0.025 g, 78%); m.p. 153−155 °C; IR (film) ν_{max} 1725, 1613, 1544, 1345, 1204, 1019, 787, 696 cm^{-1}; ^{1}H NMR (400 MHz, $CDCl_3$) δ: 8.62 (d, J = 6.6 Hz, 1H), 8.31 (s, 1H), 7.96 (d, J = 8.8 Hz, 1H), 4.10 (s, 3H) ppm; $^{13}C\{^1H\}$ NMR (100 MHz, $CDCl_3$) δ: 164.6, 158.7 (d, J = 255 Hz), 148.1, 145.4 (d, J = 1 Hz), 143.2 (d, J = 6 Hz), 136.4 (d, J = 2 Hz), 127.9 (d, J = 9 Hz), 122.1, 115.9 (d, J = 25 Hz), 108.8 (d, J = 26 Hz), 53.6 ppm; ^{19}F NMR (376 MHz, $CDCl_3$) δ: −102 ppm; HRMS (ESI-TOF) m/z: $[M + H]^+$ calcd for $C_{11}H_7BrClFNO_2$: 317.9327; found: 317.9328.

*7-Bromo-6-fluoro-4-methoxyquinoline (**3e**).* Prepared *via* the general procedure using **1f** (35.4 mg, 0.2 mmol, 1.0 equiv). White solid (0.021 g, 41%); m.p. 139−141 °C; IR (film) ν_{max} 1596, 1570, 1499, 1348, 1181, 1093, 717 cm^{-1}; ^{1}H NMR (400 MHz, $CDCl_3$) δ: 8.72 (d, J = 5.2 Hz, 1H), 8.30 (d, J = 6.6 Hz, 1H), 7.85 (d, J = 9.2 Hz, 1H), 6.77 (d, J = 5.2 Hz, 1H), 4.06 (s, 3H) ppm; $^{13}C\{^1H\}$ NMR (100 MHz, $CDCl_3$) δ: 162.0 (d, J = 5 Hz), 156.2 (d, J = 248 Hz), 151.6 (d, J = 3 Hz), 146.3 (d, J = 1 Hz), 133.9, 121.2 (d, J = 8 Hz), 113.6 (d, J = 24 Hz), 106.8 (d, J = 25 Hz), 100.7, 56.0 ppm; ^{19}F NMR (376 MHz, $CDCl_3$) δ: −109 ppm; HRMS (ESI-TOF) m/z: $[M + H]^+$ calcd for $C_{10}H_8BrFNO$: 255.9768; found: 255.9767.

*Ethyl 7-bromo-4-chloro-6-fluoroquinoline-3-carboxylate (**3f**).* Prepared *via* the general procedure using **1e** (25.4 mg, 0.1 mmol, 1.0 equiv) and B_2pin_2 (55.9 mg, 0.22 mmol, 2.2 equiv) and purified *via* column chromatography (hexane/Et_2O, 9:1). 95% yield **2c** by ^{1}H NMR analysis using 1,3,5-trimethoxybenzene as an internal standard. White solid (0.029 g, 88%); m.p. 119−120 °C; IR (film) ν_{max} 1727, 1609, 1551, 1336, 1153, 1037, 788, 689 cm^{-1}; ^{1}H NMR (400 MHz, $CDCl_3$) δ: 9.17 (s, 1H), 8.42 (d, J = 6.6 Hz, 1H), 8.08 (d, J = 9.2 Hz, 1H), 4.51 (q, J = 7.1 Hz, 2H), 1.47 (q, J = 7.1 Hz, 3H) ppm; $^{13}C\{^1H\}$ NMR (100 MHz, $CDCl_3$) δ: 164.0, 157.9 (d, J = 252 Hz), 150.5, 142.6, 142.6 (d, J = 6 Hz), 135.1, 126.6 (d, J = 8 Hz), 123.7, 116.6 (d, J = 25 Hz), 110.1 (d, J = 26 Hz), 62.4, 14.2 ppm; ^{19}F NMR (376 MHz, $CDCl_3$) δ: −104 ppm; HRMS (ESI-TOF) $m/zm/z$: $[M + H]^+$ calcd for $C_{12}H_9BrClFNO_2$: 331.9484; found: 331.9481.

Derivatization of C7-Borylated-6-fluoroquinolines. *4-Chloro-6-fluoro-7-iodo-2-methylquinoline (**4a**).* A 15 mL Schlenk flask was oven-dried (150 °C) and cooled under vacuum. The Schlenk flask was refilled with nitrogen, and all reagents were added under a positive pressure of nitrogen in the order: **1a** (39.1 mg, 0.2 mmol, 1.0 equiv), dtbpy (1.6 mg, 0.006 mmol, 3 mol %), B_2pin_2 (55.9 mg, 0.22 mmol, 1.1 equiv), and $[Ir(OMe)COD]_2$ (2.0 mg, 0.003 mmol, 1.5 mol %). The Schlenk flask was then placed under vacuum for 20 min before being refilled with nitrogen 3 times. THF (0.5 mL) was added *via* syringe through a septum, the reaction was sealed, and the mixture was heated to 80 °C in an aluminum heating block for 14 h, cooled to r.t., and concentrated under reduced pressure. The residue was dissolved in MeOH (1.6 mL) and added to a 5 mL screw-capped vial containing CuI (3.8 mg, 0.02 mmol, 10 mol %), 1,10-phenanthroline (7.2 mg, 0.04 mmol, 0.2 equiv), and KI (49.8 mg, 0.3 mmol, 1.5 equiv). The mixture was stirred at r.t. for 5 min, H_2O (0.4 mL) was then added, the vial was sealed, and the solution was heated to 80 °C in an aluminum heating block for 2 h.[25] The solution was cooled to r.t., diluted with DCM and H_2O, and the layers were separated. The aqueous portion was extracted with DCM (2 ×5 mL), and the combined organic layers were then washed with brine (10 mL), dried over $MgSO_4$, filtered, and concentrated under reduced pressure. The product was purified *via* column chromatography (DCM/EtOAc, 95:5). White solid (0.038 g, 64%); m.p. 108−111 °C; IR (film) ν_{max} 1594, 1538, 1097, 704, 628 cm^{-1}; ^{1}H NMR (300 MHz, $CDCl_3$) δ: 8.52 (d, J = 6.0 Hz, 1H), 7.76 (d, J = 8.4 Hz, 1H), 7.41 (s, 1H), 2.70 (s, 3H) ppm; $^{13}C\{^1H\}$ NMR (75 MHz, $CDCl_3$) δ: 159.1 (d, J = 3 Hz), 159.0 (d, J = 247 Hz), 146.1, 141.7, 140.8 (d, J = 3 Hz), 125.6 (d, J = 9 Hz), 122.9, 107.5 (d, J = 27 Hz), 87.2 (d, J = 29 Hz), 25.0 ppm; ^{19}F NMR (282 MHz, $CDCl_3$) δ: −95 ppm; HRMS (ESI-TOF) m/z: $[M + H]^+$ calcd for $C_{10}H_7ClFIN$: 321.9290; found: 321.9286.

*4-Chloro-6-fluoro-2-methylquinoline-7-d (**5a**).* A 15 mL Schlenk flask was flame-dried and cooled under vacuum. The Schlenk flask was refilled with nitrogen, **2a** (64.3 mg, 0.2 mmol, 1.0 equiv) and $[Ir(OMe)COD]_2$ (1.3 mg, 0.002 mmol, 1.0 mol %) were added, and the Schlenk flask was evacuated and backfilled with nitrogen 3 times.

https://doi.org/10.1021/acs.joc.2c00973
J. Org. Chem. 2022, 87, 9977−9987

THF (0.8 mL) and D_2O (0.2 mL) were added, the vessel was sealed, and the mixture was heated to 80 °C in an oil bath for 12 h. The solution was cooled to r.t. and extracted with Et_2O (2 ×5 mL).[26] The combined organic layers were washed with brine (10 mL), dried over $MgSO_4$, filtered, and concentrated under reduced pressure. The product was purified *via* column chromatography (DCM/EtOAc, 95:5). Colorless crystalline solid (0.022 g, 57%); m.p. 85−86 °C; IR (film) ν_{max} 1617, 1555, 1025, 830 cm^{-1}; ^1H NMR (400 MHz, $CDCl_3$) δ: 8.02 (d, J = 5.2 Hz, 1H), 7.79 (d, J = 9.4 Hz, 1H), 7.41 (s, 1H), 2.71 (s, 3H) ppm; $^{13}C\{^1H\}$ NMR (100 MHz, $CDCl_3$) δ: 160.8 (d, J = 249 Hz), 158.3 (d, J = 3 Hz), 145.6, 142.1 (d, J = 5 Hz), 131.5 (d, J = 9 Hz), 125.8 (d, J = 11 Hz), 122.7, 121.0−120.0 (m), 107.9 (d, J = 24 Hz), 25.0 ppm; ^{19}F NMR (282 MHz, $CDCl_3$) δ: −113 ppm; HRMS (ESI-TOF) m/z: $[M + H]^+$ calcd for $C_{10}H_7DClFN$: 197.0387; found: 197.0380.

*(4-Chloro-6-fluoro-2-methylquinolin-7-yl)trifluoroborate potassium salt (**6a**).* A 15 mL Schlenk flask was oven-dried (150 °C) and cooled under vacuum. The Schlenk flask was refilled with nitrogen, and all reagents were added under a positive pressure of nitrogen in the order: **1a** (195.6 mg, 1.0 mmol, 1.0 equiv), dtbpy (8.1 mg, 0.03 mmol, 3 mol %), B_2pin_2 (279.3 mg, 1.1 mmol, 1.1 equiv), and $[Ir(OMe)COD]_2$ (9.9 mg, 0.015 mmol, 1.5 mol %). The Schlenk flask was then placed under vacuum for 20 min before being refilled with nitrogen 3 times. THF (5 mL) was added *via* a syringe through a septum, the reaction was sealed, and the mixture was heated to 80 °C in an oil bath for 18 h. The solution was cooled, H_2O (3 mL) and KHF_2 (468.6 mg, 6.0 mmol, 6.0 equiv) were added, and the mixture was allowed to stir for a further 24 h before being diluted with acetone and H_2O. Volatiles were removed under reduced pressure, and the resulting precipitate was isolated by suction filtration and washed with H_2O (15 mL) and cold hexane (15 mL).[27] Beige solid (0.215 g, 71%); m.p. >250 °C; IR (film) ν_{max} 1640, 1583, 1120, 1033, 799 cm^{-1}; ^1H NMR (600 MHz, $(CD_3)_2SO$) δ: 7.93 (d, J = 5.6 Hz, 1H), 7.56 (s, 1H), 7.45 (d, J = 9.2 Hz, 1H), 2.61 (s, 3H) ppm; $^{13}C\{^1H\}$ NMR (150 MHz, $(CD_3)_2SO$) δ: 164.8 (d, J = 245 Hz), 156.7 (d, J = 2 Hz), 145.2, 139.8, 134.3 (d, J = 15 Hz), 123.5 (d, J = 11 Hz), 121.1, 104.8 (d, J = 30 Hz), 24.4 ppm; a signal for the carbon directly attached to the boron atom was not observed; ^{19}F NMR (282 MHz, $(CD_3)_2SO$) δ: −105, −138 ppm; ^{11}B NMR (96 MHz, $(CD_3)_2SO$) δ: 2 ppm; HRMS (ESI-TOF) m/z: $[M + H]^+$ calcd for $C_{10}H_7BClF_3N$: 244.0307; found: 244.0311.

*(6-Fluoro-4-methoxy-2-methylquinolin-7-yl)trifluoroborate potassium salt (**6b**).* Prepared *via* the procedure described for **6a** using **1b** (153 mg, 0.8 mmol, 1.0 equiv). Brown solid (0.174 g, 73%); m.p. >250 °C; IR (film) ν_{max} 1645, 1592, 1146, 1017, 834 cm^{-1}; ^1H NMR (600 MHz, $(CD_3)_2SO$) δ: 8.01 (d, J = 4.6 Hz, 1H), 7.59 (d, J = 8.4 Hz, 1H), 7.38 (s, 1H), 4.21 (s, 3H), 2.80 (s, 3H) ppm; $^{13}C\{^1H\}$ NMR (150 MHz, $(CD_3)_2SO$) δ: 166.9 (d, J = 5 Hz), 164.6 (d, J = 247 Hz), 156.8, 135.4, 125.1 (d, J = 14 Hz), 118.7 (d, J = 10 Hz), 104.7 (d, J = 30 Hz), 102.4, 58.2, 20.7 ppm; a signal for the carbon directly attached to the boron atom was not observed; ^{19}F NMR (282 MHz, $(CD_3)_2SO$) δ: −103, −139 ppm; ^{11}B NMR (96 MHz, $(CD_3)_2SO$) δ: 2 ppm; HRMS (ESI-TOF) m/z: $[M + H]^+$ calcd for $C_{11}H_{10}BF_3NO$: 240.0802; found: 240.0807.

*(6-Fluoro-4-methoxy-2-methylquinolin-7-yl)boronic Acid (**7b**).* **6b** (98 mg, 0.33 mmol, 1.0 equiv) was suspended in THF (11 mL), and a solution of $LiOH.H_2O$ (124.6 mg, 2.97 mmol, 9.0 equiv) in H_2O (2.5 mL) was added. The resulting mixture was stirred at r.t. for 24 h. THF was removed under reduced pressure, and the mixture was acidified to pH∼5 using saturated NH_4Cl (4 mL) and 1 M HCl (2 mL). The resulting precipitate was collected by suction filtration, redissolved in 1 M HCl, and extracted once with Et_2O. The aqueous portion was then neutralized using solid $NaHCO_3$ and extracted with DCM/iPrOH (9:1, 3 × 10 mL). The organic layers were dried over $MgSO_4$, filtered, and concentrated under reduced pressure. White solid (0.058 g, 75%); m.p. >250 °C; IR (film) ν_{max} 1646, 1504, 1362, 1250, 1202, 1091 cm^{-1}; ^1H NMR (600 MHz, $(CD_3)_2SO$) δ: 8.52 (s, 2H), 8.04 (d, J = 5.7 Hz, 1H), 7.56 (d, J = 9.6 Hz, 1H), 6.95 (s, 1H), 4.01 (s, 3H), 2.59 (s, 3H) ppm; $^{13}C\{^1H\}$ NMR (150 MHz, $(CD_3)_2SO$) δ: 161.8 (d, J = 243 Hz), 160.9 (d, J = 5 Hz), 159.2 (d, J = 2 Hz), 144.9, 136.1 (d, J = 10 Hz), 120.6 (d, J = 10 Hz), 104.3 (d, J = 27 Hz), 101.9, 56.1, 25.4 ppm; a signal for the carbon directly attached to the boron atom was not observed; ^{19}F NMR (282 MHz, $(CD_3)_2SO$) δ: −108 ppm; ^{11}B NMR (96 MHz, $(CD_3)_2SO$) δ: 27 ppm; HRMS (ESI-TOF) m/z: $[M + H]^+$ calcd for $C_{11}H_{12}BFNO_3$: 236.0889; found: 236.0894.

*7-Benzyl-4-chloro-6-fluoro-2-methylquinoline (**8a**).* A 15 mL Schlenk flask was dried under vacuum, cooled to r.t., and refilled with nitrogen. **2a** (64.3 mg, 0.2 mmol, 1.0 equiv), $Pd_2(dba)_3$ (1.8 mg, 0.002 mmol, 1.0 mol %), PPh_3 (2.1 mg, 0.008 mmol, 4.0 mol %), and K_2CO_3 (110.6 mg, 0.8 mmol, 4.0 equiv) were added, and the Schlenk flask was evacuated and backfilled with nitrogen 3 times. Benzyl bromide (0.03 mL, 0.24 mmol, 1.2 equiv), THF (1 mL), and H_2O (0.02 mL) were added, the vessel was sealed, and the mixture was heated to 100 °C in an aluminum heating block for 24 h.[24] The solution was cooled to r.t., diluted with H_2O, and extracted with EtOAc (3 × 10 mL). The combined organic layers were washed with brine (10 mL), dried over $MgSO_4$, filtered, and concentrated under reduced pressure. The product was purified *via* column chromatography (DCM). Off-white solid (0.049 g, 86%); m.p. 94−96 °C; IR (film) ν_{max} 1635, 1598, 1551, 1027, 871 cm^{-1}; ^1H NMR (400 MHz, $CDCl_3$) δ: 7.88−7.66 (m, 2H), 7.39−7.14 (m, 6H), 4.16 (s, 2H), 2.66 (s, 3H) ppm; $^{13}C\{^1H\}$ NMR (100 MHz, $CDCl_3$) δ: 159.7 (d, J = 250 Hz), 158.1 (d, J = 2 Hz), 145.6, 141.6 (d, J = 5 Hz), 138.5, 134.3 (d, J = 20 Hz), 131.0 (d, J = 6 Hz), 129.1, 128.7, 126.6, 124.4 (d, J = 10 Hz), 121.9, 107.7 (d, J = 26 Hz), 35.5 (d, J = 3 Hz), 24.9 ppm; ^{19}F NMR (376 MHz, $CDCl_3$) δ: −117 ppm; HRMS (ESI-TOF) m/z: $[M + H]^+$ calcd for $C_{17}H_{14}ClFN$: 286.0793; found: 286.0785.

*Ethyl-4-(4-chloro-6-fluoro-2-methylquinolin-7-yl)benzoate (**9a**).* A 15 mL Schlenk flask was oven-dried (150 °C) and cooled under vacuum. The Schlenk flask was refilled with nitrogen, and all reagents were added under a positive pressure of nitrogen in the order: **1a** (39.1 mg, 0.2 mmol, 1.0 equiv), dtbpy (1.6 mg, 0.006 mmol, 3 mol %), B_2pin_2 (55.9 mg, 0.22 mmol, 1.1 equiv), and $[Ir(OMe)COD]_2$ (2.0 mg, 0.003 mmol, 1.5 mol %). The Schlenk flask was then placed under vacuum for 20 min before being refilled with nitrogen 3 times. THF (0.5 mL) was added *via* septum, the reaction was sealed, and the mixture was heated to 80 °C in an aluminum heating block for 14 h, cooled to r.t., and concentrated under reduced pressure. A 15 mL Schlenk was heated under vacuum, cooled to r.t., and refilled with nitrogen. The crude reaction mixture for **2a** (0.2 mmol, 1.0 equiv), $Pd(PPh_3)_4$ (11.6 mg, 0.01 mmol, 5.0 mol %), and K_3PO_4 (127.4 mg, 0.6 mmol, 3.0 equiv) was added, and the Schlenk flask was evacuated and backfilled with nitrogen 3 times. Ethyl-4-bromobenzoate (0.05 mL, 0.3 mmol, 1.5 equiv), THF (2 mL), and H_2O (0.4 mL) were added, the vessel was sealed, and the mixture was heated to 60 °C for 18 h.[3l] The solution was cooled to r.t., diluted with H_2O, and extracted with Et_2O (3 × 10 mL). The combined organic layers were washed with brine (10 mL), dried over $MgSO_4$, filtered, and concentrated under reduced pressure. The product was purified *via* column chromatography (DCM:Et_2O, 90:10); X-ray quality crystals were obtained *via* vapor diffusion from a saturated solution of DCM in Et_2O; and the CCDC number is 2159957. White solid (0.052 g, 76%); m.p. 120−122 °C; IR (film) ν_{max} 1710, 1610, 1598, 1383, 1291, 1027, 857 cm^{-1}; ^1H NMR (300 MHz, $CDCl_3$) δ: 8.25−8.09 (m, 3H), 7.89 (d, J = 11.2 Hz, 1H), 7.81−7.67 (m, 2H), 7.42 (s, 1H), 4.42 (q, J = 7.1 Hz, 2H), 2.73 (s, 3H), 1.43 (t, J = 7.1 Hz, 3H) ppm; $^{13}C\{^1H\}$ NMR (75 MHz, $CDCl_3$) δ: 166.2, 158.9 (d, J = 2 Hz), 158.1 (d, J = 251 Hz), 145.6, 141.5 (d, J = 6 Hz), 139.1 (d, J = 2 Hz), 133.1 (d, J = 18 Hz), 131.3 (d, J = 4 Hz), 130.4, 129.8, 129.2 (d, J = 3 Hz), 125.3 (d, J = 10 Hz), 122.6, 108.9 (d, J = 26 Hz), 61.1, 25.1, 14.4 ppm; ^{19}F NMR (282 MHz, $CDCl_3$) δ: −116 ppm; HRMS (ESI-TOF) m/z: $[M + H]^+$ calcd for $C_{19}H_{16}ClFNO_2$: 344.0848; found: 344.0839.

*Ethyl-4-(6-fluoro-4-methoxy-2-methylquinolin-7-yl)benzoate (**9b**).* Prepared *via* the procedure described for **9a** using **1b** (57.4 mg, 0.3 mmol, 1.0 equiv). White solid (0.063 g, 62%); m.p. 93−95 °C; IR (film) ν_{max} 1712, 1608, 1556, 1348, 1280, 1201, 1107, 1024 cm^{-1}; ^1H NMR (300 MHz, $CDCl_3$) δ: 8.19−8.11 (m, 2H), 8.06 (d, J = 7.3 Hz, 1H), 7.84 (d, J = 11.4 Hz, 1H), 7.79−7.69 (m, 2H), 6.66 (s, 1H),

https://doi.org/10.1021/acs.joc.2c00973
J. Org. Chem. 2022, 87, 9977−9987

4.42 (q, J = 7.1 Hz, 2H), 4.05 (s, 3H), 2.71 (s, 3H), 1.42 (t, J = 7.1 Hz, 3H) ppm; $^{13}C\{^1H\}$ NMR (75 MHz, $CDCl_3$) δ: 166.4, 161.7 (d, J = 5 Hz), 160.1 (d, J = 2 Hz), 157.1 (d, J = 248 Hz), 145.8, 139.9, 132.0 (d, J = 17 Hz), 130.4 (d, J = 4 Hz), 130.0, 129.7, 129.2 (d, J = 3 Hz), 120.2 (d, J = 10 Hz), 106.8 (d, J = 25 Hz), 101.2, 61.1, 55.7, 25.9, 14.4 ppm; ^{19}F NMR (282 MHz, $CDCl_3$) δ: −120 ppm; HRMS (ESI-TOF) m/z: $[M + H]^+$ calcd for $C_{20}H_{19}FNO_3$: 340.1343; found: 340.1336.

*4-Chloro-6-fluoro-7-(1H-indol-5-yl)-2-methylquinoline (**10a**).* A 15 mL Schlenk flask was oven-dried (150 °C), cooled to r.t. under vacuum, and refilled with nitrogen. 5-Bromoindole (23.5 mg, 0.12 mmol, 1.0 equiv), **2a** (48.2 mg, 0.15 mmol, 1.25 equiv), $Pd(dba)_2$ (1.4 mg, 0.0024 mmol, 2.0 mol %), P(o-tol)$_3$ (2.2 mg, 0.0072 mmol, 6.0 mol %), and Na_2CO_3 (50.9 mg, 0.48 mmol, 4.0 equiv) were added, and the Schlenk flask was evacuated and backfilled with nitrogen 3 times. THF (0.45 mL) and H_2O (0.05 mL) were added, the vessel was sealed, and the mixture was heated to 50 °C in an oil bath for 24 h.[28] The mixture was cooled to r.t., filtered through a short plug of Celite with DCM, and concentrated under reduced pressure. The product was purified *via* column chromatography (DCM/EtOAc, 98:2). Bright yellow solid (0.032 g, 86%); m.p. 160−162 °C; IR (film) ν_{max} 3415, 1626, 1596, 1545, 1011, 867 cm^{-1}; ^1H NMR (400 MHz, $(CD_3)_2SO$) δ: 11.30 (bs, 1H), 8.06 (d, J = 7.5 Hz, 1H), 7.97−7.77 (m, 2H), 7.66 (s, 1H), 7.55 (d, J = 8.4 Hz), 7.51−7.32 (m, 2H), 6.54 (bs, 1H), 2.64 (s, 3H) ppm; $^{13}C\{^1H\}$ NMR (100 MHz, $(CD_3)_2SO$) δ: 158.9 (d, J = 2 Hz), 158.0 (d, J = 249 Hz), 145.2, 140.1 (d, J = 5 Hz), 135.9, 135.1 (d, J = 18 Hz), 130.4 (d, J = 3 Hz), 128.0, 126.4, 124.7 (d, J = 1 Hz), 123.4 (d, J = 11 Hz), 122.27, 122.24, 121.1 (d, J = 3 Hz), 111.8, 108.0 (d, J = 26 Hz), 101.8, 24.5 ppm; ^{19}F NMR (282 MHz, $(CD_3)_2SO$) δ: −116 ppm; HRMS (ESI-TOF) m/z: $[M + H]^+$ calcd for $C_{18}H_{13}ClFN_2$: 311.0746; found: 311.0741.

*6-Fluoro-4-methoxy-2-methyl-7-(piperidin-1-yl)quinoline (**11b**).* A 15 mL Schlenk flask was dried under vacuum, cooled to r.t., and refilled with nitrogen. **3b** (27.0 mg, 0.1 mmol, 1.0 equiv), RuPhos (2.8 mg, 0.006 mmol, 6.0 mol %), and NaO*t*-Bu (24 mg, 0.25 mmol, 2.5 equiv) were added, and the Schlenk flask was evacuated and backfilled with nitrogen 3 times. Piperidine (0.02 mL, 0.2 mmol, 2.0 equiv) and toluene (1 mL) were added, and the mixture was degassed with nitrogen for 5 min. $Pd_2(dba)_3$ (2.7 mg, 0.003 mmol, 2.0 mol %) was then added, the vessel was sealed, and the suspension was heated to 80 °C in an oil bath for 16 h. The product was purified *via* column chromatography (DCM/EtOAc, 98:2 with 1% NEt_3 as modifier). Yellow oil (0.024 g, 88%); IR (film) ν_{max} 1605, 1514, 1381, 1350, 1241, 1131, 1019 cm^{-1}; ^1H NMR (500 MHz, $CDCl_3$) δ: 7.64 (d, J = 13.5 Hz, 1H), 7.41 (d, J = 8.3 Hz, 1H), 6.51 (s, 1H), 3.99 (s, 3H), 3.23−3.09 (m, 4H), 2.67 (s, 3H), 1.86−1.70 (m, 4H), 1.68−1.56 (m, 2H) ppm; $^{13}C\{^1H\}$ NMR (125 MHz, $CDCl_3$) δ: 161.9 (d, J = 5 Hz), 159.2 (d, J = 2 Hz), 154.5 (d, J = 249 Hz), 146.6, 145.9 (d, J = 12 Hz), 115.5 (d, J = 3 Hz), 114.3 (d, J = 10 Hz), 106.4 (d, J = 24 Hz), 99.3, 55.6, 51.9 (d, J = 4 Hz), 26.0, 25.5, 24.2 ppm; ^{19}F NMR (282 MHz, $CDCl_3$) δ: −120 ppm; HRMS (ESI-TOF) m/z: $[M + H]^+$ calcd for $C_{16}H_{20}FN_2O$: 275.1554; found: 275.1555.

*4-Chloro-6-fluoro-2-methylquinolin-7-ol (**12a**).* A solution of **2a** (64.3 mg, 0.2 mmol, 1.0 equiv) in MeOH (0.5 mL) in a 5 mL screw-capped vial was cooled to 0 °C over ice. 30% H_2O_2 solution (0.02 mL, 0.24 mmol, 1.18 equiv) was gradually added, and the mixture was allowed warm slowly to r.t. and stirred at this temperature for 16 h. The reaction mixture was diluted with MeOH, quenched using saturated $Na_2S_2O_3$ solution (∼1 mL), and MeOH was removed under reduced pressure. The mixture was then extracted with EtOAc (3 × 10 mL), dried over $MgSO_4$, filtered, and concentrated under reduced pressure. White solid (0.036 g, 85%); m.p. 192−195 °C; IR (film) ν_{max} 1629, 1539, 1261, 1032, 797 cm^{-1}; ^1H NMR (600 MHz, $(CD_3)_2SO$) δ: 11.09 (bs, 1H), 7.78 (d, J = 11.7 Hz, 1H), 7.49 (s, 1H), 7.40 (d, J = 8.5 Hz, 1H), 2.58 (s, 3H) ppm; $^{13}C\{^1H\}$ NMR (150 MHz, $(CD_3)_2SO$) δ: 158.7 (d, J = 2 Hz), 152.1 (d, J = 249 Hz), 149.2 (d, J = 15 Hz), 146.5, 140.0 (d, J = 5 Hz), 119.8, 117.8 (d, J = 9 Hz), 113.2 (d, J = 3 Hz), 108.1 (d, J = 21 Hz), 24.5 ppm; ^{19}F NMR (282 MHz, $(CD_3)_2SO$) δ: −131 ppm; HRMS (ESI-TOF) m/z: $[M + H]^+$ calcd for $C_{10}H_8ClFNO$: 212.0273; found: 212.0269.

Methods to Access 4-Fluoroquinolones. *(6-Fluoro-2-methyl-4-oxo-1,4-dihydroquinolin-7-yl)boronic Acid (**13a**).* A 15 mL Schlenk flask was oven-dried (150 °C) and cooled under vacuum. The Schlenk flask was refilled with nitrogen, and all reagents were added under a positive pressure of nitrogen in the order: **1a** (39.1 mg, 0.2 mmol, 1.0 equiv), dtbpy (1.6 mg, 0.006 mmol, 3 mol %), B_2pin_2 (55.9 mg, 0.22 mmol, 1.1 equiv), and $[Ir(OMe)COD]_2$ (2.0 mg, 0.003 mmol, 1.5 mol %). The Schlenk flask was then placed under vacuum for 20 min before being refilled with nitrogen 3 times. THF (0.5 mL) was added *via* a syringe through a septum, the reaction was sealed, and the mixture was heated to 80 °C in an aluminum heating block for 14 h, cooled to r.t., and concentrated under reduced pressure. The crude reaction mixture for **2a** (0.2 mmol, 1.0 equiv) and NaOAc (32.8 mg, 0.4 mmol, 2.0 equiv) was added to a 5 mL screw-capped vial followed by glacial acetic acid (1.25 mL). The vial was sealed and stirred at 120 °C in an aluminum heating block for 1 h, cooled to r.t., concentrated under reduced pressure, diluted with H_2O, and allowed to stand for 1 h. The resulting precipitate was isolated by suction filtration and washed with H_2O and cold Et_2O. Pink solid (0.030 g, 69%); m.p. 245−249 °C; IR (film) ν_{max} 1655, 1608, 1505, 1375, 1275, 1110 cm^{-1}; ^1H NMR (300 MHz, $(CD_3)_2SO$) δ: 11.68 (bs, 1H), 8.48 (s, 2H), 7.67 (d, J = 4.8 Hz, 1H), 7.56 (d, J = 9.3 Hz, 1H), 5.90 (s, 1H), 2.34 (s, 3H) ppm; $^{13}C\{^1H\}$ NMR (75 MHz, $(CD_3)_2SO$) δ: 176.0 (d, J = 3 Hz), 160.9 (d, J = 241 Hz), 149.9, 136.3, 126.4 (d, J = 7 Hz), 125.0 (d, J = 10 Hz), 108.0 (d, J = 26 Hz), 107.6, 19.5 ppm; a signal for the carbon directly attached to the boron atom was not observed; ^{19}F NMR (282 MHz, $(CD_3)_2SO$) δ: −111 ppm; ^{11}B NMR (96 MHz, $(CD_3)_2SO$) δ: 27 ppm; HRMS (ESI-TOF) m/z: $[M + H]^+$ calcd for $C_{10}H_{10}BFNO_3$: 222.0732; found: 222.0738.

*7-Bromo-6-fluoro-2-methylquinolin-4(1H)-one (**13b**).* **3b** (27.0 mg, 0.1 mmol, 1.0 equiv) was added to a 5 mL screw-capped vial followed by 48% HBr solution (0.25 mL) and glacial acetic acid (0.5 mL). The vial was sealed and stirred at 150 °C in an aluminum heating block for 6 h, cooled to r.t., diluted with H_2O, and neutralized using 6 M NaOH. The resulting precipitate was isolated by suction filtration and washed with H_2O and cold Et_2O. Off-white solid (0.021 g, 82%); m.p. >250 °C; IR (film) ν_{max} 1639, 1601, 1558, 1272, 1021, 751 cm^{-1}; ^1H NMR (600 MHz, $(CD_3)_2SO$) δ: 11.73 (bs, 1H), 8.00−7.62 (m, 2H), 5.95 (s, 1H), 2.36 (s, 3H) ppm; $^{13}C\{^1H\}$ NMR (150 MHz, $(CD_3)_2SO$) δ: 175.4, 154.2 (d, J = 242 Hz), 150.5, 137.3, 125.0 (d, J = 5 Hz), 122.8, 113.0 (d, J = 24 Hz), 110.4 (d, J = 23 Hz), 108.1, 19.5 ppm; ^{19}F NMR (282 MHz, $(CD_3)_2SO$) δ: −115 ppm; HRMS (ESI-TOF) m/z: $[M + H]^+$ calcd for $C_{10}H_8BrFNO$: 255.9768; found: 255.9772.

*6-Fluoro-2-methyl-7-(4,4,5,5-tetramethyl-1,3,2-dioxaborolan-2-yl)quinolin-4(1H)-one (**13c**).* A 15 mL Schlenk flask was oven-dried (150 °C) and cooled under vacuum. The Schlenk flask was refilled with nitrogen, and all reagents were added under a positive pressure of nitrogen in the order: **1c** (59.1 mg, 0.2 mmol, 1.0 equiv), dtbpy (1.6 mg, 0.006 mmol, 3 mol %), B_2pin_2 (55.9 mg, 0.22 mmol, 1.1 equiv), and $[Ir(OMe)COD]_2$ (2.0 mg, 0.003 mmol, 1.5 mol %). The Schlenk flask was then placed under vacuum for 20 min before being refilled with nitrogen 3 times. THF (0.5 mL) was added *via* a syringe through a septum, the reaction was sealed, and the mixture was heated to 80 °C in an aluminum heating block for 16 h. The reaction was cooled to r.t., diluted with MeOH, and concentrated under reduced pressure. The residue was dissolved in MeOH (2 mL) and added to a small Schlenk flask, followed by 10% Pd/C (2.0 mg, 0.02 mmol, 10 mol %). The resulting suspension was purged with H_2 and then stirred under a balloon of H_2 at 50 °C for 16 h. The mixture was cooled to r.t., diluted with DCM, filtered through a short plug of Celite, and concentrated under reduced pressure. The product was purified *via* trituration from DCM/Et_2O (1:1). Beige solid (0.032 g, 53%); m.p. >250 °C; IR (film) ν_{max} 1643, 1561, 1373, 1340, 1265, 1142, 1035 cm^{-1}; ^1H NMR (600 MHz, $(CD_3)_2SO$) δ: 11.71 (bs, 1H), 7.92 (d, J = 4.8 Hz, 1H), 7.60 (d, J = 9.5 Hz, 1H), 5.93 (s, 1H), 2.34 (s, 3H), 1.34 (s, 12H) ppm; $^{13}C\{^1H\}$ NMR (150 MHz, $(CD_3)_2SO$) δ: 175.7, 161.4 (d, J = 246 Hz), 150.2, 136.2, 127.9 (d, J = 7 Hz), 127.4 (d, J = 8 Hz), 108.7 (d, J = 25 Hz), 107.9, 84.2, 24.7, 19.5 ppm; a signal for the carbon directly attached to the boron atom was not observed; ^{19}F

https://doi.org/10.1021/acs.joc.2c00973
J. Org. Chem. 2022, 87, 9977−9987

NMR (282 MHz, $(CD_3)_2SO$) δ: −110 ppm; ^{11}B NMR (96 MHz, $(CD_3)_2SO$) δ: 30 ppm; HRMS (ESI-TOF) m/z: $[M + H]^+$ calcd for $C_{16}H_{20}BFNO_3$: 304.1515; found: 304.1515. *Note that compound **13c** contained a trace impurity **13a**; over time, complete conversion from **13c** to **13a** was observed in solution.

*Ethyl 6-fluoro-4-oxo-7-(4,4,5,5-tetramethyl-1,3,2-dioxaborolan-2-yl)-1,4-dihydroquinoline-3-carboxylate (**13d**).* Prepared *via* the procedure described for **13a** using **1f** (50.7 mg, 0.2 mmol, 1.0 equiv), with the acid-catalyzed hydrolysis step being carried out for 2 h at 120 °C. The product was purified *via* trituration from a mixture of hot acetone/MeOH. White solid (0.039 g, 53%); m.p. >250 °C; IR (film) ν_{max} 1694, 1613, 1534, 1401, 1334, 1265, 1143, 1043 cm^{-1}; ^1H NMR (600 MHz, $(CD_3)_2SO$) δ: 8.60 (s, 1H), 8.01 (d, J= 4.8 Hz, 1H), 7.71 (d, J = 9.4 Hz, 1H), 4.21 (q, J = 7.1 Hz, 2H), 1.39−1.18 (m, 15H) ppm; $^{13}C\{^1H\}$ NMR (150 MHz, $(CD_3)_2SO$) δ: 172.5, 164.8, 162.5 (d, J = 248 Hz), 145.5, 135.6, 131.0 (d, J = 6 Hz), 128.6, 109.8 (d, J = 25 Hz), 109.1, 84.2, 59.6, 26.7, 14.3 ppm; a signal for the carbon directly attached to the boron atom was not observed; ^{19}F NMR (282 MHz, $(CD_3)_2SO$) δ: −108 ppm; ^{11}B NMR (96 MHz, $(CD_3)_2SO$) δ: 30 ppm; HRMS (ESI-TOF) m/z: $[M + H]^+$ calcd for $C_{18}H_{22}BFNO_5$: 362.1570; found: 362.1577. *Note that compound **13d** was highly insoluble in $(CD_3)_2SO$ and degraded in solution over a matter of hours; once synthesized, the compound (∼2 mg) was dissolved in $(CD_3)_2SO$ with gentle heating and immediately taken for NMR analysis.

*Ethyl 7-bromo-6-fluoro-4-oxo-1,4-dihydroquinoline-3-carboxylate (**13e**).* **3f** (30 mg, 0.09 mmol, 1.0 equiv) was dissolved in EtOH (2.5 mL), and 1 M HCl (0.5 mL) was added. The mixture was stirred at 100 °C in an oil bath for 3 h. Upon cooling, a white precipitate formed, which was isolated *via* suction filtration and rinsed with H_2O, cold EtOH, and Et_2O to give **13e** as a white solid (0.018 g, 64%); m.p. >250 °C; IR (film) ν_{max} 1694, 1549, 1507, 1358, 1250, 1192, 1103 cm^{-1}; ^1H NMR (water suppression, 600 MHz, 313 K, $(CD_3)_2SO$) δ: 8.59 (s, 1H), 7.98 (d, J = 5.8 Hz, 1H), 7.91 (d, J = 9.1 Hz, 1H), 4.22 (q, J = 7.1 Hz, 2H), 1.28 (q, J = 7.1 Hz, 3H) ppm; $^{13}C\{^1H\}$ NMR (150 MHz, 313 K, $(CD_3)_2SO$) δ: 172.2, 164.8, 155.2 (d, J = 244 Hz), 146.3 (d, J = 2 Hz), 137.3 (d, J = 3 Hz), 128.2 (d, J = 6 Hz), 124.8, 113.7 (d, J = 25 Hz), 111.3 (d, J = 23 Hz), 109.4, 59.7, 14.3 ppm; ^{19}F NMR (282 MHz, $(CD_3)_2SO$) δ: −113 ppm; HRMS (ESI-TOF) m/z: $[M + H]^+$ calcd for $C_{12}H_{10}BrFNO_3$: 313.9823; found: 313.9826.

■ ASSOCIATED CONTENT

Supporting Information

The Supporting Information is available free of charge at https://pubs.acs.org/doi/10.1021/acs.joc.2c00973.

Supplementary experiments, experimental details, and copies of NMR spectra (PDF)

Accession Codes

CCDC 2159956−2159957 contain the supplementary crystallographic data for this paper. These data can be obtained free of charge via www.ccdc.cam.ac.uk/data_request/cif, or by emailing data_request@ccdc.cam.ac.uk, or by contacting The Cambridge Crystallographic Data Centre, 12 Union Road, Cambridge CB2 1EZ, UK; fax: +44 1223 336033.

CCDC (2159956 (**2a**) and 2159957 (**9a**)) contain the supplementary crystallographic data for this paper. These data can be obtained free of charge *via* www.ccdc.cam.ac.uk/data_request/cif, by emailing data_request@ccdc.cam.ac.uk, or by contacting The Cambridge Crystallographic Data Centre, 12 Union Road, Cambridge, CB2 1EZ, U.K.; Fax: +44 1223 336033.

■ AUTHOR INFORMATION

Corresponding Author

Gerard P. McGlacken − *School of Chemistry & Analytical and Biological Chemistry Research Facility, University College Cork, Cork T12 YN60, Ireland; Synthesis and Solid State Pharmaceutical Centre, University College Cork, Cork T12 YN60, Ireland;* orcid.org/0000-0002-7821-0804; Email: g.mcglacken@ucc.ie

Authors

Aobha Hickey − *School of Chemistry & Analytical and Biological Chemistry Research Facility, University College Cork, Cork T12 YN60, Ireland*

Julia Merz − *Institute for Inorganic Chemistry, and Institute for Sustainable Chemistry & Catalysis with Boron, Julius-Maximilians-Universität Würzburg, 97074 Würzburg, Germany*

Hamad H. Al Mamari − *Institute for Inorganic Chemistry, and Institute for Sustainable Chemistry & Catalysis with Boron, Julius-Maximilians-Universität Würzburg, 97074 Würzburg, Germany; Department of Chemistry, College of Science, Sultan Qaboos University, Muscat, Sultanate of Oman*

Alexandra Friedrich − *Institute for Inorganic Chemistry, and Institute for Sustainable Chemistry & Catalysis with Boron, Julius-Maximilians-Universität Würzburg, 97074 Würzburg, Germany;* orcid.org/0000-0002-1411-7336

Todd B. Marder − *Institute for Inorganic Chemistry, and Institute for Sustainable Chemistry & Catalysis with Boron, Julius-Maximilians-Universität Würzburg, 97074 Würzburg, Germany;* orcid.org/0000-0002-9990-0169

Complete contact information is available at: https://pubs.acs.org/10.1021/acs.joc.2c00973

Notes

The authors declare no competing financial interest.

■ ACKNOWLEDGMENTS

GMG thanks the Irish Research Council for funding (IRC GOIPG/2017/255), the Science Foundation Ireland (grant number SFI/12/IP/1315), and the Synthesis and Solid State Pharmaceutical Centre (SSPC) (SFI/12/RC/2275 and SFI/12/RC2275_P2). TBM thanks the Julius-Maximilians-Universität Würzburg. Sabbatical leave granted to HAM by Sultan Qaboos University is gratefully acknowledged.

■ REFERENCES

(1) (a) Girard, S. A.; Knauber, T.; Li, C.-J. The Cross-Dehydrogenative Coupling of C-H bonds: A Versatile Strategy for C-C Bond Formations. *Angew. Chem., Int. Ed.* **2014**, *53*, 74−100. (b) Gensch, T.; Hopkinson, M. N.; Glorius, F.; Wencel-Delord, J. Mild metal-catalyzed C−H activation: examples and concepts. *Chem. Soc. Rev.* **2016**, *45*, 2900−2936. (c) Moselage, M.; Lie, J.; Ackermann, L. Cobalt-Catalyzed C−H Activation. *ACS Catal.* **2016**, *6*, 498−525. (d) Shang, R.; Ilies, L.; Nakamura, E. Iron-Catalyzed C−H Bond Activation. *Chem. Rev.* **2017**, *117*, 9086−9139. (e) Yamaguchi, J.; Yamaguchi, A. D.; Itami, K. C-H Bond Functionalization: Emerging Synthetic Tools for Natural Products and Pharmaceuticals. *Angew. Chem., Int. Ed.* **2012**, *51*, 8960−9009. (f) Cano, R.; Pérez, J. M.; Ramón, D. J.; McGlacken, G. P. Impregnated palladium on magnetite as catalyst for direct arylation of heterocycles. *Tetrahedron* **2016**, *72*, 1043−1050.

(2) Welsch, M. E.; Snyder, S. A.; Stockwell, B. R. Privileged Scaffolds for Library Design and Drug Discovery. *Curr. Opin. Chem. Biol.* **2010**, *14*, 347−361.
(3) (a) Cho, J.-Y.; Tse, M. K.; Holmes, D.; Maleczka, R. E.; Smith, M. R. Remarkably Selective Iridium Catalysts for the Elaboration of Aromatic C−H Bonds. *Science* **2002**, *295*, 305−308. (b) Hartwig, J. F. Regioselectivity of The Borylation of Alkanes And Arenes. *Chem. Soc. Rev.* **2011**, *40*, 1992−2002. (c) Ishiyama, T.; Nobuta, Y.; Hartwig, J. F.; Miyaura, N. Room Temperature Borylation of Arenes and Heteroarenes Using Stoichiometric Amounts of Pinacolborane Catalyzed by Iridium Complexes in an Inert Solvent. *Chem. Commun.* **2003**, 2924−2925. (d) Ishiyama, T.; Takagi, J.; Hartwig, J. F.; Miyaura, N. A Stoichiometric Aromatic C−H Borylation Catalyzed by Iridium(I)/2,2′-Bipyridine Complexes at Room Temperature. *Angew. Chem., Int. Ed.* **2002**, *41*, 3056−3058. (e) Boller, T. M.; Murphy, J. M.; Hapke, M.; Ishiyama, T.; Miyaura, N.; Hartwig, J. F. Mechanism of the Mild Functionalization of Arenes by Diboron Reagents Catalyzed by Iridium Complexes. Intermediacy and Chemistry of Bipyridine-Ligated Iridium Trisboryl Complexes. *J. Am. Chem. Soc.* **2005**, *127*, 14263−14278. (f) Ishiyama, T.; Takagi, J.; Ishida, K.; Miyaura, N.; Anastasi, N. R.; Hartwig, J. F. Mild Iridium-Catalyzed Borylation of Arenes. High Turnover Numbers, Room Temperature Reactions, and Isolation of a Potential Intermediate. *J. Am. Chem. Soc.* **2002**, *124*, 390−391. (g) Mkhalid, I. A. I.; Coventry, D. N.; Albesa-Jove, D.; Batsanov, A. S.; Howard, J. A. K.; Perutz, R. N.; Marder, T. B. Ir-Catalyzed Borylation of C−H Bonds in N-Containing Heterocycles: Regioselectivity in the Synthesis of Heteroaryl Boronate Esters. *Angew. Chem., Int. Ed.* **2006**, *45*, 489−491. (h) Wright, J. S.; Scott, P. J. H.; Steel, P. G. Iridium-Catalysed C−H Borylation of Heteroarenes: Balancing Steric and Electronic Regiocontrol. *Angew. Chem., Int. Ed.* **2021**, *60*, 2796−2821. (i) Tian, Y.-M.; Guo, X.-N.; Wu, Z.; Friedrich, A.; Westcott, S. A.; Braunschweig, H.; Radius, U.; Marder, T. B. Ni-Catalyzed Traceless, Directed C3-Selective C−H Borylation of Indoles. *J. Am. Chem. Soc.* **2020**, *142*, 13136−13144. (j) Sadler, S. A.; Tajuddin, H.; Mkhalid, I. A. I.; Batsanov, A. S.; Albesa-Jove, D.; Cheung, M. S.; Maxwell, A. C.; Shukla, L.; Roberts, B.; Blakemore, D. C.; Lin, Z.; Marder, T. B.; Steel, P. G. Iridium-Catalyzed C−H Borylation of Pyridines. *Org. Biomol. Chem.* **2014**, *12*, 7318−7327. (k) Sadler, S. A.; Hones, A. C.; Roberts, B.; Blakemore, D.; Marder, T. B.; Steel, P. G. Multidirectional Synthesis of Substituted Indazoles via Iridium-Catalyzed C−H Borylation. *J. Org. Chem.* **2015**, *80*, 5308−5314. (l) Konishi, S.; Kawamorita, S.; Iwai, T.; Steel, P. G.; Marder, T. B.; Sawamura, M. Site-Selective C-H Borylation of Quinolines at the C8 Position Catalyzed by a Silica-Supported Phosphane-Iridium System. *Chem. Asian J.* **2014**, *9*, 434−438. (m) Ishiyama, T.; Takagi, J.; Yonekawa, Y.; Hartwig, J. F.; Miyaura, N. Iridium-Catalyzed Direct Borylation of Five-Membered Heteroarenes by Bis(pinacolato)diboron: Regioselective, Stoichiometric, and Room Temperature Reactions. *Adv. Synth. Catal.* **2003**, *345*, 1103−1106. (n) Takagi, J.; Sato, K.; Hartwig, J. F.; Ishiyama, T.; Miyaura, N. Iridium-Catalyzed C−H Coupling Reaction of Heteroaromatic Compounds with Bis(pinacolato)diboron: Regioselective Synthesis of Heteroarylboronates. *Tetrahedron Lett.* **2002**, *43*, 5649−5651. (o) Hartwig, J. F. Borylation and Silylation of C−H Bonds: A Platform for Diverse C−H Bond Functionalizations. *Acc. Chem. Res.* **2012**, *45*, 864−873. (p) Mkhalid, I. A. I.; Barnard, J. H.; Marder, T. B.; Murphy, J. M.; Hartwig, J. F. C−H Activation for the Construction of C−B Bonds. *Chem. Rev.* **2010**, *110*, 890−931. (q) Larsen, M. A.; Hartwig, J. F. Iridium-Catalyzed C−H Borylation of Heteroarenes: Scope, Regioselectivity, Application to Late-Stage Functionalization, and Mechanism. *J. Am. Chem. Soc.* **2014**, *136*, 4287−4299. (r) Haldar, C.; Hoque, M. E.; Chaturvedi, J.; Hassan, M. M. M.; Chattopadhyay, B. Ir-Catalyzed Proximal and Distal C−H Borylation of Arenes. *Chem. Commun.* **2021**, *57*, 13059−13074. (s) Bisht, R.; Haldar, C.; Hassan, M. M. M.; Hoque, M. E.; Chaturvedi, J.; Chattopadhyay, B. Metal-catalysed C−H Bond Activation and Borylation. *Chem. Soc. Rev.* **2022**, *51*, 5042−5100.
(4) Neeve, E. C.; Geier, S. J.; Mkhalid, I. A. I.; Westcott, S. A.; Marder, T. B. Diboron(4) Compounds: From Structural Curiosity to Synthetic Workhorse. *Chem. Rev.* **2016**, *116*, 9091−9161.
(5) (a) Taylor, R. D.; MacCoss, M.; Lawson, A. D. G. Rings in Drugs. *J. Med. Chem.* **2014**, *57*, 5845−5859. (b) Michael, J. P. Quinoline, Quinazoline and Acridone Alkaloids. *Nat. Prod. Rep.* **2008**, *25*, 166−187. (c) Marella, A.; Tanwar, O. P.; Saha, R.; Ali, M. R.; Srivastava, S.; Akhter, M.; Shaquiquzzaman, M.; Alam, M. M. Quinoline: A Versatile Heterocyclic. *Saudi Pharm. J.* **2013**, *21*, 1−12. (d) Chan, P.; Shao, L.; Tomlinson, B.; Zhang, Y.; Liu, Z.-M. An Evaluation of Pitavastatin For The Treatment of Hypercholesterolemia. *Expert Opin. Pharmacother.* **2019**, *20*, 103−113. (e) Van Deun, A.; Decroo, T.; Tahseen, S.; Trébucq, A.; Schwoebel, V.; Ortuno-Gutierrez, N.; de Jong, B. C.; Rieder, H. L.; Piubello, A.; Chiang, C.-Y. World Health Organization 2018 Treatment Guidelines for Rifampicin-Resistant Tuberculosis: Uncertainty, Potential Risks and the Way Forward. *Int. J. Antimicrob. Agents* **2020**, *55*, 105822.
(6) (a) Harrisson, P.; Morris, J.; Marder, T. B.; Steel, P. G. Microwave-Accelerated Iridium-Catalyzed Borylation of Aromatic C−H Bonds. *Org. Lett.* **2009**, *11*, 3586−3589. (b) Tajuddin, H.; Harrisson, P.; Bitterlich, B.; Collings, J. C.; Sim, N.; Batsanov, A. S.; Cheung, M. S.; Kawamorita, S.; Maxwell, A. C.; Shukla, L.; Morris, J.; Lin, Z.; Marder, T. B.; Steel, P. G. Iridium-Catalyzed C−H Borylation of Quinolines and Unsymmetrical 1,2-Disubstituted Benzenes: Insights into Steric and Electronic Effects on Selectivity. *Chem. Sci.* **2012**, *3*, 3505−3515. (c) Harrisson, P.; Morris, J.; Steel, P. G.; Marder, T. B. A One-Pot, Single-Solvent Process for Tandem, Catalyzed C−H Borylation-Suzuki-Miyaura Cross-Coupling Sequences. *Synlett* **2009**, *2009*, 147−150. (d) Iwai, T.; Sawamura, M. Transition-Metal-Catalyzed Site-Selective C−H Functionalization of Quinolines beyond C2 Selectivity. *ACS Catal.* **2015**, *5*, 5031−5040.
(7) (a) Suda, K. J.; Hicks, L. A.; Roberts, R. M.; Hunkler, R. J.; Matusiak, L. M.; Schumock, G. T. Antibiotic Expenditures by Medication, Class, and Healthcare Setting in the United States, 2010−2015. *Clin. Infect. Dis.* **2018**, *66*, 185−190. (b) Almalki, Z. S.; Yue, X.; Xia, Y.; Wigle, P. R.; Guo, J. J. Utilization, Spending, and Price Trends for Quinolones in the US Medicaid Programs: 25 Years' Experience 1991−2015. *PharmacoEconomics - Open* **2017**, *1*, 123−131.
(8) World Health Organization. Model List of Essential Medicines − 22nd List, 2021.
(9) (a) Emmerson, A. M.; Jones, A. M. The Quinolones: Decades of Development and Use. *J. Antimicrob. Chemother.* **2003**, *51*, 13−20. (b) Pham, T. D. M.; Ziora, Z. M.; Blaskovich, M. A. T. Quinolone Antibiotics. *MedChemComm* **2019**, *10*, 1719−1739. (c) Andersson, M. I.; MacGowan, A. P. Development of the Quinolones. *J. Antimicrob. Chemother.* **2003**, *51*, 1−11. (d) Heeb, S.; Fletcher, M. P.; Chhabra, S. R.; Diggle, S. P.; Williams, P.; Cámara, M. Quinolones: From Antibiotics to Autoinducers. *FEMS Microbiol. Rev.* **2011**, *35*, 247−274. (e) Mitscher, L. A. Bacterial Topoisomerase Inhibitors: Quinolone and Pyridone Antibacterial Agents. *Chem. Rev.* **2005**, *105*, 559−592.
(10) (a) Grohe, K. The Chemistry of the Quinolones: Methods of Synthesizing the Quinolone Ring System. In *Quinolone Antibacterials*, Kuhlmann, J.; Dalhoff, A.; Zeiler, H. J., Eds.; Springer: Berlin, Heidelberg, 1998; pp 13−62. (b) Li, J. J., *Name Reactions: A Collection of Detailed Mechanisms and Synthetic Applications Fifth Edition*. Springer International Publishing: Cham, 2014. (c) Ghosh, P.; Das, S. Synthesis and Functionalization of 4-Quinolones—A Progressing Story. *Eur. J. Org. Chem.* **2019**, *2019*, 4466−4516.
(11) Or need to be (i) halogenated for further functionalisation see: (a) Clarke, S. L.; McGlacken, G. P. Access to trifluoromethylated 4-alkoxy-2-pyrones, pyridones and quinolones. *Tetrahedron* **2015**, *71*, 2906−2913. or (ii) intramolcular see: (b) Nolan, M.-T.; Bray, J. T. W.; Eccles, K.; Cheung, M. S.; Lin, Z.; Lawrence, S. E.; Whitwood, A. C.; Fairlamb, I. J. S. F.; McGlacken, G. P. Pd-catalysed intramolecular regioselective arylation of 2-pyrones, pyridones, coumarins and quinolones by C−H bond functionalization. *Tetrahedron* **2014**, *70*, 7120−7127.

https://doi.org/10.1021/acs.joc.2c00973
J. Org. Chem. 2022, 87, 9977−9987

(12) Shen, C.; Wang, A.; Xu, J.; An, Z.; Loh, K. Y.; Zhang, P.; Liu, X. Recent Advances in the Catalytic Synthesis of 4-Quinolones. *Chem* **2019**, *5*, 1059−1107.
(13) (a) Kuleshova, O.; Asako, S.; Ilies, L. Ligand-Enabled, Iridium-Catalyzed ortho-Borylation of Fluoroarenes. *ACS Catal.* **2021**, *11*, 5968−5973. (b) Pabst, T. P.; Obligacion, J. V.; Rochette, É.; Pappas, I.; Chirik, P. J. Cobalt-Catalyzed Borylation of Fluorinated Arenes: Thermodynamic Control of C(sp2)-H Oxidative Addition Results in ortho-to-Fluorine Selectivity. *J. Am. Chem. Soc.* **2019**, *141*, 15378−15389. (c) Eisenstein, O.; Milani, J.; Perutz, R. N. Selectivity of C−H Activation and Competition between C−H and C−F Bond Activation at Fluorocarbons. *Chem. Rev.* **2017**, *117*, 8710−8753. (d) Budiman, Y. P.; Westcott, S. A.; Radius, U.; Marder, T. B. Fluorinated Aryl Boronates as Building Blocks in Organic Synthesis. *Adv. Synth. Catal.* **2021**, *363*, 2224−2255. (e) Miller, S. L.; Chotana, G. A.; Fritz, J. A.; Chattopadhyay, B.; Maleczka, R. E.; Smith, M. R. C−H Borylation Catalysts that Distinguish Between Similarly Sized Substituents Like Fluorine and Hydrogen. *Org. Lett.* **2019**, *21*, 6388−6392.
(14) Purser, S.; Moore, P. R.; Swallow, S.; Gouverneur, V. Fluorine in medicinal chemistry. *Chem. Soc. Rev.* **2008**, *37*, 320−330.
(15) (a) Bannen, L. C.; Bui, M.; Jiang, F.; Wang, Y.; Xu, W. Compounds for the Treatment of Kinase-Dependent Disorders. WO2019/148043, 2019. (b) Heindel, N. D.; Fine, S. A. Alcoholysis of 4-Chloroquinolines to 4(1H)-Quinolones. *J. Org. Chem.* **1970**, *35*, 796−798. (c) Pou, S.; Dodean, R. A.; Frueh, L.; Liebman, K. M.; Gallagher, R. T.; Jin, H.; Jacobs, R. T.; Nilsen, A.; Stuart, D. R.; Doggett, J. S.; Riscoe, M. K.; Winter, R. W. New Scalable Synthetic Routes to ELQ-300, ELQ-316, and Other Antiparasitic Quinolones. *Org. Process Res. Dev.* **2021**, *25*, 1841−1852. (d) Rádl, S.; Rezková, H.; Obadalová, I.; Srbek, J.; Břicháč, J.; Pekárek, T. Synthesis of 2-(4-Isopropylthiazol-2-yl)-7-methoxy-8-methylquinolin-4-ol; A Quinoline Building Block for Simeprevir Synthesis. *Synthesis* **2014**, *46*, 899−908.
(16) Llinàs-Brunet, M.; Bailey, M. D.; Bolger, G.; Brochu, C.; Faucher, A.-M.; Ferland, J. M.; Garneau, M.; Ghiro, E.; Gorys, V.; Grand-Maître, C.; Halmos, T.; Lapeyre-Paquette, N.; Liard, F.; Poirier, M.; Rhéaume, M.; Tsantrizos, Y. S.; Lamarre, D. Structure−Activity Study on a Novel Series of Macrocyclic Inhibitors of the Hepatitis C Virus NS3 Protease Leading to the Discovery of BILN 2061. *J. Med. Chem.* **2004**, *47*, 1605−1608.
(17) (a) Thompson, A. L. S.; Kabalka, G. W.; Akula, M. R.; Huffman, J. W. The Conversion of Phenols to the Corresponding Aryl Halides Under Mild Conditions. *Synthesis* **2005**, *2005*, 547−550. (b) Murphy, J. M.; Liao, X.; Hartwig, J. F. Meta Halogenation of 1,3-Disubstituted Arenes via Iridium-Catalyzed Arene Borylation. *J. Am. Chem. Soc.* **2007**, *129*, 15434−15435.
(18) (a) Caço, A. I.; Varanda, F.; Pratas de Melo, M. J.; Dias, A. M. A.; Dohrn, R.; Marrucho, I. M. Solubility of Antibiotics in Different Solvents. Part II. Non-Hydrochloride Forms of Tetracycline and Ciprofloxacin. *Ind. Eng. Chem. Res.* **2008**, *47*, 8083−8089. (b) Zhang, Z.; Xiao, X.; Su, T.; Wu, J.; Ren, J.; Zhu, J.; Zhang, X.; Cao, R.; Du, R. Synthesis, Structure-Activity Relationships and Preliminary Mechanism of Action of Novel Water-Soluble 4-Quinolone-3-carboxamides as Antiproliferative Agents. *Eur. J. Med. Chem.* **2017**, *140*, 239−251. (c) Reen, F. J.; Phelan, J. P.; Woods, D. F.; Shanahan, R.; Cano, R.; Clarke, S.; McGlacken, G. P.; O'Gara, F. Harnessing Bacterial Signals for Suppression of Biofilm Formation in the Nosocomial Fungal Pathogen Aspergillus fumigatus. *Front. Microbiol.* **2016**, *7*, 2074. (d) Shanahan, R.; Reen, F. J.; Cano, R.; O'Gara, F.; McGlacken, G. P. The Requirements at the C-3 Position Of Alkylquinolones for Signalling in Pseudomonas Aeruginosa. *Org. Biomol. Chem.* **2017**, *15*, 306−310. (e) Ramos, A. F.; Woods, D. F.; Shanahan, R.; Cano, R.; McGlacken, G. P.; Serra, C.; O'Gara, F.; Reen, F. J. A Structure-Function Analysis of Interspecies Antagonism by the 2-Heptyl-4-alkylquinolone Signal Molecule from Pseudomonas Aeruginosa. *Microbiology* **2020**, *166*, 169−179. (f) Reen, F. J.; Phelan, J. P.; Gallagher, L.; Woods, D. F.; Shanahan, R. M.; Cano, R.; Ó Muimhneacháin, E.; McGlacken, G. P.; O'Gara, F. Exploiting Interkingdom Interactions for Development of Small-Molecule Inhibitors of Candida albicans Biofilm Formation. *Antimicrob. Agents Chemother.* **2016**, *60*, 5894−5905.
(19) (a) Ji, Y.; Brueckl, T.; Baxter, R. D.; Fujiwara, Y.; Seiple, I. B.; Su, S.; Blackmond, D. G.; Baran, P. S. Innate C−H Trifluoromethylation of Heterocycles. *Proc. Natl. Acad. Sci. U.S.A.* **2011**, *108*, 14411−14415. (b) Fujiwara, Y.; Dixon, J. A.; O'Hara, F.; Funder, E. D.; Dixon, D. D.; Rodriguez, R. A.; Baxter, R. D.; Herlé, B.; Sach, N.; Collins, M. R.; Ishihara, Y.; Baran, P. S. Practical and Innate Carbon−Hydrogen Functionalization of Heterocycles. *Nature* **2012**, *492*, 95−99. (c) Fujiwara, Y.; Domingo, V.; Seiple, I. B.; Gianatassio, R.; Del Bel, M.; Baran, P. S. Practical C−H Functionalization of Quinones with Boronic Acids. *J. Am. Chem. Soc.* **2011**, *133*, 3292−3295. (d) Schröter, S.; Stock, C.; Bach, T. Regioselective Cross-Coupling Reactions of Multiple Halogenated Nitrogen-, Oxygen-, And Sulfur-containing Heterocycles. *Tetrahedron* **2005**, *61*, 2245−2267. (e) Düfert, M. A.; Billingsley, K. L.; Buchwald, S. L. Suzuki-Miyaura Cross-Coupling of Unprotected, Nitrogen-Rich Heterocycles: Substrate Scope and Mechanistic Investigation. *J. Am. Chem. Soc.* **2013**, *135*, 12877−12885. (f) Rossi, R.; Bellina, F.; Lessi, M.; Manzini, C. Cross-Coupling of Heteroarenes by C−H Functionalization: Recent Progress towards Direct Arylation and Heteroarylation Reactions Involving Heteroarenes Containing One Heteroatom. *Adv. Synth. Catal.* **2014**, *356*, 17−117.
(20) Uson, R.; Oro, L. A.; Cabeza, J. A.; Bryndza, H. E.; Stepro, M. P. Dinuclear Methoxy, Cyclooctadiene, and Barrelene Complexes of Rhodium(I) and Iridium(I). In *Inorganic Syntheses*, John Wiley & Sons: New York, NY, 1985; pp 126−130.
(21) Sellam, Z.; Brandam, G.; Blanc, R.; Mouad, A.; Hamze, A.; Provot, O.; Khélifi, I. New Targeted Cytotoxic Isocombretaquinoline Derivatives And Conjugates Thereof, WO2018/1782772018.
(22) Nayak, N.; Ramprasad, J.; Dalimba, U. Synthesis and Antitubercular and Antibacterial Activity of Some Active Fluorine Containing Quinoline−Pyrazole Hybrid Derivatives. *J. Fluor. Chem.* **2016**, *183*, 59−68.
(23) Goncalves, V.; Brannigan, J. A.; Whalley, D.; Ansell, K. H.; Saxty, B.; Holder, A. A.; Wilkinson, A. J.; Tate, E. W.; Leatherbarrow, R. J. Discovery of Plasmodium vivaxN-Myristoyltransferase Inhibitors: Screening, Synthesis, and Structural Characterization of their Binding Mode. *J. Med. Chem.* **2012**, *55*, 3578−3582.
(24) Takada, S.; Shindo, H.; Sasatani, T.; Chomei, N.; Matsushita, A.; Eigyo, M.; Kawasaki, K.; Murata, S.; Takahara, Y.; Shintaku, H. Thienylpyrazoloquinolines: Potent Agonists and Inverse Agonists to Benzodiazepine Receptors. *J. Med. Chem.* **1988**, *31*, 1738−1745.
(25) Chen, G.; Shigenari, T.; Jain, P.; Zhang, Z.; Jin, Z.; He, J.; Li, S.; Mapelli, C.; Miller, M. M.; Poss, M. A.; Scola, P. M.; Yeung, K.-S.; Yu, J.-Q. Ligand-Enabled β-C−H Arylation of α-Amino Acids Using a Simple and Practical Auxiliary. *J. Am. Chem. Soc.* **2015**, *137*, 3338−3351.
(26) Chaturvedi, J.; Haldar, C.; Bisht, R.; Pandey, G.; Chattopadhyay, B. Meta Selective C−H Borylation of Sterically Biased and Unbiased Substrates Directed by Electrostatic Interaction. *J. Am. Chem. Soc.* **2021**, *143*, 7604−7611.
(27) Crawford, A. G.; Liu, Z.; Mkhalid, I. A. I.; Thibault, M.-H.; Schwarz, N.; Alcaraz, G.; Steffen, A.; Collings, J. C.; Batsanov, A. S.; Howard, J. A. K.; Marder, T. B. Synthesis of 2- and 2,7-Functionalized Pyrene Derivatives: An Application of Selective C−H Borylation. *Chem.-Eur. J.* **2012**, *18*, 5022−5035.
(28) Robbins, D. W.; Hartwig, J. F. A C−H Borylation Approach to Suzuki−Miyaura Coupling of Typically Unstable 2−Heteroaryl and Polyfluorophenyl Boronates. *Org. Lett.* **2012**, *14*, 4266−4269.

https://doi.org/10.1021/acs.joc.2c00973
J. Org. Chem. 2022, 87, 9977−9987

JOURNAL OF CHEMICAL EDUCATION
Cite This: J. Chem. Educ. 2020, 97, 200−206
Laboratory Experiment
pubs.acs.org/jchemeduc

Synthesis of a Diaryliodonium Salt and Its Use in the Direct Arylation of Indole: A Two-Step Experiment for the Organic Teaching Laboratory

Aisling M. Prendergast,[†] Rachel Shanahan,[†] Aobha Hickey,[†] Francis Harrington,[†] David Schönbauer,[‡] Peter A. Byrne,[†,§] Michael Schnürch,[‡] and Gerard P. McGlacken*[,†,§]

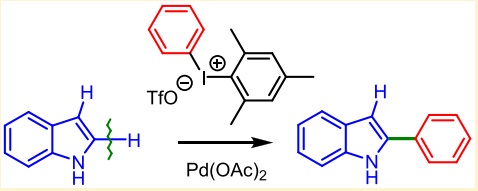
[†]School of Chemistry and Analytical & Biological Chemistry Research Facility (ABCRF), University College Cork, College Road, Cork, Ireland

[‡]Institute of Applied Synthetic Chemistry, Technische Universität Wien, Getreidemarkt 9/163-OC, Vienna 1060, Austria

[§]Solid State Pharmaceutical Centre, Cork, Ireland

Supporting Information

ABSTRACT: In the past decade, C−H functionalization has been a very active topic of research in both academia and industry. When a H atom is replaced by an aryl (or heteroaryl) group, the transformation is termed "direct arylation". This approach to the formation of key (hetero)aryl−(hetero)aryl bonds is complementary to traditional methods, such as the Suzuki−Miyaura and Stille reactions. Direct arylation/C−H functionalization is not represented in the majority of undergraduate chemistry laboratory curricula. An experiment is described here in which students carry out a multistep process, synthesizing a diaryliodonium salt and using it in the direct arylation of indole. Important organic and organometallic chemistry concepts are covered, including catalysis, traditional cross-coupling, C−H functionalization, multistep reaction processes, and regioselectivity. The experiment was successfully carried out by third- and fourth-year students in two universities over a two-year period (four times in total). Both high-yielding and low-yielding chemical steps were encountered, and a number of pedagogical approaches evolved.



KEYWORDS: *Upper-Division Undergraduate, Organic Chemistry, Laboratory Instruction, Hands-On Learning/Manipulatives, Synthesis, Catalysis*

INTRODUCTION

The formation of aryl−aryl and aryl−heteroaryl bonds are key transformations in organic chemistry.[1] The reaction can be carried out using well-known, named reactions such as the Suzuki−Miyaura,[2] Stille,[3] and Negishi reactions[4] and related processes. Indeed, Suzuki and Negishi shared the Nobel Prize in Chemistry in 2010 (along with Richard F. Heck) for their contributions to these types of reactions.[5] The aryl−heteroaryl products that arise from cross-coupling are very prominent throughout medicinal chemistry and also in the agrichemical and energy sectors (Figure 1).

Suzuki−Miyaura and related reactions can be executed under mild reaction conditions, in excellent selectivity and yields,[6] and these transformations have been carried out at the undergraduate level very successfully.[7]

Despite the broad usefulness of traditional cross-coupling reactions, they require the installation of an activating group on each coupling partner (Figure 2i). For example, Suzuki−Miyaura coupling usually involves a boronic acid and an aryl halide, and Stille coupling utilizes tin-based reagents and aryl halides. The installation of these activating groups has time and cost implications, especially on a large scale. There is also the associated waste after the reaction. Tin-based residues, in particular, are usually toxic, and their disposal has environmental issues.[8]

In the past decade, organic chemists have begun to replace one (or sometimes both) reactants with "unactivated" coupling partners (Figure 2ii). The unactivated coupling partner contains a C−H group, and the H is substituted in the reaction process. The methodology is termed "C−H activation" or "C−H functionalization".[9] The direct functionalization of the C−H group in cross-coupling has a number of major advantages:

(1) The substrate does not have to be preactivated.
(2) The waste is H, which can usually be picked up in its H^+ form using base; thus, it can present fewer environmental concerns.
(3) Direct C−H functionalization can provide advantages in situations where halogenated, borylated, or stannylated coupling partners are difficult to prepare.
(4) Because of the number of C−H bonds present in many molecules of biological relevance and because chemists

Received: June 5, 2019
Revised: October 8, 2019
Published: November 4, 2019

Downloaded via UNIV COLG CORK on April 12, 2022 at 15:31:13 (UTC).
See https://pubs.acs.org/sharingguidelines for options on how to legitimately share published articles.

ACS Publications
© 2019 American Chemical Society and Division of Chemical Education, Inc.

DOI: 10.1021/acs.jchemed.9b00525
J. Chem. Educ. 2020, 97, 200−206

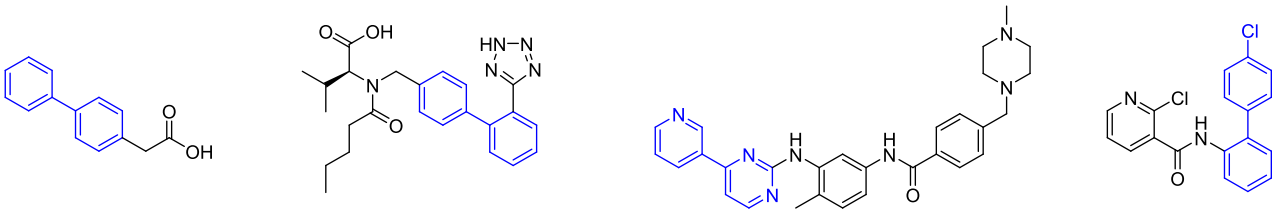


Figure 1. Important compounds containing key aryl−aryl bonds and their heterocyclic counterparts. (Het)aryl−(Het)aryl moieties are in blue.

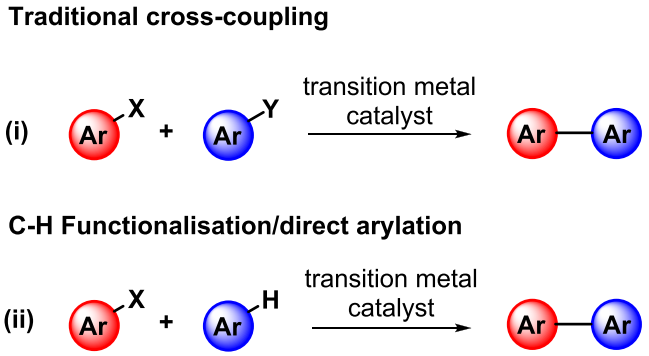


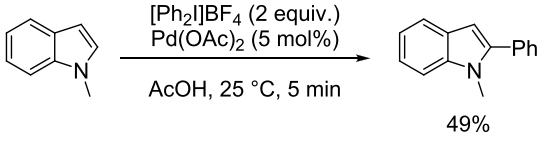
Figure 2. Traditional cross-coupling and C−H functionalization (X = halide; Y = boronic acid, stannyl group, etc.)

are continuing to develop new C−H functionalization chemistry, molecular entities that are difficult to prepare via traditional cross-coupling can become accessible.

However, there are many challenges in the field of C−H functionalization. For example, in aryl compounds (and often in heteroaryl compounds), the C−H bond is quite strong and thus can be difficult to cleave.

Indoles comprise the structural cores of many biologically active natural (e.g., serotonin, a neurotransmitter) and unnatural (e.g., sertindole, an antipsychotic drug) compounds.[10] Aryl indoles, in particular, are prevalent in a range of therapeutics.[11] Initial work by Sanford (Scheme 1),[12]

Scheme 1. Arylation of Indoles under Mild Conditions, Demonstrated by Sanford and Co-workers[12]



Gaunt,[13] and others demonstrated that certain C−H bonds in indole could be broken using transition metal catalysts and coupled with aryl iodonium salts to form new C−C bonds. Aryl iodonium salts[14] involve iodine in a +III oxidation state, which has the consequence of making the attached aryl group quite reactive.

Since the seminal publications, a number of groups have reported alternative reaction conditions. For example Malmgren et al.[15] published the arylation of indoles at the 2-position in water. Fairlamb and co-workers carried out C−H functionalization reactions on tryptophan derivatives without the need for acidic solvents, base, or additional oxidants.[16]

Herein, a laboratory experiment involving the synthesis of a diaryliodonium salt and its application in the direct arylation of indole is described. This experiment is aimed at students at an upper undergraduate or Masters of Science level. It was undertaken by four sets of undergraduate chemistry students at University College Cork (UCC), Ireland, and at Technische Universität Wien (TU Wien), Austria, over two academic years.

During the experiment, the students synthesized the diaryliodonium salt and employed the salt in the Pd-catalyzed arylation of indole. The pedagogical goals that we aimed to achieve and the learning outcomes that we envisaged for the participating students are listed and described in detail in the Supporting Information (SI).

EXPERIMENTAL OVERVIEW

In summary, the diaryliodonium salt synthesis and subsequent direct arylation reaction were carried out without the need for specialized glassware or prior purification of reagents or solvents. The diaryliodonium salt prepared in step 1 did not require purification prior to use, and the direct arylation product was purified using flash column chromatography in step 2.

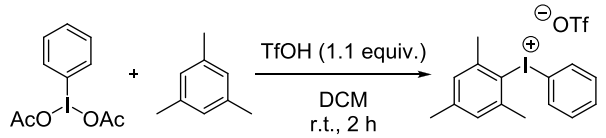
Course instructors can tailor the experiment to suit their needs, allowing them to highlight themes from the experiment that are relevant to their pedagogical goals and course content.

The two parts of the laboratory experiment were completed across three 3 h laboratory sessions. This, along with the scientific content, makes it an ideal exercise for third- and fourth-year undergraduates as part of a Bachelor of Science degree or for Master of Science or Master of Chemistry programs. Detailed experimental procedures can be found in the SI.

Diaryliodonium Salt Synthesis

The diaryliodonium salt was synthesized from commercially available phenyliodo(III)diacetate (PIDA) (Scheme 2).[15]

Scheme 2. Synthesis of Diaryliodonium Salt



PIDA and mesitylene were suspended in dichloromethane (DCM), and the suspension was cooled to 0 °C using an ice bath. Trifluoromethanesulfonic acid (TfOH) was added dropwise to the stirring mixture. Once addition was complete, the mixture was stirred for 2 h and then concentrated under reduced pressure. Diethyl ether (Et_2O) was added to the residue, and a solid precipitated. The solid was isolated using a

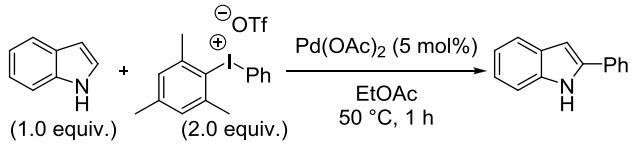
DOI: 10.1021/acs.jchemed.9b00525
J. Chem. Educ. 2020, 97, 200−206

Büchner funnel and washed further with Et_2O until the filtrate ran clear of colored components. The solid was left to dry in air in an oven at 65 °C for 1 h prior to use. Students were expected to obtain a yield of >90% from a well-executed experiment. Purity was checked by melting point analysis and ^{1}H NMR spectroscopy. If desired, this step of the procedure could be performed in pairs, as an excess of diaryliodonium salt was usually obtained relative to the amount required for the subsequent direct arylation step. The compound is a stable solid and can be stored at ambient temperature for extended periods of time. Additional tests showed the solid is stable at 65 °C for several days. This gives flexibility with regard to the scheduling of laboratory classes: both reactions (Sessions 1 and 2) may be performed in 1 day or scheduled over a couple of weeks.

Direct Arylation Reaction

The direct arylation reaction was performed using commercially available $Pd(OAc)_2$ and indole (Scheme 3). The

Scheme 3. Direct Arylation Reaction



conditions are based on reported conditions for the arylation of tryptophan derivatives.[16] None of the reagents or solvents were purified prior to use. The catalyst was employed at 5 mol % loading and ethyl acetate (EtOAc) was used as the solvent. The mixture was stirred at 50 °C for 1 h. Once consumption of the starting material was confirmed by TLC, the reaction was cooled to ambient temperature. The organic layer was washed with a saturated solution of sodium bicarbonate and brine, dried over $MgSO_4$, filtered, and concentrated onto Celite under reduced pressure. The crude residue on Celite was loaded onto a column of silica gel, and the product was eluted with a mixture of EtOAc and cyclohexane in moderate yields (typical student yield was ca. 30%).

It should be emphasized to students that care must be taken to ensure complete removal of residual solvent. Some yields reported by students were inflated because of residual solvent and poor drying. Again, this was recognized by students in their reports.

Following their experimental work, participating students completed written reports, which were structured to each include a title, date, introduction, results, discussion, experimental section, and conclusion. Details of the NMR spectra used to establish product purity were included, as were details of the yields of the iodonium salt and 2-arylindole products.

HAZARDS

Students must wear safety glasses, lab coats, and gloves. These reactions should be performed in a fume hood or similarly well-ventilated workspace. The experiment must be fully risk-assessed by all participants. This was performed as part of a prelaboratory assessment to ensure compliance. PIDA and sodium bicarbonate are not classified as hazardous substances or mixtures, although caution should always be taken. Mesitylene, diethyl ether, and ethyl acetate are flammable and can cause skin and respiratory irritation, as well as dizziness on inhalation. Trifluoromethanesulfonic acid is corrosive. Dichloromethane causes skin and serious eye irritation and may cause respiratory irritation and damage to organs. The diaryliodonium salt synthesized causes skin and serious eye irritation and may cause respiratory irritation. Indole is toxic in contact with skin, causes skin and serious eye irritation, and may cause respiratory irritation. Palladium(II) acetate causes serious eye damage. Chloroform-d_3 is a potential carcinogen, is harmful if swallowed, causes skin and serious eye irritation, is toxic if inhaled, and causes damage to organs. Please treat the isolated phenyl indole and all side products or byproducts as toxic, and avoid contact with skin.

RESULTS AND DISCUSSION

Experimental Sessions at University College Cork (UCC), Ireland

At UCC, third-year undergraduate chemistry students undertook the experiment in three 3 h sessions over 2 days. In the first year (2018) in which this experiment was run, nine students participated and worked individually. In the second year (2019), 17 students participated and worked mainly in pairs. Very little difference was noticed between both cohorts, and thus, the results will be taken together. Laboratory demonstrators were on hand throughout to assist the students if necessary. On the first day, students synthesized the diaryliodonium salt (Session 1, average yield of 91%).

Two students obtained material that would correspond to yields >100% as a result of insufficient drying of the salt. This was recognized by both students in their reports. The melting point of the diaryliodonium salt was obtained by each student to confirm that the salt had been successfully synthesized. The ^{1}H NMR spectrum of the newly formed salt was also obtained by each student or student pair. A representative example of a ^{1}H spectrum obtained by a student is shown in Figure S1 in the SI.

Next (Session 2), the students used the iodonium salt in the direct arylation reaction as described in detail in the SI; this was followed by an aqueous workup and concentration of the organic layers onto Celite for loading onto flash chromatography columns. On the second day (Session 3), the students purified their products using flash chromatography. The ^{1}H NMR spectrum of each student's product was recorded. Of the nine students (year 1), six successfully isolated the 2-phenylindole product from the crude reaction mixture. The yields ranged from 13 to 55%. A sample spectrum from one student is shown in Figure S3 in the SI. The success of the reaction was determined by ^{1}H NMR spectroscopy through comparison of the starting materials and the product spectra. In particular, students were able to recognize the shift in the C3 proton resonance (from ca. 6.6 to 6.8 ppm), as well as the absence of the C2 proton resonance of the indole starting material (7.4 ppm) in the spectrum of the arylated product. The increased complexity of the aromatic region was also noted by students. Finally, it was relayed to students that the purity of the final product would, in some cases, not be sufficient for publication in scientific research journals. For the students that did not isolate pure 2-phenylindole, the ^{1}H NMR spectra showed, in some cases, that the product was contaminated with suspected 2-mesitylindole (a side product), mesityl iodide (a byproduct), or a combination of both. Additionally, the NMR spectra of some students revealed residual solvent as a result of incomplete drying of the product

DOI: 10.1021/acs.jchemed.9b00525
J. Chem. Educ. 2020, 97, 200−206

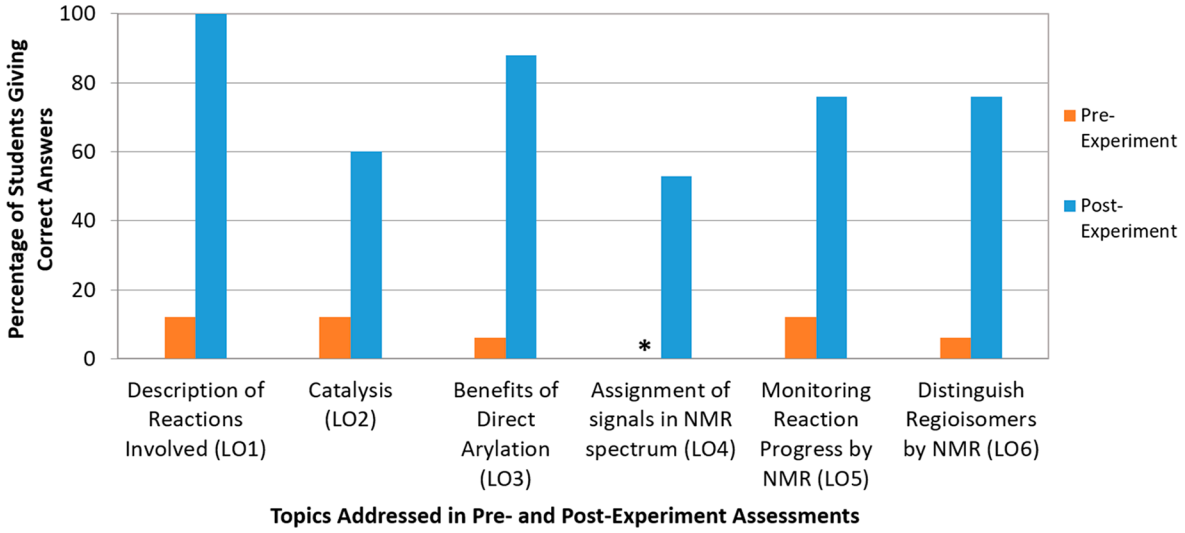


Figure 3. Bar chart showing student performance in pre- and postexperiment assessments questions relating to fulfilment of learning outcomes (LOs) 1−6 for students from the UCC 2019 cohort. For the LO marked with an asterisk (*), we did not attempt to assess students' prior knowledge of this topic (interpretation and assignment of signals the ^{1}H NMR spectrum of the product). See the main text for details.

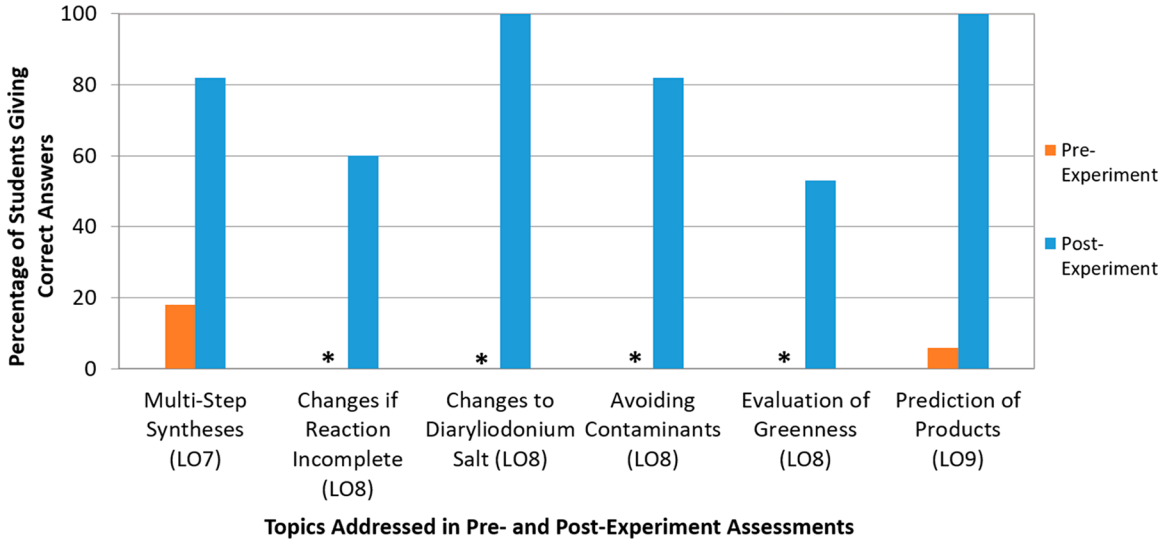


Figure 4. Bar chart showing student performance in pre- and postexperiment assessment questions relating to fulfilment of learning outcomes (LOs) 7−9 for students from the UCC 2019 cohort. For the LOs marked with asterisks (*), we did not attempt to assess students' prior knowledge of these topics. See the main text for details.

prior to measuring the yield and preparing the NMR sample. As such, some yields reported by students were inflated.

Experimental Sessions at Technische Universität Wien (TU Wien), Austria

At TU Wien, the two-step sequence was embedded in the Advanced Synthetic Chemistry laboratory course, which is a mandatory course for fourth-year students pursuing a Master's Degree in synthetic chemistry. Therefore, the students at TU Wien are effectively one year more advanced than the students at UCC. Eight students participated in each of the 2 years (16 in total) the experiment was run. In the aforementioned laboratory course, students prepare two polymer chemistry experiments, four organometallic experiments, and four mainstream organic experiments. Students are free to execute the 10 experiments in any order within a given time period, and so the experiments were not carried out on the same day by all students. The experimental procedure was identical to that used at UCC.

On average, the synthesis of the diaryliodonium salt gave 95% yield (88−99%). The purity of the compound was determined by ^{1}H NMR spectroscopy, and the results were similar to those reported at UCC.

The subsequent arylation of indole was carried out as per the procedure described, and the results of this step were also comparable. As at UCC, the purification of the 2-phenylindole via column chromatography was challenging for students at TU Wien. The yields ranged from 10 to 39%. Two students obtained an unexpectedly high yield of >80%. However, it was quickly identified that this was due to the presence of some impurities, mainly resulting from incomplete drying of the product after column chromatography. In cases of sufficient drying, the spectra were similar to those obtained at UCC.

DOI: 10.1021/acs.jchemed.9b00525
J. Chem. Educ. 2020, 97, 200−206

APPRAISAL OF ACHIEVEMENT OF PEDAGOGICAL GOALS AND LEARNING OUTCOMES

In order to enable evaluation of the extent to which the learning outcomes were achieved by the students, we conducted pre- and postexperiment assessments of the 17 students in the UCC 2019 cohort in which they were asked to answer a series of questions (included on pp S17−S20 of the SI) focused on the topics covered in our intended learning outcomes.[17] Comparison of students' answers to questions in the pre-experiment assessment (administered prior to the pre-experiment introductory lecture) with their postexperiment assessment answers enabled us to establish whether their understanding of several key concepts of relevance to intended learning outcomes 1−9 had been improved, specifically through their engagement in this experiment. Figure 3 shows a graphical summary of our conclusions on the achievement of intended learning outcomes 1−6 by this group of students. Figure 4 shows a similar graphical summary related to pre- and postexperiment assessment questions of relevance to learning outcomes 7−9. Note that we did not attempt to assess students' prior knowledge of material relevant to learning outcomes 4 and 8, as we felt that it would be unreasonable to expect students of the target level to have experience of these relatively high level outcomes (analysis of reactions and NMR spectra of cross-coupling or direct arylation products).

In general, we observed that students' prior knowledge of the material relevant to intended learning outcomes 1−3, 5−7, and 9 was very limited. Only a small percentage of the students were able to give satisfactory answers to pre-experiment assessment questions on any of the various topics covered (see Figures 3 and 4).

The results displayed in Figure 3 show that learning outcomes 1, 3, 5, and 6 were achieved by at least 76% of the participating students on the basis of their answers to postexperiment assessment questions (see pp S17−S20 in the SI). Learning outcomes 2 and 4 were achieved by 60 and 53%, respectively, of the students involved. It can be seen from Figure 3 that significant improvements in students' understanding of the topics of learning outcomes 1−3, 5, and 6 came about as a direct result of their engagement with the experiment and associated material.

As shown in Figure 4, learning outcomes 7 and 9 were well-achieved by this group of students (82 and 100%, respectively) according to their answers to questions 3 and 6 on the postexperiment assessment. Four questions relevant to learning outcome 8 were included in this assessment. These were intended to assess the student's ability to analyze the reactions they had carried out and improve them, that is, to discern what changes could be made to improve the yield, prevent side reactions, and avoid the presence of contaminants in the products and to evaluate the "greenness" of the process. All students identified suitable modifications to the structure of the diaryliodonium salt to minimize side product formation, and over 80% were able to recognize potential contaminants that could be formed and suggest means of avoiding them. Only 60% put forward adequate suggestions for how to modify reaction conditions to improve the yield of the reaction. Although most students were capable of enunciating the benefits of the direct arylation process in the context of Green Chemistry, only 53% successfully identified drawbacks that compromise the "greenness" of this process (e.g., the use of diaryliodonium salt as a coupling partner, resulting in the formation of a stoichiometric amount of an aryl iodide byproduct). On the basis of this, we conclude that learning outcome 8 was well-achieved by 53% of the participating students and partially achieved by most students (at least 82%).

Learning outcomes 7−9 were more challenging for students than learning outcomes 1−6. By demonstrating their ability to evaluate the factors that dictate success in multistep syntheses, analyze the reactions they had carried out, appraise potential improvements, and predict products of unfamiliar reactions (thereby fulfilling learning outcomes 7−9), the students demonstrated evidence of higher order thinking in the context of Bloom's taxonomy of educational objectives.[18]

On the basis of our analysis of these data, and the extent to which learning outcomes 1−9 were achieved by the 17 students involved in UCC in 2019, we conclude that pedagogical goals 1−3, 5−7, and 9 were well-achieved, whereas pedagogical goals 4 and 8 were partly achieved.

CONCLUSIONS

This laboratory experiment allowed students to work on a multistep reaction by synthesizing a diaryliodonium salt and using it in a subsequent direct arylation reaction. Important organic and organometallic chemistry concepts are covered, including catalysis, traditional cross-coupling, direct arylation/C−H functionalization, multistep reactions, and regioselectivity. Techniques to focus on include NMR spectroscopy and TLC. The emphasis placed on each concept and on the analytical techniques can be at the instructor's discretion. This allows flexibility with respect to the availability of equipment. The experiment can also be tailored to the needs of the student group.

The first part of the experiment demonstrated the synthesis of a diaryliodonium salt. Sufficient quantities were produced to allow this part of the experiment to be conducted in pairs if needed.

The second part of the experiment allowed the students to use the previously synthesized diaryliodonium salt in a direct arylation reaction. This aided the students' understanding of the importance of taking care with each synthetic step, as they can impact subsequent steps. A reaction carried out by a demonstrator in the absence of palladium catalyst showed that only the diaryliodonium salt and the indole starting material were present, as observed by TLC and ^{1}H NMR spectroscopy. This facilitated student understanding of the role of a catalyst in an organic chemistry reaction. The direct arylation reaction can generate a mixture of arylated indoles, which were not always separated by the students after purification by flash chromatography. An example of a student's ^{1}H NMR spectrum after purification is shown in the SI. Students were able to assign key product ^{1}H NMR signals.

To conclude, this laboratory experiment was undertaken by undergraduate chemistry students at University College Cork, Ireland, and at Technische Universität Wien, Austria, over 2 years (four times in total). The experiments can be used to demonstrate a number of important topics and analytical techniques in organic chemistry. As discussed, key topics include catalysis, traditional cross-coupling, and C−H functionalization, as well as NMR spectroscopy and TLC. Links can also be made to the movement toward more environmentally responsible organic synthesis, such as the use of EtOAc as a solvent, no addition of ligand, the use of a low reaction temperature, and of course the inherent avoidance of

DOI: 10.1021/acs.jchemed.9b00525
J. Chem. Educ. 2020, 97, 200−206

one activation partner with C−H functionalization. However, the C−H functionalization step does utilize iodonium salts, which are atom uneconomic, and thus there is scope for some in-class debate. As such, a variety of students should find the experiment engaging. The practical experience will help students in their understanding of what can be challenging techniques to adequately portray in lectures. For example, students performed work-ups and column chromatography. The latter in particular proved an excellent training output. Given that the yields were moderate, separation of the pure arylated indole was challenging; however, importantly, it mimics many of the necessary purifications encountered on a daily basis in research laboratories. The range of concepts and techniques employed gives the instructor a lot of flexibility to tailor the laboratory experience to best suit their course content.

■ ASSOCIATED CONTENT

Supporting Information

The Supporting Information is available on the ACS Publications website at DOI: 10.1021/acs.jchemed.9b00525.

Instructions for students, safety information, sample preparation (^{1}H and ^{13}C NMR spectroscopy), and notes for instructors (PDF, DOCX)

■ AUTHOR INFORMATION

Corresponding Author

*E-mail: g.mcglacken@ucc.ie.

ORCID

Aisling M. Prendergast: 0000-0002-6332-0525

Gerard P. McGlacken: 0000-0002-7821-0804

Notes

The authors declare no competing financial interest.

■ ACKNOWLEDGMENTS

The authors wish to thank Pamela Mackey, Katrina Mackey, and Emma Alcock for acting as laboratory demonstrators for the students at UCC. In addition, the authors are grateful to the third-year Chemistry, Chemistry of Pharmaceutical Compounds, and Chemistry with Forensic Science students at UCC and the fourth-year students at TUW who performed this experiment. G.M.G. wishes to acknowledge funding from Science Foundation Ireland (SFI) and the Synthesis and Solid State Pharmaceutical Centre (SSPC), Grant numbers SFI/12/IP/1315 and SFI/12/RC/2275. Finally, the authors wish to acknowledge the contribution of the European COST, Action CA15106 (C−H Activation in Organic Synthesis, CHAOS).

■ REFERENCES

(1) (a) McGlacken, G. P.; Bateman, L. M. Recent advances in aryl-aryl bond formation by direct arylation. *Chem. Soc. Rev.* **2009**, *38*, 2447−2464. (b) Alberico, D.; Scott, M. E.; Lautens, M. Aryl-Aryl Bond Formation by Transition-Metal-Catalyzed Direct Arylation. *Chem. Rev.* **2007**, *107*, 174−238. (c) Ackermann, L.; Vicente, R.; Kapdi, A. R. Transition-metal-catalyzed direct arylation of (hetero)-arenes by C-H bond cleavage. *Angew. Chem., Int. Ed.* **2009**, *48*, 9792−9826.

(2) (a) Miyaura, N.; Yamada, K.; Suzuki, A. A new stereospecific cross-coupling by the palladium-catalyzed reaction of 1-alkenylboranes with 1-alkenyl or 1-alkynyl halides. *Tetrahedron Lett.* **1979**, *20*, 3437−3440. (b) Miyaura, N.; Suzuki, A. Stereoselective synthesis of arylated (E)-alkenes by the reaction of alk-1-enylboranes with aryl halides in the presence of palladium catalyst. *J. Chem. Soc., Chem. Commun.* **1979**, 866−867.

(3) Milstein, D.; Stille, J. K. Palladium-catalyzed coupling of tetraorganotin compounds with aryl and benzyl halides. Synthetic utility and mechanism. *J. Am. Chem. Soc.* **1979**, *101*, 4992−4998.

(4) (a) Negishi, E.-i.; Baba, S. Novel stereoselective alkenyl-aryl coupling via nickel-catalysed reaction of alkenylanes with aryl halides. *J. Chem. Soc., Chem. Commun.* **1976**, 596b−597b. (b) Baba, S.; Negishi, E. A novel stereospecific alkenyl-alkenyl cross-coupling by a palladium- or nickel-catalyzed reaction of alkenylalanes with alkenyl halides. *J. Am. Chem. Soc.* **1976**, *98*, 6729−6731. (c) Negishi, E.; King, A. O.; Okukado, N. Selective carbon-carbon bond formation via transition metal catalysis. 3. A highly selective synthesis of unsymmetrical biaryls and diarylmethanes by the nickel- or palladium-catalyzed reaction of aryl- and benzylzinc derivatives with aryl halides. *J. Org. Chem.* **1977**, *42*, 1821−1823. (d) King, A. O.; Okukado, N.; Negishi, E.-i. Highly general stereo-, regio-, and chemoselective synthesis of terminal and internal conjugated enynes by the Pd-catalysed reaction of alkynylzinc reagents with alkenyl halides. *J. Chem. Soc., Chem. Commun.* **1977**, 683−684.

(5) Johansson Seechurn, C. C. C.; Kitching, M. O.; Colacot, T. J.; Snieckus, V. Palladium-catalyzed cross-coupling: a historical contextual perspective to the 2010 Nobel Prize. *Angew. Chem., Int. Ed.* **2012**, *51*, 5062−5085.

(6) (a) Suzuki, A. Cross Coupling Reactions Of Organoboranes: An Easy Way To Construct C-C Bonds (Nobel Lecture). *Angew. Chem., Int. Ed.* **2011**, *50*, 6722−6737. (b) Nicolaou, K. C.; Bulger, P. G.; Sarlah, D. Palladium-catalyzed cross-coupling reactions in total synthesis. *Angew. Chem., Int. Ed.* **2005**, *44*, 4442−4489.

(7) (a) Hamilton, A. E.; Buxton, A. M.; Peeples, C. J.; Chalker, J. M. An Operationally Simple Aqueous Suzuki−Miyaura Cross-Coupling Reaction for an Undergraduate Organic Chemistry Laboratory. *J. Chem. Educ.* **2013**, *90*, 1509−1513. (b) Aktoudianakis, E.; Chan, E.; Edward, A. R.; Jarosz, I.; Lee, V.; Mui, L.; Thatipamala, S. S.; Dicks, A. P. Greening Up" the Suzuki Reaction. *J. Chem. Educ.* **2008**, *85*, 555−557. (c) Soares, P.; Fernandes, C.; Chavarria, D.; Borges, F. Microwave-Assisted Synthesis of 5-Phenyl-2-hydroxyacetophenone Derivatives by a Green Suzuki Coupling Reaction. *J. Chem. Educ.* **2015**, *92*, 575−578.

(8) (a) Appel, K. E. Organotin compounds: toxicokinetic aspects. *Drug Metab. Rev.* **2004**, *36*, 763−786. (b) Graceli, J. B.; Sena, G. C.; Lopes, P. F.; Zamprogno, G. C.; da Costa, M. B.; Godoi, A. F.; Dos Santos, D. M.; de Marchi, M. R.; Dos Santos Fernandez, M. A. Organotins: a review of their reproductive toxicity, biochemistry, and environmental fate. *Reprod. Toxicol.* **2013**, *36*, 40−52. (c) Gajda, T.; Jancso, A. Organotins. Formation, Use, Speciation, and Toxicology. In *Organometallics in Environment and Toxicology*; Sigel, A., Sigel, H., Sigel, R. K. O., Eds.; Metal Ions in Life Sciences 7; Royal Society of Chemistry: London, 2010; pp 111−151.

(9) The term C—H activation is also used. However, this term is associated with specific mechanistic pathways: (a) Bergman, R. G. C-H activation. *Nature* **2007**, *446*, 391−393. (b) Godula, K.; Sames, D. C-H Bond Functionalization in Complex Organic Synthesis. *Science* **2006**, *312*, 67−72.

(10) Wu, Y.-J. New Indole-Containing Medicinal Compounds. In *Heterocyclic Scaffolds II: Reactions and Applications of Indoles*; Gribble, G. W., Ed.; Topics in Heterocyclic Chemistry *26*; Springer-Verlag: Berlin, 2010; pp 1−29.

(11) Cacchi, S.; Fabrizi, G. Synthesis and Functionalization of Indoles Through Palladium-catalyzed Reactions. *Chem. Rev.* **2005**, *105*, 2873−2920.

(12) Deprez, N. R.; Kalyani, D.; Krause, A.; Sanford, M. S. Room Temperature Palladium-Catalyzed 2-Arylation of Indoles. *J. Am. Chem. Soc.* **2006**, *128*, 4972−4973.

(13) Phipps, R. J.; Grimster, N. P.; Gaunt, M. Cu(II)-Catalyzed Direct and Site-Selective Arylation of Indoles Under Mild Conditions. *J. Am. Chem. Soc.* **2008**, *130*, 8172−8174.

(14) Zhdankin, V. V. *Hypervalent Iodine Chemistry: Preparation, Structure, and Synthetic Applications of Polyvalent Iodine Compounds*; John Wiley & Sons: New York, NY, 2013.
(15) Malmgren, J.; Nagendiran, A.; Tai, C. W.; Bäckvall, J. E.; Olofsson, B. C 2 Selective Arylation of Indoles with Heterogeneous Nanopalladium and Diaryliodonium Salts. *Chem. - Eur. J.* **2014**, *20*, 13531−13535.
(16) Reay, A. J.; Williams, T. J.; Fairlamb, I. J. Unified mild reaction conditions for C2-selective Pd-catalysed tryptophan arylation, including tryptophan-containing peptides. *Org. Biomol. Chem.* **2015**, *13*, 8298−8309.
(17) Two different approaches to these assessments were employed. Details on the first approach are included in the Instructors' Notes section of the Supporting Information for readers interested in the development of our assessment plan. The second of these approaches, described in the main text, was informed by our observations obtained from the results of the first approach.
(18) Krathwohl, D. R. A Revision of Bloom's Taxonomy: An Overview. *Theory Pract.* **2002**, *41*, 212−218.

DOI: 10.1021/acs.jchemed.9b00525
J. Chem. Educ. 2020, 97, 200−206